Faculty of Sciences
Department of Physics and Astronomy

Variational Renormalization Group Methods for Extended Quantum Systems

Jutho Haegeman

Thesis submitted in fulfillment of the requirements for the degree of
Doctor (Ph.D.) in Sciences: Physics

Year 2010-2011

Supervisor : Prof. Dr. Henri Verschelde

Word of thanks

Preparing for a Ph.D. is not a short trip; it is a long journey. Along this journey, guidance and support of many people has been indispensable. Having reached the destination, it is time to look back and honor those without which this dissertation would not have been. Four years of meeting people is a long time, and despite my best effort, the list below is only a poor and incomplete summary.

At first I would like to thank my supervisor Henri Verschelde, who enabled me to start this journey. I myself could not have foreseen the destination. I am very grateful for pointing me in the right direction, both at the start and whenever I got lost. Secondly, I greatly acknowledge the support I have received from three people during the last year and a half of this journey: Frank Verstraete, Tobias J. Osborne and J. Ignacio Cirac. They are digging into new and fascinating unexplored territories of the land of Theoretical Physics, and were so kind to include me in their team. In a short amount of time, I gathered a lot of knowledge from their experience and expertise. Without their guidance through the rugged terrain that is scientific research, I would not have been able to complete the final rush toward my goal. Hopefully this will be, not the end, but only the beginning of an exciting expedition with many treasures yet to be discovered. Finally, I would also like to thank Guifre Vidal and Dimitri Van Neck. While we have not yet shared common goals —who knows what the future might bring— I strongly appreciate the interest they have shown in my journey.

Acknowledgement is also due to the sponsor of this journey, the Research Fund Flanders, for providing financial support with minimal administrative overhead.

All long journeys require time to relax and to rest. For this, I would like to thank the fellow-minded travelers on my path. Office mates and colleagues, plenty art thou, each with gifts and specialties. Nele (1), Dirk, Benjamin, Nele (2), Hans, David, Jos, Karel, Virginie, as well as many others: thank you for the occasional chats, (semi-) scientific discussions, practical support with matters of all kind, and last but not least, the tradition of Wednesday soccer games. All of us are indebted to our secretary Inge, system administrator Gerbrand and technician Guy for allowing us to focus solely on research and making sure that everything around us keeps running smoothly.

In the same spirit of rest and relaxation, a second paragraph is devoted to all my friends and buddies out there, to whom I am grateful for giving me the chance to revitalize from time to time. My hike through physics was often exchanged for physical hikes through the beautiful landscapes of Mother Earth thanks to Isabelle en Nelson. Reinvigorating fluids were absorbed with Matthieu, Stephane, Wouter and Piet during our biweekly exploration of the many bars in Ghent, or with Jan, Sarah, Dieter, Inge, Soetkin,

Boudewijn, Pieter and Anneleen during the weekends. *Mens sana in corpore sano* and therefore I am grateful to Tomas for the physical labor of Sunday morning mountain biking. And a final word of thanks goes out to Soetkin for the many evenings filled with home-made pizza and British comedy, which were of utmost importance after long and tiring days.

As we have already reached a second page, it is time to thank those people that have been there during a great part of my life. I would like to thank my mother and Jan, for giving me the chance not only to undertake this journey, but also to prepare for it, by enabling me to study both Engineering and Physics, and in the broader sense, for everything they have given me in life. I should not fail to mention my brother Dietwin, although our passions in life are different, for always being interested in my well-being. And as tradition dictates, the final place is reserved for the most important person. I wouldn't know where to start with thanking my girlfriend —or should I say wife— Karo for her unlimited support throughout my whole journey, and these last tough months in particular. I am grateful for the many things, small and large. Providing me with delicious meals every evening, proofreading my papers and dissertation, being my personal scheduler, having such wonderful and helpful parents; it is only the beginning of a very long list. Thank you for always being there for me and for helping me to accomplish my goals. Thank you for your existence.

Jutho Haegeman
September 23rd, 2011

Preface

This dissertation focusses on the application of variational methods to the setting of extended quantum systems. Two major types of extended systems are lattice systems and field theories. The start of this line of research can arguably be dated back to 1992, when White developed its renowned density-matrix renormalization group. It was later realized that the density-matrix renormalization group can be reformulated as a variational method that optimizes over a class of variational ansatz states called matrix product states. This area of research benefited greatly from insights and concepts that were developed in quantum information theory and are now successfully applied to quantum lattice systems and quantum field theories, with a central role being played by the characterization of entanglement in such systems. We contribute by developing a new method for studying time evolution of one-dimensional quantum lattices with matrix product states, based on the time-dependent variational principle. In addition, we introduce a new variational ansatz for studying the dispersion relation of low-lying excitations of one-dimensional lattices, including topologically non-trivial excitations in systems with spontaneous symmetry breaking. We also show how this ansatz is related to the time-dependent variational principle. The same techniques for time evolution and excitations are then applied to the setting of continuous matrix product states, which were recently developed by Verstraete and Cirac (2010). Thirdly, we develop a continuum formulation of the process of entanglement renormalization, introduced by Vidal in 2005. This results in a new variational ansatz that can be used to study quantum field theories at criticality and also has great theoretical value in the search for the relation between entanglement renormalization and the AdS/CFT correspondence. Finally, we devote a separate chapter to the application of these variational strategies to relativistic field theories, where the the absence of an ultraviolet cutoff poses a major difficulty.

Keywords

entanglement, area laws, variational methods, renormalization group, holography, quantum lattice systems, quantum field theories, matrix product states, continuous matrix product states, entanglement renormalization, quantum dynamics, excitations, symmetry breaking, domain walls and kinks, transverse Ising model, Heisenberg model, XXZ model, Gross-Neveu model, Dirac model, Klein-Gordon model

Dutch summary — Nederlandstalige samenvatting

The following pages provide a Dutch summary of the contents of this thesis.

Plaatsing van het onderzoek

Deze thesis behandelt kwantummechanische veeldeeltjessystemen van macroscopische omvang. In tegenstelling tot microscopische systemen zoals moleculen of atoomkernen bevatten zulke systemen een macroscopisch groot aantal deeltjes of vrijheidsgraden. Meestal zijn we dan geïnteresseerd in de eigenschappen van de bulk, zodat de thermodynamische limiet genomen wordt waarbij het aantal vrijheidsgraden oneindig wordt en alle randeffecten verdwijnen. Macroscopische systemen vallen op te delen in twee grote klassen: roostersystemen en veldentheorieën. Beide komen in deze thesis aan bod.

Centraal bij onze studie van kwantummechanische roostersystemen en veldentheorieën is een bepaling van de grondtoestand en de laagste geëxciteerde toestanden. In de terminologie van statistische fysica werken we dus steeds bij de absolute minimumtemperatuur van 0 K. In een kwantummechanische formulering beogen we een accurate bepaling van de laagste eigenwaarden, en bijbehorende eigentoestanden, van de Hamiltoniaan die het systeem modelleert. Hiervoor gebruiken we methoden gebaseerd op het variationele principe, dat heel krachtig is voor de benadering van kwantummechanische ééndeeltjesproblemen. Ook voor veeldeeltjessystemen bieden variationele methoden een aantal interessante vooruitzichten. In tegenstelling tot Monte Carlo gebaseerde technieken voor de bemonstering van de partitiefunctie hebben variationele methoden geen last van het beruchte tekenprobleem, dat verantwoordelijk is voor de ontoepasbaarheid van Monte Carlo technieken op fermionische systemen of gefrustreerde spinsystemen. Bovendien herleiden Monte Carlo technieken de kwantummechanische partitiefunctie tot een groot aantal —hopelijk representatieve— klassieke configuraties. Informatie over geëxciteerde toestanden kan slechts onrechtstreeks worden bekomen. Bij toepassing van het variationele principe wordt een rechtstreekse benadering van de eigentoestanden van de Hamiltoniaan bepaald —zowel voor de grondtoestand als mogelijks voor geëxciteerde toestanden— wat toelaat om fundamenteel kwantummechanische eigenschappen zoals verstrengeling te onderzoeken. Zulke eigenschappen kunnen niet of moeilijk met Monte Carlo technieken worden bepaald. Zoals verderop wordt aangetoond, kunnen we zelfs variationele methoden formuleren die rechtstreeks in de thermodynamische limiet of in

het continuum werken. Onze variationele toestanden zijn intelligent genoeg geconstrueerd om een grondtoestand met oneindig veel vrijheidsgraden te comprimeren in een eindig aantal variationele parameters.

Inleiding en achtergrond

Hoofdstuk 1 introduceert en bespreekt algemene begrippen en concepten die belangrijk blijken voor de verdere studie van kwantummechanische roosterssytemen en veldentheorieën. Sectie 1 behandelt algemene eigenschappen van kwantummechanische systemen in de thermodynamische limiet. Vooraf wordt kort ingegaan op enkele moeilijkheden geassocieerd aan de traditionele beschrijving in termen van Hilbertruimten. Wanneer zulke beschrijving wordt toegepast op kwantumsystemen met oneindig veel vrijheidsgraden, leidt dit tot het probleem van unitair inequivalente representaties en —als manifestatie hiervan— de orthogonaliteitscatastrofe: elke twee inequivalente grondtoestanden zijn noodzakelijk orthogonaal. Een wiskundig rigoureuze behandeling vereist een formulering in termen van C^*-algebra's, maar met enige voorzichtigheid en welwillendheid zullen we ons in deze thesis toch beperken tot de traditionele Hilbertruimte. Vervolgens komt de algemene structuur van het spectrum van geëxciteerde toestanden aan bod voor systemen die invariant zijn onder translaties, een gangbare veronderstelling doorheen de rest van dit werk. De thermodynamische limiet laat toe dat de grondtoestand ontaard is en spontane symmetriebreking vertoont. Bepaalde symmetrieën van het systeem komen niet tot uiting in de grondtoestand en de gebroken symmetrieën transformeren de ene grontoestand in andere grondtoestanden met dezelfde energie. Net zoals in thermodynamische systemen kan de realisatie van symmetrie in de grondtoestand veranderen als functie van de parameters van het systeem, wat aanleiding geeft tot het concept van kwantummechanische fasetransities. Deze spelen zich af bij temperatuur $T = 0$ en worden dus niet geïnduceerd door thermische fluctuaties maar eerder door kwantumfluctuaties.

Sectie 2 van Hoofdstuk 1 gaat dieper in op de aard van deze kwantumfluctuaties in de meest interessante klasse van systemen: sterk gecorreleerde systemen met interacties met korte dracht. Net zoals in statistische fysica maken de sterke correlaties deze systemen ontoegankelijk voor gemiddeld-veld technieken. Deze correlaties worden nu echter veroorzaakt door kwantummechanische eerder dan thermische fluctuaties en zijn daardoor van een totaal verschillende aard. Een enorme vooruitgang van ons inzicht in kwantumfluctuaties werd geboekt door de toepassing van concepten uit kwantuminformatietheorie. Centraal staat het begrip 'verstrengeling', dat uitdrukt in welke mate twee deelsystemen van een kwantumsysteem gecorreleerd zijn op een manier die klassiek onmogelijk is. Verstrengeling is een gevolg van de mogelijke superpositie van klassieke toestanden in één kwantummechanische toestand. In geïsoleerde bipartiete systemen kan deze best worden gekwantificeerd met behulp van de verstrengelingsentropie, hoewel ook andere maten bestaan. Er bestaat geen unieke maat die optimaal is in alle om-

standigheden, bijvoorbeeld wanneer ook klassieke correlaties aanwezig zijn (zoals bij eindige temperatuur). Hoewel kwantumcorrelaties sterker zijn dan klassieke correlaties in termen van de Bell-ongelijkheden, zijn ze ook aan restricties gebonden en voldoen ze in het bijzonder aan de monogamiteitseigenschap: twee maximaal verstrengelde deelsystemen kunnen niet verstrengeld zijn met een derde deelsysteem. In het begin van de jaren '90 groeide het besef dat verstrengeling tevens een belangrijke eigenschap is om het fasediagram van kwantummechanische veeldeeltjessystemen te onderzoeken. Hoewel de verstrengelingsentropie van een deelsysteem met de rest van het systeem evenredig is met het volume van het deelsysteem voor willekeurige kwantumtoestanden, blijkt een evenredigheid met de oppervlakte van de rand van het deelsysteem de gangbare regel in de grondtoestand en laagste geëxciteerde toestanden van systemen met korte-dracht interacties. Enkel voor de kwantummechanische kritische punten in een fasetransitie is een logaritmische afwijking mogelijk. De determinerende grootheid blijkt het bereik van interagerende lengteschalen, gaande van een ultraviolette minimumlengte zoals de roosterparameter of de gemiddelde afstand tussen twee deeltjes in een niet-relativistische veldentheorie tot een infrarode maximumlengte, zijnde de correlatielengte. In kritische theorieën of relativistische veldentheorieën divergeert de verhouding tussen beide omdat de correlatielengte oneindig wordt of de ultraviolette minimumlengte naar nul gaat. In alle andere systemen blijkt deze 'schaling met de oppervlakte' een feit en duidt ze op een soort intrinsieke holografische eigenschap: de informatie in de grondtoestand van een d-dimensionaal systeem kan worden gecomprimeerd in een equivalent $(d-1)$-dimensionaal systeem. Dergelijke oppervlakteschaling werd ook gevonden voor de entropie van een zwart gat. Theorieën voor kwantumgravitatie worden eveneens gekenmerkt door een holografische principe, zoals aangetoond door 't Hooft en Susskind (1993). De overeenkomst tussen beide is niet enkel vanuit theoretisch oogpunt belangrijk. De oppervlakteschaling van verstrengelingsentropie toont aan dat grondtoestanden van systemen met korte-dracht interacties slechts een klein hoekje van de totale Hilbertruimte kunnen bezetten. De holografische eigenschap blijkt de sleutel tot een efficiënte parameterisatie van dit hoekje als een klasse van variationele toestanden. Voor kritische systemen, tenslotte, is een andere vorm van holografie belangrijk. Kritische systemen blijken immers schaalinvariant. Maldacena was in 1999 de eerste die een holografische equivalentie vermoedde waarbij de fysische, schaalinvariante theorie in d dimensies nu op de rand leeft van een $(d+1)$-dimensionale gravitatietheorie in een zogenaamde anti-de Sitter ruimte. De verstrengeling van een fysisch deelsysteem werd door Ryu en Takayanagi in 2006 gerelateerd aan de lengte of oppervlakte van de geodetische curve of het geodetische oppervlak die het deelsysteem omgeeft in de $(d+1)$-dimensionale bulk. Op deze manier krijgt verstrengeling eveneens een geometrische betekenis, wat in verband blijkt te staan met een andere klasse van variationele toestanden die onder meer geschikt blijkt voor de beschrijving van kritische kwantumsystemen.

Ten slotte wordt in Sectie 3 van Hoofdstuk 1 de renormalisatiegroep geïntroduceerd. Deze is uitermate belangrijk voor de studie van systemen met oneindig veel vrijheidsgraden die over een groot bereik van lengteschalen met elkaar interageren. Vertrekkende

van de gekende renormalisatiegroep in relativistische kwantumveldentheorieën en statistische fysica belichten we ook enkele moderne ontwikkelingen. Zo valt de extra dimensie van de anti-de Sitter ruimte in de conjectuur van Maldacena te interpreteren als een renormalisatieschaal. Voortbouwend op Wilson's pionierend werk introduceren we ook het gebruik van de renormalisatiegroep als numerieke methode, in nauwe overeenstemming met het variationele principe. Wilson, die bijdroeg tot de ontwikkeling van zowel de correcte interpretatie van de renormalisatiegroep als verschillende analytische renormalisatieschema's, was tevens de eerste om renormalisatie te gebruiken als een numerieke procedure om de grondtoestand van een onoplosbare Hamiltoniaan te benaderen. Hij bedacht reeds in 1974 een manier om het Kondo probleem —de verstrooiing van conductie-elektronen aan een gelokaliseerde magnetische onzuiverheid in een metaal— af te beelden op een equivalent roosterprobleem, dat dan iteratief kan aangroeien en waarbij de laagste energietoestanden van het vorige rooster kunnen worden gebruikt om de grondtoestand van het huidige rooster te benaderen. Helaas werkte Wilson's aanpak niet voor algemene roosterproblemen, en dit bleef zo tot White in 1992 zijn dichtheidsmatrix-renormalisitatiegroep formuleerde. Deze methode was in staat heel accurate waarden voor de grondtoestandsenergie van allerhande ééndimensionale spinroosters te produceren en vormt nog steeds de meest krachtige methode om ééndimensionale kwantummechanische roostersystemen te bestuderen. Enkele jaren later werd de dichtheidsmatrix-renormalisatiegroep geherformuleerd als een variationele methode over de klasse van matrix product toestanden. Deze doorbraken gaven het startschot voor een hele resem aan nieuwe ontwikkelingen, geïnspireerd door inzichten uit kwantuminformatietheorie. Renormalisatie wordt nu opgevat als een actief proces dat inwerkt op kwantumtoestanden en iteratief informatie verwijdert, wat tot gevolg geeft dat de verstrengeling in opeenvolgens gerenormaliseerde toestanden afneemt (of constant wordt voor kritische punten). Dit culmineert uiteindelijk in de idee dat elke renormalisatiegroeptransformatie voor kwantumtoestanden op zichzelf een klasse van variationele toestanden definieert, zoals wordt aangetoond in Sectie 1 van Hoofdstuk 5. Voor de dichtheidsmatrix-renormalisatiegroep zijn dit de matrix product toestanden, maar deze missen de eigenschap dat ze in staat zijn verstrengeling te verminderen omdat ze niet op een correcte manier over de verschillende schalen werken. Een correcte implementatie leidt uiteindelijk tot het proces van verstrengelingsrenormalisatie, dat aanleiding geeft tot variationele toestanden die ook kritische grondtoestanden kunnen beschrijven.

Daar waar Hoofdstuk 1 alle noodzakelijke achtergrond samenvat die nodig is voor de formulering van geschikte klasses van variationele toestanden voor de beschrijving van sterk gecorreleerde kwantummechanische veeldeeltjesssystemen, richt Hoofdstuk 2 zich op de theorie die toelaat om deze variationele toestanden concreet toe te passen op interessante systemen. Centraal is het alom gekende variationele principe, dat stelt dat de beste benadering voor de grondtoestand van een Hamiltoniaan binnen een variationele variëteit die toestand is die de verwachtingswaarde van de Hamiltoniaan minimaliseert. Wanneer de variationele variëteit zelf een vectorruimte vormt die opgespannen wordt

door een aantal basisvectoren gekozen binnen de totale Hilbertruimte leidt dit tot de zogenaamde Rayleigh-Ritz methode. Voor een meer algemene variëteit leidt het variationele principe tot een stelsel niet-lineaire vergelijkingen waarvoor in het meest algemene geval een benaderde oplossingsmethode nodig is. Het variationele principe is echter niet beperkt tot het bepalen van eigentoestanden van de Hamiltoniaan. In Sectie 2 van Hoofdstuk 2 formuleren we het zogenaamde tijdsafhankelijke variationele principe van Dirac, dat in staat stelt de volledige dynamica van een systeem te projecteren binnen de variationele subruimte. We tonen aan onder welke voorwaarde deze geprojecteerde evolutie de symmetrieën van de exacte evolutie in de totale Hilbertruimte behoudt, en construeren een foutmaat die op elk moment aangeeft hoe sterk de exacte evolutie afwijkt van de geprojecteerde evolutie. Wanneer het tijdsafhankelijke variationele principe gebruikt wordt om een evolutie in imaginaire tijd te beschrijven, bekomen we een krachtige methode om het stelsel van niet-lineaire vergelijkingen van het tijdsonafhankelijke variationele principe op te lossen en om dus de optimale variationele benadering van grondtoestanden te vinden. Nadien wordt in Sectie 3 van Hoofdstuk 2 aangetoond hoe een linearisatie van het tijdsafhankelijk variationele principe rond een optimum van het tijdsonafhankelijk variationele principe kan gebruikt worden om te besluiten dat het raakvlak aan het optimum een goede variationele variëteit vormt voor de beschrijving van de laagste geëxciteerde toestanden van de Hamiltoniaan. Een benadering voor de laagste geëxciteerde eigentoestanden van de Hamiltoniaan kan dus worden gevonden door toepassing van de Rayleigh-Ritz methode op de vectorruimte opgespannen door de raakvectoren van de variationele variëteit in het variationele optimum voor de benadering van de grondtoestand. Tenslotte bespreken we in Sectie 4 van Hoofdstuk 2 nog enkele bijzonderheden van het variationele principe wanneer het wordt toegepast op systemen met oneindig veel vrijheidsgraden. We besteden in het bijzonder de nodige aandacht aan Feynman's ontevredenheid met het variationele principe. Feynman gaf in 1987 drie sterke argumenten waarom hij geloofde dat het variationele principe nooit succesvol toepasbaar zou zijn op systemen met oneindig veel vrijheidgraden. Hoewel Feynman in de eerste plaats dacht aan relativistische kwantumveldentheorieën, gaan zijn argumenten ook op voor de andere systemen die in deze thesis bestudeerd worden. Vooreerst bekritiseerde Feynman het variationele principe ervan te gevoelig te zijn aan hoge frequenties. In systemen waarbij vrijheidsgraden over een groot bereik van lengteschalen interageren, wordt de grondtoestandsenergie typisch gedomineerd door de vrijheidsgraden op de kortste lengteschalen. Alle variationele parameters in de variëteit zullen door toepassing van het variationele principe zo afgestemd worden om de best mogelijke benadering te verkrijgen van het gedrag op korte afstandsschalen. Fysische observabelen daarentegen worden bepaald door het lange afstandsgedrag van de golffunctie en zullen heel slecht benaderd worden. Verder was Feynman de mening toegedaan dat het quasi onmogelijk is om een variationele ansatz te construeren die enerzijds de extensiviteit van de grondtoestand respecteert, en anderzijds toelaat om efficiënt en nauwkeurig verwachtingswaarden te berekenen. Dit zijn uiteraard noodzakelijke eisen om het variationele principe succesvol te kunnen toepassen. Deze thesis stelt tot doel om een variationale ansatz te ontwikkelen die elk van Feynman's argumenten overwint.

Matrix product toestanden voor roosters en velden

Hoofdstuk 3 beschrijft de variationale variëteit van matrix product toestanden, die het laatste decennium succesvol werd toegepast op talloze ééndimensionale roostermodellen. Sectie 1 van dit hoofdstuk introduceert de noodzakelijke definities en vat de bestaande literatuur in verband met de eigenschappen van deze fysische toestanden en van hun parameterisatie als matrix product toestand samen. In de eerste plaats wordt aangetoond waarom deze klasse van toestanden in staat is de grondtoestand van Hamiltonianen met korte-dracht interacties accuraat te benaderen. Belangrijk is dat de verstrengelingsentropie van elk deelsysteem eindig blijft, zodat matrix product toestanden niet kunnen worden gebruikt voor kritische grondtoestanden. Elke matrix product toestand heeft een eindige correlatielengte. Er wordt aangetoond hoe verwachtingswaarden efficiënt kunnen worden berekend —in het bijzonder in geval van open randvoorwaarden— en hoe systemen in de thermodynamische limiet kunnen worden beschreven. Een nieuwe bijdrage in deze sectie is een systematische studie van het raakvlak aan de variëteit. In het bijzonder wordt uitgebreid bestudeerd hoe de ijkvrijheid die aanwezig is in de representatie van matrix product toestanden tot uiting komt in het raakvlak. Aan deze raakvectoren werd tot voor kort geen belang gehecht, en pas met de toepassing van het tijdsafhankelijke variationele principe en onze ansatz voor excitaties is het belang van een grondige studie van het raakvlak duidelijk geworden. De toepassing van het tijdsafhankelijke variationele principe vormt het onderwerp van Sectie 2 van Hoofdstuk 3. Er wordt besproken hoe dit algoritme numeriek kan worden geïmplementeerd, zowel voor eindige roostersystemen met open randvoorwaarden als voor systemen in de thermodynamische limit. In imaginaire tijd ontspruit hieruit een krachtig optimalisatie-algoritme dat een heel accurate bepaling van het variationele optimum toelaat. Voor eindige systemen zou dit algoritme vergeleken kunnen worden met de bestaande variationele strategie gebaseerd op de dichtheidsmatrix-renormalisatiegroep en wordt een hogere effeciëntie verwacht. Het resulterende algoritme werd echter enkel geïmplementeerd in de thermodynamische limiet, omdat op deze systemen de nadruk ligt in deze thesis. Voor dynamische simulaties in reële tijd wordt beschreven hoe een symmetrische numerieke integrator kan worden geconstrueerd die de tijdsomkeringsinvariantie van de differentiaalvergelijkingen respecteert. Het resulterende algoritme overtreft bestaande algoritmes voor tijdsevolutie met matrix product toestanden op het vlak van behoud van symmetrieën, zoals wordt geïllustreerd aan de hand van een voorbeeld. Sectie 3 van Hoofdstuk 3 behandelt ten slotte het gebruik van het raakvlak als ansatz voor geëxciteerde toestanden. Een efficiënte implementatie wordt geconstrueerd. Verder wordt ook een sterk gelijkende ansatz voorgesteld die kan gebruikt worden om topologisch niet-triviale excitaties te beschrijven in systemen met spontane symmetriebreking. Aan de hand van verschillende voorbeelden wordt aangetoond dat een uiterst accurate bepaling van dispersierelaties in spinsystemen mogelijk is met bescheiden computationele vereisten. Tevens wordt aangetoond hoe de bekomen dispersierelaties kunnen helpen bij de studie van kwantummechanische fasetransities en wordt de relatie met de linearisatie van het tijdsafhankelijk variationele

principe expliciet geïllustreerd.

In 2010 werd door Verstraete en Cirac een continue matrix product toestand ontwikkeld, die kan gebruikt worden voor de rechtstreekse studie van ééndimensionale veldentheorieën. Voordien was het enkel mogelijk om veldentheorieën te bestuderen door ze eerst te discretiseren en op een rooster te plaatsen. De variationele variëteit van continue matrix product toestanden wordt behandeld in Hoofdstuk 4. Deze klasse van toestanden werd ontwikkeld door het nemen van een continuumlimiet voor een speciale subklasse van matrix product toestanden, en is uitermate geschikt voor de beschrijving van niet-relativistische systemen met een eindige dichtheid aan deeltjes. De gemiddelde afstand tussen twee deeltjes speelt nu de rol van een effectieve ultraviolette lengteschaal. Relativistische theorieën missen zulke ultraviolette minimumlengte en vereisen een speciale behandeling, wat het onderwerp vormt van Hoofdstuk 6. De volledige analyse van Hoofdstuk 3 kan worden overgedaan voor continue matrix product toestanden. Gezien de recente ontwikkeling van deze klasse van toestanden zijn de meeste resultaten in Hoofdstuk 4 nieuw en tot op heden ongepubliceerd. Bovendien zijn er weinig of geen referentiemogelijkheden, op exacte modellen na. De implementatie van het tijdsafhankelijk variationele principe en van de Rayleigh-Ritz methode voor excitaties in het raakvlak wordt ontwikkeld in Sectie 2 van Hoofdstuk 4. Aangezien de interpretatie parallel is aan deze uit Secties 2 en 3 van Hoofdstuk 3, ligt de nadruk op de afleiding en de implementatie. De resulterende algoritmen worden toegepast op twee eenvoudige voorbeelden in Sectie 3, waar wordt aangetoond dat een vergelijkbare nauwkeurigheid als voor roostersystemen met matrix product toestanden haalbaar is.

Renormalisatie van verstrengeling

Matrix product toestanden —voor roostersystemen of voor veldentheorieën— zijn extensieve toestanden die toelaten om op efficiënte wijze verwachtingswaarden exact te berekenen. Op deze manier overwinnen ze reeds twee van Feynman's argumenten. Ze worden echter geplaagd door de gevoeligheid aan hoge frequenties wanneer het bereik van interagerende schalen divergeert, wat verklaart waarom ze niet kunnen worden toegepast op kritische theorieën. In Hoofdstuk 5 wordt dit probleem geanalyseerd in de context van renormalisatiegroeptransformaties die werkzaam zijn op kwantumtoestanden. De renormalisatiegroeptransformatie geassocieerd aan matrix product toestanden is niet voldoende in staat om de verschillende lengteschalen die werkzaam zijn in het systeem te scheiden. Een verbeterde poging leidt tot de zogenaamde 'renormalisatie van verstrengeling', een proces dat werd geïntroduceerd voor roostersystemen door Vidal in 2005. Deze verbeterde renormalisatiegroeptransformatie definieert een nieuwe variationele klasse die het concept van matrix producten veralgemeent tot een contractie van een tensornetwerk en wel in staat blijkt om kritische grondtoestanden te beschrijven. De eigenschappen van deze variationele ansatz voor roostersystemen in willekeurige dimensies d worden besproken in Sectie 1 van Hoofdstuk 5. In het bijzonder ondersteunen deze

toestanden algebraïsch afvallende correlatiefuncties (dus met oneindige correlatielengte) en logarithmisch divergerende verstrengelingsentropie in ééndimensionale systemen. Bovendien laten deze toestanden eenvoudig toe om kritische exponenten te berekenen in de buurt van kwantummechanische fasetransities, en vertoont de geometrie van het tensornetwerk een kwalitatieve overeenkomst met de geometrie van de anti-de Sitter ruimte in de Maldacena-conjectuur.

Sectie 2 van Hoofdstuk 5 bespreekt hoe we er in geslaagd zijn om een continuüformulering van het concept 'renormalisatie van verstrengeling' te definiëren. De geassocieerde variationele ansatz kan eveneens gebruikt worden voor een rechtstreekse studie van veldentheorieën. We tonen aan dat deze toestanden dezelfde eigenschappen hebben als hun roostervariant. Bovendien illustreren we hoe deze toestanden een renormalisatiegroeptransformatie induceren die rechtstreeks toepasbaar is op operatoren eerder dan op verwachtingswaarden van operatoren. Deze continuümformulering zal hopelijk bruikbaar zijn in verder onderzoek naar het verband tussen renormalisatie van verstrengeling en de Maldacena-conjectuur. De variationele parameters van onze ansatz zijn nu kwantummechanische veldoperatoren en niet langer tensoren, wat nadelig is vanuit praktisch oogpunt. De renormalisiegroepvergelijking voor operatoren wordt in het meest algemene geval sterk niet-linear en kan niet exact worden geïntegreerd. Een numerieke implementatie van het variationele principe voor de meest algemene ansatz is dan niet meer vanzelfsprekend en vormt stof voor verder onderzoek. Desalniettemin kunnen we enkele interessante eigenschappen van onze ansatz illustreren door te beperken tot een subklasse van Gaussische toestanden, wat het onderwerp vormt van Sectie 3 van het desbetreffende hoofdstuk. In het bijzonder tonen we aan dat deze in staat zijn om quasi exact de grondtoestand van vrije theorieën te beschrijven. In de buurt van een kritisch punt kunnen we uit de renormalisatiegroepvergelijking voor schalingsexponenten en bijbehorende schalingsoperatoren afleiden. Tot slot onderzoeken we ook hoe een uitbreiding van onze ansatz aanleiding kan geven tot logaritmische afwijkingen van de schalingswet voor verstrengelingsentropie voor dimensies $d > 1$, zoals wordt waargenomen in kritische fermionsystemen.

Relativistische kwantumveldentheorieën

Doorheen deze thesis werden nieuwe methoden ontwikkeld die werden getoetst aan gebruikelijke referentiemodellen. Eén van de initiële doelstellingen van deze thesis was ook om deze verschillende klassen van variationele methoden toe te passen op relativistische kwantumveldentheorieën. Door het gebrek aan een expliciete ultraviolette minimumlengte vereisen deze een speciale behandeling en vormen ze het onderwerp van Hoofdstuk 6. Sectie 1 beschrijft de traditionele aanpak. Een interessante relativistische veldentheorie in één dimensie, het Gross-Neveu model, wordt gediscretiseerd en de veldoperatoren worden op roostersites geplaatst. Dit lost het divergentieprobleem op, aangezien de momentumruimte en dus het bereik van interagerende schalen eindig wordt.

We kunnen deze roostertheorie bestuderen met onze methoden uit Hoofdstuk 3 gebaseerd op de klasse van matrix product toestanden. Onze resultaten kunnen echter pas worden vergeleken met analytische oplossingen van de veldentheorie als we de gepaste continuümlimiet nemen. Deze vereist dat de correlatielengte constant wordt gehouden terwijl de roosterparameter naar nul wordt geschaald en correspondeert dus met een kritische punt van de roostertheorie. In deze limiet wordt het moeilijk om accurate resultaten te bekomen met de matrix product toestand. In Sectie 2 van Hoofdstuk 6 trachten we daarom rechtstreeks de continue matrix product toestand toe te passen. In het continuüm is de afwezigheid van een minimale lengteschaal echt catastrofaal, zoals voorspeld door Feynman. Zonder een manuele toevoeging van een ultraviolette schaal kunnen geen zinvolle resultaten worden bekomen. We bespreken hoe de continue matrix product toestand ons dus tot een nieuwe manier leidt om relativistische kwantumveldentheorieën te regulariseren en niet-perturbatieve resultaten te bekomen. We passen dit toe op zowel vrije Dirac-fermionen, waarvan we tevens de Casimir-energie berekenen met onze numerieke aanpak, als op het Gross-Neveu-model. Tot slot schakelen we in Sectie 3 van dit hoofdstuk over op de continue verstrengelingsrenormalisatie-ansatz. Hoewel we voorlopig beperkt zijn tot vrije theorieën levert dit toch reeds enkele nuttige inzichten op. Ook bij deze strategie zijn we verplicht om handmatig een ultraviolette momentumschaal in te voeren, maar nu kunnen we deze terug naar oneindig zenden op het einde van het proces. We bestuderen vrije fermionen (Dirac-veld) en bosonen (Klein-Gordon-veld) in een willekeurig aantal dimensies.

Besluiten en vooruitzichten

In dit gebied van de fysica zijn we op een uiterst interessant punt gekomen waar er sterke kruisbestuiving is tussen vele verschillende onderzoeksdomeinen die elk op zich reeds hun diensten bewezen hebben. De samenkomst van ideeën uit vaste-stoffysica, kwantuminformatietheorie, renormalisatiegroeptheorie en zelfs kwantumgravitatie heeft tot een resem aan baanbrekende ontwikkelingen geleid. Centraal staat de vaststelling dat verstrengelingsentropie schaalt als de oppervlakte van de rand, die toelaat te besluiten dat ook in kwantumveeldeeltjessystemen een holografisch principe werkzaam is. Dit heeft geleid tot de formulering van nieuwe klassen van variationele toestanden die willekeurig ver kunnen afwijken van de Gaussische toestand uit de gemiddeld-veld theorie, en toch toelaten om efficiënt en nauwkeurig verwachtingswaarden te berekenen. We zijn tevreden om een bescheiden bijdrage aan dit gebied te kunnen leveren, en voorzien een aantal intrigerende ontwikkelingen die hieruit zouden kunnen voortvloeien.

In Hoofdstuk 3 werd een nieuw algoritme voorgesteld om tijdsevolutie in ééndimensionale kwantummechanische roostersystemen te simuleren met matrix product toestanden, alsook een nieuwe variationele ansatz voor excitaties. Deze blijken extreem nauwkeurig en bovendien computationeel efficiënt. Het expliciet inbouwen van bepaalde symmetrievoorwaarden zou de methoden verder ten goede komen. Het meest uitdagende

vooruitzicht is echter om deze technieken ook toe te passen op meer algemene tensor netwerk toestanden die de veralgemening vormen van de matrix product toestand voor hogerdimensionale roostersystemen. Hoewel dit eenvoudige idee vrij snel zal leiden tot een heel complex algoritme met vele iteratieve en benaderde stappen, toch is het vooruitzicht van een accurate bepaling van dispersierelaties in willekeurige roostersystemen uitermate aanlokkelijk. Aangezien onze methoden polynomiaal schalen in de parameter die de nauwkeurigheid bepaald, zal zulke implementatie zeker haalbaar worden naarmate de rekenkracht van computers verder toeneemt.

Totaal vernieuwend is de formulering van een niet-Gaussische variationele ansatz die rechtstreeks op kwantumveldentheorieën kan worden toegepast, zoals ontwikkeld door Verstraete en Cirac in 2010. In deze thesis werden de variationale technieken uit Hoofdstuk 3 ook toegepast op deze continue matrix product toestand, zowel voor niet-relativistische veldentheorieën in Hoofdstuk 4 als voor relativistische theorieën in Sectie 2 van Hoofdstuk 6. Relativistische theorieën vereisen de invoering van een nieuwe regularisatiestrategie die voorlopig enkel toepasbaar is op fermionische systemen. Hoewel ééndimensionale relativistische bosontheorieën een andere regularisatiestrategie vereisen, staat er verder niets in de weg om deze ook met de continue matrix product toestand te bestuderen. Verder dringt de vraag zich op of ook deze ansatz een veralgemening kent voor hoger-dimensionale systemen. Hoewel er reeds een voorstel werd gegeven in de literatuur, moet nog worden uitgezocht of het mogelijk is om het variationele optimum op een numerieke manier te bepalen. Zelfs indien dit niet mogelijk blijkt, kunnen zulke meer-dimensionale ansätze toch nut hebben voor theoretische doeleinden.

Tot slot is er de continuümformulering van 'renormalisatie van verstrengeling'. De meest fundamentele vraag betreft hier de mogelijkheid om het variationele principe toe te passen op een niet-Gaussisch element uit deze variationale variëteit. Dit zou toe laten om de renormalisatiegroep op een variationele manier te implementeren: de aanwezige vrijheidsgraden zouden optimaal gekozen worden om de beste benadering te vinden voor de grondtoestand van algemene veldentheorieën, zonder dat er gevreesd moet worden voor Feynman's gevoeligheid aan hoge frequenties. De variationele vrijheidsgraden bepalen het gedrag op een specifieke lengteschaal en worden niet beïnvloed door de kortste lengteschalen die de energie domineren. Een andere beloftevolle denkpiste is het vinden van een kwantitatief verband tussen 'verstrengeling van renormalisatie' en de Maldacena-conjectuur met behulp van onze continuümansatz. Een formele afleiding zou kunnen dienen als bewijs van deze conjectuur en zou tevens toelaten om holografisch duale theorieën te construeren voor modellen die niet schaalinvariant zijn.

Table of Contents

Introductory remarks

General introduction

This dissertation deals with extended quantum systems, which, in contrast to microscopic systems such as molecules and nuclei, contain a macroscopic number of particles or degrees of freedom. The main focus of this dissertation is on the bulk properties of such systems, which allows us to take the thermodynamic limit: the number of degrees of freedom becomes infinite and all boundary effects or finite size effects disappear. Extended quantum systems contain two major classes: lattice systems and field theories. Both are studied in this dissertation.

The main objective of our study is a determination of the ground state and possibly lowest excited states of a quantum lattice system or a quantum field theory. In terms of statistical physics, we are always working at the absolute zero temperature. Our main objective is thus to find the lowest eigenvalues and corresponding eigenvectors of the Hamiltonian that describes the system. Our toolbox contains methods based on the variational principle, which has proven extremely powerful for single particle quantum mechanics. Additionally, it offers interesting prospects for quantum many body systems as well. In contrast to techniques based on Monte Carlo sampling of the partition function, variational strategies do not suffer from the notorious sign problem, that hinders the applicability of Monte Carlo methods to fermionic systems and frustrated spin systems. Since Monte Carlo methods reduce the partition function to a number of classical configurations, which are hopefully representative, information about *e.g.* excited states can only be extracted indirectly. This is in sharp contrast to variational approaches, where a direct approximation of the eigenvectors of the Hamiltonian —both the ground state as well as excited states— can be constructed, allowing a direct exploration of fundamental quantum mechanical properties such as entanglement. Such properties are hard to probe with techniques based on Monte Carlo sampling of the classical partition function. As will be illustrated throughout this dissertation, variational ansätze can be constructed that can directly be applied in the thermodynamic limit or in the continuum (*i.e.* to field theories). The variational classes explored in this dissertation are constructed in such an intelligent manner that they can compress the ground state of systems with an infinite number of degrees of freedom into a finite set of variational parameters.

Overview

This area of research has progressed quickly over the last two decades thanks to a cross fertilization between different branches of theoretical physics, including condensed matter physics, quantum information theory and renormalization group theory, with even some ingredients of quantum gravity added to the picture. Chapter 1 extracts a general background from each of these fields. Section 1 introduces basic notions about quantum lattice systems and quantum field theories. While the mathematically rigorous framework for quantum systems with an infinite number of degrees of freedom is briefly highlighted, we choose to stick to a traditional description in terms of Hilbert spaces and only remind to be cautious. The nature of the spectrum of excited states for translation invariant systems is discussed, as well as the aspect of symmetry and breaking thereof. The concept of quantum phase transitions is introduced. The true quantum nature of these systems is only fully appreciated thanks to insights from quantum information theory, which awards a key role to the concept of entanglement, as discussed in Section 2. The pursuit of the characterization of entanglement in quantum many body systems has resulted in the observation that ground states of quantum theories with short-ranged interactions are special. The entanglement of a subsystem with the remainder scales only as the area of its boundary in gapped systems, with possible logarithmic corrections at quantum critical points. This observation implies that quantum ground states have a holographic property which reminds strongly of similar statements in quantum gravity theories. Section 3 discusses the basics of renormalization group theory, which is the required tool to deal with systems with degrees of freedom interacting over a large range of length scales. Starting from the traditional framework in relativistic quantum field theory and statistical physics, we also discuss the revolutionary work of Wilson and later White to use renormalization as a numerical approach to approximate eigenstates of quantum Hamiltonians. In addition, we discuss the modern approach to apply renormalization group transformations as an active process on quantum states, which removes short distance information and hence reduces entanglement under successive transformations.

While Chapter 1 summarizes all necessary background information to formulate adequate variational ansätze for ground states of extended quantum systems, Chapter 2 discusses in great detail the set of tools that can be used to actually apply these ansätze in approximation methods for eigenstates of the Hamiltonian. After discussing the well known time-independent variational principle in Section 1, we devote Section 2 to the time-dependent variational principle of Dirac, which allows to project a complete quantum dynamical time evolution into the variational manifold. Furthermore, Section 3 illustrates how the time-dependent variational principle associates to any variational manifold a new variational manifold, namely the tangent plane of the original manifold at the variational optimum, for studying excited states of the system. Finally, Section 4 discusses some peculiarities regarding the application of the variational principle to quantum systems with an infinite number of degrees of freedom, with in particular

some important arguments of Feynman that need to be kept in mind throughout the remainder of this dissertation.

Chapter 3 introduces the variational manifold of matrix product states for studying one-dimensional quantum lattice systems. Its main properties are well studied in the literature and summarized in Section 1. In addition to a literature survey, this section provides a systematic study of the tangent vectors of matrix product states, as required for the remainder of this chapter. Section 2 discusses how to apply the time-dependent variational principle to the class of matrix product states and explains its benefits over existing methods for both real and imaginary time evolution, which are then also illustrated with numerical examples. The third section elaborates on the implementation of our ansatz for excitations and introduces a similar ansatz for topologically non-trivial excitations in systems with spontaneous symmetry breaking. The adequacy of these ansätze are illustrated using examples.

Chapter 4 applies the same analysis to the variational manifold of continuous matrix product states, a revolutionary new ansatz developed by Verstraete and Cirac in 2010, that can be directly applied to quantum field theories. Section 1 discusses their basic properties and their close relationship with matrix product states for lattice systems. The application of the time-dependent variational principle and the ansatz for excitations to continuous matrix product states is completely parallel to the case of matrix product states, so that Section 2 of Chapter 4 focusses mainly on the derivation of the required formulae and the construction of an efficient implementation. The power and possibilities of continuous matrix product states are illustrated in Section 3 using two simple benchmark models.

Chapter 5 starts with an exploration of the general relationship between renormalization strategies and variational ansätze in Section 1. This allows to conclude that the renormalization scheme associated to matrix product states is not able to separate degrees of freedom living at different length scales and can thus be improved, resulting in the entanglement renormalization scheme developed by Vidal in 2005. Fundamental properties of the associated multi-scale entanglement renormalization ansatz are discussed. In Section 2, we develop a continuum formulation of the process of entanglement renormalization and hence define a new variational ansatz for quantum field theories. While a direct application of the variational principle to this manifold is far from trivial, we do show that our ansatz has very promising features. We further illustrate this in Section 3 by using a restricted submanifold of Gaussian instances that are used to approximate the ground states of free field theories.

The last chapter is devoted to the study of relativistic theories, which require a separate treatment due to the lack of an ultraviolet cutoff scale. The traditional approach is to discretize the fields and put them on the sites of a lattice, to which we can now apply the matrix product state. This approach is explored in Section 1 of Chapter 6. In the second section, we try to use the newly developed continuous matrix product state, which automatically directs us towards a new regularization scheme for relativistic quantum

field theories. In Section 3, we use the continuous entanglement renormalization ansatz of Chapter 5 to describe the ground state of free field theories and show that we can easily send the cutoff scale back to infinity.

A note on notation

We have tried to maintain a consistent notation throughout this dissertation. The following conventions were used. General sets or manifolds are denoted with a calligraphic font $\mathcal{S}$, $\mathcal{L}$, $\mathcal{M}$, ... If a set $\mathcal{S}$ has a notion of cardinality or volume, this value is denoted as $|\mathcal{S}|$. Vector spaces and Hilbert spaces as well as the elementary fields of the natural, integral, real and complex numbers are denoted with a blackboard bold font $\mathbb{V}$, $\mathbb{H}$, $\mathbb{N}$, $\mathbb{Z}$, $\mathbb{R}$ and $\mathbb{C}$. Elements of a general vector space are denoted using a bold font $\boldsymbol{v}$, unless they correspond to spatial vectors in the Euclidean space $\mathbb{R}^d$, in which case an arrow notation $\vec{v}$ is employed. The norm of the vector is denoted as $||\vec{v}||$. The symbol d is reserved for the number of spatial dimensions. The standard notation $\mathbb{L}(\mathbb{V})$ is used for the space of linear transformations or homomorphisms of a vector space $\mathbb{V}$, while the notation $\mathbb{T}_{\mathcal{M}}$ is reserved for the tangent plane of a manifold $\mathcal{M}$. Endomorphisms or general linear maps between different vector spaces are denoted using a script font $\mathcal{M}$, $\mathcal{E}$, $\mathcal{P}$, ..., which should be distinguishable from the calligraphic font $\mathcal{S}$, $\mathcal{L}$, $\mathcal{M}$ for sets and manifolds. The symbol $\mathcal{O}$ is reserved for the mathematical 'order' operator, used in both series expansions and in the specification of computational complexity. Symmetry groups are denoted with a sans serif font G. For example, the standard groups of unitary and special unitary transformations of degree D are denoted as $\mathsf{U}(D)$ and $\mathsf{SU}(D)$. The general linear group of degree D over the real or complex numbers is denoted as $\mathsf{GL}(D;\mathbb{R})$ or $\mathsf{GL}(D;\mathbb{C})$. Algebras are denoted using a fraktur font $\mathfrak{A}$. In particular, the group algebra corresponding to a group G is denoted using a small latter $\mathfrak{g}$. For the standard groups, this results in the notations $\mathfrak{u}(D)$, $\mathfrak{su}(D)$, $\mathfrak{gl}(D;\mathbb{R})$ or $\mathfrak{gl}(D;\mathbb{C})$.

This dissertation deals with extended quantum systems, which, as we explain in the next chapter, should in principle be described using a C^*-algebra $\mathfrak{A}$ of observables, where quantum states correspond to linear functionals on $\mathfrak{A}$. We always use capital greek letters Ψ, Φ, Ξ for pure quantum states, while sticking to the traditional notation ρ for a mixed state. Small greek symbols ψ, ϕ are reserved for one-particle quantum states, which are not encountered often. In the traditional description in terms of a Hilbert space $\mathbb{H}$, the pure states Ψ corresponds to kets $|\Psi\rangle \in \mathbb{H}$, whereas mixed states ρ correspond to density operators $\hat{\rho} \in \mathbb{L}(\mathbb{H})$. All operators in $\mathbb{L}(\mathbb{H})$ are denoted with a hat, including the unit operator $\hat{\mathbb{1}}$. Hermitian conjugation of operators is denoted using the dagger $\dagger$ superscript. We also introduce the bras $\langle\Psi|$ as linear functionals on $\mathbb{H}$. Unless specified otherwise, the symbol Ψ is reserved for ground states, while Φ and Ξ correspond to topologically trivial and topologically non-trivial excitations respectively. In quantum field theories, the field operators in real-space are denoted as $\hat{\psi}(\vec{x})$, $\hat{\phi}(\vec{x})$ or $\hat{\pi}(\vec{x})$, corresponding to the interpretation of 'second quantized' one-particle functions.

The Fourier transformed fields in momentum space are denoted as $\hat{\Psi}(\vec{p})$, $\hat{\Phi}(\vec{p})$ and $\hat{\Pi}(\vec{p})$, which should be distinguishable from quantum states since slanted greek capitals are used (and the hat points to their operator character). The notation p is reserved for momentum, both on the lattice ($p \in [-\pi, \pi)$) as in the continuum ($p \in \mathbb{R}$). The gradient is denoted as $\vec{\nabla}$ in real space, while the analogous gradient in momentum space is denoted as $\vec{\blacktriangledown}$ (which is not the Fourier transform of $\vec{\nabla}$).

In Chapters 3 and 4 we will encounter virtual systems or ancillae corresponding to a virtual Hilbert space $\mathbb{H}_{\text{ancilla}} = \mathbb{C}^D$. Elements of $\mathbb{H}_{\text{ancilla}}$ are denoted using the standard vector notation $\boldsymbol{v}$, whereas operators ($D \times D$ matrices) are denoted without special indication. We do however introduce a special notation for the Hilbert space $\mathbb{H}_{\text{ancilla}} \otimes \overline{\mathbb{H}}_{\text{ancilla}}$. Elements and linear functionals of this Hilbert space are denoted using a rounded braket notation $|v)$ and $(v|$, while operators of $\mathbb{L}(\mathbb{H}_{\text{ancilla}} \otimes \overline{\mathbb{H}}_{\text{ancilla}})$ are denoted using a breve $\breve{E}$. While this summarizes most of the special notations encountered throughout dissertation, any additional non-standard notation will be properly defined at time of introduction.

1

The cornerstones

This chapter introduces some basic notions about *extended systems* that are governed by the laws of *quantum mechanics*. Fundamental properties of quantum systems are revised. The concept of *entanglement* is defined and its importance is motivated. Entanglement characterizes the strong quantum fluctuations that are present in ground states of quantum mechanical systems. In extended systems, these fluctuations exist over a wide range of scales. Another important development that enables us to deal with phenomena occuring at such wide range of scales is *renormalization*, which is the topic of the last section. This chapter thus summarizes some hallmarks of modern theoretical physics that are of key importance for the developments in the remainder of this thesis.

1. Quantum mechanics of extended systems

This dissertation treats many-body theories and field theories that are described by the postulates of quantum mechanics. *Extended* systems or field theories have degrees of freedom associated to every site or point of a lattice or a continuum of macroscopic dimensions. For all practical purposes, the volume of the system can be considered infinite, and so is the number of degrees of freedom. In addition, we often assume that these systems are translation invariant, unlike finite systems such as molecules, nuclei, *etc*.

The physical state Ψ of a quantum system at a certain point of time t is described by a wave vector $|\Psi(t)\rangle$ that lives in a Hilbert space $\mathbb{H}$, or more generally by a density operator $\hat{\rho}(t) \in \mathbb{L}(\mathbb{H})$, which is a self-adjoint, positive, linear operator of unit trace [1]. A general density operator $\hat{\rho}$ describes a mixed state ρ. The density matrix of a pure state Ψ is given by $\hat{\rho}_\Psi = |\Psi\rangle\langle\Psi|$ and has a single eigenvalue 1. Physical observables A are identified with self-adjoint operators $\hat{A} \in \mathbb{L}(\mathbb{H})$, and its expectation value for a system in state ρ is given by

$$\langle \hat{A} \rangle = \mathrm{tr}[\hat{\rho}\hat{A}] \tag{1.1}$$

The density operator $\hat{\rho}$ itself is associated to the observable corresponding to the statement "the system is in the state ρ". While this formalism is highly successful for single particle and few-particle quantum mechanics, it is plagued by difficulties for systems

with an infinite number of degrees of freedom, *i.e.* for the systems under study in this dissertation. This was first noted in [2, 3, 4, 5, 6].

From an operational point of view, a more general algebraic construction of quantum mechanics is obtained by specifying the set of observables A of the theory. One can easily show that this set has an identity and can be given the structure of a C^*-algebra $\mathfrak{A}$ [7, 8], for which the observables correspond to the self-adjoint elements. The state of the system is then given by a linear functional $\rho : \mathfrak{A} \mapsto \mathbb{C}$ that satisfies

- $\forall A \in \mathfrak{A} : \rho(A^\dagger A) > 0$ (positivity),
- $\rho(\mathbb{1}_{\mathfrak{A}}) = 1$ (normalization).

As linear functionals, a pure state Ψ is set apart from a mixed state ρ by the fact that the latter can be decomposed as a convex sum

$$\rho = \lambda\rho_1 + (1-\lambda)\rho_2, \quad 0 < \lambda < 1. \tag{1.2}$$

while this is impossible for the former. From this abstract setting, a representation of observables as operators acting on a Hilbert space of states can be recovered through the Gelfand-Naimark-Segal (GNS) construction [9, 10]. A brief elaboration is in order, as the GNS construction will implicitly be used a number of times in the remainder of this section. A *-representation of a C^*-algebra $\mathfrak{A}$ is in this context formally defined as a mapping π from $\mathfrak{A}$ to the algebra $\mathfrak{B}(\mathbb{H}) \subset \mathbb{L}(\mathbb{H})$ of bounded operators on a Hilbert space $\mathbb{H}$ (*i.e.* $\pi : \mathfrak{A} \mapsto \mathfrak{B}(\mathbb{H}) : A \mapsto \pi(A) = \hat{A}$), such that

- π is a ring homomorphism ($\pi(A+B) = \pi(A) + \pi(B)$ and $\pi(AB) = \pi(A)\pi(B)$, $\forall A, B \in \mathfrak{A}$) which carries involution on $\mathfrak{A}$ into involution of operators;
- π is non-degenerate (*i.e.* the set $\{\pi(A)|\Psi\rangle, \forall A \in \mathfrak{A}, \forall |\Psi\rangle \in \mathbb{H}\}$ is dense in $\mathbb{H}$), which implies that $\pi(\mathbb{1}_{\mathfrak{A}}) = \hat{\mathbb{1}}$.

If there exists a vector $|\Psi\rangle \in \mathbb{H}$, such that the set $\{\pi(A)|\Psi\rangle, \forall A \in \mathfrak{A}\}$ is norm-dense in $\mathbb{H}$, then the representation π is cyclic and $|\Psi\rangle$ is called the cyclic vector. The GNS construction asserts that for a given pure state Ψ (a linear functional on $\mathfrak{A}$) there is a cyclic *-representation π of $\mathfrak{A}$ with a cyclic vector $|\Psi\rangle$ such that $\langle\Psi|\hat{A}|\Psi\rangle = \Psi(A)$, $\forall A \in \mathfrak{A}$. The GNS construction is typically used in combination with the ground state of a given Hamiltonian H. In the resulting Hilbert space, $|\Psi\rangle$ is the ground state of the Hamiltonian operator $\hat{H} = \pi(H)$, and $\hat{H}$ can be diagonalized to yield the full spectrum of excitations. If the representation π is irreducible, every vector in $\mathbb{H}$ is a cyclic vector, so the construction also works by starting from excited states. Difficulties arise in systems with an infinite number of degrees of freedom, because the observables $A \in \mathfrak{A}$ that define the theory and the canonical commutation relations between them can have different unitarily inequivalent representations. Different states Ψ then define different Hilbert spaces $\mathbb{H}^{(\Psi)}$ that can be completely disjoint (*i.e.* any vector from one Hilbert space has zero overlap with any vector from another Hilbert space).

This dissertation restricts to a description in terms of Hilbert spaces and operators. For

systems with an infinite number of degrees of freedom we often implicitly assume that this Hilbert space was obtained by applying the GNS construction to the ground state. Some of the 'complications' related to this approach are mentioned throughout this section and will also be encountered in later chapters. Nevertheless, we will not use an explicit description in terms of C^*-algebras and will always assume that we can embed the relevant physical states in a total Hilbert space $\mathbb{H}$. We thus take a pragmatic view: we use the nice properties of systems with an infinite number of degrees of freedom —*e.g.* possibility for translation invariance, symmetry breaking, *etc* in the thermodynamic limit— but avoid the mathematical difficulties as much as possible by assuming, when necessary, that the number of degrees of freedom is finite. Hereto we assume that *e.g.* the volume is finite, albeit macroscopically large, or that a continuous system has an intrinsic cutoff at some fundamental scale. This seems to correspond to the physical reality, since no physical system (including the universe) is truly infinitely large and since fundamental field theories are predicted to have a discrete structure at the Planck scale by quantum gravity.

1.1. Quantum lattice models

A lattice $\mathscr{L}$ can formally be defined as a discrete subset $\mathscr{L} \subset \mathbb{R}^d$, where d can be identified with the number physical space dimensions. To every site $\vec{n} \in \mathscr{L}$, we associate an elementary quantum variable with Hilbert space $\mathbb{H}_{\vec{n}}$. The dimension $q_{\vec{n}} = \dim \mathbb{H}_{\vec{n}}$ can be finite, *e.g.* when the site contains a elementary spin J variable ($q = 2J+1$) or accomodates N species of particles with fermion statistics ($q = 2^N$), or can be denumerably infinite, *e.g.* when the site accomodates one or more species of particles with bosonic statistics. The state of the quantum system defined on the lattice $\mathscr{L}$ is given by a wave vector in or a density operator on the Hilbert space

$$\mathbb{H}_{\mathscr{L}} = \bigotimes_{\vec{n}\in\mathscr{L}} \mathbb{H}_{\vec{n}}. \tag{1.3}$$

In most physical systems, all sites are equivalent and $q_{\vec{n}} = q$, $\forall \vec{n} \in \mathscr{L}$. If we assume that we can construct the Hilbert space $\mathbb{H}_{\vec{n}}$ by acting with creation operators $\hat{c}^\dagger_{\vec{n}}$ on a reference state $|0_{\vec{n}}\rangle \in \mathbb{H}_n$ that is annihilated by the corresponding annihilation operator $\hat{c}_{\vec{n}}$ (*i.e.* $\hat{c}_{\vec{n}}|0\rangle_{\vec{n}} = 0$), then

$$\mathbb{H}_{\vec{n}} = \mathrm{span}\left\{ \frac{(\hat{c}^\dagger_{\vec{n}})^s}{\sqrt{s!}} |0\rangle_{\vec{n}}, \forall s \in \mathbb{Z}_q \right\}. \tag{1.4}$$

This construction is valid for fermions, bosons and spin-½ systems (where $\hat{c}_{\vec{n}} = \sigma^-_{\vec{n}}$ and $\hat{c}^\dagger_{\vec{n}} = \sigma^+_{\vec{n}}$). The generalization to a multi-particle setting or general spin-J systems is

straightforward. We can then directly construct $\mathbb{H}_{\mathscr{L}}$

$$\mathbb{H}_{\mathscr{L}} = \mathrm{span}\left\{ \prod_{\vec{n}\in\mathscr{L}} \frac{(\hat{c}_{\vec{n}}^{\dagger})^{s_{\vec{n}}}}{\sqrt{s_{\vec{n}}!}} |\mathbf{0}\rangle , \forall \boldsymbol{s} \in \mathbb{Z}_q^{\otimes_{\mathscr{L}}} \right\}, \tag{1.5}$$

where the product $\prod_{\vec{n}\in\mathscr{L}}$ has a fixed order if the creation operators at different sites anticommute (fermion statistics), and the reference state $|\mathbf{0}\rangle$ is defined as

$$|\mathbf{0}\rangle = \bigotimes_{\vec{n}\in\mathscr{L}} |0\rangle_{\vec{n}} . \tag{1.6}$$

The dimension of $\mathbb{H}_{\mathscr{L}}$ is

$$\dim \mathbb{H}_{\mathscr{L}} = q^{|\mathscr{L}|} \tag{1.7}$$

and scales exponentially in the number of sites $|\mathscr{L}|$. This exponential scaling is the basis for the complexity of quantum systems. It restricts the application of exact numerical techniques (exact diagonalization) to very low values of $|\mathscr{L}|$. Even for the simplest quantum system with $q = 2$, a doubling in computing power only enables an increase of the maximal system size that can be studied by one site.

The above construction starts from the full Hilbert space $\mathbb{H}_{\vec{n}}$ of a single site $\vec{n}$ (*i.e.* any number of particles) and subsequently adds other sites to construct $\mathbb{H}_{\mathscr{L}}$. It can only formally be defined through a limit procedure if $|\mathscr{L}| = +\infty$. A Hilbert space for a quantum lattice model can also be defined using the Fock construction [11], even when $|\mathscr{L}| = \infty$. The Fock construction starts from the single-particle problem on the lattice $\mathscr{L}$, corresponding to the Hilbert space

$$\mathbb{H}_{\mathscr{L}}^{(1)} = \mathrm{span}\left\{ |\vec{n}\rangle , \forall \vec{n} \in \mathscr{L} \right\}, \tag{1.8}$$

where the basis vector $|\vec{n}\rangle = \hat{c}_{\vec{n}}^{\dagger}|\mathbf{0}\rangle$ indicates that the particle is localized at site $\vec{n}$ and $\langle\vec{n}|\vec{m}\rangle = \delta_{\vec{n},\vec{m}}$. Next, the Hilbert space for the N-particle problem is defined as

$$\mathbb{H}_{\mathscr{L}}^{(N)} = \mathrm{span}\left\{ \prod_{\vec{n}\in\mathscr{L}} \frac{(\hat{c}_{\vec{n}}^{\dagger})^{s_{\vec{n}}}}{\sqrt{s_{\vec{n}}!}} |\mathbf{0}\rangle , \forall s_{\vec{n}} \in \mathbb{Z}_q | \sum_{\vec{n}\in\mathscr{L}} s_{\vec{n}} = N \right\}, \tag{1.9}$$

resulting in $\dim \mathbb{H}_{\mathscr{L}}^{(N)} = \binom{|\mathscr{L}|+N-1}{N}$ if q is denumerably infinite and $\dim \mathbb{H}_{\mathscr{L}}^{(N)} = \binom{|\mathscr{L}|}{N}$ if $q = 2$. Finally, the Fock space is constructed as

$$\mathbb{H}_{\mathscr{L}}^{\mathrm{F}} = \bigoplus_{N=0}^{(q-1)|\mathscr{L}|} \mathbb{H}_{\mathscr{L}}^{(N)}. \tag{1.10}$$

The standard procedure is to first construct Fock space and then define the creation and annihilation operators afterwards, as we will do for continuous systems in the next subsection. For bosons (fermions), the N-particle Hilbert space $\mathbb{H}_{\mathscr{L}}^{(N)}$ contains all

symmetric (antisymmetric) tensors of rank N, where the indices can take values in $\mathscr{L}$. $\mathbb{H}^{(0)}_{\mathscr{L}}$ is identified with $\mathbb{C}$. For a lattice $\mathscr{L}$ of finite size $|\mathscr{L}|$, the Fock construction is equivalent to the previous construction (*i.e.* $\mathbb{H}_{\mathscr{L}} \equiv \mathbb{H}^{\mathrm{F}}_{\mathscr{L}}$). However, problems arise in the thermodynamic limit ($|\mathscr{L}| \to \infty$), since the corresponding limit of the dimension of $\mathbb{H}_{\mathscr{L}}$ given in Eq. (1.7) ($\lim_{|\mathscr{L}|\to+\infty} q^{|\mathscr{L}|}$) represents a non-denumerable infinity, both for q finite and q denumerably infinite. In contrast, the Fock construction $\mathbb{H}^{\mathrm{F}}_{\mathscr{L}}$ can be obtained as the direct sum of the N-particle Hilbert spaces $\mathbb{H}^{(N)}_{\mathscr{L}}$ directly in the thermodynamic limit, and thus has a denumarably infinite dimension by construction. Indeed, $\lim_{|\mathscr{L}|\to\infty} \dim \mathbb{H}^{(N)}_{\mathscr{L}} = \lim_{|\mathscr{L}|\to\infty} \mathcal{O}(|\mathscr{L}|^N)$ represents a denumerable infinity and thus so does $\dim \mathbb{H}^{\mathrm{F}}_{\mathscr{L}} = \sum_{N=0}^{+\infty} \dim \mathbb{H}^{(N)}_{\mathscr{L}}$. The difference between both Hilbert spaces can be understood by noting that every state $|\Psi\rangle \in \mathbb{H}^{\mathrm{F}}_{\mathscr{L}}$ produces a finite expectation value for the number operator:

$$\frac{\langle\Psi|\hat{N}|\Psi\rangle}{\langle\Psi|\Psi\rangle} < \infty, \forall\, |\Psi\rangle \in \mathbb{H}^{\mathrm{F}}_{\mathscr{L}}, \tag{1.11}$$

with

$$\hat{N} = \sum_{\vec{n}\in\mathscr{L}} \hat{c}^{\dagger}_{\vec{n}} \hat{c}_{\vec{n}}, \tag{1.12}$$

while it is easy to construct a normalized state $|\widetilde{\Psi}\rangle \in \mathbb{H}_{\mathscr{L}}$ for which the expectation value of $\hat{N}$ diverges.

If we construct a different set of creation operators $\hat{\tilde{c}}^{\dagger}_{\vec{n}}$ —related to $\hat{c}^{\dagger}_{\vec{n}}$ and $\hat{c}_{\vec{n}}$ through a local Bogoliubov transform [12]— with corresponding annihilation operator $\hat{\tilde{c}}_{\vec{n}}$ and vacuum $|\tilde{0}_{\vec{n}}\rangle$ (such that $\hat{\tilde{c}}_{\vec{n}}|\tilde{0}_{\vec{n}}\rangle = 0$), then the Hilbert space of the single sites $\vec{n}$ can also be constructed as

$$\mathbb{H}_{\vec{n}} = \mathrm{span}\left\{ \frac{(\hat{\tilde{c}}^{\dagger}_{\vec{n}})^s}{\sqrt{s!}} |\tilde{0}\rangle_{\vec{n}}, \forall s \in \mathbb{Z}_q \right\}.$$

We can then define the Hilbert space $\tilde{\mathbb{H}}^{\mathrm{F}}_{\mathscr{L}}$ by applying the Fock construction to the *different* one-particle Hilbert space

$$\tilde{\mathbb{H}}^{(1)}_{\mathscr{L}} = \mathrm{span}\left\{ |\tilde{\vec{n}}\rangle = \hat{\tilde{c}}^{\dagger}_{\vec{n}} |\tilde{\mathbf{0}}\rangle, \forall \vec{n} \in \mathscr{L} \right\} \tag{1.13}$$

with $|\tilde{\mathbf{0}}\rangle = \otimes_{\vec{n}\in\mathscr{L}} |\tilde{0}\rangle_{\vec{n}}$. If $|\mathscr{L}| = \infty$, the overlap between any state $|\Psi\rangle \in \mathbb{H}^{\mathrm{F}}_{\mathscr{L}}$ and any state $|\tilde{\Psi}\rangle \in \tilde{\mathbb{H}}^{\mathrm{F}}_{\mathscr{L}}$ satisfies $\langle\Psi|\tilde{\Psi}\rangle = 0$. The Hilbert spaces $\mathbb{H}^{\mathrm{F}}_{\mathscr{L}}$ and $\tilde{\mathbb{H}}^{\mathrm{F}}_{\mathscr{L}}$ constitute inequivalent representations of the algebra of observables of the theory. In particular, the expectation value of the number operator $\hat{N}$ defined with respect to the operators $(\hat{c}^{\dagger}_{\vec{n}}, \hat{c}_{\vec{n}})$ diverges for any state $|\tilde{\Psi}\rangle \in \tilde{\mathbb{H}}^{(\mathrm{F})}_{\mathscr{L}}$, indicating that $\tilde{\mathbb{H}}^{(\mathrm{F})}_{\mathscr{L}}$ is not in the domain of definition of $\hat{N}$. The different Fock spaces $\mathbb{H}^{(\mathrm{F})}_{\mathscr{L}}$ and $\tilde{\mathbb{H}}^{(\mathrm{F})}_{\mathscr{L}}$ divide the formally defined Hilbert space $\mathbb{H}_{\mathscr{L}}$ into mutually exclusive "equivalence classes", where states within an equivalence class differ from each other by at most a finite number of occupation numbers. There are no proper unitary operators transforming a set of states from one equivalence class to another. The

number of equivalence classes is also denumerably infinite. The implications of these observations are studied in the next subsection.

1.2. Quantum field theories

Let now the region $\mathscr{R}$ be a continuous subset $\mathscr{R} \subset \mathbb{R}^d$, with a corresponding size or volume $|\mathscr{R}|$. To every point $\vec{x} \in \mathscr{R}$, we can associate an elementary Hilbert space $\mathbb{H}(\vec{x})$. The Hilbert space of a quantum system defined on $\mathscr{R}$ can formally be defined through the *continuum limit* of some lattice approximation of $\mathscr{R}$. More precisely, if $\{\mathscr{L}_k, \forall k \in \mathbb{N}\}$ represents a set of lattices that satisfy $\mathscr{L}_k \subset \mathscr{R}$, $\forall k \in \mathbb{N}$ and $\lim_{k\to+\infty} \mathscr{L}_k$ is dense in $\mathscr{R}$, then we can formally define

$$\mathbb{H}_{\mathscr{R}} = \lim_{k\to+\infty} \mathbb{H}_{\mathscr{L}_k}. \tag{1.14}$$

An example is to take $\mathscr{R} = [0,1] \subset \mathbb{R}$ and $\mathscr{L}_k = \{i/2^k, \forall i \in \mathbb{Z}_{2^k+1}\}$. Since $\lim_{k\to\infty} |\mathscr{L}_k| = +\infty$, this construction indicates that problems that were encountered for lattice models in the thermodynamic limit can already appear for quantum field theories in regions $\mathscr{R}$ of finite size $|\mathscr{R}| < \infty$.

A rigorous definition of a Hilbert space for a non-relativistic quantum field theory on $\mathscr{R}$ is obtained through the Fock construction. The quantum mechanical wave function of a non-relativistic particle on $\mathscr{R}$ is a vector in the Hilbert space of square integrable functions on the region $\mathscr{R}$, so that $\mathbb{H}^{(1)}_{\mathscr{R}} = L^2(\mathscr{R})$. In order to define the N-particle Hilbert space, we define the symmetric (S) or antisymmetric (A) subspace $\mathscr{R}^{(N)}_{\mathrm{S,A}}$ of $\mathscr{R}^{(N)} = \mathscr{R} \times \mathscr{R} \times \cdots \times \mathscr{R}$ (Cartesian product of N copies of $\mathscr{R}$), and define $\mathbb{H}^{(N)}_{\mathscr{R}} = L^2(\mathscr{R}^{(N)}_{\mathrm{S,A}})$, with S for bosons and A for fermions. Finally, the Fock space is constructed as

$$\mathbb{H}^{(\mathrm{F})}_{\mathscr{R}} = \bigoplus_{N=0}^{+\infty} \mathbb{H}^{(N)}_{\mathscr{R}}. \tag{1.15}$$

In Fock space, we can construct for every point $\vec{x} \in \mathscr{R}$ creation and annihilation operators $\hat{\psi}^\dagger(\vec{x})$ and $\hat{\psi}(\vec{x})$ that satisfy

$$\{\hat{\psi}(\vec{x}), \hat{\psi}^\dagger(\vec{y})\}_\mp = \delta(\vec{x}-\vec{y}), \qquad \forall \vec{x}, \vec{y} \in \mathbb{R}^n, \tag{1.16}$$

with $\{\cdot,\cdot\}_\mp$ representing a commutator $(-)$ for bosons and an anticommutator $(+)$ for fermions. The number operator is defined as

$$\hat{N} = \int_{\mathscr{R}} \mathrm{d}^d x\, \hat{\psi}^\dagger(\vec{x})\hat{\psi}(\vec{x}) \tag{1.17}$$

and has a finite expectation value with respect to all states $|\Psi\rangle \in \mathbb{H}^{\mathrm{F}}_{\mathscr{R}}$.

If $|\mathscr{R}|$ is finite, $\mathbb{H}^{(1)}_{\mathscr{R}}$ has a denumerably infinite dimension and an orthonormal basis $\{|\varphi_k\rangle, k \in \mathbb{N}\}$ can be constructed. We can define then creation and annihilation opera-

tors

$$\hat{c}_k^\dagger = \int_{\mathscr{R}} \mathrm{d}^d x \, \varphi_k(\vec{x}) \hat{\psi}^\dagger(\vec{x}), \qquad \hat{c}_k = \int_{\mathscr{R}} \mathrm{d}^d x \, \overline{\varphi}_k(\vec{x}) \hat{\psi}(\vec{x}), \tag{1.18}$$

so that the reference vacuum $|\Omega\rangle \in \mathbb{H}_{\mathscr{R}}^{(0)}$ is completely characterized by $\hat{c}_k |\Omega\rangle = 0$ and the one-particle states $|\varphi_k\rangle$ are obtained as $|\varphi_k\rangle = \hat{c}_k^\dagger |\Omega\rangle$. All N-particle Hilbert spaces $\mathbb{H}_{\mathscr{R}}^{(N)}$ are denumerably infinite-dimensional, and so is $\mathbb{H}_{\mathscr{R}}^{\mathrm{F}}$. Ground states and excited states of non-relativistic field theories on finite regions $\mathscr{R}$ ($|\mathscr{R}| < \infty$) have a finite number of particles and can thus be described in $\mathbb{H}_{\mathscr{R}}^{\mathrm{F}}$. Despite the infinite number of degrees of freedom in a field theory, non-relativistic field theories are well behaved because they possess an intrinsic cutoff: the finite number of particles in the ground state $|\Psi\rangle$ of a Hamiltonian defines a particle density $\rho = \langle\Psi|\hat{N}|\Psi\rangle / |\mathscr{R}|$ that will be related to a real space cutoff length $a = \rho^{-1/d}$, with d the number of dimensions of space. As for quantum lattice models, the mathematical complications only appear in the thermodynamic limit. As a particular example, the vacuum state $|\Omega\rangle$ is the only translation invariant state that can be normalized to one in the thermodynamic limit. All other translation invariant states (momentum zero) in $\mathbb{H}$ satisfy a δ-normalization. A nontrivial, normalizable and translation invariant ground state of a translation invariant Hamiltonian is thus unitarily inequivalent to the vacuum state $|\Omega\rangle$ and lives in a different Hilbert space. This phenomenon is called the *orthogonality catastrophe* by Anderson [13]. Because it depends on the system size, it is an infrared effect.

Matters are more complicated for relativistic theories, as they cannot easily be described in a fixed Fock space. Relativistic theories should be described in the Hilbert space created using the GNS constructions starting from the exact ground state (as linear functional in the C^*-algebra of observables). Thus, constructing the Hilbert space requires knowledge of the exact ground state. Consider as an example a scalar massive boson (such as the scalar meson) described by the free Klein-Gordon Hamiltonian with mass parameter m. While this model is typically defined in $\mathscr{R} = \mathbb{R}^d$, problems already arise in regions $\mathscr{R}$ with finite size. We therefore consider a Klein-Gordon Hamiltonian in a subspace $\mathscr{R} = [0, L]^d$ and introduce periodic boundary conditions, so that $\mathscr{R}$ is topologically equivalent to the d-dimensional torus $\mathscr{T}^{(d)}$. The relevant Hilbert space for this theory can be obtained by applying the Fock construction to the single particle Hilbert space, which is given by $\mathbb{H}_{\mathscr{R}}^{(1)} = L^2_\mu(\mathscr{R})$, *i.e.* the space of functions that are square integrable with respect to the measure μ, *i.e.*

$$\forall \phi, \psi \in \mathbb{H}_{\mathscr{R}}^{(1)} : (\phi, \psi)_\mu = \int_{\mathscr{R}} \mathrm{d}^d x \int_{\mathscr{R}} \mathrm{d}^d y \, \mu(\vec{x}, \vec{y}) \overline{\phi}(\vec{x}) \psi(\vec{y}) < \infty \tag{1.19}$$

with

$$\mu(\vec{x}, \vec{y}) = \frac{1}{L^d} \sum_{\vec{k} \in \mathbb{Z}^d} \frac{\mathrm{e}^{\mathrm{i} \frac{2\pi \vec{k}}{L} \cdot (\vec{x} - \vec{y})}}{\sqrt{\left(\frac{2\pi \|\vec{k}\|}{L}\right)^2 + m^2}}. \tag{1.20}$$

As the measure μ depends on the parameter m of the Hamiltonian, so does the single particle subspace $\mathbb{H}^{(1)}_{\mathscr{R}}$. The resulting Fock spaces $\mathbb{H}^{\mathrm{F}}_{\mathscr{R}}$ corresponding to different values of the mass parameter m are unitarily inequivalent. Since this is already true at systems of finite size $|\mathscr{R}| < \infty$, there is now an ultraviolet orthogonality catastrophe. More generally, Haag's theorem proofs that any two inequivalent ground states of relativistic theories (as linear functionals on the C^*-algebra of observables) define unitarily inequivalent Hilbert spaces [14, 15], based on the following assumptions:

1. Lorentz covariance of the Hamiltonian;
2. the existence of a positive-definite norm in each Hilbert space;
3. local commutativity, *i.e.* operators at spacelike different spacetime points commute;
4. existence of a Lorentz invariant and normalizable vacuum;
5. positive-definiteness of the excitation spectrum.

Within each Hilbert space $\mathbb{H}^{\mathrm{F}}$, there is a unique normalizable and Lorentz invariant state. This has serious implications, since ground states corresponding to slightly different values of the parameters in the theory are unitarily inequivalent. Hence, the interaction picture, which forms the basis for perturbation theory, does not even exist! Now suppose that the Hilbert spaces corresponding to all possible ground states can be embedded in a formally defined Hilbert space $\mathbb{H}$ (e.g. using the lattice approximation), that contains several (non-denumerably infinitely many) normalizable and Lorentz invariant states. Then we can conclude that the difference between the expectation value of a Lorentz covariant Hamiltonian with respect to its ground state and with respect to another Lorentz-invariant normalizable state is a Lorentz invariant quantity. But since it is an energy (difference), the only Lorentz-invariant possibilities are either zero or infinity. The Hamiltonian can thus have a degenerate ground state subspace, but the energy expectation value with respect to any other Lorentz-invariant normalizable state diverges! This explains the divergence of the ground state energy of an interacting field theory when it is evaluated in the Hilbert space constructed for the free theory.

Most of these problems can be avoided by introducing a cutoff into the theory, which will also be our strategy henceforth. Obtaining physically unambiguous results from this strategy requires the introduction of the renormalization group, to be developed in Section 3.

1.3. Ground states and excitations of physical systems

Let us now assume that the correct Hilbert space $\mathbb{H}$ for a particular system has been constructed, so that the Hamiltonian has a representation as a linear operator $\hat{H} \in \mathbb{L}(\mathbb{H})$. We are most often interested in the ground state and lowest lying excited states of this Hamiltonian, *i.e.* its lowest lying eigenvalues and the corresponding eigenvectors. Most physically interesting models have local interactions, so that the Hamiltonian can be

written as

$$\hat{H} = \sum_{\vec{n} \in \mathscr{L}} \hat{h}_{\vec{n}} \quad \text{or} \quad \hat{H} = \int_{\mathscr{R}} \mathrm{d}^d x \, \hat{h}(\vec{x}) \tag{1.21}$$

where $\hat{h}_{\vec{n}}$ or $\hat{h}(\vec{x})$ acts non-trivially only on a small region around site $\vec{n} \in \mathscr{L}$ or point $\vec{x} \in \mathscr{R}$. No attempt is made to define the necessary conditions more formally. In addition, one can often assume that the Hamiltonian is translation invariant, so that all operators $\hat{h}_{\vec{n}}$ or $\hat{h}(\vec{x})$ are shifted versions of a unique operator $\hat{h}$ with compact support. The Hilbert space can then be divided into sectors with different momentum, and the Hamiltonian will be block diagonal with respect to this division. It can thus be diagonalized within the different momentum sectors. The resulting eigenvalues for different values of the momentum constitute the spectrum of the Hamiltonian. We have assumed that the ground state is unique and falls in the trivial representation of the translation symmetry (*i.e.* in the momentum zero sector). If the ground state manifold would be degenerate, then we know from the previous subsections that different ground states generate inequivalent Hilbert spaces (through the GNS construction) in the thermodynamic limit. In particular, if some of these ground states break translation invariance, the corresponding Hilbert space would not even constitute a representation for the group of translations. This more general scenario is treated in the next subsection.

Let us now quantify these statements. For lattice systems, translations constitute a discrete symmetry group and there is no generator that can be identified with the momentum operator. We can however introduce a unitary translation operator $\hat{T}_i$ that shifts a state $|\Psi\rangle \in \mathbb{H}$ over a single lattice site in dimension $i = 1, 2, \ldots, d$. Shifts over $m \in \mathbb{Z}$ lattice sites in dimension i are obtained by acting with $(\hat{T}_i)^m$. Translation invariance of the system is thus characterized by $[\hat{T}_i, \hat{H}] = 0$, $\forall i = 1, 2, \ldots, d$. For a system with periodic boundary conditions of length N_i in dimension i, we obtain $(\hat{T}_i)^{N_i} = \pm 1$ (+ for bosons and even number of fermions, − for odd number of fermions). The spectrum of eigenvalues of $\hat{T}_i$ is then given by

$$\sigma(\hat{T}_i) = \left\{ \lambda_i^{(k)} = \exp\left[-\mathrm{i} \frac{2\pi k}{N_i} \right], \forall k \in \mathbb{Z}_{N_i} \right\} \tag{1.22}$$

or by

$$\sigma(\hat{T}_i) = \left\{ \lambda_i^{(k)} = \exp\left[-\mathrm{i} \frac{2\pi}{N_i} \left(k + \frac{1}{2} \right) \right], \forall k \in \mathbb{Z}_{N_i} \right\} \tag{1.23}$$

respectively. In the thermodynamic limit ($N_i \to \infty$), the distinction between both cases disappear and the spectrum becomes continuous:

$$\sigma(\hat{T}_i) = \left\{ \lambda_i^{(k)} = \exp[-\mathrm{i}k], \forall k \in [-\pi, +\pi) \right\}. \tag{1.24}$$

The values $p_i = \mathrm{i} \log(\lambda_i) \in [-\pi, +\pi)$ can be identified with the momentum in dimension $i = 1, 2, \ldots, d$ of the corresponding eigenstates.

For field theories, translations constitute a continuous symmetry group that is generated by Hermitian operators which are identified with the momentum operator. A translation over a distance $x \in \mathbb{R}$ in a dimension i is obtained by the action of the unitary operator $\hat{T}_i(x) = \exp(-\mathrm{i}x\hat{P}_i)$. Translation invariance is obtained if $[\hat{H}, \hat{P}_i] = 0$, $\forall i = 1, 2, \ldots, d$. If the system is periodic in dimension i with total length L_i, then the spectrum of $\hat{P}_i$ is given by

$$\sigma(\hat{P}_i) = \left\{ p_i^{(k)} = \frac{2\pi k}{L_i}, \forall k \in \mathbb{Z} \right\} \tag{1.25}$$

or by

$$\sigma(\hat{P}_i) = \left\{ p_i^{(k)} = \frac{2\pi}{L_i}\left(k + \frac{1}{2}\right), \forall k \in \mathbb{Z} \right\} \tag{1.26}$$

when an odd number of fermions are present. In the thermodynamic limit ($L_i \to \infty$), the continuous spectrum is given by

$$\sigma(\hat{P}_i) = \{ p_i, \forall\, p_i \in \mathbb{R} \}. \tag{1.27}$$

The corresponding eigenspaces divide $\mathbb{H}$ into the aforementioned momentum sectors which are labeled by the eigenvalue p_i.

Every eigenstate of the Hamiltonian represents a physical state with a real energy expectation value that is stable (*i.e.* it does not decay) and does not interact with other states (since the matrix element of $\hat{H}$ with respect to two different eigenstates is zero by definition). For extended systems with translation invariance and short-ranged interaction, the spectrum of eigenstates is expected to have some nice properties. It should be possible to create states that look similar to the ground state[1] in most of $\mathscr{L}$ or $\mathscr{R}$, and deviate only in a compact subspace of $\mathscr{L}$ or $\mathscr{R}$. Because of the assumed locality of the terms $\hat{h}_n$ or $\hat{h}(x)$ in the Hamiltonian, this disturbance is only felt in a (slightly larger) compact region, resulting in a finite increase in energy for this state. These local clumps of energy are henceforth referred to as *elementary excitations*. Of course, eigenstates of momentum represent superpositions of these local disturbances that are spread out all over space. Nevertheless, because the system is supposed to be in the thermodynamic limit, it should even be able to support any finite number of these elementary excitations —each with fixed momentum— and still keep them sufficiently far apart so that they do not feel each others presence (because the interaction is assumed to be short-ranged). If these properties are fulfilled, the spectrum of excited states has a special structure that was described by Lieb [16]:

> " ...and as is undoubtedly true, in general, the spectrum of low-lying states falls into a pattern. There exists one or more sets of energy vs momentum curves such that: (a) For each point on one of these curves there is an eigenstate; (b) if we add together the energy and momenta corresponding to several points on one or more of the curves, we obtain (in the thermody-

[1] This qualitative statement is to be made more precise in the next subsection.

namic limit) a resultant energy and momentum corresponding to an exact wave function of the system. The converse is also true: every state can be thought of as a sum of the elementary states.

These basic energy vs momentum curves we call elementary excitations. From this point of view, elementary excitations are a bookkeeping arrangement. There does not exist any simple operator which, acting on the ground state, gives these elementary states, nor can "compound" states be obtained from the elementary ones by simple operators. Nevertheless, when one attempts to diagonalize the many-body Hamiltonian by some method, it is the elementary excitations in the above sense that one is calculating ... "

The elementary excitations correspond to the physical notion of a particle, which have a specific energy versus momentum relationship that is called the *dispersion relation*.

1.4. Symmetries and spontaneous breaking thereof

In the previous subsection, translation invariance was used to divide the Hilbert space $\mathbb{H}$ into different sectors in which the Hamiltonian is block diagonal. Let us first assume that the number of degrees of freedom is finite, so that there are no representation problems and there is a unique and well-defined Hilbert space $\mathbb{H}$. In general, any symmetry of the Hamiltonian can be used to further divide the Hilbert space. Let thus $g \in \mathsf{G}$ be a symmetry transformation corresponding to a symmetry group G that can be discrete or continuous. The Hilbert space $\mathbb{H}$ constitutes a representation of G in terms of unitary (or anti-unitary) operators $\hat{U}(g)$, as was proven by Wigner [17]. If the symmetry transformations in G leave the Hamiltonian invariant (*i.e.* $[\hat{U}(g), \hat{H}] = 0$, $\forall g \in \mathsf{G}$), then we can use the decomposition of $\mathbb{H}$ into irreducible representations of G to bring the Hamiltonian into block-diagonal form. Translation invariance that was exploited in the previous subsection is a particular example of this general result. Other symmetry transformations related to the spacetime structure of the system are rotations, Galileo or Lorentz transformations, parity transformations and time-reversal transformations. These last two are discrete symmetry transformations that are obtained by the unitary operator $\hat{\Pi}_i$ (for a reflection through the hyperplane orthogonal to dimension i at the origin) and by the anti-unitary operator $\hat{R}$ (for a time-reversal transformation). For bosonic systems, the parity transformation and the time-reversal transformation are idempotent (as in classical physics), so that $\hat{\Pi}_i = \hat{\Pi}_i^\dagger = \hat{\Pi}_i^{-1}$ ($\forall i = 1, 2, \ldots, d$) and $\hat{R} = \hat{R}^{-1}$ (one cannot define the adjoint of an anti-linear operator). Fermionic systems are more complicated, since a state $|\Psi\rangle$ with half-integral spin satisfies $\hat{R}^2 |\Psi\rangle = -|\Psi\rangle$ and $\hat{\Pi}_i^2 |\Psi\rangle = -|\Psi\rangle$. Note that $\hat{\Pi}_i \hat{T}_i \hat{\Pi}_i^\dagger = \hat{T}_i^\dagger$, so that parity transformations and translations do not commute. As a consequence, they cannot be diagonalized simultaneously. A state with momentum p_i is transformed into a state with momentum $-p_i$ by the parity transform. Only the zero momentum sector can be further subdivided into sectors corresponding to even or odd parity.

Besides symmetries related to the spacetime structure of the model, the Hamiltonian can also be invariant with respect to a group of internal symmetry transformations. These act on the quantum variables within the local Hilbert spaces $\mathbb{H}_{\vec{n}}$ ($\vec{n} \in \mathscr{L}$) or $\mathbb{H}(\vec{x})$ ($\vec{x} \in \mathscr{R}$) rather than on the spacetime structure of the model. Most common are *global symmetries* where the transformation can be defined locally as $\hat{u}_{\vec{n}}(g) \in \mathbb{L}(\mathbb{H}_{\vec{n}})$ or $\hat{u}(g;\vec{x}) \in \mathbb{L}(\mathbb{H}(\vec{x}))$, $\forall g \in \mathsf{G}$ and $\forall \vec{n} \in \mathscr{L}$ or $\forall \vec{x} \in \mathscr{R}$, but where the Hamiltonian is only invariant under the global transformations $\hat{U}(g) \in \mathbb{L}(\mathbb{H})$, defined by

$$\hat{U}(g) = \bigotimes_{\vec{n}\in\mathscr{L}} \hat{u}_{\vec{n}}(g) \quad \text{or} \quad \hat{U}(g) = \bigotimes_{\vec{x}\in\mathscr{R}} \hat{u}(g;\vec{x}), \tag{1.28}$$

so that $[\hat{H}, \hat{U}(g)] = 0$, $\forall g \in \mathsf{G}$. Note that transformation operators that can be defined in this way are translation invariant ($[\hat{U}(g), \hat{T}] = 0$). A different class of symmetries are the local or gauge symmetries, for which the Hamiltonian commutes with transformation operators that are non-trivial only at a small number of sites of $\mathscr{L}$ or a small region of $\mathscr{R}$. No attempt is made to define these in a general setting, since they are not used in this dissertation.

Global symmetries can manifest themselves in two ways: In the Wigner-Weyl realization, the ground state is unique and transforms according to a one-dimensional representation. Typically, the ground state is assumed to transform according to the trivial representation. One notable exception is the abelian group $\mathsf{U}(1)$ corresponding to particle number or charge conservation, for which all irreducible representations are one-dimensional, and ground states corresponding to each irreducible representation can be created by adding a suitable chemical potential to the Hamiltonian. Since the Hamiltonian commutes with all symmetry operators, all eigenstates of the Hamiltonian can be labeled by irreducible representations of the symmetry group G. All eigenstates within a certain irreducible representation have the same energy eigenvalue, which can thus also be labeled by these quantum numbers. If the Wigner-Weyl realization survives the thermodynamic limit or continuum limit, these statements remain true and the Hilbert space associated to the ground state through the GNS construction still constitutes a representation for the symmetry group. Another possibility in the thermodynamic limit is the Nambu-Goldstone realization, where there exists a higher-dimensional manifold of ground states that are not individually invariant under the symmetry transformations: this corresponds to the well-known phenomenon of *symmetry breaking*. This realization is a consequence of the infinite number of degrees of freedom and cannot exist for systems with a finite number of degrees of freedom (except for some pathologically simple models where quantum fluctuations are totally absent, *i.e.* classical models). At finite size, different candidate ground states can tunnel into each other and quantum fluctuations restore the symmetry. A gap opens between the nondegenerate ground state and the lowest lying excited state. This gap vanishes exponentially in the system size. In the Nambu-Goldstone realization, a Hilbert space $\mathbb{H}^{(\Psi)}$ can be constructed from every symmetry breaking ground state $|\Psi\rangle$ through the GNS construction. This Hilbert space does not constitute a representation of the symmetry group, *i.e.* the transformation operators

$\hat{U}(g)$ do not even exist within this $\mathbb{H}^{(\Psi)}$[2].

Because the Nambu-Goldstone realization cannot be described within a single Hilbert space, we would need to resort to a description in terms of the C^*-algebra $\mathfrak{A}$ of observables for a further discussion of the properties of this realization (see [18]). For the sake of simplicity, we assume that the relevant problem can be described in a 'total' Hilbert space $\mathbb{H}$, *e.g.* by taking the direct sum of all inequivalent Hilbert spaces $\mathbb{H}^{(\Psi)}$ obtained by applying the GNS construction to all possible ground states Ψ. The different ground states Ψ can then be represented as vectors $|\Psi\rangle \in \mathbb{H}$ and span a subspace $\mathbb{S}^{(g)} \subset \mathbb{H}$. The transformation operators are improper unitary operators in $\mathbb{H}$. They can be used to map different ground states, and in fact their corresponding Hilbert spaces, to each other. We can then also try to decompose the ground state subspace into the different irreducible representations of G. Let now $\mathsf{S} \subset \mathsf{G}$ be the largest subgroup of G, which leaves every state within the ground state subspace $\mathbb{S}^{(g)}$ unchanged. For any $g \in \mathsf{G}$ and $s \in \mathsf{S}$, and for an arbitrary ground state $|\Psi\rangle \in \mathbb{S}^{(g)}$ we find

$$\hat{U}(g)\hat{U}(s)\hat{U}(g)^\dagger|\Psi\rangle = \hat{U}(g)\hat{U}(s)|\Psi'\rangle = \hat{U}(g)|\Psi'\rangle = |\Psi\rangle$$

so that every ground state is also invariant under the action of $\hat{U}(gsg^{-1})$ and S must be an normal subgroup of G. The Hilbert space $\mathbb{H}^{(\Psi)}$ obtained from an arbitrary ground state $|\Psi\rangle \in \mathbb{H}^{(\Psi)} \subset \mathbb{H}$ only constitutes a representation of the smaller group S (*i.e.* the operators $\hat{U}(s)$ are proper unitary operators in $\mathbb{H}^{(\Psi)}$, $\forall s \in \mathsf{S}$) and the ground state $|\Psi\rangle$ is in the trivial representation of S. In the total Hilbert space $\mathbb{H}$, the ground state subspace $\mathbb{S}^{(g)}$ constitutes an improper representation of the quotient group $\mathsf{Z} = \mathsf{G}/\mathsf{S}$. Define $g_z \in \mathsf{G}$ as the group element that corresponds to the elements $z \in \mathsf{Z}$ of the quotient group, so that $\mathsf{G} = \bigcup_{z\in\mathsf{Z}}\{g_z s, \forall s \in \mathsf{S}\}$. Because infinitely many quantum variables are non-trivially affected by the improper operators $\hat{U}(g_z)$, they can be collected into effectively classical variables that can be identified with the elements $z \in \mathsf{Z}$. More precisely, the ground state subspace $\mathbb{S}^{(g)}$ can be identified with the regular representation[3] of Z. It is possible to choose a ground state $|\Psi_1\rangle$ and identify ground states to any $z \in \mathsf{Z}$ as

$$|\Psi_z\rangle = \hat{U}(g_z)|\Psi_1\rangle\,, \tag{1.29}$$

so that $\langle\Psi_z|\Psi_{z'}\rangle = \delta_{z,z'}$ and

$$\mathbb{S}^{(g)} = \mathrm{span}\{|\Psi_z\rangle\,, \forall z \in \mathsf{Z}\}. \tag{1.30}$$

These special states $|\Psi_z\rangle$ correspond to our intuitive notion of classical symmetry breaking solutions (*e.g.* a ferromagnet pointing in a specific direction), whereas a general quantum mechanical ground state can be in any superposition of these 'classical states'. Using these states $|\Psi_z\rangle$ as basis for $\mathbb{S}^{(g)}$ does identify the ground state subspace with

[2] Unless the Hilbert space is constructed using a ground state in the trivial representation [see Eq. (1.31)].

[3] In principle, it is also possible that $\mathbb{S}^{(g)}$ contains the regular representation an integral number of times. As this is often a consequence of a remaining hidden symmetry that has not been exploited, we ignore this subtlety.

the regular representation of Z, since $\hat{U}(g_{z'})|\Psi_z\rangle = \hat{U}(g_{z'}g_z)|\Psi_1\rangle = |\Psi_{z'z}\rangle$, $\forall z, z' \in \mathsf{Z}$. The ground state subspace $\mathbb{S}^{(\mathrm{g})}$ thus contains all irreducible representations of Z, and in particular it contains one state $|\Psi_{\mathrm{triv}}\rangle$ in the trivial representation of Z and of G. This state can be obtained as

$$|\Psi_{\mathrm{triv}}\rangle \sim \int_{\mathsf{G}} \mathrm{d}g\, \hat{U}(g)|\Psi\rangle = \int_{\mathsf{Z}} \mathrm{d}z\, \hat{U}(g_z)|\Psi\rangle \tag{1.31}$$

for any ground state $|\Psi\rangle \in \mathbb{S}^{(\mathrm{g})}$. Different Hilbert spaces $\mathbb{H}^{(\Psi_z)}$ and $\mathbb{H}^{(\Psi_{z'})}$ are completely disjoint and the 'total' Hilbert space $\mathbb{H}$ is obtained as $\mathbb{H} = \bigoplus_{z\in\mathsf{Z}} \mathbb{H}^{(\Psi_z)}$. Furthermore, we can use the improper unitary transformations to map these Hilbert spaces onto each other as $\hat{U}(g_{z'})\mathbb{H}^{(\Psi_z)} = \{\hat{U}(g_{z'})|\Phi\rangle, \forall\, |\Phi\rangle \in \mathbb{H}^{(\Psi_z)}\} = \mathbb{H}^{(\Psi_{z'z})}$.

We now introduce the concept of an order parameter, which is an observable that maps to an operator $\hat{O} \in \mathbb{L}(\mathbb{H})$ —we still assume the existence of the total Hilbert space $\mathbb{H}$— and satisfies

$$\int_{\mathsf{G}} \mathrm{d}g\, \hat{U}(g)\hat{O}\hat{U}(g)^\dagger = 0. \tag{1.32}$$

The order parameter can be a scalar, vector or tensor quantity. For a ground state $|\Psi\rangle$ in the trivial representation (which is typically the case in the Wigner-Weyl realization), $\langle\Psi|\hat{O}|\Psi\rangle = 0$. However, when the ground state subspace is higher-dimensional and contains non-trivial irreducible representations (Nambu-Goldstone realization), the restriction of $\hat{O}$ to the ground state subspace $\mathbb{S}^{(\mathrm{g})}$, to which we henceforth refer as $\hat{O}^{(\mathrm{g})}$, is not trivially zero. We can then try to diagonalize $\hat{O}^{(\mathrm{g})}$ and use the set of eigenvectors as a basis for the ground state manifold $\mathbb{S}^{(\mathrm{g})}$. One can easily be convinced (intuitively) that these states also correspond to the notion of classical symmetry breaking solutions, so that the eigenvectors of $\hat{O}^{(\mathrm{g})}$ are precisely the states $|\Psi_z\rangle$. Henceforth, we refer to these states as the ground states with maximal symmetry breaking. A specific state $|\Psi_z\rangle$ can be physically obtained by coupling the order parameter to some external field in a suitable manner, and determining the ground state of the system in the limit for which the field strength goes to zero. For symmetries that can be defined from local transformation operators [as in Eq. (1.28)], it is possible to also define the order parameter locally, which we denote as $\hat{o}_{\vec{n}}$ ($\vec{n} \in \mathscr{L}$) or $\hat{o}(\vec{x})$ ($\vec{x} \in \mathscr{R}$). The ground state subspace always contains linear superpositions $|\Psi\rangle$ of the states $|\Psi_z\rangle$, in particular the state $|\Psi_{\mathrm{triv}}\rangle$ in the trivial representation [see Eq. (1.31)], that have $\langle\Psi|\hat{O}|\Psi\rangle = 0$. Symmetry breaking can thus not always be detected from the expectation value of the order parameter. However, for a given ground state $|\Psi\rangle \in \mathbb{S}^{(\mathrm{g})}$, the Nambu-Goldstone realization can be detected by a non-vanishing limit

$$\lim_{\|\vec{m}-\vec{n}\|\to\infty} G^{(o)}_{\vec{m},\vec{n}} \neq 0 \quad \text{or} \quad \lim_{\|\vec{x}-\vec{y}\|\to\infty} G^{(o)}(\vec{x},\vec{y}) \neq 0 \tag{1.33}$$

where the correlation function of the local order parameter is defined as

$$G^{(o)}_{\vec{m},\vec{n}} = \langle\Psi|\hat{o}_{\vec{m}}\hat{o}_{\vec{n}}|\Psi\rangle, \forall \vec{m},\vec{n} \in \mathscr{L} \quad \text{or} \quad G^{(o)}(\vec{x},\vec{y}) = \langle\Psi|\hat{o}(\vec{x})\hat{o}(\vec{y})|\Psi\rangle, \forall \vec{x},\vec{y} \in \mathscr{R}. \tag{1.34}$$

This definition also allows to illustrate the difference between the ground states $|\Psi_z\rangle$ of maximal symmetry breaking and a general superposition

$$|\Psi\rangle = \sum_{z\in\mathbb{Z}} c_z\,|\Psi_z\rangle\,. \tag{1.35}$$

The ground states of maximal symmetry breaking satisfy the property

$$\begin{aligned}\lim_{\|\vec{m}-\vec{n}\|\to\infty} \langle\Psi_z|\hat{o}_{\vec{m}}\hat{o}_{\vec{n}}|\Psi_z\rangle &= \langle\Psi_z|\hat{o}_{\vec{m}}|\Psi_z\rangle\,\langle\Psi_z|\hat{o}_{\vec{n}}|\Psi_z\rangle \\ \text{or}\quad \lim_{\|\vec{x}-y\|\to\infty} \langle\Psi_z|\hat{o}(\vec{x})\hat{o}(\vec{y})|\Psi_z\rangle &= \langle\Psi_z|\hat{o}(\vec{x})|\Psi_z\rangle\,\langle\Psi_z|\hat{o}(\vec{y})|\Psi_z\rangle\end{aligned} \tag{1.36}$$

so that the long-range limit of the connected correlation function

$$\begin{aligned}&\Gamma^{(o)}_{\vec{m},\vec{n}} = \langle\Psi|(\hat{o}_{\vec{m}} - \langle\Psi|\hat{o}_{\vec{m}}|\Psi\rangle)(\hat{o}_{\vec{n}} - \langle\Psi|\hat{o}_{\vec{n}}|\Psi\rangle)|\Psi\rangle\,, \forall\,\vec{m},\vec{n}\in\mathscr{L} \\ &\text{or}\quad \Gamma^{(o)}(\vec{x},\vec{y}) = \langle\Psi|(\hat{o}(\vec{x}) - \langle\Psi|\hat{o}(\vec{x})|\Psi\rangle)(\hat{o}(\vec{y}) - \langle\Psi|\hat{o}(\vec{y})|\Psi\rangle)|\Psi\rangle\,, \forall\,\vec{x},\vec{y}\in\mathscr{R}.\end{aligned} \tag{1.37}$$

vanishes, a property that is called *clustering*. In contrast, for the superposition $|\Psi\rangle$ of Eq. (1.35) we obtain

$$\begin{aligned}\lim_{\|\vec{m}-\vec{n}\|\to\infty} \langle\Psi|\hat{o}_{\vec{m}}\hat{o}_{\vec{n}}|\Psi\rangle &= \sum_{z\in\mathbb{Z}} c_z\,\langle\Psi_z|\hat{o}_{\vec{m}}|\Psi_z\rangle\,\langle\Psi_z|\hat{o}_{\vec{n}}|\Psi_z\rangle \\ &\neq \langle\Psi|\hat{o}_{\vec{m}}|\Psi\rangle\,\langle\Psi|\hat{o}_{\vec{n}}|\Psi\rangle \\ \text{or}\quad \lim_{\|\vec{x}-\vec{y}\|\to\infty} \langle\Psi|\hat{o}(\vec{x})\hat{o}(\vec{y})|\Psi\rangle &= \sum_{z\in\mathbb{Z}} c_z\,\langle\Psi_z|\hat{o}(\vec{x})|\Psi_z\rangle\,\langle\Psi_z|\hat{o}(\vec{y})|\Psi_z\rangle \\ &\neq \langle\Psi|\hat{o}(\vec{x})|\Psi\rangle\,\langle\Psi|\hat{o}(\vec{y})|\Psi\rangle\end{aligned} \tag{1.38}$$

and the connected correlation function does not vanish in the long-range limit. The importance of the clustering property will become clear in the next sections.

So far, only properties of the ground states of systems with symmetry breaking have been discussed. For every ground state $|\Psi\rangle\in\mathbb{S}^{(\mathrm{g})}$, the corresponding Hilbert space $\mathbb{H}^{(\Psi)}$ constitutes a representation of the Hamiltonian as a Hermitian operator $\hat{H}$, that can be diagonalized to yield the excitation spectrum. If $|\Psi\rangle$ is translation invariant and the Hamiltonian is local [as in Eq. (1.21)], the excitation spectrum has the same properties as for the case of a unique ground state discussed in the previous subsection, *i.e.* all states will either describe an elementary excitation or a finite number thereof. The same spectrum is obtained for any chosen ground state $|\Psi\rangle$ and corresponding eigenvectors can be mapped across different Hilbert spaces with the improper unitary operators $\hat{U}(g_z)$, $\forall z\in\mathbb{Z}$. In addition, the local order parameter $\hat{o}$ will map to $\langle\Psi|\hat{o}|\Psi\rangle\,\hat{\mathbb{1}}$, since a finite number of excitations cannot change its value. These states are said to describe topologically trivial excitations.

In local systems with a Nambu-Goldstone realization of symmetry, it is also possible

to have topologically non-trivial excitations [19]. These go under the name of solitons, kinks, domain walls, ... Like particles, they represent states with a finite amount of energy that is localized in a space. At the boundary of $\mathscr{L}$ or $\mathscr{R}$ —which lies at infinite in the thermodynamic limit— these states are also locally similar to a ground state. But since there is now a range of ground states, it is possible to construct states with this property that have a non-trivial topology. Assume for the sake of simplicity that the state under construction is locally similar to a ground state $|\Psi_z\rangle$ of maximal symmetry breaking, where the index z can smoothly change along the boundary $\partial\mathscr{L}$ or $\partial\mathscr{R}$. Imposing that a state looks similar to a ground state at the boundary $\partial\mathscr{L}$ or $\partial\mathscr{R}$ thus boils down to specifying a continuous[4] map φ from $\partial\mathscr{L}$ or $\partial\mathscr{R}$ to Z. If these maps can be continuously deformed to a single point $z \in \mathsf{Z}$, the state is topologically trivial. More generally, we define an equivalence relation between maps such that two maps are equivalent if they are homotopic (*i.e.* if they can be continuously deformed into each other). The physical motivation for this definition is the assumption that a local Hamiltonian can only induce a local change to a state, corresponding to a continuous deformation. The different equivalence classes of all possible maps $\varphi : \partial\mathscr{L} \to \mathsf{Z}$ or $\varphi : \partial\mathscr{R} \to \mathsf{Z}$ constitute a group, the homotopy group H. Excited states with a finite, localized energy can thus be labeled by an element $h \in \mathsf{H}$, which is often called the topological quantum number. Topologically trivial excited states correspond to the unit element $h = \mathbb{1}$. Topologically non-trivial excitations correspond to the other elements $h \in \mathsf{H}$. The group multiplication rules dictate the possible scattering processes that are allowed between these kind of excitations, *e.g.* an excitation with topological quantum number h can combine with an excitation with topological quantum number h^{-1} in order to decay into a topologically trivial excitation, or a ground state. A single topological excitation with $h \neq 1$ is automatically stable against decay into the ground state. A simple example is that of a one-dimensional system (so that $\partial\mathscr{L}$ or $\partial\mathscr{R}$ contains two separated points) that breaks a discrete $\mathbb{Z}_N$ symmetry, the corresponding homotopy group of which is $\mathbb{Z}_N$. For two-dimensional systems on a flat surface, $\partial\mathscr{R}$ is topologically equivalent to S_1 (the circle), and the homotopy group is given by the first fundamental homotopy group $\pi_1(\mathsf{Z})$. In particular, $\pi_1(\mathsf{Z}) = 0$ for all discrete groups Z. Finally, note that systems with periodic boundary conditions have $\partial\mathscr{L} = \emptyset$ or $\partial\mathscr{R} = \emptyset$, and topologically non-trivial excitations are impossible.

We conclude this subsection by stating some interesting theorems related to symmetry breaking in quantum systems. Firstly, Goldstone's theorem (and its non-relativistic counterpart) states that the breaking of a continuous symmetry results in the existence

[4] This definition only works well for systems in the continuum (*i.e.* field theories), since a continuous map cannot be defined on the discrete space $\partial\mathscr{L}$. The underlying physical assumption is that the change of the index z that labels the ground state to which the excitation is locally similar, is sufficiently slow and hence negligable within the support of a single term $h(x)$. This term can thus not detect the difference between the true ground state $|\Psi_z\rangle$ and the excited state. For lattice systems, we analoguously assume that a map is 'continuous' if the change in the index z is arbitrarily small over a number of sites given by the support of the local energy terms h_i. More formally, since $\partial\mathscr{L}$ contains infinitely many points (in the thermodynamic limit), we can embed it in a compact continuous space $\mathscr{K}$ such that $\partial\mathscr{L}$ is dense in $\mathscr{K}$. The map φ on $\partial\mathscr{L}$ can then be called continuous if it has a continuous extension on $\mathscr{K}$.

of massless excitations with boson statistics, called Nambu-Goldstone bosons [20, 21, 22, 23]. If the symmetry group G is a Lie group with Lie algebra $\mathfrak{g}$, and the unbroken subgroup S corresponds to the Lie algebra $\mathfrak{s}$, then the number of Goldstone bosons is given by $\dim \mathfrak{g} - \dim \mathfrak{s} = \dim \mathfrak{z}$, with $\mathfrak{z}$ the Lie algebra of the quotient group Z. However, Goldstone bosons are very uncommon in $d = 1$ (spatial) dimension, since continuous symmetries corresponding to an order parameter that does not commute with the Hamiltonian cannot be broken in one-dimensional quantum systems at zero temperature (*i.e.* ground states) according to Coleman's theorem [24]. This is the quantum version of the Mermin-Wagner-Hohenberg theorem in statistical mechanics [25, 26]. The massless Nambu-Goldstone bosons that would result from such breaking restore the symmetry for $d = 1$ spatial dimensions due to their strong contribution to the quantum fluctuations in the ground state. At finite temperature, thermal fluctuations of these massless excitations can similarly restore the symmetry in $d = 2$ (spatial) dimensions. Local symmetries can never be broken according to Elitzur's theorem [27]. This can easily be understood in the same way that spontaneous breaking of global symmetries is not possible for a finite number of degrees of freedom. Since local symmetries only act locally, they can only detect a finite number of degrees of freedom and fluctuations are always able to restore the symmetry. Nevertheless, there is the possibility of the Englert-Brout-Higgs-Guralnik-Hagen-Kibble mechanism [28, 29, 30], which corresponds to a breaking of the global symmetry that remains after the gauge degrees of freedom have been fixed. Finally, we note that it is possible for quantum systems to have a degenerate ground state manifold without breaking any symmetry. This is discussed in the next subsection.

1.5. Quantum phases and quantum order

As discussed in the previous subsection, Hamiltonians that are invariant with respect to the action of some symmetry transformations can roughly be divided into two classes, depending on how this symmetry is manifested in the ground state. Consequently, it is possible —in the thermodynamic limit— that the symmetry manifestation changes from the Wigner-Weyl realization to the Nambu-Goldstone realization as a parameter in the Hamiltonian is varied. This process is very familiar to the statistical mechanics of classical models, where such a 'classical' phase transition is triggered by a change of temperature T. Analoguously, the corresponding transition in the ground state (thus at $T = 0$) of a quantum Hamiltonian is called a *quantum phase transition* [31, 32]. More specifically, we are discussing second order quantum phase transitions where the energy is continuous but not analytical at the point of the transition. As mentioned, this requires an infinite number of degrees of freedom, as the ground state energy should be analytical in all parameters of the Hamiltonian for any model with a finite number of degrees of freedom (except in the case of a simple level crossing). A quantum phase transition —just like a classical phase transition— separates two phases of matter that differ in the type of order and correlations that are present in the ground state. But this transition is now triggered by quantum fluctuations rather than thermal fluctuations. These quantum

fluctuations behave differently —they can have quantum statistics— and the difference between quantum and classical (thermodynamic) phase transitions that originate from this are outlined in the following sections.

All second order classical phase transistions are captured by the Landau-Ginzburg-Wilson paradigm [33, 34, 35, 36], that links all phase transitions to a change in the manifestation of a symmetry of the model, as measurable by a local order parameter. This framework explains the universality hypothesis, since observational physics near the critical point is determined by the long-wavelength (low-energy) fluctuations of the order-parameter degree of freedom, so that the only relevant parameters are the number of spatial dimensions d and the type of order parameter. However, not all quantum phase transitions correspond to a change in the symmetry pattern in the ground state. Quantum systems do allow for other types of order that are not related to symmetry and have no classical analogon. In particular, quantum systems can undergo phase transitions without changing the realization of the symmetry, or without having any symmetry at all! In such a phase transition, the quantum state develops *topological order*[37]. The effective low energy behavior is then not described by a Landau-Ginzburg-Wilson field theory for the order parameter, since topological order cannot be detected with local order parameters. Topological order is even hard to define in general. Some properties of a topologically ordered phase are:

- gapped spectrum (*i.e.* finite separation between the lowest eigenvalue (possibly degenerate) and the second lowest eigenvalue of the Hamiltonian);
- ground state degeneracy depends on the topology of $\mathscr{L}$ or $\mathscr{R}$;
- different ground states seem 'locally' similar;
- elementary excitations with fractional statistics (anyons).

The third property indicates that no local order parameter can detect the presence of topological order. Whereas a phase transition towards an ordered state in the previous case resulted in symmetry breaking, topological order is associated with an increase of symmetry: it looks very much like a liquid phase and the corresponding phase is often called a quantum liquid. Topological order can be explained through the physical mechanism of string-net condensation[38], which shows that infinitely many different topological orders can exist. The best known example of topological order in nature is the fractional quantum Hall effect[39, 40], but other realizations have been found. Whereas the mathematical foundation of symmetry-breaking order is group theory, a complete classification of the possible topological orders is attempted through tensor category theory [41].

As a last point, we introduce the *fidelity F* between two quantum states. The fidelity is a measure for the "closeness" of two quantum states, and is for pure states Ψ and Ψ' given

by the absolute value of the overlap

$$F(\Psi,\Psi') = \frac{|\langle\Psi|\Psi'\rangle|}{\sqrt{\langle\Psi|\Psi\rangle\,\langle\Psi'|\Psi'\rangle}}. \tag{1.39}$$

A generalized definition for mixed states also exists [42, 43]. If $F = 1$, the states are identical. In the thermodynamic limit, the fidelity scales to zero due to the orthogonality castrastrophe. The rate of "orthogonalization" r_0 can be defined through

$$\lim_{|\mathscr{L}|\to\infty} F \sim \mathrm{e}^{-r_0|\mathscr{L}|} \qquad \text{or} \lim_{|\mathscr{R}|\to\infty} F(\Psi,\Psi') \sim \mathrm{e}^{-r_0|\mathscr{R}|} \tag{1.40}$$

for two states Ψ or Ψ' living on the lattice $\mathscr{L}$ or in the continuum $\mathscr{R}$. In the continuum, r_0 scales as $r_0 \sim a^{-d}$ with a the cutoff length, and hence diverges for relativistic theories. Either $r_0 = 0$ if Ψ and Ψ' live in the same Hilbert space, or $r_0 = +\infty$ if the states Ψ and Ψ' live in unitarily inequivalent Hilbert spaces. Consequently, $F = 0$ already occurs for systems of finite size, corresponding to the ultraviolet character of the orthogonality catastrophe in relativistic theories. On the lattice, r_0 is dimensionless and can be used to define a *fidelity per site* $d(\Psi,\Psi') = \mathrm{e}^{r_0}$, or thus directly as

$$d(\Psi,\Psi') = \exp\left(\lim_{|\mathscr{L}|\to\infty} \frac{\log F(\Psi,\Psi')}{|\mathscr{L}|}\right). \tag{1.41}$$

Recently, it has been shown that $d(\Psi,\Psi')$ is an important quantity for characterizing quantum phase transitions. For $\Psi = \Psi(\boldsymbol{\lambda})$ and $\Psi' = \Psi(\boldsymbol{\lambda}')$ with $\Psi(\boldsymbol{\lambda})$ the ground state of a Hamiltonian $\hat{H}(\boldsymbol{\lambda})$ with parameters $\boldsymbol{\lambda}$, the fidelity per site is defined as $d(\boldsymbol{\lambda},\boldsymbol{\lambda}') = d(\Psi(\boldsymbol{\lambda}),\Psi(\boldsymbol{\lambda}'))$. Near a critical point $\boldsymbol{\lambda} = \boldsymbol{\lambda}_c$, the ground state fidelity per site develops singular behavior that encodes universal information about the quantum phase transition [44, 45, 46, 47] and can be characterized using the curvature of the surface $d(\boldsymbol{\lambda},\boldsymbol{\lambda}')$ [48, 49, 50]. See also [51] for a review on fidelity and [52] for the relation with topological order.

2. Quantum correlations and entanglement

While the previous section has summarized the most important properties of extended quantum systems, it did not discuss the quantum nature of these systems by which they are set apart from classical systems. By far the utmost important and astonishing property of quantum systems is *entanglement*. The concept of entanglement was introduced by Schrödinger [53] and was the cause of Einstein's dissatisfaction with quantum mechanics [54], because it resulted in a "*Spukhafte Fernwirkung*". It is most easily introduced for a system C that can be divided into two disjoint subsystems or parties A and B, so that $A \cup B = C$ and $A \cap B = \emptyset$. The bipartition of C into subsystems A and B can correspond to a bipartition of the spatial region $\mathscr{L}$ or $\mathscr{R}$ on which C is defined, but a more general

abstract bipartition is equally possible. If $O^{(A)}$ and $O^{(B)}$ represent two observables that act non-trivially only on party A, respectively on party B, then the connected correlation function $\Gamma_{A,B}$ is defined as

$$\Gamma_{A,B} = \langle O^{(A)} \otimes O^{(B)} \rangle - \langle O^{(A)} \rangle \langle O^{(B)} \rangle . \tag{1.42}$$

For local classical theories, these correlations are bound by the Bell inequality [55] or the Clauser-Horne-Shimony-Holt inequality [56], whereas entanglement allows for a violation of these inequalities for quantum theories, thus indicating that quantum theories cannot be explained by underlying classical models. Entanglement is made possible by the tensor product construction of Hilbert spaces for composite systems. A simple classical state $\rho^{(C)}$ of the system C would look like $\rho^{(C)} = \rho^{(A)} \otimes \rho^{(B)}$ so that $\rho^{(C)}(O^{(A)} \otimes O^{(B)}) = \rho^{(A)}(O^{(A)})\rho^{(B)}(O^{(B)}) = \rho^{(C)}(O^{(A)})\rho^{(C)}(O^{(B)})$ and $\Gamma_{A,B} = 0$. Classical systems can of course have non-zero correlations due to probabilistic mixtures (*e.g.* due to thermal fluctuations). The most general class of states that do not violate the Bell inequalities for classical correlations is called the class of *separable states* $\rho^{(C)}_{\text{sep}}$ and are given by [57]

$$\rho^{(C)}_{\text{sep}} = \sum_k p_k \rho^{(A)}_k \otimes \rho^{(B)}_k . \tag{1.43}$$

A general quantum state $\rho^{(C)}$ cannot be decomposed in this way. The subsystems A and B are then entangled, resulting in non-classical correlations between them. Nevertheless, the fundamental role of entanglement did at first not get widely accepted in standard quantum mechanics. Only after quantum information theory identified entanglement as the key resource for an exponential speedup with quantum computers, the importance of entanglement in strongly correlated quantum systems became clear.

2.1. Measures and properties

The concept of entanglement is most easily introduced for isolated systems C that allow for a bipartition into a subsystem A and B. By the assumption of isolation of C, we imply that the quantum state of C is given by a pure state $\rho^{(C)} = \Psi$, to which corresponds a state vector $|\Psi\rangle \in \mathbb{H}^{(C)} = \mathbb{H}^{(A)} \otimes \mathbb{H}^{(B)}$ or a density operator $\hat{\rho}^{(C)}_{\Psi} = |\Psi\rangle\langle\Psi|$. We henceforth assume that $\dim \mathbb{H}^{(C)} = \dim \mathbb{H}^{(A)} + \dim \mathbb{H}^{(B)}$ is finite so that there is no problem with defining these Hilbert spaces. If we introduce orthogonal bases $\{|\Phi^{(A)}_\alpha\rangle ; \alpha = 1, \ldots, \dim \mathbb{H}^{(A)}\}$ and $\{|\Phi^{(B)}_\beta\rangle ; \beta = 1, \ldots, \dim \mathbb{H}^{(B)}\}$ for $\mathbb{H}^{(A)}$ and $\mathbb{H}^{(B)}$, then we can construct the product basis $\{|\Phi^{(A)}_\alpha\rangle \otimes |\Phi^{(B)}_\beta\rangle ; \alpha = 1, \ldots, \dim \mathbb{H}^{(A)}; \beta = 1, \ldots, \dim \mathbb{H}^{(B)}\}$ for $\mathbb{H}^{(C)}$ and expand $|\Psi\rangle$ as

$$|\Psi\rangle = \sum_{\alpha=1}^{\dim \mathbb{H}^{(A)}} \sum_{\beta=1}^{\dim \mathbb{H}^{(B)}} c_{\alpha,\beta} |\Phi^{(A)}_\alpha\rangle \otimes |\Phi^{(B)}_\beta\rangle . \tag{1.44}$$

For an unentangled system, the coefficient matrix $c_{\alpha,\beta}$ has rank 1 and can be written as $c_{\alpha,\beta} = c^{(A)}_{\alpha} c^{(B)}_{\beta}$ so that the state $|\Psi\rangle$ factorizes into

$$|\Psi\rangle = |\Psi^{(A)}\rangle \otimes |\Psi^{(B)}\rangle$$
$$\text{with} \quad |\Psi^{(A)}\rangle = \sum_{i=1}^{\dim \mathbb{H}^{(A)}} c^{(A)}_{\alpha} |\Phi^{(A)}_{\alpha}\rangle, \quad |\Psi^{(B)}\rangle = \sum_{j=1}^{\dim \mathbb{H}_B} c^{(B)}_{\beta} |\Phi^{(B)}_{\beta}\rangle \quad (1.45)$$

and the state of subsystem A (respectively B) is given by the pure state $|\Psi^{(A)}\rangle$ (respectively $|\Psi^{(B)}\rangle$). All separable pure states are thus product states and result in a total absence of correlations, since this corresponds to $\Gamma_{A,B} = 0$. For the more general case, the singular-value decomposition or Schmidt decomposition [58] of the coefficient matrix $c_{\alpha,\beta} = \sum_{\gamma=1}^{D} U_{\alpha,\beta} \lambda_{\gamma} V_{\beta,\gamma}$ (with $D = \min(\dim \mathbb{H}^{(A)}, \dim \mathbb{H}^{(B)})$ allows to write

$$|\Psi\rangle = \sum_{\gamma=1}^{D} \lambda_{\gamma} |\Psi^{(A)}_{\gamma}\rangle \otimes |\Psi^{(B)}_{\gamma}\rangle$$
$$\text{with} \quad |\Psi^{(A)}_{\gamma}\rangle = \sum_{\alpha=1}^{\dim \mathbb{H}^{(A)}} U_{\alpha,\gamma} |\Phi^{(A)}_{\alpha}\rangle, \quad |\Psi^{(B)}\rangle = \sum_{\beta=1}^{\dim \mathbb{H}^{(B)}} V_{\beta,\gamma} |\Phi^{(B)}_{\beta}\rangle, \quad (1.46)$$

which is called the Schmidt decomposition of the state $|\Psi\rangle$. Since U and V are unitary operators (or can be expanded to be unitary if $D < \dim \mathbb{H}^{(A)}$ or $D < \dim \mathbb{H}^{(B)}$), the states $|\Psi^{(A)}_{\gamma}\rangle$ are mutually orthogonal (and idem ditto for the states $|\Psi^{(B)}_{\gamma}\rangle$). The singular values $\lambda_{\gamma} \geq 0$ are called the Schmidt coefficients and satisfy $\sum_{\gamma=1}^{D} \lambda^2_{\gamma} = 1$ because of normalization. Subsystem A and B are now described by the mixed state $\rho^{(A)}$ and $\rho^{(B)}$ corresponding to the density operators

$$\begin{aligned} \hat{\rho}^{(A)} &= \mathrm{tr}_B \left(\hat{\rho}^{(C)} \right) = \sum_{\gamma=1}^{D} \lambda^2_{\gamma} |\Psi^{(A)}_{\gamma}\rangle \langle \Psi^{(A)}_{\gamma}|, \\ \hat{\rho}^{(B)} &= \mathrm{tr}_A \left(\hat{\rho}^{(C)} \right) = \sum_{\gamma=1}^{D} \lambda^2_{\gamma} |\Psi^{(B)}_{\gamma}\rangle \langle \Psi^{(B)}_{\gamma}|. \end{aligned} \quad (1.47)$$

The density operators $\hat{\rho}^{(A)}$ and $\hat{\rho}^{(B)}$ thus have the same spectrum of eigenvalues, given by the square of the Schmidt coefficients. The vectors $|\Psi^{(A)}_{\gamma}\rangle$, $|\Psi^{(B)}_{\gamma}\rangle$ are the corresponding eigenvectors and are henceforth called the Schmidt vectors. The entanglement between the complementing subsystems A and B is measured by the *entanglement entropy* $S^{(A,B)}$, which is defined as

$$S^{(A,B)} = -\mathrm{tr} \left[\hat{\rho}^{(A)} \ln \hat{\rho}^{(A)} \right] = -\mathrm{tr} \left[\hat{\rho}^{(B)} \ln \hat{\rho}^{(B)} \right] = -\sum_{\gamma=1}^{D} \lambda^2_{\gamma} \ln \lambda^2_{\gamma}. \quad (1.48)$$

The spectrum of (the square of) the Schmidt-coefficients is therefore called the *entanglement spectrum*. A *maximally entangled state* is obtained when $\lambda_\gamma = 1/\sqrt{D}$, $\forall \gamma = 1, \ldots, D$ resulting in $S = \log D$. For a bipartite system in a pure state, the entanglement entropy is the unique measure of entanglement that satisfies the following properties [59]:

- $S^{(A,B)}$ is invariant under local unitary operations in A or B;
- S is continuous (see [60] for a precise definition);
- S is additive, *i.e.* if we add a second bipartite system $C' = A' \cup B'$ so that the total state of $C \cup C'$ is given by $\rho^{(C \cup C')} = \rho^{(C)} \otimes \rho^{(C')}$, we obtain $S^{(A \cup A', B \cup B')} = S^{(A,B)} + S^{(A',B')}$.

When system $C = A \cup B$ itself is in a mixed state, classical correlations are present: *e.g.* thermal correlations corresponding to thermal equilibrium at temperature $T = \beta^{-1}$ are obtained when the system C is in the Gibbs state ρ_β corresponding to the density operator $\hat{\rho}_\beta^{(C)} \sim \exp(-\beta \hat{H})$. The spectrum of $\hat{\rho}^{(A)}$ is no longer equal to the spectrum of $\hat{\rho}^{(B)}$ and the entanglement entropy is no longer well defined. It is difficult to find a measure that fully separates the pure quantum correlations from the classical correlations. Even for the simplest case where A and B both represent a single qubit (*i.e.* $\mathbb{H}^{(A)} \equiv \mathbb{H}^{(B)} \equiv \mathbb{C}^2$), there is no unique measure for entanglement. Similar problems arise if one tries to quantify the entanglement corresponding to a multipartite division ($C = \cup_{i=1}^m A_i$ with $A_i \cap A_j = \emptyset$ if $i \neq j$) of the system. General properties of a good entanglement measure $E^{(A_1,\ldots,A_m)}$ corresponding to such a division can be formulated [61, 60]:

- Separable states contain no entanglement:
  $E^{(A_1,\ldots,A_m)} = 0$ if $\rho^{(C)} = \sum_k p_k \bigotimes_{i=1}^m \rho_k^{(A_i)}$.
- All non-separable states have non-zero entanglement:
  $E^{(A_1,\ldots,A_m)} > 0 \Leftrightarrow \rho^{(C)} \neq \sum_k p_k \bigotimes_{i=1}^m \rho_k^{(A_i)}$.
- The measure E is an *entanglement monotone*:
  $E^{(A_1,\ldots,A_m)}$ cannot be increased with local operations (*i.e.* quantum measurements or unitary operations restricted to the individual subsystems A_i) or classical communication between the subsystems.

Unlike for bipartitions, it is not possible to define maximally entangled states for entanglement measures corresponding to multipartite divisions. Since this dissertation is concerned with isolated systems at zero temperature, the state of the system C can always be assumed to be a pure state Ψ. A suitable multipartite entanglement measure is then given by the geometric entanglement measure $E_{\text{geom}}(A_1, \ldots, A_m)$, defined as [62]

$$E_{\text{geom}}^{(A_1,\ldots,A_m)} = -\ln\left(\max_{\{\psi_i\}} |\langle \psi_1 \cdots \psi_m | \Psi \rangle|^2\right), \tag{1.49}$$

with $|\psi_1 \cdots \psi_m\rangle = |\psi_1\rangle_1 \otimes \cdots \otimes |\psi_m\rangle_m$.

For any state ρ and any $0 < \alpha \leq \infty$ we now define the *Rényi entropy* $S_\alpha(\rho)$ as

$$S_\alpha(\rho) = \frac{1}{1-\alpha} \ln(\operatorname{tr} \hat{\rho}^\alpha). \tag{1.50}$$

In the limit $\alpha \to 1$, the Rényi entropy yields the *von Neumann entropy*

$$S(\rho) = S_1(\rho) = \lim_{\alpha \to 1} \frac{1}{1-\alpha} \ln(\operatorname{tr} \hat{\rho}^\alpha) = -\operatorname{tr}[\hat{\rho} \ln \hat{\rho}]. \tag{1.51}$$

The entanglement entropy $S^{(A,B)}$ of a system $C = A \cup B$ corresponding to a bipartition into complementary subsystems A and B given in Eq. (1.48) can thus be recognized as the von Neumann entropy of either subsystem A or B: $S^{(A,B)} = S(\rho^{(A)}) = S(\rho^{(B)})$. Both notations will be used interchangeably. We can now also define a generalized bipartite entangled entropy as

$$S_\alpha^{(A,B)} = S_\alpha(\rho^{(A)}) = S_\alpha(\rho^{(B)}). \tag{1.52}$$

If system C is not in a pure state then $S_\alpha(\rho^{(A)}) \neq S_\alpha(\rho^{(B)})$ so that this definition is still restricted to the setting of isolated systems C.

Let A and B now represent general subsystems of system C, so that not necessarily $A \cap B = \emptyset$ nor $A \cup B = C$. The von Neumann entropy satisfies a very interesting property called *strong subadditivity* [63, 64, 65]:

$$S(\rho^{(A\cup B)}) + S(\rho^{(A\cap B)}) \leq S(\rho^{(A)}) + S(\rho^{(B)}). \tag{1.53}$$

In particular, for disjoint subsystems $A \cap B = \emptyset$, this allows to define the *mutual information* between subsystems A and B as

$$I(A:B) = S(\rho^{(A)}) + S(\rho^{(B)}) - S(\rho^{(A\cup B)}). \tag{1.54}$$

The mutual information is restricted to the range $0 \leq I(A:B) \leq 2\min[S_1(\rho^{(A)}), S_1(\rho^{(B)})]$. It is directly related to the connected correlation function $\Gamma_{A,B}$ since [66]

$$(\Gamma_{A,B})^2 \leq 2||\hat{O}^{(A)}||^2 ||\hat{O}^{(B)}||^2 I(A:B). \tag{1.55}$$

Entanglement between parties A and B (as measured by the mutual information) thus yields an upper bound for the maximum correlation, or —vice versa— the connected correlation function yields a lower bound for the minimum amount of entanglement required to sustain these correlations. This relation is further investigated in the case of extended systems in the next subsection.

2.2. Quantum correlations in extended systems

In an extended system, the connected correlation function becomes position dependent. More precisely, if at every site $\vec{n} \in \mathscr{L}$ or any point $\vec{x} \in \mathscr{R}$ a complete set of observables is given by $O_{\vec{n}}^{(\alpha)}$ or $O^{(\alpha)}(\vec{x})$, then all two-point connected correlation functions can be obtained from

$$\Gamma^{(\alpha,\beta)}_{\vec{m},\vec{n}} = \langle O^{(\alpha)}_{\vec{m}} \otimes O^{(\beta)}_{\vec{n}} \rangle - \langle O^{(\alpha)}_{\vec{m}} \rangle \langle O^{(\beta)}_{\vec{n}} \rangle \quad \text{or}$$
$$\Gamma^{(\alpha,\beta)}(\vec{x},\vec{y}) = \langle O^{(\alpha)}(\vec{x}) \otimes O^{(\beta)}(\vec{y}) \rangle - \langle O^{(\alpha)}(\vec{x}) \rangle \langle O^{(\beta)}(\vec{y}) \rangle . \quad (1.56)$$

In translation invariant systems, the connected correlation function only depends on the distance $||\vec{m} - \vec{n}||$ or $||\vec{x} - \vec{y}||$ and allows to define a physical correlation length ξ_c as

$$\xi_c^{-1} = \lim_{||\vec{m}-\vec{n}||\to\infty} \max_{\alpha,\beta} \left(-\frac{\log \left[\Gamma^{(\alpha,\beta)}_{\vec{m},\vec{n}} \right]}{a||\vec{m} - \vec{n}||} \right), \quad \xi_c^{-1} = \lim_{||\vec{x}-\vec{y}||\to\infty} \max_{\alpha,\beta} \left(-\frac{\log \left[\Gamma^{(\alpha,\beta)}(\vec{x},\vec{y}) \right]}{||\vec{x} - \vec{y}||} \right), \quad (1.57)$$

where one also needs rotation invariance or parity invariance for this limit to be direction independent. For lattice systems, we have introduced the lattice spacing a in order to give ξ_c the physical dimension of a length in lattice and continuum systems alike. Note that the clustering property of connected correlation function is a necessary (but not sufficient) condition to obtain a finite correlation length; a finite correlation length requires the connected correlation functions to be *exponentially clustering*.

Since correlations only offer a lower bound for entanglement, a similar construction is needed to evaluate the entanglement between points that are separated over a long distance. In principle, we could use the mutual information with party A equal to site $\vec{m} \in \mathscr{L}$ or point $\vec{x} \in \mathscr{R}$ and party B equal to site $\vec{n} \in \mathscr{L}$ or point $\vec{y} \in \mathscr{R}$. This allows to similarly define an entanglement length ξ_e as

$$\xi_e^{-1} = \lim_{||\vec{m}-\vec{n}||\to\infty} \left(-\frac{\log \left[I(\vec{m} : \vec{n}) \right]}{2a||\vec{m} - \vec{n}||} \right), \quad \xi_e^{-1} = \lim_{||\vec{x}-\vec{y}||\to\infty} \left(-\frac{\log \left[I(\vec{x} : \vec{y}) \right]}{2||\vec{x} - \vec{y}||} \right). \quad (1.58)$$

The inequality in Eq. (1.55) allows to conclude that

$$\xi_e \geq \xi_c. \quad (1.59)$$

However, mutual information is still not the best measure to fully separate classical from quantum correlations. For spin systems on a lattice $\mathscr{L}$, a more operational construction was already provided in [67], hereby defining the measure of *localizable entanglement* $E_{\vec{m},\vec{n}}$ $(\forall \vec{m}, \vec{n} \in \mathscr{L})$ as follows. By performing a series of local measurements $\mathcal{M}$ on all $|\mathscr{L}| - 2$ spins in the lattice $\mathscr{L}$ except for spin $\vec{m}$ and spin $\vec{n}$, the subsystem containing the

two spins ends up in a pure state $|\phi_s\rangle$ with a probability p_s (due to the collapse postulate). Using an entanglement measure $E(\phi)$ for this simple bipartite system in pure state ϕ, the localizable entanglement is obtained as

$$E_{\vec{m},\vec{n}} = \max_{\mathcal{M}} \sum_s p_s E(\phi_s), \tag{1.60}$$

where the maximization is performed with respect to all possible series of local measurements $\mathcal{M}$. Rather than $I(\vec{m} : \vec{n})$, one can then use $E_{\vec{m},\vec{n}}$ in the definition of the entanglement length ξ_e [Eq. (1.58)]. While the difference between the entanglement length and the correlation length can be small, it can also be extreme. In particular, it is possible to construct quantum states for which all correlations $\Gamma^{(\alpha,\beta)}_{\vec{m},\vec{n}} = 0$ but which are nevertheless in a strongly entangled state [68].

Even though quantum correlations can violate bounds on maximal correlations as expressed by the Bell inequalities, entanglement is not an unlimited resource. More precisely, it satisfies a fundamental property called *entanglement monogamy* [69, 70, 71, 72]. If a single party A_1 of a quantum system is maximally entangled with another party A_2, there can be no entanglement between either A_1 or A_2 and any other party A_i, $i > 2$. Let $E^{(A_i,A_j)}$ be a bipartite entanglement measure that quantifies the entanglement between two parties A_i and A_j. Unfortunately, we cannot use the entanglement entropy for this, and a different measure was used in the proof in [72]. The entanglement $E^{(A_1,C\setminus A_1)}$ between a single party A_1 and the rest of the system is limited to some amount $E^{(A_1)}_{\max}$ depending on the entanglement measure E. If party A_1 has to share this entanglement with many other parties A_i, $i = 2,\ldots,k$ (*e.g.* due to symmetry), it can only be weakly entangled with each of them. The quantitative statement is given by

$$E^{(A_1,A_2)} + E^{(A_1,A_3)} + \ldots + E^{(A_1,A_k)} \leq E^{(A_1,\bigcup_{i=2}^k A_k)} \leq E^{(A_1)}_{\max} \tag{1.61}$$

Ultimately, entanglement monogomy is a consequence of the no-cloning theorem [73, 74]. Classical correlations can easily be shared, since it is sufficient to copy the state of A_2 to all other parties A_i, $i = 3,\ldots,k$ in order to obtain equally strong correlations between A_1 and any of the A_i, $\forall i = 2,\ldots,k$. This operational strategy is not feasible for quantum systems because the quantum state of party A_2 cannot be copied to all other parties. Hence, the monogamy of entanglement also induces a strong limitation on the shareability of non-local quantum correlations (*i.e.* on correlations that violate the Bell inequalities) [75, 76, 77, 78]. In particular, in symmetric systems with an infinite coordination number (*e.g.* Bethe lattice) quantum correlations are completely absent and mean-field theory is able to provide an exact solution.

The limited shareability of quantum entanglement combined with the non-commutativity of the different terms $\hat{h}$ in the Hamiltonian $\hat{H}$ of a system [see Eq. (1.21)] induces a kind of *frustration* in quantum systems [79, 80]. Frustration is defined as the inability to minimize simultaneously the energy of all competing interactions. In classical systems, frustration is of geometric origin, because the order that is favored by the interactions

cannot propagate throughout space as a result of an incompatibility between correlations along closed loops [81, 82, 83]. This incompatibility is a consequence of different competing interactions or because of the lattice geometry. The most simple example is the impossibility of having antiferromagnetic correlations on a triangular lattice. The relation between frustration and the Bell inequality for classical correlations are explored in [84]. Classically frustrated systems possess a ground state degeneracy that increases exponentially in the volume of the system —and thus violate the third law of thermodynamics— as well as local zero energy modes and algebraically decaying correlations. However, they are not critical, as they do not separate a disordered phase from an ordered phase. The most famous example of a classically frustrated system is (water) ice [85], but similar effects occur in magnetic systems (*e.g.* spin ice). In quantum systems, the many classical ground states that are induced by geometric frustration can tunnel into each other and exotic phases of matter (*e.g.* topological order) can be created [86]. However, quantum systems can also be frustrated without any classical counterpart. As a simple example, an antiferromagnetic Heisenberg interaction $J\vec{S}_{\vec{m}} \cdot \vec{S}_{\vec{n}}$ ($J > 0$) between spin-½ systems on sites $\vec{m}$ and $\vec{n}$ is minimized by putting sites $\vec{m}$ and $\vec{n}$ into a singlet state $|\phi\rangle = (|\uparrow_{\vec{m}}\downarrow_{\vec{n}}\rangle - |\downarrow_{\vec{m}}\uparrow_{\vec{n}}\rangle)/\sqrt{2}$. However, since this is a maximally entangled state, sites $\vec{m}$ and $\vec{n}$ can no longer be entangled with any other sites. Vice versa, if site $\vec{n}$ has an antiferromagnetic Heisenberg interaction with each of its neighbors, entanglement monogomy prevents the interactions to all be minimized individually. By expanding $\vec{S}_{\vec{m}} \cdot \vec{S}_{\vec{n}}$ as $\hat{\sigma}^x_{\vec{m}}\hat{\sigma}^x_{\vec{n}} + \hat{\sigma}^y_{\vec{m}}\hat{\sigma}^y_{\vec{n}} + \hat{\sigma}^z_{\vec{m}}\hat{\sigma}^z_{\vec{n}}$, this frustration can also be attributed to the non-commutativity of the individual terms. The individual Hamiltonians $\hat{H}^{(x,y,z)}$ given by

$$\hat{H}^{(x)} = \sum_{\langle \vec{m},\vec{n}\rangle} \hat{\sigma}^x_{\vec{m}}\hat{\sigma}^x_{\vec{n}}, \qquad \hat{H}^{(y)} = \sum_{\langle \vec{m},\vec{n}\rangle} \hat{\sigma}^y_{\vec{m}}\hat{\sigma}^y_{\vec{n}}, \qquad \hat{H}^{(z)} = \sum_{\langle \vec{m},\vec{n}\rangle} \hat{\sigma}^z_{\vec{m}}\hat{\sigma}^z_{\vec{n}}, \tag{1.62}$$

would each produce classical ground states with corresponding ground state energies $E_0^{(x,y,z)}$. However, the non-commutativity of the terms $H^{(x,y,z)}$ in the total Hamiltonian $\hat{H} = \hat{H}^{(x)} + \hat{H}^{(y)} + \hat{H}^{(z)}$ requires the ground state of the total system to be in some superposition and thus induces entanglement [87]. If the ground state energy of $\hat{H}$ is given by E_0, we can define the frustration energy as $E^{(\mathrm{f})} = E_0 - E_0^{(x)} - E_0^{(y)} - E_0^{(z)}$ and relate it to the entanglement in the ground state (see *e.g.* [88] for the application to a different model). This opens up the idea to use the Hamiltonian of the system as an *entanglement witness*, which is the general name for an observable that is able to discriminate between entangled and factorizing states [89, 90, 91]. A unified treatment of geometric and quantum contributions to frustration is endeavored in [92].

2.3. Scaling of quantum correlations near quantum critical points

Quantum phase transition, as classical phase transitions, are generally accompanied by a diverging correlation length ξ_c (as defined in Eq. (1.57)). At the critical point, the correlations decay algebraically. Since we are working at $T = 0$, there are no thermal

fluctuations and all correlations are of quantum nature. The divergence of the correlation length implies the lack of an intrinsic length scale in the system, so that fluctuations at different length scales are self-similar. The long distance behavior (far away from the ultraviolet cutoff length a) becomes scale invariant at the critical point. Similarly, the temporal coherence length τ_c diverges as ξ_c^z, thereby defining a dynamic scaling exponent z. With ξ_c and τ_c being the only relevant time and length scales in the neighborhood of the critical point, an observable O measured at wave vector k and frequency ω must satisfy

$$O(k,\omega) = \xi_c^{d_O} f_O(k\xi_c, \omega\tau_c) \tag{1.63}$$

where d_O is the scaling dimension of the observable and the scaling function $f_O(x,y)$ must satisfy for large values of the arguments x and y

$$f_O(x,y) = x^{-d_O} \tilde{f}_O(x^z/y) \tag{1.64}$$

in order for the observable to have a sensible limit as the critical point is approached. At the critical point, we then obtain

$$O(k,\omega) = k^{-d_O} \tilde{f}_O(k^z/\omega), \tag{1.65}$$

which indicates the presence of fluctuations at all length scales. Similar scaling behaviors and relations between the different scaling dimensions d_O were first proposed by Essam and Fisher [93] and by Widom [94, 95] in the context of classical phase transitions. Kadanoff was the first to use renormalization group arguments to explain these relations [96]. For classical phase transitions, the dynamic exponent z only enters when studying dynamic behavior of systems in the neighborhood of their critical points. For example, static connected correlation functions $\Gamma(\vec{x},\vec{y})$ at the critical point scale as $\Gamma(\vec{x},\vec{y}) \sim 1/||\vec{x}-\vec{y}||^{d-2+\eta}$ so that its Fourier transform diverges at small values of k as k^{-d_Γ} with thus $d_\Gamma = 2-\eta$.

For quantum critical points, the dynamics cannot be decoupled from the static properties due to Heisenberg's uncertainty relation. Algebraically decaying correlations at the critical point require the closing of the energy gap $\Delta E \to 0$ in the system, as was proven in [97] for a general class of lattice systems. Vice versa, if a system has a finite energy gap $\Delta E > 0$ away from the critical point, then correlations decay exponentially with the size of the gap ΔE, which was proven for lattice systems in [98, 99]. Near the critical point, we can write $\Delta E \sim \xi_c^{-z}$, where the dynamic exponent z reappears in order to conserve Heisenberg's relation $\Delta E \Delta t \geq \hbar$. As a result, the dynamic exponent even enters in static correlation functions $\Gamma(\vec{x},\vec{y})$ as $\Gamma(\vec{x},\vec{y}) \sim 1/||\vec{x}-\vec{y}||^{d+z-2+\eta}$. The origin of the effective dimension $d+z$ of quantum phase transitions is explained in Section 3.

A quantum phase transition thus characterizes a transition where the nature of quantum correlations changes drastically from one side of the critical point to the other. This drastic change is accompanied by singular behavior in physical observables, which is characterized by a universal set of critical exponents. The intimate connection between

correlations and entanglement explored in the previous subsections indicates that this difference may propagate into the entanglement structure of the ground state. In particular, investigating whether the entanglement also has singular and/or universal behavior in the neighborhood of the critical point is the logical next step.

2.4. Entanglement and quantum phases

The study of entanglement in strongly correlated quantum systems —more specifically spin systems— was initiated in [100, 101, 102]. The behavior of entanglement in the neighborhood of critical points in one-dimensional lattice models was first investigated in [103, 104, 105]. These papers focussed on pairwise entanglement between two sites m and n (nearest neighbors or next-nearest neighbors), which is non-analytic at the phase transition but does not develop a universal behavior. The pairwise entanglement can be discontinuous (in case of a level crossing) but can just as well be smooth. It attains a maximum close to but not necessarily at the phase transition point. Because the correlation length ξ_c diverges at the transition point, Eq. (1.59) automatically implies a diverging entanglement length ξ_e [5]. So a site m is strongly entangled with all sites n at arbitrarily large distances. Because of the monogamy of entanglement, this is not automatically compatible with a maximal pairwise entanglement between two specific sites m and n. The pairwise entanglement is not a good measure of the global entanglement in the ground state.

The global entanglement can be studied by evaluating the entanglement of a block of spins as function of the size of the block. In the remainder of this chapter, we will often consider a bipartition $C = A \cup B$ of a system C where A is associated to a spatial region $\mathscr{A} \subset \mathscr{L}$ or $\mathscr{A} \subset \mathscr{R}$ with $\mathscr{L}$ or $\mathscr{R}$ the lattice or continuum on which C lives. We then simply denote subsystem A by its spatial region $\mathscr{A}$. For the complementary region $\mathscr{L} \setminus \mathscr{A}$ or $\mathscr{R} \subset \mathscr{A}$ associated to B, we introduce the notation $-\mathscr{A}$. The entanglement entropy $S^{(\mathscr{A},-\mathscr{A})}$ is then abbreviated as $S^{(\mathscr{A})}$. In exactly solvable one-dimensional lattice models, the entanglement entropy $S^{(\mathscr{A})}$ of a block $\mathscr{A}$ of physical length of ℓ containing ℓ/a contiguous spins was found to diverge as $S^{(\mathscr{A})} \sim \log(\ell/a)$ in [107, 108] at the critical point, indicating that the long-range fluctuations responsible for the phase transition are indeed of quantum mechanical origin. For one-dimensional lattice systems, it can also be proven (see [109, 110]) that the presence of a finite gap $\Delta E > 0$ implies that the entanglement entropy S of a block $\mathscr{A}$ of ℓ spins necessarily saturates to some constant value $S^{(\mathscr{A})} \sim \log \xi_c$ for $\ell \to \infty$, a result that is known as an *area law* (since the area of a one-dimensional interval $\mathscr{A}$ of length ℓ is constant: $|\partial\mathscr{A}| = 2$). A similar proof of the intimate connection between a gapped spectrum and an area law for the entanglement entropy does not (yet) exist in higher dimensions. In (quasi) free bosonic system an

[5] Note that Eq. (1.59) allows for the possibility that $\xi_e \to \infty$ whereas $\xi_c < \infty$. As shown in [106], the energy gap does not need to close and this is not a critical point. The diverging entanglement length is caused by the hidden topological order in the model under investigation. A diverging entanglement length is also obtained for a general superposition of ground states with maximal symmetry breaking due to its violation of the clustering property, as explained further on in this subsection.

area law for the entanglement entropy was analytically found even at the critical point [111, 112], but in fermionic systems a multiplicative logarithmic violation of the area law is possible for critical systems with a finite Fermi surface [113, 114, 115].

Two ground states $|\Psi(0)\rangle$ and $|\Psi(1)\rangle$ of respective Hamiltonians $\hat{H}(0)$ and $\hat{H}(1)$ are defined to be *equivalent* if there exists a smooth path of short-ranged Hamiltonians $\hat{H}(g)$ ($g \in [0,1]$) such that there is no quantum phase transition along the path. A sufficient criterion[6] is thus that the spectrum of $\hat{H}(g)$ is gapped $\forall g \in [0,1]$. This definition of an equivalence relation allows to interpret different phases of matter as different equivalence classes. It can then also be shown that different states within a single equivalence class can be transformed into each other by acting with local unitary transformations [116, 117]. These local unitary transformations can alter the short-range entanglement in the ground state, but not the long-range entanglement. For example, it is shown in [118] that all gapped one-dimensional short-range interacting systems are equivalent to frustration free systems with an increased interaction length. For lattice systems in arbitrary dimensions, the ground state of frustration-free systems can efficiently be determined, and the entanglement entropy of a region $\mathscr{A}$ can be proven to satisfy an area law $S_{\mathscr{A}} \sim |\partial\mathscr{A}|$ [119]. Unfortunately, for $d > 1$ spatial dimension, it is not generally proven that all ground states of gapped Hamiltonians are equivalent to frustration-free states and hence satisfy an area law.

Results in the previous paragraphs were obtained for lattice models. For a field theory on the continuum $\mathscr{R}$, the definition of the entanglement entropy $S^{(\mathscr{A})}$ of a spatial region $\mathscr{A} \subset \mathscr{R}$ is more intricate. In non-relativistic theories, the Fock construction of the Hilbert space $\mathbb{H}^{(\mathrm{F})}_{\mathscr{R}}$ [see Eq. (1.15)] satisfies

$$\mathbb{H}^{(\mathrm{F})}_{\mathscr{R}} = \mathbb{H}^{(\mathrm{F})}_{\mathscr{A}} \otimes \mathbb{H}^{(\mathrm{F})}_{-\mathscr{A}}$$

and the entanglement entropy can straightforwardly be defined. Similar results as for lattice models are obtained, where physical lengths are weighted by the inverse cutoff length $a^{-1} = \rho^{1/d}$ with ρ the finite particle density. Matters are more complicated for relativistic field theories. Whereas the operator algebra defining the field can unambiguously be localized in a part $\mathscr{A} \subset \mathscr{R} = \mathbb{R}^d$, there is no Lorentz invariant partition of the Hilbert space $\mathbb{H}^{(\mathrm{F})}$ corresponding to a spatial region $\mathscr{A}$ and its complement. Due to the presence of the measure in the definition of $\mathbb{H}^{(1)}_{\mathscr{R}}$, there is no covariant definition of localization of single-particle states and $\mathbb{H}^{(1)}_{\mathscr{A}}$ cannot be defined. A manifestation of this fact for a scalar field theory is that it is impossible to choose a single particle state $|\Psi\rangle \in \mathbb{H}^{(1)}_{\mathscr{R}}$ such that $\langle 0|\hat{\phi}(x)|\Psi\rangle$ and $\langle 0|\hat{\pi}(x)|\Psi\rangle$ vanish in the same region $x \in -\mathscr{A}$. If the entanglement entropy $S^{(\mathscr{A})} = S(\rho^{(\mathscr{A})})$ would be finite, combining the positivity of the von Neumann entropy S with strong subadditivity and the Poincaré-invariance of the vacuum would suffice to prove an area law and to conclude that the mutual information $I(\mathscr{A} : \mathscr{B})$ between any two disjoint spatial regions $\mathscr{A} \cap \mathscr{B} = \emptyset$ is identically zero [120].

[6] Note that this is not a required criterion, since the Hamiltonian of a system with spontaneous breaking of a continuous symmetry is gapless arbitrarily far away from the critical point.

Entanglement entropy may thus not have a finite covariant meaning in quantum field theory. However, the mutual information $I(\mathscr{A}:\mathscr{B})$ is well defined and only diverges when the distance between $\mathscr{A}$ and $\mathscr{B}$ goes to zero. By lifting the restriction of positivity, a finite entropy function $\tilde{S}(\rho^{(\mathscr{A})})$ for relativistic field theories can be constructed that produces the same mutual information [121].

For practical purposes, an ultraviolet cutoff length scale a is introduced in order to render the entanglement entropy $S^{(\mathscr{A})}$ finite. In $d=1$ spatial dimensions, a special role is played by the class of conformal field theories, characterized by a central charge c. They serve as effective field theories for the low-energy behavior of critical quantum models, such as the lattice models discussed in the beginning of this subsection. For these conformal field theories, the entanglement entropy of an interval $\mathscr{A}$ of length ℓ can be exactly computed [122, 123, 124] for many different scenarios. For a conformal field theory having periodic boundary conditions on a line of length L, the generalized entanglement entropy $S_\alpha^{(\mathscr{A})}$ [see Eq. (1.52)] of a block $\mathscr{A}$ of length ℓ is given by

$$S_\alpha^{(\mathscr{A})} = \frac{c+\overline{c}}{12}\left(1+\frac{1}{\alpha}\right)\log\left[\frac{L}{\pi a}\sin\left(\frac{\pi}{L}\ell\right)\right]+k, \tag{1.66}$$

with c and $\overline{c}$ the holomorphic and antiholomorphic central charge of the theory and k a non-universal constant depending on the regularization scheme. In the thermodynamic limit ($L\to\infty$), the entanglement entropy thus reduces to $S^{(\mathscr{A})}=2(c+\overline{c})/12\log(\ell/a)+k$, where the explicit factor 2 represents the area (number of boundary points) of the interval $\mathscr{A}$. If a chain of finite length L with open boundary condition is divided into a left part $\mathscr{A}$ with length ℓ and a right part $-\mathscr{A}$ with length $L-\ell\geq\ell$, then there is only one internal boundary point and the generalized entanglement entropy $S_\alpha^{(\mathscr{A})}$ is exactly half the value of Eq. (1.66). These results thus proof the findings of [107, 108] for critical lattice models. The prefactor of the logarithmic scaling is universal and only depends on the central charges c and $\overline{c}$ of the theory. As for lattice systems, analytic results for the entanglement entropy of higher-dimensional quantum field theories can only be obtained for free theories. Calculations supporting the area law were performed much earlier [125, 126] in the context of black hole entropy, a relation that is discussed in more detail in the next subsection. A recent overview of different methods to obtain analytic results can be found in [127]. The general expression for the entanglement entropy of a subsystem A corresponding to the spatial region $\mathscr{A}$ in n spatial dimensions is given by [128]

$$S^{(\mathscr{A})} = g_{d-1}(\partial\mathscr{A})a^{-(d-1)}+g_{d-2}(\partial\mathscr{A})a^{-(d-2)}+\ldots+g_0(\partial\mathscr{A})\log(a)+f(\mathscr{A}) \tag{1.67}$$

where $f(\mathscr{A})$ is a finite part and the functions g_i are local and extensive functions on the boundary $\partial\mathscr{A}$, which are homogeneous of degree i. For $i\geq 1$, they depend on the regularization procedure and are not universal. They are not physical since they are not related to continuum quantities. Only for spherical regions $\mathscr{A}$ is it possible to conclude that $g_{d-1}(\partial\mathscr{A})\sim|\partial\mathscr{A}|$, hence producing the area law. The function $g_0(\partial\mathscr{A})$

is independent of the regularization scheme. Universal contributions can be present in $f(\mathscr{A})$, but they have to be carefully extracted since the finite part is affected by changes in the cutoff.

This subsection is concluded by discussing the influence of quantum order on the entanglement entropy. Firstly, for the classical paradigm of symmetry-breaking order, the ground state manifold is degenerate. If a discrete symmetry is broken, the lowest excited state above the ground state manifold (which can be topologically non-trivial) is massive (gapped) away from the critical point. In contrast, when a continuous symmetry is broken, Goldstone's theorem ensures the presence of massless (gapless) excitations. The previous section has introduced ground states $|\Psi_z\rangle$ with maximal symmetry breaking ($\forall z \in \mathsf{Z}$ with Z the quotient group that is spontaneously broken) and illustrated that they are clustering [see Eq. (1.37)]. Let a bipartition into a region $\mathscr{A}$ and its complement produce a Schmidt decomposition for the state $|\Psi_z\rangle$

$$|\Psi_z\rangle = \sum_\alpha \lambda_\alpha |\Psi_{z,\alpha}^{(\mathscr{A})}\rangle |\Psi_{z,\alpha}^{(-\mathscr{A})}\rangle . \tag{1.68}$$

If we assume, as in the definition in Eq. (1.29), that $|\Psi_z\rangle$ is obtained by acting with an (improper) unitary operator $\hat{U}(g_z)$ on $|\Psi_1\rangle$, where $\hat{U}(g_z)$ is a product of local operators $\hat{u}(g_z)$ and can thus be decomposed as $\hat{U}(g_z) = \hat{U}^{(\mathscr{A})}(g_z) \otimes \hat{U}^{(-\mathscr{A})}(g_z)$, then the Schmidt coefficients are independent of the label z and the corresponding Schmidt vectors can be obtained as $|\Psi_{z,\alpha}^{(\mathscr{A})}\rangle = \hat{U}^{(\mathscr{A})}(g_z)|\Psi_{1,\alpha}^{(\mathscr{A})}\rangle$ and $|\Psi_{z,\alpha}^{(-\mathscr{A})}\rangle = \hat{U}^{(-\mathscr{A})}(g_z)|\Psi_{1,\alpha}^{(-\mathscr{A})}\rangle$, $\forall \alpha$. Indeed, the locality of these unitary transformations implies that the different ground states with maximal symmetry breaking are in the same phase. If an area law for the states $|\Psi_z\rangle$ is assumed, then

$$S_z^{(\mathscr{A})} = S(\rho_z^{(\mathscr{A})}) = -\sum_\alpha \lambda_\alpha^2 \log \lambda_\alpha^2 \sim |\partial\mathscr{A}|. \tag{1.69}$$

The complement $-\mathscr{A}$ is infinite so that the Schmidt vectors automatically fulfill the orthonormalization condition $\langle \Psi_{z,\alpha}^{(\mathscr{A})} | \Psi_{z',\alpha'}^{(-\mathscr{A})} \rangle = \delta_{z,z'}\delta_{\alpha,\alpha'}$ due to the orthogonality catastrophe. For a general superposition $|\Psi\rangle$ as in Eq. (1.35), this can be used to compute

$$\hat{\rho}^{(\mathscr{A})} = \sum_{z\in\mathsf{Z}} \sum_\alpha |c_z|^2 \lambda_\alpha^2 |\Psi_{z,\alpha}^{(\mathscr{A})}\rangle \langle \Psi_{z,\alpha}^{(A)}| . \tag{1.70}$$

The entanglement entropy of the superposition $|\Psi\rangle$ is thus given by

$$\begin{aligned} S^{(\mathscr{A})} = S(\rho^{(\mathscr{A})}) &= -\sum_{z\in\mathsf{Z}} \sum_\alpha |c_z|^2 \lambda_\alpha^2 \log |c_z|^2 \lambda_\alpha^2 \\ &= -\sum_\alpha \lambda_\alpha^2 \log \lambda_\alpha^2 - \sum_{z\in\mathsf{Z}} |c_z|^2 \log |c_z|^2 . \end{aligned} \tag{1.71}$$

The superposition $|\Psi\rangle$ thus has a higher entanglement content, which is required to explain the violation of the clustering property by the connected correlation function of the order parameter [see Eq. (1.38)]. The states $|\Psi_z\rangle$ of maximal symmetry breaking

can therefore also be identified as the minimally entangled ground states. If Z is a discrete group with a finite number of elements, then the additive contribution is finite. But for infinite groups or continuous symmetry groups, there might be a diverging additive contribution to the entanglement entropy and thus a very peculiar violation of the area law. The macroscopic extent of this entanglement makes these states extremely vulnerable against decoherence. Interactions with the environment can collapse a general superposition $|\Psi\rangle$ to one of the ground states of maximal symmetry breaking $|\Psi_z\rangle$.

Finally, states with topological order are also characterized by a higher entanglement entropy. For a bipartition into the spatial region $\mathscr{A}$ and its complement $-\mathscr{A}$, the entropy of a state $|\Psi\rangle$ with topological order is given by

$$S^{(\mathscr{A})} = \alpha|\partial A| - \gamma + \mathcal{O}(1/|\partial\mathscr{A}|), \tag{1.72}$$

where the prefactor α depends on the ultraviolet cutoff and the geometry of $\mathscr{A}$. But now, the additive contribution γ is universal and is called the *topological entanglement entropy* [129, 130]. It is given by $\gamma = \log Q$, where Q is called the *quantum dimension* [131]. The topic of topological entanglement entropy is not further explored in this dissertation.

2.5. Area laws and holography

The previous subsection sketched the most important feature of the entanglement structure in ground states of short-ranged Hamiltonians: the entanglement $S^{(\mathscr{A})}$ between a subsystem $\mathscr{A}$ and its compliment scales as the area $|\partial\mathscr{A}|$, with at most logarithmic violations for critical systems. For arbitrary quantum states, the entropy $S^{(A)}$ is upper bounded by $\log(\dim \mathbb{H}^{(\mathscr{A})})$ (assuming that $\mathscr{A}$ is smaller than its complement). Since $\dim \mathbb{H}^{(\mathscr{A})}$ scales exponentially with the volume of $\mathscr{A}$, the entanglement entropy in a general quantum state is extensive (*i.e.* it scales with the volume). An area law thus indicates that ground states of short-ranged Hamiltonians are special and only occupy a small part of the total Hilbert space. This observation is of major importance for the formulation of efficient variational ansätze in the remainder of this dissertation.

Before trying to interpret the physical origin of the area law, it is possible to extend its validity beyond the case of ground states. For free field theories, power-law corrections to the area law were found when the field is in a superposition of its ground state and low-lying excited states [132, 133, 134]. For large areas, these are negligable and the area law still holds. An area law was also found for low-lying excited states in an integrable one-dimensional lattice model [135]. In [136] an area law is proven for all low-energy states —not restricted to eigenstates— of short-range interacting lattice models under some technical conditions, including a sufficiently rapid decay of connected correlation functions and an upper bound on the number of low-lying excitations in a subsystem A corresponding to a compact spatial region $\mathscr{A}$. More precisely, if $\hat{O}^{(\mathscr{A})}$ has non-trivial

support on the spatial region $\mathscr{A}$ and $\hat{O}^{(\mathscr{B})}$ acts non-trivially only in a compact spatial region $\mathscr{B}$ at a distance $d(\mathscr{A},\mathscr{B})$ of $\mathscr{A}$, then the proof requires that

$$\left|\langle\hat{O}^{(\mathscr{A})}\hat{O}^{(\mathscr{B})}\rangle - \langle\hat{O}^{(\mathscr{A})}\rangle\,\langle\hat{O}^{(\mathscr{B})}\rangle\right| \leq (d(\mathscr{A},\mathscr{B}) - \xi\,\ln|\mathscr{A}|)^{-d}\,,$$

with ξ some constant. Secondly, if $\hat{H}_{\mathscr{A}}$ contains all terms of the Hamiltonian $\hat{H}$ with spatial support completely contained in $\mathscr{A}$, then the number $\Omega_{\mathscr{A}}(e)$ of eigenvalues of $\hat{H}_{\mathscr{A}}$ smaller than e should fulfill

$$\Omega_{\mathscr{A}}(e) \leq (\tau|\mathscr{A}|)^{\gamma(e-e_0)+\eta|\partial\mathscr{A}|},$$

with τ, γ and η some constants and e_0 the lowest eigenvalue of $\hat{H}_{\mathscr{A}}$.

If a system is at thermal equilibrium for a finite temperature $T=\beta^{-1}$, then the von Neumann entropy of the total state ρ_β [associated to the thermal density operator $\hat{\rho}_\beta = \exp(-\beta\hat{H})/\operatorname{tr}\{\exp(-\beta\hat{H})\}$] returns the thermodynamic entropy of the state, which is proportional to the volume. Thus, the entanglement of a compact region $\mathscr{A}$ as measured by the von Neumann entropy $S^{(\mathscr{A})}$ also contains a contribution of the thermal entropy proportional to the volume $|\mathscr{A}|$. This is of course a consequence of the von Neumann entropy not being able to separate classical and quantum correlations. In [66] an area law is exactly proven for short-ranged lattice model, if as entanglement measure the mutual information $I(\mathscr{A}:-\mathscr{A})$ between a subsystem $\mathscr{A}$ and its complement is used. More precisely

$$I(\mathscr{A}:-\mathscr{A}) \leq 2||\hat{h}||\beta|\partial\mathscr{A}|, \tag{1.73}$$

where $||\hat{h}||$ denotes the largest eigenvalue of any term $\hat{h}$ in the Hamiltonian that acts across the boundary $\partial\mathscr{A}$. At zero temperature, β diverges and the area law can be violated.

Finally, area laws even exist beyond equilibrium. If a (possibly time-dependent) Hamiltonian $\hat{H}(t)$ on a bipartite lattice $\mathscr{L}=\mathscr{A}\cup-\mathscr{A}$ can be written as

$$\hat{H}(t) = \hat{H}^{(\mathscr{A})}(t) + \hat{H}^{(-\mathscr{A})}(t) + \sum_k r_k(t)\hat{J}^{(\mathscr{A})}(t)\otimes\hat{J}^{(-\mathscr{A})}(t), \tag{1.74}$$

where $\hat{H}^{(\pm\mathscr{A})}(t)$ and $\hat{J}^{(\pm\mathscr{A})}(t)$ act non-trivially only on region $\pm\mathscr{A}$ and $||\hat{J}^{(\pm\mathscr{A})}(t)|| \leq 1$, then the increase of entanglement for a random intitial state $\Psi(0)$ under time evolution with $\hat{H}(t)$ is given by (see [137, 138])

$$\frac{\mathrm{d}S^{(\mathscr{A})}}{\mathrm{d}t}(t) \leq \eta\sum_k |r_k(t)| \tag{1.75}$$

with η some absolute constant smaller than 2. Thus, if the initial state $\Psi(0)$ satisfies an area law and the number of terms $r_k(t)$ is proportional to the area $|\partial A|$ —which is the case in short-range interacting systems— then the state $\Psi(t)$ satisfies an area law for

any finite time t. These results are derived using the *Lieb-Robinson bound* [139] for lattice systems, which states that for operators $\hat{O}^{(\mathscr{A})}$ and $\hat{O}^{(\mathscr{B})}$ acting non-trivially only at disjoint compact spatial regions $\mathscr{A}$ and $\mathscr{B}$, time dependent correlations satisfy

$$\frac{\left\|[\hat{O}^{(\mathscr{B})}(t),\hat{O}^{(\mathscr{A})}]\right\|}{||\hat{O}^{(\mathscr{A})}||\,||\hat{O}^{(\mathscr{B})}||} \leq \eta \min(|\mathscr{A}|,|\mathscr{B}|)\exp\left(-\frac{d(\mathscr{A},\mathscr{B})-vt}{\xi}\right) \tag{1.76}$$

with η, v and ξ some constants and $\hat{O}^{(\mathscr{B})}(t)=\mathrm{e}^{+\mathrm{i}\hat{H}t}\hat{O}^{(\mathscr{B})}(t)\mathrm{e}^{-\mathrm{i}\hat{H}t}$ for some short-ranged Hamiltonian $\hat{H}$. The Lieb-Robinson bound thus provides a notion of causality for non-relativistic systems, since the commutator between two operators at distance $d(\mathscr{A},\mathscr{B})$ and time-difference t is exponentially small if $d(\mathscr{A},\mathscr{B})>vt$, where v is the effective speed of light —or speed of information— of the lattice model. While the original proof was restricted to bounded operators for a lattice systems with bounded interactions, it has been generalized to many different scenarios in [140, 98, 99, 141, 142, 143, 144, 145, 146, 147].

Now that the validity of the area law is established for a number of cases, an elaboration on its interpretation is in order. For arbitrary quantum states, a bipartition of the system into a spatial region $\mathscr{A}$ and its complement results in an entanglement $S^{(\mathscr{A},-\mathscr{A})}$ that can only be bounded by $S^{(\mathscr{A},-\mathscr{A})}\leq \min(\dim\mathbb{H}^{(\mathscr{A})},\dim\mathbb{H}^{(-\mathscr{A})})\sim\min(|\mathscr{A}|,|-\mathscr{A}|)$. However, since $S^{(\mathscr{A},-\mathscr{A})}$ is a common property of subsystem $\mathscr{A}$ and its complement, a short-range interacting Hamiltonian should not be able to detect the volumes of $\mathscr{A}$ or $-\mathscr{A}$ individually, but only the shared area $|\partial\mathscr{A}|$. Only when the correlation length diverges is it possible for the interaction to penetrate the complete regions $\mathscr{A}$ and $-\mathscr{A}$. On the other hand, thermodynamic entropy is almost always an extensive quantity, with one well-known example being the entropy of a black hole, which is given by [148, 149, 150]

$$S_{\mathrm{BH}}=\frac{|\partial\mathscr{A}|}{4G_d}, \tag{1.77}$$

where $\mathscr{A}$ is the part of space taken by the black hole and G_d is Newton's gravitional constant in d spatial dimensions, so that $G_d=\ell_{\mathrm{P}}^{d-1}$ with ℓ_{P} the Planck length in these units. The attempt to explain the black hole area law as the entanglement entropy of the quantum fields obscured by the horizon of the black hole was the original motivation for the computation of the entanglement entropy in free field theories [125, 126] and conformal field theories [151] (see also [152] for a review).

Since entropy also serves as a measure of the information contained in a system, the area law for black holes indicates that the maximal amount of information that can be encoded in any subsystem of the universe scales as the area rather than the volume of the system. This allows to conclude that the universe itself can be interpreted as the hologram of a theory that completely lives at the boundary [153, 154, 155]. Even though the *holographic principle* is believed to be an exclusive feature of gravity, the area law in the ground states of short-range interacting Hamiltonians also indicates that such

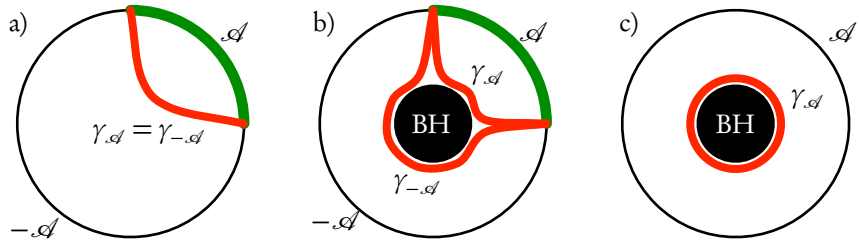

Figure 1.1: Holographic interpretation of von Neumann entropy $S^{(\mathscr{A})}$ of a spatial region $\mathscr{A}$ as the length or area $|\gamma_{\mathscr{A}}|$ of the geodesic or minimal surface $\gamma_{\mathscr{A}}$ that encapsulates $\mathscr{A}$ in the AdS bulk (up to a factor): a) if the system is in a pure state, $\gamma_{\mathscr{A}} = \gamma_{-\mathscr{A}}$ and the entanglement entropy is defined as $S^{(\mathscr{A})} = S_1(\rho^{(\mathscr{A})}) = S_1(\rho^{(-\mathscr{A})})$; b) at thermal equilibrium, the presence of a black hole creates two different minimal surfaces and $S_1(\rho^{(\mathscr{A})}) \neq S_1(\rho^{(-\mathscr{A})})$; c) if $\mathscr{A}$ equals to complete domain $\mathscr{R}$ on which the system lives, $S_1(\rho^{(\mathscr{A})})$ represents the thermodynamic entropy of the system, which is equal to the black hole entropy of the corresponding black hole in the AdS space.

a holographic description is possible, an observation that characterizes the corner of Hilbert space in which these ground states live and can be used to interpret the variational ansätze in Chapters 3 and 4.

Another realization of the holographic principle is the duality between conformal field theories in d spatial dimensions and quantum gravity theories living in the product space of a $d+1$ dimensional anti-de Sitter space[7] and some closed manifold, known as the *Maldacena conjecture* or the *AdS/CFT correspondence* [156, 157, 158]. Here, the theory of interest (the conformal theory) is living at the boundary and is itself acting as the holographic screen that encodes a gravity theory in one higher dimension. It can also be used to study systems at thermal equilibrium, by placing a black hole at the center of the gravity theory with a Hawking-temperature corresponding to the temperature of the boundary system. It was used by Ryu and Takayanagi to postulate that the von Neumann entropy of a subregion $\mathscr{A}$ of the boundary theory is related to the length or area of the geodesic or minimal surface $\gamma_{\mathscr{A}}$ encapsulating this boundary region $\mathscr{A}$ in the AdS bulk [159, 160] by

$$S_1(\rho^{(A)}) = \frac{|\gamma_{\mathscr{A}}|}{4G_d}. \tag{1.78}$$

This endows the entanglement entropy with the geometric interpretation in Figure 1.1, that also allows to very easily derive the "strong subadditivity" property [161] (see Figure 1.2). An overview of results obtained with this approach is given in [162] and a first contribution towards deriving the postulate of Ryu and Takayanagi can be found in [163].

[7] This is the maximally symmetric vacuum solution of Einstein's field equations with constant negative curvature.

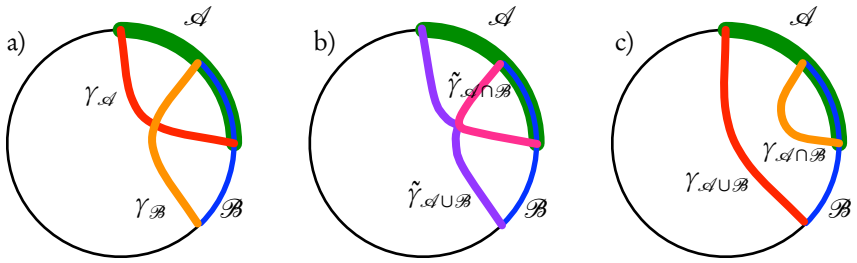

Figure 1.2: Holographic derivation of "strong subadditivity" [161]: $|\gamma_{\mathscr{A}}|+|\gamma_{\mathscr{B}}| = |\tilde{\gamma}_{\mathscr{A}\cup\mathscr{B}}|+|\tilde{\gamma}_{\mathscr{A}\cap\mathscr{B}}| \geq |\gamma_{\mathscr{A}\cup\mathscr{B}}|+|\gamma_{\mathscr{A}\cap\mathscr{B}}|$ where the last inequality follows from the fact that $\tilde{\gamma}_{\mathscr{A}\cup\mathscr{B}}$ and $\tilde{\gamma}_{\mathscr{A}\cap\mathscr{B}}$ are not guaranteed to be geodesics or minimal surfaces.

3. Renormalization of quantum systems

Critical phenomena (both classical and quantum mechanical) and relativistic quantum field theories are both characterized by fluctuations (quantum mechanical or statistical) over an infinitely large range of scales. In critical phenomena, there is often an explicit ultraviolet cutoff scale in terms of a lattice spacing a or the inter-particle separation $a = \rho^{-1/d}$ (with ρ the particle density), but the infrared scale ξ_c diverges. In relativistic field theories, the infrared cutoff ξ_c may (or may not) be finite, but there is no finite ultraviolet cutoff ($a \to 0$). Thus, the range of scales ξ_c/a over which fluctuations act diverges in both cases. There is no definite length or energy scale in the system for which the fluctuations dominate and that can thus be used in a dimensional analysis. Fluctuations on all scales from a to ξ_c are equally important. Even when a system is very simple at the fundamental scale (the Hamiltonian), very complex dynamics at the observational scale can *emerge* [164]. The mathematical tool to study the change of behavior along a shift in the observational scale is the *renormalization group*, which is studied in this section.

The renormalization group was developed simultaneously for classical phase transitions and for relativistic quantum field theories. Classical and quantum systems differ in terms of the number of relevant dimensions. Criticality corresponds to a diverging correlation length $\xi_c \to \infty$, which requires the presence of at least one spatial dimension that is of infinite size. For a quantum theory in d spatial dimensions, Feynman's path integral formalism or other approaches exist to bring the partition function in an equivalent classical form

$$\begin{aligned} Z = \mathrm{tr}\left[\exp(-\beta\hat{H})\right] &= \int [\mathcal{D}\phi_\alpha] \exp\left\{-\int_{-\beta/2}^{+\beta/2} \mathrm{d}\tau\, L_{\mathrm{E}}(\phi_\alpha(\tau))\right\} \\ &= \int [\mathcal{D}\phi^\alpha] \exp\{-S_{\mathrm{E}}[\phi_\alpha(\tau)]\}, \end{aligned} \tag{1.79}$$

where the quantum theory is assumed to be defined in terms of a set variables ϕ_α that

can live in the continuum (for a field theory) or on a lattice (for a lattice theory). Even though we are studying equilibrium systems, capturing the quantum fluctuations requires the introduction of an explicit (imaginary) time τ dependence of the fields $\phi_\alpha(\tau)$. Time appears as additional dimension in the partition function: the quantum partition function thus looks like a classical partition function in $d+1$ dimensions, where the role of the Hamiltonian is now played by an object that can often be interpreted as the Euclidean action $S_\mathrm{E}[\phi^\alpha] = \int_{-\beta/2}^{+\beta/2} \mathrm{d}\tau\, L_\mathrm{E}(\phi^\alpha(\tau))$. At finite temperature, this additional dimension is finite. In particular, near thermodynamic phase transitions, the thermal fluctuations are much more important than the quantum fluctuations and the model can be considered effectively classical. When studying quantum phase transitions, *i.e.* transitions in quantum systems at zero temperature, the length of this additional dimension also diverges ($\beta \to \infty$)[8]. Properties of thermodynamic phase transitions in d dimensions are then valid for quantum phase transitions in $d-1$ dimensions. For example, the Mermin-Wagner-Hogenberg theorem [26, 25] states that interacting thermal fluctuations of a system with continuous symmetry will always restore the symmetry for $d \leq 2$, so that a thermodynamic phase transition towards a phase with symmetry breaking is only possible in $d \geq 3$. Quantum fluctuations are able to restore the same symmetry only for $d \leq 1$ and a symmetry broken ground state exists for $d \geq 2$ [24]. Therefore, a quantum system is often labeled by the number of spacetime dimensions $(d+1)$. This is only correct for relativistic systems, where time and space coordinates enter the action S_E on the same footing: Lorentz invariance becomes Euclidean invariance in the Euclidean action S_E. For non-relativistic systems, interactions in the action S_E can differ between the temporal direction and the spatial directions, and the temporal coherence length τ_c is related to the spatial correlation length ξ_c by the dynamic exponent z. Under a change of scale, we need to map $x \mapsto bx$ and $\tau \mapsto b^z\tau$, so that the volume element $\mathrm{d}\tau\mathrm{d}^d x \mapsto b^{d+z}\mathrm{d}\tau\mathrm{d}^d x$. The effective number of relevant dimensions for the quantum phase transition is given by $d+z$, where z can be positive (the general case), zero (the marginal case generally associated to the quantum critical point being the $T=0$ endpoint of a thermodynamic critical line), or negative (a peculiar case that occurs in some random magnetic systems and results in dimensional reduction).

3.1. Perturbative renormalization and divergences

The infinite range of fluctuations in critical phenomena and quantum field theories are responsible for non-analytic behavior. In particular, the absence of an ultraviolet cutoff scale in (relativistic) quantum field theories leads to divergences in the expectation value of physical observables. This interpretation should be contrasted to the statements in Subsection 1.1, where the divergences were attributed to the evaluation of physical observables in the wrong Hilbert space. Expectation values of observables with respect to the ground state of an interacting theory should not be evaluated by computing

[8] At small nonzero temperature near a quantum phase transition, a crossover region exists [32]. This dissertation is restricted to $T=0$.

the expectation value of the representation of this observable as an operator acting on the Hilbert space of a free theory. However, since the ground state of the interacting theory is not exactly known, there is no other possibility then to regularize the theory by explicitly introducing an ultraviolet cutoff scale $a = \Lambda^{-1}$, where Λ is henceforth called the cutoff frequency. The number of degrees of freedom in a finite volume is then finite, and most problems with inequivalent representations and divergences are cured. However, results should not depend on this cutoff frequency and it should be possible to consistently take the limit $\Lambda \to \infty$ at the end of the calculation.

The first person to compute a finite value for a physical observable from the difference of two diverging quantities was Bethe, who computed the Lamb shift —the difference in the $2s$ and $2p$ energy levels of the hydrogen atom caused by quantizing the electromagnetic field— in 1947 [165]. Shortly after, Schwinger computed the anomalous magnetic momentum of the electron [166]. Both computations were in very good agreement with the experimental results (respectively [167] and [168]). The theory of "Quantum electrodynamics" was further developed by Tomonaga [169], Schwinger [170, 171, 172] and Feynman [173, 174, 175]. In 1949, Dyson proved that the application of the renormalization procedure to quantum electrodynamics leads to finite values up to every order in perturbation theory [176, 177].

A basic outline of the renormalization procedure that was unfolded by these pioneers can now be given. Starting from a bare (fundamental) Lagrangian with bare parameters e_0 (electron charge) and m_0 (electron mass), one introduces a regularization procedure (depending on a cutoff frequency Λ) and computes finite renormalized (physical) values e and m for the electron charge and mass (using perturbation theory). It is then possible to invert these relations in order to obtain

$$e_0 = e + \frac{1}{2} c_1 e^3 \ln(\Lambda/m) + \ldots, \qquad m_0 = m + c_2 m e^2 \ln(\Lambda/m),$$

so that all occurrences of the bare parameters e_0 and m_0 in physical quantities can be replaced by the physical values e and m. One can then consistently send $\Lambda \to \infty$ and still obtain finite values for physical observables. While highly succesfull, it was a miracle that this procedure worked. In effect, this procedure does not work for all theories but only for the so-called *renormalizable* field theories. Hence, the renormalization procedure was considered an embarrassment by many theorists (including Dirac). The bare parameters e_0 and m_0 diverge in the limit $\Lambda \to \infty$ and their interpretation is unclear. A solution was sought along several lines:

- The origin of the problem is perturbation theory and would disappear in exact solutions or summations up to all order [178], a hypothesis which was very quickly abandoned as it proved to be untrue [179].
- The problem was of mathematical nature: the procedure for generating renormalized perturbation theory had to be modified to avoid introducing unphysical divergences and automatically generating finite terms, so that the bare Lagrangian

has no physical meaning. This line of thought led to the Bogoliubov-Parasiuk-Hepp-Zimmerman formalism [180, 181, 182] and later to the causal perturbation theory of Epstein and Glaser [183], where the problem of divergences in position space (rather than momentum space) was reduced to a proper definition of products of singular distributions.

- Quantum electrodynamics was only an effective theory and the cutoff scale was physical because of a more fundamental theory with unknown interactions at very small scale. This point of view corresponds best to our current interpretation of the standard model.

In the mid-fifties, it was noted by Stueckelberg and independently by Gell-Mann and Low that a theory of massless electrons lacks a natural energy scale on which the renormalization procedure should be based [184, 185]. In terms of dimensional analysis, a dimensionless coupling constant e cannot be related to a cutoff frequency Λ if there is no other energy scale present. A new mass scale μ has to be introduced in order to define a renormalized coupling constant e. This mass scale is completely arbitrary, and other couples $\{\mu', e'\}$ should yield the same physical results. This implies the existence of an equivalence class of parametrizations $\{\mu, e(\mu)\}$ and different couples within the equivalence class are related through a reparametrization transformation that has to satisfy a (semi) group law. This *renormalization group* does not provide any new intelligence for exact solutions of the field theory. But since its group character is violated by perturbation theory, a restoration of the group character can be used to improve the perturbative results. The flow $e(\mu)$ of the renormalization group is captured by a differential equation

$$\frac{\mathrm{d}e(\mu)^2}{\mathrm{d}\ln\mu} = \beta(e(\mu)^2) \tag{1.80}$$

where the *beta function* $\beta(e^2)$ is analytic and can be expanded in a power series of e^2. The different terms can be computed in different orders of perturbation theory. Integrating the RG flow improves the perturbation results as it boils down to an automatic resummation of a subclass of the perturbation terms to all orders. The renormalization group predicts *running coupling constants*, *i.e.* the value of the coupling constant $e(\mu)$ depends on the energy scale μ with which the theory is probed, as was later established experimentally.

In 1970, the relation between the renormalization group and scale invariance was discovered by Callen [186], Symanzik [187, 188]. In particular, they related the β function to the canonical trace anomaly, indicating the breaking of scale invariance in massless quantum field theories. Critical quantum field theories do not break this scale invariance and have $\beta = 0$. In addition, they formulated the Callan-Symanzik equation for n-point

correlation functions $G^{(n)}(x_1,\ldots,x_n;\{g_\beta\};\mu)=\langle\phi_1(x_1)\cdots\phi_n(x_n)\rangle$, given by

$$\left[\mu\frac{\partial}{\partial\mu}+\sum_k\beta_k(g_k)\frac{\partial}{\partial g_k}+\sum_{i=1}^{n}\gamma_i\right]G^{(n)}(x_1,\ldots,x_n;\{g_k\};\mu)=0 \qquad (1.81)$$

for a theory of fields ϕ_i with scaling dimension γ_i, where the theory contains the dimensionless renormalized coupling constants g_k defined at renormalization scale μ and the corresponding beta functions $\beta_k(g_k)$ are given by $\beta_k=\mu\partial g_k/\partial\mu$. This equation expresses the independence of physical correlation functions on the renormalization scale μ. When dimensional parameters such as masses are present, a mass-independent renormalization scheme is required in order to be able to trivially generalize the Callan-Symanzik equation.

3.2. Development of the renormalization group: from scaling to holography

Wilson was the first to realize that the way fluctuations are summed over in the perturbative renormalization procedure developed for quantum electrodynamics is not appropriate since fluctuations at all scales are treated on the same footing in Feynman diagrams. This only works when the expansion parameter for the Feynman diagram expansion is small so that there is only a small coupling between fluctuations at different scales. As Wilson stated: " This procedure is only safely applicable when the basic physics is already well understood." Wilson thus had to idea to organize the summation over fluctuations in a better way, based on the underlying idea that fluctuations at different scales are locally coupled: *i.e.* the behavior of fluctuations at one scale is only strongly influenced by fluctuations at nearby scales [189]. This cascade picture has two principal features. Firstly, the scaling feature expresses that the behavior of fluctuations at intermediate scales (far from the ultraviolet or infrared scale) should be identical, up to a scale transformation. Secondly, fluctuations can add up coherently resulting in an amplification or deamplification of certain effects as the cascade develops. Deamplification washes out the details of the fundamental theory at the ultraviolet scale and underlies the *universality hypothesis*. When Wilson, who was working in high energy field theory, learned about the theory of critical phenomena, he discovered that he had been scooped by Kadanoff, who applied a real space version of the renormalization group argument to the Ising model [96] in order to explain the scaling relations, as discussed in the context of quantum critical points in Subsection 2.3. Kadanoff assumed that a block of spins should behave like a single spin, only interacting with the nearest neighbor blocks but with modified coupling constants (temperature and magnetic field strength). He did not construct the actual transformation. This assumption was on itself sufficient to explain the scaling relations that were proposed by Essam and Fisher [93] and by Widom [94, 95].

To actually compute the scaling dimensions, an explicit construction of the renormaliza-

tion group transformation is required. In contrast to the common approach in relativistic field theories and to Kadanoff's approach, Wilson learned that the effective action generated by the renormalization group transform does not necessarily need to be identical, but rather that a complicated effective action containing infinitely many interactions —and thus infinitely many coupling constants— can arise, without this being a disaster [190]. This major breakthrough paved the way for the interpretation of the renormalization group as a flow in the space of all possible Hamiltonians. Wilson reanalyzed Kadanoff's real-space renormalization group transformation and was able to recast it in a differential form [191], which he then used to show that the critical point corresponds to a fixed point of the differential equations and that critical exponents follow from a linearization of the differential equations around the critical point. He visualized this flow for an extended toy model and discussed the effect of irrelevant variables, which were just ignored by Kadanoff. In the second paper in this series [192], Wilson used a phase-space analysis[9] to study the Landau-Ginzburg model —the effective field theory of a symmetry breaking phase transition— in three dimensions for the Ising-like case ($\mathbb{Z}_2$ breaking). The resulting renormalization iterations could numerically be solved in order to obtain estimates for the critical exponents that deviate from the mean-field prediction (the classical solution of the Landau-Ginzburg model) and agree impressively well with known estimates. Wilson also realized that the non-trivial critical point of the Landau-Ginzburg model describing the symmetry breaking phase transition becomes trivial (*i.e.* the fixed point is a quadratic theory and the mean-field solution becomes exact) for dimensions $d \geq 4$. Soon after, he and Fisher analytically studied the critical points of the Landau-Ginzburg model in $d = 4 - \epsilon$ dimensions as a perturbative expansion in ϵ, and obtained the critical exponents for the Ising-like and the XY-like case ($\mathbb{Z}_2$ breaking and O(2) breaking respectively) [193]. Using his background in field theory, Wilson then constructed a diagrammatic approach to facilitate these integrations and he computed the ϵ expansion of general Heisenberg models (O(m) breaking for arbitrary m) [194]. These papers gave light to the *momentum-shell renormalization group*, where fluctuations with momenta $\vec{p}$ satisfying $\Lambda/b < |\vec{p}| < \Lambda$ are (approximately) integrated out, followed by a scaling $\vec{p} \mapsto \vec{p}\,' = b\,\vec{p}$ to bring the maximal momentum back to $||\vec{p}\,'|| = \Lambda$ [10]. This formalism was further strengthened by Wegner [195, 196, 197] and formed the basis for some high-precision computations of the critical exponents for $d = 3$ ($\epsilon = 1$) using expansions to high orders in ϵ [198].

For $d = 2$ ($\epsilon = 2$), the ϵ expansion is no longer valid and another expansion for $d = 2 + \epsilon$ had to be developed [199, 200, 201]. Real-space approaches were also being explored: transformation schemes for integrating out blocks of spins by replacing them with effective spins —a step often called *decimation* or *coarse graining*— were first constructed in [202, 203, 204, 189] for the Ising model and one was able to very accurately reproduce the exact Onsager solution [205]. Continuous symmetries cannot be broken for $d = 2$, but there is the possibility of the infinite order phase transition called the Berezin-

[9] Wilson devised a kind of wavelet that was maximally localized both in momentum-space and in real-space to the extent allowed by Heisenberg's uncertainty relation $\Delta x_i \Delta p_j \leq \delta_{i,j}/2$.

[10] From hereon, the symbol Λ is exclusively reserved for the momentum cutoff.

skiĭ-Kosterlitz-Thouless transition that separates a phase with exponentially decaying correlation funtions from a phase with algebraically decaying correlation functions with a temperature-dependent power [206, 207, 208, 209]. No true long-range order develops in the low-temperature phase, but the high-temperature phase is set apart because entropy considerations allow the spontaneous formation of vortices (*i.e.* topologically non-trivial configurations[11]).

It was noted by Wegner and Houghton [210] that the renormalization group transformation law of the ϵ expansion of Wilson and Fisher can be computed exactly by integrating out only an infinitesimally small momentum-shell of fluctuations ($b = \mathrm{e}^{\mathrm{d}s}$ with $\mathrm{d}s \to 0$). By iterating this process, an exact renormalization group in differential form can be constructed. A similar *exact renormalization group* was proposed even earlier by Wilson, although it was only published in [36]. Wilson proposed to use a smooth cutoff rather than the sharp cutoff of Wegner and Houghton, as this last choice results in strongly non-local interactions in position space. Polchinski [211] used Wilson's construction to prove the perturbative renormalizability of the four-dimensional $\lambda\phi^4$ theory to all orders, without having to resort to complicated techniques that are required when using perturbative renormalization (*e.g.* superficial degrees of divergence, topology of graphs, ...). While it is often impossible to integrate the exact renormalization group equations, it is possible to construct approximation schemes that are non-perturbative in nature, hence the name *non-perturbative renormalization group equations*. Initially, the non-perturbative renormalization group was not often used, because of the success of perturbation theory for both the $\mathrm{O}(m)$ models for critical phenomena and for the relevant field theories for particle physics, and because the non-perturbative approximations in the non-perturbative renormalization group seemed uncontrolled. However, perturbative expansions do not converge and are asymptotic series at best. They require resummation methods which often fail to produce converged results. Results obtained with the non-perturbative renormalization group have good convergence properties (see [212] and references therein) and eventually the non-perturbative renormalization group became adopted in particle physics. However, the renormalized action S_s —the *Wilsonian effective action* for degrees of freedom below scale $\mathrm{e}^{-s}\Lambda$— that appears in the Wilson-Polchinski approach after having integrated out all modes between scale $\mathrm{e}^{-s}\Lambda$ and cutoff scale Λ, is a highly abstract object. It does not contain all the information in the initial theory, as it does not allow to compute correlation functions of the degrees of freedom that have been integrated out. A different formulation under the name of *effective average action method* was introduce by Wetterlich [213]. Rather than computing a Wilsonian action for the remaining degrees of freedom, the central object is now the vertex function or Legendre effective action Γ (also called the Gibbs free energy in statistical physics) of the degrees of freedom that have been integrated out. Hence, the free energy Γ_s at some scale s is obtained by applying an *infrared* cutoff $\Lambda e^{-s} \leq ||\vec{p}||$ to the computation of the free energy. All information on the model (fixed points,

[11] Note that this phenomenon is totally unrelated to a topologically ordered quantum phase, where correlations still decay exponentially away from the critical point.

correlation functions, ...) is contained within this single object Γ_s.

The latest development in renormalization group theory is given by the insight that the renormalization scale s can be interpreted as an additional dimension of a holographic nature. Vice versa, it was soon realized that in the particular example of the AdS/CFT correspondence, the additional dimension into the bulk of the anti-de Sitter space can indeed be interpreted as a renormalization scale [214]. This has resulted into the formulation of the *holographic renormalization group* [215, 216, 217, 218], where the equations of motion for the fields living in the anti-de Sitter bulk correspond to the renormalization group equations (*i.e.* Callan-Symanzik equations) for the boundary theory [219].

3.3. Renormalization group flow: critical phenomena and field theories

Different formulations of the renormalization group exist. For example, the exact renormalization group can be represented as a functional differential equation or as a functional integral for the Wilsonian action S_s, or as an infinite set of differential equations in the coupling constants. This last formulation, thanks to Wilson [36], might not be the best formulation for practical computations but is the most intuitive one. Let $S[\phi_\alpha; \boldsymbol{K}, \Lambda]$ represent a general family of field theory actions in d spatial dimensions with a built in regularization scheme associated to the ultraviolet scale Λ, given in terms of momentum or energy units. The regularization can be in terms of a hard or soft momentum cutoff around Λ. The dimensional parameter Λ can be used to map all coupling constants in the action to the set of dimensionless parameters $\boldsymbol{K} \in \mathscr{K}$. The space $\mathscr{K}$ of coupling constants is assumed to correspond to all short-range interaction terms that respect a certain group of symmetry transformations. 'Short-range' interactions have an interaction length of the order of the cutoff. Long-range interactions are excluded as they interfere with the qualitative ideas about critical behavior: *e.g.* the universality hypothesis is known to be false if long range interactions are permitted [220]. The renormalization group flow is now interpreted as a flow of the set of coupling constants $\boldsymbol{K}$ in the space $\mathscr{K}$ as a function of the renormalization group parameter s. Let us now describe the qualitative features that will be used in the remainder of this dissertation.

Integrating out degrees of freedom maps the initial action $S[\phi_\alpha; \boldsymbol{K}_0, \Lambda]$ to a new action $S[\phi'_\alpha; \boldsymbol{K}', \mathrm{e}^{-s}\Lambda]$, where ϕ'_α represents the new set of fields that remain after the integration, *i.e.* $\phi'_\alpha(\vec{p}') = \phi_\alpha(\vec{p}')\theta(|\vec{p}'| < \mathrm{e}^{-s}\Lambda)$ in the case of a hard cutoff. The new action $S[\phi'_\alpha; \boldsymbol{K}', \mathrm{e}^{-s}\Lambda]$ produces the same result as the action $S[\phi_\alpha; \boldsymbol{K}, \Lambda]$ for observables sufficiently far below the cutoff $\mathrm{e}^{-s}\Lambda$. In particular, they have the same correlation length ξ_c. In order to obtain fixed point behavior, two additional steps are necessary. Firstly, a scaling transformation with scale parameter $b = \mathrm{e}^s$ restores the cutoff at its original value Λ. Alternatively, we can convert all dimensional observables to dimensionless values using the cutoff scale. Hence, the dimensionless set $\boldsymbol{K}$ uniquely determines a

dimensionless correlation length $\tilde{\xi} = \xi_c \Lambda$, which can clearly not depend on the only dimensional parameter Λ. Similarly, the parameter set $\boldsymbol{K}'$ corresponds to a dimensionless correlation length $\tilde{\xi}' = \tilde{\xi}_c \Lambda / b = \tilde{\xi} / b$. Working with dimensionless parameters thus eliminates the need to apply the additional scale transformation. The parameter space $\mathscr{K}$ can be divided into surfaces of parameter configurations resulting in dimensionless correlation lengths $\tilde{\xi}$, $\forall 0 \leq \tilde{\xi} \leq +\infty$.

Secondly, the path integral $Z = \int [\mathcal{D}\phi] \exp(-S[\phi^\alpha; \boldsymbol{K}, \lambda])$ has a general reparametrization invariance in the fields ϕ_α, that induces a 'gauge invariance' in the coupling constants $\boldsymbol{K}$: different 'gauge-equivalent' values of the coupling constants define the same theory. In order to detect a fixed point $\boldsymbol{K}^*$ of the renormalization group, it is necessary to fix this gauge freedom. A (partial) gauge fixing is possible by *e.g.* bringing the kinetic part of the action in standard form, for which we rescale the fields as $\phi'_\alpha = \zeta_\alpha(\phi_\beta; s)$. Inserting this scaling law in $S[\phi'_\alpha; \boldsymbol{K}', \mathrm{e}^{-s}\Lambda]$, we can write $S[\zeta_\alpha(\phi_\beta; s); \boldsymbol{K}', \mathrm{e}^{-s}\Lambda] = S[\phi_\alpha; \boldsymbol{K}(s), \mathrm{e}^{-s}\Lambda]$. The renormalization group flow is now captured by a differential equation, the *renormalization group equation*, given by

$$\frac{\mathrm{d}\boldsymbol{K}}{\mathrm{d}s}(s) = \boldsymbol{R}(\boldsymbol{K}(s)) \tag{1.82}$$

with $\boldsymbol{R}$ the renormalization group transformation law. Note that the transformation law does not depend explicitly on s as a consequence of the self-similarity of the process. If the initial theory has a dimensionless correlation length $\tilde{\xi}(0) = \tilde{\xi}_0$, then the set of parameters $\boldsymbol{K}(s)$ lies somewhere in the surface corresponding to $\tilde{\xi}(s) = \mathrm{e}^{-s}\tilde{\xi}_0$. The renormalization group equation allows to transform the complete space $\mathscr{K}$ into a subspace $\mathscr{K}(s) \subset \mathscr{K}$ for any $s > 0$. While a differential equation is invertible in principle, an arbitrary action $S[\phi_\alpha; \boldsymbol{K}, \Lambda]$ corresponding to a point $\boldsymbol{K} \in \mathscr{K}$ that is not in $\mathscr{K}(s)$ will be mapped to a Hamiltonian with long-range interactions if it is integrated over a time $-s$. The resulting Hamiltonian can thus not be described by a set of parameters in $\mathscr{K}$.

For $s \to \infty$, it is assumed that $\boldsymbol{K}(s)$ converges to some fixed point $\boldsymbol{K}^*$. Fixed points $\boldsymbol{K}^*$ correspond to $\boldsymbol{R}(\boldsymbol{K}^*) = 0$ and have either $\xi_c = 0$ or $\xi_c = +\infty$. While a different limiting behavior is possible in principle, convergence to fixed points is generally assumed. For any starting point $\boldsymbol{K}_0$ corresponding to $\tilde{\xi}_0 < +\infty$, the renormalization group trajectory $\boldsymbol{K}(t)$ has to converge to a fixed point with $\tilde{\xi}^* = 0$. Figure 1.3 depicts a very simple sketch of the parameter space $\mathscr{K}$. A particular physical model corresponds to the surface $\boldsymbol{K}_0(\boldsymbol{\lambda})$ where $\boldsymbol{\lambda}$ describes the physically accessible range of parameters. The renormalization group trajectories originating from these points leave this subspace, and do thus not correspond to physically accessible transformations. As the physical parameters $\boldsymbol{\lambda}$ vary across the value $\boldsymbol{\lambda}_c$, the renormalization group trajectory converge to two distinct fixed points $\boldsymbol{K}^*_a$ and $\boldsymbol{K}^*_b$, indicating a phase transition from a phase a to some phase b. Precisely at the configuration $\boldsymbol{\lambda}_c$, the correlation length in the physical model diverges, indicating the presence of a critical point. The renormalization group trajectory starting in $\boldsymbol{K}_0(\boldsymbol{\lambda}_c)$ converges to the fixed point $\boldsymbol{K}^*_c$. The low-energy behavior of the model is

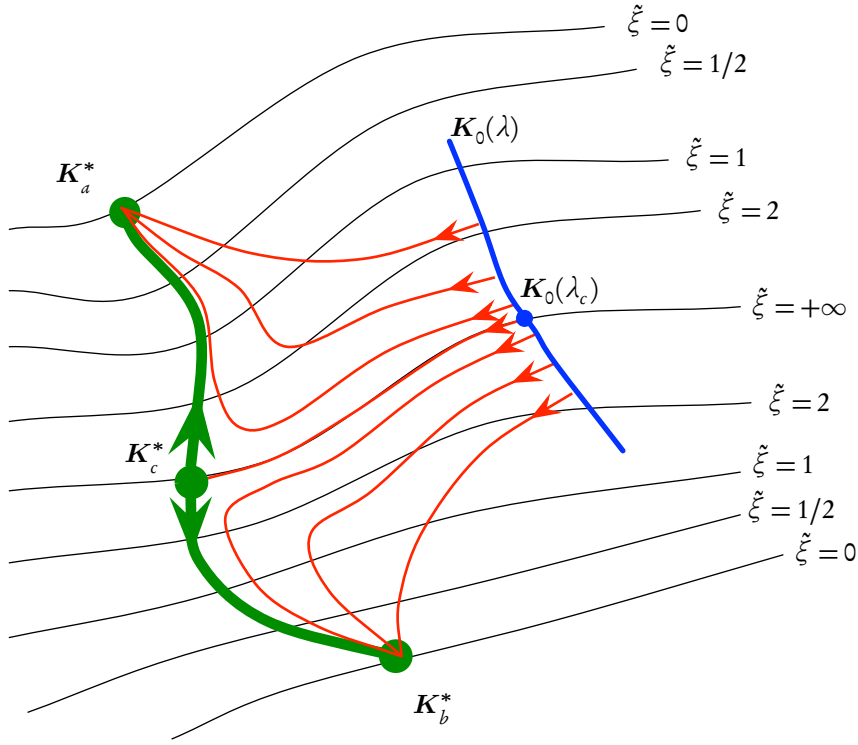

Figure 1.3: Space $\mathscr{K}$ of dimensionless coupling constants with indication of surfaces of constant $\tilde{\xi}$ (black lines), some renormalization group trajectories $\boldsymbol{K}(t)$ (red lines) originating from physically accessible parameter configurations $\boldsymbol{K}_0(\lambda)$ (blue line), two fixed points $\boldsymbol{K}_a^*$ and $\boldsymbol{K}_b^*$ with $\tilde{\xi}_{a,b}^*=0$ and one fixed point $\boldsymbol{K}_c^*$ with $\tilde{\xi}_c^*=+\infty$ (green dots).

determined by the corresponding fixed points $\boldsymbol{K}_a^*$, $\boldsymbol{K}_b^*$ or $\boldsymbol{K}_c^*$. All configurations $\boldsymbol{\lambda}$ to one side of the critical point correspond to the same phase and the same low-energy physics. Two points $\boldsymbol{\lambda}$ and $\boldsymbol{\lambda}'$ close to the critical point (thus with very large correlation length $\tilde{\xi}_0$) remain close to the surface $\tilde{\xi}=+\infty$ and thus close to each other as long as $\mathrm{e}^{-t}\tilde{\xi}_0 \gg 1$. But if they are at different sides of the critical point $\boldsymbol{\lambda}_c$, they will eventually flow away from each other and end up in different fixed points.

Different physical models $\boldsymbol{K}_0(\lambda)$ and $\widetilde{\boldsymbol{K}}_0(\tilde{\lambda})$ that are described in the same parameter space $\mathscr{K}$ can have critical points λ_c and $\tilde{\lambda}_c$ such that the renormalization group trajectories starting in $\boldsymbol{K}_0(\lambda_c)$ and $\widetilde{\boldsymbol{K}}_0(\tilde{\lambda}_c)$ end up at the same fixed point $\boldsymbol{K}_c^*$. Their low energy physics are then equivalent, which explains the universality hypothesis. If the renormalization group transformation $\boldsymbol{R}$ is analytic near $\boldsymbol{K}_c^*$, we can linearize it in order to obtain $\boldsymbol{R}\left(\boldsymbol{K}_c^*+\epsilon\boldsymbol{K}\right)=\epsilon R_c^*\cdot\boldsymbol{K}$. The matrix R_c^* can be diagonalized[12]

[12] This is an assumption, as R_c^* is not symmetric. It can have complex eigenvalues (in conjugate pairs) resulting in a spiral-like renormalization group flow around the fixed point, or it can only have a Jordan normal form.

with eigenvalues $d^{(i)}$ and corresponding eigenvectors $\boldsymbol{K}^{(i)}$ that constitute a complete set[13]. A renormalization group trajectory starting at $\boldsymbol{K}_0 = \boldsymbol{K}_c^* + \epsilon \sum_i c^{(i)} \boldsymbol{K}^{(i)}$ flows as $\boldsymbol{K}(t) = \boldsymbol{K}_c^* + \epsilon \sum_i c^{(i)} \mathrm{e}^{d^{(i)} t} \boldsymbol{K}^{(i)}$. Since any coupling constant K_j is associated to an 'operator' O_j in the action $S[\phi_\alpha, \boldsymbol{K}, \Lambda]$, we can define scaling operators $O^{(i)} = \sum_j K_j^{(i)} O_j$ for which $d^{(i)}$ is the scaling dimension. In the action S, the scaling operators $O^{(i)}$ contain local combinations of the field operators ϕ_α and its derivatives, which are integrated over the complete spacetime: $O^{(i)} = \int \mathrm{d}\tau \int \mathrm{d}^d x \, o^{(i)}(x,\tau)$ where $o^{(i)}(x,\tau)$ is combination of $\phi_\alpha(x',\tau')$ and its derivatives with $\|(x,\tau) - (x',\tau')\| \lesssim \mathcal{O}(\Lambda^{-1})$. Typically then, the local operators $o^{(i)}(x,\tau)$ are in itself scaling operators and can be associated to true local operators $\hat{o}^{(i)}(x)$ acting on the Hilbert space of the problem. One particular example of scaling operators are the field operators ϕ_α: the field rescaling $\phi'_\alpha = \zeta_\alpha(\phi_\beta; s)$ is for an infinitesimal renormalization step ds given by $\zeta_\alpha(\phi_\beta; \mathrm{d}s) = (\delta_{\alpha,\beta} + \mathrm{d}s [d_\phi]_{\alpha,\beta}) \phi_\beta$. By choosing the fields ϕ_α such that $[d_\phi]$ is diagonal, we obtain the scaling dimension of field ϕ_α as the eigenvalue $[d_\phi]_{\alpha,\alpha} = d^{(\phi_\alpha)}$.

Scaling operators $O^{(i)}$ with $d^{(i)} > 0$ are relevant, they correspond to directions in which the renormalization group flow moves away from the fixed point. They define the scaling functions that were defined in Subsection 2.3. Scaling operators $O^{(i)}$ with $d^{(i)} < 0$ are called irrelevant and determine the small corrections to the scaling laws away from the critical point. Finally, if $d^{(i)} = 0$, the corresponding scaling operators are marginal and a higher order expansion is required to determine whether the renormalization group flow moves towards (marginally irrelevant) or away from (marginally relevant) the fixed point along this direction [196]. Note that the scaling dimension of an operator decreases as the number of spatial dimensions d is increased. Consequently, an upper critical dimension d_c is associated to every relevant operator, such that this operator becomes marginal at $d = d_c$ and irrelevant for $d > d_c$. In addition to scaling operators, there are also redundant operators, which follow from the invariance of the physical model under *e.g.* field reparametrizations. The scaling fields of physical observables do not depend on these redundant operators and the associated eigenvalues, which can be non-universal.

We can conclude this subsection by discussing the relation with renormalizable quantum field theories. Renormalizable interactions correspond to marginal operators, super-renormalizable interactions to relevant operators and non-renormalizable interactions to irrelevant operators. Renormalization is then equivalent to starting with a bare action $S_0(\phi_\alpha; \boldsymbol{\lambda}_\Lambda, \Lambda) = S(\phi_\alpha; \boldsymbol{K}_0(\boldsymbol{\lambda}_\Lambda), \Lambda)$ with only a few interaction terms and associated bare coupling constants $\boldsymbol{\lambda}_\Lambda$ at cutoff scale Λ, and taking the limit $\Lambda \to \infty$ in such a way that the low energy physics remains unchanged. Since the renormalization group transformation decreases the cutoff, taking this limit boils down to inverting the renormalization group to $s = -\infty$. For general points $\boldsymbol{K} \in \mathscr{K}$, this operation is impossible, so that a special fine tuning is required. In order to obtain a fixed physical correlation length

[13] This too is an assumption, since the set of parameters is infinite dimensional and it is not guaranteed that the eigenvectors of R_c^* constitute a complete set.

ξ_c, the bare action (*i.e.* its coupling constants $\boldsymbol{K}_0(\boldsymbol{\lambda}_\Lambda)$) has to lie in the surface with dimensionless coupling constant $\tilde{\xi} = \xi_c \Lambda$. For $\Lambda \to \infty$, the bare action has to approach the critical surface with $\tilde{\xi} = \infty$, so that the bare coupling constants have to be tuned to a critical value $\lim_{\Lambda\to\infty} \boldsymbol{\lambda}_\Lambda = \boldsymbol{\lambda}_{\text{crit}}$. In this limit, the renormalization group trajectory of the bare action decomposes into two parts: the renormalized coupling constants first evolve along the critical surface until they approach an ultraviolet (unstable) fixed point $\boldsymbol{K}_c^*$ and then they move away along the line or surface connecting this ultraviolet fixed point with an infrared (stable) fixed point. This limit represents a singular point of the renormalization group differential equations, since the initial conditions no longer uniquely determine the trajectory. Instead, the theory is now determined by the renormalization prescriptions at an arbitrary observational scale μ. The number of conditions required to fix the theory is given by the dimensionality of the surface from the ultraviolet fixed point to the infrared fixed point, or thus by the number of relevant directions. The renormalized theory lives in this surface and is completely determined by fixing the relevant couplings, *i.e.* by specifying renormalized couplings $\boldsymbol{\lambda}_\mu$ at scale μ. As we increase the observational scale μ, we run backwards along the trajectory towards the ultraviolet fixed point. Note that the renormalized theory contains interactions that were not initially present in $S_0(\phi_\alpha; \boldsymbol{\lambda}_\Lambda, \Lambda)$, but these are completely fixed by specifying $\boldsymbol{\lambda}_\Lambda$ as function of $\boldsymbol{\lambda}_\mu$, μ and Λ. If on the other hand we try to fix an irrelevant interaction, we take the renormalized theory away from the surface between the ultraviolet and the infrared fixed point. The limit $\Lambda \to \infty$ of this theory cannot correspond to the submanifold spanned by $S_0(\phi_\alpha; \boldsymbol{\lambda}_\Lambda, \Lambda)$ and requires in general infinitely many other interactions to be introduced and corresponding coupling constants to be fixed. The theory then loses its predictive power.

3.4. Numerical real-space renormalization group methods

Not only did Wilson massively contribute to the consistent modern framework of renormalization group theory, he also initiated the use of numerical renormalization group methods to obtain highly non-trivial information about models that are not exactly solvable. Wilson's first attempt in [221] failed for the particular model under study, but when he applied a similar approach to the Kondo model, he was able to obtain very accurate information [189]. The Kondo model is a basic model to capture the effect of a magnetic impurity to a conduction band electrons and is described by the Hamiltonian (in dimensionless units)

$$\hat{H}_{\text{K}} = \int_{-1}^{+1} \mathrm{d}k \sum_s \epsilon_k \hat{a}^\dagger_{k,s} \hat{a}_{k,s} - J \sum_{s,s'} \left(\hat{A}^\dagger_s \vec{\sigma}_{s,s'} \hat{A}_{s'} \right) \cdot \hat{\vec{S}} \tag{1.83}$$

with $\vec{a}_{k,s}$ the annihilator of a conduction electron with momentum k and spin s, $\vec{\sigma}$ the vector of Pauli-matrices, $\hat{\vec{S}}$ the quantum spin of the impurity, and $\hat{A}_s$ the real-space

annihilator of a conduction electron with spin s at position zero:

$$\hat{A}_{s'} = \int_{-1}^{+1} \mathrm{d}k\, \hat{a}_{k,s}. \tag{1.84}$$

The momentum index k is scalar, since this model only describes the s-wave electrons. Higher partial waves do not couple to the impurity. Wilson discretized the conduction band into energy levels $\pm\Lambda^{-n}$ with exponential scaling. By only retaining a single electron per energy level, he obtained a good approximation for $\hat{H}_{\mathrm{K}}$ in terms of the lattice model

$$\hat{H} = \sum_{n=0}^{+\infty} \sum_{s} \Lambda^{-n/2} \left(\hat{f}^{\dagger}_{n,s} \hat{f}_{n+1,s} + \hat{f}^{\dagger}_{n+1,s} \hat{f}_{n,s} \right) - \hat{J} \sum_{s,s'} \left(\hat{f}^{\dagger}_{0,s} \vec{\sigma}_{s,s'} \hat{f}_{0,s} \right) \cdot \hat{\vec{S}}. \tag{1.85}$$

If we now define the Hamiltonian of a block of L sites by restricting the sum over n to values $n = 0, \ldots, L$, a renormalization group equation is obtained as

$$\hat{H}^{(L+1)} = \sum_{s} \left(\hat{f}^{\dagger}_{L,s} \hat{f}_{L+1,s} + \hat{f}^{\dagger}_{L+1,s} \hat{f}_{L,s} \right) + \Lambda^{1/2} \hat{H}^{(L)}. \tag{1.86}$$

A fixed point is obtained when the lowest eigenvalues of $\hat{H}_L$ become independent of L. Rather than computing these exactly, which is computationally intractable except for very small values of L, Wilson devised the following renormalization group procedure to iteratively increase L, starting from a small value where exact diagonalization is still possible:

1. Diagonalize $\hat{H}^{(L)}$ numerically.

2. Reduce the Hilbert space $\mathbb{H}^{(L)}$ to the linear span of the eigenvectors corresponding to the D lowest eigenvalues of $\hat{H}^{(L)}$: $\widetilde{\mathbb{H}}^{(L)} = \mathrm{span}\{|\Psi^{(L)}_{\alpha}\rangle, \alpha = 1, \ldots, D\}$. Project all relevant operators $\hat{O} \in \mathbb{L}(\mathbb{H}^{(L)})$ to $D \times D$-dimensional operators $\hat{O}' = \hat{P}_D \hat{O} \hat{P}^{\dagger}_D$ on $\widetilde{\mathbb{H}}^{(L)}$.

3. Add a site using Eq. (1.86) in the tensor product space $\mathbb{H}^{(L+1)} = \widetilde{\mathbb{H}}^{(L)} \otimes \mathbb{H}_{\mathrm{site}}$.

4. Set $L \to L + 1$ and reiterate.

With two spin-components per electron, $\dim \mathbb{H}_{\mathrm{site}} = 4$ and the dimension of the Hamiltonian $\hat{H}_L$ that has to be diagonalized never exceeds $4D$. The error in each step can be shown to be $\Lambda^{-1/2}$. In addition, the error resulting from the discretization of the conduction band is of order $(1 - \Lambda^{-1})$ and the value of Λ should be chosen close to $\Lambda = 1$. At this point, errors from reducing the Hilbert space $\mathbb{H}_L$ grow large and the renormalization group procedure no longer converges. However, by starting from $\Lambda \approx 2$ and extrapolating results for $\Lambda \to 1$, Wilson was able to obtain very accurate estimates for the expectation value of relevant operators with respect to the ground state.

The key to the success of Wilson's numerical renormalization group procedure is the exponential decrease of the interaction strength along the chain, which is a consequence of the sites representing spherical shells at increasing distance beyond the magnetic impurity. When applied to one-dimensional quantum lattice models with equally strong interactions between every two nearest neighbors, Wilson's real-space renormalization group procedure fails. While the basic ingredient —namely that configurations corresponding to high local energies should be irrelevant for the description of low-energy states of the total lattice— is still valid, the way to reduce the local Hilbert space should be modified. At an informal lecture in 1986, Wilson did himself isolate the problem for a very simple toy model describing a single particle hopping on a lattice of finite size (*i.e.* a lattice version of a particle in a box), corresponding to the Hamiltonian

$$\hat{H}^{(L)} = -\sum_{n=1}^{L-1} (|n\rangle\langle n+1| + |n+1\rangle\langle n|) - 2\sum_{n=1}^{L} |n\rangle\langle n|. \tag{1.87}$$

Since the dimension of the single particle Hilbert space $\mathbb{H}^{(L)}$ now only increases linearly in L, a single renormalization step should double the length L. Since all lowest eigenstates of $\hat{H}^{(L)}$ have nodes at the boundaries, so will any state in the reduced Hilbert space $\widetilde{\mathbb{H}}^{(L)}$. On a lattice of size $2L$, all states in the tensor product $\widetilde{\mathbb{H}}^{(L)} \otimes \widetilde{\mathbb{H}}^{(L)}$ have a node in the middle, whereas the exact ground state of $\hat{H}^{(2L)}$ reaches a maximum in the middle and is thus not well represented in $\widetilde{\mathbb{H}}^{(L)} \otimes \widetilde{\mathbb{H}}^{(L)}$. For this toy model, a simple solution is obtained by adding to $\widetilde{\mathbb{H}}^{(L)}$ states with different boundary conditions [222]. These boundary conditions can be specified explicitly, or implicitly by embedding the subsystem into a larger superblock of $L' > L$ sites. The reduced Hilbert space $\widetilde{\mathbb{H}}^{(L)}$ is then obtained as the linear span of the restriction of the lowest lying excited states of $\hat{H}^{(L')}$ onto the L sites under consideration. While it was at first not clear how this approach could be generalized to ordinary lattice models with interactions in the full Hilbert space $\mathbb{H}^{(L)}$ (whose dimension scales exponentially in L), it is the idea of the superblock that eventually provided the answer.

In 1992, White introduced the *density matrix renormalization group* [223, 224]. The isolated smaller subsystems that were considered by Wilson are not representative for the total system, because they interact with their environment, hence creating entanglement. This can be modeled by considering a superblock of $2L$ sites: the left L sites are called the system block S, the right L sites the environment block E. Unlike in the previous case, the ground state of the Hamiltonian $\hat{H}^{(S\cup E)}$ of the superblock cannot be projected to a single state on the system block, but requires many different states for its description. However, using the Schmidt decomposition from the previous section and its relation to the important resource that is entanglement, it goes without saying that the most important states to keep in a reduced Hilbert space $\mathbb{H}'_L$ are the Schmidt vectors corresponding to the largest Schmidt coefficients. This observation results in the following renormalization algorithm:

1. Having a system S of L sites with (reduced) Hilbert space $\widetilde{\mathbb{H}}^{(S)} = \text{span}\{|\Psi_\alpha^{(S)}\rangle, \alpha =$

$1,\ldots,D\}$, add a site to obtain the enlarged system S' with Hilbert space $\mathbb{H}^{(S')} = \widetilde{\mathbb{H}}^{(S)} \otimes \mathbb{H}_{\text{site}} = \text{span}\{|\Psi_\alpha^{(S)}\rangle \otimes |s\rangle ; \alpha = 1,\ldots,D; s = 1,\ldots,d\}$. Similarly, define a new environment E' by adding a site to the existing environment E of L sites with reduced Hilbert space $\widetilde{\mathbb{H}}^{(E)} = \text{span}\{|\Psi_\alpha^{(E)}\rangle, \alpha = 1,\ldots,D\}$.

2. Define the superblock $S' \cup E'$, construct the Hamiltonian $\hat{H}^{(S'\cup E')}$ and determine its ground state $|\Psi^{(S'\cup E')}\rangle \in \mathbb{H}^{(S')} \otimes \mathbb{H}^{(E')}$, where $\dim \mathbb{H}^{(S')} = \dim \mathbb{H}^{(E')} = Dd$.

3. Determine the Schmidt decomposition $|\Psi^{(S'\cup E')}\rangle = \sum_{\alpha=1}^{dD} \lambda_\alpha |\Psi_\alpha^{(S')}\rangle |\Psi_\alpha^{(E')}\rangle$, where the Schmidt coefficients λ_α are ordered in decreasing order.

4. Define the reduced Hilbert spaces for the system block S' and the environment block E' by retaining only the Schmidt vectors corresponding to the D largest Schmidt coefficients: $\widetilde{\mathbb{H}}^{(S')} = \text{span}\{|\Psi_\alpha^{(S)}\rangle, \alpha = 1,\ldots,D\}$ and $\widetilde{\mathbb{H}}^{(E')} = \text{span}\{|\Psi_\alpha^{(E)}\rangle, \alpha = 1,\ldots,D\}$. Project relevant operators into these reduced Hilbert spaces.

5. Set $S = S'$ and $E = E'$. Reiterate.

This algorithm is called the *infinite size algorithm*, as the lattice steadily grows with two sites per iteration. The resulting ground state can be further improved by applying the following *finite size algorithm*, which requires that the bases $\{|\Psi_\alpha^{(S)}\rangle, \alpha = 1,\ldots,D\}$ and $\{|\Psi_\alpha^{(E)}\rangle, \alpha = 1,\ldots,D\}$ were stored for all sizes of the system block S and environment block E. Now the system S is shrunk by one site and the environment E is enlarged by one site, keeping the total superblock length constant. A new ground state calculation and its Schmidt decomposition redefines the optimal basis for a system block S with $L-1$ sites and an environment block with $L+1$ sites. This process is repeated untill the system S has reached a minimal size where its D dimensional basis spans the complete Hilbert space. Then the system is grown and the environment is shrunk. This whole process defines one sweep of the finite size algorithm. Since this approach is variational, the energy exceptation value monotonically decreases in every step of the sweeping process. Convergence is often obtained after a small number of sweeps. The basis of the Hilbert space $\mathbb{H}^{(S'\cup E')}$ of the superblock is d^2D^2 dimensional, and by exploiting symmetries and using a sparse eigensolver for finding the ground state of $\hat{H}^{(S'\cup E')}$ large values of D (up to $D \approx 10^5$) can be obtained [225, 226]. Soon after, it was realized by Östlund and Rommer [227, 228] that the infinite size algorithm gives rise to a class of variational ansatz states called *matrix product states*, to be discussed in Chapter 3, and that the finite size algorithm is a procedure to optimize over this variational class. The number D of states kept determines the maximal number of non-zero Schmidt values and is thus strongly related to the maximal amount of entanglement in the state. In particular, the entanglement between two halves of arbitrary length L of the chain is limited by $\log D$. For large values of D, this limit is sufficient to determine the ground state energy of gapped systems and critical systems of sufficiently small size to machine precision, thanks to the area law (and the fact that it is only logarithmically violated by critical systems).

3.5. Quantum aspects of the renormalization group

Despite the success of the density matrix renormalization group, it does not constitute a genuine renormalization group transformation: the fixed points are matrix product states with an area law for the entanglement entropy; they are not scale invariant and cannot accurately represent the ground states of critical points in the thermodynamic limit (see Chapter 3). The density matrix renormalization group fails to exploit the behavior of quantum states along the renormalization group flow. Let us now investigate precisely what these quantum aspects of the renormalization group entail. We therefore assume to have at our disposal a renormalization group transformation that applies to quantum states, either by defining a renormalized quantum state as the ground state of a corresponding renormalized Hamiltonian, or by a direct scheme to integrate out short-range fluctuations (see *e.g.* [229]).

Firstly, we can study the evolution of fidelity as function of the renormalization group time s. Let $|\Psi(\boldsymbol{\lambda})\rangle$ and $|\Psi(\boldsymbol{\lambda}')\rangle$ represent the ground states of a Hamiltonian $\hat{H}(\boldsymbol{\lambda})$ at different values $\boldsymbol{\lambda}$ and $\boldsymbol{\lambda}'$ of the coupling constants between which the fidelity is computed. If these states are in the same phase a, both states flow to the same fixed point $|\Psi_a^*\rangle$ at $s \to \infty$. The fidelity $F(s)$ monotonically increases as a function of s. At the fixed point, the fidelity reaches its maximal value $F(+\infty) = F(\Psi_a^*, \Psi_a^*) = 1$. The states are completely indistinguishable. At finite renormalization group times s, short range fluctuations that are still present in the ground states hide the fact that these states are in the same phase and make the two states distinguishable. Contrastingly, if these states were initially in different phases a and b, they flow for $s \to \infty$ to different fixed points $|\Psi_a^*\rangle$ and $|\Psi_b^*\rangle$ respectively. The fidelity $F(s)$ decreases monotonically to reach its minimal value $F(+\infty) = F(\Psi_a^*, \Psi_b^*)$, where the two phases are most distinguishable. At finite renormalization group times s, the short range fluctuations present in the ground states partially hide the distinguishability of the two phases. Due to the orthogonality catastrophe, it is better to rephrase this paragraph in terms of a local fidelity measure, such as the fidelity per site [46].

It is also possible to investigate the properties of a single state $|\Psi\rangle$ under the renormalization group flow, and entanglement turns out to be an interesting quantity to look at. For quantum systems in $d = 1$ spatial dimension, it can be shown that the entanglement entropy of a subsystem of length ℓ decreases monotonically under renormalization group transformations, both for lattice systems [230, 231] and for relativistic field theories [121, 232]. Because of the appearance of the central charge c in the block entanglement entropy near the critical point, this result is inspired by Zamolodchikov's c-theorem, which states that the central charge —a measure for the degrees of freedom in a theory— decreases monotonically under the renormalization group flow. Zamolodchikov's c-theorem is based on the correlation function of the energy-momentum tensor and thus involves the complete Hilbert space. However, the monotonic decrease of the entanglement can be proven independently from the existing c-theorem, and allows to formulate an entropic c-theorem, based entirely on properties of the ground state.

Rather than using the energy momentum correlation function, the central quantity is now the function

$$c(\ell) = \ell \frac{\mathrm{d}S(\ell)}{\mathrm{d}\ell}, \tag{1.88}$$

with $S(\ell) = S^{(\mathscr{A}_\ell)}$ the entropy of a block $\mathscr{A}_\ell$ of length ℓ. Under the renormalization group transformation, this function flows as $c(\ell; s) = c(\mathrm{e}^s \ell)$ and thus converges to $c(\ell; +\infty) = c(\infty)$ for every value of the arugment. For conformal theories, Eq. (1.66) indicates that $c(+\infty)$ is proportional to the conformal charge of the theory. For systems with an area law, $S(\ell)$ saturates to a horizontal asymptote for large values of the argument and $c(\ell, s)$ decreases monotonically to $c(+\infty) = 0$. This monotonic decrease of entanglement is not only present in the global entanglement entropy. There is a fine grained loss of entanglement as expressed by the fact that some density matrix $\hat{\rho}(s_1)$ at a point s_1 along the renormalization group flow is majorized by the same density matrix at a point $s_2 > s_1$: $\hat{\rho}(s_1) \prec \hat{\rho}(s_2)$ [231]. This topic is not further explored in this dissertation. For higher dimensional systems, few analogous results are known. In particular, there is no c-theorem due to the wide range of shapes of two-dimensional subsets and other intrinsic problems [232].

We can now return to the first paragraph of this subsection: the loss of entanglement along the renormalization group flow is not exploited by the density matrix renormalization group. It is therefore not able to accurately capture critical points. A different variational ansatz that does capture the hierarchical structure of quantum fluctuations and of the entanglement created by these fluctuations will be encountered in Chapter 5.

2

VARIATIONAL PRINCIPLE IN QUANTUM MECHANICS

This chapter recapitulates the fundamental methods that will be used in the remainder of this thesis. Firstly, the time-independent variational principle is developed in full detail. Secondly, a time-dependent variational principle is formulated that transforms the time-dependent Schrödinger equation (a linear differential equation) for any quantum system (including many body systems) into a non-linear one-body problem (a set of coupled non-linear differential equations for the variational parameters). In combination with imaginary time evolution, the time-dependent variational principle yields a powerful method to find an optimal solution for the time-independent variational method. The time-dependent variational principle can also be used to study real-time evolution, which is often used to extract information about the dynamic properties of a system. In particular, the third section discusses how a linearization of the time-dependent variational principle equations can provide information about the low-lying excited states of a quantum Hamiltonian. While none of the material in this chapter is new, it constitutes the foundation for the material in the subsequent chapters and is therefore treated in full detail.

Results in this chapter are formulated for general quantum systems that live in a Hilbert space $\mathbb{H}$. The dynamics of this quantum system are described by a Hamiltonian $\hat{H} \in \mathbb{L}(\mathbb{H})$ that can possibly be time-dependent (in the second section). As we are discussing variational methods, we have to define a class of *variational ansatz* states. We introduce the general set of states $|\Psi(\boldsymbol{z})\rangle$, where $\boldsymbol{z}$ denotes a finite or countably infinite set of complex parameters $z^i \in \mathbb{C}$. In principle, we can also deal with a continuous set of parameters — which is required in Chapters 4 and 5 — by replacing derivatives with respect to the parameters z^i by functional derivatives. For the sake of simplicity, we restrict to ordinary derivatives in this chapter. Alternatively, we could say that we are using the DeWitt notation when having a continuous set of parameters. We furthermore assume that any combination of complex numbers $\boldsymbol{z}$ yields a valid state $|\Psi(\boldsymbol{z})\rangle \in \mathbb{H}$, and that the dependence on all parameters z^i is holomorphic. We can then define the *variational manifold* $\mathcal{M}$ as

$$\mathcal{M} = \{|\Psi(\boldsymbol{z})\rangle \mid \forall z^i \in \mathbb{C}, \forall i\} \tag{2.1}$$

We explicitly denote the antiholomorphic character of the linear functional $\langle\Psi(\overline{z})|$, introduce the short-hand notation $\partial_i = \partial\ /\partial z^i$ and use barred indices $\overline{\imath}$ for complex conjugate parameters $\overline{z}^{\overline{\imath}}$, which constitute an independent set of parameters. We also use Einstein's summation convention, unless specified otherwise.

1. Time-independent variational principle

The variational principle is a general name for a number of methods in physics, chemistry and mathematical physics that try to find a particular solution by finding the function or functional that this solution should minimize or —more generally— extremize. Examples include Fermat's principle in optics and the principle of least action in classical mechanics. The quantum mechanical version of the principle of least action is studied in the next section. However, for quantum mechanics, the best known variational principle is the time-indepedent variant, which asserts that for any state $|\Psi\rangle \in \mathbb{H}$, one obtains an energy expectation value that exceeds the ground state energy, *i.e.*

$$E^{(0)} \leq \frac{\langle\Psi|\hat{H}|\Psi\rangle}{\langle\Psi|\Psi\rangle},$$

with $E^{(0)}$ the ground-state energy (lowest eigenvalue) of the Hamiltonian $\hat{H}$. This assertion also applies to the variational ansatz states $|\Psi(z)\rangle \in \mathscr{M}$. If we define the energy function

$$H(\overline{z}, z) = \frac{\langle\Psi(\overline{z})|\hat{H}|\Psi(z)\rangle}{\langle\Psi(\overline{z})|\Psi(z)\rangle}, \tag{2.2}$$

then the variational principle could allow to conclude that the best approximation of the ground state of $\hat{H}$ within the variational class $\mathscr{M}$ can be found by looking for the set of the parameters $z^\star$ that minimize the energy function $H(\overline{z}, z)$. An optimum $z^\star$ is thus characterized by the set of equations

$$\begin{cases} \partial_i H(\overline{z}^\star, z^\star) = 0, \\ \partial_{\overline{\imath}} H(\overline{z}^\star, z^\star) = 0. \end{cases} \tag{2.3}$$

However, this result should be used with caution. There is no unique definition of "the best approximation" of a state, and an approximation that has the lowest ground state energy can produce an incorrect description of other physical quantities, as we discuss at the end of this section.

This version of the variational principle is not restricted to finding approximations of ground states of quantum Hamiltonians $\hat{H}$. By using an ansatz state that is orthogonal to the ground state (or an approximation thereof) one can try to construct approximations for low-lying excited states of the Hamiltonian. (Single-particle) quantum mechanics is

just a special case of a general class of boundary value problems with Sturm-Liouville operators, to which the variational method can be applied. One particular example of ansatz states that has proven to be very succesfull for this class of problems is the expansion into a finite basis $\{|\Psi_i\rangle, i = 1,2,\ldots,I\}$, such that $|\Psi(\boldsymbol{z})\rangle = z^i |\Psi_i\rangle$. The variational manifold is then an I-dimensional vector space

$$\mathscr{M} = \text{span}\{|\Psi_i\rangle, i = 1,2,\ldots,I\}.$$

The resulting approach is known as the Rayleigh-Ritz method [233, 234]. Applying Eq. (2.3) learns that

$$H_\Psi \boldsymbol{z} = E N_\Psi \boldsymbol{z} \quad \text{with} \quad [H_\Psi]_{\bar{\imath},j} = \langle \Psi_{\bar{\imath}} | \hat{H} | \Psi_j \rangle \quad \text{and} \quad [N_\Psi]_{\bar{\imath},j} = \langle \Psi_{\bar{\imath}} | \Psi_j \rangle . \tag{2.4}$$

The Rayleigh-Ritz method thus boils down to solving a generalized eigenvalue equation (H_Ψ, N_Ψ). The eigenvalues E give variational estimates for the exact eigenvalues of $\hat{H}$, and the corresponding eigenvectors $\boldsymbol{z}$ provide an estimate $|\Psi(\boldsymbol{z})\rangle$ for the corresponding eigenstate of the $\hat{H}$. The Rayleigh-Ritz method can successfully be applied to single-particle and many body quantum physics alike. A typical approach would be to include in the basis $\{|\Psi_i\rangle\}$ the ground state and lowest lying excited states of a nearby or related Hamiltonian $\hat{H}'$ that can be diagonalized exactly.

However, the variational principle is more generally applicable to any variational manifold $\mathscr{M}$, even when it is not a vector space. Its success depends on the adequacy of the variational manifold to capture the relevant physical effects present in the exact ground state, and on the applicability of an efficient method to find the variational optimum. When applicable, the variational method offers some powerful advantages over alternative approaches. It is free of any sign problem that hinders the application of Monte-Carlo sampling to many interesting problems, and it is perfectly able to reproduce non-perturbative effects. It lies at the basis for a tremendous number of highly successful tools in many-body physics. Examples include self-consistent (mean) field theory (Hartree-Fock [235, 236, 237, 238] or Hartree-Fock-Bogoliubov theory [239]), density functional theory [240, 241], Wilson's numerical renormalization group and finally the density matrix renormalization group, the variational manifold of which will be studied in the next chapter.

Let us conclude this section by evaluating the accuracy that can be obtained by a variational optimum $|\Psi(\boldsymbol{z}^\star)\rangle$. Most of these results are only valid for systems with a small number of degrees of freedom. Since the main interest of this thesis is in extended systems with a large or infinite number of degrees freedom, we return to this question in Section 4. Let now $\{E^{(n)}, |\Psi^{(n)}\rangle, n = 0,1,\ldots\}$ be the set of exact eigenvalues and corresponding normalized eigenvectors of a Hamiltonian $\hat{H}$, with $E^{(0)}$ the ground state energy. Suppose that the best variational approximation within the manifold $\mathscr{M}$ is given by $|\Psi^\star\rangle = |\Psi(\boldsymbol{z}^\star)\rangle$ satisfying

$$|\Psi^\star\rangle = \sqrt{1-\epsilon^2}\,|\Psi^{(0)}\rangle + \epsilon\,|\Psi^\star_{\text{err}}\rangle, \qquad \text{with } \langle \Psi^\star_{\text{err}} | \Psi^\star_{\text{err}} \rangle = 1,\ \langle \Psi^{(0)} | \Psi^\star_{\text{err}} \rangle = 0. \tag{2.5}$$

The state error between the exact solution $|\Psi^{(0)}\rangle$ and the variational approximation $|\Psi^\star\rangle$ is given by

$$\||\Psi^\star\rangle - |\Psi^{(0)}\rangle\| = \sqrt{|\sqrt{1-\epsilon^2}-1|^2+\epsilon^2} = \epsilon + \mathcal{O}(\epsilon^3) \tag{2.6}$$

so that ϵ is a good first order approximation of the state error. For the expectation value of the Hamiltonian we obtain

$$\langle\Psi^\star|\hat{H}|\Psi^\star\rangle - E^{(0)} = \epsilon^2 \langle\Psi^\star_{\text{err}}|\hat{H}|\Psi^\star_{\text{err}}\rangle - \epsilon^2 E^{(0)} = \mathcal{O}(\epsilon^2) \tag{2.7}$$

which implies that the energy is already accurate up to second order in ϵ, provided that $\langle\Psi^\star_{\text{err}}|\hat{H}|\Psi^\star_{\text{err}}\rangle$ is finite. Even with ansätze that are only moderately adequate, a good approximation of the ground state energy can be obtained. The reason for the quadratic convergence in ϵ of the energy expectation value is of course that we are approximating an eigenvector of $\hat{H}$. An error of $\mathcal{O}(\epsilon^2)$ is also obtained for the expectation value $\langle\Psi^\star|\hat{O}|\Psi^\star\rangle - \langle\Psi^{(0)}|\hat{O}|\Psi^{(0)}\rangle$ of any operator that has $|\Psi^{(0)}\rangle$ as eigenvector, since

$$\langle\Psi^\star|\hat{O}|\Psi^\star\rangle - \langle\Psi^{(0)}|\hat{O}|\Psi^{(0)}\rangle = -\epsilon^2 \langle\Psi^{(0)}|\hat{O}|\Psi^{(0)}\rangle + \epsilon^2 \langle\Psi^\star_{\text{err}}|\hat{O}|\Psi^\star_{\text{err}}\rangle = \mathcal{O}(\epsilon^2). \tag{2.8}$$

For all other operators however, the state error ϵ is important, since we obtain

$$\langle\Psi^\star|\hat{O}|\Psi^\star\rangle - \langle\Psi^{(0)}|\hat{O}|\Psi^{(0)}\rangle = 2\epsilon\sqrt{1-\epsilon^2}\Re\left(\langle\Psi^{(0)}|\hat{O}|\Psi^\star_{\text{err}}\rangle\right) + \mathcal{O}(\epsilon^2) = \mathcal{O}(\epsilon). \tag{2.9}$$

This is a bad sign, since we are often more interested in the expectation value of such operators then in the energy: *e.g.* order parameters, correlation functions, … A good convergence of the energy does not necessarily indicate a good convergence of the physically relevant observables. In practice, we would like to be able to estimate ϵ. An estimate of the order of ϵ can be obtained by the error measure $\varepsilon(\overline{z}^\star, z^\star) = \Delta H(\overline{z}^\star, z^\star)$, which satisfies

$$\varepsilon(\overline{z}^\star, z^\star)^2 = \Delta H(\overline{z}^\star, z^\star)^2 = \langle\Psi^\star|(\hat{H} - \langle\Psi^\star|\hat{H}|\Psi^\star\rangle)^2|\Psi^\star\rangle = \epsilon^2 \langle\Psi^\star_{\text{err}}|(\hat{H} - E^{(0)})^2|\Psi^\star_{\text{err}}\rangle. \tag{2.10}$$

In addition, it is easy to prove that if an arbitrary state $|\Psi\rangle$ has energy expectation value $\langle\Psi|\hat{H}|\Psi\rangle$ and $\Delta H^2 = \langle\Psi|\hat{H}^2|\Psi\rangle - \langle\Psi|\hat{H}|\Psi\rangle^2$, then an exact eigenvalue of $\hat{H}$ must exist in the interval $[\langle\Psi|\hat{H}|\Psi\rangle - \Delta H, \langle\Psi|\hat{H}|\Psi\rangle + \Delta H]$. In combination with the variational principle, we thus hope to be able to refine this statement for a good variational approximation $|\Psi^\star\rangle$ to

$$E^{(0)} \in [\langle\Psi^\star|\hat{H}|\Psi^\star\rangle - \varepsilon(\overline{z}^\star, z^\star), \langle\Psi^\star|\hat{H}|\Psi^\star\rangle] \tag{2.11}$$

This result is however suboptimal, since we know that the error between $\langle\Psi^\star|\hat{H}|\Psi^\star\rangle$ and $E^{(0)}$ is $\mathcal{O}(\epsilon^2)$, whereas the lower bound of this estimate is $\mathcal{O}(\epsilon)$. Other variational approaches for finding a lower bound of the ground state energy can be found in [242, 243].

2. Time-dependent variational principle

The (time-independent) variational principle [244, 245, 246] is a very powerful approach to find good approximations of the lowest lying eigenstates of a time-independent Hamiltonian $\hat{H}$ within a variational manifold $\mathscr{M}$. The variational manifold can also be used to study quantum dynamics, which are governed by the time-dependent Schrödinger equation

$$\mathrm{i}\frac{\mathrm{d}}{\mathrm{d}t}|\Psi(t)\rangle = \hat{H}(t)|\Psi(t)\rangle\,, \tag{2.12}$$

which is a linear first-order differential equation in $\mathbb{H}$. Note that we now allow for the Hamiltonian $\hat{H}$ to be time-dependent. An initial state $|\Psi(z(0))\rangle$ in the variational manifold $\mathscr{M}$ will in general leave the manifold under time evolution. This section introduces the time-dependent variational principle, which allows to construct an approximation $|\Psi(z(t))\rangle$ of the exact time evolution of $|\Psi(z(0))\rangle$ that is confined to $\mathscr{M}$.

When applied to a mean-field ansatz for a many-body wave function, the time-dependent variational principle results in the the time-dependent Hartree-Fock method [244] or the time-dependent Gross-Pitaevskii equation (for bosons) [247, 248]. The time-dependent variational principle is here discussed in full generality, and will be applied to some specific variational manifolds $\mathscr{M}$ in the subsequent chapters.

2.1. Principle of least action

The time-dependent Schrödinger equation can be derived by applying the variational principle of least action to the action functional

$$S_{\mathbb{H}}[\overline{\Psi},\Psi] = \int_{-\infty}^{+\infty}\left(\frac{\mathrm{i}}{2}\langle\Psi(t)|\dot{\Psi}(t)\rangle - \frac{\mathrm{i}}{2}\langle\dot{\Psi}(t)|\Psi(t)\rangle - \langle\Psi(t)|\hat{H}(t)|\Psi(t)\rangle\right)\mathrm{d}t. \tag{2.13}$$

Indeed, requiring stability with respect to an infinitesimal variation $\langle\Psi(t)| \to \langle\Psi(t)| + \langle\delta\Psi(t)|$ results in the time-dependent Schrödinger equation [Eq. (2.12)], whereas stability with respect to $|\Psi(t)\rangle \to |\Psi(t)\rangle + |\delta\Psi(t)\rangle$ requires the complex conjugate of the Schrödinger equation to hold.

In order to confine the dynamics of a quantum state to the variational manifold $\mathscr{M}$, we can analoguously apply the principle of least action to

$$S_{\mathscr{M}}[\overline{z},z] = \int_{-\infty}^{+\infty}\left(\frac{\mathrm{i}}{2}\left[\dot{z}^j(t)\partial_j - \dot{\overline{z}}^{\bar{\jmath}}(t)\partial_{\bar{\jmath}}\right]\langle\Psi(\overline{z}(t))|\Psi(z(t))\rangle \right.$$
$$\left. - \langle\Psi(\overline{z}(t))|\hat{H}(t)|\Psi(z(t))\rangle\right)\mathrm{d}t. \tag{2.14}$$

Stability of the action functional $S_{\mathscr{M}}$ with respect to a variation $\overline{z}(t) \mapsto \overline{z}(t) + \overline{\delta z}(t)$ or

$z(t) \mapsto z(t) + \delta z(t)$ is obtained by imposing the Euler-Lagrange equations

$$\begin{cases} +\mathrm{i}\,\langle \partial_{\bar{i}}\Psi(\bar{z}(t))|\partial_j\Psi(z(t))\rangle\,\dot{z}^j(t) = \langle \partial_{\bar{i}}\Psi(\bar{z}(t))|\hat{H}(t)|\Psi(z(t))\rangle\,, \\ -\mathrm{i}\dot{\bar{z}}^{\bar{j}}(t)\,\langle \partial_{\bar{j}}\Psi(\bar{z}(t))|\partial_i\Psi(z(t))\rangle = \langle \Psi(\bar{z}(t))|\hat{H}(t)|\partial_i\Psi(z(t))\rangle\,. \end{cases} \tag{2.15}$$

We can define the Hermitian matrix $G(\bar{z}, z)$ as

$$G_{\bar{i},j}(\bar{z}, z) = \langle \partial_{\bar{i}}\Psi(\bar{z})|\partial_j\Psi(z)\rangle \tag{2.16}$$

and interpret $G(\bar{z}, z)$ as the metric of the manifold $\mathscr{M}$ in the point $(\bar{z}, z)$. This metric appears in Eq. (2.15) in order to map the contravariant vector $\dot{z}^i$ to a covariant vector. The matrix $G(\bar{z}, z)$ can also be recognized as the Gram matrix containing the scalar product between any two tangent vectors. If the map $\Psi : z \mapsto |\Psi(z)\rangle$ is injective, the inverse function theorem guarantees that this metric can be inverted for every $(\bar{z}, z)$ such that the Euler-Lagrange equations [Eq. (2.15)] define a unique solution $z(t)$. As is common in differential geometry, the inverse metric is denoted by the same symbol G, and the only distinction is in the position of the indices. The inverse metric satisfies $G^{i,\bar{j}}(\bar{z}, z)G_{\bar{j},k}(\bar{z}, z) = \delta^i_k$ and $G_{\bar{i},j}(\bar{z}, z)G^{j,\bar{k}}(\bar{z}, z) = \delta^{\bar{k}}_{\bar{i}}$ and allows to rewrite the Euler-Lagrange equations [Eq. (2.15)] as

$$\begin{cases} +\mathrm{i}\dot{z}^i(t) = G^{i,\bar{j}}(\bar{z}(t), z(t))\,\langle \partial_{\bar{i}}\Psi(\bar{z}(t))|\hat{H}(t)|\Psi(z(t))\rangle\,, \\ -\mathrm{i}\dot{\bar{z}}^{\bar{i}}(t) = G^{\bar{i},j}(\bar{z}(t), z(t))\,\langle \Psi(\bar{z}(t))|\hat{H}(t)|\partial_j\Psi(z(t))\rangle\,. \end{cases} \tag{2.17}$$

These equations are henceforth referred to as the *flow equations* of the time-dependent variational principle. The time-dependent variational principle thus approximates the linear Schrödinger equation in $\mathbb{H}$ by a set of non-linear first order differential equations in the variational parameters z. Since the number of variational parameters is ideally much smaller than the dimension of $\mathbb{H}$, these non-linear differential equations can more easily be dealt with, *e.g.* with numerical methods. It is however not guaranteed that a variational manifold $\mathscr{M}$ can successfully capture the long-time dynamics of an initial state $|\Psi(z(0))\rangle$ under the real time evolution corresponding to a Hamiltonian $\hat{H}$, even when $\mathscr{M}$ is capable of capturing the ground state and low-lying excited states of $\hat{H}$. As was explained in Subsection 2.5 of the previous chapter, the entanglement in a state generally increases linearly under time evolution. This will turn out to be the effect that limits the length of the maximal time interval that can accurately be captured by the variational manifolds in the next chapters.

2.2. Geometric construction

The flow equations [Eq. (2.17)] of the time-dependent variational principle can also be obtained from a purely geometric construction, which is sketched here in order to improve the insight into the precise nature of the approximation made by the time-dependent variational principle. If time evolution could be exactly captured within the variational manifold $\mathcal{M}$, the time-dependent state $|\Psi(\boldsymbol{z}(t))\rangle$ would need to satisfy the time-dependent Schrödinger equation [Eq. (2.12)], resulting in

$$\mathrm{i}\dot{z}^j(t)\,|\partial_j\Psi(\boldsymbol{z}(t))\rangle = \hat{H}(t)\,|\Psi(\boldsymbol{z}(t))\rangle\,. \tag{2.18}$$

Note that the left hand side of this equation is a vector living in the tangent plane $\mathbb{T}_{\mathcal{M}}(\boldsymbol{z}(t))$ of $\mathcal{M}$ in the point $|\Psi(\boldsymbol{z}(t))\rangle$, which is defined as

$$\mathbb{T}_{\mathcal{M}}(\boldsymbol{z}) = \mathrm{span}\{|\partial_i\Psi(\boldsymbol{z})\rangle\,, \forall i\}. \tag{2.19}$$

A general tangent vector $|\Phi(\boldsymbol{c};\boldsymbol{z})\rangle \in \mathbb{T}_{\mathcal{M}}(\boldsymbol{z})$ is defined as

$$|\Phi(\boldsymbol{c};\boldsymbol{z})\rangle = c^j\,|\partial_j\Psi(\boldsymbol{z})\rangle\,. \tag{2.20}$$

Only when the right hand side of Eq. (2.18) is exactly captured by the tangent plane $\mathbb{T}_{\mathcal{M}}(\boldsymbol{z}(t))$ is it possible to describe the exact quantum-mechanical time evolution. Since in general the right hand side can be any vector in $\mathbb{H}$, we need to look for an approximate solution of Eq. (2.18). By using the standard norm defined in $\mathbb{H}$, we can approximate $\hat{H}(t)|\Psi(\boldsymbol{z}(t))\rangle$ by the tangent vector $|\Phi(\boldsymbol{c}^\star(t);\boldsymbol{z}(t))\rangle$ where

$$\boldsymbol{c}^\star(t) = \arg\min_{\boldsymbol{c}} \left\| |\Phi(\boldsymbol{c};\boldsymbol{z}(t))\rangle - \hat{H}(t)\,|\Psi(\boldsymbol{z}(t))\rangle \right\|^2.$$

The least square solution $\boldsymbol{c}^\star(t)$ can be obtained by expanding this norm and solving the quadratic minimization problem in the expansion coefficients $\boldsymbol{c}$. Equivalently, we can just project the Schrodinger equation [Eq. (2.18)] onto the basis of tangent vectors $\langle\partial_{\bar{i}}\Psi(\overline{\boldsymbol{z}}(t))|$, resulting in the first line of Eq. (2.17). By using the inverse of the Gram matrix of the tangent vectors, we can define an orthogonal projector $\hat{P}_{\mathbb{T}_{\mathcal{M}}}(\overline{\boldsymbol{z}},\boldsymbol{z})$ as

$$\hat{P}_{\mathbb{T}_{\mathcal{M}}}(\overline{\boldsymbol{z}},\boldsymbol{z}) = |\partial_j\Psi(\boldsymbol{z})\rangle\, G^{j,\bar{i}}(\overline{\boldsymbol{z}},\boldsymbol{z})\,\langle\partial_{\bar{i}}\Psi(\overline{\boldsymbol{z}})|\,, \tag{2.21}$$

which allows to rewrite the flow equations [Eq. (2.17)] in wave vector format

$$\begin{cases} +\mathrm{i}\frac{\mathrm{d}}{\mathrm{d}t}\,|\Psi(\boldsymbol{z}(t))\rangle = \hat{P}_{\mathbb{T}_{\mathcal{M}}}(\overline{\boldsymbol{z}}(t),\boldsymbol{z}(t))\hat{H}(t)\,|\Psi(\boldsymbol{z}(t))\rangle\,, \\ -\mathrm{i}\frac{\mathrm{d}}{\mathrm{d}t}\,\langle\Psi(\overline{\boldsymbol{z}}(t))| = \langle\Psi(\overline{\boldsymbol{z}}(t))|\,\hat{H}(t)\hat{P}_{\mathbb{T}_{\mathcal{M}}}(\overline{\boldsymbol{z}}(t),\boldsymbol{z}(t)). \end{cases} \tag{2.22}$$

The time-dependent variational principle thus projects the exact evolution onto the tangent plane of the manifold, as is illustrated in Figure 2.1.

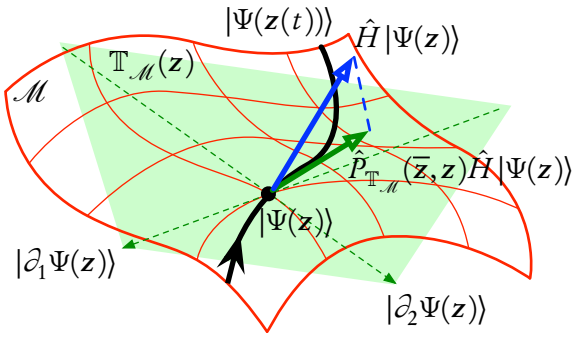

Figure 2.1: Sketch of the variational manifold $\mathcal{M}$ (red) with indication of the tangent vectors (green dashes) and the resulting tangent plane $\mathbb{T}_{\mathcal{M}}(z)$ in the point $|\Psi(z)\rangle$. The exact dynamics are given by the evolution vector $\hat{H}|\Psi(z)\rangle$ (blue arrow), whereas the evolution according to the time-dependent variational principle follows the projected vector $\hat{P}_{\mathbb{T}_{\mathcal{M}}}\hat{H}|\Psi(z)\rangle$ (green arrow). This results in the flow $|\Psi(z(t))\rangle$ (black curve).

2.3. Norm-preserving dynamics

While the previous subsections summarize the basic ingredients of the time-dependent variational principle, it is necessary to introduce some essential modifications. Whereas the exact solution of the Schrödinger equation is a unitary process (norm-preserving), this is not guaranteed for the solution of the flow equations [Eq. (2.17)] of the time dependent variational principle. Norm-preserving dynamics are obtained by defining a modified action

$$\begin{aligned}\widetilde{S}_{\mathcal{M}} &= \int_{-\infty}^{+\infty} \frac{\frac{\mathrm{i}}{2}\left[\dot{z}^j(t)\partial_j - \dot{\bar{z}}^j(t)\partial_{\bar{j}}\right]\langle\Psi(\bar{z}(t))|\Psi(z(t))\rangle - \langle\Psi(\bar{z}(t))|\hat{H}|\Psi(z(t))\rangle}{\langle\Psi(\bar{z}(t))|\Psi(z(t))\rangle}\,\mathrm{d}t \\ &= \int_{-\infty}^{+\infty}\left(\frac{\mathrm{i}}{2}\left[\dot{z}^j(t)\partial_j - \dot{\bar{z}}^j(t)\partial_{\bar{j}}\right]\ln N(\bar{z}(t),z(t)) - H(\bar{z}(t),z(t))\right)\mathrm{d}t,\end{aligned} \tag{2.23}$$

where

$$N(\bar{z},z) = \langle\Psi(\bar{z})|\Psi(z)\rangle \tag{2.24}$$

and $H(\bar{z},z)$ was defined in Eq. (2.2). Note that we henceforth omit the explicit time-dependence of the Hamiltonian $\hat{H}$ for the sake of simplicity. For a time-dependent Hamiltonian $\hat{H}(t)$, the energy function H would have an explicit time-dependence [*i.e.* $H(\bar{z},z,t)$], but this has no other effect on the resulting expressions.

Firstly, note that the stability of $\widetilde{S}_{\mathbb{H}}$ with respect to variations $\langle\Psi(t)| \mapsto \langle\Psi(t)| + \langle\delta\Psi(t)|$ requires

$$\left(\hat{\mathbb{1}} - \frac{|\Psi(t)\rangle\langle\Psi(t)|}{\langle\Psi(t)|\Psi(t)\rangle}\right)\left(\mathrm{i}\frac{\mathrm{d}}{\mathrm{d}t}|\Psi(t)\rangle - \hat{H}|\Psi(t)\rangle\right) = 0. \tag{2.25}$$

Applying the variational principle to the modified action $\widetilde{S}_{\mathbb{H}}$ thus imposes the Schrö-

dinger equation in the plane orthogonal to the vector $|\Psi(t)\rangle$, whereas it leaves the evolution in the direction of the current vector $|\Psi(t)\rangle$ unspecified. Since a nonzero parallel component of the evolution vector ($\langle\Psi(t)|\dot{\Psi}(t)\rangle \neq 0$) results in norm or phase changes, the use of the modified action unties the restriction to a specific choice of phase and normalization of the state.

The Euler-Lagrange equations for the modified action $\widetilde{S}_{\mathscr{M}}$ are given by

$$\begin{cases} +\mathrm{i}\widetilde{G}_{\bar{\imath},j}(\overline{z}(t),z(t))\dot{z}^{j}(t) = H_{\bar{\imath}}(\overline{z}(t),z(t)), \\ -\mathrm{i}\dot{\overline{z}}^{\bar{\jmath}}(t)\widetilde{G}_{\bar{\jmath},i}(\overline{z}(t),z(t)) = H_{i}(\overline{z}(t),z(t)). \end{cases} \tag{2.26}$$

We have introduced the modified metric

$$\widetilde{G}_{\bar{\imath},j}(\overline{z},z) = \partial_{\bar{\imath}}\partial_{j}\ln N(\overline{z},z) = \frac{G_{\bar{\imath},j}(\overline{z},z)}{N(\overline{z},z)} - \frac{\langle\partial_{\bar{\imath}}\Psi(\overline{z})|\Psi(z)\rangle\,\langle\Psi(\overline{z})|\partial_{j}\Psi(z)\rangle}{N(\overline{z},z)^{2}} \tag{2.27}$$

and the gradients

$$\begin{aligned} H_{\bar{\imath}}(\overline{z},z) &= \partial_{\bar{\imath}}H(\overline{z},z) = \frac{\langle\partial_{\bar{\imath}}\Psi(\overline{z})|\hat{H}|\Psi(z)\rangle}{N(\overline{z},z)} - \frac{\langle\partial_{\bar{\imath}}\Psi(\overline{z})|\Psi(z)\rangle\,\langle\Psi(\overline{z})|\hat{H}|\Psi(z)\rangle}{N(\overline{z},z)^{2}}, \\ H_{i}(\overline{z},z) &= \partial_{i}H(\overline{z},z) = \frac{\langle\Psi(\overline{z})|\hat{H}|\partial_{i}\Psi(z)\rangle}{N(\overline{z},z)} - \frac{\langle\Psi(\overline{z})|\partial_{i}\Psi(z)\rangle\,\langle\Psi(\overline{z})|\hat{H}|\Psi(z)\rangle}{N(\overline{z},z)^{2}}. \end{aligned} \tag{2.28}$$

As for the evolution produced by $\widetilde{S}_{\mathbb{H}}$ in the full Hilbert space, one can now define the orthogonal projector onto the space orthogonal to $|\Psi(z)\rangle$ as

$$\hat{P}_{0}(\overline{z},z) = \hat{\mathbb{1}} - \frac{|\Psi(z)\rangle\,\langle\Psi(\overline{z})|}{\langle\Psi(\overline{z})|\Psi(z)\rangle} = \hat{\mathbb{1}} - \frac{|\Psi(z)\rangle\,\langle\Psi(\overline{z})|}{N(\overline{z},z)} \tag{2.29}$$

and observe that

$$\begin{aligned} \widetilde{G}_{\bar{\imath},j}(\overline{z},z) &= \frac{\langle\partial_{\bar{\imath}}\Psi(\overline{z})|\hat{P}_{0}(\overline{z},z)|\partial_{j}\Psi(z)\rangle}{N(\overline{z},z)}, \\ H_{\bar{\imath}}(\overline{z},z) &= \frac{\langle\partial_{\bar{\imath}}\Psi(\overline{z})|\hat{P}_{0}(\overline{z},z)\hat{H}|\Psi(z)\rangle}{N(\overline{z},z)}. \end{aligned}$$

The modified Euler-Lagrange equations [Eq. (2.26)] thus encode the projection of the modified Schrödinger equation [Eq. (2.25)] onto the tangent plane $\mathbb{T}_{\mathscr{M}}(z)$.

We can now not straightforwardly assume that the modified metric $\widetilde{G}$ can be inverted. In the full Hilbert space, the Euler-Lagrange equation [Eq. (2.25)] does not fix the component of $|\dot{\Psi}(t)\rangle$ parallel with $|\Psi(t)\rangle$, as discussed above. For general manifolds $\mathscr{M}$, we have to distinguish between two cases.

(a) If the manifold $\mathscr{M}$ allows for norm and phase variations of states, *i.e.* if $|\Psi(z)\rangle \in \mathbb{T}_{\mathscr{M}}(z)$, one can define the contravariant vector $\Psi^i(z)$ such that $\Psi^i(z)|\partial_i\Psi(z)\rangle = |\Psi(z)\rangle$. By definition we have that $\hat{P}_0(\overline{z},z)|\Psi(z)\rangle = \hat{P}_0(\overline{z},z)|\partial_i\Psi(z)\rangle\,\Psi^i(z) = 0$ and we can conclude that $\widetilde{G}_{\overline{\imath}j}(\overline{z},z)$ has an eigenvalue zero, since $\widetilde{G}_{\overline{\imath},j}(\overline{z},z)\Psi^j(z) = 0 = \overline{\Psi}^{\overline{\imath}}(\overline{z})\widetilde{G}_{\overline{\imath},j}(\overline{z},z)$, from which we immediately obtain the corresponding eigenvector. The metric $G(\overline{z},z)$ allows to also define the covariant vector $\Psi_{\overline{\imath}}(\overline{z},z) = G_{\overline{\imath}j}(\overline{z},z)\Psi^j(z) = \langle\partial_{\overline{\imath}}\Psi(\overline{z})|\Psi(z)\rangle$ so that $\overline{\Psi}_i(\overline{z},z)\Psi^i(z) = \langle\Psi(\overline{z})|\Psi(z)\rangle = N(\overline{z},z)$. With these definitions, we can write

$$\widetilde{G}_{\overline{\imath},j}(\overline{z},z) = \frac{G_{\overline{\imath},j}(\overline{z},z)}{N(\overline{z},z)} - \frac{\Psi_{\overline{\imath}}(\overline{z},z)\overline{\Psi}_j(\overline{z},z)}{N(\overline{z},z)^2}. \tag{2.30}$$

Even though $\widetilde{G}(\overline{z},z)$ is not invertible, we can still define a pseudo-inverse as

$$\widetilde{G}^{i,\overline{\jmath}}(\overline{z},z) = N(\overline{z},z)G^{i,\overline{\jmath}}(\overline{z},z) - \Psi^i(z)\overline{\Psi}^{\overline{\jmath}}(\overline{z}), \tag{2.31}$$

such that

$$\widetilde{G}^{i,\overline{\jmath}}(\overline{z},z)\widetilde{G}_{\overline{\jmath},k}(\overline{z},z) = \delta^i_k - \frac{\Psi^i(z)\overline{\Psi}_k(\overline{z},z)}{N(\overline{z},z)},$$

$$\widetilde{G}_{\overline{\imath},j}(\overline{z},z)\widetilde{G}^{j,\overline{k}}(\overline{z},z) = \delta^{\overline{k}}_{\overline{\imath}} - \frac{\Psi_{\overline{\imath}}(\overline{z},z)\overline{\Psi}^{\overline{k}}(\overline{z})}{N(\overline{z},z)}.$$

Since we can rewrite $H_{\overline{\imath}}(\overline{z},z)$ as

$$N(\overline{z},z)^{-1}(\delta_{\overline{\imath}}^{\ \overline{k}} - N(\overline{z},z)^{-1}\Psi_{\overline{\imath}}(\overline{z},z)\overline{\Psi}^{\overline{k}}(\overline{z},z))\,\langle\delta_{\overline{k}}\Psi(\overline{z})|\hat{H}|\Psi(z)\rangle\,,$$

we are allowed to apply this pseudo-inverse to the Euler-Lagrange equations given by Eq. (2.26) in order to obtain

$$\begin{cases} +\mathrm{i}\dot{z}^i(t) = \widetilde{G}^{i,\overline{\jmath}}(\overline{z}(t),z(t))H_{\overline{\jmath}}(\overline{z}(t),z(t)), \\ -\mathrm{i}\dot{\overline{z}}^{\overline{\imath}}(t) = \widetilde{G}^{j,\overline{\imath}}(\overline{z}(t),z(t))H_i(\overline{z}(t),z(t)). \end{cases} \tag{2.32}$$

These equations are henceforth called the *(modified) flow equations*. In principle, the component of $\dot{z}(t)$ along the zero eigenspace $\Psi^i(z(t))$ of $\widetilde{G}(\overline{z}(t),z(t))$ can be chosen freely. But, with the particular solution in the equation above, we satisfy

$$\overline{\Psi}_i(\overline{z}(t),z(t))\dot{z}^i(t) = \langle\Psi(\overline{z}(t))|\partial_i\Psi(z(t))\rangle\,\dot{z}^i(t) = 0$$

and

$$\dot{\overline{z}}^{\overline{\imath}}(t)\Psi_{\overline{\imath}}(\overline{z}(t),z(t)) = \dot{\overline{z}}^{\overline{\imath}}(t)\,\langle\partial_{\overline{\imath}}\Psi(\overline{z}(t))|\Psi(z(t))\rangle = 0.$$

We hence obtain

$$\frac{\mathrm{d}}{\mathrm{d}t}\langle\Psi(\overline{z}(t))|\Psi(z(t))\rangle = \dot{\overline{z}}^{\bar{i}}(t)\langle\partial_{\bar{i}}\Psi(\overline{z}(t))|\Psi(z(t))\rangle + \langle\Psi(\overline{z}(t))|\partial_i\Psi(z(t))\rangle\dot{z}^i(t) = 0, \quad (2.33)$$

so that the norm of the state $|\Psi(z(t))\rangle$ is fixed to its initial value at $t = 0$ and we can also refer to Eq. (2.32) as the norm-preserving flow equations. In the full Hilbert space, adding norm preservation to Eq. (2.25) results in a norm- and phase preserving Schrödinger equation

$$\mathrm{i}\frac{\mathrm{d}}{\mathrm{d}t}|\Psi(t)\rangle = \hat{P}_0(\overline{\Psi}(t),\Psi(t))\hat{H}|\Psi(t)\rangle = \left[\hat{H} - H(\overline{\Psi}(t),\Psi(t))\right]|\Psi(t)\rangle. \quad (2.34)$$

More generally, for any variational manifold for which $|\Psi(z)\rangle \in \mathbb{T}_{\mathscr{M}}(z)$, it is clear from the definition of the pseudo-inverse $\widetilde{G}^{i,\bar{j}}(\overline{z},z)$ that

$$\begin{aligned}\widetilde{G}^{i,\bar{j}}(\overline{z},z)H_{\bar{j}}(\overline{z},z) &= N(\overline{z},z)^{-1}G^{i,\bar{j}}(\overline{z},z)H_{\bar{j}}(\overline{z},z)\\ &= G^{i,\bar{j}}(\overline{z},z)\langle\partial_j\Psi(\overline{z})|\hat{P}_0(\overline{z},z)\hat{H}|\Psi(z)\rangle.\end{aligned}$$

We thus obtain the modified Euler-Lagrange equations [Eq. (2.26)] from the geometric construction by projecting the modified Schrödinger equation [Eq. (2.25)] onto the tangent plane $\mathbb{T}_{\mathscr{M}}(z(t))$. The specific choice of pseudo-inverse in the modified flow equations [Eq. (2.32)] corresponds to a projection of the exact evolution vector $\hat{P}_0(\overline{z},z)\hat{H}|\Psi(z)\rangle$ of the norm- and phase-preserving Schrödinger equation [eq. (2.34)] into the tangent plane $\mathbb{T}_{\mathscr{M}}(z(t))$. This observation results in an alternate formulation of the modified flow equations [Eq. (2.32)] as

$$\begin{cases}+\mathrm{i}\frac{\mathrm{d}}{\mathrm{d}t}|\Psi(z(t))\rangle = +\mathrm{i}\dot{z}^j(t)|\partial_j\Psi(z(t))\rangle\\ \qquad\qquad = \hat{P}_{\mathbb{T}_{\mathscr{M}}}(\overline{z}(t),z(t))\hat{P}_0(\overline{z}(t),z(t))\hat{H}|\Psi(z(t))\rangle,\\ -\mathrm{i}\frac{\mathrm{d}}{\mathrm{d}t}\langle\Psi(\overline{z}(t))| = -\mathrm{i}\dot{\overline{z}}^{\bar{j}}(t)\langle\partial_{\bar{j}}\Psi(\overline{z}(t))|\\ \qquad\qquad = \langle\Psi(\overline{z}(t))|\hat{H}\hat{P}_0(\overline{z}(t),z(t))\hat{P}_{\mathbb{T}_{\mathscr{M}}}(\overline{z}(t),z(t)).\end{cases}$$

Alternatively, by restricting the tangent plane to the set of tangent vectors that are orthogonal to $|\Psi(z)\rangle$, there is no difference between the Euler-Lagrange equations in Eq. (2.15) and in Eq. (2.26). Indeed, since we have assumed that $|\Psi(z)\rangle \in \mathbb{T}_{\mathscr{M}}(z)$ or thus $\hat{P}_{\mathbb{T}_{\mathscr{M}}}(\overline{z},z)|\Psi(z)\rangle = |\Psi(z)\rangle$, we obtain

$$\hat{P}_0(\overline{z},z)\hat{P}_{\mathbb{T}_{\mathscr{M}}}(\overline{z},z) = \hat{P}_0(\overline{z},z)\hat{P}_{\mathbb{T}_{\mathscr{M}}}(\overline{z},z)\hat{P}_0(\overline{z},z) = \hat{P}_{\mathbb{T}_{\mathscr{M}}}(\overline{z},z)\hat{P}_0(\overline{z},z).$$

We henceforth denote the orthogonal complement of $|\Psi(z)\rangle$ in the tangent plane

$\mathbb{T}_{\mathscr{M}}(z)$ as $\mathbb{T}^{\perp}_{\mathscr{M}}(z)$, and thus define

$$\hat{P}_{\mathbb{T}^{\perp}_{\mathscr{M}}}(\overline{z},z) = \hat{P}_0(\overline{z},z)\hat{P}_{\mathbb{T}_{\mathscr{M}}}(\overline{z},z)\hat{P}_0(\overline{z},z). \tag{2.35}$$

We now obtain the wave vector formulation of the modified flow equations

$$\begin{cases} +\mathrm{i}\frac{\mathrm{d}}{\mathrm{d}t}|\Psi(z(t))\rangle = +\mathrm{i}\dot{z}^j(t)|\partial_j\Psi(z(t))\rangle = \hat{P}_{\mathbb{T}^{\perp}_{\mathscr{M}}}(\overline{z}(t),z(t))\hat{H}|\Psi(z(t))\rangle\,, \\ -\mathrm{i}\frac{\mathrm{d}}{\mathrm{d}t}\langle\Psi(\overline{z}(t))| = -\mathrm{i}\dot{\overline{z}}^{\overline{j}}(t)\langle\partial_{\overline{j}}\Psi(\overline{z}(t))| = \langle\Psi(\overline{z}(t))|\hat{H}\hat{P}_{\mathbb{T}^{\perp}_{\mathscr{M}}}(\overline{z}(t),z(t)). \end{cases} \tag{2.36}$$

(b) In contrast, if the manifold $\mathscr{M}$ does not contain the freedom to change the norm and phase of a state, the modified metric $\widetilde{G}$ has the same rank as the original metric G, which we assumed to be invertible. The inverse of $\widetilde{G}$ can thus be defined without any problem and the same set of modified flow equations in Eq. (2.32) are formally reproduced. In general, the dynamics extracted from the modified action $\widetilde{S}_{\mathscr{M}}$ will be different from the dynamics obtained from $S_{\mathscr{M}}$. The modified metric can be recognized as the Gram matrix of the set of vectors $\{\hat{P}_0(\overline{z},z)|\partial_i\Psi(z)\rangle\,,\forall i\}$. We can thus define a generalized 'projector'

$$\hat{Q}_{\mathbb{T}_{\mathscr{M}}}(\overline{z},z) = |\partial_i\Psi(z)\rangle\,\widetilde{G}^{i,\overline{j}}(\overline{z},z)\,\langle\partial_{\overline{j}}\Psi(\overline{z})| \tag{2.37}$$

that satisfies

$$\hat{Q}_{\mathbb{T}_{\mathscr{M}}}(\overline{z},z)\hat{P}_0(\overline{z},z)\hat{Q}_{\mathbb{T}_{\mathscr{M}}}(\overline{z},z) = \hat{Q}_{\mathbb{T}_{\mathscr{M}}}(\overline{z},z) \tag{2.38}$$

in order to rewrite the modified flow equations [Eq. (2.32)] in vector format as

$$\begin{cases} +\mathrm{i}\frac{\mathrm{d}}{\mathrm{d}t}|\Psi(z(t))\rangle = +\mathrm{i}\dot{z}^j(t)|\partial_j\Psi(z(t))\rangle \\ \qquad\qquad = \hat{Q}_{\mathbb{T}_{\mathscr{M}}}(\overline{z}(t),z(t))\hat{P}_0(\overline{z}(t),z(t))\hat{H}|\Psi(z(t))\rangle\,, \\ -\mathrm{i}\frac{\mathrm{d}}{\mathrm{d}t}\langle\Psi(\overline{z}(t))| = -\mathrm{i}\dot{\overline{z}}^{\overline{j}}(t)\langle\partial_{\overline{j}}\Psi(\overline{z}(t))| \\ \qquad\qquad = \langle\Psi(\overline{z}(t))|\hat{H}\hat{P}_0(\overline{z}(t),z(t))\hat{Q}_{\mathbb{T}_{\mathscr{M}}}(\overline{z}(t),z(t)). \end{cases} \tag{2.39}$$

This equation indicates that

$$\begin{aligned} \frac{\mathrm{d}}{\mathrm{d}t}N(\overline{z}(t),z(t)) = &-\mathrm{i}\,\langle\Psi(\overline{z}(t))|\hat{Q}_{\mathbb{T}_{\mathscr{M}}}(\overline{z}(t),z(t))\hat{P}_0(\overline{z}(t),z(t))\hat{H}|\Psi(z(t))\rangle \\ &+\mathrm{i}\,\langle\Psi(\overline{z}(t))|\hat{H}\hat{P}_0(\overline{z}(t),z(t))\hat{Q}_{\mathbb{T}_{\mathscr{M}}}(\overline{z}(t),z(t))|\Psi(z(t))\rangle \neq 0. \end{aligned} \tag{2.40}$$

Indeed, since the manifold $\mathscr{M}$ has a unique norm $N(\overline{z},z)$ associated to every state $|\Psi(z)\rangle$, the norm cannot be kept constant in general. Hence, the modified flow equations are not norm-preserving in this case.

Clearly, the physically most relevant scenario is a variational manifold $\mathscr{M}$ in which the normalization is equal for all states. This requires that $|\Psi(z)\rangle \perp \mathbb{T}_{\mathscr{M}}(z)$ such

that $\forall i : \hat{P}_0(\overline{z},z)|\partial_i\Psi(z)\rangle = |\partial_i\Psi(z)\rangle$ and allows to define $\mathbb{T}^{\perp}_{\mathscr{M}}(z) = \mathbb{T}_{\mathscr{M}}(z)$. One then obtains

$$\begin{aligned}\widetilde{G}_{\bar{\imath},j}(\overline{z},z) &= N(\overline{z},z)^{-1}G_{\bar{\imath},j}(\overline{z},z),\\ H_{\bar{\imath}}(\overline{z},z) &= N(\overline{z},z)^{-1}\langle\partial_{\bar{\imath}}\Psi(\overline{z})|\hat{H}|\Psi(z)\rangle,\end{aligned}$$

so that the modified flow equations [Eq. (2.32)] are identical to the original flow equations [Eq. (2.17)]. $\hat{Q}_{\mathbb{T}_{\mathscr{M}}}$ is then equivalent to the ordinary projector $\hat{P}_{\mathbb{T}_{\mathscr{M}}}$, which can also be written as $\hat{P}_{\mathbb{T}^{\perp}_{\mathscr{M}}}$, so that Eq. (2.39) can also be written as in the form of Eq. (2.36). The equivalence between both cases is evident. Any manifold $\mathscr{M}$ with fixed normalization can be converted into a manifold that allows norm and phase variation by adding an additional variational parameter that multiplies every state. Vice versa, in any manifold $\mathscr{M}$ that allows norm and phase variations, a fixed point on every ray of states can be chosen, which effectively reduces the number of variational parameters by one. This norm (and phase) fixing removes the direction $|\Psi(A)\rangle$ from the tangent plane $\mathbb{T}_{\mathscr{M}}(\overline{A},A)$.

2.4. Symplectic properties of real time evolution

One can define for every pair of functions $f : \mathscr{M} \mapsto \mathbb{C} : (\overline{z},z) \mapsto f(\overline{z},z)$ and $g : \mathscr{M} \mapsto \mathbb{C} : (\overline{z},z) \mapsto g(\overline{z},z)$ a Poisson bracket

$$\{f,g\}(\overline{z},z) = \partial_i f(\overline{z},z)\widetilde{G}^{i,\bar{\jmath}}(\overline{z},z)\partial_{\bar{\jmath}}g(\overline{z},z) - \partial_i g(\overline{z},z)\widetilde{G}^{i,\bar{\jmath}}(\overline{z},z)\partial_{\bar{\jmath}}f(\overline{z},z). \tag{2.41}$$

The modified flow equations [Eq. (2.32)] can then be written down as

$$\begin{cases}\dot{z}^j(t) = \mathrm{i}\{H,z^j\}(\overline{z}(t),z(t)),\\ \dot{\overline{z}}^{\bar{\jmath}}(t) = \mathrm{i}\{H,\overline{z}^{\bar{\jmath}}\}(\overline{z}(t),z(t)).\end{cases} \tag{2.42}$$

In addition, if we now associate to any operator $\hat{O} \in \mathbb{L}(\mathbb{H})$ the function

$$O : (\overline{z},z) \mapsto \frac{\langle\Psi(\overline{z})|\hat{O}|\Psi(z)\rangle}{\langle\Psi(\overline{z})|\Psi(z)\rangle} \tag{2.43}$$

that maps the coordinates $(\overline{z},z)$ of a state $|\Psi(z)\rangle$ in the manifold $\mathscr{M}$ to its expectation value, then we can write the evolution of this expectation value under the (modified) flow of the time-dependent variational principle as

$$\frac{\mathrm{d}}{\mathrm{d}t}O(\overline{z}(t),z(t)) = \mathrm{i}\{H,O\}(\overline{z}(t),z(t)). \tag{2.44}$$

The generalization for time-dependent operators $\hat{O}(t)$ is straightforwardly given by

$$\frac{\mathrm{d}}{\mathrm{d}t}O(\overline{z}(t),z(t),t)=\mathrm{i}\{H,O\}(\overline{z}(t),z(t),t)+\frac{\partial O}{\partial t}(\overline{z}(t),z(t),t). \tag{2.45}$$

The manifold $\mathscr{M}$ is thus a symplectic manifold, which was first derived in [249]. From the antisymmetry of the Poisson bracket we find $\{H,H\}=0$, which implies that the energy expectation value $H(\overline{z}(t),z(t))$ of the state $|\Psi\rangle\in\mathscr{M}$ is conserved under exact integration of the flow equations of the time-dependent variational principle for a time-independent Hamiltonian $\hat{H}$.

The symplectic properties of the time-dependent variational principle also conserve other symmetries. Assume that the Hamiltonian is invariant under the action of a symmetry operator $\hat{U}$ (which should be a unitary operator), such that $[\hat{H},\hat{U}]=0$. In order to be able to transfer this symmetry to the manifold $\mathscr{M}$, we need to assume that for any state $|\Psi(z)\rangle\in\mathscr{M}$, the action of $\hat{U}$ is mapped to a new state $|\Psi(\boldsymbol{u}(z))\rangle=\hat{U}|\Psi(z)\rangle\in\mathscr{M}$. Because of the unitarity of $\hat{U}$, we have $N(\overline{\boldsymbol{u}}(\overline{z}),\boldsymbol{u}(z))=N(\overline{z},z)$, from which we obtain

$$\partial_{\bar{i}}\overline{u}^{\bar{j}}(\overline{z})\widetilde{G}_{\bar{j},k}(\overline{\boldsymbol{u}}(\overline{z}),\boldsymbol{u}(z))\partial_l u^k(z)=\widetilde{G}_{\bar{i},l}(\overline{z},z), \tag{2.46}$$

The condition $[\hat{H},\hat{U}]=0$ also allows to conclude $H(\overline{\boldsymbol{u}}(\overline{z}),\boldsymbol{u}(z))=H(\overline{z},z)$ and thus

$$\begin{aligned}&\partial_{\bar{i}}\overline{u}^{\bar{j}}(\overline{z})H_{\bar{j}}(\overline{\boldsymbol{u}}(\overline{z}),\boldsymbol{u}(z))=H_{\bar{i}}(\overline{z},z),\\&H_j(\overline{\boldsymbol{u}}(\overline{z}),\boldsymbol{u}(z))\partial_i u^j(z)=H_i(\overline{z},z).\end{aligned} \tag{2.47}$$

The (modified) metric and the gradient thus transform covariantly under the symmetry transformation and can be used to transform Eq. (2.32) into

$$\begin{cases}+\mathrm{i}\partial_{\bar{i}}\overline{u}^{\bar{j}}(\overline{z}(t))\widetilde{G}_{\bar{j},k}(\overline{\boldsymbol{u}}(\overline{z}(t)),\boldsymbol{u}(z(t)))\frac{\mathrm{d}}{\mathrm{d}t}u^k(z(t))=\partial_{\bar{i}}\overline{u}^{\bar{j}}(\overline{z}(t))H_{\bar{j}}(\overline{\boldsymbol{u}}(\overline{z}(t)),\boldsymbol{u}(z(t))),\\-\mathrm{i}\frac{\mathrm{d}}{\mathrm{d}t}\overline{u}^{\bar{i}}(z(t))\widetilde{G}_{\bar{i},j}(\overline{\boldsymbol{u}}(\overline{z}(t)),\boldsymbol{u}(z(t)))\partial_k u^j(z(t))=H_j(\overline{\boldsymbol{u}}(\overline{z}(t)),\boldsymbol{u}(z(t)))\partial_k u^j(z(t)).\end{cases}$$

By using the injectivity of the map $\boldsymbol{u}(z)$, we can eliminate the Jacobians $\partial_{\bar{i}}\overline{u}^{\bar{j}}$ and $\partial_k u^j$ in order to obtain the correct flow equations in terms of the new coordinates $(\boldsymbol{u}(t),\overline{\boldsymbol{u}}(t))$.

One case that is not covered by the general derivation of the previous paragraph is when $\hat{U}$ is an anti-linear operator, since $\boldsymbol{u}$ will then depend on z anti-holomorphically. Anti-linear transformations appear in quantum mechanics exclusively for time-reversal transformations. However, since $\overline{z}$ denotes a set of coordinates that is independent of z, we temporarily use an asterisk to denote complex conjugation, so that z^* represents the complex conjugate of the set of coordinates z. Let us define the vector function $\boldsymbol{r}$ that depends anti-holomorphically on z as $\hat{R}|\Psi(z)\rangle=|\Psi(\boldsymbol{r}(z^*))\rangle$ with $\hat{R}$ the operator of an elementary time-reversal transformation. Because of the anti-unitarity of $\hat{R}$ and its commutation relation with the Hamiltonian (*i.e.* $[\hat{H},\hat{R}]=0$ where we assume $\hat{H}$ to be

time-reversal invariant), we obtain $N(\overline{\boldsymbol{r}}(\overline{\boldsymbol{z}}^*), \boldsymbol{r}(\boldsymbol{z}^*)) = [N(\overline{\boldsymbol{z}}, \boldsymbol{z})]^*$ and $H(\overline{\boldsymbol{r}}(\overline{\boldsymbol{z}}^*), \boldsymbol{r}(\boldsymbol{z}^*)) = [H(\overline{\boldsymbol{z}}, \boldsymbol{z})]^*$. We can derive

$$\widetilde{G}_{\bar{\imath},j}(\overline{\boldsymbol{z}}, \boldsymbol{z}) = \frac{\partial \left[\overline{r}^{\bar{k}}(\overline{\boldsymbol{z}}^*)\right]^*}{\partial \overline{z}^{\bar{\imath}}} \left[\widetilde{G}_{\bar{k},l}(\overline{\boldsymbol{r}}(\overline{\boldsymbol{z}}^*), \boldsymbol{r}(\boldsymbol{z}^*))\right]^* \frac{\partial \left[r^l(\boldsymbol{z}^*)\right]^*}{\partial z^j} \tag{2.48}$$

and

$$\begin{aligned} H_j(\overline{\boldsymbol{z}}, \boldsymbol{z}) &= \frac{\partial \left[r^l(\boldsymbol{z}^*)\right]^*}{\partial z^j} \left[H_l(\overline{\boldsymbol{r}}(\overline{\boldsymbol{z}}^*), \boldsymbol{r}(\boldsymbol{z}^*))\right]^*, \\ H_{\bar{\imath}}(\overline{\boldsymbol{z}}, \boldsymbol{z}) &= \frac{\partial \left[\overline{r}^{\bar{k}}(\overline{\boldsymbol{z}}^*)\right]^*}{\partial \overline{z}^{\bar{\imath}}} \left[H_{\bar{k}}(\overline{\boldsymbol{r}}(\overline{\boldsymbol{z}}^*), \boldsymbol{r}(\boldsymbol{z}^*))\right]^*. \end{aligned} \tag{2.49}$$

Inserting these relations into Eq. (2.32) and taking the complex conjugate, we obtain

$$\begin{cases} -\mathrm{i}\frac{\partial \overline{r}^{\bar{k}}}{\partial \overline{z}^{*\bar{\imath}}}(\overline{\boldsymbol{z}}^*(t))\widetilde{G}_{\bar{k},l}(\overline{\boldsymbol{r}}(\overline{\boldsymbol{z}}^*(t)), \boldsymbol{r}(\boldsymbol{z}^*(t)))\frac{\mathrm{d}}{\mathrm{d}t} r^l(\boldsymbol{z}^*(t)) \\ \qquad = \frac{\partial \overline{r}^{\bar{k}}}{\partial \overline{z}^{*\bar{\imath}}}(\overline{\boldsymbol{z}}^*(t)) H_{\bar{k}}(\overline{\boldsymbol{r}}(\overline{\boldsymbol{z}}^*(t)), \boldsymbol{r}(\boldsymbol{z}^*(t))), \\ +\mathrm{i}\frac{\mathrm{d}}{\mathrm{d}t}\overline{r}^{\bar{k}}(\overline{\boldsymbol{z}}^*(t))\widetilde{G}_{\bar{k},l}(\overline{\boldsymbol{r}}(\overline{\boldsymbol{z}}^*(t)), \boldsymbol{r}(\boldsymbol{z}^*(t)))\frac{\partial r^l}{\partial z^{*j}}(\boldsymbol{z}^*(t)) \\ \qquad = H_l(\overline{\boldsymbol{r}}(\overline{\boldsymbol{z}}^*(t)), \boldsymbol{r}(\boldsymbol{z}^*(t)))\frac{\partial r^l}{\partial z^{*j}}(\boldsymbol{z}^*(t)), \end{cases}$$

or, by eliminating the Jacobian of the transformation and introducing the new coordinates $(\overline{\boldsymbol{r}}(t), \boldsymbol{r}(t))$

$$\begin{cases} -\mathrm{i}\widetilde{G}_{\bar{\imath},j}(\overline{\boldsymbol{r}}(t), \boldsymbol{r}(t))\frac{\mathrm{d}}{\mathrm{d}t} r^j(t) = H_{\bar{\imath}}(\overline{\boldsymbol{r}}(t), \boldsymbol{r}(t)), \\ +\mathrm{i}\frac{\mathrm{d}}{\mathrm{d}t}\overline{r}^{\bar{\jmath}}(t)\widetilde{G}_{\bar{\jmath},i}(\overline{\boldsymbol{r}}(t), \boldsymbol{r}(t)) = H_i(\overline{\boldsymbol{r}}(t), \boldsymbol{r}(t)) \end{cases} \tag{2.50}$$

Note that the signs of the two equations have been switched due to the complex conjugation, which is necessary to revert the time evolution for the new coordinates $(\overline{\boldsymbol{r}}(t), \boldsymbol{r}(t))$. For a time-reversal invariant Hamiltonian $\hat{H}$ and a variational manifold $\mathcal{M}$ that contains the time-reversed state $\hat{R}|\Psi(\boldsymbol{z})\rangle \in \mathcal{M}$ for each of its elements $|\Psi(\boldsymbol{z})\rangle \in \mathcal{M}$, the flow equations of the time-dependent variational principle are also time-reversal invariant. This can be exploited in numerical integration schemes in order to construct symmetric schemes with improved stability (see next chapter).

Returning to the case of linear symmetry transformations $\hat{U}$, the expectation value $U(\overline{\boldsymbol{z}}, \boldsymbol{z})$ is a constant of motion of the exact evolution according to the Schrödinger equation [Eq. (2.12) or Eq. (2.25)]. For the evolution according to the time-dependent

variational principle, we obtain

$$\frac{\mathrm{d}}{\mathrm{d}t}U(\overline{z}(t),z(t)) = \mathrm{i}\{H,U\}(\overline{z}(t),z(t)).$$

and by combining this with the modified flow equation [Eq. (2.39)]

$$\{H,U\}(\overline{z},z) = \frac{\langle\Psi(\overline{z})|\hat{H}\hat{P}_0(\overline{z},z)\hat{Q}_{\mathbb{T}_{\mathscr{M}}}(\overline{z},z)\hat{P}_0(\overline{z},z)\hat{U}|\Psi(z)\rangle}{\langle\Psi(\overline{z})|\Psi(z)\rangle} - \frac{\langle\Psi(\overline{z})|\hat{U}\hat{P}_0(\overline{z},z)\hat{Q}_{\mathbb{T}_{\mathscr{M}}}(\overline{z},z)\hat{P}_0(\overline{z},z)\hat{H}|\Psi(z)\rangle}{\langle\Psi(\overline{z})|\Psi(z)\rangle}. \quad (2.51)$$

The constant of motion is thus not automatically reproduced by the evolution according to the time-dependent variational principle. However, the expectation value of a symmetry operator is often not an interesting quantity. For extended systems, one typically has that either $U(\overline{z},z) = 1$ (if $|\Psi(z)\rangle$ is invariant under the action of $\hat{U}$) or $U(\overline{z},z) = 0$ (due to the orthogonality catastrophe if $|\Psi(z)\rangle$ is not invariant). In the first case, $\hat{P}_0(\overline{z},z)\hat{U}|\Psi(z)\rangle \sim (\hat{U}-1)|\Psi(z)\rangle = 0$ and it is clear from the previous equation that $\{H,U\} = 0$, so that the invariance of $|\Psi(z)\rangle$ under $\hat{U}$ is conserved by the evolution according to the time-dependent variational principle.

Finally, we study the case where the symmetry operator $\hat{U}$ corresponds to a continuous symmetry generated by the Hermitian generator $\hat{K} \in \mathbb{L}(\mathbb{H})$, with $[\hat{K},\hat{H}] = 0$. Thus, the expectation value of the generator $\hat{K}$ is also conserved under exact evolution. In contrast to the expectation value of the symmetry operator $\hat{U}$, this is an interesting constant of motion. We define a one-parameter family of transformations $\hat{U}(\epsilon) = \exp(\mathrm{i}\epsilon\hat{K})$. Since we require that for every state $|\Psi(z)\rangle$ in the manifold $\mathscr{M}$, $\hat{U}(\epsilon)|\Psi(z)\rangle = |\Psi(\boldsymbol{u}(z,\epsilon))\rangle \in \mathscr{M}$, we can differentiate this defining relation with respect to ϵ and set $\epsilon = 0$ in order to learn

$$\mathrm{i}\hat{K}|\Psi(z)\rangle = \frac{\partial u^i}{\partial \epsilon}(z,0)|\partial_i\Psi(z)\rangle\,. \quad (2.52)$$

The action of $\hat{K}$ on a state $|\Psi(z)\rangle$ thus has to be exactly captured in $\mathbb{T}_{\mathscr{M}}(z)$, resulting in

$$\hat{P}_0(\overline{z},z)\hat{Q}_{\mathbb{T}_{\mathscr{M}}}(\overline{z},z)\hat{P}_0(\overline{z},z)\hat{K}|\Psi(z)\rangle = \hat{P}_0(\overline{z},z)\hat{K}|\Psi(z)\rangle\,,$$

from which we obtain

$$\{H,K\}(\overline{z},z) = \frac{\langle\Psi(\overline{z})|\hat{H}\hat{P}_0(\overline{z},z)\hat{K}|\Psi(z)\rangle}{\langle\Psi(\overline{z})|\Psi(z)\rangle} - \frac{\langle\Psi(\overline{z})|\hat{K}\hat{P}_0(\overline{z},z)\hat{H}|\Psi(z)\rangle}{\langle\Psi(\overline{z})|\Psi(z)\rangle} = \frac{\langle\Psi(\overline{z})|[\hat{H}-H(\overline{z},z),\hat{K}-K(\overline{z},z)]|\Psi(z)\rangle}{\langle\Psi(\overline{z})|\Psi(z)\rangle} = 0. \quad (2.53)$$

Generators of continuous symmetry transformations are thus constants of motion of

the evolution according to the time-dependent variational principle, provided that the symmetry transformation can be captured exactly in the manifold $\mathcal{M}$.

2.5. Properties of imaginary time evolution

The flow equations [Eq. (2.32)] can also be used to simulate imaginary time evolution by setting $t = -i\tau$. In the full Hilbert space $\mathbb{H}$, imaginary time evolution will converge any random initial state to the exact ground state, provided that the initial state is not orthogonal to this ground state. Note that imaginary time evolution in combination with the modified Schrödinger equation [Eq. (2.34)] does not change the norm of the state. Imaginary time evolution then describes a continuous steepest descent for a convex energy function $H(\overline{\Psi}, \Psi)$ in the convex subspace of constant norm $\langle\Psi|\Psi\rangle$ and thus converges monotonically to the unique minimum[1].

The flow of the time-dependent variational principle given by Eq. (2.32) does not represent a simple steepest descent in parameter space, unless the parameterization of the states $|\Psi(z)\rangle$ is chosen such that the metric $\widetilde{G}$ is proportional to the unit matrix. The flow equations offer the best approximation to a steepest descent flow in the physical Hilbert space $\mathbb{H}$. For this flow, the rate of change of the energy expectation value is given by

$$\frac{\mathrm{d}}{\mathrm{d}\tau} H(\overline{z}(\tau), z(\tau)) = -2 H_i(\overline{z}(\tau), z(\tau)) \widetilde{G}^{i,\bar{j}}(\overline{z}(\tau), z(\tau)) H_{\bar{j}}(\overline{z}(\tau), z(\tau)) \leq 0. \qquad (2.54)$$

The energy expectation value thus decreases monotonically until the flow reaches a minimum $(\overline{z}^\star, z^\star)$ of the time-independent variational principle [characterized by Eq. (2.3)]. If the energy functional $H(\overline{z}, z)$ on $\mathcal{M}$ has many local minima, there is no guarantee that the flow of the time-dependent variational principle converges towards the global minimum (which is assumed to provide the best approximation of the exact ground state). However, if the variational manifold $\mathcal{M}$ is able to accurately approximate the exact imaginary time evolution, one can hope that the flow inherits the global minimization character of the exact imaginary time flow and does indeed converge to the global optimum for most random initial states.

2.6. Convergence and error measures

We refer once again to the (modified) flow equations in the format of Eq. (2.39). At a point $(\overline{z}, z)$ corresponding to $|\Psi(z)\rangle \in \mathcal{M}$, the evolution vector for the time-dependent variational principle is given by $\hat{Q}_{\mathbb{T}_{\mathcal{M}}}(\overline{z}, z)\hat{P}_0(\overline{z}, z)\hat{H}|\Psi(z)\rangle$. Note that there is no significant difference between real and imaginary time evolution, since we work with a

[1] The full energy function $H(\overline{\Psi}, \Psi)$ in the restriction of $\mathbb{H}$ to a convex subspace of constant norm and phase can have saddle points corresponding to higher eigenstates, but has a single minimum corresponding to the ground state.

complex representation. It thus does not matter whether the time derivative of the variational parameters z contains an additional factor i. Since only the component of the evolution orthogonal to $|\Psi(z)\rangle$ is of importance, we can evaluate the 'norm' of the evolution vector as

$$\begin{aligned}\eta(\overline{z},z) &\triangleq \left\| \hat{P}_0(\overline{z},z)\hat{Q}_{\mathbb{T}_{\mathscr{M}}}(\overline{z},z)\hat{P}_0(\overline{z},z)\hat{H}\,|\Psi(z)\rangle \right\| \\ &= \langle\Psi(\overline{z})|\hat{H}\hat{P}_0(\overline{z},z)\hat{Q}_{\mathbb{T}_{\mathscr{M}}}(\overline{z},z)\hat{P}_0(\overline{z},z)\hat{H}|\Psi(z)\rangle^{1/2} \\ &= \left[H_i(\overline{z},z)\widetilde{G}^{i,\bar{j}}(\overline{z},z)H_{\bar{j}}(\overline{z},z)\right]^{1/2}\end{aligned} \tag{2.55}$$

Note that this is not the true norm due to the appearance of an additional $\hat{P}_0(\overline{z},z)$. But when $|\Psi(z)\rangle \in \mathbb{T}_{\mathscr{M}}(z)$ or $|\Psi(z)\rangle \perp \mathbb{T}_{\mathscr{M}}(z)$ (these cases result in a conserved norm under the modified flow equations), one has $\hat{Q}_{\mathbb{T}_{\mathscr{M}}}(\overline{z},z) = \hat{P}_0(\overline{z},z)\hat{P}_{\mathbb{T}_{\mathscr{M}}}(\overline{z},z)\hat{P}_0(\overline{z},z)$ and $\eta(\overline{z},z) = \left\|\hat{Q}_{\mathbb{T}_{\mathscr{M}}}(\overline{z},z)\hat{P}_0(\overline{z},z)\hat{H}\,|\Psi(z)\rangle\right\|$, such that $\eta(\overline{z},z)$ measures the true norm of the evolution vector.

When applying the time-dependent variational principle to simulate imaginary time evolution, one tries to converge the state to a fixed point $z^\star$ where $\eta(\overline{z}^\star,z^\star) = 0$. The measure $\eta(\overline{z},z)$ can be interpreted as the norm of the physical gradient and can thus be used as a measure of convergence towards the steady state solution $(\overline{z}^\star,z^\star)$. Note that the rate of decrease of the energy expectation value in Eq. (2.54) is given by $\mathrm{d}H(\overline{z}(\tau),z(\tau))/\mathrm{d}\tau = -2\eta(\overline{z}(\tau),z(\tau))^2$. The energy thus converges quadratically faster than the state itself, which is also a manifestation of the quadratic convergence of energy encountered in the time-independent case of the previous section.

On the other hand, we can also assess the error between the evolution according to the time-dependent variational principle and the exact evolution given by the Schrödinger equation [Eq. (2.34)], which is relevant both for real and imaginary time evolution. We thereto define the error measure $\varepsilon(\overline{z},z)$ as

$$\begin{aligned}\varepsilon(\overline{z},z) &\triangleq \left\| \hat{P}_0(\overline{z},z)\big(\hat{\mathbb{1}} - \hat{Q}_{\mathbb{T}_{\mathscr{M}}}(\overline{z},z)\big)\hat{P}_0(\overline{z},z)\hat{H}\,|\Psi(z)\rangle \right\|, \\ &= \left[\langle\Psi(\overline{z})|\hat{H}\hat{P}_0(\overline{z},z)\hat{H}|\Psi(z)\rangle - \eta(\overline{z},z)^2\right]^{1/2}, \\ &= \left[\Delta H(\overline{z},z)^2 - \eta(\overline{z},z)^2\right]^{1/2},\end{aligned} \tag{2.56}$$

with $\Delta H(\overline{z},z) = \left\|\hat{P}_0(\overline{z},z)\hat{H}\,|\Psi(z)\rangle\right\| = \langle\Psi(\overline{z})|(\hat{H}-H(\overline{z},z))^2|\Psi(z)\rangle^{1/2}$. In the steady state solution $(\overline{z}^\star,z^\star)$ of the imaginary time evolution ($\eta(\overline{z}^\star,z^\star)=0$), we trivially obtain $\varepsilon(\overline{z}^\star,z^\star) = \Delta H(\overline{z}^\star,z^\star)$ as it was defined in Eq. (2.10).

3. Probing the excitation spectrum

The flow equations of the time-dependent variational principle [Eq. (2.32)] can be used to study dynamic properties of quantum systems, and to acquire information about

the excitation spectrum. In particular, the stability of the steady state solution $(\overline{z}^\star, z^\star)$ can be examined by linearizing the flow equations: inserting the solution $\big(\overline{z}(t) = \overline{z}^\star + \epsilon \overline{z}_1(t), z(t) = z^\star + \epsilon z_1(t)\big)$ into Eq. (2.32) yields at $\mathcal{O}(\epsilon)$

$$\begin{cases} +\mathrm{i}\widetilde{G}_{\bar{\imath},j}(\overline{z}^\star, z^\star)\dot{z}_1^j(t) = H_{\bar{\imath},j}(\overline{z}^\star, z^\star) z_1^j(t) + H_{\bar{\imath},\bar{\jmath}}(\overline{z}^\star, z^\star)\overline{z}_1^{\bar{\jmath}}(t), \\ -\mathrm{i}\dot{\overline{z}}_1^{\bar{\jmath}}(t)\widetilde{G}_{\bar{\jmath},i}(\overline{z}^\star, z^\star) = \overline{z}_1^j(t) H_{\bar{\jmath},i}(\overline{z}^\star, z^\star) + z_1^j(t) H_{j,i}(\overline{z}^\star, z^\star). \end{cases}$$

where we have assumed that the energy function $H \in C^2(\mathscr{M})$ so that Schwarz's theorem can be applied, and we have defined

$$\begin{aligned} H_{\bar{\imath},j}(\overline{z}, z) = \partial_{\bar{\imath}}\partial_j H(\overline{z}, z) = & \frac{\langle \partial_{\bar{\imath}}\Psi(\overline{z})|\hat{P}_0(\overline{z}, z)\hat{H}\hat{P}_0(\overline{z}, z)|\partial_j\Psi(z)\rangle}{\langle\Psi(\overline{z})|\Psi(z)\rangle} \\ & - H(\overline{z}, z)\frac{\langle \partial_{\bar{\imath}}\Psi(\overline{z})|\hat{P}_0(\overline{z}, z)|\partial_j\Psi(z)\rangle}{\langle\Psi(\overline{z})|\Psi(z)\rangle} \end{aligned} \tag{2.57a}$$

together with

$$\begin{aligned} H_{i,j}(\overline{z}, z) = \partial_i\partial_j H(\overline{z}, z) = & \frac{\langle\Psi(\overline{z})|\hat{H}\hat{P}_0(\overline{z}, z)|\partial_i\partial_j\Psi(z)\rangle}{\langle\Psi(\overline{z})|\Psi(z)\rangle} \\ & - \frac{\langle\Psi(\overline{z})|\hat{H}\hat{P}_0(\overline{z}, z)|\partial_j\Psi(z)\rangle\,\langle\Psi(\overline{z})|\partial_i\Psi(z)\rangle}{\langle\Psi(\overline{z})|\Psi(z)\rangle^2} \\ & - \frac{\langle\Psi(\overline{z})|\hat{H}\hat{P}_0(\overline{z}, z)|\partial_i\Psi(z)\rangle\,\langle\Psi(\overline{z})|\partial_j\Psi(z)\rangle}{\langle\Psi(\overline{z})|\Psi(z)\rangle^2}. \end{aligned} \tag{2.57b}$$

In the steady state solution $(\overline{z}^\star, z^\star)$ the last two terms of Eq. (2.57b) cancel. If we now introduce the Hermitian matrices $N^\star$ and $H^\star$, and the symmetric matrix $M^\star$, as

$$[N^\star]_{\bar{\imath},j} = \widetilde{G}_{\bar{\imath},j}(\overline{z}^\star, z^\star) \tag{2.58a}$$

$$[H^\star]_{\bar{\imath},j} = H_{\bar{\imath},j}(\overline{z}^\star, z^\star) \tag{2.58b}$$

$$[M^\star]_{\bar{\imath},\bar{\jmath}} = H_{\bar{\imath},\bar{\jmath}}(\overline{z}^\star, z^\star) \tag{2.58c}$$

and set $z_1(t) = z_+ \mathrm{e}^{-\mathrm{i}\omega t} + z_- \mathrm{e}^{+\mathrm{i}\omega t}$, we can rewrite the linearized flow equation as a generalized Hermitian eigenvalue equation

$$\omega \begin{bmatrix} N^\star & 0 \\ 0 & -\overline{N^\star} \end{bmatrix} \begin{bmatrix} z_+ \\ \overline{z}_- \end{bmatrix} = \begin{bmatrix} H^\star & M^\star \\ \overline{M^\star} & \overline{H^\star} \end{bmatrix} \begin{bmatrix} z_+ \\ \overline{z}_- \end{bmatrix}. \tag{2.59}$$

The matrix appearing in the right hand side of Eq. (2.59) is the Hessian of the energy functional $H(\overline{z}, z)$ in the steady state solution $(\overline{z}^\star, z^\star)$. If the variational extremum

$(\overline{z}^\star, z^\star)$ is a minimum, this matrix should be positive definite. Note that $\overline{M^\star} = (M^\star)^\dagger$ and that $[M^\star]_{\bar{i},\bar{j}}$ contains $\langle \partial_{\bar{i}} \partial_{\bar{j}} \Psi(\overline{z}) | \hat{P}_0(\overline{z}, z) \hat{H} | \Psi(z) \rangle$. Thus, $M^\star$ measures the projection of the exact evolution vector $\hat{P}_0(\overline{z}, z)\hat{H}\,|\Psi(z)\rangle$ of the Schrödinger equation [Eq. (2.34)] onto the double tangent plane

$$\mathbb{T}^{(2)}_{\mathscr{M}}(z) = \text{span}\left\{ |\partial_i \partial_j \Psi(z)\rangle, \forall i, j \right\} \tag{2.60}$$

which is much larger (higher-dimensional vector subspace of $\mathbb{H}$) than the tangent plane $\mathbb{T}^{(1)}_{\mathscr{M}}(z) = \mathbb{T}_{\mathscr{M}}(z)$ to which $\hat{P}_0(\overline{z}, z)\hat{H}\,|\Psi(z)\rangle$ is projected in the framework of the time-dependent variational principle, as discussed in Subsection 2.2. Indeed, when this linear response theory is applied to the time-dependent Hartree-Fock theory, one obtains the Random Phase Approximation [250], which goes well beyond the mean-field ansatz of the Hartree-Fock theory. For the Gross-Pitaevskii equation, the linearization in Eq. (2.59) is called the Bogoliubov-de Gennes equation [251]. Note that for any eigenvalue $\omega = \omega^{(k)}$ with corresponding eigenvector $(z_+^{(k)}, z_-^{(k)})$, we obtain another eigenvalue $\omega^{(-k)} = -\omega^{(k)}$ with corresponding eigenvector $(z_+^{(-k)} = \overline{z}_-^{(k)}, z_-^{(-k)} = \overline{z}_+^{(k)})$. The spectrum of eigenvalues is thus symmetric around zero.

Since $||M^\star|| \leq ||\hat{P}_0(\overline{z}, z)\hat{H}\,|\Psi(z^\star)\rangle|| = \varepsilon(\overline{z}^\star, z^\star)$, it can be expected that be small when $|\Psi(z^\star)\rangle$ is a good approximation to the exact ground state of $\hat{H}$. In contrast, $H^\star$ is independent of $\varepsilon(\overline{z^\star}, z^\star)$ and contains the restriction of $\hat{H}$ to $\mathbb{T}_{\mathscr{M}}(z^\star)$. We can thus expect $||H^\star|| \gg ||M^\star||$ and we can approximate Eq. (2.59) by

$$\omega \begin{bmatrix} N^\star & 0 \\ 0 & -\overline{N^\star} \end{bmatrix} \begin{bmatrix} z_+ \\ \overline{z}_- \end{bmatrix} = \begin{bmatrix} H^\star & 0 \\ 0 & \overline{H^\star} \end{bmatrix} \begin{bmatrix} z_+ \\ \overline{z}_- \end{bmatrix}.$$

The two different components z_+ and z_- then decouple. Note that the matrix $H^\star$ is in itself positive semidefinite if $(\overline{z}^\star, z^\star)$ represents a variational minimum. We thus find eigenvalues $\omega^{(k)} \geq 0$ for which the $z_-^{(k)} = \mathbf{0}$ and, by using the mapping discussed in the previous paragraph, eigenvalues $\omega^{(-k)} = -\omega^{(k)} \leq 0$ with $z_-^{(-k)} = \overline{z}_+^{(k)}$ and $z_+^{(-k)} = \mathbf{0}$. These eigenvalues and corresponding eigenvectors produce identical solutions $z_1(t)$. We can thus restrict to the z_+ component, which can be interpreted as an application of the time-independent variational principle to the variational manifold $\mathbb{T}_{\mathscr{M}}(z^\star)$. Indeed, this generalized eigenvalue problem is also obtained by applying the Rayleigh-Ritz method to the set of states $\{|\Phi(z_+; z^\star)\rangle = z_+^i\,|\partial_i \Psi(z^\star)\rangle\}$ with $z^\star$ fixed. Thus, if $|\Psi(z^\star)\rangle$ accurately approximates the exact ground state of $\hat{H}$ (such that $\varepsilon(\overline{z}^\star, z^\star) \ll 1$), then we can hope that the tangent plane $\mathbb{T}_{\mathscr{M}}(z^\star)$ contains a good approximation for the lowest excited state(s).

If $\epsilon(\overline{z}^\star, z^\star) \not\ll 1$, then the generalized eigenvalue equation [Eq. (2.59)] can still give a reasonable estimate for the excitation energies, but there is no associated variational ansatz that can be interpreted as an approximation for the corresponding eigenvectors of the Hamiltonian $\hat{H}$.

4. Variational principle for extended quantum systems

Despite the many successes of the (time-independent) variational principle, it should be used carefully. As was already illustrated in Section 1 that the energy converges quadratically faster than most other expectation values, so that a good estimate of the energy in the variational optimum $|\Psi^\star\rangle = |\Psi(z^\star)\rangle$ not necessarily implies a good approximation of physical observables and the general physical behavior of the state. For systems with an infinite number of degrees of freedom, the results at the end of Section 1 are rendered moot due to the orthogonality catastrophe (see Section 1 of the previous chapter). Almost any variational approximation $|\Psi^\star\rangle$ of an extended system without ultraviolet (relativistic theories) or infrared (thermodynamic limit) cutoff that is not the exact ground state $|\Psi^{(0)}\rangle$ satisfies $\langle\Psi^\star|\Psi^{(0)}\rangle = 0$, hence invalidating the starting expression in Eq. (2.5).

4.1. Local error and convergence measures

If the variational approximation is locally similar to the exact ground state, in terms of a local state error $\tilde{\epsilon}$ so that

$$||\hat{\rho}^\star_A - \hat{\rho}^{(0)}_A|| \leq \tilde{\epsilon} \tag{2.61}$$

with $\hat{\rho}^\star_{\mathscr{A}}$ and $\hat{\rho}^{(0)}_{\mathscr{A}}$ the density matrix of the variational approximation and of the exact ground state in some compact subspace $\mathscr{A}$, it should still be possible to accurately obtain the expectation value of local observables. A suitable length scale of $\mathscr{A}$ that guarantees good global properties of the state is given by the correlation length ξ_c.

We now evaluate the $\Delta H(\overline{z}^\star, z^\star)$ for a translation invariant local Hamiltonian $\hat{H} = \sum_{n\in\mathscr{L}} \hat{h}_n$ or $\hat{H} = \int_{\mathscr{R}} \mathrm{d}x \hat{h}(x)$ as in Eq. (1.21), for a system living on a lattice $\mathscr{L}$ or a continuum $\mathscr{R}$. Using translation invariance of the ground state approximation $|\Psi^\star\rangle$ and defining $h(\overline{z}^\star, z^\star) = \langle\Psi^\star|\hat{h}_n|\Psi^\star\rangle$ or $h(\overline{z}^\star, z^\star) = \langle\Psi^\star|\hat{h}(x)|\Psi^\star\rangle$, we obtain

$$\begin{aligned}
\Delta H(\overline{z}^\star, z^\star)^2 &= \sum_{m,n\in\mathscr{L}} \langle\Psi^\star| \left(\hat{h}_n - h(\overline{z}^\star, z^\star)\right)\left(\hat{h}_m - h(\overline{z}^\star, z^\star)\right)|\Psi^\star\rangle \\
&= |\mathscr{L}| \sum_{n\in\mathscr{L}} \langle\Psi^\star| \left(\hat{h}_0 - h(\overline{z}^\star, z^\star)\right)\left(\hat{h}_n - h(\overline{z}^\star, z^\star)\right)|\Psi^\star\rangle \\
\text{or } \Delta H(\overline{z}^\star, z^\star)^2 &= \int_{\mathscr{R}} \mathrm{d}x\mathrm{d}y \, \langle\Psi^\star| \left(\hat{h}(x) - h(\overline{z}^\star, z^\star)\right)\left(\hat{h}(y) - h(\overline{z}^\star, z^\star)\right)|\Psi^\star\rangle \\
&= |\mathscr{R}| \int_{\mathscr{R}} \mathrm{d}x \, \langle\Psi^\star| \left(\hat{h}(0) - h(\overline{z}^\star, z^\star)\right)\left(\hat{h}(x) - h(\overline{z}^\star, z^\star)\right)|\Psi^\star\rangle .
\end{aligned} \tag{2.62}$$

In the thermodynamic limit, the prefactor $|\mathscr{L}|$ or $|\mathscr{R}|$ is diverging. The remaining factor represents the connected correlation function of the terms of the Hamiltonian: due to the expected clustering properties of physical states, this sum or integrand should produce a finite result, since the terms should converge rapidly to zero for $|n| \geq \xi_c/a$ or

$|x| \geq \xi_c$ (with a the lattice spacing; see Eq. (1.57)). An estimate $\tilde{\varepsilon}(\overline{z}^\star, z^\star)$ of the local state error $\tilde{\epsilon}$ (see Eq. (2.61)) in the variational optimum $|\Psi(z^\star)\rangle$ is thus given by

$$\tilde{\varepsilon}(\overline{z}^\star, z^\star) = \sqrt{\Delta H(\overline{z}^\star, z^\star)^2/|\mathscr{L}|} = \varepsilon(\overline{z}^\star, z^\star)/|\mathscr{L}|^{1/2}$$
$$\text{or } \tilde{\varepsilon}(\overline{z}^\star, z^\star) = \sqrt{\Delta H(\overline{z}^\star, z^\star)^2/|\mathscr{R}|} = \varepsilon(\overline{z}^\star, z^\star)/|\mathscr{R}|^{1/2} \quad (2.63)$$

If $|\Psi(z)\rangle$ represents a translation invariant variational ansatz for systems in the thermodynamic limit, then all of its tangent vectors $|\partial_i \Psi(z)\rangle$ are also translation invariant. Assuming that $|\Psi(z)\rangle$ and the tangent plane $\mathbb{T}_{\mathscr{M}}(z)$ live in the same Hilbert space, the normalizability of $|\Psi(z)\rangle$ automatically implies that the tangent vectors cannot be normalized and thus satisfy

$$\langle \partial_i \Psi(\overline{z}) | \partial_j \Psi(z) \rangle \sim |\mathscr{L}| \qquad \text{or} \qquad \langle \partial_i \Psi(\overline{z}) | \partial_j \Psi(z) \rangle \sim |\mathscr{R}|.$$

As a generalization of Subsection 2.6, we can now define local convergence and error measures $\tilde{\eta}(\overline{z}, z)$ and $\tilde{\varepsilon}(\overline{z}, z)$ for the time-dependent variational principle in all points $|\Psi(z)\rangle \in \mathscr{M}$ using the identification

$$\tilde{\eta}(\overline{z}, z) \triangleq \eta(\overline{z}, z)/|\mathscr{L}|^{-1/2} \qquad \text{or} \qquad \tilde{\eta}(\overline{z}, z) \triangleq \eta(\overline{z}, z)/|\mathscr{R}|^{-1/2}, \quad (2.64)$$
$$\tilde{\varepsilon}(\overline{z}, z) \triangleq \varepsilon(\overline{z}, z)/|\mathscr{L}|^{-1/2} \qquad \text{or} \qquad \tilde{\varepsilon}(\overline{z}, z) \triangleq \varepsilon(\overline{z}, z)/|\mathscr{R}|^{-1/2}. \quad (2.65)$$

4.2. Feynman's objections

Unfortunately, it turns out a small local error $\tilde{\epsilon}(\overline{z}^\star, z^\star)$ is hard to obtain in systems where the the range of interacting scales ξ_c/a grows very large, with a representing any kind of ultraviolet cutoff. Three conceptual issues standing in the way of a successful application of the variational principle in this regime where outlined by Feynman in a talk given in 1987 [252]. While Feynman focussed on the case of relativistic quantum field theories (where $a = 0$), his arguments can easily be extended to any system having a large ratio ξ_c/a and are thus worth studying in some detail.

Sensitivity to high frequencies

We have already seen how the energy expectation value of the variational approximation $|\Psi^\star\rangle$ has a much smaller error with respect to the exact solution then the expectation value of most other operators. In systems with a large number of degrees of freedom, this dominance of the ground state energy is much more dramatic. In systems with a large range of interacting energy scales, the ground state energy is typically dominated by the degrees of freedom living at the ultraviolet scales. However, observable physical quantities, *i.e.* the expectation values that we are interested in computing, are related to the degrees of freedom living at the infrared scale. But since the only driving force for any

variational approach is the ground state energy (density), all variational parameters z will be exploited to obtain the best possible description of the ultraviolet degrees of freedom. Variational methods do in general not care about the relatively tiny energy penalty resulting from having an ill-described infrared behavior. Interesting physical expectation values will then be very badly approximated when using the variationally optimized state $|\Psi(z^\star)\rangle$. This argument can even lead to the paradoxical situation where the addition of variational parameters provides a *worse* approximation to physical quantities.

While this problem is a major issue for any system with a large range of relevant energy scales, it is truly catastrophic when the range of energy scales ξ/a diverges: relativistic field theories and critical systems. In relativistic systems, the ultraviolet scales are often associated to the high momentum modes or high frequencies. Feynman was thus accusing the variational principle of being too "sensitive to the high frequencies". To lowest order, the ground state of a relativistic quantum field theory contains the zero-point fluctuations from all energy scales. But since these energy contributions are in itself proportional to the frequency which they are at, the corresponding ground-state energy is dominated by the contribution of the high frequencies. Since there is no ultraviolet cutoff, these high frequency modes are infinitely abundant and create a divergence in the ground state energy (density). Hence, the prime quantity of interest for the application of the variational principle is ill-defined, which already signals a difficulty that the variational principle will face.

In principle, this sensitivity only poses an issue in interacting theories, since free (quadratic) theories can be diagonalized exactly by going to momentum space. The different momentum scales decouple and an exact solution for each scale independently is possible. Only when interactions are present is there no longer an obvious way to decouple the different scales of the system. However, any variational method where the variational parameters z affect both ultraviolet and infrared scales suffer from Feynman's first argument. In particular, this dissertation focusses on variational ansätze formulated in real space, where variational parameters are associated to a specific point of the lattice $\mathscr{L}$ or continuum $\mathscr{R}$. These variational parameters influence both the infrared and ultraviolet behavior of the theory. Hence the sensitivity to high frequencies of the variational classes of the next chapters can already be investigated for free theories.

Only Gaussians

Feynman's second concern is on the nature of suitable variational ansatz states, rather than on an inherent feature of the variational method. His observation was again formulated for relativistic theories, but applies equally to all extended quantum systems. Feynman remarks that a suitable ansatz for an extended quantum system should be extensive or size consistent, *i.e.* the expectation value of any extensive observable —in particular the Hamiltonian– with respect to the trial states $|\Psi(\overline{z}, z)\rangle$ should be proportional to the volume $|\mathscr{L}|$ or $|\mathscr{R}|$ of the system. For compact systems, one can easily construct a set of variational ansatz states by taking the span of the ground state

and a few of the excited states of a nearby free Hamiltonian that can be diagonalized exactly, to which the Rayleigh-Ritz method can then be applied. One famous example in this class is the 'configuration interaction method' for quantum chemistry problems, where first the Hartree-Fock problem is solved and then a basis is constructed from the Hartree-Fock ground state and its lowest lying excitations.

For extended systems, this approach fails because the excited states are not extensive and can thus not contribute to the energy expectation value. We thus end up trying to apply the variational method by using the ground state of a free theory —a *Gaussian* state— as variational ansatz, which is thus equivalent to mean field theory.

We still have to compute expectation values

Feynman's third objection is closely related to the previous. Starting from the ground state of a nearby free theory, it is clear that extensive states can be obtained by creating states with a finite density of excitations. The creation of excitations should then appear inside the argument of an exponential. In quantum chemistry, such an approach is know as coupled cluster theory [253], which has also been used in combination with lattice field theory [254, 255, 256]. However, Feynman argued that for (relativistic) field theories (in the continuum), evaluating expectation values with an analoguous ansatz is as difficult as computing the path integral describing the quantum field theory, but in one dimension less: time has disappeared from this Hamiltonian framework. For non-Gaussian states, Feynman believed that it is impossible to accurately calculate expectation values, as he considered perturbation theory the only means possible to compute these integrals. The resulting errors have a strong influence on the optimal state $|\Psi(z^\star)\rangle$ obtained by applying the variational method and thus on observable quantities derived from it.

4.3. Outlook

Feynman's argument present three major barriers that need to be overcome by any variational approach for extended quantum systems. Not only do we need a good variational class of ansatz states $|\Psi(\overline{z}, z)\rangle$ that is both extensive and is capable of capturing a wide range of physical effects, we also need to ensure that we can efficiently compute expectation values with these ansatz states, either exactly or approximative with a very good accuracy. Preferably, we would like to be able to decouple the different scales in the system in order to also escape Feynman's first argument. If we are not able to do so, the variational approach will inevitably run into trouble in the neighborhood of critical systems and for relativistic theories.

Feynman himself seemed very pessimistic at first and concluded his plea with the following conclusion:

> "I'am going to give away what I want to say, which is that I didn't get anywhere. I got very discouraged and I think I can see why the variational principle is not very useful. So I want to take, for the sake of argument, a very strong view —which is stronger than I really believe— and argue that it is no damn good at all!"

However, in the discussion after his talk, Feynman gave away that he already had a strong suspicion that there might be a way out:

> "Now, in field theory, what's going on over here and what's going on over there and all over space is more or less the same. Why do we have to keep track in our functional of all things going on over there while we are looking at the things that are going on over here? ... It's really quite insane, actually: we are trying to find the energy by taking the expectation value of an operator which is located here and we present ourselves with a functional which is dependent on everything all over the map. That's something wrong. Maybe there is some way to surround the object, or the region where we want to calculate things, by a surface and describe what things are coming in across the surface. It tells us everything that's going on outside."

Feynman even had an intuition for how such a construction could look like:

> "I think it should be possible some day to describe field theory in some other way than with the wave functions and amplitudes. It might be something like the density matrices where you concentrate on quantities in a given locality and in order to start to talk about it you don't immediately have to talk about what's going on everywhere else ... "

Clearly, in light of recent discoveries about the behavior of entanglement in such systems and the relationship with holography (as discussed in Section 2 of the previous chapter), Feynman's intuition was correct. It should be possible to holographically encode the information in a region by a theory living on its boundary and this insight turns out to be crucial in the construction of very flexible variational classes in the next chapters, while still allowing an efficient evaluation by using the boundary theory. Insights from renormalization group theory can provide methods for decoupling the interacting degrees of freedom and eventually lead to algorithms and even a variational ansatz that naturally supersedes Feynman's first objection in Chapter 5.

3

MATRIX PRODUCT STATES FOR QUANTUM LATTICES

A first answer to Feynman's supposed lack of good variational ansätze is the class of matrix product states, a very powerful ansatz for strongly correlated quantum lattice systems in $d = 1$ spatial dimension. Matrix product states arise as the variational ansatz underlying the density matrix renormalization group (see Subsection 3.4 of Chapter 1), even though this was not immediately clear from the original formulation. This observation, first made by Östlund and Rommer [227, 228], allowed for an explosion in the power of this approach. While the density matrix renormalization group was originally a method for computing ground states (and a few excited stated) of finite chains with open boundary conditions, the matrix product state formalism together with quantum information theoretical insights concerning entanglement in extended systems have resulted in the development of powerful extensions for chains with periodic boundary conditions, infinite chains, higher-dimensional systems, finite-temperature properties and nonequilibrium physics (see [257, 258, 259] for an overview). This chapter starts with a summary of definitions and properties regarding matrix product states. Next, the general variational methods for time dependence and excitations that were introduced in the previous chapter are being applied to the variational class of matrix product states. Despite the generality of these methods, this had not been done before and new powerful algorithms for studying the dynamical properties of one-dimensional quantum lattice systems are obtained.

1. Definition and properties of the manifold $\mathcal{M}_{\mathrm{MPS}}$

Consider a one-dimensional lattice $\mathcal{L}$ with $|\mathcal{L}| = N$ sites labeled by the integer $n \in \mathcal{L} = \{1, \ldots, N\}$. The physical length of the system is given by $L = Na$ with a the lattice spacing. Every site n contains a q_n-dimensional quantum variable, so that local Hilbert space $\mathbb{H}_n \cong \mathbb{C}^{q_n}$ is spanned by a basis $\{|s_n\rangle \mid s_n = 1, \ldots, q_n\}$. The total Hilbert space is given by $\mathbb{H}_{\mathcal{L}} = \bigotimes_{n=1}^{N} \mathbb{H}_n$ and spanned by the product basis

$$\mathbb{H}_{\mathcal{L}} = \mathrm{span}\{|s_1 s_2 \ldots s_N\rangle = |s_1\rangle_1 \otimes |s_2\rangle_2 \otimes \cdots \otimes |s_N\rangle_N \mid \forall s_n = 1, \ldots, q_n, \forall n = 1, \ldots, N\}. \quad (3.1)$$

The dimension of $\mathbb{H}_{\mathscr{L}}$ is thus given by $\dim \mathbb{H}_{\mathscr{L}} = \prod_{n=1}^{N} q_n$, and the specification of an arbitrary state $|\Psi\rangle \in \mathbb{H}_{\mathscr{L}}$ requires a value for each of the coefficients $c_{s_1,s_2,\ldots,s_N}$ corresponding to the element $|s_1 s_2 \ldots s_N\rangle$ of the basis.

A matrix product state $|\Psi[A]\rangle \in \mathbb{H}_{\mathscr{L}}$ is defined as

$$|\Psi[A]\rangle \triangleq \sum_{s_1=1}^{q_1} \sum_{s_2=1}^{q_2} \cdots \sum_{s_N=1}^{q_N} \mathrm{tr}\left[A^{s_1}(1) A^{s_2}(2) \cdots A^{s_N}(N)\right] |s_1 s_2 \cdots s_N\rangle, \tag{3.2}$$

where we misuse the functional notation $[A]$ for the dependence on a discrete set of objects $A = \{A(n) \mid n = 1, \ldots, N\}$. For every value of $s_n = 1, \ldots, q_n$, the quantity $A^{s_n}(n)$ represents a matrix of size $D_{n-1} \times D_n$, with $D_0 = D_N$. The coefficients $c_{s_1,s_2,\ldots,s_N}$ are thus obtained as a product of matrices, hence the name. The objects $A(n)$ can also be interpreted as rank 3 tensors with entries $A^{s_n}_{\alpha,\beta}(n)$, where there is one physical index $s_n = 1, \ldots, q_n$ and two virtual indices $\alpha = 1, \ldots, D_{n-1}$ and $\beta = 1, \ldots, D_n$. The integers D_n are called the bond dimension or virtual dimension of the matrix product state. Note that it is always useless to choose $D_n > q_n D_{n-1}$ or $D_{n-1} > q_n D_n$. For example, if $D_n > D_{n-1} q_n$ then define the $(D_{n-1} q_n \times D_n)$-matrix $A_{(\alpha s),\beta}(n)$ from reordering and grouping the indices of the tensor $A(n)$. The rank of the matrix $A_{(\alpha s),\beta}(n)$ is limited by $D_{n-1} q_n$, and there exists a $D_{n-1} q_n \times D_{n-1} q_n$ matrix $B_{(\alpha s),\gamma}(n)$ and $D_{n-1} q_n \times D_n$ matrix $Q_{\gamma,\beta}$ such that $A_{(\alpha s),\beta}(n) = \sum_{\gamma=1}^{D_{n-1} q_n} B_{(\alpha s),\gamma} Q_{\gamma,\beta}$. Without loss of accuracy, we can redefine $A^s(n) \leftarrow B^s$, $A^s(n+1) \leftarrow Q A^s(n+1)$ and $D_n \leftarrow D_{n-1} q_n$. A similar proof holds for the case $D_{n-1} > q_n D_n$.

For a given lattice $\mathscr{L}$ with local Hilbert spaces $\mathbb{H}_n$ and fixed bond dimensions $\{D_n, \forall n = 1, \ldots, L\}$, the variational manifold $\mathscr{M}_{\mathrm{MPS}} \subset \mathbb{H}_{\mathscr{L}}$ is thus given by

$$\mathscr{M}_{\mathrm{MPS}} = \left\{ |\Psi[A]\rangle, \forall A^{s_n}(n) \in \mathbb{C}^{D_{n-1} \times D_n} \mid \forall s_n = 1, \ldots, q_n, \forall n = 1, \ldots, L \right\}. \tag{3.3}$$

The notation $\mathscr{M}_{\mathrm{MPS}}$ will not be cluttered with explicit notation of the lattice $\mathscr{L}$ or the local Hilbert dimensions $\{q_n\}$. This information will always be clear from the context. The bond dimensions $\{D_n\}$ can be indicated explicitly as $\mathscr{M}_{\mathrm{MPS}\{D_n\}}$ when confusion between different choices of $\{D_n\}$ is possible. If a different set of bond dimensions $\{D'_n\}$ satisfies $D'_n \leq D_n$, $\forall n = 1, \ldots, N$, then $\mathscr{M}_{\mathrm{MPS}\{D'_n\}} \subset \mathscr{M}_{\mathrm{MPS}\{D_n\}}$. A matrix product state $|\Psi[A']\rangle \in \mathscr{M}_{\mathrm{MPS}\{D'_n\}}$ can be identified with a state $|\Psi[A]\rangle \in \mathscr{M}_{\mathrm{MPS}\{D_n\}}$ by setting, $\forall s = 1, \ldots, q_n$, $A^s_{\alpha,\beta}(n) = (A')^s_{\alpha,\beta}(n)$ for $\alpha = 1, \ldots, D'_{n-1}$ and $\beta = 1, \ldots, D'_n$, and $A^s_{\alpha,\beta}(n) = 0$ for all other combinations of α and β. The manifold $\mathscr{M}_{\mathrm{MPS}\{D_n\}}$ is definitely not a vector space, since for two states $|\Psi[A_1]\rangle, |\Psi[A_2]\rangle \in \mathscr{M}_{\mathrm{MPS}\{D_n\}}$, the matrix product state representation of $|\Psi[A_1]\rangle + |\Psi[A_2]\rangle$ requires in the most general case a set of bond dimensions $\{D'_n = 2D_n\}$. Put differently, in the most general case we obtain $|\Psi[A_1]\rangle + |\Psi[A_2]\rangle = |\Psi'[A']\rangle \in \mathscr{M}_{\mathrm{MPS}\{D'_n\}}$, where $(A')^s(n)$ is constructed as $(A')^s(n) = A^s_1(n) \oplus A^s_2(n)$, $\forall s = 1, \ldots, q_n$, $\forall n = 1, \ldots, N$. The variational manifold does however contain complete rays of states, since for a state $|\Psi[A]\rangle \in \mathscr{M}_{\mathrm{MPS}\{D_n\}}$ and $\lambda \in \mathbb{C}$, the

state $\lambda|\Psi[A]\rangle \in \mathscr{M}_{\mathrm{MPS}\{D_n\}}$ and a matrix product state representation can be obtained by multiplying the matrices $A^s(n)$ for one particular value of n by λ. The arbitrariness in the value of n already indicates that there is some redundancy in the matrix product state representation. We now define the matrix product state parameter space $\mathbb{A}_{\mathrm{MPS}}$ as

$$\mathbb{A}_{\mathrm{MPS}} = \bigoplus_{n=1}^{N} \mathbb{C}^{D_{n-1}\times q_n \times D_n}, \tag{3.4}$$

with

$$\dim \mathbb{A}_{\mathrm{MPS}} = \sum_{n=1}^{N} D_{n-1} q_n D_n. \tag{3.5}$$

The matrix product state then represents a map

$$\Psi : \mathbb{A}_{\mathrm{MPS}} \mapsto \mathscr{M}_{\mathrm{MPS}} \subset \mathbb{H}_{\mathscr{L}} : A = \{A(n) \mid n = 1,\ldots,N\} \mapsto |\Psi[A]\rangle \tag{3.6}$$

that is not injective. We thus have $\dim \mathscr{M}_{\mathrm{MPS}} < \dim \mathbb{A}_{\mathrm{MPS}}$.

We now also define the tangent plane $\mathbb{T}_{\mathscr{M}_{\mathrm{MPS}}}[A] = \mathbb{T}_{\mathrm{MPS}}[A] \subset \mathbb{H}_{\mathscr{L}}$ at a certain point $A = \{A(n) \mid n = 1,\ldots,N\} \in \mathbb{A}_{\mathrm{MPS}}$. For the tangent vectors, the general notation

$$\begin{aligned} |\Phi^{[A]}[B]\rangle = |\Phi[B;A]\rangle &\triangleq \sum_{n=1}^{N} \sum_{i=1}^{D_{n-1}q_nD_n} B^i(n) \frac{\partial}{\partial A^i(n)} |\Psi[A(n)]\rangle \\ &= \sum_{n=1}^{N} \left(\sum_{s_1=1}^{q_1} \cdots \sum_{s_n=1}^{q_n} \cdots \sum_{s_N=1}^{q_N} \mathrm{tr}\left[A^{s_1}(1)\cdots B^{s_n}(n)\cdots A^{s_N}(N)\right] |s_1 s_2 \cdots s_N\rangle \right) \end{aligned} \tag{3.7}$$

is introduced, where i is a collective index $i = (\alpha, s, \beta)$ that contains both the physical index s and the matrix indices α and β. A general tangent vector $|\Phi[B;A]\rangle$ is thus built from N matrix product states, where one of the tensors $A(n)$ is replaced by $B(n)$. Given the remark above, the smallest manifold $\mathscr{M}_{\mathrm{MPS}\{D'_n\}}$ in which $\mathbb{T}_{\mathrm{MPS}}[A]$ for a general point $A = \{A(n) \mid n = 1,\ldots,N\}$ can be embedded has bond dimensions $\{D'_n = ND_n\}$. Obviously, the tangent plane $\mathbb{T}_{\mathrm{MPS}}[A]$ is a vector space, and we can define $\Phi^{[A]}$ as the linear homomorphism

$$\Phi^{[A]} : \mathbb{A}_{\mathrm{MPS}} \mapsto \mathbb{T}_{\mathrm{MPS}}[A] \subset \mathbb{H}_{\mathscr{L}} : \{B(n) \mid n = 1,\ldots,N\} \mapsto |\Phi^{[A]}[B]\rangle = |\Phi[B;A]\rangle \tag{3.8}$$

for every fixed value of $A = \{A(n) \mid n = 1,\ldots,N\}$. Note in particular that $|\Phi[A;A]\rangle = N|\Psi[A]\rangle$, so that $|\Psi[A]\rangle \in \mathbb{T}_{\mathrm{MPS}}[A]$. This will proof relevant want applying the time dependent variational principle, as was discussed in general in Subsection 2.3 of the previous chapter. We thus also define the orthogonal complement of $|\Psi[A]\rangle$ in $\mathbb{T}_{\mathrm{MPS}}[A]$ as $\mathbb{T}^{\perp}_{\mathrm{MPS}}[A]$. $\mathbb{T}^{\perp}_{\mathrm{MPS}}[A]$ only contains tangent vectors $|\Phi[B;A]\rangle$ that do not induce a in the norm of $|\Psi[A+\eta B]\rangle$ up to the first order of η. This requires that B is restricted to those values for which $\langle\Psi[\overline{A}]|\Phi[B;A]\rangle = 0$. When no confusion is possible, the

point $A = \{A(n) \mid n = 1,\ldots,N\}$ at which the tangent plane is constructed will be omitted from the notation of the tangent vectors and the tangent plane. Both the mathematical as well as the physical properties of the non-linear map Ψ, the linear map Φ and the corresponding sets $\mathscr{M}_{\mathrm{MPS}}$, $\mathbb{A}_{\mathrm{MPS}}$ and $\mathbb{T}_{\mathrm{MPS}}$ are studied in the remainder of this section.

1.1. Density matrix renormalization group and Schmidt decompositions

A suitable variational ansatz for a system on a lattice with open boundary conditions can be obtained by choosing $D_0 = D_N = 1$ in the general form of Eq. (3.2). The trace in the definition of $|\Psi[A(n)]\rangle$ then becomes redundant. As was realized by Östlund and Rommer in [227, 228], the infinite size algorithm of density matrix renormalization group (see Subsection 3.4 of Chapter 1) implicitly creates such matrix product states with open boundary conditions. Indeed, in every step, the ground state on a superblock $(S' \cup E')$ corresponding to a lattice $\mathscr{L}'$ with $|\mathscr{L}'| = N+2$ is computed. The respective Hilbert spaces of $S' = \{1,\ldots,n+1\}$ and $E' = \{n+2,\ldots,|\mathscr{L}'||\}$ (with $n = N/2$) are given by $\mathbb{H}^{(S')} = \mathrm{span}\{|\Phi_\alpha^{(S)}\rangle \otimes |s\rangle_{n+1} \mid \alpha = 1,\ldots,D_n; s = 1,\ldots,q_{n+1}\}$ and $\mathbb{H}^{(E')} = \mathrm{span}\{|s\rangle_{n+2} \otimes |\Phi_\alpha^{(E)}\rangle \mid s = 1,\ldots,q_{n+2}; \alpha = 1,\ldots,D_{n+2}\}$, with $\{|\Phi_\alpha^{(S)}\rangle \mid \alpha = 1,\ldots,D_n\}$ and $\{|\Phi_\alpha^{(E)}\rangle \mid \alpha = 1,\ldots,D_{n+2}\}$ the left (system) and right (environment) Schmidt vectors corresponding to the $D_n = D_{n+2}$ largest Schmidt vectors of the ground state on the superblock from the previous iteration. If the new ground state $|\Psi'\rangle$ has a Schmidt decomposition

$$|\Psi'\rangle = \sum_{\alpha=1}^{\min(q_{n+1},q_{n+2})D_n} \lambda'_\alpha(n+1)|\Phi_\alpha^{(S')}\rangle \otimes |\Phi_\alpha^{(E')}\rangle, \tag{3.9}$$

then new reduced Hilbert spaces for S' and E' can be constructed as $\mathbb{H}^{(S')} = \mathrm{span}\{|\Phi_\alpha^{(S')}\rangle \mid \alpha = 1,\ldots,D_{n+1}\}$ and $\mathbb{H}^{(E')} = \mathrm{span}\{|\Phi_\alpha^{(E')}\rangle \mid \alpha = 1,\ldots,D_{n+1}\}$ where the new bond dimension D_{n+1} satisfies $D_{n+1} < \min(q_{n+1},q_{n+2})D_n$. We can then express the new Schmidt vectors as

$$|\Phi_\alpha^{(S')}\rangle = \sum_{\beta=1}^{D_n}\sum_{s=1}^{q_{n+1}} L^s_{\beta,\alpha}(n+1)|\Phi_\beta^{(S)}\rangle \otimes |s\rangle_{n+1}, \quad \forall \alpha = 1,\ldots,D_{n+1} \tag{3.10}$$

and

$$|\Phi_\alpha^{(E')}\rangle = \sum_{s=1}^{q_{n+2}}\sum_{\beta=1}^{D_{n+2}} R^s_{\alpha,\beta}(n+2)\lambda_\beta(n+2)|s\rangle_{n+2} \otimes |\Phi_\beta^{(E)}\rangle, \quad \forall \alpha = 1,\ldots,D_{n+1}. \tag{3.11}$$

Grouping everything together and shifting $n \leftarrow n-1$, we obtain as final ground state $|\Psi\rangle$ on the lattice $\mathscr{L}$

$$|\Psi\rangle = \sum_{s_1=1}^{q_1}\sum_{s_2=1}^{q_2}\cdots\sum_{s_N=1}^{q_N} L^{s_1}(1)\cdots L^{s_n}(n) C R^{s_{n+1}}(n+1)\cdots R^{s_N}(N)\,|s_1\ldots s_n s_{n+1}\ldots s_N\rangle, \quad (3.12)$$

with $n = N/2$ and where C is a diagonal matrix of size $D_n \times D_n$ that contains on its diagonal the Schmidt values of the last iteration. The matrix C is sometimes called the center matrix and can be absorbed into either $L(n)$ or $R(n+1)$. A matrix product state with bond dimensions $\{D_n\}$ satisfying $D_n = D_{N-n}$ is obtained, where n is henceforth again an arbitrary site label (*i.e.* $n = 1,\ldots,N$) is obtained. Because of the orthonormality of the Schmidt vectors, the matrices $L^s(n)$ and $R^s(n)$ satisfy respectively left and right orthogonality conditions given by

$$\sum_{s=1}^{q_n} L^s(n)^\dagger L^s(n) = \mathbb{1}_{D_n}, \qquad \forall n = 1,\ldots,\frac{N}{2}, \quad (3.13a)$$

$$\sum_{s=1}^{q_n} R^s(n) R^s(n)^\dagger = \mathbb{1}_{D_{n-1}} \qquad \forall n = \frac{N}{2}+1,\ldots,N. \quad (3.13b)$$

The normalization of the state is given by $\langle\Psi|\Psi\rangle = \mathrm{tr}(C^\dagger C)$. In the infinite size algorithm, the ground state on the new superblock $(S' \cup E')$ is constructed from the reduced Hilbert spaces $\widetilde{\mathbb{H}}^{(S)}$ and $\widetilde{\mathbb{H}}^{(E)}$ that were optimal for the representation of the ground state on $(S \cup E)$. It is not automatically true that these reduced Hilbert spaces are also optimal for the ground state on $(S' \cup E')$. The finite size algorithm sets as it goal to further refine the reduced Hilbert spaces with respect to every bipartition of the lattice $\mathscr{L} = \{1,\ldots,N\}$ into a left part $\mathscr{L}_{\mathrm{L}}^{(n)} = \{1,\ldots,n\}$ and a right part $\mathscr{L}_{\mathrm{R}}^{(n)} = \{n+1,\ldots,N\}$, corresponding to a cut in the chain between site n and site $n+1$. It hereto optimizes over sites n and $n+1$ while keeping the Schmidt vectors of the system $\{1,\ldots,n-1\}$ and the environment $\{n+2,\ldots,N\}$ fixed, where the position n is swept from left to right and back several times. This algorithm served as an inspiration for a variational strategy for matrix product states. Since the matrix product state ansatz is linear in each of the tensors $A(n)$ individually, when all other tensors are kept fixed, the variational optimization with respect to $A(n)$ alone is a simple eigenvalue equation. The non-linearity stems from the coupling between the different tensors. However, good convergence is obtained by fixing all tensors but $A(n)$, optimizing $A(n)$ and sweeping n back and forth several times. This is *the* standard method for solving the time-independent variational optimization problem in case of matrix product states with open boundary conditions. It differs from the original formulation of the density matrix renormalization group in the fact that now a single site is optimized and it therefore is truly variational: the energy decreases monotonically in every step.

If the bond dimensions $\{D_n\}$ can grow unboundedly, an exact matrix product state representation of any state $|\Psi\rangle \in \mathbb{H}_{\mathscr{L}}$ can be constructed —following the analysis of

[260]— by successive Schmidt decompositions. Let the Schmidt decomposition of $|\Psi\rangle$ corresponding to the cut between sites n and site $n+1$ be given by

$$|\Psi\rangle = \sum_{\alpha=1}^{D_n} \lambda_\alpha(n) |\Phi_\alpha^{[1\cdots n]}\rangle \otimes |\Phi_\alpha^{[(n+1)\cdots N]}\rangle \tag{3.14}$$

where $\lambda_\alpha(n)$ are the Schmidt coefficients and $|\Phi_\alpha^{[1\cdots n]}\rangle$, $|\Phi_\alpha^{[(n+1)\cdots N]}\rangle$ are respectively the left and right orthonormal Schmidt vectors ($\forall \alpha = 1,\ldots,D_n$), with the Schmidt number D_n given by

$$\begin{aligned} D_n &= \min\left(\dim \mathbb{H}_{\mathscr{L}_{\mathrm{L}}^{(n)}}, \dim \mathbb{H}_{\mathscr{L}_{\mathrm{R}}^{(n)}}\right) \\ &= \min\left(\prod_{m=1}^{n} q_m, \prod_{m=n+1}^{N} q_m\right), \quad \forall n = 1,\ldots,N-1. \end{aligned} \tag{3.15}$$

In addition, we define $D_0 = D_N = 1$. The right Schmidt vectors according to the cut between site $n-1$ and n can be expressed in terms of the local basis at site n and the right Schmidt vectors according to the cut between site n and $n+1$, resulting in

$$|\Phi_\alpha^{[n\cdots N]}\rangle = \sum_{s=1}^{q_n} \sum_{\beta=1}^{D_n} \Gamma^s_{\alpha,\beta}(n) \lambda_\beta(n) |s\rangle_n \otimes |\Phi_\beta^{[(n+1)\cdots N]}\rangle . \tag{3.16}$$

Reiterating this equation from $n=2$ to $n=N-1$, and using that the left Schmidt vector for the cut between site 1 and site 2 can be written in terms of the local basis at site 1 as

$$|\Phi_\alpha^{[1]}\rangle = \sum_{s=1}^{q_1} \Gamma^s_\alpha(1) |s\rangle_1 \tag{3.17}$$

and the right Schmidt vector for the cut between site $N-1$ and site N can be written in terms of the local basis at site N as

$$|\Phi_\alpha^{[N]}\rangle = \sum_{s=1}^{q_N} \Gamma^s_\alpha(N) |s\rangle_N , \tag{3.18}$$

we obtain

$$|\Psi\rangle = \sum_{s_1=1}^{q_1} \sum_{s_2=1}^{q_2} \cdots \sum_{s_N=1}^{q_N} \Gamma^{s_1}(1)\Lambda(1)\Gamma^{s_2}(2)\Lambda(2)\cdots\Gamma^{s_N}(N) |s_1 s_2 \ldots s_N\rangle , \tag{3.19}$$

where the $\Gamma^s(n)$ are $D_{n-1} \times D_n$ matrices ($\forall s = 1,\ldots,q_n$) and $\Lambda(n)$ is a $D_n \times D_n$ diagonal matrix containing the Schmidt spectrum of the state $|\Psi\rangle$ according to cut between sites n and $n+1$. Every state in $\mathbb{H}_{\mathscr{L}}$ can thus be represented as a matrix product state, provided

that the maximally allowed bond dimension D can grow to

$$D \geq \max_n \left[\min \left(\dim \mathbb{H}_{\mathscr{L}_{\mathrm{L}}^{(n)}}, \dim \mathbb{H}_{\mathscr{L}_{\mathrm{R}}^{(n)}} \right) \right]. \tag{3.20}$$

There is plethora of choices for defining the matrices $A^s(n)$ in terms of $\Lambda(n-1)$, $\Gamma^s(n)$ and $\Lambda(n)$, which is related to the redundancy in the matrix product state representation. Up to a reordering in the Schmidt spectra on the diagonal of $\Lambda(n)$, the current decomposition of a state is unique. The left Schmidt vectors corresponding to a cut between site n and site $n+1$ can now also be expressed in terms of the local basis at site n and the left Schmidt vectors corresponding to a cut between site $n-1$ and site n as

$$|\Phi_\alpha^{[1\cdots n]}\rangle = \sum_{\beta=1}^{D_{n-1}} \sum_{s=1}^{q_n} \lambda_\beta(n-1) \Gamma^s_{\beta,\alpha}(n) |\Phi_\beta^{[1\cdots(n-1)]}\rangle \otimes |s\rangle_n . \tag{3.21}$$

The orthonormality of the Schmidt vectors and the normalization of the state (*i.e.* $\langle\Psi|\Psi\rangle = 1$) now imply left and right orthogonality conditions in the form

$$\sum_{s=1}^{q_n} \Gamma^s(n)^\dagger \Lambda(n-1)^2 \Gamma^s(n) = \mathbb{1}_{D_n}, \tag{3.22a}$$

$$\sum_{s=1}^{q_n} \Gamma^s(n) \Lambda(n)^2 \Gamma^s(n)^\dagger = \mathbb{1}_{D_{n-1}}, \qquad \forall n = 1, \ldots, N. \tag{3.22b}$$

1.2. Entanglement scaling and representation accuracy

Even though it is nice to know by choosing the set of bond dimensions $\{D_n\}$ according to Eq. (3.15) we obtain $\mathscr{M}_{\mathrm{MPS}\{D_n\}} = \mathbb{H}_{\mathscr{L}}$, the matrix product state formalism will then be more complex then just working with the original coefficients $c_{s_1,s_2,\ldots,s_N}$, because of the redundancy in the representation. In practice, we are interested in matrix product states where $D = \max_n D_n$ is much smaller than the bound given in Eq. (3.20), which results in $D = q^{L/2}$ if $q_n = q$ for all sites and would thus requires an exponential scaling in the system size. For a maximum bond dimension D, the maximal amount of bipartite entanglement corresponding to a cut between two sites is given by $S_{\max} = \log D$, by choosing all Schmidt values $\lambda_\alpha = 1/\sqrt{D}$, $\forall \alpha = 1, \ldots, D$. Since our goal is an accurate representation of ground states of locally interacting quantum systems, the worst case scaling of entanglement is found for critical systems [one half of Eq. (1.66) for a system with open boundary conditions]. A very naive comparison would allow to conclude that $D \sim (L/2)^{(c+\bar{c})/12}$ with c and $\bar{c}$ the holomorphic and antiholomorphic central charge of the conformal theory that describes the low-energy behavior of the critical point. This polynomial scaling in the system size is already a big improvement on the exponential scaling required to represent the complete Hilbert space $\mathbb{H}_{\mathscr{L}}$ and is a first indication

that ground states of short-range interacting Hamiltonians can be encoded *efficiently*[1] by matrix product states.

However, this naive argument cannot be considered a proof, since the spectrum of Schmidt values λ_α in extended quantum systems is not constant up to some value $\alpha = D$ and zero beyond. The asymptotic formula for the entanglement spectrum $\lambda_\alpha^2 \sim \exp(-k \ln^2 \alpha)$ (with k some arbitrary constant) was derived in [261]. The strategy of the density matrix renormalization group is to retain the Schmidt vectors corresponding to the largest Schmidt values. It can be shown that this is a good strategy that keeps errors small. For a general bipartite system $C = A \cup B$, let $|\Psi\rangle$ be a given state with Schmidt decomposition $|\Psi\rangle = \sum_{\alpha=1}^{D} \lambda_\alpha |\Phi_\alpha^{(A)}\rangle \otimes |\Phi_\alpha^{(B)}\rangle$, where there are D non-zero Schmidt coefficients[2] λ_α which are assumed to be ordered in decreasing order $\lambda_1 \geq \lambda_2 \geq \ldots \geq \lambda_D$. If $|\Psi\rangle$ has to be approximated by a state $|\Psi'\rangle$ where only $D' < D$ non-zero Schmidt coefficients are allowed, then the best approximation —in terms of minimizing $\big\||\Psi\rangle - |\Psi'\rangle\big\|$— is obtained by choosing $|\Psi'\rangle = \sum_{\alpha=1}^{D'} \lambda_\alpha |\Phi_\alpha^{(A)}\rangle \otimes |\Phi_\alpha^{(B)}\rangle$. Indeed, this statement is equivalent to stating that the best approximation of a matrix $\Psi_{i,j}$ with rank D by a matrix $\Psi'_{i,j}$ with rank D' is obtained by computing the singular value decomposition of Ψ and only retaining the D' largest singular values, which is a well known property of the singular value decomposition. The total error is given by the sum of the squares of the neglected Schmidt coefficients, *i.e.*

$$\epsilon^2 = \min_{\Psi'} \big\||\Psi\rangle - |\Psi'\rangle\big\|^2 = \sum_{\alpha=D'+1}^{D} \lambda_\alpha^2. \tag{3.23}$$

In addition, for every operator $\hat{O}$ having non-trivial support either in subsystem A or B, we obtain

$$\Big|\langle\Psi|\hat{O}|\Psi\rangle - \langle\Psi'|\hat{O}|\Psi'\rangle\Big| = \epsilon^2 \|\hat{O}\|. \tag{3.24}$$

If on a lattice $\mathscr{L}$ with open boundary conditions, the state $|\Psi\rangle \in \mathbb{H}_{\mathscr{L}} = \mathscr{M}_{\mathrm{MPS}\{D_n\}}$ has an exact matrix product state representation $|\Psi[A(n)]\rangle$ and it has to be approximated by a state $|\Psi'[A'(n)]\rangle \in \mathscr{M}_{\mathrm{MPS}\{D'_n\}}$ with $D'_n \leq D_n$, $\forall n = 1, \ldots, N$, then a trivial generalization of the above construction fails as the approximation made in one set of Schmidt coefficients $\lambda_\alpha(n)$ corresponding to a cut between sites n and $n+1$ influences the Schmidt vectors corresponding to a cut between sites n' and $n'+1$. It can however be shown that the best approximation $|\Psi'[A'(n)]\rangle$ satisfies (see [262])

$$\epsilon^2 = \min_{\{A'(n)\}} \big\||\Psi[A(n)]\rangle - |\Psi'[A'(n)]\rangle\big\|^2 \leq 2 \sum_{n=1}^{N-1} \epsilon(n)^2, \tag{3.25}$$

[1] For $D \sim \mathcal{O}(\mathrm{poly}(N))$, the number of parameters in the matrix product state representation is much smaller than $\dim \mathbb{H}_{\mathscr{L}} \sim \exp(N)$ and the coding scheme is thus efficient. That matrix product states also allow for efficient simulability (*e.g.* computing expectation values, simulating time evolution, ...) is illustrated further on.

[2] The number of non-zero Schmidt coefficients can be counted by using the Rényi entropy $S_\alpha(\rho^{(A)}) = S_\alpha(\rho^{(B)})$ for $\alpha \to 0$.

with

$$\epsilon(n)^2 = \sum_{\alpha=D'_n+1}^{D_n} \lambda_\alpha(n)^2. \tag{3.26}$$

Proving that this bound implies an efficient encoding of ground states satisfying area laws (with at most logarithmic violations) requires some additional steps. Unfortunately, such a statement cannot be proven using the Von Neumann block entropy as entanglement measure. Such a proof is however possible by using the generalized bipartite entanglement entropy $S_\alpha^{(\mathscr{A})} = S_\alpha(\rho^{(\mathscr{A})})$ of a region $\mathscr{A}$ and its compliment, with $S_\alpha(\rho^{(\mathscr{A})})$ the Rényi entropy of the reduced density matrix of $\mathscr{A}$. If a density matrix $\hat{\rho}$ has to be approximated by at most D' of its largest eigenvalues, one can proof that ($\forall 0 < \alpha < 1$)

$$\ln\left(\epsilon^2\right) = \ln\left(\sum_{\alpha=D'+1}^{+\infty}\right) \leq \frac{1-\alpha}{\alpha}\left[S_\alpha(\rho) - \ln\left(\frac{D'}{1-\alpha}\right)\right], \tag{3.27}$$

where we have symbolically set $+\infty$ for the number of non-zero eigenvalues of $\hat{\rho}$. Combining this relation with Eq. (3.25) and using the worst-case scaling of the generalized entanglement entropy for critical theories [one half of Eq. (1.66)], we obtain a sufficient condition for the bond dimension D' to approximate a critical state on a finite lattice with N sites up to a state error ϵ as

$$D' \geq (1-\alpha)\left(\frac{2N}{\epsilon^2}\right)^{\frac{\alpha}{1-\alpha}} N^{\frac{c+\bar{c}}{12}(1+1/\alpha)}. \tag{3.28}$$

This polynomial scaling in N is much slower than the exponential scaling of the bond dimension D of the exact representation [Eq. (3.20)]. For the ordinary entanglement entropy $\alpha \to 1$, this bound diverges so that knowledge about the Rényi entropy of a block is required in order to conclude efficient representability. Not even a strict area law (gapped systems) for the entanglement entropy is sufficient to conclude efficient representability with matrix product states. This was shown in [263], where the relation between efficient representability and scaling of the generalized entanglement entropy for $\alpha < 1$, $\alpha = 1$ and $\alpha > 1$ was further investigated. Henceforth, we reserve the symbol D for the bond dimension of the matrix product state approximation and do no longer refer to the bond dimension of the exact representation.

1.3. Alternative constructions

While the Schmidt decomposition is very powerful and allows to derive analytic representability bounds, it is restricted to the setting of one-dimensional lattices with open boundary conditions. If the lattice $\mathscr{L}$ has periodic boundary conditions, a single cut between two sites does not result in a bipartition of $\mathscr{L}$. The original formulation of the density matrix renormalization group was therefore not able to obtain the same accu-

racy for systems with periodic boundary conditions and new concepts from quantum information theory were necessary. We discuss here three different interpretations of the variational class of matrix product states that highlight different aspects and have proven relevant in the construction of generalizations beyond matrix product state with open boundary conditions.

Matrix product states as valence bond solids

The concept of a *valence bond* was introduced in chemistry in 1916 by Lewis: a covalent bond between two atoms is formed by a pairing of two electrons, each living —initially unpaired— in a valence atomic orbital of either atom. The availability of different yet equivalent valence bond configurations gives rise to the phenomenon of *resonance* —the quantum state is a superposition over all different valence bond configurations— as pointed out by Pauling. The idea of resonating valence bond states for extended systems, where a macroscopic number of equivalent configurations are available, was adopted by Anderson as a proposal for a new type of insulator [264] and later as a proposal to explain high temperature superconductivity [265, 266].

The seminal work of Affleck, Kennedy, Lieb and Tasaki introduced a different kind of valence bond state, the *valence bond solid* [267, 268]. With respect to our purpose, a valence bond solid for a lattice $\mathscr{L}$ can be introduced by adding to every site n a number of ancillas a_n, b_n, ... describing a D-dimensional quantum variable. Valence bonds can be constructed by placing ancillas of different sites in a maximally entangled state, *e.g.* $|\mathrm{VB}\rangle_{a_n,b_{n+1}} = \sum_{\alpha=1}^{D} |\alpha\rangle_{a_n} \otimes |\alpha\rangle_{b_{n+1}}$. For $D = 2$, the maximally entangled state is equivalent to (but not equal to) the spin singlet of two pairing electrons. When all valence bonds have been created, the joint state of all ancillas of a particular site n are projected to a physical state of the site with a projection operator

$$\mathcal{A}(n) = \sum_{s=1}^{q_n} \sum_{\{\alpha,\beta,\ldots\}=1}^{D} A^{s}_{\alpha,\beta,\ldots}(n) |s\rangle_n \left(\langle\alpha|_{a_n} \otimes \langle\beta|_{b_n} \otimes \cdots \right). \tag{3.29}$$

This construction was introduced in quantum information theory in [269] as a scheme for universal quantum computation based on local measurements. For nearest-neighbor or other short-range interacting Hamiltonians, the number of ancillas per site can be chosen equal to the coordination number of the lattice, and a valence bond between each site and its nearest neighbors can be constructed. Through the projection, a physical state with long-range entanglement is obtained. For a one-dimensional lattice with periodic boundary conditions, this gives rise to the matrix product states and indicates the necessity of the trace in Eq. (3.2) in order to establish a bond between site 1 and site N [270], as in Figure 3.1(a). This construction can also be used to define general variational classes for lattice systems in arbitrary dimensions, where the rank N coefficient tensor $c_{s_1,s_2,\ldots,s_N}$ is obtained through the contraction of a network of lower rank tensors. The straightforward generalization of matrix product states to higher dimensions are the so-

called *projected entangled pair states* [271], sketched in Figure 3.1(b). As will be explained in the next subsection, the computational complexity of evaluating expectation values increases as the number of loops of valence bonds increases. Hence, the matrix product state with open boundary conditions (zero loops) is more efficient than the matrix product state with periodic boundary conditions (one loop), whereas the projected entangled pair state (macroscopic number of loops) requires approximate methods for the evaluation of expectation values.

Finally, as a generalization of the proof in [272] for valence bond solids, it was proven in [273] that every matrix product state is the exact ground state (uniqueness is only guaranteed under additional conditions) of a frustration free Hamiltonian (see Subsection 2.2 of Chapter 1) with interaction length $2\log D/\log q$.

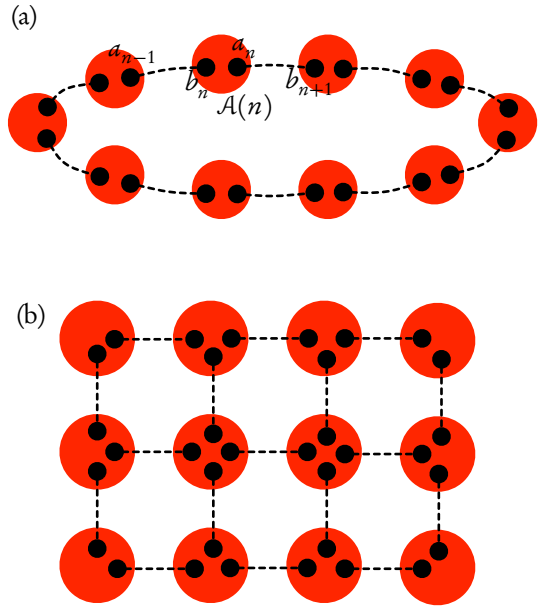

Figure 3.1: Tensor networks as valence bond solids: (a) the matrix product state for a lattice with periodic boundary conditions; (b) the projected entangled pair state for two-dimensional lattices. The dashed lines indicate valence bonds created between the ancillas (black dots). The red circles represent the projectors $A(n)$.

Matrix product states through sequential generation

Another idea that traces back to quantum information theory is to generate states with long-range entanglement sequentially. One of the most promising candidates for implementing a quantum computer is by using photons as qubits, since they can easily be transported over long distances. Entangled multiqubit states can be prepared sequentially, as photons that are created inside a resonator and gradually leave the cavity

[274]. Through an abstraction of this process, matrix product states can be interpreted as entangled multiqubit states that are sequentially generated through interaction with a D-dimensional ancilla [275]. Let the ancilla start in a state $\boldsymbol{v}_{\mathrm{R}} \in \mathbb{H}_{\mathrm{ancilla}} \equiv \mathbb{C}^D$ and the physical system in the state $|\mathbf{1}\rangle = |1\rangle_1 \otimes |1\rangle_2 \otimes \cdots \otimes |1\rangle_N \in \mathbb{H}_{\mathscr{L}}$. We now assume that the ancilla interacts with the physical system at site $N-n$ during the time interval $[n\triangle t,(n+1)\triangle t]$ according to the unitary interaction $U_{(\alpha,s);(\alpha',s')}(N-n)$, after which this site is 'emitted' and the ancilla interacts with the next site. At the end of the process, the ancilla is projected onto the state $\boldsymbol{v}_{\mathrm{L}}$ in order to disentangle it from the physical system, leaving the physical system in the pure state $|\Psi\rangle$ given by

$$|\Psi[A]\rangle = \sum_{s_1=1}^{q_1}\sum_{s_2=1}^{q_2}\cdots\sum_{s_N=1}^{q_N} \boldsymbol{v}_{\mathrm{L}}^{\dagger} A^{s_1}(1)A^{s_2}(2)\cdots A^{s_N}(N)\boldsymbol{v}_{\mathrm{R}}|s_1 s_2 \ldots s_N\rangle\,, \tag{3.30}$$

with $A^s_{\alpha,\beta}(n) = U_{(\alpha,s);(\beta,1)}(n)$. Because of the unitarity of the evolution, the matrices $A^s(n)$ now satisfy

$$\sum_{s=1}^{q_n} A^s(n)^{\dagger}A^s(n) = \mathbb{1}_D \quad \forall n = 1,\ldots,N. \tag{3.31}$$

The boundary vectors v_{L} and v_{R} can easily be absorbed into the matrices $A^s(1)$ and $A^s(L)$ respectively, although this alternative representation with boundary vectors is used occasionally throughout the remainder of this chapter. The boundary vectors can be chosen fixed, and are not included in the set of the variational parameters. Note that, before the projection onto $\boldsymbol{v}_{\mathrm{L}}$ the total state of the physical system and the ancilla is normalized to $||\boldsymbol{v}_{\mathrm{R}}||$. The projection of the ancilla will leave the physical system in an unnormalized state unless $\boldsymbol{v}_{\mathrm{L}}$ is properly chosen. This process is sketched in Figure 3.2.

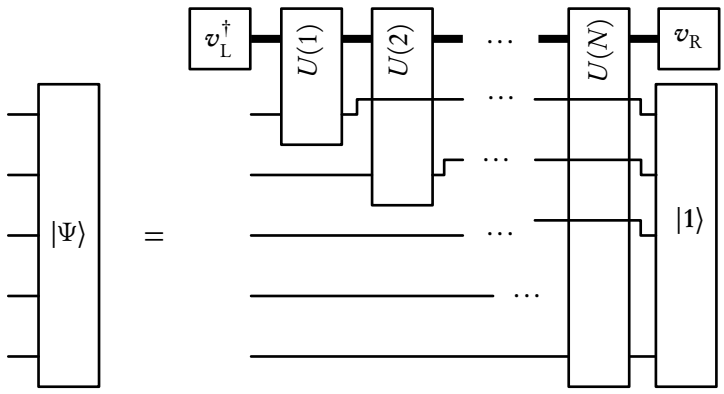

Figure 3.2: The sequential generation of matrix product states.

This picture of sequential generation learns that the quantum state of the one-dimensional physical system, as described by the matrix product state, is encoded by an ancilla that lives in zero spatial dimensions. It is thus a realization of the holographic principle,

described in Subsection 2.5 of Chapter 1, and automatically implies an exact area law for matrix product states. Hence, for a fixed bond dimension D, a matrix product state description of critical systems eventually fails if the system size is increased. This formulation is explored in more detail in the next chapter, where it becomes the natural strategy to formulate *holographic quantum states* in the continuum [276].

Other formulations of the sequential generation picture for matrix product states do exist, with or without an explicit ancilla, and it can also be used to generate a subclass of projected entangled pair states that allow for a more efficient evaluation of expectation value by exploiting the unitarity properties [277]. In fact, many different variational ansätze can be unified by rewriting them solely in terms of unitary matrices, for which a suitable variational optimization strategy can then be constructed [278].

Matrix product states and exactly solvable models

For exactly solvable models, the solution obtained by the Bethe ansatz can also be cast in a matrix product state representation [279, 280]. For example, for the $S = 1/2$ Heisenberg model, which is critical, an explicit matrix product state representation was derived in [281]. By defining a reference state $|\Downarrow\rangle = \bigotimes_{n=1}^{N} |\downarrow\rangle_n$, the eigenstates of the Heisenberg model can be labeled by the number k of 'particles' $\uparrow$ living in the reference vacuum $|\Downarrow\rangle$, which is equivalent to specifying the eigenvalue $M = (2k - N)/2$ of the total spin component $\hat{S}^z$. The bond dimension D in the matrix product state representation of an eigenstate k is $D = 2^k$. For the ground state, which has $k = L/2$, the exponential scaling $D = 2^{L/2}$ is reproduced. While reassuring that the matrix product state ansatz can reproduce the Bethe ansatz, this connection is not further explored.

Closely related is the strategy to replace the matrices in the matrix product state by physical operators, and hence replacing the finite-dimensional Hilbert space $\mathbb{C}^D$ of the ancilla with an infinite-dimensional Hilbert space, which allows to accurately describe critical systems and violate the area law [282, 283].

1.4. Computation of expectation values

We now evaluate the expectation value of an operator $\hat{O} \in \mathbb{L}(\mathbb{H}_{\mathscr{L}})$ with respect to a matrix product state $|\Psi[A(n)]\rangle \in \mathbb{H}_{\mathscr{L}}$, where $\hat{O}$ is given by

$$\hat{O} = \bigotimes_{n=1}^{N} \hat{O}_n, \tag{3.32}$$

with $\hat{O}_n$ a local operator acting non-trivially only on $\mathbb{H}_n$. Any operator can be expressed as a sum of such elementary 'product' operators. Using $\mathrm{tr}(A)\,\mathrm{tr}(B) = \mathrm{tr}(A \otimes B) = \mathrm{tr}(B \otimes A)$ we obtain

$$\langle \Psi[\overline{A}] | \hat{O} | \Psi[A] \rangle = \mathrm{tr}\left[\check{E}_{O_1}(1) \check{E}_{O_2}(2) \cdots \check{E}_{O_N}(N) \right], \tag{3.33}$$

where the superoperators $\check{E}_O(n)$, denoted by an inverse hat, are given by

$$\check{E}_O(n) \triangleq \sum_{s,s'=1}^{q_n} \langle s|\hat{O}|s'\rangle A^{s'}(n) \otimes \overline{A^s(n)}. \tag{3.34}$$

The superoperator $\check{E}_O(n)$ acts in the tensor product space of the ancilla and its complex conjugate $\mathbb{C}^{D_n} \otimes \overline{\mathbb{C}^{D_n}}$ and has its range in $\mathbb{C}^{D_{n-1}} \otimes \overline{\mathbb{C}^{D_{n-1}}}$. Each superoperator $\check{E}_O(n)$ can be represented as a matrix of size $D_{n-1}^2 \times D_n^2$. For the evaluation of the expectation value, these superoperators have to be multiplied, which is in general an operation with computational complexity $\mathcal{O}(D^6)$. By exploiting the tensor product structure of $\check{E}_O(n)$, a reduction of the computational complexity to $\mathcal{O}(D^5)$ is possible.

To every superoperator $\check{E}_O(n)$ we can associate a map $\mathcal{E}_O^{(n)} : \mathbb{L}(\mathbb{C}^{D_n}) \mapsto \mathbb{L}(\mathbb{C}^{D_{n-1}})$ from operators x acting on the ancilla space $\mathbb{C}^{D_n}$ to operators $\mathcal{E}_O^{(n)}[x]$ acting on the previous ancilla space $\mathbb{C}^{D_{n-1}}$ through the prescription

$$\mathcal{E}_O^{(n)} : \mathbb{L}(\mathbb{C}^{D_n}) \mapsto \mathbb{L}(\mathbb{C}^{D_{n-1}}) : x \mapsto \mathcal{E}_O^{(n)}[x] \triangleq \sum_{s,s'=1}^{q_n} \langle s|\hat{O}|s'\rangle A^{s'}(n) x A^s(n)^\dagger. \tag{3.35}$$

Analogously, a second map $\widetilde{\mathcal{E}}_O^{(n)}$ is defined as

$$\widetilde{\mathcal{E}}_O^{(n)} : \mathbb{L}(\mathbb{C}^{D_{n-1}}) \mapsto \mathbb{L}(\mathbb{C}^{D_n}) : x \mapsto \widetilde{\mathcal{E}}_O^{(n)}[x] \triangleq \sum_{s,s'=1}^{q_n} \langle s|\hat{O}|s'\rangle A^s(n)^\dagger x A^{s'}(n). \tag{3.36}$$

Through the Choi-Jamiołkowski isomorphism [284, 285, 286, 287], operators x in $\mathbb{L}(\mathbb{C}^{D_n})$ can be associated to vectors $|x)$ in the ancilla product space $\mathbb{C}^{D_n} \otimes \overline{\mathbb{C}^{D_n}}$, for which we introduce a rounded braket notation. The relation between the maps $\mathcal{E}_O$, $\widetilde{\mathcal{E}}_O$ and the superoperator $\check{E}_O$ is given by $\check{E}_O(n)|x) = |\mathcal{E}_O^{(n)}[x])$ and $(y|\check{E}_O(n) = (\widetilde{\mathcal{E}}_O^{(n)}[y]|$. Note that these maps only require multiplication of matrices in the original ancilla space, and can thus be implemented as operations with computational complexity $\mathcal{O}(D^3)$. A particular role is played by the map $\mathcal{E}_{\mathbb{1}}^{(n)} = \mathcal{E}^{(n)}$, which is completely positive and for which the matrices $A^s(n)$ are the Kraus operators. This map appears whenever $\hat{O}_n$ acts trivially (*i.e.* $\hat{O}_n = \hat{\mathbb{1}}$) which is almost everywhere for most relevant operators. The corresponding superoperator $\check{E}_{\mathbb{1}}(n) = \check{E}(n)$ is reminiscent of the concept of transfer operators in statistical mechanics and is henceforth referred to as such. In the remainder of this section, we will often use the generalized superoperator

$$\check{E}_B^A \triangleq \sum_{s=1}^{q} A^s \otimes \overline{B^s}, \tag{3.37}$$

so that $\check{E}(n) = \check{E}_{A(n)}^{A(n)}$.

In a system with open boundary conditions, the trace is absent and the expectation value

can be computed through a successive application of the maps $\mathcal{E}_O^{(n)}$ as

$$\begin{aligned}&\langle\Psi[\overline{A}]|\hat{O}|\Psi[A]\rangle\\&\qquad=\mathcal{E}_{O_1}^{(1)}\left[\mathcal{E}_{O_2}^{(2)}\left[\dots\left[\mathcal{E}_{O_N}^{(N)}[1]\right]\dots\right]\right]=\widetilde{\mathcal{E}}_{O_N}^{(N)}\left[\dots\left[\widetilde{\mathcal{E}}_{O_2}^{(2)}\left[\widetilde{\mathcal{E}}_{O_1}^{(1)}[1]\right]\right]\dots\right]\end{aligned}\tag{3.38}$$

or thus ($\forall n=1,\dots,N$)

$$\begin{aligned}&\langle\Psi[\overline{A}]|\hat{O}|\Psi[A]\rangle\\&\qquad=\mathrm{tr}\left(\widetilde{\mathcal{E}}_{O_n}^{(n)}\left[\dots\left[\widetilde{\mathcal{E}}_{O_2}^{(2)}\left[\widetilde{\mathcal{E}}_{O_1}^{(1)}[1]\right]\right]\dots\right]\mathcal{E}_{O_{n+1}}^{(n+1)}\left[\mathcal{E}_{O_2}^{(2)}\left[\dots\left[\mathcal{E}_{O_N}^{(N)}[1]\right]\dots\right]\right]\right).\end{aligned}\tag{3.39}$$

For a lattice with open boundary conditions, the expectation value of product operators $\hat{O}$ can be computed with computational complexity $\mathcal{O}(D^3)$. Most interesting operators (*e.g.* local operators, short-range interaction terms in the Hamiltonian, correlation functions) can be written as a small sum of such product operators, so that the computation of their expectation values inherit this very favorable computational complexity. Since most operators are trivial ($\hat{O}(n)=\hat{\mathbb{1}}$) on the majority of sites, we define the set of virtual density matrices $l(n)$ and $r(n)$ for the auxiliary system through the recursive definitions

$$l(0)=1,\qquad l(n)=\widetilde{\mathcal{E}}_{\mathbb{1}}^{(n)}[l(n-1)],\qquad \forall n=1,\dots,N;\tag{3.40a}$$

$$r(N)=1,\qquad r(n-1)=\mathcal{E}_{\mathbb{1}}^{(n)}[r(n)],\qquad \forall n=1,\dots,N;\tag{3.40b}$$

all of which can be computed with computational complexity $\mathcal{O}(D^3)$. The expectation value of a strictly local operator is then given by $\langle\Psi[A]|\hat{O}_n|\Psi[A]\rangle=(l(n-1)|\check{E}_{O_n}(n)|r(n))$ and the normalization of the state is given by $\langle\Psi[A]|\Psi[A]\rangle=l(N)=r(0)=\mathrm{tr}[l(n)r(n)]=(l(n)|r(n))$, $\forall n=0,\dots,N$. For systems with periodic boundary conditions, a similar simplification does not occur due to the lack of a starting point. Alternative schemes have been constructed for obtaining a $\mathcal{O}(D^3)$ complexity for lattice with periodic boundary conditions, based on approximations of the transfer operator [288, 289] or the variational Quantum Monte Carlo approach [290]. The increased computational complexity of contracting the tensor network for periodic matrix product states is part of a general rule, where the complexity increases as the number of loops increases. For every loop, a pair of open legs has to be dragged along. Consequently, tensor networks with a macroscopic number of loops such as projected entangled pair states cannot be contracted efficiently. However, an efficient scheme has been developed to approximately evaluate expectation values with projected entangled pair states to great numerical accuracy [257, 291], and Monte Carlo strategies can be used as well [292, 293].

One particular set of operators that straightforwardly generalizes the set of product operators is the so-called class of *matrix product operators*, which were introduced in

[294, 295] as density operators to describe quantum systems at thermal equilibrium. A matrix product operator has the general form

$$\hat{O}[C] = \sum_{t_1=1}^{q_1^2} \sum_{t_2=1}^{q_2^2} \cdots \sum_{t_N=1}^{q_N^2} \mathrm{tr}\left[C^{t_1}(1) C^{t_2}(2) \cdots C^{t_N}(N)\right] \hat{O}_1^{t_1} \otimes \hat{O}_2^{t_2} \otimes \cdots \otimes \hat{O}_N^{t_N}, \qquad (3.41)$$

where $C^t(n)$ is a $\widetilde{D}_{n-1} \times \widetilde{D}_n$ matrix ($\forall t = 1, \ldots, q_n^2$) and $\{O_n^t \mid t = 1, \ldots, q_n^2\}$ is a complete set of local operators on site n ($\forall n = 1, \ldots, N$). The expectation value of this class of operators is given by

$$\langle \Psi[\overline{A}] | \hat{O}[C] | \Psi[A] \rangle = \mathrm{tr}\left[\check{F}(1) \check{F}(2) \cdots \check{F}(N)\right], \qquad (3.42)$$

where the quantities $\check{F}(n)$ now represent $D_{n-1}^2 \widetilde{D}_{n-1} \times D_n^2 \widetilde{D}_n$ matrices given by

$$\check{F}(n) = \sum_{s,s'=1}^{q_n} \sum_{t=1}^{q_n^2} \langle s | \hat{O}_n^t | s' \rangle A^{s'}(n) \otimes \overline{A^s(n)} \otimes C^t(n). \qquad (3.43)$$

In many occasions, the label t is just a combined label $t = (s, s')$ and $\hat{O}_n^t = |s\rangle \langle s'|$. Even for small values of $\widetilde{D}$, the class of matrix product operators can encode short-range and certain long-range interacting Hamiltonians, as well as a Lie-Trotter-Suzuki decomposed step of the exponential of short-range interacting Hamiltonians [296, 297, 298].

1.5. Gauge invariance in the manifold and its tangent plane

In the previous subsections, we have encountered different formulations of the matrix product state, or different constraints satisfied by the matrices $A^s(n)$. These constraints do not result in a restriction of the variational class, since they can always be imposed as a consequence of the representation redundancy present in the original definition of $|\Psi[A(n)]\rangle$ in Eq. (3.2). Indeed, the matrix product state $|\Psi[A(n)]\rangle$ is equal to $|\Psi[\tilde{A}(n)]\rangle$ where $\tilde{A}^s(n) = g(n-1) A^s(n) g(n)^{-1}$ with $g(n) \in \mathsf{GL}(D_n; \mathbb{C})$, $\forall n = 1, \ldots, N$ and $g(0) = g(N)$[3]. The representations $A = \{A(n) \mid n = 1, \ldots, N\} \in \mathbb{A}_{\mathrm{MPS}\{D_n\}}$ and $\tilde{A} = \{\tilde{A}(n) \mid n = 1, \ldots, N\} \in \mathbb{A}_{\mathrm{MPS}\{D_n\}}$ are thus equivalent representations, as defined by the action of the group of local, multiplicative gauge transformations $\mathsf{G}_{\mathrm{MPS}\{D_n\}} = \{g(n) \in \mathsf{GL}(D_n; \mathbb{C}) \mid n = 1, \ldots, N\}$, with

$$\dim \mathsf{G}_{\mathrm{MPS}\{D_n\}} = \sum_{n=1}^{N} D_n^2. \qquad (3.44)$$

Put differently, the parameter space $\mathbb{A}_{\mathrm{MPS}\{D_n\}}$ is intersected by gauge orbits corresponding to $\mathsf{G}_{\mathrm{MPS}\{D_n\}}$, where all points on a gauge orbit correspond to equivalent representations.

[3] Note that the condition $g(0) = g(N)$ is required for both open and periodic boundary conditions, since having $g(0) \neq g(N)$ in the case of open boundary conditions ($D_0 = D_N = 1$) would produce a change in phase or normalization $|\Psi[\tilde{A}]\rangle = g(0) g(N)^{-1} |\Psi[A]\rangle$.

Vice versa, $\mathsf{G}_{\mathrm{MPS}\{D_n\}}$ describes the most general equivalence relations between to matrix product state representations. Thus, if $|\Psi[A]\rangle = |\Psi[\tilde{A}]\rangle$ then there necessarily exist matrices $g(n) \in \mathsf{GL}(D_n, \mathbb{C})$ $(\forall n = 1, \ldots, \mathscr{L})$ such that

$$\tilde{A}^s(n) = g(n-1) A^s(n) g(n)^{-1}. \tag{3.45}$$

We will proof below that the only transformation $\{g(n)\} \in \mathsf{G}_{\mathrm{MPS}\{D_n\}}$ that maps A to itself is given by the choice $\{g(n) = c\mathbb{1}_{D_n} \mid n = 1, \ldots, N\}$, such that the dimension of the gauge orbits is given by $\dim \mathsf{G}_{\mathrm{MPS}\{D_n\}} - 1$. Because $\mathsf{GL}(D; \mathbb{C})$ is a connected group and the equivalence relation is continuous, the gauge orbits are connected too. The dimension of the manifold then follows from the quotient space $\mathbb{A}_{\mathrm{MPS}\{D_n\}}/\mathsf{G}_{\mathrm{MPS}\{D_n\}}$ as

$$\dim \mathscr{M}_{\mathrm{MPS}\{D_n\}} = \dim \left(\mathbb{A}_{\mathrm{MPS}\{D_n\}}/\mathsf{G}_{\mathrm{MPS}\{D_n\}} \right) = \dim \mathbb{A}_{\mathrm{MPS}\{D_n\}} - \dim \mathsf{G}_{\mathrm{MPS}\{D_n\}} + 1. \tag{3.46}$$

By restricting to normalized states (*i.e.* $\langle \Psi[A] | \Psi[A] \rangle = 1$), the dimensionality of the manifold is further reduced by one.

It is now possible to specify gauge fixing constraints such that each state $|\Psi\rangle \in \mathscr{M}_{\mathrm{MPS}}$ is linked to a unique set of matrices $A = \{A(n) | n = 1, \ldots, N\} \in \mathbb{A}_{\mathrm{MPS}\{D_n\}}$. These matrices $\{A(n)\}$ label the different orbits living in the quotient space $\mathbb{A}_{\mathrm{MPS}\{D_n\}}/\mathsf{G}_{\mathrm{MPS}\{D_n\}}$. A matrix product state $|\Psi[A]\rangle$ is then said to be in the *canonical form*. Canonical forms for matrix product states were derived in [273]. For a matrix product state with open boundary conditions, a unique decomposition is obtained in Eq. (3.19). If we want to express this form in terms of a representation with matrices $A^s(n)$, we can choose to set $A^s(n) = \Gamma^s(n)\Lambda(n)$, which corresponds to the following conditions for the right-canonical form[4]:

- Right orthonormalization condition: $\sum_{s=1}^{q_n} A^s(n) A^s(n)^\dagger = \mathcal{E}^{(n)}(\mathbb{1}_{D_n}) = \mathbb{1}_{D_{n-1}}$ so that $r(n) = \mathbb{1}_{D_n}$ and the gauge freedom is reduced from $g(n) \in \mathsf{GL}(n; \mathbb{C})$ to $g(n) \in \mathsf{U}(n; \mathbb{C})$ $(\forall n = 1, \ldots, N+1)$;
- $\sum_{s=1}^{q_n} A^s(n)^\dagger l(n-1) A^s(n) = \widetilde{\mathcal{E}}^{(n)}[l(n-1)] = l(n)$ with $l(0) = l(N) = 1$ (for a normalized state $\langle \Psi[A] | \Psi[A] \rangle = 1$), where $l(n)$ is strictly positive definite, satisfies $\mathrm{tr}[l(n)] = 1$ and can be diagonalized, hence fixing the remaining unitary gauge freedom. Clearly, $l(n) = \Lambda(n)^2$ and contains the entanglement spectrum.

Alternatively, we could have chosen $A^s(n) = \Lambda(n-1)\Gamma^s(n)$, corresponding to the left-canonical form, which is characterized by the gauge fixing conditions

- Left orthonormalization condition: $\sum_{s=1}^{q_n} A^s(n)^\dagger A^s(n) = \widetilde{\mathcal{E}}^{(n)}(\mathbb{1}_{D_{n-1}}) = \mathbb{1}_{D_n}$ so that $l(n) = \mathbb{1}_{D_n}$ and the gauge freedom is reduced from $g(n) \in \mathsf{GL}(n; \mathbb{C})$ to $g(n) \in \mathsf{U}(n; \mathbb{C})$ $(\forall n = 0, \ldots, N)$;
- $\sum_{s=1}^{q_n} A^s(n) r(n) A^s(n)^\dagger = \mathcal{E}^{(n)}[r(n)] = r(n-1)$ with $r(0) = r(N) = 1$ (for a

[4] We assume that all Schmidt values are $\lambda_\alpha(n)$ are strictly nonzero. Otherwise, the state can exactly be described by a matrix product state with lower bond dimension.

normalized state), where $r(n)$ is diagonal, strictly positive definite and satisfies $\mathrm{tr}[r(n)] = 1$ ($\forall n = 1,\ldots,N$).

We refer to [273, 259] for more information on how to obtain the canonical form starting from an arbitrary matrix product state. For systems with periodic boundary conditions, a canonical form is more difficult to derive. The result for a translation invariant state will be stated in the next subsection.

We similarly derive the effect of gauge invariance on the tangent plane $\mathbb{T}_{\mathrm{MPS}\{D_n\}}[A]$, for which it is sufficient to consider infinitesimal transformations. Let $\{g(n;\eta) \mid n = 1,\ldots,N\}$ represent a one-parameter family of gauge transformations so that

$$\frac{\mathrm{d}}{\mathrm{d}\eta} g(n;\eta)\bigg|_{\eta=0} = x(n) \quad \text{with} \quad x(n) \in \mathfrak{gl}(D_n;\mathbb{C}) \equiv \mathbb{C}^{D_n \times D_n}. \tag{3.47}$$

We now define $\mathfrak{g}_{\mathrm{MPS}\{D_n\}} = \bigoplus_{n=1}^{N} \mathfrak{gl}(D_n;\mathbb{C})$ with

$$\dim \mathfrak{g}_{\mathrm{MPS}\{D_n\}} = \dim \mathsf{G}_{\mathrm{MPS}\{D_n\}} = \sum_{n=1}^{N} D_n^2, \tag{3.48}$$

such that a one-parameter family of gauge transformations is characterized around $\eta = 0$ by a point $x = \{x(n) \mid n = 1,\ldots,N\} \in \mathfrak{g}_{\mathrm{MPS}\{D_n\}}$. The corresponding family of points $A(\eta) = \{A(n;\eta) \mid n = 1,\ldots,N\}$ with $A^s(n;\eta) = g(n-1;\eta)A^s g(n;\eta)^{-1}$ lies within a gauge orbit, so that the matrix product state $|\Psi[A(\eta)]\rangle$ is independent of η. We hence obtain

$$|\Phi[\mathcal{N}_\Phi[x];A]\rangle = \frac{\mathrm{d}}{\mathrm{d}\eta} |\Psi[A(\eta)]\rangle\bigg|_{\eta=0} = 0 \tag{3.49}$$

so that $\mathcal{N}_\Phi^{[A]}$, which is given by the prescription

$$\mathcal{N}_\Phi^{[A]}[x] = \mathcal{N}_\Phi[x;A] \quad \text{with} \quad \mathcal{N}_\Phi^s[x;A](n) = x(n-1)A^s(n) - A^s(n)x(n), \tag{3.50}$$

represents a linear homomorphism from $\mathfrak{g}_{\mathrm{MPS}\{D_n\}}$ to the null space $\mathbb{N}_\Phi[A] \in \mathbb{A}_{\mathrm{MPS}\{D_n\}}$ of the map $\Phi^{[A]}$:

$$\mathcal{N}_\Phi^{[A]} : \mathfrak{g}_{\mathrm{MPS}\{D_n\}} \mapsto \mathbb{A}_{\mathrm{MPS}\{D_n\}} : x = \{x(n) \in \mathfrak{gl}(D_n;\mathbb{C}) \mid n = 1,\ldots N\} \mapsto \mathcal{N}_\Phi[x;A]. \tag{3.51}$$

For every tangent vector $|\Phi[B;A]\rangle$, we obtain $|\Phi[B]\rangle = |\Phi[B + \mathcal{N}_\Phi[x;A];A]\rangle$, so that the point $B \in \mathbb{A}_{\mathrm{MPS}\{D_n\}}$ is gauge equivalent to $B + \mathcal{N}_\Phi[x;A]$, $\forall x \in \mathfrak{g}_{\mathrm{MPS}\{D_n\}}$. The multiplicative gauge invariance of the matrix product state representation has turned into an additive gauge invariance in the representation of the tangent plane. We henceforth discard the explicit notation of the point A.

We can now relate the description of gauge invariance in both the tangent plane and the variational manifold. The null space $\mathbb{N}_\Phi$ can be considered as the tangent plane to

the gauge orbit of equivalent parameterizations in $\mathbb{A}_{\mathrm{MPS}\{D_n\}}$. Gauge transformations that map A to itself are generated by choices of x such that $\mathcal{N}_\Phi[x] = 0$, *i.e.* they are generated by points x in the kernel of $\mathcal{N}_\Phi^{[A]}$, which we now investigate for the case of a matrix product state with open boundary conditions. Let $\mathcal{N}_\Phi^s[x](n) = 0$, $\forall s = 1,\ldots,q_n$, $\forall n = 1,\ldots N$. We can choose $x(0) = c \in \mathfrak{gl}(D_0,\mathbb{C}) \equiv \mathbb{C}$. Using the full rank assumption of $\sum_{s=1}^{q_n} A^s(n)^\dagger A^s(n)$ at $n = 1$, it automatically follows that $x(1) = c\mathbb{1}_{D_1}$. Continuing along this way proofs $x(n) = c\mathbb{1}_{D_n}$ $\forall n = 1,\ldots,N$, such that the kernel of $\mathcal{N}_\Phi$ is one-dimensional. This corresponds to the transformation $g(n) = \mathrm{e}^{\eta c}\mathbb{1}_{D_n}$ that we introduced above. The case of periodic boundary conditions will be treated in the next subsection, but only for the restricted case of translation invariance. We thus obtain that $\dim \mathbb{N}_\Phi = \dim \mathfrak{g}_{\mathrm{MPS}\{D_n\}} - 1$ and thus $\dim \mathbb{T}_{\mathrm{MPS}\{D_n\}} = \dim \mathbb{A}_{\mathrm{MPS}\{D_n\}} - \dim \mathfrak{g}_{\mathrm{MPS}\{D_n\}} + 1$. However, $\mathbb{T}_{\mathrm{MPS}\{D_n\}}$ also contains the state $|\Psi[A]\rangle$ which has to be eliminated for the application of the time-dependent variational principle, as discussed in Subsection 2.3 of Chapter 2. The part $\mathbb{T}^\perp_{\mathrm{MPS}\{D_n\}}$ of the tangent plane that is orthogonal to $|\Psi[A]\rangle$ satisfies

$$\dim \mathbb{T}^\perp_{\mathrm{MPS}\{D_n\}} = \dim \mathbb{A}_{\mathrm{MPS}\{D_n\}} - \dim \mathfrak{g}_{\mathrm{MPS}\{D_n\}}. \tag{3.52}$$

Finally, we try to specify a set of gauge fixing conditions for the representation $B \in \mathbb{A}_{\mathrm{MPS}\{D_n\}}$ of the tangent vectors $|\Phi[B]\rangle$, such that every tangent vector in $\mathbb{T}_{\mathrm{MPS}\{D_n\}}$ is associated to a unique representation B, living in the quotient space $\mathbb{A}_{\mathrm{MPS}\{D_n\}}/\mathbb{N}_\Phi$. We restrict again to the case of open boundary conditions, and postpone the case of periodic boundary conditions to the next subsection. Let now $A^s(n;\eta)$ represent a general one-parameter family of points in $\mathbb{A}_{\mathrm{MPS}\{D_n\}}$ and let

$$B^s(n) = \left.\frac{\mathrm{d}}{\mathrm{d}\eta} A^s(n;\eta)\right|_{\eta=0} \tag{3.53}$$

represent the infinitesimal variation of A around $\eta = 0$. In the following sections, two different gauge fixing conditions turn out to be beneficial. Either of the following two conditions *completely* specify a unique representation B:

- *Left-gauge fixing condition*:

$$\sum_{s=1}^{q_n} A^s(n)^\dagger l(n-1) B^s(n) = 0 \quad \Leftrightarrow \quad (l(n-1)|\check{E}^{B(n)}_{A(n)} = 0, \quad \forall n = 1,\ldots,N. \tag{3.54}$$

- *Right-gauge fixing condition*:

$$\sum_{s=1}^{q_n} B^s(n) r(n) A^s(n)^\dagger = 0 \quad \Leftrightarrow \quad \check{E}^{B(n)}_{A(n)}|r(n)) = 0, \quad \forall n = 1,\ldots,N. \tag{3.55}$$

The left [right] gauge fixing condition ensures that the density matrix $l(n)$ [$r(n)$] is

not changed at first order in η under a substitution $A^s(n) \to A^s(n) + \eta B^s(n)$. These conditions do more than fixing the gauge, as they also include norm preservation to first order, *i.e.* they guarantee that

$$\langle \Psi[\overline{A}] | \Phi[B] \rangle = \sum_{n=1}^{N} (l(n-1) | \check{E}^{B(n)}_{A(n)} | r(n)) = 0. \tag{3.56}$$

An efficient implementation to impose these conditions is presented in the following section. We conclude this subsection by proving that the gauge freedom can indeed be used to impose the left gauge fixing conditions in Eq. (3.54). Let thus $\tilde{B}$ be a parameterization of a tangent vector that does not satisfy the left gauge fixing conditions, and define $B = \tilde{B} + \mathbb{N}_\Phi^{[A]}[x]$. We explicitly construct the choice x such that B satisfies Eq. (3.54). The proof for the right gauge fixing condition in Eq. (3.55) is analogous. Since $\langle \Psi[\overline{A}] | \Phi[B] \rangle$ is a gauge invariant, its value cannot be changed by gauge transformations, and we need to start from a tangent vector $|\Phi[\tilde{B}]\rangle$ orthogonal to $|\Psi[\overline{A}]\rangle$, such that $\langle \Psi[\overline{A}] | \Phi[\tilde{B}] \rangle = \langle \Psi[\overline{A}] | \Phi[B] \rangle = 0$.

Because of the condition $g(0) = g(N)$ for gauge transformations of the matrix product state $|\Psi[A]\rangle$, the gauge transformations in the tangent plane also satisfy $x(0) = x(N)$. Let the required gauge transformation to map $\tilde{B}$ to B start with some value $x(0) = c \in \mathbb{C}$. Now assume that $x(k)$ has been fixed up to some value $k = n-1$. We find for the left gauge fixing condition on $B^s(n)$:

$$A^s(n)^\dagger l(n-1)[\tilde{B}^s(n) + x(n-1)A^s(n) - A^s(n)x(n)] = 0,$$

from which we can solve

$$l(n)x(n) = A^s(n)^\dagger l(n-1)[\tilde{B}^s(n) + x(n-1)A^s(n)], \tag{3.57}$$

with $x(n-1)$ already determined and $l(n)$ assumed to have full rank, hence fixing $x(n)$ completely. Repeating this process from $n = 1$ to $n = N$ fixes all $x(n)$ including $x(N)$. But we should have $x(N) = x(0) = c$ for consistency, which turns out to be the condition that requires $\langle \Psi[\overline{A}] | \Phi[\tilde{B}] \rangle = 0$. Indeed, we can reiterate

$$\begin{aligned} l(n)x(n) &= A^s(n)^\dagger l(n-1)[\tilde{B}^s(n) + A^s(n)^\dagger l(n-1)x(n-1)A^s(n)] \\ &= \sum_{k=1}^{n} A^s(n)^\dagger \cdots A^s(k+1)^\dagger A^s(k)^\dagger l(k-1)\tilde{B}^s(k)A^s(k+1)\cdots A^s(n) \\ &\qquad + A^s(n)^\dagger A^s(n-1)^\dagger \cdots A^s(1)^\dagger l(0)x(0)A^s(1)\cdots A^s(n-1)A^s(n). \end{aligned}$$

Now, for $n = N$, we can use that $D_N = 1$, and furthermore use $l(0) = 1$ and $l(N) = \langle \Psi[A] | \Psi[A] \rangle$ to obtain

$$\langle \Psi[A] | \Psi[A] \rangle \, x(N) = \langle \Psi[A] | \Phi[\tilde{B}] \rangle + \langle \Psi[A] | \Psi[A] \rangle \, x(0).$$

Hence, $x(N) = x(0)$ requires that $\langle\Psi[A]|\Phi[\tilde{B}]\rangle = 0$. When this condition is fulfilled, the choice of the initial value $x(0) = c$ is completely free. Suppose we now define a different gauge transformation starting with $\tilde{x}(0) = x(0) + \tilde{c}$. Then we find

$$l(1)\tilde{x}(1) = A^s(1)^\dagger l(0)[\tilde{B}^s(1) + x(0)A^s(1)] + \tilde{c}A^s(1)^\dagger l(0)A^s(1) = l(1)x(1) + \tilde{c}\,l(1) \quad (3.58)$$

so that $\tilde{x}(1) = x(1) + \tilde{c}\mathbb{1}_{D_1}$. Continuing along this line, we find $\tilde{x}(n) = x(n) + \tilde{c}\mathbb{1}_{D_n}$, $\forall n = 1,\ldots,N$. Hence, this freedom of choice just corresponds to the kernel of the map $\mathcal{N}_\Phi^{[A]}$, so that $\mathcal{N}_\Phi^{[A]}(x) = \mathcal{N}_\Phi^{[A]}(\tilde{x})$.

1.6. Translation invariance and the thermodynamic limit

Because of the macroscopic size of interesting extended quantum systems, one is often interested in the bulk properties of these systems, far away from any boundary. In addition, our main interest goes out to systems which are translation invariant. These requirements vote in favor of systems with periodic boundary conditions, where there are no boundary effects —only finite-size effects with nice scaling behavior— and translation invariance can easily be reproduced. On a lattice with periodic boundary conditions (where translation invariance of the models dictates a site-independent $q_n = q$), a translation invariant subclass of matrix product state can be obtained by choosing the bond dimensions $D_n = D$ site-independent and using a translation invariant representation, *i.e.* by also choosing the matrices site independent: $A_n^s = A^s$, $\forall s = 1,\ldots,q$, $\forall n = 1,\ldots,L$. The resulting variational class is called the class of *uniform matrix product states* $\mathscr{M}_{\mathrm{uMPS}(D)} \subset \mathscr{M}_{\mathrm{MPS}\{D_n=D\}}$. Uniform matrix product states are denoted as $|\Psi(A)\rangle \in \mathscr{M}_{\mathrm{uMPS}(D)}$, with $A \in \mathbb{A}_{\mathrm{uMPS}(D)} \equiv \mathbb{C}^{D\times q\times D}$. Note that a general (translation non-invariant) gauge transformation will ruin the translation invariance of the representation. The only allowed gauge transformation in $\mathbb{A}_{\mathrm{uMPS}(D)}$ is a global transformation with site-indepedent matrices $g(n) = g$, $\forall n = 1,\ldots,N$, where $g \in \mathsf{G}_{\mathrm{uMPS}(D)} \equiv \mathsf{GL}(D;\mathbb{C})$. Vice versa, a translation invariant matrix product state might only have a representation as uniform matrix product state after a suitable site-dependent gauge transform. In addition, some translation invariant matrix product states do not allow for a translation invariant representation without enlarging the bond dimension (see [273]). Thus, $\mathscr{M}_{\mathrm{uMPS}(D)}$ does not contain all translation invariant states of $\mathscr{M}_{\mathrm{MPS}\{D_n=D\}}$.

As before, the equivalence relation given by the gauge transformations $g \in \mathsf{G}_{\mathrm{uMPS}(D)}$ traces out gauge orbits in $\mathbb{A}_{\mathrm{uMPS}(D)}$. These gauge orbits have dimension $\dim \mathsf{G}_{\mathrm{uMPS}(D)} - 1 = D^2 - 1$, since the trivial elements $g = c\mathbb{1}_D$ with $c \in \mathbb{C}$ map any $A \in \mathbb{A}_{\mathrm{uMPS}(D)}$ to itself. The variational manifold thus has a dimension given by $\dim \mathscr{M}_{\mathrm{uMPS}(D)} = (q-1)D^2 + 1$. By imposing a normalization condition, the dimension is further reduced to $(q-1)D^2$. An important role is played by the transfer matrix $\breve{E} = \sum_{s=1}^q A^s \otimes \overline{A^s}$ and its associated completely positive maps $\mathcal{E}$ and $\widetilde{\mathcal{E}}$, all of which are now site-independent. The transfer matrix $\breve{E}$ has eigenvalues $\omega^{(k)}$ and corresponding left and right eigenvectors which we denote as $(l^{(k)}|$ and $|r^{(k)}) \in \mathbb{C}^D \otimes \overline{\mathbb{C}}^D$. They correspond to linear operators $l^{(k)}, r^{(k)} \in$

$\mathbb{L}(\mathbb{C}^D)$, with $\mathbb{C}^D$ being the ancilla space, and are related to the associated maps by $\mathcal{E}(r^{(k)}) = \omega^{(k)} r^{(k)}$ and $\widetilde{\mathcal{E}}(l^{(k)}) = \omega^{(k)} l^{(k)}$. A canonical representation labeling the states in $\mathscr{M}_{\mathrm{uMPS}(D)}$ was derived in [273]. For a uniform matrix product $|\Psi(A)\rangle \in \mathscr{M}_{\mathrm{uMPS}(D)}$, the $D \times D$ matrices A^s have a *block decomposition* into $J \geq 1$ blocks as

$$A^s = \begin{bmatrix} \lambda_1 A_1^s & 0 & \cdots & 0 \\ 0 & \lambda_2 A_2^s & \cdots & 0 \\ \vdots & \vdots & \ddots & \vdots \\ 0 & 0 & \cdots & \lambda_J A_J^s \end{bmatrix}, \tag{3.59}$$

where A_j^s are matrices of size $D_j \times D_j$, $\forall j = 1, \ldots, J$, with $\sum_{j=1}^J D_j = D$. The coefficients λ_j satisfy $0 < \lambda_j \leq 1$ and are chosen such that the corresponding transfer operators $\check{E}_j = \sum_{s=1}^q A_j^s \otimes \overline{A}_j^s$ have 1 as eigenvalue with largest absolute value. The block decomposition is constructed such that this eigenvalue is non-degenerate for each block. The remaining gauge invariance is reduced to gauge transformation matrices g that decompose as $g = \bigoplus_{j=1}^J g_j$, with $g_j \in \mathrm{GL}(D_j; \mathbb{C}_n)$. These can be used to impose the following conditions on A_j^s:

- $\sum_{s=1}^q A_j^s A_j^{s\dagger} = \mathcal{E}_j(\mathbb{1}_{D_j}) = \mathbb{1}_{D_j}$,
- $\sum_{s=1}^q A_j^{s\dagger} l_j A_j^s = \widetilde{\mathcal{E}}_j(l_j) = l_j$ where l_j is a diagonal matrix with strictly positive eigenvalues.

The remaining gauge freedom is thus fixed by bringing the left and right eigenvectors $(l_j^{(1)}|$ and $|l_j^{(1)})$ of $\check{E}_j$ corresponding to its unique eigenvalue $\omega_j^{(1)} = 1$ into the specific format $l_j^{(1)} = l_j$ (diagonal) and $r_j^{(1)} = \mathbb{1}_{D_j}$. If $J > 1$, the block decomposition states that the uniform matrix product state $|\Psi(A)\rangle$ can be written as a superposition

$$|\Psi(A)\rangle = \sum_{j=1}^J \lambda_j^N |\Psi_j(A_j)\rangle, \tag{3.60}$$

where $|\Phi_j(A_j)\rangle \in \mathscr{M}_{\mathrm{uMPS}(D_j)}$ is a uniform matrix product state with lower bond dimension $D_j < D$. Let now A^s be the (set of) matrices appearing in a single block, so that the spectral radius $\rho(\check{E}) = 1$ and the transfer operator has a unique eigenvalue 1. It can be shown that $\check{E}$ then has P eigenvalues $\omega^{(p)} = \exp(\mathrm{i}2\pi(p-1)/P)$ $(p \in \mathbb{Z}_P)$ on the unit circle. A further decomposition, called the *periodic decomposition*, is possible:

$$A^s = \begin{bmatrix} 0 & A_1^s & 0 & \cdots & 0 \\ 0 & 0 & A_2^s & \cdots & 0 \\ \vdots & \vdots & \vdots & \ddots & \vdots \\ A_P^s & 0 & 0 & \cdots & 0 \end{bmatrix}, \tag{3.61}$$

where A_p^s is a matrix of size $D_{p-1} \times D_p$ with $D_0 = D_P$ and $\sum_{p=1}^{P} D_p = D$. The eigenstates $l^{(p)}$ and $r^{(p)}$ corresponding to the eigenvalues $\omega^{(p)}$ ($p \in \mathbb{Z}_P$) of unit magnitude correspondingly decompose into

$$l^{(p)} = \begin{bmatrix} l_1 & 0 & 0 & \cdots & 0 \\ 0 & \mathrm{e}^{-\mathrm{i}\frac{2\pi}{P}(p-1)} l_2 & 0 & \cdots & 0 \\ \vdots & \vdots & \vdots & \ddots & \vdots \\ 0 & 0 & 0 & \cdots & \mathrm{e}^{-\mathrm{i}(P-1)\frac{2\pi}{P}(p-1)} l_P \end{bmatrix}, \tag{3.62a}$$

$$r^{(p)} = \begin{bmatrix} \mathrm{e}^{+\mathrm{i}(P-1)\frac{2\pi}{P}(p-1)} r_P & 0 & 0 & \cdots & 0 \\ 0 & r_1 & 0 & \cdots & 0 \\ \vdots & \vdots & \vdots & \ddots & \vdots \\ 0 & 0 & 0 & \cdots & \mathrm{e}^{+\mathrm{i}(P-2)\frac{2\pi}{P}(p-1)} r_{P-1} \end{bmatrix}, \tag{3.62b}$$

where $\sum_{s=1}^{q} A_p^{s\,\dagger} l_p A_p^s = l_{p+1} \in \mathbb{C}^{D_p \times D_p}$ and $\sum_{s=1}^{q} A_p^s r_p A_p^{s\,\dagger} = r_{p-1} \in \mathbb{C}^{D_{p-1} \times D_{p-1}}$ ($\forall p \in \mathbb{Z}_p$). If P is a factor of N, the state $|\Psi(A)\rangle$ can be written as

$$|\Psi(A)\rangle = \sum_{p \in \mathbb{Z}_p} \hat{T}^p \, |\tilde{\Psi}[\tilde{A}]\rangle, \tag{3.63}$$

where $|\tilde{\Psi}[\tilde{A}]\rangle \in \mathscr{M}_{\mathrm{MPS}\{\tilde{D}_n\}}$ is a non-uniform matrix product state with $\tilde{A}^s(n) = A^s_{n \bmod P}$ and $\tilde{D}_n = D_{n \bmod P}$. The state $|\tilde{\Psi}[\tilde{A}]\rangle$ is thus P-periodic ($\hat{T}^P |\tilde{\Psi}[\tilde{A}]\rangle = |\tilde{\Psi}[\tilde{A}]\rangle$) and $|\Psi(A)\rangle$ is a translation invariant superposition of $|\tilde{\Psi}[\tilde{A}]\rangle$ and its shifted versions. If P is not a factor of N, $|\Psi(A)\rangle = 0$.

Despite the nice properties of systems with periodic boundary conditions, the increased computational complexity of evaluating expectation values with respect to matrix product states with periodic boundary conditions has hindered their applicability. This increased computational complexity is caused by the fact that correlations between two points can travel along two different ways on the circle. In contrast, systems with open boundary conditions can have strong boundary effects (*e.g.* Friedel oscillations) that extend deeply into the bulk, especially for (near)-critical systems. However, for very large systems —which are finite size restrictions of translation invariant Hamiltonians in the thermodynamic limit— we still expect the matrices of the matrix product state approximation of the ground state to become site-independent when sufficiently far from the boundaries. By exploiting the translation invariance in either a matrix product state with periodic boundary conditions or in the bulk of a matrix product state with open boundary conditions, we can directly define a uniform matrix product state representation in the thermodynamic limit. The computational disadvantages of the matrix product state with periodic boundary conditions disappear, since observable with compact support cannot distinguish between open or periodic boundary conditions. On the other hand, boundary effects are also undetectable by operators that live deep in the

bulk. We can therefore discard them and restrict to the translation invariant bulk of a system with open boundary conditions.

A quantitative verification of these statements requires the definition of the class of uniform matrix product states $|\Psi(A)\rangle$ in the thermodynamic limit. Starting with a system with periodic boundary conditions on the lattice $\mathscr{L} = \{-N, -N+1, \ldots, N-1, N\}$, this limit is straightforwardly obtained as

$$|\Psi(A)\rangle = \lim_{N\to\infty} \sum_{\{s_n\}=1}^{q} \mathrm{tr}\left[\prod_{n=-N}^{+N} A^{s_n}\right] |\{s_n\}\rangle = \sum_{\{s_n\}=1}^{q} \mathrm{tr}\left[\prod_{n\in\mathbb{Z}} A^{s_n}\right] |\{s_n\}\rangle . \tag{3.64}$$

The norm of the state is given by $\langle\Psi(A)|\Psi(A)\rangle = \lim_{N\to\infty} \mathrm{tr}[\check{E}^{2N+1}]$, so that normalizability requires that $\rho(\check{E}) = 1$. Let $z^{(k)}$ for $k = 1, \ldots, K$ be the eigenvalues on the unit circle with corresponding left and right eigenvectors ($\langle l^{(k)}|$ and $|r^{(k)}\rangle$), which are normalized as $\langle l^{(k)}|r^{(k)}\rangle$ so that $\check{S}^{(k)} = |r^{(k)}\rangle\langle l^{(k)}|$ is a projector onto the corresponding eigenspace. For the normalization of the state, we obtain

$$\langle\Psi(\overline{A})|\Psi(A)\rangle = \lim_{N\to\infty} \sum_{k=1}^{K} (\omega^{(k)})^{2N+1}. \tag{3.65}$$

If a product operator $\hat{O}$ has non-trivial support only on the sites $\{-M, -M+1, \ldots, +M\}$ with M some constant, then the correlations acting along the other side of the circle have to travel over an infinite distance. They are thus transported by the eigenvalues of $\check{E}$ on the unit circle and we obtain

$$\langle\Psi(\overline{A})|\hat{O}|\Psi(A)\rangle = \lim_{N\to\infty} \sum_{k=1}^{K} (\omega^{(k)})^{2N-2M} \langle l^{(k)}|\check{E}_{O(-M)}\check{E}_{O(-M+1)}\cdots\check{E}_{O(M)}|r^{(k)}\rangle. \tag{3.66}$$

This expectation value can be computed using the iterative construction for matrix product states with open boundary conditions, resulting in a computational complexity $\mathcal{O}(KD^3)$. Since the number of eigenvalues K on the unit circle is typically much smaller than D^2, the increased computational complexity of periodic boundary conditions disappears, provided that we can efficiently determine the K eigenvalues and their corresponding eigenvectors using an iterative eigensolver.

Starting from a lattice with open boundary conditions, we use the sequential generation picture to define [see Eq. (3.30)]

$$|\Psi(A)\rangle = \lim_{N\to\infty} \sum_{\{s_n\}=1}^{q} v_{\mathrm{L}}^{\dagger}\left[\prod_{n=-N}^{+N} A^{s_n}\right] v_{\mathrm{R}} |\{s_n\}\rangle = \sum_{\{s_n\}=1}^{q} v_{\mathrm{L}}^{\dagger}\left[\prod_{n\in\mathbb{Z}} A^{s_n}\right] v_{\mathrm{R}} |\{s_n\}\rangle . \tag{3.67}$$

The normalization of the state is given by

$$\langle\Psi(\overline{A})|\Psi(A)\rangle = \lim_{N\to\infty}\sum_{k=1}^{K}(\omega^{(k)})^{2N+1}(\boldsymbol{v}_{\mathrm{L}}^{\dagger}r^{(k)}\boldsymbol{v}_{\mathrm{L}})(\boldsymbol{v}_{\mathrm{R}}^{\dagger}l^{(k)}\boldsymbol{v}_{\mathrm{R}}) \tag{3.68}$$

and the expectation value of $\hat{O}$ is given by

$$\langle\Psi(\overline{A})|\hat{O}|\Psi(A)\rangle = \lim_{N\to\infty}\sum_{k=1}^{K}(\omega^{(k)})^{2N-2M}(\boldsymbol{v}_{\mathrm{L}}^{\dagger}r^{(k)}\boldsymbol{v}_{\mathrm{L}})(\boldsymbol{v}_{\mathrm{R}}^{\dagger}l^{(k)}\boldsymbol{v}_{\mathrm{R}}) \times (l^{(k)}|\check{E}_{O(-M)}\check{E}_{O(-M+1)}\cdots\check{E}_{O(M)}|r^{(k)}). \tag{3.69}$$

When there is a unique eigenvalue on the unit circle ($K=1$ with thus $z^{(1)}=1$), both formulations produce the same normalized expectation values. In the remainder of this chapter, we always assume that such states are then normalized to unity, which is automatically fulfilled for the formulation with periodic boundary conditions and requires $(\boldsymbol{v}_{\mathrm{L}}^{\dagger}r^{(k)}\boldsymbol{v}_{\mathrm{L}})(\boldsymbol{v}_{\mathrm{R}}^{\dagger}l^{(k)}\boldsymbol{v}_{\mathrm{R}})=1$ in the case of open boundary conditions. The next subsection discusses for which systems $K=1$ is a valid assumption. Note that, while open and periodic boundary conditions produce the same result in the thermodynamic limit, the possibility of using open boundary conditions will prove essential for studying topologically non-trivial excitations (see Subection 1.4 of Chapter 1), which do not exist on a lattice with periodic boundary conditions. Henceforth, we always assume to be working in the setting of an infinite lattice with open boundary conditions [Eq. (3.67)] when talking about uniform matrix product states $|\Psi(A)\rangle$, unless explicitly stated otherwise.

Note that these uniform matrix product states are also known as *finitely correlated states* and were studied —as a generalization of the valence bond solid— by Fannes, Nachtergaele and Werner in [299], before the advent of the density matrix renormalization group. The class of finitely correlated states is even more general, and the subclass that corresponds to the uniform matrix product states are the so-called *purely generated* finitely correlated states. When the transfer matrix $\check{E}$ has a unique eigenvalue 1 (*i.e.* $J=1$ in the block decomposition), the state is called *ergodic*, and when this is also the only eigenvalue with modulus 1 (*i.e.* $P=1$ in the periodic decomposition), the state is called a *pure* finitely correlated state. Unlike the ordinary matrix product state $|\Psi[A]\rangle$, which is linear in each of its arguments $A(n)$ separately, the uniform matrix product state $|\Psi(A)\rangle$ is highly non-linear in its argument. It took some major breakthroughs before an algorithm was constructed that allowed the variational optimization of the uniform matrix product state ansatz [300].

One particularly interesting operator is the connected correlation function of Eq. (1.56), which is now given by

$$\Gamma^{(\alpha,\beta)}(n) = (l|\check{E}_{O^{\alpha}}\check{E}^{n-1}\check{E}_{O^{\beta}}|r) - (l|\check{E}_{O^{\alpha}}|r)(l|\check{E}_{O^{\beta}}|r) = (l|\check{E}_{O^{\alpha}}\check{Q}\check{E}^{n-1}\check{Q}\check{E}_{O^{\beta}}|r). \tag{3.70}$$

The correlation length ξ_c is thus determined by the largest eigenvalue of $\breve{Q}\breve{E}\breve{Q}$ as

$$\xi_c = \frac{a}{\log\left[\rho(\breve{Q}\breve{E}\breve{Q})\right]}. \tag{3.71}$$

If the uniform matrix product state is pure, so that $\breve{E}$ contains a unique eigenvalue on the unit circle, then $\rho(\breve{Q}\breve{E}\breve{Q}) < 1$ and the correlation length ξ_c is finite. Hence, all pure uniform matrix product states are exponentially clustering. The correlation length is determined by $\rho(\breve{Q}\breve{E}\breve{Q})$, which is equal to the eigenvalue of the transfer matrix $\breve{E}$ that is second largest in absolute value.

The overlap between two uniform matrix product states is given by

$$F(\overline{A},\tilde{A}) = |\langle\Psi(\overline{A})|\Psi(\tilde{A})\rangle| \sim \lim_{N\to\infty} \rho\left(\breve{E}_A^{\tilde{A}}\right)^{2N+1}, \tag{3.72}$$

where the states $|\Psi(A)\rangle$ and $|\Psi(\tilde{A})\rangle$ are assumed to be normalized to unity. We can thus define $d(\overline{A},\tilde{A}) = \rho(\breve{E}_A^{\tilde{A}})$ as the fidelity per site between the two uniform matrix product states $|\Psi(A)\rangle$ and $|\Psi(\tilde{A})\rangle$. If both states are pure, so that $\breve{E}_A^A$ and $\breve{E}_{\tilde{A}}^{\tilde{A}}$ have a unique eigenvalue 1 with corresponding left and right eigenvectors ($\langle l|$, ($\langle\tilde{l}|$ and $|r\rangle$), $|\tilde{r}\rangle$), and all other eigenvalues lie strictly within the unit circle, then there are two possibilities. Either $d(A,\tilde{A}) < 1$, and $F(A,\tilde{A}) = 0$ due to the orthogonality catastrophe (see Subsection 1.1 of Chapter 1), or $d(A,\tilde{A}) = 1$ and the two states are equivalent. Indeed, for $\rho(\breve{E}_A^{\tilde{A}}) = 1$, we denote the largest eigenvalue of $\breve{E}_A^{\tilde{A}}$ as $e^{i\varphi}$ and the corresponding left and right eigenvector as ($\langle g_L|$ and $|g_R\rangle$). We thus obtain $\sum_{s=1}^q \tilde{A}^s g_R A^{s\dagger} = e^{i\varphi} g_R$, which implies [due to $\rho(\breve{E}_A^A) = 1$ and $\rho(\breve{E}_{\tilde{A}}^{\tilde{A}}) = 1$] that $\tilde{A}^s = e^{i\varphi} g A^s g^{-1}$ with $g = g_R r^{-1} = g_L^{-1} l$. When the uniform matrix product states are not pure, it is sufficient that they contain an equivalent pair of blocks in order to obtain $\rho(\breve{E}_A^{\tilde{A}}) = 1$. Note that the presence of the infrared orthogonality catastrophe within the variational manifold $\mathscr{M}_{\mathrm{uMPS}}$ indicates that uniform matrix product states are not tied to a single Fock space. Many different translation invariant states defining completely separated Hilbert spaces can be represented by a uniform matrix product state with fixed bond dimension D.

This subsection is concluded by a quick study of the tangent plane $\mathbb{T}_{\mathrm{uMPS}(D)}(A)$. A simple repetition of previous derivations starts with the introduction of

$$\begin{aligned} |\Phi(B;A)\rangle = |\Phi^{(A)}(B)\rangle &= B_i \frac{\partial}{\partial A_i} |\Psi(A)\rangle \\ &= \sum_{n\in\mathbb{Z}} \sum_{\{s_n\}=1}^{q} v_L^\dagger \left[\left(\prod_{m<n} A^{s_m} \right) B^{s_n} \left(\prod_{m'>n} A^{s_{m'}} \right) \right] v_R |\{s_n\}\rangle . \end{aligned} \tag{3.73}$$

For the application of the variational principle to the study of translation invariant phenomena, this tangent plane —consisting completely out of translation invariant

states— is sufficient. However, we can also interpret $|\Psi(A)\rangle$ as a special point in the larger class $\mathcal{M}_{\text{MPS}\{D_n=D\}} = \mathcal{M}_{\text{MPS}(D)}$ and define tangent vectors

$$|\Phi^{(A)}[B]\rangle = \sum_{n\in\mathbb{Z}} \sum_{\{s_n\}=1}^{q} v_{\text{L}}^{\dagger} \left[\left(\prod_{m<n} A^{s_m} \right) B^{s_n}(n) \left(\prod_{m'>n} A^{s_{m'}} \right) \right] v_{\text{R}} |\{s_n\}\rangle \tag{3.74}$$

with site dependent matrices $B^s(n)$. These vectors span $\mathbb{T}_{\text{MPS}(D)}(A)$. This larger tangent plane turns out to be important when studying excited states, for which translation invariance is no longer a good assumption. However, when both the Hamiltonian and its ground state is translation invariant, we know that we can label the excited states by a momentum quantum number $p \in [-\pi, \pi)$ (see Subsection 1.3 of Chapter 3). The momentum p sector of the tangent plane $\mathbb{T}_{\text{MPS}(D)}(A)$ is obtained by choosing $B^s(n) = B^s e^{ipn}$, and we define

$$|\Phi_p(B;A)\rangle = |\Phi_p^{(A)}(B)\rangle = \sum_{n\in\mathbb{Z}} e^{ipn} \sum_{\{s_n\}=1}^{q} v_{\text{L}}^{\dagger} \left[\left(\prod_{m<n} A^{s_m} \right) B^{s_n} \left(\prod_{m'>n} A^{s_{m'}} \right) \right] v_{\text{R}} |\{s_n\}\rangle, \tag{3.75}$$

with thus $|\Phi_0(B;A)\rangle = |\Phi(B;A)\rangle$. Thus, $\Phi_p^{(A)}$ represents a linear map from $\mathbb{A}_{\text{uMPS}(D)}$ to the momentum p sector of the tangent plane $\mathbb{T}_{\text{MPS}(D)}(A)$ at the translation invariant point $|\Psi(A)\rangle$, the explicit notation of which is henceforth discarded. This momentum p sector of the tangent plane is denoted as $\mathbb{T}_{\Phi_p} \subset \mathbb{T}_{\text{MPS}(D)} \subset \mathbb{H}_{\mathscr{L}}$, so that $\mathbb{T}_{\text{MPS}(D)} = \bigotimes_{p\in[-\pi,+\pi)} \mathbb{T}_{\Phi_p}$ and $\mathbb{T}_{\text{uMPS}(D)} = \mathbb{T}_{\Phi_0}$. These notations are used interchangeably. The null space $\mathbb{N}_{\Phi_p} \subset \mathbb{A}_{\text{uMPS}(D)}$ follows from applying infinitesimal site-dependent gauge transformations $g(n;\eta) = \mathbb{1}_D + \eta x(n)$ where $x(n) = x e^{ipn}$ with $x \in \mathfrak{gl}(D;\mathbb{C})$. Expressing the invariance of $|\Psi(A)\rangle$ under such infinitesimal gauge transformations allows to define a linear map

$$\mathcal{N}_{\Phi_p} : \mathfrak{gl}(D;\mathbb{C}) \mapsto \mathbb{N}_{\Phi_p} : x \mapsto \mathcal{N}_{\Phi_p}(x) \quad \text{with} \quad \mathcal{N}^s_{\Phi_p}(x) = e^{-ip} x A^s - A^s x, \forall s = 1,\ldots,q. \tag{3.76}$$

The dimensionality of $\mathbb{N}_{\Phi_p}$, and hence of $\mathbb{T}_{\Phi_p}$, can be obtained from the dimension of the null space of $\mathcal{N}_{\Phi_p}$. We assume that the uniform matrix product state $|\Psi(A)\rangle$ is pure, *i.e.* that $\check{E}$ has a unique eigenvalue 1 with eigenvectors $(l|$ and $|r)$, which is also the only eigenvalue on the unit circle. If $\mathcal{N}^s_{\Phi_p}(x) = 0$ $(\forall s = 1,\ldots,q)$, this requires that

$$\check{E}|xr) = e^{-ip}|xr). \tag{3.77}$$

For $p \neq 0$, this equation has no solutions, so that $\dim \mathbb{N}_{\Phi_p} = D^2$ and $\dim \mathbb{T}_{\Phi_p} = (q-1)D^2$. For $p = 0$, this equation has the unique solution $x = \mu \mathbb{1}_D$ with $\mu \in \mathbb{C}$, so that $\dim \mathbb{N}_{\Phi_0} = D^2 - 1$ and $\dim \mathbb{T}_{\Phi_0} = (q-1)D^2 + 1$. But of course, $|\Psi(A)\rangle \in \mathbb{T}_{\Phi_0}$, and restricting to the part $\mathbb{T}^{\perp}_{\Phi_0}$ that is orthogonal to $|\Psi(A)\rangle$ also reduces the dimension to $\dim \mathbb{T}^{\perp}_{\Phi_0} = (q-1)D^2$.

The additive gauge freedom in the representation $|\Phi_p(B)\rangle$ can be removed by restricting to tensors B satisfying either of the following gauge fixing conditions:

- *Left-gauge fixing condition*:

$$\sum_{s=1}^{q} A^{s\dagger} l B^s = 0 \qquad \Leftrightarrow \qquad (l|\check{E}_A^B = 0. \tag{3.78}$$

- *Right-gauge fixing condition*:

$$\sum_{s=1}^{q} B^s r A^{s\dagger} = 0 \qquad \Leftrightarrow \qquad \check{E}_A^B|r) = 0. \tag{3.79}$$

Since these conditions are D^2 dimensional, they fix all D^2 linearly independent gauge transformations in $\mathbb{N}_{\Phi_p}$ for $p \neq 0$. For $p = 0$, there are only $D^2 - 1$ linearly independent gauge transformations, and these D^2 gauge fixing conditions also include norm preservation, *i.e.* they imply $\langle\Psi(A)|\Phi_0(B)\rangle = 0$ or thus $|\Phi_0(B)\rangle \in \mathbb{T}_{\Phi_0}^{\perp}$. For $p \neq 0$, all states automatically satisfy $\langle\Psi(\overline{A})|\Phi_p(B)\rangle = 0$ due to the orthogonality of the different momentum sectors, so that $\mathbb{T}_{\Phi_p}^{\perp} = \mathbb{T}_{\Phi_p}$.

As in the previous subsection, we can actually construct the gauge transformation x that maps an arbitrary choice $\tilde{B}$ satisfying $\langle\Psi(\overline{A})|\Phi_p(\tilde{B})\rangle = 0$ to a different parameterization $B = \tilde{B} + \mathbb{N}_{\Phi_p}(x)$ that satisfies the left-gauge fixing condition in Eq. (3.78). Inserting this transformation and imposing the gauge fixing condition on B as

$$(A^s)^\dagger l[\tilde{B}^s + \mathrm{e}^{-\mathrm{i}p} x A^s - A^s x] = 0$$

results in

$$(lx|(\check{\mathbb{1}} - \mathrm{e}^{-\mathrm{i}p}\check{E}) = (l|\check{E}_A^{\tilde{B}}, \tag{3.80}$$

with $|lx)$ the D^2-component vector associated to the matrix product lx. For $p \neq 0$, the operator $\check{\mathbb{1}} - \mathrm{e}^{-\mathrm{i}p}\check{E}$ is non-singular and can be inverted, hence fixing lx and thus x, since l is assumed to have full rank. For $p = 0$, $\check{\mathbb{1}} - \check{E}$ has a single eigenvalue zero with left and right eigenvectors $(l|$ and $|r)$. We thus have to take a pseudo-inverse, which is only possible if $(l|\check{E}_A^{\tilde{B}}$ has no support in the eigenspace corresponding to eigenvalue zero. Hence, we need to restrict to choices $\tilde{B}$ that satisfy $(l|\check{E}_A^{\tilde{B}}|r) = 0$. If this equation is fulfilled, then we can take the pseudo-inverse, and $(lx|$ is only determined up to an additive part in the zero subspace, *i.e.* if x is a solution, then so is $\tilde{x}$ satisfying $(l\tilde{x}| = (lx| + c(l|$, or thus $\tilde{x} = x + c\mathbb{1}_D$. This freedom corresponds of course to the kernel of $\mathcal{N}_{\Phi_0}$, so that $\mathcal{N}_{\Phi_0}(\tilde{x}) = \mathcal{N}_{\Phi_0}(x)$.

1.7. Symmetries and quantum phases

Finally, a quick note on symmetry and symmetry breaking phases in relation to matrix product states is in order. When a matrix product state $|\Psi[A]\rangle \in \mathscr{M}_{\mathrm{MPS}}$ is expected to be invariant under the action of a symmetry transformation, the point $\{A(n)\} \in \mathbb{A}_{\mathrm{MPS}}$ in its representation must be transformed to some point $\{\tilde{A}(n)\} \in \mathbb{A}_{\mathrm{MPS}}$ that is gauge equivalent to the original. In particular, when applying an internal symmetry transformation $\hat{U} = \bigotimes_{n\in\mathscr{L}} \hat{u}_n$ that is expected to leave the state $|\Psi[A]\rangle$ unchanged, this requires

$$\tilde{A}^s(n) = \sum_{s'=1}^{q} \langle s|\hat{u}_n|s'\rangle A^{s'}(n) = g(n-1)A^s g(n)^{-1}, \forall n = 1,\ldots,D. \tag{3.81}$$

By imposing a gauge fixing condition on A, the transformation matrices g in the virtual space can easily be shown to be unitary. If the symmetry group of the problem is given by G, then we can define for every $h \in \mathsf{G}$ a physical transformation $\hat{U}_h$, and define the associated transformation in the virutal space as g_h. By applying $\hat{U}_{h_1}\hat{U}_{h_2} = \hat{U}_{h_1 h_2}$, we can proof that we must have $g_{h_1 h_2} = \mathrm{e}^{\mathrm{i}\omega(h_1,h_2)} g_{h_2} g_{h_1}$. The additional phase does not feature in $\tilde{A}^s$, so that the matrices g_h constitute a projective representation of G. The phase $\omega(h_1,h_2)$ can be non-trivial throughout the group, which implies that it cannot be gauged away to $\tilde{\omega}(h_1,h_2) = 0$ $(\forall h_1,h_2 \in \mathsf{G})$ by redefining $\tilde{g}_h = \mathrm{e}^{\mathrm{i}\alpha(h)} g_h$ with $\alpha(h)$ some phase for every element $h \in \mathsf{G}$. The corresponding redefinition for ω is given by $\tilde{\omega}(h_1,h_2) = \omega(h_1,h_2) + \alpha(h_1) + \alpha(h_2) - \alpha(h_1 h_2) \mod 2\pi$. This equivalence relation defines different cohomology classes which cannot be transformed into each other [301]. Among them is the trivial class which contains $\omega(h_1,h_2) = 0$ $(\forall h_1,h_2 \in \mathsf{G})$ but non-trivial can classes also exist. The (projective) representation g_h allows us to decompose the decompose the virtual space into irreducible transformations of the group G, so that the entries $A^s_{\alpha,\beta}$ within an irreducible representation are completely determined by the Clebsch?Gordan coefficients, as is dictated by the Wigner-Eckart theorem [302, 303]. Since all elementary operations can then be applied to the different irreducible representations separately, a big gain in computational efficiency is obtained. In addition, by exploiting the decomposition into irreducible representations, quantum states with specific quantum numbers can be constructed and the variational optimization can be restricted to certain symmetry sectors. In particular, the variational wave function for the ground state can be forced to transform according to the trivial representation, whereas a variational optimization in the full space could result in an approximation that does not perfectly fall into this representation. However, as shown in the next section, using the time-dependent variational principle with imaginary time is a very good strategy to reproduce the expected symmetry of the ground state without enforcing it. We do not exploit symmetry in this chapter and refer to [304, 305, 306, 302, 303, 307] for more information about the use of internal symmetries in combination with the density matrix renormalization group, matrix product states or general tensor network states.

Another class of symmetries are the spacetime symmetries. Translation invariance has already been discussed at length in the previous subsection. For one-dimensional systems, other possible spacetime symmetries of the model are parity and time-reversal invariance. A time-reversal transformation in an elementary quantum spin-S systems is obtained by acting with the anti-unitary operator

$$\hat{R} = \exp\left(-\mathrm{i}\pi \hat{S}^y\right)\hat{K}, \tag{3.82}$$

with $\hat{S}_y$ the total spin operator in the y-direction and $\hat{K}$ the anti-linear operator that acts trivially on the standard basis of $\hat{S}_z$ (*i.e.* it transforms the expansion coefficients of the state in the basis $\{|s\rangle, s = -S, \ldots, S\}$ into their complex conjugate values). The generalization to a lattice $\mathscr{L}$ of spin-S systems is straightforward, by introducing the total spin operator $\hat{\vec{J}} = \sum_{n\in\mathscr{L}} \hat{\vec{S}}_n$. We henceforth ignore the additional factor $\exp(-\mathrm{i}\pi\hat{J}^y)$ that rotates the spin of the system around the y-axis and identify the effect of the anti-linear operator $\hat{K}$ with a time-reversal transformation. A Hamiltonian $\hat{H}$ is time-reversal invariant if $[\hat{K}, \hat{H}] = 0$, which implies that $\hat{H}$ has real matrix entries in the standard basis. Since $\hat{K}|\Psi[A]\rangle = |\Psi[A_K]\rangle$ with $A^s_K(n) = \overline{A^s(n)}$ ($\forall s = 1, \ldots, q_n$; $\forall n = 1, \ldots, N$) time-reversal invariance is obtained if there exists a gauge transform $\{g_K(n)\}$ that establishes $\overline{A^s(n)} = g_K(n-1)A^s(n)g_K(n)^{-1}$, $\forall s = 1, \ldots, q_n$, $\forall n = 1, \ldots, N$. Applying $\hat{K}$ again learns that $\overline{g_K(n)}g_K(n) = \mathbb{1}_{D_n}$, $\forall n = 1, \ldots, N$ (by using the assumption that the matrix product state representation has full rank). It is now interesting to ask whether a gauge transformed representation $\tilde{A}^s(n) = g(n-1)A^s(n)g(n)^{-1}$ can be chosen such that it transforms trivially, *i.e.* such that $\tilde{A}^s(n)$ is real, $\forall s = 1, \ldots, q_n$, $\forall n = 1, \ldots, N$. The required condition is that $g_K(n) = \overline{g(n)}^{-1} g(n)$, $\forall n = 1, \ldots, N$. Note that this decomposition is compatible with $\overline{g_K(n)}g_K(n) = \mathbb{1}_{D_n}$. It can be constructed by computing the logarithm of $g_K(n)$, which exists for every invertible matrix. Imposing that $\overline{g_K(n)}g_K(n) = \mathbb{1}_{D_n}$ requires $\log g_K(n)$ to be purely imaginary, or thus, $g_K(n) = \exp[\mathrm{i}x(n)]$ with $x(n)$ a real matrix. It is then sufficient to choose $g(n) = \exp[\mathrm{i}x(n)/2]$. A matrix product state that is time-reversal invariant can thus always be written in a gauge where the matrices are real.

The effect of parity transformation $\hat{\Pi}$ is most easily discussed for a translation invariant state $|\Psi(A)\rangle$, where the specific origin of the reflection does not contribute. We then obtain $\hat{\Pi}|\Psi(A)\rangle = |\Psi(A_\Pi)\rangle$ where $A^s_\Pi = \sum_{s'=1}^q \pi_{s,s'}(A^{s'})^\mathsf{T}$, $\forall s = 1, \ldots, q$, with π an idempotent $q \times q$ matrix (for fermionic systems, it is possible that $\pi^2 = -\hat{\mathbb{1}}$). We henceforth ignore the appearance of π (*i.e.* $\pi_{s,s'} = \delta_{s,s'}$), similar to ignoring the unitary matrix in front of $\hat{K}$ for time-reversal transformations. Parity invariance of the uniform matrix product state $|\Psi(A)\rangle$ then requires the existence of a gauge transformation $g_\Pi \in \mathrm{GL}(D, \mathbb{C})$ such that $(A^s)^\mathsf{T} = g_\Pi A^s g_\Pi^{-1}$, $\forall s = 1, \ldots, q$. Applying the parity transformation again learns that $g_\Pi^{-1} g_\Pi^T = \mathbb{1}_D$, so that g_Π is a complex-symmetric matrix. We now define a gauge transformed set of matrices $\tilde{A}^s = gA^s g^{-1}$ where we would like to choose g such that $\tilde{A}$ transforms trivially under the parity transform (*i.e.* $\tilde{A}^s$ is a complex-symmetric

matrix, $\forall s = 1,\ldots,q$). This requires that $g_\Pi = g^\mathsf{T} g$, which is compatible with g_Π being complex symmetric. Defining the (complex-symmetric) matrix $x = \log g_\Pi$, we can set $g = \exp(x/2)$ in order to obtain $g^\mathsf{T} = g$ and $g_\Pi = g^2$. A matrix product state that is parity-invariant can thus be written in a gauge where the matrices are complex-symmetric.

We now start from a time-reversal invariant matrix product state that is written down using real matrices. If we know that this state is also parity-invariant, can we then further tune the gauge so as to obtain real symmetric matrices? Repeating the analysis from the previous paragraph, we now find in general $A^s_\Pi = [A^s]^\mathsf{T} = g_\Pi A^s g_\Pi^{-1}$ where the real matrix $g_\Pi \in \mathsf{GL}(D,\mathbb{R})$ is symmetric ($g_\Pi^T = g_\Pi$) and thus has real eigenvalues. Can we now find a real gauge transform $g \in \mathsf{GL}(D,\mathbb{R})$ such that $g_\Pi = g^\mathsf{T} g$? Clearly, this is only possible if g_Π is positive definite, which is not true in general. We can try to loosen the restriction of real symmetric matrices, and perform a general complex gauge transform $g \in \mathsf{GL}(D,\mathbb{C})$ so as to obtain a Hermitian matrices $\widetilde{A}^s = g A^s g^{-1}$. This requires $g_\Pi = g^\dagger g$ and is also only possible when g_Π is positive definite. By starting from a parity invariant matrix product state and trying to impose time-reversal invariance, one runs into similar trouble. Clearly, the K-gauge, in which A transforms trivially under the action of $\hat{K}$, is in general not compatible with the Π-gauge, in which A transforms trivially under the action of $\hat{\Pi}$. Because of the computational advantage of working with real variables, the parity invariance is often sacrificed. It is of course recovered, either exactly or approximately, in a good approximation of the ground state. A physical motivation for the incompatibility between the two gauges can be found by noting that real-symmetric or hermitean matrices A^s would imply that the transfer matrix $\check{E}$ has real eigenvalues $x^{(k)}$ only. Since these eigenvalues feature in correlation functions as

$$\langle\Psi(A)|\hat{O}_m\hat{O}_{m+n}|\Psi(A)\rangle = \sum_{k=1}^{D^2} c_k (x^{(k)})^n, \tag{3.83}$$

all correlation functions can at most have an oscillating behavior with period 2. Oscillations with longer periods, which are very common in systems with finite density, would be excluded.

We conclude this section with a discussion of the relation between matrix product state and spontaneous symmetry breaking, for which we necessarily work in the thermodynamic limit. Let us first assume that the ground state manifold $\mathbb{S}^{(\mathrm{g})}$ does not break translation invariance, so that we can use the uniform matrix product state ansatz. Because the approximation accuracy of matrix product states is related to the amount of entanglement in the state, a variational optimization algorithm starting from a set of random matrices A^s will end up in a state $|\Psi(A_z)\rangle$ that (hopefully) provides a good approximation for one of the minimally entangled ground states $|\Psi_z\rangle$ (see Subsections 1.4 and 2.4 in Chapter 1). Away from the critical point, the system is gapped in the symmetry broken regime (for discrete symmetry breaking) and the corresponding ground states are exponentially clustering. We can thus expect that $\check{E}_z$ has a unique eigenvalue 1, and all

other eigenvalues are inside the unit circle. Let now $|\Psi(A_z)\rangle$ and $|\Psi(A_{z'})\rangle$ represent the best uniform matrix product state approximation for the exact ground states $|\Psi_z\rangle$ and $|\Psi_{z'}\rangle$. Note that, using Eq. (1.29), the matrices $A^s_{z'}$ can be derived from A^s_z by acting on $|\Psi(A_z)\rangle$ with $\hat{U}(g_{z'})\hat{U}(g_z)^\dagger$, thus yielding $A^s_{z'} = \sum_{s'=1}^{z} \langle s|\hat{u}(g_{z'})\hat{u}(g_z)^\dagger|s'\rangle A^{s'}_z$, with $\hat{u}(g)$ the local transformations associated to the symmetry group. All minimally entangled ground states thus have an equally good approximation within the variational manifold $\mathscr{M}_{\mathrm{uMPS}(D)}$ for a fixed value of D. An equally good uniform matrix product state representation of a general superposition $|\Psi\rangle$ of the minimally entangled ground states requires a set of matrices $A^s = \bigoplus_z A^s_z$, where the range of z contains all ground states z that are present in $|\Psi\rangle$. The increased entanglement thus requires a much larger bond dimension. Finally, we can require normalizability and orthogonality of the different ground state approximations ($\langle\Psi(A_z)|\Psi(A_{z'})\rangle = \delta_{z,z'}$. Using

$$\langle\Psi(A_z)|\Psi(A_{z'})\rangle \sim \lim_{N\to\infty} \left\| \check{E}^{A_{z'}}_{A_z} \right\|^{2N+1}, \tag{3.84}$$

this boils down to

$$\rho(\check{E}^{A_z}_{A_z}) = 1, \qquad \text{and} \qquad \rho(\check{E}^{A_{z'}}_{A_z}) < 1 \text{ for } z \neq z'. \tag{3.85}$$

If on the other hand $\rho(\check{E}^{A_{z'}}_{A_z}) = 1$ where $A_{s'}$ is obtained as $\hat{U}(g_{z'})\hat{U}(g_z)^\dagger|\Psi(A_z)\rangle = |\Psi(A_{z'})\rangle$, then we can conclude that there exists a gauge transformation g such that $A^s_{z'} = \mathrm{e}^{\mathrm{i}\varphi} g A^s_z g^{-1}$ (see previous subsection) and the matrix products states $|\Psi(A_z)\rangle$ and $|\Psi(A_{z'})\rangle$ are equal. The fidelity per site $d(A_z, A_{z'}) = 1$ and the system is in a symmetric phase, provided that the matrix product states approximate the exact ground states accurately. Note that continuous symmetries for which the order parameter does not commute with the Hamiltonian cannot be broken in one-dimensional systems. They can however be critical. Close to the critical point, a matrix product state approximation of the ground state might falsely predict symmetry breaking, whenever it can create an excited state with nearly massless excitations that has much less entanglement than the ground state (see [308] for an example).

If the ground state manifold $\mathbb{S}^{(\mathrm{g})}$ of a system breaks translation invariance and is only invariant under $\hat{T}^P$, the minimally entangled ground states $|\Psi_z\rangle$ cannot be described by a uniform matrix product state. Applying the variational manifold within the class of uniform matrix product states then results in an approximation of some translation invariant superposition $\sum_{p\in\mathbb{Z}_P} \hat{T}^p|\Psi_z\rangle = \sum_{p\in\mathbb{Z}_P} |\Psi_{(z+p) \bmod P}\rangle$. The matrices A^s then have a periodic decomposition with period P. A description of the minimally entangled ground states $|\Psi_q\rangle$ requires a P-periodic matrix product states. An alternative approach is to group P sites into one effective site. And sometimes it is possible to transform the Hamiltonian $\hat{H}$ of the system by local unitary operators $\hat{U}$ such that the new Hamiltonian $\hat{H}' = \hat{U}\hat{H}\hat{U}^\dagger$ is still translation invariant and has a ground state manifold $\mathbb{S}^{(\mathrm{g})\prime}$ that does not break translation invariance.

Different theoretical results regarding the relation between symmetry breaking and matrix product or finitely correlated states have been obtained. In particular, one can proof that, if a uniform matrix product state $|\Psi(A)\rangle$ has a canonical representation with J blocks ($A = \bigoplus_{j=1}^{J} A_j$), it is the ground state of a parent Hamiltonian for which the ground state manifold has a degeneracy J. All the states $|\Psi(A^{(k)})\rangle$ are exact ground states of this Hamiltonian [299, 273]. In fact, for any set of given uniform matrix states $|\Psi(A_j)\rangle$ with $j = 1,\ldots,J$, a parent Hamiltonian can be constructed for which the ground state manifold is exactly spanned by these uniform matrix product states. The corresponding broken symmetry in this Hamiltonian is in general highly complex and unphysical [309]. Note that a matrix product state description can aid in the characterization of quantum phases with both local order parameters [310] or string order parameters [311]. In addition, because the fidelity is very easily evaluated for (uniform) matrix product states, it can be used to characterize a phase transition [312]. The formalism of matrix product states and higher dimensional generalizations can even be used to characterize all phases (including topological phases) in physical systems [301], based on previous ideas regarding renormalization group transformations of quantum states described by tensor networks [229, 313]. These renormalization group transformations do however fail to include critical points as fixed points, and a matrix product description of second order phase transitions including non-analytic ground state energy, algebraically decaying correlations and a diverging entanglement entropy is impossible for finite values of the bond dimension D. Very close to the critical point, the matrix product state description eventually reproduces the mean field result for *e.g.* the value of the critical exponents [314]. It is however possible to engineer special quantum phase transitions which are not characterized by these properties and do allow an exact matrix product state description [315, 316].

2. Time-dependent variational principle for $\mathscr{M}_{\text{MPS}}$

Jutho Haegeman, J. Ignacio Cirac, Tobias J. Osborne, Iztok Pižorn,
Henri Verschelde, Frank Verstraete.
"*Time-dependent variational principle for quantum lattices*".
Physical Review Letters 107, 070601 (2011).

2.1. Introduction

In this section we apply the time-dependent variational principle (see Section 2 of Chapter 2) to the variational manifold $\mathscr{M}_{\text{MPS}\{D_n\}}$ and $\mathscr{M}_{\text{uMPS}(D)}$. Despite the generality of the time-dependent variational principle, it had not been used in previous algorithms for time evolution with matrix product states. Initial attempts to expand the possibilities of the density matrix renormalization group beyond the case of ground states did not rely on the matrix product state concept. Rather than trying to fully approximate the

time-evolving wave function, these early algorithms centered on a direct evaluation of the spectral function

$$G^{\alpha,\beta}_{m,n}(\omega+\mathrm{i}\eta) \triangleq \langle\Psi|\hat{O}^{\alpha}_{m}(E_{\Psi}+\omega+\mathrm{i}\eta-\hat{H})^{-1}\hat{O}^{\beta}_{n}|\Psi\rangle\,, \tag{3.86}$$

with $|\Psi\rangle$ the ground state (approximation), E_{Ψ} the corresponding (approximate) ground state energy and η some small constant that should be scaled to zero. The spectral function $g^{\alpha,\beta}_{m,n}(\omega)$ is obtained as the Fourier transform of the time-dependent correlation function

$$G^{\alpha,\beta}_{m,n}(t-t') \triangleq \langle\Psi|\hat{O}^{\alpha}_{m}(t)\hat{O}^{\beta}_{n}(t')|\Psi\rangle\,. \tag{3.87}$$

Using a full set of eigenvectors $|\Psi_k\rangle$ and corresponding eigenvalues E_k of the Hamiltonian $\hat{H}$ (with $|\Psi\rangle$ exactly or approximately equal to $|\Psi_0\rangle$ and E_{Ψ} exactly or approximately equal to E_0), the spectral function $g^{\alpha,\beta}_{m,n}(\omega)$ can be expanded as

$$G^{\alpha,\beta}_{m,n}(\omega+\mathrm{i}\eta) = \sum_{k}\langle\Psi|\hat{O}^{\alpha}_{m}|\Psi_k\rangle\,\langle\Psi_k|\hat{O}^{\beta}_{n}|\Psi\rangle\,\frac{1}{\omega+\mathrm{i}\eta-(E_k-E_{\Psi})}. \tag{3.88}$$

For $\eta\to 0$, the spectral function has poles at the (exact or approximate) excitation energies $E_k - E_{\Psi}$, so that the spectral function can be used to probe the spectrum of excited states. The pioneering algorithms for evaluating the spectral function in Eq. (3.86) were based on a variety of techniques. Examples include Lanczos vector dynamics [317] and the correction vector method [318, 319]. This last method was reformulated in terms of a variational principle under the name of "dynamical density matrix renormalization group" [320]. A recent overview of these methods can be found in [321].

The use of spectral functions is restricted to studying the time evolution of localized perturbations with respect to a time-independent Hamiltonian. Time-dependent perturbations and parameter quenches require an approximation of the full time evolution of the initial state. Early algorithms based on the density matrix renormalization group for directly simulating time evolution of quantum states were constructed in [322, 323, 324]. However, all modern approaches are based on the *time evolving block decimation*, which was first developed in the context of matrix product states [325]. It was later reformulated in order to be compatible with traditional density matrix renormalization group implementations [326, 327]. It is based on an iterative application of a Lie-Trotter-Suzuki decomposition [328, 329] of the exact evolution operator for a small time step $\mathrm{d}t$ as

$$\exp(\mathrm{i}\hat{H}\mathrm{d}t) = \exp(\mathrm{i}\hat{H}^{(A)}\mathrm{d}t)\exp(\mathrm{i}\hat{H}^{(B)}\mathrm{d}t) + \mathcal{O}(\mathrm{d}t^2). \tag{3.89}$$

Higher order decompositions with an error of $\mathcal{O}(\mathrm{d}t^p)$ are also possible [330]. $\hat{H}^{(A)}$ and $\hat{H}^{(B)}$ provide a decomposition of the (possibly time-dependent) Hamiltonian $\hat{H} = \hat{H}^{(A)} + \hat{H}^{(B)}$, such that $\hat{H}^{(A)}$ and $\hat{H}^{(B)}$ separately contain local terms that all commute. If necessary, a decomposition into more than two parts is also possible. For a nearest-neighbor Hamiltonian $\hat{H} = \sum_{n\in\mathbb{Z}}\hat{h}_{n,n+1}$, a possible decomposition scheme is into even and odd terms: $\hat{H}^{(A)} = \sum_{n\in\mathbb{Z}}\hat{h}_{2n,2n+1}$ and $\hat{H}^{(B)} = \sum_{n\in\mathbb{Z}}\hat{h}_{2n+1,2n+2}$. The individual

operators $\exp(\mathrm{i}\hat{H}^{(A)})$ and $\exp(\mathrm{i}\hat{H}^{(B)})$ then split into a product of local unitaries, that can be dealt with in a parallelized and efficient way. When applied to a matrix product state $|\Psi[A]\rangle \in \mathscr{M}_{\mathrm{MPS}\{D_n\}}$, these individual evolution operators take the state outside the original manifold to a state $|\Psi'[A']\rangle \in \mathscr{M}_{\mathrm{MPS}\{D'_n\}}$, since they have the effect of increasing the virtual bond dimension. To proceed, one then approximates the new state $|\Psi'[A']\rangle$ by a matrix product state $|\Psi[\tilde{A}]\rangle$ in the original variational manifold $\mathscr{M}_{\mathrm{MPS}\{D_n\}}$. The best strategy for truncating a single bond dimension is obtained by discarding the smallest Schmidt values (see Subsection 1.1). When several bond dimensions are simultaneously truncated, this strategy still serves as a good initial guess but is not globally optimal. For lattices $\mathscr{L}$ of finite size, the global minimization of $\| |\Psi'[A']\rangle - |\Psi[\tilde{A}]\rangle \|$ can accurately be solved using algorithms inspired by the sweeping process of the finite-size algorithm of the density matrix renormalization group.

The time evolving block decimation can also be applied to translation invariant systems in the thermodynamic limit. By combining it with an imaginary time evolution, this allowed for the first time to use the class of uniform matrix product states as a variational ansatz [300]. However, no globally optimal strategy for truncation of the bond dimension is known. In addition, the strategy based on locally discarding the smalllest Schmidt values assumes that the local time evolution operators are unitary, which is no longer true for imaginary time evolution. As a variational strategy, the infinite size time evolving block decimation then requires a scaling of $\mathrm{d}t \to 0$ as the optimal approximation is approached. Since the exact imaginary time evolution automatically slows down in the neighborhood of the ground state (approximation), the need for scaling induces an additional unfavorable slowing down.

In addition, both for finite and infinite systems, not all symmetries of the Hamiltonian $\hat{H}$ are inherited by the individual Trotter evolution operators $\exp(\mathrm{i}\hat{H}^{(A)}\mathrm{d}t)$ and $\exp(\mathrm{i}\hat{H}^{(B)}\mathrm{d}t)$. In itself, the Lie-Trotter-Suzuki decomposition is symplectic and under an exact iterative application of the Trotter operators, errors resulting from these broken symmetries would be strongly bound. However, the additional truncation after every evolution step ruins the symplecticity and drifting errors are possible. In particular, for a time-independent Hamiltonian $\hat{H}$, the expectation value of the Hamiltonian is a constant of motion, but will drift away in a simulation based on the time evolving block decimation. The time-dependent variational principle provides a solution to these problems, as it is a symplectic method that is globally optimal (also in the thermodynamic limit) and never leaves the variational manifold, so that no truncation of any kind is necessary. There is no need for a Trotter decomposition and hence no corresponding Trotter error. This approach is also perfectly applicable in case of imaginary time evolution (there is no symplecticity of course). Since only the computation of expectation values is required, the time-dependent variational principle can also perfectly be combined with strategies for exploiting symmetry. So far, this has not been done.

The time-dependent variational principle produces a highly non-linear set of coupled differential equations and thus requires a numerical integration scheme with time step

$\mathrm{d}t$. Time discretization errors are thus present, but they can easily be controlled. For imaginary time evolution, a simple first order Euler-step algorithm is sufficient. The relevant formulae for the variational manifolds $\mathscr{M}_{\mathrm{MPS}\{D_n\}}$ and $\mathscr{M}_{\mathrm{uMPS}(D)}$ are presented in Subsection 2.2 and 2.3 respectively and an efficient implementation, based on the Euler algorithm, is sketched. Even though large (second-order) errors can be present, this is not an issue since imaginary time evolution is extremely stable and self-correcting, and always strives to end up in an energy minimum. For imaginary time evolution with the time-dependent variational principle we expect a monotonically decreasing energy expectation value. As long as the step size $\mathrm{d}t$ is small enough to reproduce this monotonic decrease, there is no need to change it. A decrease of the time step should thus only be considered when higher-order effects result in an energy increase. In contrast to the time-evolving block decimation, no scaling of $\mathrm{d}t \to 0$ is necessary, since the algorithm automatically slows down near the minimum.

For real time-evolution, it is often important that the numerical integration scheme inherits the symplectic properties and a more advanced numerical integration scheme is necessary, to be discussed in Subsection 2.5. Since entanglement grows linearly under real time evolution [see Eq. (1.75) in Subsection 2.5 of Chapter 1], a dynamic increase of the bond dimension is sometimes useful. This is straightforwardly accomplised in the time evolving block decimation (by skipping the truncation step), but requires more effort in combination with the time-dependent variational principle, which naturally stays in the original manifold. Subsection 2.6 describes a strategy for a dynamical increase of the bond dimension. Subsection 2.7 concludes this section by showing some exemplary results.

2.2. Generic matrix product states

The flow equations of the time-dependent variational principle [Eq. (2.17)] for the variational manifold $\mathscr{M}_{\mathrm{MPS}\{D_n\}}$ of generic matrix product states on lattices $\mathscr{L}$ of finite size were written down for the first time in [331], but they were not further investigated and no attempt was made to implement these equations into an efficient algorithm for real or imaginary time evolution. Setting $\mathrm{d}A^s(n;t)/\mathrm{d}t = B(n;t)$, we obtain

$$\frac{\mathrm{d}}{\mathrm{d}t}\,|\Psi[A(t)]\rangle = |\Phi^{[A(t)]}[B(t)]\rangle\,, \tag{3.90}$$

where the tangent vectors $|\Phi^{[A]}[B]\rangle$ were defined in Eq. (3.7). According to Subsection 2.2 of the previous chapter, the flow equations boil down to finding the set of tensors $B(n;t)$ from

$$B(t) = \arg\min_{B} \left\| |\Phi[B;A(t)]\rangle - \hat{H}\,|\Psi[A(t)]\rangle \right\|^2 . \tag{3.91}$$

The expansion of Eq. (3.91) contains the metric of the tangent vectors, which is encoded in the overlap elements

$$\begin{aligned}\langle\Phi[\overline{B};\overline{A}]|\Phi[B';A]\rangle = &\sum_{n<n'=1}^{N}(l(n-1)|\check{E}^{A(n)}_{B(n)}\left(\prod_{m=n+1}^{n'-1}\check{E}^{A(m)}_{A(m)}\right)\check{E}^{B'(n')}_{A(n')}|r(n'))\\ &+\sum_{n'<n=1}^{N}(l(n'-1)|\check{E}^{B(n')}_{A(n')}\left(\prod_{m=n'+1}^{n-1}\check{E}^{A(m)}_{A(m)}\right)\check{E}^{A(n)}_{B(n)}|r(n))+\sum_{n=1}^{N}(l(n-1)|\check{E}^{B'(n)}_{B(n)}|r(n)),\end{aligned} \tag{3.92}$$

where the definitions in Eq. (3.37) and Eq. (3.40) were used. The metric is thus a complicated matrix of size $\dim\mathbb{A}_{\mathrm{MPS}\{D_n\}}\times\dim\mathbb{A}_{\mathrm{MPS}\{D_n\}}$, that couples all variations $B(n)$ and $B'(n')$ at different sites n and n'. It seems like an impossible task to invert this gigantic matrix, which is required by the time-dependent variational principle. This problem could be solved by using an iterative implementation, but the evaluation of $\langle\Phi^{[A]}[B]|\Phi^{[A]}[B']\rangle$ would still scale as $\mathcal{O}(L^2)$, which is also very unfavorable. However, we still have to fix the gauge of B and can exploit this to simplify the overlap, as will now become clear. In addition, we also have to pay attention to the fact that $|\Phi[A;A]\rangle = N|\Psi[A]\rangle\in\mathbb{T}_{\mathrm{MPS}\{D_n\}}[A]$, which requires to use the modified time-dependent variational principle discussed in Subsection 2.3 of the previous chapter. Rather than defining a modified metric and gradient as in Eq. (2.27) and (2.28), we can simply restrict to tensors B such that $|\Phi[B;A]\rangle\in\mathbb{T}^{\perp}_{\mathrm{MPS}\{D_n\}}[A]$. Both fixing the gauge freedom and restricting to $\mathbb{T}^{\perp}_{\mathrm{MPS}\{D_n\}}[A]$ is obtained by imposing the gauge fixing conditions in Eq. (3.54) or (3.55). Either of these gauge fixing conditions simplify the overlap to

$$\langle\Phi[\overline{B};\overline{A}]|\Phi[B';A]\rangle = \sum_{n=1}^{N}(l(n-1)|\check{E}^{B'(n)}_{B(n)}|r(n)) \tag{3.93}$$

and eliminate all non-local terms. We henceforth omit the explicit notation $[A]$ in the tangent vectors.

It is now easy to find a linear parameterization[5] $B=\mathcal{B}_\Phi[x]$ depending on N matrices $x(n)$ $(n=1,\ldots,N)$ of size $D_{n-1}\times(q_nD_n-D_{n-1})$, where $\mathcal{B}_\Phi[x](n)$ depends only on $x(n)$, so that $\mathcal{B}_\Phi[x]$ satisfies the right gauge fixing conditions [Eq. (3.55)] and so that the effective Gram matrix becomes the unit matrix. We thereto define the $q_nD_n\times D_{n-1}$ matrices $R(n)$ as

$$[R(n)]_{(\alpha,s);\beta} = [r(n)^{1/2}A^s(n)^\dagger]_{\alpha,\beta} \tag{3.94}$$

and then construct a $(q_nD_n-D_{n-1})\times q_nD_n$ matrix $V_R(n)$ so that $V_R(n)^\dagger$ contains an orthonormal basis for the null space of $R(n)^\dagger$, *i.e.* $V_R(n)R(n)=0$ and $V_R(n)V_R(n)^\dagger = \mathbb{1}_{q_nD_n-D_{n-1}}$, for all $n=1,\ldots,N$. Setting $[V^s_R(n)]_{\alpha,\beta}=[V_R(n)]_{\alpha;(\beta,s)}$, we then define the

[5] It is important that this representation is linear in order to preserve the vector space structure of the tangent plane, and in particular to preserve the quadratic character of the optimization problem in Eq. (3.91).

representation $\mathcal{B}^s[x](n)$ as

$$\mathcal{B}^s[x](n) = l(n-1)^{-1/2} x(n) V_R^s r(n)^{-1/2} \tag{3.95}$$

in order to obtain

$$\langle \Phi[\overline{\mathcal{B}_\Phi}[\overline{x}]] | \Phi[\mathcal{B}_\Phi[y]] \rangle = \sum_{n=1}^{L} \mathrm{tr}\left[x(n)^\dagger y(n) \right] \tag{3.96}$$

and $\sum_{s=1}^{q_n} \mathcal{B}_\Phi^s[x](n) r(n+1) A^s(n)^\dagger = 0$, $\forall n = 1,\ldots,N$. Analogously, an alternative representation $\widetilde{\mathcal{B}}_\Phi[x]$ in terms of matrices $x(n)$ of size $(q_n D_{n-1} - D_n) \times D_n$ ($\forall n = 1,\ldots,N$) can be constructed, so that the matrices $B^s(n) = \widetilde{\mathcal{B}}_\Phi^s[x](n)$ satisfy the left gauge fixing conditions [Eq. (3.54)]. Define thereto the $D_n \times q_n D_{n-1}$ matrix $L(n)$ as

$$[L(n)]_{\alpha;(s,\beta)} = [A^s(n)^\dagger l(n-1)^{1/2}]_{\alpha,\beta} \tag{3.97}$$

and then construct a $q_n D_{n-1} \times (q_n D_{n-1} - D_n)$ matrix $V_L(n)$ that contains an orthonormal basis for the null space of $L(n)$, *i.e.* $L(n)V_L(n) = 0$ and $V_L(n)^\dagger V_L(n) = 1$, for all $n = 1,\ldots,N$. By defining $[V_L^s(n)]_{\alpha,\beta} = [V_L(n)]_{(s\alpha),\beta}$, the representation $\widetilde{\mathcal{B}}_\Phi[x]$ is obtained as

$$\widetilde{\mathcal{B}}_\Phi^s[x](n) = l(n-1)^{-1/2} V_L^s x(n) r(n)^{-1/2}. \tag{3.98}$$

For evaluating $\langle \Phi[\overline{B}] | \hat{H} | \Psi[A] \rangle$, we assume that $\hat{H}$ is a nearest neighbor Hamiltonian $\hat{H} = \sum_{n=1}^{L-1} \hat{h}_{n,n+1}$ with $\hat{h}_{n,n+1}$ acting non-trivially only on sites n and $n+1$. The generalization to Hamiltonians with interactions over three or more sites is straightforward. Assuming that B satisfies the right gauge fixing condition, we obtain

$$\begin{aligned} \langle \Phi[\overline{B}] | \hat{H} | \Psi[A] \rangle = \sum_{n=1}^{L} \Bigg[& \theta(n<N)(l(n-1)|\check{E}^{C(n)}_{B(n)A(n+1)}|r(n+1)) \\ & + \theta(n>1)(l(n-2)|\check{E}^{C(n-1)}_{A(n-1)B(n)}|r(n)) \\ & + \theta(n<N-1) \sum_{m=n+1}^{N-1} (l(n-1)|\check{E}^{A(n)}_{B(n)} \left(\prod_{k=n+1}^{m-1} \check{E}^{A(k)}_{A(k)} \right) \check{E}^{C(m)}_{A(m)A(m+1)}|r(m+1)) \Bigg], \end{aligned} \tag{3.99}$$

where θ is a discrete Heaviside function that yields one if its argument is true and zero otherwise, where

$$C^{s,t}(n) = \sum_{u=1}^{q_n} \sum_{v=1}^{q_{n+1}} \langle s,t|\hat{h}_{n,n+1}|u,v\rangle A^u(n) A^v(n+1) \tag{3.100}$$

and where we have extended the definition of $\check{E}_B^A$ in order to include

$$\check{E}^{C(n)}_{A(n)B(n+1)} = \sum_{s=1}^{q_n}\sum_{t=1}^{q_{n+1}} C^{s,t}(n) \otimes \overline{A^s(n)B^t(n+1)}. \tag{3.101}$$

In case of left gauge fixing, the last term in Eq. (3.99) would be replaced by a term containing all contributions of the Hamiltonian acting to the left of $B(n)$. These terms are familiar from the standard variational sweeping algorithm for matrix product states, and it is well known how to construct them efficiently and iteratively. Note that $\langle\Phi[\overline{B}]|\hat{H}|\Psi[A]\rangle$ can be interpreted as the energy gradient, which had been computed before in a matrix product state framework [289], in order to apply a steepest descent algorithm. However, the time-dependent variational principle together with a detailed study of the representation of the tangent plane $\mathbb{T}_{\mathrm{MPS}\{D_n\}}$ learns that the best direction to travel along for converging to the optimum is not the mere gradient, except when a suitable representation is chosen for which the metric is the identity matrix.

We now have all the ingredients to evaluate

$$\begin{aligned}\Big\| |\Phi[B;A]\rangle - \hat{H}\,|\Psi[A]\rangle \Big\|^2 = \langle\Phi[\overline{B};\overline{A}]|\Phi[B;A]\rangle - \langle\Phi[\overline{B};\overline{A}]|\hat{H}|\Psi[A]\rangle \\ - \langle\Psi[\overline{A}]|\hat{H}|\Phi[B;A]\rangle + \langle\Psi[\overline{A}]|\hat{H}^2|\Psi[A]\rangle\,. \end{aligned}\tag{3.102}$$

Inserting the current solution $A(t)$ and a representation $B = \mathcal{B}_\Phi[x]$ and differentiating with respect to $x(n)^\dagger$ produces the solution $x^\star(t)$ that minimizes Eq. (3.102); we obtain

$$\begin{aligned}|\Phi[\mathcal{B}_\Phi[x^\star(t)];A(t)]\rangle &= \hat{P}_{\mathbb{T}^\perp_{\mathrm{MPS}}}[\overline{A(t)},A(t)]\hat{H}\,|\Psi[A(t)]\rangle \\ \Leftrightarrow \quad x^\star(n;t) &= \frac{\partial}{\partial\, x(n)^\dagger}\,\langle\Phi[\overline{\mathcal{B}_\Phi}[\overline{x}];A(t)]|\hat{H}|\Psi[A(t)]\rangle\,. \end{aligned}\tag{3.103}$$

Let us now outline all the necessary steps in a single iteration of a simple Euler implementation for imaginary time evolution, where the value of A is overwritten after every step:

1. Define $K(N+1) = 0$ (scalar) and $K(N) = 0$ ($D_{N-1}\times D_{N-1}$ matrix) and compute the $D_{n-1}\times D_{n-1}$ matrices $K(n)$ as

$$K(n) = \sum_{s=1}^{q_n}\sum_{t=1}^{q_{n+1}} C^{s,t}(n)\,r(n+1)A^t(n+1)^\dagger A^s(n)^\dagger + \sum_{s=1}^{q_n} A^s(n)K(n+1)A^s(n)^\dagger \tag{3.104}$$

   for $n = N-1, N-2, \ldots, 1$, with $C(n)$ given in Eq. (3.100). $K(1)$ corresponds to the energy expectation value $H[\overline{A},A]$ if $|\Psi[A]\rangle$ is normalized to unity.

2. Define, for $n = 1,\ldots,N$, the $q_nD_n\times D_{n-1}$ matrices $R(n)$ as in Eq. (3.94) and

construct the $(q_n D_n - D_{n-1}) \times q_n D_n$ matrices $V_R(n)$ so that $V_R(n)R(n) = 0$ and $V_R(n)V_R(n)^\dagger = \mathbb{1}_{q_n D_n - D_{n-1}}$.

3. Define the $(q_n D_{n-1} - D_n) \times D_n$ matrices $F(n)$ $(n = 1, \ldots, N)$ as

$$\begin{aligned} F(n) = & \\ & \theta(n < N) \sum_{s=1}^{q_n} \sum_{t=1}^{q_{n+1}} l(n-1)^{1/2} C^{s,t}(n) r(n+1) A^t(n+1)^\dagger r(n)^{-1/2} V_R^s(n)^\dagger \\ & + \theta(n > 1) \sum_{t=1}^{q_{n-1}} \sum_{s=1}^{q_n} l(n-1)^{-1/2} A^t(n-1)^\dagger l(n-2) C^{t,s}(n-1) r(n)^{1/2} V_R^s(n)^\dagger \\ & + \theta(n < N-1) \sum_{s=1}^{q_n} l(n-1)^{1/2} A^s(n) K(n+1) r(n)^{-1/2} V_R^s(n)^\dagger, \end{aligned} \quad (3.105)$$

so that $\langle \Phi^{[A]}[\overline{\mathcal{B}_\Phi}[\overline{x}]] | \hat{H} | \Psi[A] \rangle = \sum_{n=1}^{N} \mathrm{tr}[x(n)^\dagger F(n)]$.

4. Set $x^\star(n) = F(n)$, $\forall n = 1, \ldots, N$. Take a step $A^s(n) \leftarrow A^s(n) - \mathrm{d}\tau\, \mathcal{B}^s[x^\star](n)$.

5. Set $l(0) = 1$ and compute $l(n) = \sum_{s=1}^{q_n} A^s(n)^\dagger l(n-1) A^s(n)$ for $n = 1, \ldots, N$. The norm of the new state is given by $l(N)$; renormalize if necessary. Set $r(N) = 1$ and compute

$$r(n) = \sum_{s=1}^{q} A^s(n+1) r(n+1) A^s(n+1)^\dagger$$

for $n = N-1, \ldots, 0$. Bring A back to chosen canonical representation (optional).

6. Repeat step 1 and evaluate the energy $H[\overline{A}, A]$ of the new state. Change $\mathrm{d}t$ if necessary.

Every step can be computed with computational complexity $\mathcal{O}(ND^3)$, just as in the standard time-independent sweeping algorithm. However, unlike in the sweeping algorithm, the determination of the change $A^s(n) \leftarrow A^s(n) - \mathrm{d}t\, \mathcal{B}^s[x](n)$ — even though only valid for $\mathrm{d}t$ not too large — is globally optimal and thus includes all correlations from the changes at every other site in the lattice. This has to be compared to the variational sweeping algorithm, where the energy is minimized with respect to a single tensor $A(n)$ while keeping all other tensors fixed. While the update of $A(n)$ is not restricted to small variations —the optimization problem for $A(n)$ alone is quadratic and can be solved exactly— it is possible that the large update is only locally optimal and receives large corrections in the next sweep, when the other tensors in the sites have been updated. In addition, solving this quadratic problem is an eigenvalue problem, which is done iteratively in order to keep the computational complexity at $\mathcal{O}(D^3)$. This operation dominates the computational speed at large values of the bond dimension D. When using the time-dependent variational principle as a variational optimization method, the update for the matrices $A(n)$ is straightforwardly computed through a number of $D \times D$ matrix multiplications. No iterative eigensolver or linear solver is required. Hence,

one 'sweep' (iteration step) of the time-dependent variational principle will be much faster than a corresponding sweep in the traditional variational sweeping algorithm. It is thus interesting to see whether this implementation can outperform the traditional sweeping algorithm in convergence speed. In particular, this might be the case near critical points where the traditional algorithm also requires many sweeps due to the long range correlations which are not taken into account in the local update. However, the time-dependent variational principle for generic matrix product states has not yet been implemented. Since the focus of this dissertation is extended systems with translation invariance, only the algorithm for uniform matrix product states, to be discussed in the next subsection, has been implemented.

For lattices of finite size with periodic boundary conditions, the gauge freedom cannot be exploited to fully decouple variations at different sites. The resulting algorithm is much more complicated and an exact implementation with computational complexity $\mathcal{O}(D^3)$ is impossible. This situation is familiar from the traditional approaches for matrix product states with periodic boundary conditions.

2.3. Uniform matrix product states

The tangent vectors $|\Phi(B;A)\rangle$ in a point $|\Psi(A)\rangle$ of the variational manifold $\mathscr{M}_{\mathrm{uMPS}(D)}$ are defined in Eq. (3.73). Setting $\mathrm{d}A^s(t)/\mathrm{d}t = B^s(t)$, the time dependent variational principle dictates to choose $B(t)$ as

$$B(t) = \arg\min_B \left\| |\Phi(B;A(t))\rangle - \hat{H}\,|\Psi(A(t))\rangle \right\|^2 . \tag{3.106}$$

All relevant quantities can just as easily be computed for the generalized set of tangent vectors $|\Phi_p(B;A)\rangle$ spanning the tangent plane $\mathbb{T}_{\mathrm{MPS}(D)}(A)$, as defined in Eq. (3.75). These expressions are required in the next section anyway and it automatically follows that only $|\Phi_0(B;A)\rangle = |\Phi(B;A)\rangle$ contributes to the time-dependent variational principle when applied to translation invariant Hamiltonians.

We henceforth assume that $|\Psi(A)\rangle$ is pure, so that the transfer matrix $\check{E} = \check{E}^A_A$ has a unique eigenvalue $\omega^{(1)} = 1$ with corresponding left and right eigenvectors $(l^{(1)}| = (l|$ and $|r^{(1)}) = |r)$ that we assume to be normalized as $(l|r) = 1$, and that all other eigenvalues $\omega^{(k)}$, $k > 1$ lie strictly within the unit circle. If the largest eigenvalue $\omega^{(1)}$ of $\check{E}$ differs from one, the matrices A have to be rescaled as $A/\sqrt{\omega^{(1)}}$. We also define $\check{S}^{(1)} = \check{S} = |r)(l|$ as a projector onto the eigenspace of eigenvalue 1, and its complement $\check{Q} = \mathbb{1} - \check{S}$. We further assume that these eigenvector can be obtained from the application of an iterative eigensolver to the efficiently implementable maps $\mathcal{E}$ and $\widetilde{\mathcal{E}}$, so that all required information is available at a computational cost of $\mathcal{O}(D^3)$.

We now start by computing the overlap between two tangent vectors $\langle\Psi_{p'}(\overline{B'})|\Psi_p(B)\rangle$, which encodes the metric. We have to be very careful with the infinite sums over the

positions $n \in \mathbb{Z}$ and $n' \in \mathbb{Z}$ of B and B'. When a diverging result is obtained, it is easily possible to make errors by miscounting. Only when the result is guaranteed to be finite can we freely use index substitutions. We therefore replace every occurrence of $\check{E}^n$ by a 'regularized' operator $\check{Q}\check{E}^n\check{Q} = \check{E}^n\check{Q} = \check{Q}\check{E}^n = \check{E}^n - |r)(l| = \check{Q}(\check{Q}\check{E}\check{Q})^n\check{Q}$ with $\rho(\check{Q}\check{E}\check{Q}) < 1$ and a 'singular' part $\check{S} = |r)(l|$. The reason of this notation becomes clear if we now evaluate $\langle\Psi_p(\overline{B};\overline{A})|\Psi_{p'}(B';A)\rangle$ as

$$\begin{aligned}
&\langle\Phi_p(\overline{B};\overline{A})\,|\,\Phi_{p'}(B';A)\rangle \\
&\quad= \sum_{n=-\infty}^{+\infty}\sum_{n'=-\infty}^{+\infty} \mathrm{e}^{+\mathrm{i}p'n'-\mathrm{i}pn}\Big[\theta(n=n')(l|\check{E}_B^{B'}|r) \\
&\qquad\qquad + \theta(n'>n)(l|\check{E}_B^{A}(\check{E})^{n'-n-1}\check{E}_A^{B'}|r) \\
&\qquad\qquad + \theta(n'<n)(l|\check{E}_A^{B'}(\check{E})^{n-n'-1}E_B^{A}|r)\Big] \\
&\quad= \sum_{n_0=-\infty}^{+\infty} \mathrm{e}^{\mathrm{i}(p'-p)n_0}\sum_{\Delta n=-\infty}^{+\infty} \mathrm{e}^{\mathrm{i}p\Delta n}\Big[\theta(\Delta n=0)(l|\check{E}_B^{B'}|r) \\
&\qquad\qquad + \theta(\Delta n>0)(l|\check{E}_B^{A}\check{Q}\check{E}^{\Delta n-1}\check{Q}\check{E}_A^{B'}|r) \\
&\qquad\qquad + \theta(\Delta n<0)(l|\check{E}_A^{B'}\check{Q}\check{E}^{-\Delta n-1}\check{Q}\check{E}_B^{A}|r)\Big] \\
&\qquad + (l|\check{E}_B^{A}|r)(l|\check{E}_A^{B'}|r)\sum_{n=-\infty}^{+\infty}\sum_{n'=-\infty}^{n-1} \mathrm{e}^{\mathrm{i}p'n'-\mathrm{i}pn} \\
&\qquad\qquad + (l|\check{E}_A^{B'}|r)(l|\check{E}_B^{A}|r)\sum_{n=-\infty}^{+\infty}\sum_{n'=n+1}^{+\infty} \mathrm{e}^{\mathrm{i}p'n'-\mathrm{i}pn}.
\end{aligned}$$

By using the well known result for the geometric series of an operator with spectral radius smaller than one, we obtain

$$\sum_{n=0}^{+\infty}\check{Q}\check{E}^n\check{Q} = \sum_{n=0}^{+\infty}\check{Q}(\check{Q}\check{E}\check{Q})^n\check{Q} = \check{Q}(\check{\mathbb{1}} - \check{Q}\check{E}\check{Q})^{-1}\check{Q} \tag{3.107}$$

and thus

$$\begin{aligned}
&\langle\Phi_p(\overline{B};\overline{A})|\Phi_{p'}(B';A)\rangle = \\
&\qquad 2\pi\delta(p'-p)\Big[(l|\check{E}_B^{B'}|r) + (l|\check{E}_B^{A}\check{Q}(\check{\mathbb{1}} - \mathrm{e}^{\mathrm{i}p}\check{Q}\check{E}\check{Q})^{-1}\check{Q}\check{E}_A^{B'}|r) \\
&\qquad\qquad + (l|\check{E}_A^{B'}\check{Q}(\check{\mathbb{1}} - \mathrm{e}^{-\mathrm{i}p}\check{Q}\check{E}\check{Q})^{-1}\check{Q}\check{E}_B^{A}|r) \\
&\qquad\qquad + (2\pi\delta(p)-1)(l|\check{E}_A^{B'}|r)(l|\check{E}_B^{A}|r)\Big]
\end{aligned} \tag{3.108}$$

As expected, momentum eigenstates cannot be normalized to unity in an infinitely large system, but rather satisfy a δ normalization. For equal momenta, $\langle\Phi_p(\overline{B};\overline{A})|\Phi_p(B';A)\rangle$ contains the diverging factor $2\pi\delta(0) = |\mathbb{Z}|$ where the cardinality $|\mathbb{Z}|$ represents the diverging system size ($\mathscr{L} = \mathbb{Z}$). Inside the square brackets, the regular part $\check{Q}\check{E}\check{Q}$

produces a finite contribution where B and B' are strongly connected. We therefore also refer to these terms as the *connected contribution*. For $p = 0$, the product $\check{Q}(\check{\mathbb{1}} - e^{\pm ip}\check{Q}\check{E}\check{Q})^{-1}\check{Q}$ can be interpreted as the pseudo-inverse of the singular superoperator $\check{\mathbb{1}} - \check{E}$, which has an eigenvalue zero associated to the left and right eigenvectors $(l|$ and $|r)$. We henceforth define $(\check{\mathbb{1}} - e^{\pm ip}\check{E})^{\mathsf{P}} = \check{Q}(\check{\mathbb{1}} - e^{\pm ip}\check{Q}\check{E}\check{Q})^{-1}\check{Q}$, so that $(\check{\mathbb{1}} - \check{E})^{\mathsf{P}}(\check{\mathbb{1}} - \check{E}) = (\check{\mathbb{1}} - e^{\pm ip}\check{E})(\check{\mathbb{1}} - e^{\pm ip}\check{E})^{\mathsf{P}} = \check{Q} = \check{\mathbb{1}} - |r)(l|$. Only for zero momentum does $(\check{\mathbb{1}} - e^{\pm ip}\check{E})^{\mathsf{P}}$ denote a true pseudo-inverse. For momentum zero, there is an additional divergence inside the square brackets coming from the singular part $\check{S}$. Here B and B' appear in two separate factors, and this term is henceforth referred to as the *disconnected contribution*. It can be traced back to the component of $|\Phi_0(B)\rangle$ that is parallel to the uniform matrix product state $|\Psi(A)\rangle$. Indeed, we similarly obtain

$$\langle\Psi(\overline{A})|\Phi_p(B;A)\rangle = 2\pi\delta(p)(l|\check{E}_A^B|r) \tag{3.109}$$

so that all states $|\Phi_p(B)\rangle$ with $p \neq 0$ are automatically orthogonal to $|\Psi(A)\rangle$, but for $p = 0$ we have to restrict to tensors B that are solutions of the linear system $(l|\check{E}_A^B|r) = 0$. Put differently, $|\Phi_0(A)\rangle = |\mathbb{Z}||\Psi(A)\rangle$, and we have to impose $(l|\check{E}_A^B|r) = 0$ in order to restrict to the tangent vectors $|\Phi_0(B)\rangle \in \mathbb{T}_{\Phi_0}^{\perp}$. For any vector $|\Phi_p(B)\rangle$ in the tangent plane $\mathbb{T}_{\Phi_p}^{\perp}$, we can impose the left or right gauge fixing conditions Eq. (3.78) or (3.79). Either choice cancels the non-local terms in Eq. (3.108), resulting in

$$\langle\Phi_p(\overline{B};\overline{A})|\Phi_p(B;A)\rangle = 2\pi\delta(p'-p)(l|\check{E}_B^{B'}|r). \tag{3.110}$$

A linear parameterization $B = \mathcal{B}_\Phi(x)$ depending on a $D \times D(q-1)$ matrix x can now be constructed, analogously to the construction in the previous subsection but now in a translation invariant setting. We first define the $qD \times D$ matrices R as

$$[R]_{(\alpha,s);\beta} = [r^{1/2}A^{s\dagger}]_{\alpha,\beta} \tag{3.111}$$

and then construct a $(q-1)D \times qD$ matrix V_R such that $V_R^\dagger$ contains an orthonormal basis for the null space of $R^\dagger$, *i.e.* $V_R R = 0$ and $V_R V_R^\dagger = \mathbb{1}_{(q-1)D}$. Setting $[V_R^s]_{\alpha,\beta} = [V_R]_{\alpha;(\beta,s)}$, we then define the representation $\mathcal{B}_\Phi^s(x)$ as

$$\mathcal{B}_\Phi^s(x) = l^{-1/2}xV_R^s r^{-1/2} \tag{3.112}$$

in order to obtain

$$\langle\Phi_{p'}(\overline{\mathcal{B}_\Phi(\overline{x})})|\Phi_p(\mathcal{B}_\Phi(y))\rangle = 2\pi\delta(p-p')\mathrm{tr}\left[x^\dagger y\right], \tag{3.113}$$

in combination with the right gauge fixing condition $\sum_{s=1}^q \mathcal{B}_\Phi^s(x)rA^{s\dagger} = 0$. The representation $\widetilde{\mathcal{B}}_\Phi(x)$ satisfying the left gauge fixing conditions follows similarly.

As a last step, we have to evaluate $\langle\Phi_p(\overline{B})|\hat{H}|\Psi(A)\rangle$. We again assume that the Hamil-

tonian, which should now be translation invariant, only contains nearest-neighbor interactions, *i.e.* $\hat{H} = \sum_{n\in\mathbb{Z}} \hat{T}^n \hat{h} \hat{T}^{-n}$ where $\hat{h}$ has non-trivial support only on sites zero and one. We hence obtain

$$\begin{aligned}\langle \Phi_p(\overline{B};\overline{A}) \,|\, \hat{H}|\Psi(A)\rangle = \\ \sum_{n=-\infty}^{+\infty}\sum_{n'=-\infty}^{+\infty} \mathrm{e}^{-\mathrm{i}pn}\Big[\theta(n=n')(l|\check{H}^{AA}_{BA}|r) + \theta(n=n'+1)(l|\check{H}^{AA}_{AB}|r) \\ + \theta(n>n'+1)(l|\check{H}^{AA}_{AA}(\check{E})^{n-n'-2}\check{E}^{B}_{A}|r) \\ + \theta(n<n')(l|\check{E}^{B}_{A}(\check{E})^{n'-n-1}\check{H}^{AA}_{AA}|r)\Big],\end{aligned}$$

where we have defined a new superoperator

$$\check{H}^{A_1A_2}_{A_3A_4} \triangleq \sum_{s,t,u,v=1}^{q} \langle u,v|\hat{h}|s,t\rangle A^s_1 A^t_2 \otimes \overline{A^u_3 A^v_4}, \tag{3.114}$$

with which we can write for the expectation value of the energy density

$$h(\overline{A},A) = \langle\Psi(\overline{A})|\hat{h}|\Psi(A)\rangle = (l|\check{H}^{AA}_{AA}|r). \tag{3.115}$$

Using a translation invariant version of the definition in Eq. (3.100), namely

$$C^{s,t} = \sum_{u,v=1}^{q} \langle s,t|\hat{h}|u,v\rangle A^s A^t \tag{3.116}$$

we can rewrite $\check{H}^{AA}_{AB} = \check{E}^{C}_{AB}$ and $\check{H}^{AA}_{BA} = \check{E}^{C}_{BA}$. Repeating the same tricks as for the evaluation of $\langle\Phi_{p'}(B')|\Phi_p(B)\rangle$ leads to

$$\begin{aligned}\langle \Phi_p(\overline{B};\overline{A})|\hat{H}|\Psi(A)\rangle = \\ 2\pi\delta(p)\Big[(l|\check{H}^{AA}_{BA}|r) + (l|\check{H}^{AA}_{AB}|r) + (l|\check{H}^{AA}_{AA}(\check{\mathbb{1}}-\check{E})^{\mathsf{P}}\check{E}^{B}_{A}|r) \\ + (l|\check{E}^{B}_{A}(\check{\mathbb{1}}-\check{E})^{\mathsf{P}}\check{H}^{AA}_{AA}|r) + (|\mathbb{Z}|-2)(l|\check{H}^{AA}_{AA}|r)(l|\check{E}^{A}_{B}|r)\Big].\end{aligned} \tag{3.117}$$

As expected, the translation invariant state $\hat{H}|\Psi(A)\rangle$ has zero overlap with momentum eigenstates with $p \neq 0$. For $p = 0$, the overlap is proportional to $2\pi\delta(0) = |\mathbb{Z}|$, which matches with the same factor in $\langle\Phi_0(\overline{B};\overline{A})|\Phi_0(B;A)\rangle$. There is an additional divergence inside the brackets, which cancels due to

$$\begin{aligned}\langle \Phi_p(\overline{B};\overline{A})|\hat{P}_0\hat{H}|\Psi(A)\rangle &= \langle \Phi_p(\overline{B};\overline{A})|\hat{H} - H(\overline{A},A)|\Psi(A)\rangle \\ &= \langle \Phi_p(\overline{B};\overline{A})|\hat{H}|\Psi(A)\rangle - |\mathbb{Z}|h(\overline{A},A)2\pi\delta(p)(l|\check{E}^{A}_{B}|r),\end{aligned}$$

where we assume $|\Psi(A)\rangle$ to be normalized to unity and we have defined the (normalized) expectation values $H(\overline{A},A) = \langle\Psi(\overline{A})|\hat{H}|\Psi(A)\rangle = |\mathbb{Z}|h(\overline{A},A) = |\mathbb{Z}|(l|\check{H}^{AA}_{AA}|r)$. As before,

this divergent factor automatically cancels by restricting to tangent vectors $|\Phi_0(B)\rangle \in \mathbb{T}^{\perp}_{\Phi_0}$. By imposing the left gauge fixing condition [Eq. (3.78)], the third and the fourth term in Eq. (3.117) cancel, while for the right gauge fixing condition [Eq. (3.79)], the second and fourth term cancel.

For either choice of the gauge fixing conditions, one non-local term survives in the expression for $\langle \Phi_p(\overline{B};\overline{A})|\hat{H}|\Psi(A)\rangle$ [Eq. (3.117)], which requires the computation of the pseudo-inverse of $\check{\mathbb{1}} - \check{E}$. An exact computation of $(\check{\mathbb{1}} - \check{E})^{\mathsf{P}}$ would be an operator of $\mathcal{O}(D^6)$, but an iterative strategy is also possible. If we represent B as $\mathcal{B}_\Phi(x)$, so that the right gauge fixing conditions are fulfilled, we have to compute

$$|K) = (\check{\mathbb{1}} - \check{E})^{\mathsf{P}} \check{H}^{AA}_{AA}|r) = \check{Q}(\check{\mathbb{1}} - \check{Q}\check{E}\check{Q})^{-1}\check{Q}\check{H}^{AA}_{AA}|r) = (\check{\mathbb{1}} - \check{Q}\check{E}\check{Q})^{-1}\check{Q}\check{H}^{AA}_{AA}|r), \quad (3.118)$$

where $\check{Q}\check{H}^{AA}_{AA}|r)$ can be computed efficiently. Since the action of $(\check{\mathbb{1}} - \check{Q}\check{E}\check{Q})$ on a vector $|K)$ can also be implemented as an operation with computational efficiency $\mathcal{O}(D^3)$ using the maps $\mathcal{E}$ and $\widetilde{\mathcal{E}}$, and since $(\check{\mathbb{1}} - \check{Q}\check{E}\check{Q})$ itself is non-singular, an iterative solver such as the biconjugate gradient stabilized method can be used to compute $|K)$ with a computational cost that scales as $\mathcal{O}(D^3)$. We then also define

$$F = \sum_{s,t=1}^{q} l^{1/2} C^{s,t} r A^{t\dagger} r^{-1/2} V_R^{s\dagger} + \sum_{s,t=1}^{q} l^{-1/2} A^{t\dagger} l C^{t,s} r^{1/2} V_R^{s\dagger} + \sum_{s=1}^{q} l^{1/2} A^s K r^{-1/2} V_R^{s\dagger}, \quad (3.119)$$

in order to obtain

$$\langle \Phi_p(\overline{\mathcal{B}_\Phi}(\overline{x});A)|\hat{H}|\Psi(A)\rangle = 2\pi\delta(p)\,\mathrm{tr}\left[x^\dagger F\right]. \quad (3.120)$$

The solution to the minimization of $\left\| |\Phi_0(B;A(t))\rangle - \hat{H}\,|\Psi(A(t))\rangle \right\|^2$ is thus given by $B = \mathcal{B}_\Phi(x^\star(t))$ with $x^\star(t) = F(t)$, so that we can write

$$|\Phi(\mathcal{B}_\Phi(x^\star(t));A(t))\rangle = \hat{P}_{\mathbb{T}^{\perp}_{\mathrm{uMPS}(D)}(\overline{A(t)},A(t))\hat{H}}\,|\Psi(A(t))\rangle. \quad (3.121)$$

A simple Euler-based algorithm for imaginary time evolution can then be constructed as in the previous subsection. Rather than having to perform $\mathcal{O}(ND^3)$ operators, the implementation for uniform matrix product states rquires $\mathcal{O}(N_{\mathrm{iter}}D^3)$ operations, with N_{iter} the number of iterations necessary in the iterative eigensolvers for l, r and in the iterative linear solver for K.

2.4. Error and convergence measures

For the remainder of this section, we restrict to the setting of uniform matrix product states in the thermodynamic limit. We can compute the convergence and error measures $\eta(\overline{A},A)$ and $\varepsilon(\overline{A},A)$ as defined in Subsection 2.6 of the previous chapter [see Eq. (2.55) and (2.56) respectively]. The quantity $\eta(\overline{A},A) = \big\| |\Phi_0(\mathcal{B}_\Phi(x^\star);A)\rangle \big\|$ can be interpreted as a measure for the convergence of an imaginary time evolution. We obtain $\eta(\overline{A},A) = \left(|\mathbb{Z}|\,\mathrm{tr}[(x^\star)^\dagger(x^\star)]\right)^{1/2}$ so that the convergence measure is always infinity, unless $x^\star$ is exactly zero. This was expected for infinite systems, as was discussed in general in Subsection 4.1 of the previous chapter. This is a consequence of the infrared orthogonality catastrophe and the ability of uniform matrix product states to vary between different Fock spaces, which was discussed in Subsection 1.6. Since our interest is often restricted to expectation values of local observables such as the energy density, it is better to define a local measure of convergence as in Eq. (2.64), which now results in

$$\tilde{\eta}(\overline{A},A) \triangleq \sqrt{\mathrm{tr}[(x^\star)^\dagger(x^\star)]} = \|x^\star\|. \tag{3.122}$$

Just as the total energy expectation value $H(\overline{A},A)$ converges quadratically in $\eta(\overline{A},A)$, the expectation value of the energy density $h(\overline{A},A)$ converges quadratically in the local measure $\tilde{\eta}(\overline{A},A)$.

The error measure $\varepsilon(\overline{A},A)$ can be used to monitor the deviation between the exact evolution and the flow according to the time-dependent variational principle. It can be computed as $\varepsilon(\overline{A},A)^2 = \Delta H(\overline{A},A)^2 - \eta(\overline{A},A)^2$. With $\hat{H}$ being our nearest neighbor Hamiltonian, we obtain

$$\begin{aligned}\Delta H(\overline{A},A)^2 &= \langle\Psi(\overline{A})|\left[\sum_{n\in\mathbb{Z}}\hat{T}^n(\hat{h}-h(\overline{A},A)\hat{T}^{-n}\right]^2|\Psi(A)\rangle \\ &= |\mathbb{Z}|\Bigg(\sum_{n=-1}^{1}\langle\Psi(\overline{A})|(\hat{h}-h(\overline{A},A))\hat{T}^n(\hat{h}-h(\overline{A},A))|\Psi(A)\rangle \\ &\qquad + 2(l|\check{E}^{C}_{AA}(\check{\mathbb{1}}-\check{E})^{\mathsf{P}}\check{E}^{AA}_{C}|r)\Bigg).\end{aligned} \tag{3.123}$$

The first term results in

$$\langle\Psi|(\hat{h}-h)(\hat{h}-h)|\Psi\rangle = \sum_{s,t,u,v=1}^{q}\langle u,v|(\hat{h}-h)^2|s,t\rangle\,(l|A^sA^t\otimes\overline{A}^u\overline{A}^v|r) = \Delta h(\overline{A},A)^2$$

and

$$\langle\Psi|(\hat{h}-h)\hat{T}(\hat{h}-h)|\Psi\rangle = \sum_{r,s,t,u,v,w=1}^{q} \langle u,v,w|(\hat{h}-h)\hat{T}(\hat{h}-h)\hat{T}^{-1}|r,s,t\rangle\, (l|A^r A^s A^t \otimes \overline{A}^u \overline{A}^v \overline{A}^w|r),$$

for $n=0$ and $n=1$ respectively, and in the complex conjugate of the last expression for $n=-1$. Thus, both terms in $\varepsilon(\overline{A},A)^2$ are proportional to $|\mathbb{Z}|$, and it is better to define a local measure as in Eq. (2.65), or thus

$$\tilde{\varepsilon}(\overline{A},A) = \sqrt{\Delta H(\overline{A},A)^2/|\mathbb{Z}| - \tilde{\eta}(\overline{A},A)^2}. \tag{3.124}$$

When the exact time evolution is accurately captured in the manifold of (uniform) matrix product states, $\tilde{\varepsilon}$ contains the difference of two terms which are of comparable size. In addition, the computation of $\Delta H(\overline{A},A)^2/|\mathbb{Z}|$ contains four terms that can be both positive and negative and can neutralize each other. This can result in large numerical errors in the computation of these quantities. A better strategy for evaluating these quantities as a sum of strictly positive terms is constructed in Subsection 2.6.

While almost all technical details of the algorithm have been discussed in the previous subsection, we have left open the choice of gauge imposed on the matrices A in the uniform matrix product state representation. The choice of gauge for the tangent vectors can be combined with any choice of gauge for A. We could thus choose for the left- or right-canonical form for A, or just do not enforce any specific gauge at all (we do have to renormalize after every step though, since the norm —which is related to the largest eigenvalue of the transfer operator $\breve{E}$— is only conserved up to first order in the time step). We have chosen to use a *symmetric* gauge, where the left and right eigenvectors l and r of the transfer operator are diagonal and equal: $l=r$ (note that this does not imply that A^s or $\breve{E}$ is symmetric). In terms of the unique singular value decomposition from Subsection 1.1, we set $A^s = \Lambda^{1/2}\Gamma^s\Lambda^{1/2}$, with thus $l=r=\Lambda$. This has the advantage that the entanglement spectrum $P=\Lambda^2$, which contains many small values when D becomes large and the approximation error $\tilde{\varepsilon}$ becomes small, is evenly distributed as Schmidt values over both l and r. Since the implementation of the time-dependent variational principle depends heavily on both $l^{-1/2}$ and $r^{-1/2}$, it is important to keep both matrices as well conditioned as possible. The minimally obtainable state error $\tilde{\varepsilon}$ can roughly be estimated as follows: Since a localized state error $\tilde{\varepsilon}$ implies that the neglected Schmidt values are $\mathcal{O}(\tilde{\varepsilon})$, the condition number of l and r can be estimated as $\mathcal{O}(\tilde{\varepsilon}^{-1})$. Let δ be the relative numerical precision of the computation, with thus $\delta \approx 10^{-15}$ for the double precision floating-point number format. Since F, the most important quantity that is computed in the implementation of the time-dependent variational principle, depends on $l^{-1/2}$ and $r^{-1/2}$ separately (but not together in a single term), it can be evaluated with numerical precision $\delta/\tilde{\varepsilon}^{-1/2}$. Since the state directly depends on F, we obtain as bound on the minimal value of the convergence measure $\tilde{\eta}$ the relation $\tilde{\eta} > \delta/\tilde{\varepsilon}^{-1/2}$.

The minimal state error $\tilde{\varepsilon}$ is obtained when $\tilde{\varepsilon} = \tilde{\eta}$, resulting in $\tilde{\eta} = \tilde{\varepsilon} > \delta^{2/3} \approx 10^{-10}$. At this point, the error on the energy density expectation value is dominated by the numerical precision δ, rather than by $\tilde{\varepsilon}^2$. The practical limit will be slightly higher due to the many iterative computations involved, which have the effect of increasing δ. For smaller values of D, where the minimum value of $\tilde{\varepsilon}$ is not yet obtained, lower values of the convergence towards the variational optimum (*e.g.* $\tilde{\eta} = 10^{-12}$) are possible.

2.5. Numerical integration scheme for real time evolution

As discussed in Subsection 1.7, a Hamiltonian $\hat{H}$ with real entries is time-reversal invariant. In the case of imaginary time evolution, we can then restrict to a real representation for the matrices A^s, $x^\star$, and $\mathcal{B}_\Phi(x^\star)$. When using the time-dependent variational principle to simulate real-time evolution, we are no longer able to restrict to a real representation. The quantities A, $x^\star$, and $\mathcal{B}_\Phi(x^\star)$ become complex, even when the operator $\hat{h}$ has only real entries. Nevertheless, the algorithm sketched in the previous subsections remain valid by replacing $\mathrm{d}\tau$ with $\mathrm{i}\mathrm{d}t$. However, the second order errors that are introduced by the Euler method can now accumulate in time. A prime indicator of this is a drifting expectation value $H(\overline{A(t)}, A(t)) = \langle \Psi(\overline{A(t)}) | \hat{H} | \Psi(A(t)) \rangle$ when the state $|\Psi(A)\rangle$ is evolved in time according to a time-independent Hamiltonian $\hat{H}$. For an exact integration of the flow equations of the time-dependent variational principle, the energy expectation value should be conserved. The accumulation of systematic errors can be eliminated by implementing a numerical integrator for the Euler-Lagrange equations that respects the symplectic structure of the time-dependent variational principle. However, this structure is much more complicated than the typical structure of classical dynamics with a separable Hamiltonian $H(q,p) = T(p) + V(q)$. In particular, the relation $H(\overline{A}, A)$ is highly nonlinear and not separable. Consequently, none of the existing symplectic algorithms from classical dynamics can be applied to the time dependent variational principle.

When the Hamiltonian has real entries and is thus time-reversal invariant, this symmetry is inherited by the time-dependent variational principle (see Subsection 2.4 of the previous chapter). When a set of differential equations is invariant under time reversal, it is a good policy to at least devise a numerical integration scheme that respects this time-reversal symmetry. Numerical integration schemes that respect time-reversal symmetry are called symmetric and share many nice properties with symplectic integration schemes such as a stable long-time behavior, a linear growth of the global error and a near-preservation of first integrals [332]. The following paragraphs describe the details of a second order numerical integration scheme that respects time-reversal symmetry, although it can of course also be applied to Hamiltonians which are not invariant under time reversal or which are time-dependent, in which case it is a simple second-order numerical integrator. At any point, the projection of $\hat{H}|\Psi(A)\rangle$ into the tangent plane $\mathbb{T}_\Phi^\perp$ (*i.e.* the determination of $x^\star$) can be computed using the construction from the previous subsections.

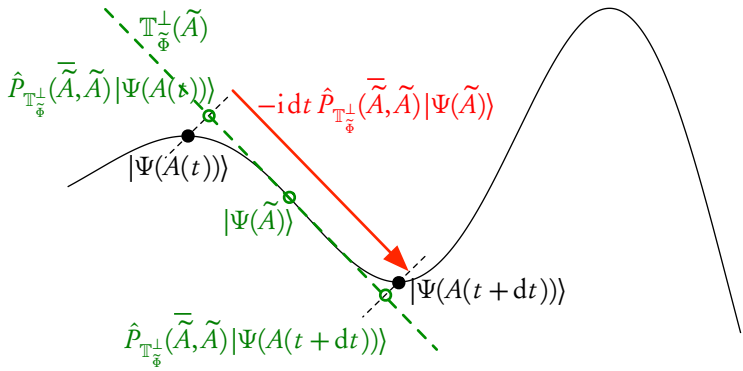

Figure 3.3: Sketch of the location of the midpoint to be used in a symmetric integration scheme on a manifold.

The main problem one encounters when trying to construct a symmetric integrator for differential equations on manifolds is that the tangent plane at the points $|\Psi(A(t))\rangle$ and $|\Psi(A(t+\mathrm{d}t))\rangle$ are different. Most algorithms thus start with the determination of a midpoint $|\Psi(\widetilde{A})\rangle$ so that

$$\hat{P}_{\mathbb{T}^{\perp}_{\widetilde{\Phi}}}(\overline{\widetilde{A}},\widetilde{A})\,|\Psi(A(t))\rangle + \hat{P}_{\mathbb{T}^{\perp}_{\widetilde{\Phi}}}(\overline{\widetilde{A}},\widetilde{A})\,|\Psi(A(t+\mathrm{d}t))\rangle = 0, \tag{3.125}$$

with $\mathbb{T}_{\widetilde{\Phi}}$ the tangent plane of the midpoint $\widetilde{A}$, spanned by the vectors $|\Phi(B;\widetilde{A})\rangle = |\widetilde{\Phi}(B)\rangle$. This relation only specifies the location of the midpoint once a relation between $A(t)$ and $A(t+dt)$ is known. In principle, the midpoint can be combined with any integration scheme that transform $\widetilde{A}$ into $A(t)$ when taking a step $-\mathrm{d}t/2$ and transforms $\widetilde{A}$ into $A(t+\mathrm{d}t)$ when taking a step $\mathrm{d}t/2$. If we thus use the simple Euler step, we obtain the additional relation

$$\begin{aligned}\hat{P}_{\mathbb{T}^{\perp}_{\widetilde{\Phi}}}(\overline{\widetilde{A}},\widetilde{A})\,|\Psi(A(t+dt))\rangle - \hat{P}_{\mathbb{T}^{\perp}_{\widetilde{\Phi}}}(\overline{\widetilde{A}},\widetilde{A})\,|\Psi(A(t))\rangle \\ = \mathrm{i}\,\mathrm{d}t\,\hat{P}_{\mathbb{T}^{\perp}_{\widetilde{\Phi}}}(\overline{\widetilde{A}},\widetilde{A})\hat{H}\,|\Psi(\widetilde{A})\rangle = -\mathrm{i}\,\mathrm{d}t\;|\widetilde{\Phi}(\mathcal{B}_{\widetilde{\Phi}}(\widetilde{x}^{\star}))\rangle\,.\end{aligned} \tag{3.126}$$

This is sketched in Figure 3.3. This specific combination of midpoint with Euler step immediately tells us that $A(t+\mathrm{d}t) = \widetilde{A} - \mathrm{i}\,\mathrm{d}t/2\,\mathcal{B}_{\widetilde{\Phi}}(\widetilde{x}^{\star})$. A similar reasoning leads to the conclusion that the midpoint is implicitly defined by $A(t) = \widetilde{A} + \mathrm{i}\,\mathrm{d}t/2\,\mathcal{B}_{\widetilde{\Phi}}(\widetilde{x}^{\star})$.

However, this reasoning was just a little bit too quick and sloppy. We also have to take into account the normalization preservation and gauge fixing that is applied in every step. Instead of setting $A(t+\mathrm{d}t) = A - \mathrm{i}\,\mathrm{d}t/2\,\mathcal{B}_{\widetilde{\Phi}}(\widetilde{x}^{\star})$, we find a scalar constant $c\in\mathbb{C}$ and a $D\times D$ matrix $g\in\mathrm{GL}(D)$ such that $A^s(t+\mathrm{d}t) = c\,g[\widetilde{A}^s - \mathrm{i}\,\mathrm{d}t/2\,\mathcal{B}_{\widetilde{\Phi}}(\widetilde{x}^{\star})]g^{-1}$, where c is chosen such that $\check{E}^{A(t+dt)}_{A(t+dt)}$ has 1 as largest eigenvalue, and g is chosen such

that $A(t+\mathrm{d}t)$ satisfies a prescribed gauge fixing condition. Analogously, we also have to look for (different) $c \in \mathbb{C}$ and $g \in \mathrm{GL}(D;\mathbb{C})$ by which the inverse Euler step is given as $c^{-1}g^{-1}A^s(t)g = \widetilde{A}^s + \mathrm{i}\,\mathrm{d}t/2\,\mathcal{B}_{\widetilde{\Phi}}(\widetilde{x}^\star)$ and which are chosen such that $c^{-1}g^{-1}A^s(t)g - \widetilde{A}^s$ is compatible with the gauge fixing constraints that are built into the representation $\mathcal{B}_{\widetilde{\Phi}}(\widetilde{x}^\star)$. Since every $\mathcal{B}_{\widetilde{\Phi}}(\widetilde{x})$ satisfies $\check{E}_{\widetilde{A}}^{\mathcal{B}_{\widetilde{\Phi}}(\widetilde{x}^\star)}|\widetilde{r}) = 0$ with $|\widetilde{r})$ the right eigenvector corresponding to eigenvalue 1 of $\check{E}_{\widetilde{A}}^{\widetilde{A}}$, we have to tune c and g such that

$$\check{E}_{\widetilde{A}}^{c^{-1}g^{-1}A(t)g-\widetilde{A}}|\widetilde{r}) = 0 \qquad \Rightarrow \qquad \check{E}_{\widetilde{A}}^{A(t)}|g\widetilde{r}) = c\,|g\widetilde{r}\rangle$$

Put differently, c is the largest eigenvalue of $E_{\widetilde{A}}^{A(t)}$ and g is chosen such that $|g\widetilde{r})$ is the corresponding right eigenvector.

Since we cannot solve the resulting implicit relation $c^{-1}g^{-1}A^s(t)g = \widetilde{A}^s - \mathrm{i}\,\mathrm{d}t/2\,\mathcal{B}_{\widetilde{\Phi}}(\widetilde{x}^\star)$ exactly, we have to devise a numerical scheme to determine the mid point $\widetilde{A}$. The resulting algorithm doesn't satisfy time-reversal symmetry exactly, but only up to the accuracy of the numerical determination of $\widetilde{A}$, which can be near machine precision. We can try to solve the implicit relation for the midpoint by a simple error correct strategy. We choose as an initial guess the forward Euler step starting at $A(t)$, so that $\widetilde{A}_0 \sim A(t) - \mathrm{i}\,\mathrm{d}t/2\,\mathcal{B}_{\Phi}(x^\star)$, where the 'similarity sign' is used to indicate that $\widetilde{A}_0$ has already been transformed in order to satisfy norm and gauge fixing constraints. Having a guess $|\Psi(\widetilde{A}_n)\rangle$ with corresponding tangent vectors $|\widetilde{\Phi}_n(B)\rangle = |\Phi(B;\widetilde{A}_n)\rangle$, we can iteratively try to improve it as follows. We calculate the difference $\widetilde{\mathrm{d}A}_n^s = c_n^{-1}g_n^{-1}A^s(t)g_n - \widetilde{A}_n^s - \mathrm{i}\,\mathrm{d}t/2\mathcal{B}_{\widetilde{\Phi}_n}(\widetilde{x}_n^\star)$, where c_n and g_n are chosen such that $\check{E}_{\widetilde{A}_n}^{A(t)}|\widetilde{r}_n g_n) = c_n|\widetilde{r}_n g_n)$. We then set $\widetilde{A}_{n+1} \sim \widetilde{A}_n + \widetilde{\mathrm{d}A}_n$ and repeat this process. At any point in the iteration, we can measure the size of the correction as $\| |\widetilde{\Phi}_n(\widetilde{\mathrm{d}A}_n)\rangle \| = |\mathbb{Z}|^{1/2}(\widetilde{l}_n|\check{E}_{\widetilde{\mathrm{d}A}_n}^{\widetilde{\mathrm{d}A}_n}|\widetilde{r}_n)^{1/2}$. As argued in the previous subsection, we can safely omit the overall $|\mathbb{Z}|^{1/2}$ in order to obtain a local measure $\tilde{\zeta} = (\widetilde{l}_n|\check{E}_{\widetilde{\mathrm{d}A}_n}^{\widetilde{\mathrm{d}A}_n}|\widetilde{r}_n)^{1/2}$. When $\tilde{\zeta}$ dives below a tolerance level that can be chosen near-machine precision, we can stop the iteration. When the chosen time step is not too big — for example $\mathrm{d}t \approx 0.01$ — this algorithm converges in a few (less then 20) iteration steps. Better strategies in terms of higher order iterative solvers for non-linear equations can be devised.

The general outline of an algorithm for real time evolution is thus:

1. iteratively determine the midpoint from $A(t) \sim \widetilde{A} + \mathrm{i}\,\mathrm{d}t/2\,\mathcal{B}_{\widetilde{\Phi}}(\widetilde{x}^\star)$
2. set $A(t+dt) \sim \widetilde{A} - \mathrm{i}\,\mathrm{d}t/2\,\mathcal{B}_{\widetilde{\Phi}}(\widetilde{x}^\star)$

Note that all operations can be implemented with computational complexity $\mathcal{O}(D^3)$. We of course have to use iterative eigensolvers to determine the eigenvalues and eigenvectors of $\check{E}_{\widetilde{A}}^{A(t)}$, $\check{E}_{\widetilde{A}}^{\widetilde{A}}$ and $\check{E}_{A(t+dt)}^{A(t+dt)}$. The midpoints $|\Psi(\widetilde{A})\rangle$ can in fact be interpreted as $|A(t+\mathrm{d}t/2)\rangle$. Thus the algorithm produces twice the resolution as initially requested.

However, it is only (approximately) time-reversal invariant after an integral number of steps $\mathrm{d}t$. Furthermore, since the (backwards) Euler method is used to step from $A(t)$ to $A(t+\mathrm{d}t/2)$, the error in this step is expected to be $\mathcal{O}(\mathrm{d}t^2/4)$. Similarly, the error in the step $A(t+\mathrm{d}t/2)$ to $A(t+\mathrm{d}t)$ is expected to be of the same order. Nevertheless, the resulting step from $A(t)$ to $A(t+\mathrm{d}t)$ is correct up to second order, and the error is actually $\mathcal{O}(\mathrm{d}t^4)$ because odd-powered effects are forbidden by the symmetry of the construction. Higher order errors are obtainable by combining the midpoint construction with more advanced Runge-Kutta schemes.

2.6. Dynamic expansion of the variational manifold

Both for real and imaginary time evolution, we have introduced the local error measure $\tilde{\epsilon}$ [see Eq. (3.124)] that captures the tendency of the exact evolution to move away from the manifold $\mathscr{M}_{\mathrm{uMPS}(D)}$. If this quantity exceeds a given tolerance value, we might try to reduce the error by expanding the variational class. For uniform matrix product states with bond dimension D, we can expand $\mathscr{M}_{\mathrm{uMPS}(D)}$ by increasing the bond dimension to some value $\widetilde{D}$. If at some point the state $|\Psi\rangle \in \mathscr{M}_{\mathrm{uMPS}(D)}$ is a uniform matrix product state with $D\times D$ matrices A^s, we can try to better approximate the exact evolution over the time step $\mathrm{d}t$ by embedding this state into a larger manifold $\mathscr{M}_{\mathrm{uMPS}(\widetilde{D})}$ by defining new $\widetilde{D}\times\widetilde{D}$ matrices $\widetilde{A}^s$ with $\widetilde{D}\geq D$ and

$$\widetilde{A}^s = \begin{bmatrix} A^s & 0 \\ 0 & 0 \end{bmatrix}. \tag{3.127}$$

For the evolution over the time step $\mathrm{d}t$, we can now use a larger variation $\widetilde{\mathrm{d}A}^s$ given by

$$\widetilde{\mathrm{d}A}^s = \begin{bmatrix} \mathrm{d}A^s_{00} & \mathrm{d}A^s_{01} \\ \mathrm{d}A^s_{10} & \mathrm{d}A^s_{11} \end{bmatrix}, \tag{3.128}$$

with $\mathrm{d}A^s_{00}$ a $D\times D$ matrix, $\mathrm{d}A^s_{01}$ a $D\times(\widetilde{D}-D)$ matrix, $\mathrm{d}A^s_{10}$ a $(\widetilde{D}-D)\times D$ matrix and $\mathrm{d}A^s_{11}$ a $(\widetilde{D}-D)\times(\widetilde{D}-D)$ matrix. However, by assuming $\widetilde{\mathrm{d}A}\sim\mathrm{d}t$, we obtain $|\widetilde{\Psi}(\widetilde{A}+\widetilde{\mathrm{d}A})\rangle - |\widetilde{\Psi}(\widetilde{A})\rangle = |\widetilde{\Psi}(\widetilde{A}+\widetilde{\mathrm{d}A})\rangle - |\Psi(A)\rangle = |\Phi(\mathrm{d}A_{00};A)\rangle$. The newly added variations do not feature to first order. The time-dependent variational prinicple is very keen to restricting its flow to the original manifold $\mathscr{M}_{\mathrm{uMPS}(D)}$. A solution is obtained by choosing $\mathrm{d}A^s_{00}$ as $\mathcal{O}(\mathrm{d}t)$, $\mathrm{d}A^s_{10}$ and $\mathrm{d}A_{01}$ as $\mathcal{O}(\mathrm{d}t^{1/2})$ and $\mathrm{d}A_{11}$ as $\mathcal{O}(\mathrm{d}t^0)$. We then obtain as first order

$$|\widetilde{\Psi}(\widetilde{A}+\widetilde{\mathrm{d}A})\rangle - |\Psi(A)\rangle = |\mathrm{d}\widetilde{\Psi}_0\rangle + |\mathrm{d}\widetilde{\Psi}_1\rangle \tag{3.129}$$

with

$$|\widetilde{\mathrm{d}\Psi_0}\rangle = |\Phi(\mathrm{d}A_{00},A)\rangle \tag{3.130}$$

and

$$|\widetilde{\mathrm{d}\Psi_1}\rangle = \sum_{n\in\mathbb{Z}} \hat{T}^n \left(\sum_{\{s_j\}=1}^{q} \sum_{m=0}^{+\infty} \boldsymbol{v}_{\mathrm{L}}^{\dagger} \Big(\cdots A^{s_{-2}} A^{s_{-1}} \big[\mathrm{d}A_{01}^{s_0} \mathrm{d}A_{11}^{s_1} \cdots \times \mathrm{d}A_{11}^{s_m} \mathrm{d}A_{10}^{s_{m+1}} \big] A^{s_{m+2}} \cdots \Big) \boldsymbol{v}_{\mathrm{R}} |\{s_n\}\rangle \right). \quad (3.131)$$

Clearly the increased bond dimension allows for an action on an arbitrary number of neighboring sites, which increases the entanglement entropy from some initial value smaller than $\log(D)$ to some new value that is smaller than the new bound $\log(\widetilde{D})$. If we try to imitate the geometric strategy of the time-dependent variational principle, we have to optimize the variation $\widetilde{\mathrm{d}A}$ so as to minimize

$$\big\| |\widetilde{\mathrm{d}\Psi_0}\rangle + |\widetilde{\mathrm{d}\Psi_1}\rangle - \hat{H}\,|\widetilde{\Psi}(\widetilde{A})\rangle \big\|^2. \quad (3.132)$$

Eq. (3.132) is a complicated expression that couples the four sets of parameters $\mathrm{d}A_{00}^s$, $\mathrm{d}A_{01}^s$, $\mathrm{d}A_{10}^s$ and $\mathrm{d}A_{11}^s$. Luckily, here too we can hope to simplify the expressions by applying gauge transformations such as

$$\widetilde{g} = \begin{bmatrix} 1+\eta x_{00} & \eta^{1/2} x_{01} \\ \eta^{1/2} x_{10} & \exp(x_{11}) \end{bmatrix} = \begin{bmatrix} 1 & 0 \\ 0 & \exp(x_{11}) \end{bmatrix} \begin{bmatrix} 1+\eta x_{00} & \eta^{1/2} x_{01} \\ \eta^{1/2} \exp(-x_{11}) x_{10} & 1 \end{bmatrix},$$

from which we obtain up to $\mathcal{O}(\eta)$

$$\begin{aligned} \widetilde{g}^{-1} &= \begin{bmatrix} 1-\eta x_{00}+\eta x_{01}\exp(-x_{11})x_{10} & -\eta^{1/2} x_{01} \\ -\eta^{1/2}\exp(-x_{11})x_{10} & 1+\eta\exp(-x_{11})x_{10}x_{01} \end{bmatrix} \begin{bmatrix} 1 & 0 \\ 0 & \exp(-x_{11}) \end{bmatrix} \\ &= \begin{bmatrix} 1-\eta x_{00}+\eta x_{01}\exp(-x_{11})x_{10} & -\eta^{1/2} x_{01}\exp(-x_{11}) \\ -\eta^{1/2}\exp(-x_{11})x_{10} & \exp(-x_{11})+\eta\exp(-x_{11})x_{10}x_{01}\exp(-x_{11}) \end{bmatrix} \end{aligned}$$

and thus

$$\widetilde{g}\widetilde{A}^s\widetilde{g}^{-1} = \widetilde{A}^s + \widetilde{\mathcal{N}}^s(x)$$

$$\text{with} \quad \widetilde{\mathcal{N}}^s(x) = \begin{bmatrix} \eta[x_{00}, A^s] + A^s x_{01} x_{10} & -\eta^{1/2} A^s x_{01}\exp(-x_{11}) \\ \eta^{1/2} x_{10} A^s & -\eta x_{10} A^s x_{01}\exp(-x_{11}) \end{bmatrix}.$$

Any variation $\widetilde{\mathrm{d}A}$ is thus gauge equivalent to $\widetilde{\mathrm{d}A} + \widetilde{\mathcal{N}}^s(x)$. Since x_{11} has prefactor η^0, it could not be considered infinitesimal. By redefining $x_{01} \leftarrow x_{01}\exp(-x_{11})$, it is clear that x_{11} does not feature explicitly in $\widetilde{\mathcal{N}}(x)$. We can use x_{00} to impose a gauge fixing condition on $\mathrm{d}A_{00}$, x_{01} to impose a condition on $\mathrm{d}A_{01}$ and x_{10} to impose a condition on $\mathrm{d}A_{10}$. There is, at first sight, no additional freedom to impose any condition on $\mathrm{d}A_{11}$. However, $\widetilde{\mathrm{d}A}$

also has a multiplicative gauge invariance, since its first order contribution $|\widetilde{\mathrm{d}\Psi_0}\rangle + |\widetilde{\mathrm{d}\Psi_1}\rangle$ is similarly obtained for the equivalent choice $\widetilde{\mathrm{d}A}'$, given by

$$\widetilde{\mathrm{d}A}'^{s} = \begin{bmatrix} \mathrm{d}A^s_{00} & \mathrm{d}A^s_{01} g_{11}^{-1} \\ g_{11}\mathrm{d}A^s_{10} & g_{11}\mathrm{d}A^s_{11} g_{11}^{-1} \end{bmatrix},$$

which can be used to impose a different kind of condition on $\mathrm{d}A_{11}$.

We first impose the following gauge fixing conditions on $\mathrm{d}A_{01}$ and $\mathrm{d}A_{10}$:

$$(l|\check{E}_A^{\mathrm{d}A_{01}} = 0, \qquad \check{E}_A^{\mathrm{d}A_{10}}|r) = 0. \tag{3.133}$$

We then obtain

$$\langle\widetilde{\mathrm{d}\Psi_1}|\Psi(A)\rangle = 0, \qquad \langle\widetilde{\mathrm{d}\Psi_1}|\widetilde{\mathrm{d}\Psi_0}\rangle = 0, \tag{3.134}$$

and

$$\langle\widetilde{\mathrm{d}\Psi_1}|\widetilde{\mathrm{d}\Psi_1}\rangle = |\mathbb{Z}|\sum_{m=0}^{+\infty}(l|\check{E}^{\mathrm{d}A_{01}}_{\mathrm{d}A_{01}}(\check{E}^{\mathrm{d}A_{11}}_{\mathrm{d}A_{11}})^m\check{E}^{\mathrm{d}A_{10}}_{\mathrm{d}A_{10}}|r). \tag{3.135}$$

Thus, $|\widetilde{\mathrm{d}\Psi_1}\rangle$ is automatically orthogonal both to the original uniform matrix product state $|\Psi(A)\rangle$ and to all of its tangent vectors $|\widetilde{\mathrm{d}\Psi_0}\rangle = |\Phi(\mathrm{d}A_{00};A)\rangle$. The optimization then completely decouples into a part in $\mathbb{T}^{\perp}_{\mathrm{uMPS}(D)}(A)$ that can be solved as in the previous subsections. In particular, we still have the gauge freedom in x_{00} at hand to impose either the left or right gauge fixing condition [Eq. (3.78) or (3.79) respectively] on $\mathrm{d}A_{00}$. In addition, the choice of gauge in Eq. (3.133) guarantees that contributions to $|\widetilde{\mathrm{d}\Psi_1}\rangle$ of length m only overlap with themselves in Eq. (3.135).

With the right choice of gauge, $|\widetilde{\mathrm{d}\Psi_1}\rangle$ thus effectively captures a part of the contribution of $\hat{P}_0\hat{H}|\Psi(A)\rangle$ that falls outside the tangent plane $\mathbb{T}_{\mathrm{uMPS}(D)}(A)$. Two cases of special interest are discussed. Firstly, if $\hat{H}$ only contains nearest neighbor interactions described by $\hat{h}$, then all contributions of length $m > 0$ in $|\widetilde{\mathrm{d}\Psi_1}\rangle$ disappear from $\langle\widetilde{\mathrm{d}\Psi_1}|\hat{H}|\Psi(A)\rangle$, so that $\mathrm{d}A_{11}$ does not feature and can be put to zero. For the optimization problem in dA_{01} and dA_{10}, we can use a parameterization that is based on the definitions in the first subsection of this section. We define $B^s_{01}(x) = l^{-1/2}V^s_L x$ with x a $(D-1)q \times (\widetilde{D} - D)$ matrix of independent components, and analogously $B^s_{10}(y) = y\,V^s_R r^{-1/2}$ with y a $(\widetilde{D} - D) \times (D-1)q$ matrix of independent components. We then define $B^{st}_1(x,y) = B^s_{01}(x)B^t_{10}(y)$ in order to find

$$\langle\widetilde{\mathrm{d}\Psi_1}|\widetilde{\mathrm{d}\Psi_1}\rangle = |\mathbb{Z}|(l|\check{E}^{B_1(x,y)}_{B_1(x,y)}|r) = |\mathbb{Z}|\mathrm{tr}\left[(xy)(xy)^\dagger\right],$$
$$\langle\widetilde{\mathrm{d}\Psi_1}|\hat{H}|\Psi(A)\rangle = |\mathbb{Z}|(l|\check{E}^{C}_{B_1(x,y)}|r) = |\mathbb{Z}|\mathrm{tr}\left[G(xy)^\dagger\right],$$

with $G = \sum_{s,t=1}^{q}(V^s_L)^\dagger l^{1/2}C^{st}r^{1/2}(V^t_R)^\dagger$ and C as in Eq. (3.116). Since we have to

minimize

$$\mathrm{tr}\left[(xy)(xy)^\dagger\right] - \mathrm{tr}\left[G(xy)^\dagger\right] - \mathrm{tr}\left[(xy)G^\dagger\right] + \text{constant},$$

we are looking for the optimal matrix xy of rank $\widetilde{D}-D$ such that $||xy-G||$ is minimized, with $||\cdot||$ the Hilbert-Schmidt norm. The best approximation (x,y) can be found by performing a singular value decomposition of the $(q-1)D\times(q-1)D$ matrix G and retaining the largest $\widetilde{D}-D$ singular values. If $\widetilde{D}=qD$, we can exactly capture one step of the discretized flow of the time-dependent variational principle applied to a nearest neighbor Hamiltonian.

Another case of a more academic interest is when $\hat{H}$ looks as

$$\hat{H} = \sum_{n\in\mathbb{Z}} \left(\hat{h}_n + \sum_{m=1}^{+\infty} \hat{p}_n \hat{s}_{n+1} \hat{s}_{n+2} \cdots \hat{s}_{n+m-1} \hat{q}_{n+m} \right), \tag{3.136}$$

where the subscripts only serve to indicate the position, but the terms are site-independent. This Hamiltonian has a one-site contribution and a string-type of interaction. This includes exponential interactions, where $\hat{s} = \mathrm{e}^{-\lambda}\hat{\mathbb{1}}$. For this Hamiltonian, an exact evolution step can be constructed by choosing $\widetilde{D}=2D$ and

$$\mathrm{d}A^s_{00} = \sum_{t=1}^{q} \langle s|\hat{h}|t\rangle A^t, \qquad \mathrm{d}A^s_{01} = \sum_{t=1}^{q} \langle s|\hat{p}|t\rangle A^t,$$
$$\mathrm{d}A^s_{10} = \sum_{t=1}^{q} \langle s|\hat{q}|t\rangle A^t, \qquad \mathrm{d}A^s_{11} = \sum_{t=1}^{q} \langle s|\hat{s}|t\rangle A^t.$$

For any other choice of $\widetilde{D}$ or when more complicated interactions are present, the optimization problem with $\mathrm{d}A_{11}$ included becomes very difficult.

The most interesting case is thus obtained for nearest-neighbor Hamiltonians. This construction is very useful in combination with imaginary time evolution in order to correctly converge a random initial state to the optimal state within the variational manifold. Rather then starting from a random uniform matrix product state for some large bond dimension $\widetilde{D}$, it is better to use a previous optimal uniform matrix product state $|\Psi(A)\rangle$ at a smaller bond dimension D and combine it with the construction above to form an initial state $\widetilde{A}+\widetilde{\mathrm{d}A}$ for the simulation at the new bond dimension $\widetilde{D}$. Note that, if A represents the optimal solution at D, we can choose $dA^s_{00}=0$, or thus $|\widetilde{\mathrm{d}\Psi_0}\rangle = 0$. This approach avoids a particular problem of the imaginary time evolution with the time-dependent variational principle: For large D, the current implementation of the flow equations is susceptible to converging some random initial states to a state where the purity assumption (*i.e.* $\check{E}^A_A$ has a unique largest eigenvalue 1 and all other eigenvalues lie inside the unit circle) no longer holds. At this point, the formulas for the gradient and the gram matrix derived in the previous subsections are no longer valid. An incorrect application of these formulas often results in the algorithm getting trapped. While we

could of course implement more advanced formula's that take this scenario into account and with which the implementation would be able to continue the convergence process, using the aforementioned construction avoids the occurrence of this problem completely. In addition, at higher values of D, fewer iterations are required by starting from a good initial guess. Clearly, this is the preferred approach.

In principle, the same construction can be used in combination with real time evolution. After quantum quenches, the entanglement entropy typically increases and so does the error measure $\tilde{\epsilon}$. When $\tilde{\epsilon}$ increases beyond a certain tolerance level, we can choose to use the above construction to dynamically increase D, which brings $\tilde{\epsilon}$ back to an acceptable level. However, since this whole step is only well defined at first order, it cannot be included in a higher order numerical integrator. The dynamic expansion of the variational manifold should thus be used carefully in real time evolution, since it breaks the time-reversal symmetry.

Finally, we can also use the results from this subsection for another purpose. With $|\widetilde{\mathrm{d}\Psi_0}\rangle$ capturing the projection of $\hat{P}_0(\overline{A},A)\hat{H}|\Psi(A)\rangle = [\hat{H} - H(\overline{A},A)]|\Psi(A)\rangle$ in the tangent plane $\mathbb{T}_{\mathrm{uMPS}(D)}$ (*i.e.* $|\widetilde{\mathrm{d}\Psi_0}\rangle = \hat{P}_{\mathbb{T}^{\perp}_{\mathrm{uMPS}(D)}}(\overline{A},A)\hat{H}|\Psi(A)\rangle = \hat{P}_{\mathbb{T}_{\mathrm{uMPS}(D)}}(\overline{A},A)\hat{P}_0(\overline{A},A)\hat{H}|\Psi(A)\rangle$), we have defined $\tilde{\eta}(\overline{A},A)^2 = |\mathbb{Z}|^{-1}\langle\widetilde{\mathrm{d}\Psi_0}|\widetilde{\mathrm{d}\Psi_0}\rangle$. By choosing $\tilde{D} = dD$, $|\widetilde{\mathrm{d}\Psi_1}\rangle$ exactly captures the remnant $[\hat{\mathbb{1}} - \hat{P}_{\mathbb{T}^{\perp}_{\mathrm{uMPS}(D)}}(\overline{A},A)][\hat{H} - H(\overline{A},A)]|\Psi(A)\rangle$ that is orthogonal to the tangent plane $\mathbb{T}_{\mathrm{uMPS}(D)}$ for a nearest-neighbor Hamiltonian. We can now redefine $\tilde{\epsilon}$ from Eq. (3.124) as $\tilde{\epsilon}(\overline{A},A)^2 = |\mathbb{Z}|^{-1}\langle\widetilde{\mathrm{d}\Psi_1}|\widetilde{\mathrm{d}\Psi_1}\rangle = \mathrm{tr}[(xy)(xy)^{\dagger}]$. Thus, $\tilde{\epsilon}$ now follows from a manifestly positive expression, and can be computed much more accurately than from Eq. (3.124), where two terms of comparable size are subtracted. In addition, the expression for $\Delta H(\overline{A},A)^2$ given in Eq. (3.123) also contains 4 contributions which might almost cancel each other if $|\Psi\rangle$ is very close to an eigenstate of $\hat{H}$. This too can produce large numerical errors, and it is better to compute $\Delta H(\overline{A},A)$ as $\Delta H(\overline{A},A) = (\langle\widetilde{\mathrm{d}\Psi_0}|\widetilde{\mathrm{d}\Psi_0}\rangle + \langle\widetilde{\mathrm{d}\Psi_1}|\widetilde{\mathrm{d}\Psi_1}\rangle)^{1/2}$ where the square root contains two positive numbers.

2.7. Exemplary results

We now illustrate the power of our approach using both an imaginary time and a real time example. For the imaginary time evolution, we stress the accuracy that can be obtained, not only in the energy but also in the state itself. For real time evolution, the focus is on the conservation of constants of motion as predicted by symmetry, which is a consequence of using an algorithm that (approximately) respects time-reversal invariance.

Imaginary time evolution as a variational optimization method

Using imaginary time evolution with the simple Euler implementation of the time-dependent variational principle we now obtain a uniform matrix product state approximation for the ground state of the $S = 1$ antiferromagnetic Heisenberg model, which is given by the Hamiltonian

$$\hat{H}^{(S=1)}_{\text{Heisenberg}} = J \sum_{n\in\mathbb{Z}} \hat{S}^x_n \hat{S}^x_{n+1} + \hat{S}^y_n \hat{S}^y_{n+1} + \hat{S}^z_n \hat{S}^z_{n+1}. \tag{3.137}$$

This model has a continuous SU(2) invariance and can thus not be in a symmetry-broken state in one spatial dimension. However, the ground state has a hidden topological order that is measured by the string order parameter S, given by [333]

$$S = \lim_{n\to\infty} G_S(n_0, n_0 + n)$$
$$\text{with} \quad G_S(n_0, n_0 + n) = \langle\Psi|\hat{S}^z_{n_0} \exp(\mathrm{i}\pi \sum_{m=n_0}^{n_0+n} \hat{S}^z_m)\hat{S}^z_{n_0+n}|\Psi\rangle\,. \tag{3.138}$$

When trying to exploit SU(2) symmetry in a matrix product state approximation for the ground state of $\hat{H}^{(S=1)}_{\text{Heisenberg}}$, one would be inclined to decompose the ancilla space into integral spin representations of SU(2), since the physical degrees of freedom are all $S = 1$ variables. It was however found that decomposing the ancilla into half-integral spin representations gives far better result [227, 228], which corresponds to the fact that the topological ordered phase of the ground state is characterized by $S = 1/2$ edge states [334]. In addition, this phase has exponentially decaying correlations and is gapped. This was first conjectured by Haldane [335, 336] for all Heisenberg antiferromagnets with integral spin S. The computation of an accurate estimate of the so-called *Haldane gap* is discussed in the next section.

Due to the $\mathcal{O}(D^3)$ computational efficiency, an ordinary laptop or personal computer allows one to find the ground state up to $D = 1024$ in less then one hour (without exploiting symmetries), resulting in a ground state energy density $h/J = -1.4014840389712(2)$ which is accurate up to 14 significant digits. This result was obtained with a constant step size $\mathrm{d}t = 0.1$. Since the gradient —expressed through the value x^*— has zero length at the variational minimum ($||x^*|| = 0$), it automatically decreases in size as we approach it, and there is typically no need to reduce the size of the time step. This should be compared with the time-evolving block decimation for infinite lattices, where reduction of the time step, and thus automatic slowing down, is necessary to overcome the Trotter error and to validate the truncation step, which was only (locally) correct for unitary operations (real-time evolution). Having a very low value of the state convergence is useful to *e.g.* obtain a very accurate convergence in the entanglement spectrum. The entanglement spectrum can offer valuable information but is hard to get converged very accurately by other approaches. Table 3.1 shows how the first Schmidt values of the uniform matrix

product state approximation for the ground state of the Heisenberg chain at $D = 128$, which was converged up to $\tilde{\eta} = 10^{-10}$, accurately reproduce the degeneracy according to half-integral spin representations, without imposing this structure in any way.

Table 3.1: First 24 Schmidt values of the $D = 128$ uMPS approximation for the ground state of the $S = 1$ Heisenberg antiferromagnet. The degeneracy in the Schmidt spectrum as a result of SU(2) symmetry manifests itself, not by exploiting the symmetry, but rather by converging up to 'state tolerance' $\tilde{\eta} = 10^{-10}$.

0.6961989782	0.0057700505	0.0014877669
0.6961989782	0.0057700505	0.0014877669
0.0860988815	0.0057700505	0.0014877669
0.0860988815	0.0057700505	0.0014877669
0.0860988815	0.0016659093	0.0014877669
0.0860988815	0.0016659093	0.0014877669
0.0200132616	0.0016659093	0.0011065273
0.0200132616	0.0016659093	0.0011065273

Color labels:
S=1/2
S=3/2
S=5/2

Real time evolution and constants of motion

Using the time-reversal invariant numerical integrator discussed in Subsection 2.5, we can simulate a real-time evolution using the flow equations of the time-dependent variational principle. We start with the $D = 128$ uniform matrix product state $|\Psi(A)\rangle$ that best approximates the ground state of the XX-model with magnetic field $\mu/J = 1/2$ along the z-axis, which is described by the Hamiltonian

$$\hat{H}_{\mathrm{XX}} = \sum_{n\in\mathbb{Z}} J(\hat{\sigma}^x_n \hat{\sigma}^x_{n+1} + \hat{\sigma}^y_n \hat{\sigma}^y_{n+1}) + \mu \hat{\sigma}^z_n. \tag{3.139}$$

For the given parameter configuration, this model is critical. The ground state has a non-zero magnetization expectation value $\langle \hat{\sigma}^z \rangle \neq 0$ along the z-axis, whereas $\langle \hat{\sigma}^x \rangle = \langle \hat{\sigma}^y \rangle = 0$ due to a U(1) symmetry (spin rotations around the z-axis as generated by $\sum_{n\in\mathbb{Z}} \hat{\sigma}^z_n$). We evolve this state according to the $S = 1/2$ antiferromagnetic Heisenberg model, given by

$$\hat{H}^{(S=1/2)}_{\mathrm{Heisenberg}} = J \sum_{n\in\mathbb{Z}} \hat{\sigma}^x_n \hat{\sigma}^x_{n+1} + \hat{\sigma}^y_n \hat{\sigma}^y_{n+1} + \hat{\sigma}^z_n \hat{\sigma}^z_{n+1}, \tag{3.140}$$

so the expectation values $\langle \hat{\sigma}^{x,y,z} \rangle$ should be conserved due to the SU(2) symmetry. Unlike the integral S cases, the Heisenberg antiferromagnets are critical for half integral spins.

Comparative results for a second order implementation of the time-dependent variational principle and a second order, translation-invariant implementation of the time-evolving block decimation (based on [298]) are shown in Fig. 3.4. They illustrate that the time-evolving block decimation is much more capable of describing the evolution of conserved

quantities. Not only does the real time flow of the time-dependent variational principle have the same advantages as the imaginary time algorithm — conservation of translational invariance and internal symmetries — the (approximate) time-reversal invariance makes the algorithm extremely stable over longer simulation times. In principle, the first step in a real time simulation based on the time-evolving block decimation is even better, because evolving over a small time using a Lie-Trotter-Suzuki decomposition is a symplectic operation. However, since the time-evolving block decimation takes the state outside the manifold of uniform matrix product states with fixed bond dimensions, this step is followed by a truncation that breaks both the symplectic symmetry and the time reversal symmetry. Consequently, the results of the time-evolving block decimation for the quantities $h(\overline{A(t)},A(t))$ and $\sigma^z(\overline{A(t)},A(t))$ start to deviate considerably from their initial value $h(\overline{A},A)$ and $\sigma^z(\overline{A},A)$ after some time t. For the results obtained with the time-dependent variational principle, no deviation is noticeable at the same scale. Small deviations at $\mathcal{O}(\mathrm{d}t^4)$ do of course exist, as is visible in the flow of $\sigma^x(\overline{A(t)},A(t))$. For the simulation based on the time-evolving block decimation, the evolution $\sigma^x(\overline{A(t)},A(t))$ fluctuates at the same order and does not show a strong deviation, which is a consequence of the invariance of the Lie-Suzuki-Trotter decomposition under the discrete symmetry transformation $\hat{U} = \exp(\mathrm{i}\pi/2\sum_{n\in\mathbb{Z}}\hat{\sigma}^z_n)$, which maps $\hat{\sigma}^x \leftrightarrow -\hat{\sigma}^x$ and $\hat{\sigma}^y \leftrightarrow -\hat{\sigma}^y$ and thus prohibits a non-zero expectation value $\sigma^x(\overline{A(t)},A(t))$ if the initial state has $\sigma^x(\overline{A},A)=0$.

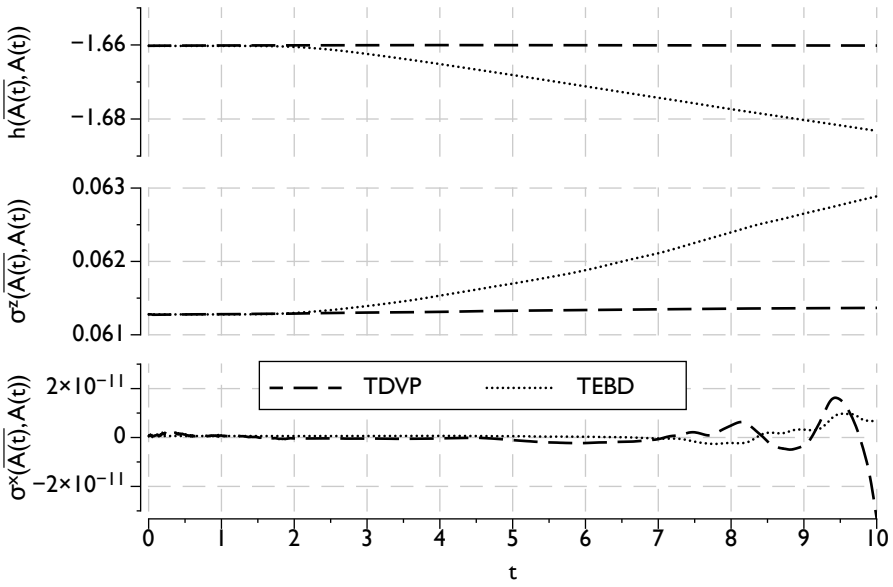

Figure 3.4: Comparison of real-time simulation results at $D = 128$ with time step $\mathrm{d}t = 5\times10^{-3}$ for conserved quantities e (energy density), $\langle\hat{S}^x\rangle$ and $\langle\hat{S}^z\rangle$ obtained with the time-dependent variational principle (TDVP, dashed lines) and the time-evolving block decimation (TEBD, dotted lines).

After having applied the real time evolution algorithm to evolve the state $|\psi(A)\rangle$ at $t = 0$ to $|\psi(A(t))\rangle$ at time t for a total time t_f, we can explicitly apply the time reversal operator $\hat{K}$ to the final state $|\psi(A(t_{\mathrm{f}}))\rangle$ and use the resulting state $|\psi(\overline{A(t_{\mathrm{f}})})\rangle$ as the initial value for a new time evolution over a total time t_f, resulting in states $|\psi(A'(t)\rangle$ at time t with thus $A'(0) = \overline{A(t_{\mathrm{f}})}$. We should then compare the states $\hat{K}\,|\psi(A'(t_{\mathrm{f}} - t))\rangle = |\psi(\tilde{A}(t))\rangle$ [with $\tilde{A}(t) = \overline{A'(t_{\mathrm{f}} - t)}$] to the states $|\psi(A(t))\rangle$. We measure the equality between two uMPS $|\psi(A)\rangle$ and $|\psi(\tilde{A})\rangle$ by the fidelity per site, which is given by the spectral radius of $\check{E}^{\tilde{A}(t)}_{A(t)}$. The fidelity per site is one for equivalent uniform matrix product states and is smaller than one for states that differ. Fig. 3.5 compares the results of this set-up for the time-reversal symmetric integrator of the time-dependent variational principle with results for the implementation based on the time-evolving block decimation. At $t = t_{\mathrm{f}}$, $A(t)$ and $\tilde{A}(t)$ are equal by definition. As t evolves towards $t = 0$, they are expected to diverge for algorithms that break the time reversal invariance. This is very clearly seen for the results obtained with the time-evolving block decimation. The result for $\rho(\check{E}^{\tilde{A}(t)}_{A(t)})$ obtained with the time-dependent variational principle stays nicely at one at the same observational scale. There are of course small fluctuations, since the numerical integration scheme is only time reversal invariant up to a precision $\tilde{\zeta}$, which was given the value $\tilde{\zeta} = 10^{-10}$.

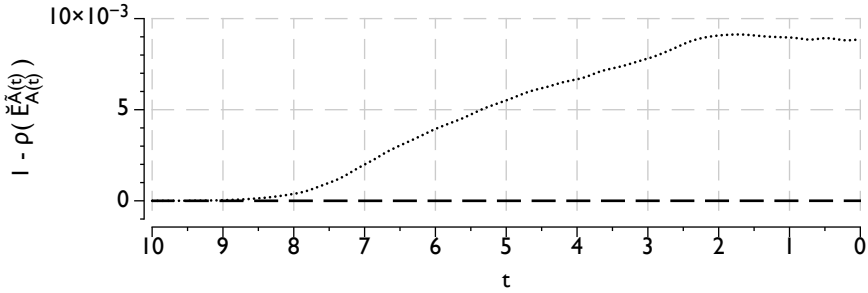

Figure 3.5: Comparison of time reversal invariance in a simulation based on the time-dependent variational principle (TDVP, dashed lines) and on the time-evolving block decimation (TEBD, dotted lines). Illustrated is (one minus) the spectral radius $\rho(\check{E}^{\tilde{A}(t)}_{A(t)})$, where $\tilde{A}(t) = \overline{A'(t_f - t)}$ ($t_f = 10$, $\mathrm{d}t = 5 \times 10^{-3}$, $\zeta = 10^{-10}$)

3. Excitations in the tangent plane $\mathbb{T}_{\mathsf{MPS}}$

Jutho Haegeman, Bogdan Pirvu, David J. Weir,
J. Ignacio Cirac, Tobias J. Osborne, Henri Verschelde, Frank Verstraete.
"*A variational matrix product ansatz for dispersion relation*".
arXiv:1103.2286 (2011).

3.1. Introduction

The density matrix renormalization group was originally developed for finding ground states of strongly correlated quantum lattice systems in one spatial dimension. By applying the variational principle to a state that is enforced to be orthogonal to previously found states, low-lying excited states on finite lattices can be found. Typically, these are not the states that one is interested in. On the finite lattice with open boundary conditions, the momentum quantum number does not exist. Low-lying excited states can easily be related to boundary effects and have no relation to the momentum eigenstates in the bulk of a macroscopic system. In the thermodynamic limit, the suggested approach fails, since any two states are likely to be orthogonal due to the orthogonality catastrophe. Even if we were able to construct a uniform matrix product state approximation for the lowest lying excited state with momentum zero, the finite excitation energy would spread out over an infinite lattice and is undetectable from computing the expectation value of the energy density. States with a different energy density as the ground state contain a finite density (and thus an infinite number) of elementary excitations. On a more mathematical level, we do not expect the class of matrix product states in the thermodynamic limit to have the correct properties for describing elementary excited states, since matrix product states are normalizable, and excited states with definite momentum are not.

Two different strategies for solving this problem emerge. Information about the spectrum of excited states can be obtained from the spectral functions $G^{\alpha,\beta}_{m,n}(\omega)$ defined in Eq. (3.86) in Subsection 2.1. Initially, algorithms for directly evaluating these spectral functions were developed. But since the development of the time-evolving block decimation, time evolution can be approximated so well that modern state-of-the-art algorithms first compute the time-dependent correlation function $G^{\alpha,\beta}_{m,n}(t)$ [see Eq. (3.87)] for some finite interval $t \in [0, T]$, and then compute the Fourier transform [337, 338]. Starting from a disturbance of the ground state of a large but finite lattice, the time evolution can be computed for any time T below which the information of the disturbance has not yet reached the edges of the lattice. The finite time T results in a broadening of the spectral function, but by combining advanced linear prediction techniques to extend T beyond the computable range with complex statistical machinery for isolating the location of the poles, a fairly accurate determination of the dispersion relation of the elementary excitation in the Heisenberg model was obtained [338]. Because of the (approximately)

linear increase of entropy under time evolution, very large bond values are required in order to accurately approximate the time evolution all the way up to time T. This is in sharp contrast with the observation that low-lying excited states also satisfy an area law for the scaling of entanglement entropy (see Subsection 2.5 of Chapter 1), and that it should thus be possible to construct a direct and efficient approximation.

A different strategy is thus to construct a variational ansatz that is suited to directly probe the spectrum of excited states. Nevertheless, variational ansätze for excited states based on the matrix product concept are rare. The interest in energy-momentum dispersion relations of translation invariant Hamiltonians automatically redirects us to a lattice with periodic boundary conditions. A direct construction in the thermodynamic limit seems impossible due to the remarks above. Together with their seminal work on matrix product states for ground states, Rommer and Östlund proposed the following ansatz for excited states with momentum p [227, 228]

$$|\tilde{\Phi}_p(x)\rangle = \sum_{n=1}^{N} \mathrm{e}^{\mathrm{i}pn} \hat{T}^n \sum_{\{s_n\}=1}^{q} \mathrm{tr}\left[x A^{s_1} A^{s_2} \cdots A^{s_N}\right] |s_1 s_2 \cdots s_N\rangle, \tag{3.141}$$

which allowed them to get an early estimate of the Haldane gap $\Delta_{\mathrm{Haldane}}$. The matrices A^s are fixed to the value for which the uniform matrix product state $|\Psi(A)\rangle$ (of finite size N) best approximates the ground state, and one can hope that several branches of the energy-momentum spectrum can be captured by different values of x. The rationale of this ansatz is that low-lying excited states can be described as a momentum superposition of a local disturbance, which is encoded in the virtual system using the virtual operator $x \in \mathbb{L}(\mathbb{C}^D)$. Using a series expansion in the system size N, Rommer and Östlund were even able to extrapolate their results to the thermodynamic limit. A different type of variational class are the so-called "projected entangled multipartite states", given by the ansatz [339]

$$|\Upsilon_p[A]\rangle = \frac{1}{\sqrt{N}} \sum_{n=1}^{N} \mathrm{e}^{\mathrm{i}pn} \hat{T}^n \sum_{\{s_n\}=1}^{q} \mathrm{tr}\left[A^{s_1}(1) A^{s_2}(2) \cdots A^{s_N}(N)\right] |s_1 s_2 \cdots s_N\rangle, \tag{3.142}$$

which contains a momentum superposition of the non-translation invariant matrix product state $|\Psi[A]\rangle$. Here all matrices $A^s(n)$ are variational parameters, and different branches of the spectrum are obtained by creating mutually orthogonal states at a fixed momentum p. This specific superposition is expected to be able to introduce long-range information: writing $|\Upsilon_0[A]\rangle$ as a uniform matrix product state $|\tilde{\Psi}(\tilde{A})\rangle$ requires a bond dimension $\tilde{D} = ND$ if D represents the bond dimension of the matrix product state $|\Psi[A]\rangle$. The computational complexity of this algorithm scales as $\mathcal{O}(N^2 D^5)$, and it is thus restricted to lattices of moderate size and small values of the bond dimension D. This last aspect is partially compensated by the higher entanglement that is allowed in this state.

The idea that low-lying excited states can be regarded as (momentum superpositions

of) local disturbances on the ground state is of course inspired by the case of quadratic theories, where creation operators $\hat{a}^\dagger(p)$ can be defined that create elementary excitations when acting on the ground state. Most elementary collective excitations do indeed have this pointlike structure. Bijl, Feynman and Cohen generalized this concept by acting on the ground state with general operators $\hat{O}(p)$, which represent the Fourier transform of some local operator $\hat{O}$ with compact support, for studying excitations in liquid Helium [340, 341, 342]. If $\{\hat{O}^\alpha\}$ represents a complete set of local observables, then the Feynman-Bijl operator $\hat{O}$ can be expanded as $\hat{O} = c_\alpha \hat{O}^\alpha$ and $\{c_\alpha\}$ can be treated as the set of variational parameters. This ansatz was first used in the context of spin systems by Arovas, Auerbach and Haldane [343] and is then referred to as the single-mode approximation. The single-mode approximation was first combined with matrix product states in [344], and generalized to local operators acting on up to 4 sites in [345].

A direct generalization of both the Östlund and Rommer ansatz, where the excitation is represented as an operator in the virtual space, and the single-mode approximation, where the excitation is represented as an operator in the physical space, was recently proposed by Pirvu *et al.* [346]. The variational ansatz

$$|\Phi_p(B)\rangle = \sum_{n=1}^{N} e^{ipn} \hat{T}^n \sum_{\{s_n\}=1}^{q} \mathrm{tr}\left[B^{s_1} A^{s_2} \cdots A^{s_N}\right] |s_1 s_2 \cdots s_N\rangle, \tag{3.143}$$

was studied, where A is kept fixed to the value for which $|\Psi(A)\rangle$ best approximates the ground state of the lattice of N sites. While we now recognize $|\Phi_p(B)\rangle$ as a tangent vector living in the momentum p sector of $\mathbb{T}_{\mathrm{MPS}}(A)$, this relation was not explored in [346]. By choosing $B^s = XA^s$, the Östlund and Rommer ansatz is reproduced, whereas the Feynman-Bijl ansatz with a one-site operator $\hat{O}$ is obtained by setting $B^s = \sum_{t=1}^{q} \langle s|\hat{O}|t\rangle A^t$. Feynman-Bijl operators with a larger support of $n > 1$ sites are not strictly included in this variational class, but by transferring information along the virtual space all operators acting on $n \approx 2\log_q D$ sites are effectively included. We can even hope that the D left and D right Schmidt vectors throw away irrelevant information on the nearest sites in favor of keeping relevant information on sites that are further away. The optimal choice of B^s for the lowest lying excitation with momentum p could then correspond to a Feynman-Bijl operator with local support that is significantly larger than $2\log_q D$ sites. It was noted in [346] that not only the lowest branches of elementary excitations, but also higher branches of composite excitations are well reproduced when the system size N is not too large.

Unfortunately, all of the existing proposals are restricted to the setting of a finite lattice with periodic boundary conditions, which implies that their computational complexity scales as $\mathcal{O}(D^5)$ and hinders their practical applicability. We now apply the variational principle to the tangent vectors $|\Phi_p(B)\rangle$ of $\mathcal{M}_{\mathrm{MPS}(D)}$ at a point $|\Psi(A)\rangle \in \mathcal{M}_{\mathrm{uMPS}(D)}$ in the thermodynamic limit. Not only does this allow for an efficient implementation, where the computational complexity scales as $\mathcal{O}(D^3)$, it is also a necessary extension in order to be able to describe topologically non-trivial excitations. In one spatial dimension,

topologically non-trivial excitations exist in a phase of discrete symmetry breaking as kinks or domain walls that interpolate between two ground states with a different value of the order parameter. This ansatz includes the topologically non-trivial analogon of the Feynman-Bijl operators, which are the Mandelstam operators [347]. We also relate our approach to the time-dependent variational principle from the previous section.

3.2. Topologically trivial states

Let $\hat{H}$ be a given translation invariant Hamiltonian on an infinite lattice, which we assume to contain only nearest-neighbor interactions: $\hat{H} = \sum_{n\in\mathbb{Z}} \hat{T}^n \hat{h} \hat{T}^{-n}$. We first look for the ground state, which we approximate with a uniform matrix product state $|\Psi(A)\rangle \in \mathscr{M}_{\text{uMPS}(D)}$. We use the time-dependent variational principle with imaginary time evolution to find an energy minimum, *i.e.* a solution of the difficult set of equations that is imposed by the time-independent variational principle. We henceforth assume that A is the value of at least a local —and hopefully the global— minimum. We again assume that the uniform matrix product state $|\Psi(A)\rangle$ is pure, so that $\check{E}$ has a unique eigenvalue 1 and all the other eigenvalues lie strictly within the unit circle.

We now apply the time-independent variational principle to the set of states $|\Phi_p(B;A)\rangle \in \mathbb{T}_{\text{MPS}(D)}(A)$. Since we are interested in excited states, we need to impose orthogonality to the ground state approximation $|\Psi(A)\rangle$. We can thus restrict to $\mathbb{T}^{\perp}_{\text{MPS}(D)}(A)$, as was also the case when applying the time-dependent variational principle. The momentum p sector of $\mathbb{T}^{\perp}_{\text{MPS}(D)}(A)$, denoted as $\mathbb{T}^{\perp}_{\Phi_p}(A)$, is $(q-1)D^2$-dimensional for any $p \in [-\pi, +\pi)$. We can recylce the parameterization $B = \mathcal{B}_\Phi(x)$ from Eq. (3.112) in terms of the $D \times (q-1)D$ matrix x. Since $|\Phi_p(B;A)\rangle$ is linear in B and $\mathcal{B}_\Phi(x)$ is linear in x, we effectively have a variational manifold that is spanned by the states $|\Phi_j\rangle = |\Phi(\mathcal{B}_\Phi(x_i);A)\rangle$ with $\{x_i \mid i = 1,\ldots,(q-1)D^2\}$ a basis for x, so that $x = z^i x_i$ and $|\Phi\rangle = z^i |\Phi_i\rangle$. The energy expectation value $\langle\Phi(\overline{\mathcal{B}}_\Phi(\overline{x});\overline{A})|\hat{H}|\Phi(\mathcal{B}_\Phi(x);A)\rangle$ is quadratic in x or thus in the coefficients z. Applying the time-independent variational principle does then not require to solve a complicated set of equations, but reduces simply to the Rayleigh-Ritz equation [see Eq. (2.4) in the previous chapter], *i.e.* a generalized eigenvalue equation.

Two remarks are in order. Firstly, the ansatz states $|\Phi_p(B)\rangle$ (we henceforth omit the explicit notation of the variational minimum A) are momentum eigenstates in an infinite volume and can thus not be normalized to unity. Secondly, unlike for the ground state, we cannot restrict to an evaluation of the energy density expectation value. As explained in the introduction, the finite excitation energy in a momentum eigenstate is spread out over the complete lattice, and the energy density

$$\frac{\langle\Phi_p(\overline{B})|\hat{h}|\Phi_{p'}(B')\rangle}{\langle\Phi_p(\overline{B})|\Phi_{p'}(B')\rangle}$$

is undistinguishable from its ground state value $h(\overline{A},A) = \langle\Psi(\overline{A})|\hat{h}|\Psi(A)\rangle$ (where $|\Psi(A)\rangle$ is assumed to be normalized to unity). We thus have to evaluate the expectation value of the full Hamiltonian $\langle\Phi_p(\overline{B})|\hat{H}|\Phi_{p'}(B')\rangle$, where the excitation energy is present as a finite shift (times the infinite normalization $\langle\Phi_p(\overline{B})|\hat{h}|\Phi_{p'}(B')\rangle$) above a divergent contribution from the extensive ground state energy $H(\overline{A},A) = |\mathbb{Z}|h(\overline{A},A)$ (times the infinite normalization $\langle\Phi_p(\overline{B})|\hat{h}|\Phi_{p'}(B')\rangle$). Subtracting this ground state energy can quickly become a source of errors, as we have to subtract precisely $|\mathbb{Z}|$ times the ground state energy density, and counting errors are easily made. The safest strategy is to subtract $H(\overline{A},A)$ from $\hat{H}$ from the beginning. Note that, unlike in the evaluation of $\langle\Phi_p(\overline{B})|\hat{H}|\Psi(A)\rangle$ that was required by the time dependent variational principle, the ground state energy contribution is not automatically subtracted by restricting to tangent vectors $|\Phi_p(B)\rangle$ that are orthogonal to $|\Psi(A)\rangle$. We thus redefine $\hat{h} \leftarrow \hat{h} - h(\overline{A},A)$, where $h(\overline{A},A) = (l|\check{H}_{AA}^{AA}|r)$ [see Eq. (3.114)]. With this newly defined $\hat{h}$, we thus obtain $(l|\check{H}_{AA}^{AA}|r) = 0$.

We are now ready to evaluate the required quantities appearing in the Rayleigh-Ritz equations. The Gram matrix $\langle\Phi_p(\overline{B})|\Phi_{p'}(B')\rangle$ appearing in the right hand side was computed in Eq. (3.108) of the previous section. Expanding $\langle\Phi_p(\overline{B})|\hat{H}|\Phi_{p'}(B')\rangle$ is a lot more involved, as we now have to deal with three infinite sums. The three summation indices indicate the position of B, B' and the first site acted upon by $\hat{h}$. In between these three positions are transfer matrices $\check{E}$, which can be decomposed into connected contributions coming from $\check{Q}\check{E}\check{Q}$ and disconnected contributions coming from $\check{S} = |r)(l|$ (see Subsection 2.3). Thanks to the redefinition of the hamiltonian terms $\hat{h}$, we obtain $(l|\check{H}_{AA}^{AA}\check{S} = 0$ and $\check{S}\check{H}_{AA}^{AA}|r) = 0$ and no disconnected contributions coming from $\check{H}_{AA}^{AA}$ can arise. The connected contributions yield finite results, and we are free to introduce substitutions of the summation indices. Disconnected contributions coming from $\check{E}_B^A$ and $\check{E}_A^{B'}$ might give rise to additional divergences and should be treated carefully. The total expression is of the general format

$$\langle\Phi_p(\overline{B})|\hat{H}|\Phi_{p'}(B')\rangle = \sum_{n=-\infty}^{+\infty}\sum_{n'=-\infty}^{+\infty}\sum_{n_0=-\infty}^{+\infty} \mathrm{e}^{\mathrm{i}p'n'-\mathrm{i}pn}\left[B \text{ at site } n,\ B' \text{ at site } n' \text{ and } \hat{h} \text{ on sites } n_0 \text{ and } n_0+1\right]$$

We first focus on the terms where everything is connected, thus where all transfer operators have been replaced by their corresponding regularized version $\check{Q}\check{E}\check{Q}$. We can now safely introduce the substitution $n' \leftarrow n_c$, $n \leftarrow n_c + \Delta n$ and $n_0 \leftarrow n_c + \Delta n_0$. The summation over n_c immediately yields the momentum conserving factor $2\pi\delta(p'-p)$, since the terms within the summation are independent of the global position n_c. If we change Δn to n and Δn_0 to n_0 for notational simplicity and omit the overall factor $2\pi\delta(p'-p)$, we are left with

$$(l|\check{H}_{BA}^{B'A}|r) + (l|\check{H}_{AB}^{AB'}|r)$$

$$
\begin{aligned}
&+\sum_{n_0=1}^{+\infty}(l|\check{E}_B^{B'}\check{Q}\check{E}^{n_0-1}\check{Q}\check{H}_{AA}^{AA}|r)+\sum_{n_0=-\infty}^{-2}(l|\check{H}_{AA}^{AA}\check{Q}\check{E}^{-n_0-2}\check{Q}\check{E}_B^{B'}|r)\\
&+\sum_{n=-\infty}^{-1}\mathrm{e}^{-\mathrm{i}pn}\Big[\theta(n=-1)(l|\check{H}_{BA}^{AB'}|r)\\
&\qquad+(l|\check{E}_B^{A}\check{Q}\check{E}^{n-1}\check{Q}\check{H}_{AA}^{B'A}|r)+(l|\check{H}_{AB}^{AA}\check{Q}\check{E}^{-n-1}\check{Q}\check{E}_A^{B'}|r)\\
&\qquad+\theta(n<-1)(l|\check{E}_B^{A}\check{Q}\check{E}^{-n-2}\check{Q}\check{H}_{AA}^{AB'}|r)\\
&\qquad+\theta(n<-1)(l|\check{H}_{BA}^{AA}\check{Q}\check{E}^{-n-2}\check{Q}\check{E}_A^{B'}|r)\\
&\qquad+\sum_{n_0=1}^{+\infty}(l|\check{E}_B^{A}\check{Q}\check{E}^{-n-1}\check{Q}\check{E}_A^{B'}\check{Q}\check{E}^{n_0-1}\check{Q}\check{H}_{AA}^{AA}|r)\\
&\qquad+\sum_{n_0=-\infty}^{n-2}(l|\check{H}_{AA}^{AA}\check{Q}\check{E}^{-n_0+n-2}\check{Q}\check{E}_B^{A}\check{Q}\check{E}^{-n-1}\check{Q}\check{E}_A^{B'}|r)\\
&\qquad+\theta(n<-2)\sum_{n_0=n+1}^{-2}(l|\check{E}_B^{A}\check{Q}\check{E}^{-n+n_0-1}\check{Q}\check{H}_{AA}^{AA}\check{Q}\check{E}^{-n_0-2}\check{Q}\check{E}_A^{B'}|r)\Big]\\
&+\sum_{n=1}^{+\infty}\mathrm{e}^{-\mathrm{i}pn}\Big[\theta(n=1)(l|\check{H}_{AB}^{B'A}|r)\\
&\qquad+(l|\check{E}_A^{B'}\check{Q}\check{E}^{n-1}\check{Q}\check{H}_{BA}^{AA}|r)+(l|\check{H}_{AA}^{AB'}\check{Q}\check{E}^{n-1}\check{Q}\check{E}_B^{A}|r)\\
&\qquad+\theta(n>1)(l|\check{E}_A^{B'}\check{Q}\check{E}^{n-2}\check{Q}\check{H}_{AB}^{AA}|r)\\
&\qquad+\theta(n>1)(l|\check{H}_{AA}^{B'A}\check{Q}\check{E}^{n-2}\check{Q}\check{E}_B^{A}|r)\\
&\qquad+\sum_{n_0=n+1}^{+\infty}(l|\check{E}_A^{B'}\check{Q}\check{E}^{n-1}\check{Q}\check{E}_B^{A}\check{Q}\check{E}^{n_0-n-1}\check{Q}\check{H}_{AA}^{AA}|r)\\
&\qquad+\sum_{n_0=-\infty}^{-2}(l|\check{H}_{AA}^{AA}\check{Q}\check{E}^{-n_0-2}\check{Q}\check{E}_A^{B'}\check{Q}\check{E}^{-n-1}\check{Q}\check{E}_B^{A}|r)\\
&\qquad+\theta(n>2)\sum_{n_0=1}^{n-2}(l|\check{E}_A^{B'}\check{Q}\check{E}^{n_0-1}\check{Q}\check{H}_{AA}^{AA}\check{Q}\check{E}^{n-n_0-2}\check{Q}\check{E}_B^{A}|r)\Big].
\end{aligned}
$$

The terms on the first line correspond to $n=0$, *i.e.* where B and B' are on the same site. Then we have all the terms corresponding to $n<0$ and all the terms corresponding to $n>0$. For most terms, we can immediately evaluate the geometric series for n_0, followed by an evaluation of the additional geometric series in n for some terms. The only exception are the terms with $\theta(n<-2)$ and $\theta(n>2)$, where it is better to first switch the two sums and express the summation bounds of n in terms of n_0. Then we first evaluate the geometric series in n, followed by the one in n_0. We obtain

$$
\begin{aligned}
&(l|\check{H}_{BA}^{B'A}|r)+(l|\check{H}_{AB}^{AB'}|r)+\mathrm{e}^{+\mathrm{i}p}(l|\check{H}_{BA}^{AB'}|r)+\mathrm{e}^{-\mathrm{i}p}(l|\check{H}_{AB}^{B'A}|r)\\
&+(l|\check{E}_B^{B'}(\check{\mathbb{1}}-\check{E})^{\mathsf{P}}\check{H}_{AA}^{AA}|r)+(l|\check{H}_{AA}^{AA}(\check{\mathbb{1}}-\check{E})^{\mathsf{P}}\check{E}_B^{B'}|r)
\end{aligned}
$$

$$
\begin{aligned}
&+\mathrm{e}^{+\mathrm{i}p}(l|\check{E}_B^A(\check{\mathbb{1}}-\mathrm{e}^{+\mathrm{i}p}\check{E})^{\mathsf{P}}\check{E}_A^{B'}(\check{\mathbb{1}}-\check{E})^{\mathsf{P}}\check{H}_{AA}^{AA}|r)\\
&+\mathrm{e}^{-\mathrm{i}p}(l|\check{E}_A^{B'}(\check{\mathbb{1}}-\mathrm{e}^{-\mathrm{i}p}\check{E})^{\mathsf{P}}\check{E}_B^{A}(\check{\mathbb{1}}-\check{E})^{\mathsf{P}}\check{H}_{AA}^{AA}|r)\\
&+\mathrm{e}^{+\mathrm{i}p}(l|\check{H}_{AA}^{AA}(\check{\mathbb{1}}-\check{E})^{\mathsf{P}}\check{E}_B^{A}(\check{\mathbb{1}}-\mathrm{e}^{+\mathrm{i}p}\check{E})^{\mathsf{P}}\check{E}_A^{B'}|r)\\
&+\mathrm{e}^{-\mathrm{i}p}(l|\check{H}_{AA}^{AA}(\check{\mathbb{1}}-\check{E})^{\mathsf{P}}\check{E}_A^{B'}(\check{\mathbb{1}}-\mathrm{e}^{-\mathrm{i}p}\check{E})^{\mathsf{P}}\check{E}_B^{A}|r)\\
&+\mathrm{e}^{+\mathrm{i}p}(l|\check{E}_B^{A}(\check{\mathbb{1}}-\mathrm{e}^{+\mathrm{i}p}\check{E})^{\mathsf{P}}\check{H}_{AA}^{B'A}|r)+\mathrm{e}^{-\mathrm{i}p}(l|\check{E}_A^{B'}(\check{\mathbb{1}}-\mathrm{e}^{-\mathrm{i}p}\check{E})^{\mathsf{P}}\check{H}_{BA}^{AA}|r)\\
&+\mathrm{e}^{+2\mathrm{i}p}(l|\check{E}_B^{A}(\check{\mathbb{1}}-\mathrm{e}^{+\mathrm{i}p}\check{E})^{\mathsf{P}}\check{H}_{AA}^{AB'}|r)+\mathrm{e}^{-2\mathrm{i}p}(l|\check{E}_A^{B'}(\check{\mathbb{1}}-\mathrm{e}^{-\mathrm{i}p}\check{E})^{\mathsf{P}}\check{H}_{AB}^{AA}|r)\\
&+\mathrm{e}^{+\mathrm{i}p}(l|\check{H}_{AB}^{AA}(\check{\mathbb{1}}-\mathrm{e}^{+\mathrm{i}p}\check{E})^{\mathsf{P}}\check{E}_A^{B'}|r)+\mathrm{e}^{-\mathrm{i}p}(l|\check{H}_{AA}^{AB'}(\check{\mathbb{1}}-\mathrm{e}^{-\mathrm{i}p}\check{E})^{\mathsf{P}}\check{E}_B^{A}|r)\\
&+\mathrm{e}^{+2\mathrm{i}p}(l|\check{H}_{BA}^{AA}(\check{\mathbb{1}}-\mathrm{e}^{+\mathrm{i}p}\check{E})^{\mathsf{P}}\check{E}_A^{B'}|r)+\mathrm{e}^{-2\mathrm{i}p}(l|\check{H}_{AA}^{B'A}(\check{\mathbb{1}}-\mathrm{e}^{-\mathrm{i}p}\check{E})^{\mathsf{P}}\check{E}_B^{A}|r)\\
&+\mathrm{e}^{+3\mathrm{i}p}(l|\check{E}_B^{A}(\check{\mathbb{1}}-\mathrm{e}^{+\mathrm{i}p}\check{E})^{\mathsf{P}}\check{H}_{AA}^{AA}(\check{\mathbb{1}}-\mathrm{e}^{+\mathrm{i}p}\check{E})^{\mathsf{P}}\check{E}_A^{B'}|r)\\
&\qquad\qquad+\mathrm{e}^{-3\mathrm{i}p}(l|\check{E}_A^{B'}(\check{\mathbb{1}}-\mathrm{e}^{-\mathrm{i}p}\check{E})^{\mathsf{P}}\check{H}_{AA}^{AA}(\check{\mathbb{1}}-\mathrm{e}^{-\mathrm{i}p}\check{E})^{\mathsf{P}}\check{E}_B^{A}|r).
\end{aligned}
$$

The symbolic notation $(\hat{\mathbb{1}}-\mathrm{e}^{\pm\mathrm{i}p}\check{E})^{\mathsf{P}}=\check{Q}(\check{\mathbb{1}}-\mathrm{e}^{\pm\mathrm{i}p}\check{Q}\check{E}\check{Q})^{-1}\check{Q}$ was introduced in the previous section. Only for $p=0$ is this truly a pseudo-inverse. For $p\neq 0$, the $\hat{\mathbb{1}}-\mathrm{e}^{\pm\mathrm{i}p}\check{E}$ is not really singular. Nevertheless, we had to separate the eigenvalue $\mathrm{e}^{\pm\mathrm{i}p}$ with modulus 1 from the operator $\mathrm{e}^{\pm\mathrm{i}p}\check{E}$ in order to use the formula for the geometric series.

We now consider the contributions resulting from disconnecting either B or B'. They cannot be disconnected both, since this would also imply that $\hat{h}$ is disconnected, which we've excluded above. Whenever B' appears on the complete left (right) side of a term, and is separated from the rest by a transfer operator $\check{E}$, there is such a disconnected contribution. We assume that we can still make the substitution to the global position n_{c} and the relative positions n and n_0. Only making substitutions that changes the value of finite bounds in the sum result in a possibility of miscounting contributions and making errors. The summation over the global position J again yields the momentum conservation. The total (left and right) contribution from disconnecting B is given by (omitting the momentum conserving factor $2\pi\delta(p'-p)$)

$$
\begin{aligned}
(l|E_B^A|r)\Bigg[&(l|\check{H}_{AA}^{B'A}|r)\Big(\sum_{n=-\infty}^{-1}\mathrm{e}^{-\mathrm{i}pn}+\sum_{n=2}^{+\infty}\mathrm{e}^{-\mathrm{i}pn}\Big)\\
&+(l|\check{H}_{AA}^{AB'}|r)\Big(\sum_{n=-\infty}^{-2}\mathrm{e}^{-\mathrm{i}pn}+\sum_{n=1}^{+\infty}\mathrm{e}^{-\mathrm{i}pn}\Big)\\
&+\sum_{n=-\infty}^{-1}\mathrm{e}^{-\mathrm{i}pn}\sum_{n_0=1}^{+\infty}(l|\check{E}_A^{B'}\check{Q}\check{E}^{n_0-1}\check{Q}\check{H}_{AA}^{AA}|r)\\
&+\sum_{n=3}^{+\infty}\mathrm{e}^{-\mathrm{i}pn}\sum_{n_0=1}^{n-2}(l|\check{E}_A^{B'}\check{Q}\check{E}^{n_0-1}\check{Q}\check{H}_{AA}^{AA}|r)\\
&+\sum_{n=-\infty}^{-3}\mathrm{e}^{-\mathrm{i}pn}\sum_{n_0=n+1}^{-2}(l|\check{H}_{AA}^{AA}\check{Q}\check{E}^{-n_0-2}\check{Q}\check{E}_A^{B'}|r)
\end{aligned}
$$

$$+\sum_{n=1}^{+\infty} \mathrm{e}^{-\mathrm{i}pn} \sum_{n_0=-\infty}^{-2} (l|\check{H}_{AA}^{AA}\check{Q}\check{E}^{-n_0-2}\check{Q}\check{E}_A^{B'}|r)\Big].$$

These terms should be treated carefully. They should generate a divergence at $p = 0$ through a $2\pi\delta(p)$, but should be finite for any other $p \neq 0$. By inserting the result for the finite geometric sums in n_0, we obtain for the terms between the square brackets

$$\begin{aligned}
&(l|\check{H}_{AA}^{B'A}|r)\Big(2\pi\delta(p) - 1 - \mathrm{e}^{-\mathrm{i}p}\Big) + (l|\check{H}_{AA}^{AB'}|r)\Big(2\pi\delta(p) - 1 - \mathrm{e}^{+\mathrm{i}p}\Big) \\
&+ \sum_{n=-\infty}^{-1} \mathrm{e}^{-\mathrm{i}pn}(l|\check{E}_A^{B'}(\check{\mathbb{1}} - \check{E})^{\mathsf{P}}\check{H}_{AA}^{AA}|r) \\
&+ \sum_{n=3}^{+\infty} \mathrm{e}^{-\mathrm{i}pn}(l|\check{E}_A^{B'}(\check{\mathbb{1}} - \check{E})^{\mathsf{P}}(\check{Q} - \check{Q}\check{E}^{n-2}\check{Q})\check{H}_{AA}^{AA}|r) \\
&+ \sum_{n=-\infty}^{-3} \mathrm{e}^{-\mathrm{i}pn}(l|\check{H}_{AA}^{AA}(\check{\mathbb{1}} - \check{E})^{\mathsf{P}}(\check{Q} - \check{Q}\check{E}^{-n-2}\check{Q})\check{E}_A^{B'}|r) \\
&+ \sum_{n=1}^{+\infty} \mathrm{e}^{-\mathrm{i}pn}(l|\check{H}_{AA}^{AA}(\check{\mathbb{1}} - \check{E})^{\mathsf{P}}\check{E}_A^{B'}|r).
\end{aligned}$$

Since $(\check{\mathbb{1}} - \check{E})^{\mathsf{P}}\check{Q} = (\check{\mathbb{1}} - \check{E})^{\mathsf{P}}$, we can now group the first and second terms for both the second and third line, and complete the sums in n to $\sum_{n=-\infty}^{+\infty} \mathrm{e}^{\pm\mathrm{i}p} = 2\pi\delta(p)$, in order to obtain

$$\begin{aligned}
&(l|\check{H}_{AA}^{B'A}|r)\Big(2\pi\delta(p) - 1 - \mathrm{e}^{-\mathrm{i}p}\Big) + (l|\check{H}_{AA}^{AB'}|r)\Big(2\pi\delta(p) - 1 - \mathrm{e}^{+\mathrm{i}p}\Big) \\
&+ \big(2\pi\delta(p) - 1 - \mathrm{e}^{-\mathrm{i}p} - \mathrm{e}^{-2\mathrm{i}p}\big)(l|\check{E}_A^{B'}(\check{\mathbb{1}} - \check{E})^{\mathsf{P}}\check{H}_{AA}^{AA}|r) \\
&- \sum_{n=3}^{+\infty} \mathrm{e}^{-\mathrm{i}pn}(l|\check{E}_A^{B'}(\check{\mathbb{1}} - \check{E})^{\mathsf{P}}\check{Q}\check{E}^{n-2}\check{Q}\check{H}_{AA}^{AA}|r) \\
&+ \big(2\pi\delta(p) - 1 - \mathrm{e}^{+\mathrm{i}p} - \mathrm{e}^{+2\mathrm{i}p}\big)(l|\check{H}_{AA}^{AA}(\check{\mathbb{1}} - \check{E})^{\mathsf{P}}\check{E}_A^{B'}|r) \\
&- \sum_{n=-\infty}^{-3} \mathrm{e}^{-\mathrm{i}pn}(l|\check{H}_{AA}^{AA}(\check{\mathbb{1}} - \check{E})^{\mathsf{P}}\check{Q}\check{E}^{-n-2}\check{Q}\check{E}_A^{B'}|r).
\end{aligned}$$

Finally, we have to compute two converging geometric series in n. Note that the power of $(\check{Q}\check{E}\check{Q})$ starts at one instead of zero (for $n = 3$ on line 3 and for $n = -3$ on line 5). We can absorb the term with factor $\mathrm{e}^{-2\mathrm{i}p}$ from line 2 and the term with factor $\mathrm{e}^{+2\mathrm{i}p}$ from line 4 respectively, in order to have a geometric series in $(\check{Q}\check{E}\check{Q})$ starting at power zero. We hence obtain for the total disconnected contribution of B

$$\begin{aligned}
(l|E_B^A|r)\Big[&(l|\check{H}_{AA}^{B'A}|r)\Big(2\pi\delta(p) - 1 - \mathrm{e}^{-\mathrm{i}p}\Big) + (l|\check{H}_{AA}^{AB'}|r)\Big(2\pi\delta(p) - 1 - \mathrm{e}^{+\mathrm{i}p}\Big) \\
&+ \big(2\pi\delta(p) - 1 - \mathrm{e}^{-\mathrm{i}p}\big)(l|\check{E}_A^{B'}(\check{\mathbb{1}} - \check{E})^{\mathsf{P}}\check{H}_{AA}^{AA}|r) \\
&- \mathrm{e}^{-\mathrm{i}2p}(l|\check{E}_A^{B'}(\check{\mathbb{1}} - \check{E})^{\mathsf{P}}(\check{\mathbb{1}} - \mathrm{e}^{-\mathrm{i}p}\check{E})^{\mathsf{P}}\check{H}_{AA}^{AA}|r)
\end{aligned}$$

$$
\begin{aligned}
&+\left(2\pi\delta(p)-1-\mathrm{e}^{+\mathrm{i}p}\right)(l|\check{H}_{AA}^{AA}(\check{\mathbb{1}}-\check{E})^{\mathsf{P}}\check{E}_{A}^{B'}|r)\\
&-\mathrm{e}^{+\mathrm{i}2p}(l|\check{H}_{AA}^{AA}(\check{\mathbb{1}}-\check{E})^{\mathsf{P}}(\check{\mathbb{1}}-\mathrm{e}^{+\mathrm{i}p}\check{E})^{\mathsf{P}}\check{E}_{A}^{B'}|r)\Big].
\end{aligned}
$$

By adding a similar result from disconnecting B', we obtain as final result

$$
\begin{aligned}
&\langle\Phi_{p}(\overline{B})|\hat{H}|\Phi_{p'}(B')\rangle = 2\pi\delta(p'-p)\times\\
&\Big\{(l|\check{H}_{BA}^{B'A}|r)+(l|\check{H}_{AB}^{AB'}|r)+\mathrm{e}^{+\mathrm{i}p}(l|\check{H}_{BA}^{AB'}|r)+\mathrm{e}^{-\mathrm{i}p}(l|\check{H}_{AB}^{B'A}|r)\\
&+(l|\check{E}_{B}^{B'}(\check{\mathbb{1}}-\check{E})^{\mathsf{P}}\check{H}_{AA}^{AA}|r)+(l|\check{H}_{AA}^{AA}(\check{\mathbb{1}}-\check{E})^{\mathsf{P}}\check{E}_{B}^{B'}|r)\\
&+\mathrm{e}^{+\mathrm{i}p}(l|\check{E}_{B}^{A}(\check{\mathbb{1}}-\mathrm{e}^{+\mathrm{i}p}\check{E})^{\mathsf{P}}\check{E}_{A}^{B'}(\check{\mathbb{1}}-\check{E})^{\mathsf{P}}\check{H}_{AA}^{AA}|r)\\
&+\mathrm{e}^{-\mathrm{i}p}(l|\check{E}_{A}^{B'}(\check{\mathbb{1}}-\mathrm{e}^{-\mathrm{i}p}\check{E})^{\mathsf{P}}\check{E}_{B}^{A}(\check{\mathbb{1}}-\check{E})^{\mathsf{P}}\check{H}_{AA}^{AA}|r)\\
&+\mathrm{e}^{+\mathrm{i}p}(l|\check{H}_{AA}^{AA}(\check{\mathbb{1}}-\check{E})^{\mathsf{P}}\check{E}_{B}^{A}(\check{\mathbb{1}}-\mathrm{e}^{+\mathrm{i}p}\check{E})^{\mathsf{P}}\check{E}_{A}^{B'}|r)\\
&+\mathrm{e}^{-\mathrm{i}p}(l|\check{H}_{AA}^{AA}(\check{\mathbb{1}}-\check{E})^{\mathsf{P}}\check{E}_{A}^{B'}(\check{\mathbb{1}}-\mathrm{e}^{-\mathrm{i}p}\check{E})^{\mathsf{P}}\check{E}_{B}^{A}|r)\\
&+\mathrm{e}^{+\mathrm{i}p}(l|\check{E}_{B}^{A}(\check{\mathbb{1}}-\mathrm{e}^{+\mathrm{i}p}\check{E})^{\mathsf{P}}\check{H}_{AA}^{B'A}|r)+\mathrm{e}^{-\mathrm{i}p}(l|\check{E}_{A}^{B'}(\check{\mathbb{1}}-\mathrm{e}^{-\mathrm{i}p}\check{E})^{\mathsf{P}}\check{H}_{BA}^{AA}|r)\\
&+\mathrm{e}^{+2\mathrm{i}p}(l|\check{E}_{B}^{A}(\check{\mathbb{1}}-\mathrm{e}^{+\mathrm{i}p}\check{E})^{\mathsf{P}}\check{H}_{AA}^{AB'}|r)+\mathrm{e}^{-2\mathrm{i}p}(l|\check{E}_{A}^{B'}(\check{\mathbb{1}}-\mathrm{e}^{-\mathrm{i}p}\check{E})^{\mathsf{P}}\check{H}_{AB}^{AA}|r)\\
&+\mathrm{e}^{+\mathrm{i}p}(l|\check{H}_{AB}^{AA}(\check{\mathbb{1}}-\mathrm{e}^{+\mathrm{i}p}\check{E})^{\mathsf{P}}\check{E}_{A}^{B'}|r)+\mathrm{e}^{-\mathrm{i}p}(l|\check{H}_{AA}^{AB'}(\check{\mathbb{1}}-\mathrm{e}^{-\mathrm{i}p}\check{E})^{\mathsf{P}}\check{E}_{B}^{A}|r)\\
&+\mathrm{e}^{+2\mathrm{i}p}(l|\check{H}_{BA}^{AA}(\check{\mathbb{1}}-\mathrm{e}^{+\mathrm{i}p}\check{E})^{\mathsf{P}}\check{E}_{A}^{B'}|r)+\mathrm{e}^{-2\mathrm{i}p}(l|\check{H}_{AA}^{B'A}(\check{\mathbb{1}}-\mathrm{e}^{-\mathrm{i}p}\check{E})^{\mathsf{P}}\check{E}_{B}^{A}|r)\\
&+\mathrm{e}^{+3\mathrm{i}p}(l|\check{E}_{B}^{A}(\check{\mathbb{1}}-\mathrm{e}^{+\mathrm{i}p}\check{E})^{\mathsf{P}}\check{H}_{AA}^{AA}(\check{\mathbb{1}}-\mathrm{e}^{+\mathrm{i}p}\check{E})^{\mathsf{P}}\check{E}_{A}^{B'}|r)\\
&+\mathrm{e}^{-3\mathrm{i}p}(l|\check{E}_{A}^{B'}(\check{\mathbb{1}}-\mathrm{e}^{-\mathrm{i}p}\check{E})^{\mathsf{P}}\check{H}_{AA}^{AA}(\check{\mathbb{1}}-\mathrm{e}^{-\mathrm{i}p}\check{E})^{\mathsf{P}}\check{E}_{B}^{A}|r)\\
&(l|\check{E}_{B}^{A}|r)\Big[\left(2\pi\delta(p)-1-\mathrm{e}^{-\mathrm{i}p}\right)\left((l|\check{H}_{AA}^{B'A}|r)+(l|\check{E}_{A}^{B'}(\check{\mathbb{1}}-\check{E})^{\mathsf{P}}\check{H}_{AA}^{AA}|r)\right)\\
&\qquad+\left(2\pi\delta(p)-1-\mathrm{e}^{+\mathrm{i}p}\right)\left((l|\check{H}_{AA}^{AB'}|r)+(l|\check{H}_{AA}^{AA}(\check{\mathbb{1}}-\check{E})^{\mathsf{P}}\check{E}_{A}^{B'}|r)\right)\\
&\qquad-\mathrm{e}^{-\mathrm{i}2p}(l|\check{E}_{A}^{B'}(\check{\mathbb{1}}-\check{E})^{\mathsf{P}}(\check{\mathbb{1}}-\mathrm{e}^{-\mathrm{i}p}\check{E})^{\mathsf{P}}\check{H}_{AA}^{AA}|r)\\
&\qquad-\mathrm{e}^{+\mathrm{i}2p}(l|\check{H}_{AA}^{AA}(\check{\mathbb{1}}-\check{E})^{\mathsf{P}}(\check{\mathbb{1}}-\mathrm{e}^{+\mathrm{i}p}\check{E})^{\mathsf{P}}\check{E}_{A}^{B'}|r)\Big]\\
&(l|\check{E}_{A}^{B'}|r)\Big[\left(2\pi\delta(p)-1-\mathrm{e}^{+\mathrm{i}p}\right)\left((l|\check{H}_{BA}^{AA}|r)+(l|\check{E}_{B}^{A}(\check{\mathbb{1}}-\check{E})^{\mathsf{P}}\check{H}_{AA}^{AA}|r)\right)\\
&\qquad+\left(2\pi\delta(p)-1-\mathrm{e}^{-\mathrm{i}p}\right)\left((l|\check{H}_{AB}^{AA}|r)+(l|\check{H}_{AA}^{AA}(\check{\mathbb{1}}-\check{E})^{\mathsf{P}}\check{E}_{B}^{A}|r)\right)\\
&\qquad-\mathrm{e}^{+\mathrm{i}2p}(l|\check{E}_{B}^{A}(\check{\mathbb{1}}-\check{E})^{\mathsf{P}}(\check{\mathbb{1}}-\mathrm{e}^{+\mathrm{i}p}\check{E})^{\mathsf{P}}\check{H}_{AA}^{AA}|r)\\
&\qquad-\mathrm{e}^{-\mathrm{i}2p}(l|\check{H}_{AA}^{AA}(\check{\mathbb{1}}-\check{E})^{\mathsf{P}}(\check{\mathbb{1}}-\mathrm{e}^{-\mathrm{i}p}\check{E})^{\mathsf{P}}\check{E}_{B}^{A}|r)\Big]\Big\}.
\end{aligned}
\tag{3.144}
$$

As expected, because of translation invariance of $\hat{H}$, the δ normalizing factor is obtained.

For momentum zero, the additional divergences $\delta(p)$ signal the need for imposing $(l|\check{E}_B^A|r) = 0$ and $(l|\check{E}_A^{B'}|r) = 0$, which boils down to restricting to tangent vectors $|\Phi_0(B)\rangle, |\Phi_0(B')\rangle \in \mathbb{T}_{\Phi_0}^{\perp}$. For other momenta, there is no need to impose these conditions and these terms (*i.e.* the terms in the square brackets) are finite. However, thanks to the gauge freedom we can still impose this condition, and even the more general right or left gauge fixing conditions in Eq. (3.78) and (3.79) respectively. The terms in the square brackets then all disappear, together with some additional terms on the upper lines. Eq. (3.144) can thus strongly be simplified by a proper choice of the gauge fixing conditions on B.

We now define the matrix representation of the effective Hamiltonian H_{Φ_p} and the effective normalization matrix $\mathsf{N}_{\Phi}(p)$ of the Rayleigh-Ritz equations Eq. (2.4) as

$$\langle \Phi_p(\overline{B})|\Phi_{p'}(B')\rangle = 2\pi\delta(p'-p)\boldsymbol{B}^\dagger N_{\Phi_p}\boldsymbol{B'}, \tag{3.145}$$

$$\langle \Phi_p(\overline{B})|\hat{H}|\Phi_{p'}(B')\rangle = 2\pi\delta(p'-p)\boldsymbol{B}^\dagger H_{\Phi_p}\boldsymbol{B'}, \tag{3.146}$$

where $\boldsymbol{B}$, $\boldsymbol{B'}$ represent vectors containing the dD^2 entries of the tensors B and B'. If B satisfies the right gauge fixing conditions [Eq. (3.79)], then we obtain

$$\boldsymbol{B}^\dagger N_{\Phi_p}\boldsymbol{B'} = (l|\check{E}_B^{B'}|r) \tag{3.147}$$

and

$$\begin{aligned}
\boldsymbol{B}^\dagger H_{\Phi_p}\boldsymbol{B'} =& (l|\check{H}_{BA}^{B'A}|r) + (l|\check{H}_{AB}^{AB'}|r) + \mathrm{e}^{+\mathrm{i}p}(l|\check{H}_{BA}^{AB'}|r) + \mathrm{e}^{-\mathrm{i}p}(l|\check{H}_{AB}^{B'A}|r) \\
&+ (l|\check{E}_B^{B'}(\check{\mathbb{1}}-\check{E})^{\mathsf{P}}\check{H}_{AA}^{AA}|r) + (l|\check{H}_{AA}^{AA}(\check{\mathbb{1}}-\check{E})^{\mathsf{P}}\check{E}_B^{B'}|r) \\
&+ \mathrm{e}^{+\mathrm{i}p}(l|\check{E}_B^{A}(\check{\mathbb{1}}-\mathrm{e}^{+\mathrm{i}p}\check{E})^{\mathsf{P}}\check{E}_A^{B'}(\check{\mathbb{1}}-\check{E})^{\mathsf{P}}\check{H}_{AA}^{AA}|r) \\
&+ \mathrm{e}^{-\mathrm{i}p}(l|\check{E}_A^{B'}(\check{\mathbb{1}}-\mathrm{e}^{-\mathrm{i}p}\check{E})^{\mathsf{P}}\check{E}_B^{A}(\check{\mathbb{1}}-\check{E})^{\mathsf{P}}\check{H}_{AA}^{AA}|r) \\
&+ \mathrm{e}^{+\mathrm{i}p}(l|\check{E}_B^{A}(\check{\mathbb{1}}-\mathrm{e}^{+\mathrm{i}p}\check{E})^{\mathsf{P}}\check{H}_{AA}^{B'A}|r) + \mathrm{e}^{-\mathrm{i}p}(l|\check{E}_A^{B'}(\check{\mathbb{1}}-\mathrm{e}^{-\mathrm{i}p}\check{E})^{\mathsf{P}}\check{H}_{BA}^{AA}|r) \\
&+ \mathrm{e}^{+2\mathrm{i}p}(l|\check{E}_B^{A}(\check{\mathbb{1}}-\mathrm{e}^{+\mathrm{i}p}\check{E})^{\mathsf{P}}\check{H}_{AA}^{AB'}|r) + \mathrm{e}^{-2\mathrm{i}p}(l|\check{E}_A^{B'}(\check{\mathbb{1}}-\mathrm{e}^{-\mathrm{i}p}\check{E})^{\mathsf{P}}\check{H}_{AB}^{AA}|r).
\end{aligned} \tag{3.148}$$

Note that these expressions are only valid if B satisfies the right gauge fixing condition. The best way to impose this is by using the linear parameterization $B = \mathcal{B}_\Phi(x)$. By defining $N_{\Phi_p(\mathcal{B}_\Phi)} = \mathcal{B}_\Phi^\dagger N_{\Phi_p}\mathcal{B}_\Phi$ and $H_{\Phi_p(\mathcal{B}_\Phi)} = \mathcal{B}_\Phi^\dagger H_{\Phi_p}\mathcal{B}_\Phi$, where $\mathcal{B}_\Phi$ should be interpreted as a $qD^2 \times (q-1)D^2$ matrix that projects the vector $\boldsymbol{x}$ onto $\boldsymbol{B}$ according to the linear relation $B = \mathcal{B}_\Phi(x)$, we obtain $N_{\Phi_p(\mathcal{B}_\Phi)} = \mathbb{1}_{(q-1)D^2}$ and we have to solve the $(q-1)D^2$ dimensional ordinary eigenvalue problem for the Hermitean matrix $H_{\Phi_p(\mathcal{B}_\Phi)}$. This provides us with a set of estimates for excitation energies of excitations with momentum p. Repeating this process for various values of p allows us to build an approximation of the spectrum and the dispersion relation of the elementary excitations.

A complete diagonalization of $H_{\Phi_p(\mathcal{B}_\Phi)}$ has a computational cost $\mathcal{O}(D^6)$ and is only feasible for low values of D. As will become clear in the results, we are only interested in the lowest eigenvalues of $H_{\Phi_p(\mathcal{B}_\Phi)}$, which correspond to elementary excitations. We can then try to apply an iterative eigensolver, which is of course only useful if we can implement $H_{\Phi_p(\mathcal{B}_\Phi)}\boldsymbol{x}$ efficiently (preferably with computational cost $\mathcal{O}(D^3)$). It was already explained in Subsection 2.3 how to efficiently construct B from x. An efficient implementation of $H_{\Phi_p}\boldsymbol{B}$ is a bit more complicated but also possible. Note that we need to iteratively determine l, r and the action of the $D^2 \times D^2$ operators $(\check{\mathbb{1}} - \check{E})^{\mathsf{P}}$ and $(\check{\mathbb{1}} - \mathrm{e}^{\pm \mathrm{i}p}\check{E})^{\mathsf{P}}$ on a D^2-dimensional vector. An algorithm for efficiently determining the pseudo-inverse $(\check{\mathbb{1}} - \check{E})^{\mathsf{P}}$ was also sketched in Subsection 2.3 and is equally applicable to $(\check{\mathbb{1}} - \mathrm{e}^{\pm \mathrm{i}p}\check{E})^{\mathsf{P}}$.

3.3. Topologically non-trivial states

In a system with symmetry breaking —necessarily discrete symmetry in one-dimensional systems— it is also possible to have topologically non-trivial states. Let $|\Psi(A)\rangle \in \mathcal{M}_{\mathrm{uMPS}(D)}$ and $|\Psi(\tilde{A})\rangle \in \mathcal{M}_{\mathrm{uMPS}(\tilde{D})}$ represent two uniform matrix product states with bond dimensions D and $\tilde{D}$ that approximate two different instances from the ground state manifold $\mathbb{S}^{(\mathrm{g})}$ of $\hat{H}$. The restriction to pure uniform matrix product states requires that $|\Psi(A)\rangle$ and $|\Psi(\tilde{A})\rangle$ represent minimally entangled ground states $|\Psi_z\rangle$ and $|\Psi_{\tilde{z}}\rangle$, *i.e.* ground states with maximal symmetry breaking. Thus, both $\check{E}^{A}_{A}$ and $\check{E}^{\tilde{A}}_{\tilde{A}}$ have a unique eigenvalue 1, and we define the corresponding left and right eigenvectors as $(l|$, $|r)$ and $(\tilde{l}|$, $|\tilde{r})$ respectively. Symmetry breaking implies that $\rho(\check{E}^{A}_{\tilde{A}}) < 1$. All of this was explained in Subsection 1.7. As was shown there, it is always possible to choose $\tilde{A}^s = \sum_{t=1}^{q} \langle s|\hat{u}(\tilde{z})\hat{u}(z)^{-1}|t\rangle A^t$, so that $\tilde{D} = D$ and $\check{E}^{\tilde{A}}_{\tilde{A}} = \check{E}^{A}_{A}$, and thus also $\tilde{l} = l$ and $\tilde{r} = r$. We allow for the more general case as well.

An ansatz for approximating the topologically non-trivial state with momentum p that asymptotically looks like $|\Psi_z\rangle$ at $-\infty$ and like $|\Psi_{\tilde{z}}\rangle$ at $+\infty$ (*i.e.* a kink or domain wall) is given by

$$|\Xi_p(B;A;\tilde{A})\rangle = \sum_{n\in\mathbb{Z}} \mathrm{e}^{\mathrm{i}pn} \sum_{\{s_n\}=1}^{q} \boldsymbol{v}_{\mathrm{L}}^{\dagger} \left[\left(\prod_{m<n} A^{s_m} \right) B^{s_n} \left(\prod_{m'>n} \tilde{A}^{s_{m'}} \right) \right] \boldsymbol{v}_{\mathrm{R}} |\{s_n\}\rangle, \qquad (3.149)$$

with B^s a set of $D \times \tilde{D}$ matrices ($\forall s = 1,\ldots,q$). We now impose $(\boldsymbol{v}_{\mathrm{L}}^{\dagger} r \boldsymbol{v}_{\mathrm{L}})(\boldsymbol{v}_{\mathrm{R}}^{\dagger} \tilde{l} \boldsymbol{v}_{\mathrm{R}}) = 1$ so as not to be troubled by the boundary vectors when computing expectation values. In order for this state to have a finite excitation energy, we need to impose $h(\overline{A},A) = h(\overline{\tilde{A}},\tilde{A})$, so that both uniform matrix product states approximate their respective ground state equally well. As for the ansatz for topologically non-trivial excitations, the rationale behind the ansatz in Eq. (3.149) is that the kink itself is a highly localized or point-like object that is in a momentum superposition. It is not completely restricted to live on

a single site, since it can spread out along the virtual dimension, and has non-trivial support over at least $\log_q D + \log_q \tilde{D}$ sites. Creating a kink through the action of a physical operator, analogously to the Feynman-Bijl operator, was first attempted by Mandelstam [347]. He proposed to use as operator the Fourier transform of

$$\hat{O}(n) = \hat{o}_n \prod_{m>n} \hat{u}_n, \tag{3.150}$$

with $\hat{o}_n$ a completely local operator on site n and $\prod_{m>n} \hat{u}_n$ a string of operators that has the effect to transform the ground state to another ground state for $m > n$, *i.e.* in our context $\hat{u}_n = \hat{u}_n(\tilde{z})\hat{u}_n(z)^{-1}$.

The states $|\Xi_p(B;A;\tilde{A})\rangle$ share many properties with the tangent vectors $|\Phi_p(B;A)\rangle$. Using $\rho(\check{E}^A_{\tilde{A}}) < 1$ even allows for some simplifications. Firstly, $\langle\Psi(\overline{A})|\Xi_p(B;A;\tilde{A})\rangle = \langle\Psi(\overline{\tilde{A}})|\Xi_p(B;A;\tilde{A})\rangle = 0$ for all values of the momentum p, including $p = 0$. The reason is the appearance of factors $\check{E}^A_{\tilde{A}}$ in a half-infinite space. Secondly, the linear map

$$\Xi_p^{(A;\tilde{A})} : \mathbb{C}^{D\times q\times\tilde{D}} \mapsto \mathbb{H}_{\mathscr{L}} : B \mapsto |\Xi_p^{(A;\tilde{A})}(B)\rangle = |\Xi_p(B;A;\tilde{A})\rangle \tag{3.151}$$

has a non-trivial null space $\mathbb{N}_{\Xi_p}(A;\tilde{A})$. We henceforth omit the explicit notation of A and $\tilde{A}$. The map

$$\mathcal{N}_{\Xi_p}^{(A;\tilde{A})} : \mathbb{C}^{D\times\tilde{D}} \mapsto \mathbb{N}_{\Xi_p} : x \mapsto \mathcal{N}_{\Xi_p}(x) \quad \text{with} \quad \mathcal{N}_{\Xi_p}(x) = e^{-ip} x\tilde{A}^s - A^s x, \forall s = 1,\ldots,q \tag{3.152}$$

defines a set of choices $B = \mathcal{N}_{\Xi_p}(x)$ that produce $|\Xi_p(B)\rangle = 0$. It is easy to see that the null space of $\mathcal{N}_{\Xi_p}$ itself is empty $\forall p$, including $p = 0$, since $\mathcal{N}^s_{\Xi_p}(x) = 0$ $(\forall s = 1,\ldots,q)$ requires that $\check{E}^A_{\tilde{A}}|x\tilde{r}\rangle = e^{-ip}|x\tilde{r}\rangle$. But since $\rho(\check{E}^A_{\tilde{A}}) < 1$, this equation can have no solution. If we define

$$\mathbb{T}_{\Xi_p} = \{|\Xi_p(B)\rangle \mid B \in \mathbb{C}^{D\times q\times\tilde{D}}\} \tag{3.153}$$

then we obtain $\dim \mathbb{T}_{\Xi_p} = \dim \mathbb{C}^{D\times q\times\tilde{D}} - \dim \mathbb{N}_{\Xi_p} = (q-1)D\tilde{D}$, $\forall p \in [-\pi,+\pi)$. To fix the additive gauge freedom in the representation B, we can impose either of the following conditions:

- *left gauge fixing condition:*

$$(l|\check{E}^B_A = 0 \qquad \Leftrightarrow \qquad \sum_{s=1}^{q} A^{s\dagger} l B^s = 0, \tag{3.154}$$

- *right gauge fixing condition:*

$$\check{E}^{B}_{\tilde{A}}|\tilde{r}) = 0 \qquad \Leftrightarrow \qquad \sum_{s=1}^{q} B^{s}\,\tilde{r}\tilde{A}^{s\dagger} = 0. \tag{3.155}$$

Both conditions impose in total $D\tilde{D}$ equations that completely fix the gauge freedom in x. Linear parameterizations of the tensor B that automatically satisfy either the left or right gauge fixing conditions are constructed below.

Applying the time-independent variational principle to $\bigotimes_{p\in[-\pi,+\pi)} \mathbb{T}_{\Xi_p}$ also boils down to solving the Rayleigh-Ritz equations [Eq. (2.4) in the previous chapter]. We first compute the overlap $\langle \Xi_p(\overline{B})|\Xi_{p'}(B')\rangle$. Since the superoperators $\check{E}^{A}_{\tilde{A}}$ and $\check{E}^{\tilde{A}}_{A}$ that appear between B and B' have a spectral radius smaller than one, they do not need 'regularizing' and we cannot have disconnected contributions at all. There is then also no need to introduce pseudo-inverses. We simply obtain

$$\begin{aligned}\langle \Xi_p(\overline{B})|\Xi_{p'}(B')\rangle = 2\pi\delta(p'-p)\Big[&(l|\check{E}^{B'}_{B}|\tilde{r}) + (l|\check{E}^{A}_{B}(\check{\mathbb{1}} - \mathrm{e}^{+\mathrm{i}p}\check{E}^{A}_{\tilde{A}})^{-1}\check{E}^{B'}_{A}|\tilde{r}) \\ &+ (l|\check{E}^{B'}_{A}(\check{\mathbb{1}} - \mathrm{e}^{-\mathrm{i}p}\check{E}^{\tilde{A}}_{A})^{-1}\check{E}^{A}_{B}|\tilde{r})\Big].\end{aligned} \tag{3.156}$$

Similarly, all disconnected contributions that were present in $\langle \Phi_p(\overline{B})|\hat{H}|\Phi_{p'}(B')\rangle$ [terms in square brackets in Eq. (3.144)] disappear in the evaluation of $\langle \Xi_p(\overline{B})|\hat{H}|\Xi_{p'}(B')\rangle$. If we also redefine $\hat{h} \leftarrow \hat{h} - h(\overline{A},A) = \hat{h} - h(\overline{\tilde{A}},\tilde{A})$, so that the correct ground state energy is subtracted and there are no disconnected contributions from $\hat{h}$ either, we immediately obtain

$$\begin{aligned}\langle \Xi_p(\overline{B})|\hat{H}|\Xi_{p'}(B')\rangle = 2\pi\delta(p'-p)\times&\\ \Big[&(l|\check{H}^{B'\tilde{A}}_{B\tilde{A}}|\tilde{r}) + (l|\check{H}^{AB'}_{AB}|\tilde{r}) + \mathrm{e}^{+\mathrm{i}p}(l|\check{H}^{AB'}_{B\tilde{A}}|\tilde{r}) + \mathrm{e}^{-\mathrm{i}p}(l|\check{H}^{B'\tilde{A}}_{AB}|\tilde{r}) \\ &+ (l|\check{E}^{B'}_{B}(\check{\mathbb{1}} - \check{E}^{\tilde{A}}_{\tilde{A}})^{\mathsf{P}}\check{H}^{\tilde{A}\tilde{A}}_{\tilde{A}\tilde{A}}|\tilde{r}) + (l|\check{H}^{AA}_{AA}(\check{\mathbb{1}} - \check{E}^{A}_{A})^{\mathsf{P}}\check{E}^{B'}_{B}|\tilde{r}) \\ &+ \mathrm{e}^{+\mathrm{i}p}(l|\check{E}^{A}_{B}(\check{\mathbb{1}} - \mathrm{e}^{+\mathrm{i}p}\check{E}^{A}_{\tilde{A}})^{-1}\check{E}^{B'}_{\tilde{A}}(\check{\mathbb{1}} - \check{E}^{\tilde{A}}_{\tilde{A}})^{\mathsf{P}}\check{H}^{\tilde{A}\tilde{A}}_{\tilde{A}\tilde{A}}|\tilde{r}) \\ &+ \mathrm{e}^{-\mathrm{i}p}(l|\check{E}^{B'}_{A}(\check{\mathbb{1}} - \mathrm{e}^{-\mathrm{i}p}\check{E}^{\tilde{A}}_{A})^{-1}\check{E}^{\tilde{A}}_{B}(\check{\mathbb{1}} - \check{E}^{\tilde{A}}_{\tilde{A}})^{\mathsf{P}}\check{H}^{\tilde{A}\tilde{A}}_{\tilde{A}\tilde{A}}|\tilde{r}) \\ &+ \mathrm{e}^{+\mathrm{i}p}(l|\check{H}^{AA}_{AA}(\check{\mathbb{1}} - \check{E}^{A}_{A})^{\mathsf{P}}\check{E}^{A}_{B}(\check{\mathbb{1}} - \mathrm{e}^{+\mathrm{i}p}\check{E}^{A}_{\tilde{A}})^{-1}\check{E}^{B'}_{\tilde{A}}|\tilde{r}) \\ &+ \mathrm{e}^{-\mathrm{i}p}(l|\check{H}^{AA}_{AA}(\check{\mathbb{1}} - \check{E}^{A}_{A})^{\mathsf{P}}\check{E}^{B'}_{A}(\check{\mathbb{1}} - \mathrm{e}^{-\mathrm{i}p}\check{E}^{\tilde{A}}_{A})^{-1}\check{E}^{\tilde{A}}_{B}|\tilde{r}) \\ &+ \mathrm{e}^{+\mathrm{i}p}(l|\check{E}^{A}_{B}(\check{\mathbb{1}} - \mathrm{e}^{+\mathrm{i}p}\check{E}^{A}_{\tilde{A}})^{-1}\check{H}^{B'\tilde{A}}_{\tilde{A}\tilde{A}}|\tilde{r}) + \mathrm{e}^{-\mathrm{i}p}(l|\check{E}^{B'}_{A}(\check{\mathbb{1}} - \mathrm{e}^{-\mathrm{i}p}\check{E}^{\tilde{A}}_{A})^{-1}\check{H}^{\tilde{A}\tilde{A}}_{B\tilde{A}}|\tilde{r}) \\ &+ \mathrm{e}^{+2\mathrm{i}p}(l|\check{E}^{A}_{B}(\check{\mathbb{1}} - \mathrm{e}^{+\mathrm{i}p}\check{E}^{A}_{\tilde{A}})^{-1}\check{H}^{AB'}_{\tilde{A}\tilde{A}}|\tilde{r}) + \mathrm{e}^{-2\mathrm{i}p}(l|\check{E}^{B'}_{A}(\check{\mathbb{1}} - \mathrm{e}^{-\mathrm{i}p}\check{E}^{\tilde{A}}_{A})^{-1}\check{H}^{\tilde{A}\tilde{A}}_{AB}|\tilde{r}) \\ &+ \mathrm{e}^{+\mathrm{i}p}(l|\check{H}^{AA}_{AB}(\check{\mathbb{1}} - \mathrm{e}^{+\mathrm{i}p}\check{E}^{A}_{\tilde{A}})^{-1}\check{E}^{B'}_{\tilde{A}}|\tilde{r}) + \mathrm{e}^{-\mathrm{i}p}(l|\check{H}^{AB'}_{AA}(\check{\mathbb{1}} - \mathrm{e}^{-\mathrm{i}p}\check{E}^{\tilde{A}}_{A})^{-1}\check{E}^{\tilde{A}}_{B}|\tilde{r})\end{aligned}$$

$$+\mathrm{e}^{+2\mathrm{i}p}(l|\check{H}^{AA}_{B\tilde{A}}(\check{\mathbb{1}}-\mathrm{e}^{+\mathrm{i}p}\check{E}^{A}_{\tilde{A}})^{-1}\check{E}^{B'}_{\tilde{A}}|\tilde{r})+\mathrm{e}^{-2\mathrm{i}p}(l|\check{H}^{B'\tilde{A}}_{AA}(\check{\mathbb{1}}-\mathrm{e}^{-\mathrm{i}p}\check{E}^{\tilde{A}}_{A})^{-1}\check{E}^{\tilde{A}}_{B}|\tilde{r})$$
$$+\mathrm{e}^{+3\mathrm{i}p}(l|\check{E}^{A}_{B}(\check{\mathbb{1}}-\mathrm{e}^{+\mathrm{i}p}\check{E}^{A}_{\tilde{A}})^{-1}\check{H}^{A\tilde{A}}_{\tilde{A}\tilde{A}}(\check{\mathbb{1}}-\mathrm{e}^{+\mathrm{i}p}\check{E}^{A}_{\tilde{A}})^{-1}\check{E}^{B'}_{\tilde{A}}|\tilde{r})$$
$$+\mathrm{e}^{-3\mathrm{i}p}(l|\check{E}^{B'}_{A}(\check{\mathbb{1}}-\mathrm{e}^{-\mathrm{i}p}\check{E}^{\tilde{A}}_{A})^{-1}\check{H}^{\tilde{A}\tilde{A}}_{AA}(\check{\mathbb{1}}-\mathrm{e}^{-\mathrm{i}p}\check{E}^{\tilde{A}}_{A})^{-1}\check{E}^{\tilde{A}}_{B}|\tilde{r})\Big]. \tag{3.157}$$

By imposing either the left or the right gauge fixing conditions of Eq. (3.154) or (3.155), many terms in Eq. (3.156) and in Eq. (3.157) cancel. In particular, with either choice, the overlap reduces to

$$\langle\Xi_p(\overline{B})|\Xi_{p'}(B')\rangle = 2\pi\delta(p'-p)(l|\check{E}^{B'}_{B}|\tilde{r}). \tag{3.158}$$

We can then construct linear parameterizations $\mathcal{B}_\Xi(x)$ and $\widetilde{\mathcal{B}}_\Xi(y)$ in terms of a $D\times(q-1)\tilde{D}$ matrix x and a $(q-1)D\times\tilde{D}$ matrix y that respectively satisfy the right and left gauge fixing conditions and that produce

$$\langle\Xi_p(\overline{\mathcal{B}_\Xi(\overline{x})})|\Xi_{p'}(\mathcal{B}_\Xi(x'))\rangle = 2\pi\delta(p'-p)\mathrm{tr}[x^\dagger x'],$$
$$\langle\Xi_p(\overline{\widetilde{\mathcal{B}}_\Xi(\overline{y})})|\Xi_{p'}(\widetilde{\mathcal{B}}_\Xi(y'))\rangle = 2\pi\delta(p'-p)\mathrm{tr}[y^\dagger y'].$$

We first define the $d\tilde{D}\times\tilde{D}$ matrices $\tilde{R}$ as

$$[\tilde{R}]_{(\alpha,s);\beta} = [\tilde{r}^{1/2}\tilde{A}^{s\dagger}]_{\alpha,\beta} \tag{3.159}$$

and then construct a $(q-1)\tilde{D}\times q\tilde{D}$ matrix $\tilde{V}_{\tilde{R}}$ so that $\tilde{V}^\dagger_{\tilde{R}}$ contains an orthonormal basis for the null space of $\tilde{R}^\dagger$, *i.e.* $\tilde{R}_{\tilde{R}}\tilde{R}=0$ and $\tilde{V}_{\tilde{R}}\tilde{V}^\dagger_{\tilde{R}}=\mathbb{1}_{(q-1)D}$. Setting $[\tilde{V}^s_{\tilde{R}}]_{\alpha,\beta}=[\tilde{V}_{\tilde{R}}]_{\alpha;(\beta,s)}$, we then define the representation $\mathcal{B}_\Xi(x)$ as

$$\mathcal{B}^s_\Xi(x) = l^{-1/2}x\tilde{V}^s_{\tilde{R}}\tilde{r}^{-1/2}. \tag{3.160}$$

The representation $\widetilde{\mathcal{B}}^s_\Xi(y)$ follows similarly from a definition of L and V_L (based on the matrix A).

We can now also define an effective Hamiltonian H_{Ξ_p} and effective normalization matrix N_{Ξ_p} for use in the Rayleigh-Ritz equation Eq. (2.4) as

$$\langle\Xi_p(\overline{B})|\Xi_{p'}(B')\rangle = 2\pi\delta(p'-p)\boldsymbol{B}^\dagger N_{\Xi_p}\boldsymbol{B'}, \tag{3.161}$$
$$\langle\Xi_p(\overline{B})|\hat{H}|\Xi_{p'}(B')\rangle = 2\pi\delta(p'-p)\boldsymbol{B}^\dagger H_{\Xi_p}\boldsymbol{B'}, \tag{3.162}$$

and then induce a second pair of matrices using the representation $\mathcal{B}_\Xi$ as $N_{\Xi_p(\mathcal{B}_\Xi)}=\boldsymbol{\mathcal{B}}^\dagger_\Xi N_{\Xi_p}\boldsymbol{\mathcal{B}}_\Xi=\mathbb{1}_{(q-1)D\tilde{D}}$ and $H_{\Xi_p(\mathcal{B}_\Xi)}=\boldsymbol{\mathcal{B}}^\dagger_\Xi H_{\Xi_p}\boldsymbol{\mathcal{B}}_\Xi$. Applying the Rayleigh-Ritz method to $\mathbb{T}_{\Xi_p}$ thus boils down to diagonalizing $H_{\Xi_p(\mathcal{B}_\Xi)}$. For large D, an iterative implementation with computational complexity $\mathcal{O}(D^3)$ can be constructed.

One final remark is in order. With two matrices A and $\tilde{A}$ present in the ansatz for topologically non-trivial states $|\Xi_p(B;A;\tilde{A})\rangle$, both of which can be defined independently from each other, there is some ambiguity present in the definition of the momentum. Suppose we have $A' = e^{i\varphi}A$. We obtain $|\Xi_p(B;A';\tilde{A})\rangle = |\Xi_p(B;e^{i\varphi}A;\tilde{A})\rangle \sim |\Xi_{p+\varphi}(B;A;\tilde{A})\rangle$, where the similarity sign means the two states are equal up to a global phase. This follows simply from inserting A' in *e.g.* Eq. (3.157). It is ultimately related to the fact that momentum is not a good quantum number to start with in a system with open boundary conditions. This problem did not occur in the ansatz for topologically trivial excitations, because $|\Psi_p(B)\rangle$ can be defined starting from a finite lattice with periodic boundary conditions, where p is a good quantum number. But for the kink states, this is not possible. Since the momentum seems tightly connected to $\check{E}^{A}_{\tilde{A}}$ in the sense that they appear together as $e^{ip}\check{E}^{A}_{\tilde{A}}$ in Eq. (3.157), it makes sense to require that the relative phase of A and $\tilde{A}$ is chosen so that the eigenvalue with largest modulus of $\check{E}^{A}_{\tilde{A}}$ is positive. This convention is adhered to in the remainder of this section.

3.4. Relation to the time-dependent variational principle

The relation between using the tangent plane of a variational manifold as variational ansatz for excitations and a linearization of the flow equations of the time-dependent variational principle around a variational optimum were discussed in full generality in Section 3 of the previous chapter. It was shown there that a linearization of the flow equations produces a generalized eigenvalue equation of twice the size, which corresponds to the Rayleigh-Ritz method for the tangent plane in the diagonal blocks. In the off-diagonal blocks a new matrix arises which contains the projection of the exact evolution vector $\hat{P}_0\hat{H}|\Psi\rangle$ onto the double tangent plane. So let us first introduce the double tangent plane $\mathbb{T}^{(2)}_{\mathrm{MPS}(D)}$ and its properties in general terms. We thereto define the family of states

$$
\begin{aligned}
|\Upsilon^{[A]}[B_+,B_-]\rangle = |\Upsilon[B_+,B_-;A]\rangle &= \sum_{m,n\in\mathbb{Z}} B^i_+(m)B^j_-(n)\frac{\partial^2}{\partial A^i(m)\partial A^j(n)}|\Psi[A]\rangle \\
&= \sum_{m<n\in\mathbb{Z}}\sum_{\{s_n\}=1}^{q} \boldsymbol{v}_{\mathrm{L}}^\dagger\Bigg[\Bigg(\prod_{k<m}A^{s_k}(k)\Bigg)B^{s_m}_+(m)\Bigg(\prod_{m<k'<n}A^{s_{k'}}(k')\Bigg) \\
&\qquad\qquad \times B^{s_n}_-(n)\Bigg(\prod_{n<k''}A^{s_{k''}}(k'')\Bigg)\Bigg]\boldsymbol{v}_{\mathrm{R}}|\{s_n\}\rangle \\
&\quad + \sum_{m>n\in\mathbb{Z}}\sum_{\{s_n\}=1}^{q} \boldsymbol{v}_{\mathrm{L}}^\dagger\Bigg[\Bigg(\prod_{k<w}A^{s_k}(k)\Bigg)B^{s_n}_-(n)\Bigg(\prod_{n<k'<m}A^{s_{k'}}(k')\Bigg) \\
&\qquad\qquad \times B^{s_m}_+(m)\Bigg(\prod_{n<k''}A^{s_{k''}}(k'')\Bigg)\Bigg]\boldsymbol{v}_{\mathrm{R}}|\{s_n\}\rangle,
\end{aligned}
$$

with i and j denoting collective indices of size D^2q. These states span the tangent plane $\mathbb{T}^{(2)}_{\text{MPS}(D)}$, but not all states in $\mathbb{T}^{(2)}_{\text{MPS}(D)}$ can be written in this format. Whereas a general state in $\mathbb{T}^{(2)}_{\text{MPS}(D)}$ would have a coefficient matrix $C^{i,j}(m,n)$ with respect to $\partial^2|\Psi[A]\rangle/\partial A^i(m)\partial A^j(n)$, the state $|\Upsilon^{(A)}[B_+,B_-]\rangle$ corresponds to the factorized case $C^{i,j}(m,n)=B^i_+(m)B^j_-(n)$: they are the product states of $\mathbb{T}^{(2)}_{\text{MPS}(D)}$. Note that $\mathbb{T}^{(2)}_{\text{MPS}(D)}$ contains $\mathbb{T}_{\text{MPS}(D)}$, since $|\Upsilon[B,A;A]\rangle=(|\mathbb{Z}|-1)|\Phi[B;A]\rangle$. From an intuitive perspective, the states $|\Upsilon^{(A)}[B_+,B_-]\rangle$ seem to be describing compound states containing two elementary excitations. Note that for the general states the coefficient matrix satisfies $C^{i,j}(m,n)=C^{j,i}(n,m)$, indicating that these excitations behave naively as bosons, due to the commutativity of $\partial/\partial A^i(m)$ and $\partial/\partial A^j(n)$. Grassmann numbers would be required to have a natural scheme for studying fermionic systems, which has also been the key for applying general tensor networks to fermionic systems in higher dimensions [348, 349, 350]. For translation invariant systems with a translation invariant ground state (approximated by $|\Psi(A)\rangle\in\mathscr{M}_{\text{uMPS}(D)}$), we can introduce the momentum modes $B^s_+(m)=B^s_+\mathrm{e}^{\mathrm{i}p_+m}$ and $B^s_-(n)=B^s_-(m)\mathrm{e}^{\mathrm{i}p_-n}$, and define

$$\begin{aligned}
|\Upsilon^{(A)}_{p_+,p_-}(B_+,B_-)\rangle &= |\Upsilon_{p_+,p_-}(B_+,B_-;A)\rangle \\
&= \sum_{m<n\in\mathbb{Z}} \mathrm{e}^{\mathrm{i}(p_+m+p_-n)} \sum_{\{s_n\}=1}^{q} \boldsymbol{v}_{\mathrm{L}}^\dagger \Bigg[\Bigg(\prod_{k<m} A^{s_k}\Bigg) B^{s_m}_+ \Bigg(\prod_{m<k'<n} A^{s_{k'}}\Bigg) \\
&\qquad\qquad \times B^{s_n}_- \Bigg(\prod_{n<k''} A^{s_{k''}}\Bigg)\Bigg] \boldsymbol{v}_{\mathrm{R}}|\{s_n\}\rangle \\
&+ \sum_{m>n\in\mathbb{Z}} \mathrm{e}^{\mathrm{i}(p_+m+p_-n)} \sum_{\{s_n\}=1}^{q} \boldsymbol{v}_{\mathrm{L}}^\dagger \Bigg[\Bigg(\prod_{k<w} A^{s_k}\Bigg) B^{s_n}_- \Bigg(\prod_{n<k'<m} A^{s_{k'}}\Bigg) \\
&\qquad\qquad \times B^{s_m}_+ \Bigg(\prod_{n<k''} A^{s_{k''}}\Bigg)\Bigg] \boldsymbol{v}_{\mathrm{R}}|\{s_n\}\rangle .
\end{aligned} \tag{3.163}$$

The total momentum of this state is $p=p_++p_-$. A general state in the momentum p sector of the double tangent plane $\mathbb{T}^{(2)}_{\text{MPS}(D)}$ has $C^{i,j}(m,n)=\mathrm{e}^{\mathrm{i}p(m+n)/2}C^{i,j}(m-n)$.

In the current translation invariant setting, the linearized flow equation Eq. (2.59) also decomposes into different diagonal blocks in the different momentum sectors. We can repeat the analysis of Section 3 of the previous chapter for a state $|\Psi[A(t)]\rangle\in\mathscr{M}_{\text{MPS}(D)}$ by expanding $A(t)$ around the uniform solution A that best approximates the ground state as $A^s(n;t)=A^s+B^s_1(n;t)$, where $B^s_1(n;t)=B^s_+(n)\mathrm{e}^{-\mathrm{i}\omega t}+B^s_-(n)\mathrm{e}^{+\mathrm{i}\omega t}$. By using $\langle\Psi(A)|\Psi(A)\rangle=1$ and defining the momentum modes $(B^{(p)}_+)^s(n)=B^s_+\mathrm{e}^{+\mathrm{i}pn}$ and $(B^{(p)}_-)^s(n)=B^s_-\mathrm{e}^{-\mathrm{i}pn}$, we can decompose the matrices $H^\star$, $N^\star$ and $M^\star$ defined in Eq. (2.58) as

$$\tilde{\boldsymbol{B}}^{(\tilde{p})\,\dagger}_+ N^\star \boldsymbol{B}^{(p)}_+ = \langle\Phi_{\tilde{p}}(\overline{\tilde{B}_+};\overline{A})|\Phi_p(B_+;A)\rangle$$

$$= 2\pi\delta(p-\tilde{p})\,\tilde{\boldsymbol{B}}_+^{\dagger} N_{\Phi_p} \boldsymbol{B}_+, \tag{3.164a}$$

$$\tilde{\boldsymbol{B}}_+^{(\tilde{p})\dagger} H^* \boldsymbol{B}_+^{(p)} = \langle \Phi_{\tilde{p}}(\overline{\tilde{B}_+};\overline{A}) | \hat{H} - H(\overline{A},A) | \Phi_p(B_+;A)\rangle$$
$$= 2\pi\delta(p-\tilde{p})\,\tilde{\boldsymbol{B}}_+^{\dagger} H_{\Phi_p} \boldsymbol{B}_+, \tag{3.164b}$$

$$\tilde{\boldsymbol{B}}_+^{(\tilde{p})\dagger} M^* \overline{\boldsymbol{B}_-^{(p)}} = \langle \Upsilon_{\tilde{p},-p}(\overline{B_+},\overline{B_-};\overline{A}) | \hat{P}_0(\overline{A},A)\hat{H} | \Psi(A)\rangle$$
$$= 2\pi\delta(p-\tilde{p})\,\tilde{\boldsymbol{B}}_+^{\dagger} M_{\Upsilon_{p,-p}} \overline{\boldsymbol{B}_-}, \tag{3.164c}$$

where we recover the matrices H_{Φ_p} and N_{Φ_p} defined in Subsection 3.2 and a new matrix M_{Υ_p} has been defined, whose existence follows from translation invariance. Note that $\boldsymbol{B}_\pm^{(p)}$ represents a $|\mathbb{Z}|qD^2$-dimensional vector containing the qD^2 entries of every tensor $B_\pm^{(p)}(n)$ on every site $n \in \mathbb{Z}$, whereas $\boldsymbol{B}_\pm$ represents a qD^2-dimensional vector containing the qD^2 entries in the constant tensor $B_\pm$. The linearized flow equations of the time-dependent variational principle can thus be grouped in blocks of momentum p as

$$\begin{bmatrix} H_{\Phi_p} & M_{\Upsilon_{p,-p}} \\ \overline{M_{\Upsilon_{-p,p}}} & \overline{H_{\Phi_p}} \end{bmatrix} \begin{bmatrix} \boldsymbol{B}_+ \\ \overline{\boldsymbol{B}_-} \end{bmatrix} = \omega \begin{bmatrix} N_{\Phi_p} & 0 \\ 0 & -\overline{N_{\Phi_p}} \end{bmatrix} \begin{bmatrix} \boldsymbol{B}_+ \\ \overline{\boldsymbol{B}_-} \end{bmatrix}, \tag{3.165}$$

with $M_{\Upsilon_{-p,p}} = M_{\Upsilon_{p,-p}}^{\mathsf{T}}$. The matrix $M_{\Upsilon_{p,-p}}$ has a similar structure as H_{Φ_p} and its action on a vector $\boldsymbol{B}_+$ can also be efficiently implemented. We refer to Section 1 of Appendix A for an explicit construction. We now discuss some details —specific to the matrix product state framework— about the relation between the linearized flow equations of the time-dependent variational principle and our ansatz for studying excited states.

We first restrict to the case of topologically trivial excitations $|\Phi_p(B;A)\rangle$. Since $|\Psi(A)\rangle$ is considered to be a variational minimum in $\mathcal{M}_{\text{uMPS}(D)}$, the effective Hamiltonian H_{Φ_0} is positive semidefinite, as it appears as a diagonal block in the Hessian of the energy function $H(\overline{A},A)$. The excitation energies we obtain from applying the Rayleigh-Ritz method to $\mathbb{T}_{\text{uMPS}(D)} = \mathbb{T}_{\Phi_0}$ are all positive or zero. While this of course corresponds to our physical expectation, it is in fact a non-trivial observation. The excitation energies follow from subtracting from the eigenvalues of the Hamiltonian $\hat{H}$ the divergent ground state energy E_0. Even though the variational principle guarantees that we always obtain an upper bound for the eigenvalues of $\hat{H}$, this is not applicable to the excitation energies since we have subtracted an estimate of the ground state energy $H(\overline{A},A)$ which might be too large (since $H(\overline{A},A) \geq E_0$, also according to the variational principle). Put differently, the excitation energies are energy differences and the variational principle is not applicable to energy differences. Errors on the excitation energies can thus be both positive and negative. But the relation with the time-dependent variational principle guarantees that we cannot obtain unphysical (*i.e.* negative) excitation energies.

By restricting to $\mathcal{M}_{\text{uMPS}(D)}$, positive semidefineteness of H_{Φ_p} can only be proven for $p = 0$. If the uMPS $|\Psi(A)\rangle$ is also a minimum in the complete manifold $\mathcal{M}_{\text{MPS}(D)}$, translation

non-invariant states included, then positive semidefineteness of H_{Φ_p} follows for every $p \in [-\pi, +\pi)$. This requires that there is no translation-invariance breaking matrix product state $|\Psi[A']\rangle$ that can produce a lower energy expectation value $H[\overline{A}', A'] < H(\overline{A}, A)$. Vice versa, if at a certain value of the parameters in the Hamiltonian, a branch of the excitation spectrum becomes negative around some momentum p, then this might be an indication for a tendency towards breaking of translation invariance. When the matrix product state approximation is good, this can be the signal for a physical phase transition where some elementary excitation of the spectrum develops a negative energy around some momentum and condenses, thereby producing a state with broken translation invariance. An example is studied in the next subsection.

The ansatz for topologically non-trivial excitations bears no immediate relationship to the tangent plane $\mathbb{T}_{\text{MPS}(D)}$. $\mathbb{T}_{\Xi_p}$ can however be interpreted as a subspace of $\mathbb{T}_{\text{MPS}(D')}$ at the uniform matrix product state $|\Psi'(A')\rangle \in \mathcal{M}_{\text{MPS}(D')}$ with $D' = D + \tilde{D}$ and $(A')^s = A^s \oplus \tilde{A}^s$. Indeed, $|\Xi_p(B)\rangle = |\Phi'_p(B')\rangle$ with[6]

$$(B')^s = \begin{bmatrix} 0 & B^s \\ 0 & 0 \end{bmatrix}. \tag{3.166}$$

While it is easy to prove that $|\Psi'(A')\rangle$ is a stationary point of the energy functional on $\mathcal{M}_{\text{MPS}(D')}$, there is no guarantee that it should be a minimum. In particular, close to the symmetry breaking phase transition, it is very likely that the energy could benefit from mixing domain walls into the ground state, so as to lower the expectation value of the order parameter and restore the symmetry. Far away from the phase transition, $|\Psi'(A')\rangle$ will definitely not be the global minimum, since it does not represent a minimally entangled ground state, but rather a superposition of the two ground states $|\Psi_q\rangle$ and $|\Psi_{\tilde{q}}\rangle$. There will be a better minimum where the complete $(D + \tilde{D})$-dimensional ancilla space is used to encode a single minimally entangled ground state. Nevertheless, $|\Psi(A')\rangle$ can be a local minimum of the energy functional and all topologically non-trivial excitation energies can be positive.

Finally we evaluate the added value of the off-diagonal blocks M_{Υ_p} in the linearized TDVP equation Eq. (3.165). If the uniform matrix product state approximation of the ground state is good (*i.e.* $\tilde{\epsilon}(\overline{A}, A) \ll 1$), we do not expect the states $|\Upsilon^{(A)}_{p_+,p_-}(B_+, B_-)\rangle$ to contribute much to the elementary excitations, since they naturally look like two-particle states and since $||M_{\Upsilon_p}|| \sim ||\hat{P}_0(\overline{A}, A)\hat{H}\,|\Psi(A)\rangle|||\mathbb{Z}|^{-1/2} = \tilde{\epsilon}(\overline{A}, A)$. If $|\Phi^{(A)}_p(B)\rangle$ also approximates a multi-particle state, then the correction of M_{Υ_p} might be significant. But for studying *e.g.* two-particle states, it should be much better to apply the Rayleigh-Ritz method to the complete double tangent plane $\mathbb{T}^{(2)}_{\text{MPS}(D)}$ anyway. The linearized flow equations of the time-dependent variational principle in Eq. (3.165) can however

[6] This correspondence is also key in proving that $\mathcal{N}_{\Xi_p}(x)$ spans the complete null space $\mathbb{N}_{\Xi_p}$, by using infinitesimal gauge transformations of $|\Psi'(A')\rangle$.

be useful to detect which pairs of excitations set the approximate ground state $|\psi(A)\rangle$ apart from the exact ground state. These claims are verified for a test model in the next subsection by solving the generalized eigenvalue equation of Eq. (3.165). Let us therefore study the properties of $\tilde{\boldsymbol{B}}_+^\dagger M_{\Upsilon_p} \overline{\boldsymbol{B}_-} \sim \langle \Upsilon^{(A)}_{p_+,p_-}(\overline{B_+},\overline{B_-})|\hat{P}_0(\overline{A},A)\hat{H}|\Psi(A)\rangle$ with $p_+ = p = -p_-$. Since B_+ and B_- arise as infinitesimal variations of A, we should be able to apply the same set of additive gauge transformations $\mathcal{N}_{\Phi_{p_\pm}}(x_\pm)$ [see Eq. (3.76)] on $B_\pm$. We obtain $|\Upsilon^{(A)}_{p_+,p_-}(B_+ + \mathcal{N}_{\Phi_{p_+}}(x_+), B_-)\rangle = |\Upsilon^{(A)}_{p_+,p_-}(B_+,B_-)\rangle + |\Phi^{(A)}_{p_+ + p_-}(B)\rangle$, with $B^s = -\mathrm{e}^{-\mathrm{i}p_+}x_+B^s_- + B^s_- x_+$. The state $|\Upsilon^{(A)}_{p_+,p_-}(B_+,B_-)\rangle$ is thus not invariant under the additive gauge transformations $\mathcal{N}_{\Phi_{p_\pm}}(x_\pm)$; the effect of such a gauge transformation is to add a contribution in $\mathbb{T}_{\mathrm{MPS}(D)}$. However, the matrix $M^\star$ is invariant, since it projects $|\Upsilon^{(A)}_{p_+,p_-}(B_+,B_-)\rangle$ onto $\hat{P}_0(\overline{A},A)\hat{H}\,|\Psi(A)\rangle$, where $\hat{P}_0(\overline{A},A)\hat{H}\,|\Psi(A)\rangle \perp \mathbb{T}_{\mathrm{MPS}(D)}$ in the variational optimum. We thus find $\langle \Upsilon^{(A)}_{p_+,p_-}(\mathcal{N}_{\Phi_{p_+}}(x_+),\overline{B_-})|\hat{P}_0(\overline{A},A)\hat{H}|\Psi(A)\rangle = 0$. Similarly, we can eliminate the direction $B_\pm \sim A$ and restrict to values of $B_\pm$ that produce tangent vectors $|\Phi_{p_\pm}(B_\pm)\rangle \in \mathbb{T}^\perp_{\mathrm{uMPS}(D)}$ for $p_\pm = 0$. While $|\Upsilon^{(A)}_{0,p_-}(A,B_-)\rangle \neq 0$, we do obtain $|\Upsilon^{(A)}_{0,p_-}(A,B_-)\rangle \sim |\Phi^{(A)}_{p_-}(B_-)\rangle \in \mathbb{T}_{\mathrm{MPS}(D)}$, so that $\langle \Upsilon^{(A)}_{p_+,p_-}(\overline{B_+},\overline{B_-})|\hat{P}_0(\overline{A},A)\hat{H}|\Psi(A)\rangle = 0$ and does not contribute. We can thus still impose the left or right gauge fixing conditions Eq. (3.78) and Eq. (3.79) on B_+ and B_-, and reuse all the techniques from the previous subsection for the (efficient) evaluation of M_{Υ_p}, which can be calculated similarly to H_{Φ_p}.

3.5. Exemplary results

We now test our variational ansatz for topologically trivial and topologically non-trivial excitations both qualitatively and quantitatively by studying some spin models.

Transverse quantum Ising model

The Hamiltonian of the transverse quantum Ising model is given by

$$\hat{H}_{\mathrm{Ising}} = \sum_{n\in\mathbb{Z}} -J\hat{\sigma}^x_n\hat{\sigma}^x_{n+1} + h\hat{\sigma}^z_n, \tag{3.167}$$

with $J > 0$ and h a magnetic field alignment term. It is invariant under the global rotation $\hat{U} = \bigotimes_{n\in\mathbb{Z}} \hat{u}_n$ with $\hat{u}_n = \exp(\mathrm{i}\frac{\pi}{2}\hat{\sigma}^z_n) = \hat{\sigma}^z_n$, which is a discrete symmetry that maps $\hat{\sigma}^x_n \leftrightarrow -\hat{\sigma}^x_n$. The transverse quantum Ising model can be solved exactly, since the Jordan-Wigner transformation [351] maps it to a quadratic fermion model that can be solved using a Bogoliubov transformation [352]. The elementary fermion excitation has a dispersion relation

$$\omega(p) = 2\sqrt{[J\cos(p) - h]^2 + J^2\sin^2(p)} = 2J\sqrt{1 + h^2/J^2 - 2h/J\cos p}. \tag{3.168}$$

The model has critical points at $h/J = \pm 1$ and the dispersion relation develops a node. For $|h/J| < 1$ it has symmetry-breaking order and develops a non-zero expectation value of the local order parameter $\hat{O}_n = \hat{\sigma}_n^x$, whereas $\langle\Psi|\hat{\sigma}_n^z|\Psi\rangle = 0$. The elementary fermion excitation then maps to a topologically non-trivial excitation of the spin model: when the elementary fermion excitation is mapped back to a spin excitation, the Jordan-Wigner string $\prod_{m<n} \sigma_m^z$ that appears in front of the creation operator maps one ground state to another. For $|h/J| > 1$ the magnetic field term dominates and aligns the spins, so that $\langle\Psi|\hat{\sigma}_n^z|\Psi\rangle \neq 0$ and the expectation value of the order parameter is given by $\langle\Psi|\hat{\sigma}_n^x|\Psi\rangle = 0$. This is a symmetric phase, and the elementary fermion excitation is topologically trivial in terms of the original spin model.

Excitation eigenvalues Δ obtained from an exact diagonalization of $H_{\Phi_p(\mathcal{B}_\Phi)}$ and $H_{\Xi_p(\mathcal{B}_\Xi)}$ are shown in Fig. 3.6 and Fig. 3.7 for respectively $h/J = 2$ and $h/J = 1/2$ at $D = \tilde{D} = 8$. Exact diagonalization is feasible up to $D = 48$, but becomes costly for values of D that are much larger. However, already at $D = 8$ the qualitative features of the spectrum are well reproduced. The lowest branch matches the exact result both for the topologically trivial and topologically non-trivial case. Inside the continuous bands of multi-particle excitations, a discrete set of eigenvalues is obtained. Our finite-dimensional eigenvalue equation can of course not produce a continuous distribution of eigenvalues, and was never meant to do so. We only argued the adequacy of our ansatz for the case of elementary excitations. For *e.g.* the band of two-particle excitations, a different ansatz such as $|\Upsilon^{(A)}_{p_1,p_2}(B_1,B_2)\rangle$ should be used. A continuum would then automatically arise from the continuous distribution of relative momentum $\Delta p = p_2 - p_1$ for every value of the total momentum $p = (p_1 + p_2)$. When both particles have fixed momentum p_1 and p_2, they are on average infinitely far apart. The states $|\Phi_p^{(A)}(B)\rangle$ seem to be able to describe some two-particle states with total momentum p, where a superposition over states with fixed relative momentum Δp is taken so as to be able to confine the particles in a region of approximate size $2\log_q D$. The lowest eigenvalue produced with $|\Phi_p^{(A)}(B)\rangle$ in the two-particle band is thus expected to have a finite size energy correction of $\mathcal{O}(1/\log_q D)$ above the minimum of the band.

Also note the identical form of Fig. 3.6 and Fig. 3.7, which is caused by an exact duality of the Ising model to itself, whereby h/J is mapped to J/h and the elementary topologically non-trivial excitation is mapped onto the topologically trivial excitation and vice versa [353]. This observation is of course very specific to this model. It can even be noticed that the higher order excitations do not exactly reproduce this duality.

We could also assess the accuracy of our approach, but we would first like to establish that our approach also works for more complicated models. In the Ising model, both in the symmetric as in the symmetry broken case, the elementary excitations can be created using Feynman-Bijl or Mandelstam operators with one-site local operators $\hat{O}_n$ (namely the creation operators obtained after solving the quadratic fermion model using the Bogoliubov transformation). Any errors in the excitation energies are thus due to errors in the ground state approximation.

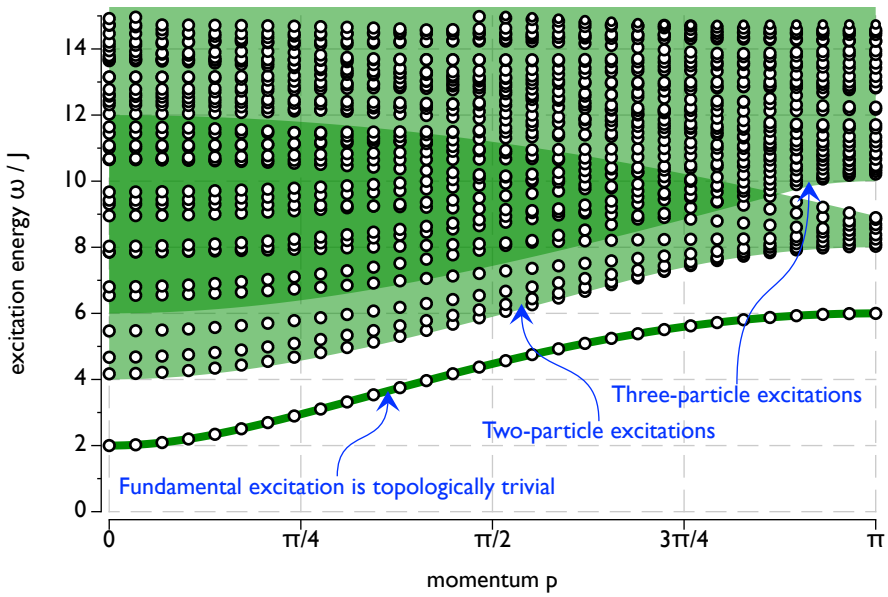

Figure 3.6: Spectrum of topologically trivial excitations (white circles) for the transverse quantum Ising model with $h/J = 2$, obtained with the variational ansatz $|\Phi_p^{(A)}(B)\rangle$ with bond dimension $D = 8$. The exact branch of the elementary excitation (green line), as well as the exact two-particle and three-particle continuum (green bands) are also shown.

$S = 1$ Bilinear-biquadratic antiferromagnetic Heisenberg model

A more complicated model that nicely illustrates many of the statements from the previous subsection is the bilinear-biquadratic antiferromagnetic Heisenberg model with $S = 1$ spins, which is described by the SU(2)-invariant Hamiltonian

$$\hat{H}_{\text{BB Heisenberg}} = J \sum_{n\in\mathbb{Z}} \cos\theta \left(\hat{\boldsymbol{S}}_n \cdot \hat{\boldsymbol{S}}_{n+1}\right) + \sin\theta \left(\hat{\boldsymbol{S}}_n \cdot \hat{\boldsymbol{S}}_{n+1}\right)^2, \tag{3.169}$$

with an energy scale $J > 0$ and an angle $\theta \in [-3\pi/4, 5\pi/4)$. This model has many interesting phases and phase transitions as a function of θ. There cannot be antiferromagnetic order due to Coleman's theorem [see Subsection 1.4 of Chapter 1]. Ferromagnetic order can exist, since the ferromagnetic order parameter commutes with the Hamiltonian, and is indeed present for $\theta \in (\pi/2, 5\pi/4)$. At $\theta = 0$, this Hamiltonian describes the antiferromagnetic Heisenberg model whose ground state was studied in the previous section [see Eq. (3.137) in Subsection 2.7]. The ground state is then in a topologically ordered phase, the Haldane phase, and the lowest lying excitation is an $S = 1$ triplet with finite mass Δ_{Haldane}, referred to as the Haldane gap [335, 336]. The same phase exists throughout $\theta \in (-\pi/4, \pi/4)$. In particular, for $\tan\theta = 1/3$ this is the model studied by Affleck, Kennedy, Lieb and Tasaki, which has an exact matrix product state representa-

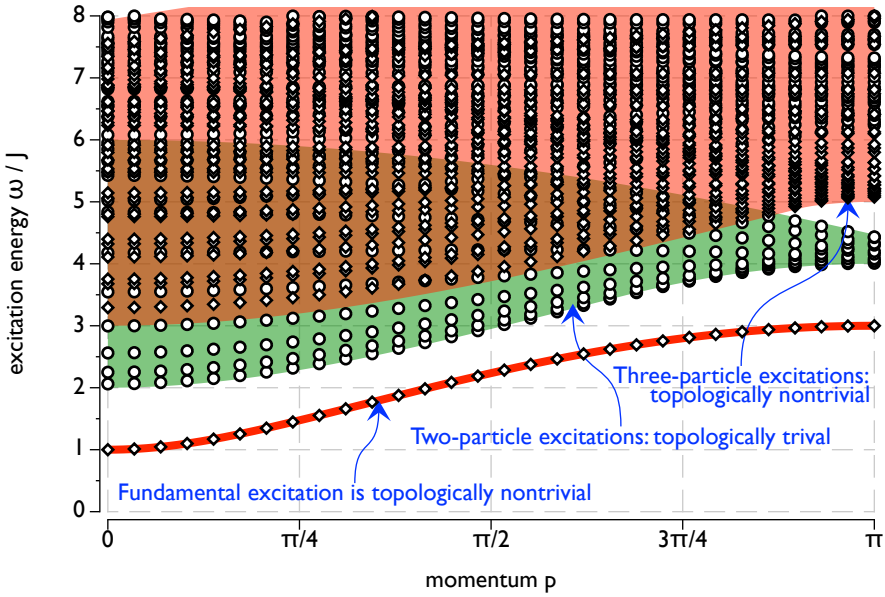

Figure 3.7: Spectrum of topologically trivial (white circles) and topologically non-trivial excitations (white diamonds) for the transverse quantum Ising model with $h/J = 1/2$, obtained with the variational ansätze $|\Phi_p^{(A)}(B)\rangle$ and $|\Xi_p^{(A)}(B)\rangle$ respectively, both with bond dimension $D = \tilde{D} = 8$. The exact branch of the elementary excitation (red line), as well as the exact two-particle continuum (green band) and three-particle continuum (red band) are also shown.

tion with bond dimension $D = 2$ [267, 268]. At $\theta = \pm\pi/4$, an exact solution in terms of the Bethe ansatz is possible and the model is critical. The dispersion relation shows nodes for $p = 0$ and $p = \pi$ for $\theta = -\pi/4$ (the Takhtajan-Babudjan point), and the model undergoes a second order phase transition to a dimer phase (only invariant under $\hat{T}^2$), which exists for $\theta \in (-3\pi/4, -\pi/4)$. The existence of a small nematic phase between the dimer phase and the ferromagnetic phase has recently been ruled out [354]. For $\theta = \pi/4$, the dispersion relation of the elementary excitation has nodes at $p = 0$ and $p = \pm 2\pi/3$ for $\theta = \pi/4$. This critical behavior exists throughout the range $\theta \in [\pi/4, \pi/2)$, no trimerization occurs and the system is a nematic phase. The transition at $\theta = \pi/4$ is supposedly of the Kosterlitz-Thouless type. The whole phase diagram is summarized in Fig. 3.8 (see [355, 356] and references therein).

We first concentrate on the point $\theta = 0$, and try to reproduce the value of the Haldane gap $\Delta_{\text{Haldane}}/J$ with our approach. Fig. 3.9 shows the spectrum of topologically trivial excitations obtained by diagonalizing H_{Ψ_p} for $D = 30$, where values are colored according to their degeneracy and scaled with respect to Δ_{Haldane}, which is determined below. Note that we did not explicitly include the SU(2) symmetry in the computation. By finding the best matrix product state representation with the time-dependent variational principle up to a state convergence of $\tilde{\eta} = 10^{-10}$, the degeneracy of the excitation spectrum is

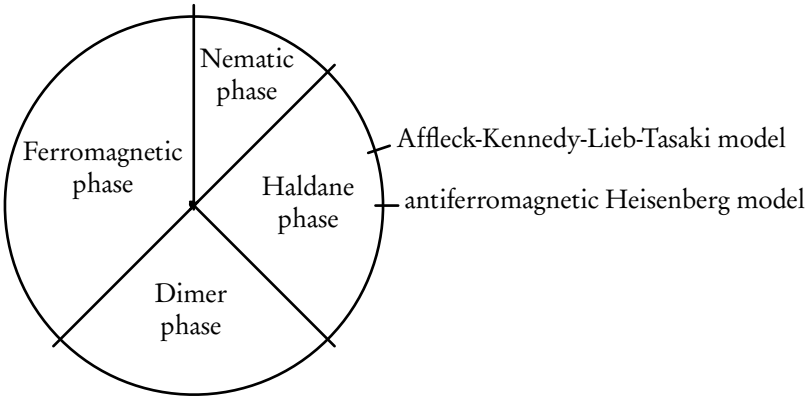

Figure 3.8: Phase diagram of the bilinear-biquadratic Heisenberg model (taken from [356]).

automatically replicated up to about the same precision $\tilde{\eta}$. This spectrum is in qualitative agreement with previous studies of Östlund and Rommer using their more restrictive ansatz [227], and by White and Affleck using a dynamic density matrix renormalization group simulation on a finite chain of up to 400 sites with values for the bond dimension up to $D = 2000$ [338]. As expected, the elementary excitation around momentum $p = \pi$ is the $S = 1$ magnon excitation. N-particle excitations arise from coupling N magnons with angular momentum $S = 1$, and can thus have all values of the angular momentum $S = 0, 1, 2, \ldots, N$. The presence of a spin S excitation thus indicates that at this place a band of N-particle excitations with $N \geq S$ is present. At $p = 0$ the two-particle band should start at $\omega/J = 2\Delta_{\text{Haldane}}$ and at $p = \pi$ the three-particle band should start at $\omega/J = 3\Delta_{\text{Haldane}}$. The disappearance of the elementary magnon excitation around $p = 0$ is addressed below. Our ansatz is not able to approximate the minimum value of these multi-particle bands, and the difference grows as the number of particles increases, which is in full correspondence with our expectation.

We now focus on the elementary magnon excitation with excitation energy $\omega(p)$. The minimum value is obtained at $p = \pi$ and defines the Haldane gap $\Delta_{\text{Haldane}} = \omega(\pi)/J$. A very accurate estimate $\Delta_{\text{Haldane}} = 0.41047925(4)$ was computed in [338]. Despite the numerical complexity of their approach for computing the magnon excitation, the obtainable accuracy on the dispersion relation $\omega(p)$ is not very high and the estimate for the Haldane gap was computed using the the ordinary ground state algorithm of the density matrix renormalization group with bond dimension $D = 500$ on the same finite lattice of 400 sites. With modest computational resources (about one hour computation time on a quad-core computer) we obtain similar results for various values of D up to $D = 192$, which were chosen so that all Schmidt values with a certain degeneracy (given by half-integral spin representations: see Table 3.1) are present. This is the only way in which the SU(2) symmetry has explicitly been exploited. We elaborate on this at the end of this paragraph when studying the relationship with the linearized time-dependent variational principle. We denote $\Delta^{(D)}_{\text{Haldane}}$ as the value of the Haldane gap obtained at

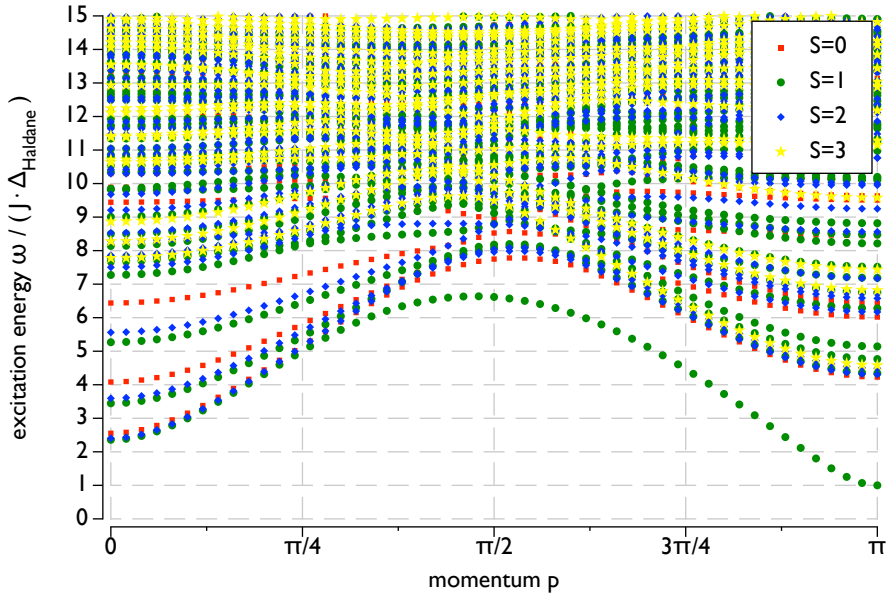

Figure 3.9: Spectrum of the lowest lying excitations of the $S = 1$ Heisenberg antiferromagnet at $D = 30$.

bond dimension D. We can expect that the error $|\Delta^{\infty}_{\mathrm{Haldane}} - \Delta^{(D)}_{\mathrm{Haldane}}|$ scales to zero as $D \to \infty$. It has been shown that near critical points errors on the ground state energy scale as a power law in D [357, 358]. However, since we are far from a critical point and we are dealing with the error on an excitation energy, this might not be the best assumption. Since we have at our disposal the local state error $\tilde{\varepsilon}(D) = \tilde{\varepsilon}(\overline{A}_D, A_D)$ in the variationally optimal uniform matrix product state approximation $|\Psi(A_D)\rangle$ at bond dimension D, it is more likely to assume a scaling

$$|\Delta^{(\infty)}_{\mathrm{Haldane}} - \Delta^{(D)}_{\mathrm{Haldane}}| = c\tilde{\varepsilon}^{\alpha}. \tag{3.170}$$

We can estimate $\Delta_{\mathrm{Haldane}} = \Delta^{(\infty)}_{\mathrm{Haldane}}$ as the value that minimizes the norm of the residuals obtained when applying linear regression to $\log|\Delta^{(\infty)}_{\mathrm{Haldane}} - \Delta^{(D)}_{\mathrm{Haldane}}|$ as function of $\log(\tilde{\varepsilon}(D))$ (see Figure 3.10). In fact, we can omit the absolute value $|\cdot|$ since the excitation energies are monotonically *increasing*. With these approach, we can improve the previous estimate for the Haldane gap by two more significant digits:

$$\Delta^{(\infty)}_{\mathrm{Haldane}} = 0.410479248463^{+6\times10^{-12}}_{-3\times10^{-12}}. \tag{3.171}$$

Error bars were obtained by taking these values where the norm of the residuals is 10% larger than at the optimal value, as indicated in Figure 3.10. It turns out that for the optimal value of $\Delta^{(\infty)}_{\mathrm{Haldane}}$, the power law dependence on $\tilde{\varepsilon}(D)$ has an exponent $\alpha \approx 2$, just as for the ground state energy (density). Recovering this theoretically expected scaling,

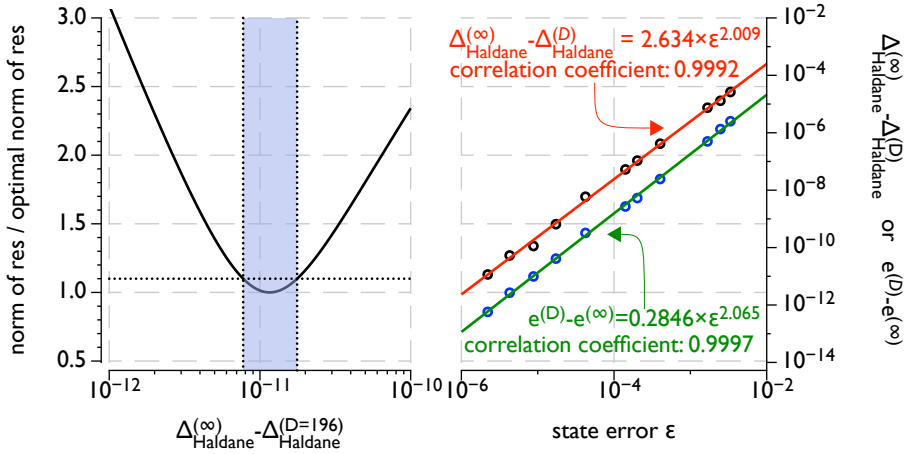

Figure 3.10: An estimate $\Delta^{(\infty)}_{\text{Haldane}}$ for the Haldane gap Δ_{Haldane} is obtained as the value that minimizes the norm of the residuals corresponding to a linear regression for the differences $\log|\Delta^{(D)}_{\text{Haldane}} - \Delta^{(\infty)}_{\text{Haldane}}|$ as function of $\log(\tilde{\varepsilon}(D))$ (note that the tilde is missing in the legend on the graph), for $D = 24$, 26, 30, 48, 64, 72, 96, 120, 142, 162 and 192. A confidence interval for $\Delta^{(\infty)}_{\text{Haldane}}$ can be obtained as the interval in which the norm of residuals is within 10% of the optimal value.

both for the ground state energy density as for the excitation energy, together with the very high value of the correlation coefficient strengthens the reliability of our approach. Indeed, the same procedure has been applied to the ground state energy density to yield (see Figure 3.10).

$$e^{(\infty)} = -1.4014840389711^{+1\times10^{-13}}_{-2\times10^{-13}}. \tag{3.172}$$

This estimate is compatible with the value obtained in the previous section at $D = 1024$. The error on the excitation energy thus scales equally fast as the ground state energy density. We can thus identify the largest contribution to the error on the excitation energy as the subtraction of an estimate of the ground state energy that is too large. Since the error on the excitation energy is about one order of magnitude larger than the error on the energy density, this indicates that the excitation is affected by about ten of these faulty subtractions. We could thus conclude that the excitation spreads out over around ten sites. This is perfectly allowed by our ansatz, which can support excitations that spread out over at least $2\log_q D + 1 \approx 11$ sites for $D = 192$ (and $q = 3$). As a final remark, it is important to note that we can now determine any point in the dispersion relation of the elementary magnon with approximately the same accuracy, in contrast to the dynamic density matrix renormalization group simulation method of [338].

Around $p = p_{\text{abs}} \approx \pi/4$, the elementary magnon excitation seems to be absorbed in the two-particle band, as is also sketched in Figure 3.11(a). It was argued in [338] that the elementary excitation with $S = 1$ ceases to exist at this point. At this point, the elementary excitation is no longer stable and decays into a two-particle excitation (with $S = 1$). The most precise estimation of this particular momentum p_{abs} made in [338]

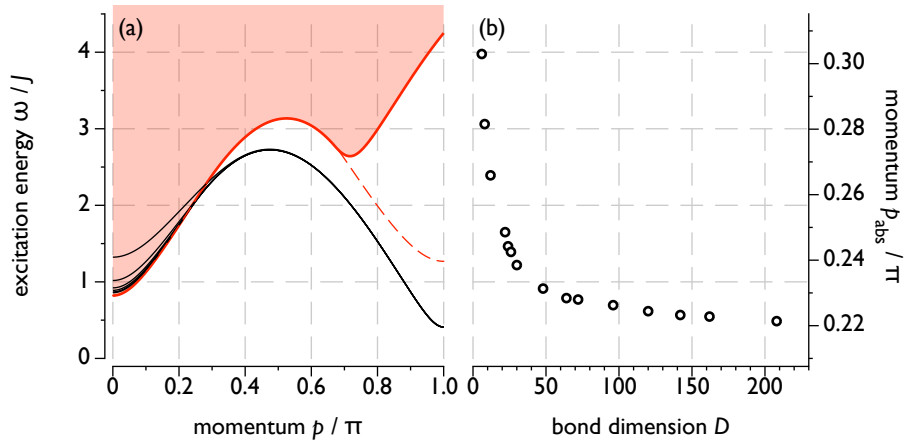

Figure 3.11: (a) The elementary magnon dispersion relations (black lines) for $D = 6$, 8, 12, 22, 24, 26, 30, 48, 64, 72, 96, 120, 142, 162 and 208, as well as the two-magnon band computed using the quasi-exact dispersion relation at $D = 208$ (red region, with the minimum of the band indicated by the solid red line). (b) The momentum p_{abs} at which the dispersion relation of the elementary magnon is absorbed into the two-magnon band as function of the bond dimension D. At the theoretically exact value of p_{abs}, the elementary magnon ceases to exist. If this does not happen, the minimum of the two-magnon band in (a) would instead be given by the dashed red line.

is about $0.23\pi - 0.24\pi$. Figure 3.11(b) indicates that the true value is definitely lower. If we perform a similar strategy as for the Haldane gap to estimate p_{abs}, we obtain (see Figure 3.12)

$$p_{\mathrm{abs}}^{(\infty)} = 0.2183^{+8\times10^{-4}}_{-22\times10^{-4}} \times \pi. \tag{3.173}$$

This value was also used in the computation of the two-magnon band in Figure 3.11(a). Note that this does not conflict, since the only part of the two magnon-band that is modified by the value of p_{abs} is not required for the computation of p_{abs}.

Unlike for the energy, there is no motivation why the error on p_{abs} should scale as a power law of the local state error $\tilde{\varepsilon}(D)$. The correlation coefficient at the optimal estimate of $p_{\mathrm{abs}}^{(\infty)}$ is slightly smaller then for the power law scaling of the energies in Figure 3.10. The biggest problem however is that the obtained optimum is very unstable at the lower side, as follows from the left side of Figure 3.12. It could just as well be that $p_{\mathrm{abs}} = 0$. Let us now try to investigate the nature of this elementary magnon excitation in some more detail. For p slightly larger than p_{abs}, the magnon excitation should not so much be regarded as a true elementary excitation but rather as a bound state of two magnons. This picture is strongly supported by the convergence behavior as a function of D. For a point-like elementary excitation, such as the magnon near $p = \pi$, the excitation energy $\omega^{(D)}(p)$ as function of the bond dimension D *increases* monotonically up to some limit value $\omega^{(\infty)}(p)$. While the excitation can spread out over a few sites, this is perfectly allowed by the ansatz. The main error in the excitation energy is the subtraction of a ground state energy density that is too large. A two-magnon bound state on the other

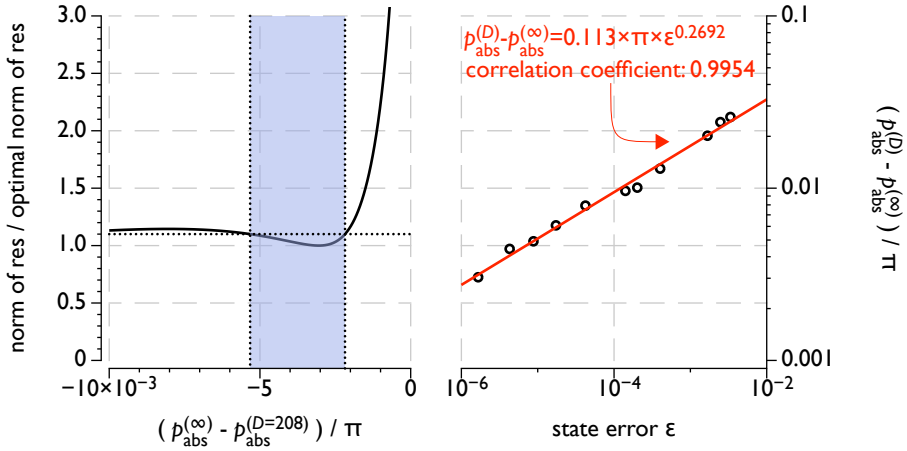

Figure 3.12: An estimate $p_{\text{abs}}^{(\infty)}$ for the momentum p_{abs} at which the elementary Heisenberg magnon is absorbed in the two-magnon continuum is obtained as the value that minimizes the norm of the residuals corresponding to a linear regression for the differences $\log|p_{\text{abs}}^{(D)} - p_{\text{abs}}^{(\infty)}|$ as function of $\log(\tilde{\varepsilon}(D))$ (note that the tilde is missing in the legend on the graph), for $D = 24$, 26, 30, 48, 64, 72, 96, 120, 142, 162 and 208. A confidence interval for $p_{\text{abs}}^{(\infty)}$ can be obtained as the interval in which the norm of residuals is within 10% of the optimal value.

hand could easily spread out over a number of sites that is much larger than $(2\log_q D+1)$. Forcing it to be described by our ansatz requires a confinement of the two particles in a smaller number of sites which results in an energy increase. If this is the major source of errors, then the dispersion relation $\omega^{(D)}(p)$ is expected to *decrease* to some limit value $\omega^{(\infty)}(p)$ as a function of D, since the particles can spread out more and more as D is increased. Figure 3.13(c) indicates that the transition between a point-like elementary excitation and a two-magnon bound state is around $p \approx 0.8\pi$. Since the separation between the two particles is finite, the convergence is expected to be fairly quick for bound states. This is in sharp contrast with a genuine two-magnon state. In particular, our ansatz is not suited for determining the minimum energy of the two-magnon band and the convergence speed decreases rapidly for $p < p_{\text{abs}}$ in Figure 3.13(c). Since this rapid decrease of convergence speed agrees nicely with the location of the estimate p_{abs} from Eq. (3.173), we can assume that the given estimate is accurate and one should not expect a much smaller or zero value for p_{abs}.

Let us now try to better understand the two-magnon bound state for $p_{\text{abs}} < p \lesssim 0.8\pi$. The minimum of the two-magnon band describes two magnons with momenta $p_\pm = \pi + (p \pm p_{\text{rel}})/2$. The minimum condition requires $\omega'\big(\pi+(p+p_{\text{rel}})/2\big) = \omega'\big(\pi+(p-p_{\text{rel}})/2\big)$, with ω' the derivative of the dispersion relation for elementary magnons. Since p_{rel} is uniquely defined, Heisenberg's uncertainty relation requires a completely undefined value for x_{rel}. In the bound state, x_{rel} can be given a finite value by making a superposition of particles with different momenta $p_\pm = \pi + (p \pm p_{\text{rel}} \pm k)/2$. This picture defines an

effective single particle problem

$$\hat{H} = \frac{\hat{k}^2}{2m_{\text{eff}}(p)} + V_{\text{eff}}(\hat{x}_{\text{rel}}; p) + \mathcal{O}(\hat{k}^3), \tag{3.174}$$

where $\hat{x}_{\text{rel}}$ and $\hat{k}$ are canonically conjugate variables satisfying $[\hat{x}_{\text{rel}}, \hat{k}] = \mathrm{i}$ and

$$\frac{1}{2m_{\text{eff}}(p)} = \frac{1}{2}\omega''(\pi + p/2 + p_{\text{rel}}) + \frac{1}{2}\omega''(\pi + p/2 - p_{\text{rel}}), \tag{3.175}$$

with ω'' the second derivative of the elementary magnon dispersion relation. V_{eff} is the p-dependent effective attraction between magnons that is required for the formation of a bound state. The effective mass $m_{\text{eff}}(p)$ is sketched in Figure 3.13(b). It becomes negative for $p \gtrsim 0.8\pi$, so that a bound state would collapse to $x_{rel} = 0$ if no higher order terms in k are present. This is compatible with the interpretation of the one-magnon curve as point-like excitation for $p \gtrsim 0.8\pi$. The easiest way to explain the sudden disappearance of the two-magnon bound state at some value $p = p_{\text{abs}}$ would be that the effective mass $m_{\text{eff}}(p)$ becomes to light for the effective potential V_{eff} to support bound states, since lighter mass results in a larger separation x_{rel} between the two particles. The effective mass $m_{\text{eff}}(p)$ is indeed decreasing around the estimated value of p_{abs}. However, it reaches a maximum value $m_{\text{eff}}(p) = +\infty$ at the very near momentum $p \approx 0.26\pi$, and the observed convergence speed is not at all compatible with the computed value of $m_{\text{eff}}(p)$ alone. A more complete model, including higher order terms in k as well as the p-dependence of $V_{\text{eff}}(x_{\text{rel}}, p)$ is required. This cannot be derived from our numerical simulation and is beyond the current scope.

As a final aspect of the Heisenberg model, we study the degeneracy in its Schmidt spectrum using the relation between our ansatz for excitations and the linearized flow equations of the time-dependent variational principle [Eq. (3.165)]. We exactly diagonalize the generalized eigenvalue problem of Eq. (3.165), where the gauge fixing conditions on $\boldsymbol{B}_+$ and $\boldsymbol{B}_-$ can be chosen such that the the matrix in the right hand side is equal to $\mathbb{1}_{(q-1)D^2} \oplus (-\mathbb{1}_{(q-1)D^2})$. For bond dimension $D = 24$, a comparative results between the eigenvalues of this larger eigenvalue problem and the eigenvalues with our variational ansatz for excitations is sketched in Figure 3.14. The doubled spectrum of eigenvalues of Eq. (3.165) is reflection invariant around zero. As argued in Subsection 3.4, the difference between the eigenvalues obtained from the linearized flow equation of the time-dependent variational principle and the eigenvalues obtained with our variational ansatz in $\mathbb{T}_{\Phi_p}$ are small for elementary excitations. The error between both is plotted for the lowest $S = 1$ excitation, which is an elementary point-like excitation around $p = \pi$. This difference should be compared to a (local) state error $\tilde{\epsilon} \approx 3 \times 10^{-3}$ for this modest value of D. Hence, for larger values of the bond dimension D, we expect the difference between the two approaches to be practically inexistent for elementary excitations. As p decreases to zero, the difference between the two curves increases, as the nature of this lowest $S = 1$ excitation changes from an elementary excitation two a two-particle bound

state and later to a true two-particle state.

Since bond dimension $D = 24$ allows to take into account all Schmidt vectors with the same degenerate Schmidt value, we expect that the minimum is unique. In contrast, at $D = 23$ or $D = 25$ the variational optimization has to choose between one of two Schmidt vectors to keep for every bipartition resulting from a cut between two sites. The variational optimum is no longer unique: there will be a flat valley of equally good choices A that produce the same energy expectation values $\langle\Psi(A)|\hat{H}|\Psi(A)\rangle$. Different values of A correspond to different choices of Schmidt vector associated to the smallest Schmidt coefficient. A first effect of this degenerate valley of energy optima is that the location of the energy optimum with an imaginary time simulation according to the time-dependent variational principle converges much slower. The effect on the excitation spectrum obtained with the variational ansatz and with the linearized flow equation is shown in Figure 3.15. While the variational ansatz $|\Phi(B;A)\rangle$ still produces the correct excitation spectrum, the linearized flow equation produces a fake zero-mode. Indeed, let $A(s)$ be a one-parameter group of tensors A that runs through this valley. Then $\langle\Psi(A(s))|\hat{H}|\Psi(A(s))\rangle$ is s-independent. Since all of these are variational optima, we automatically obtain $\langle\Psi(\overline{A(s)})|\hat{H}|\Phi_p(B;A(s))\rangle = 0$ for any $|\Phi_p(B;A(s))\rangle \in \mathbb{T}^{\perp}_{\mathrm{MPS}}(A(s))$. We also obtain

$$\left.\frac{\mathrm{d}^2}{\mathrm{d}s^2}\langle\Psi(A(s))|\hat{H}|\Psi(A(s))\rangle\right|_{s=0} =$$
$$2\langle\Phi_0(\overline{B};\overline{A})|\hat{H}|\Phi_0(B;A)\rangle + \langle\Psi(A)|\hat{H}|\Upsilon_{0,0}(B,B;A)\rangle + \langle\Upsilon_{0,0}(\overline{B},\overline{B};\overline{A})|\hat{H}|\Psi(A)\rangle =$$
$$\begin{bmatrix} B^\dagger & \overline{B}^\dagger \end{bmatrix} \begin{bmatrix} H_{\Phi_0} & M_{\Upsilon_{0,0}} \\ \overline{M_{\Upsilon_{0,0}}} & \overline{H_{\Phi_0}} \end{bmatrix} \begin{bmatrix} B \\ \overline{B} \end{bmatrix} = 0$$

with $A = A(0)$ and $B = \mathrm{d}A/\mathrm{d}s(0)$. Hence, the Hessian of the energy appearing in the left hand side of Eq. (3.165) for $p = 0$ has a zero eigenvalue, and so does the generalized eigenvalue equation of Eq. (3.165) itself. The variational ansatz that we have promoted in this section does not suffer from the same artefact. This observation can also help in detecting interesting degeneracies in the Schmidt spectrum.

We now turn to the more general bilinear-biquadratic Heisenberg model in the non-critical region $-\pi/4 < \theta < +\pi/4$. As explained in the beginning of this paragraph, the model becomes critical at the end points. As θ decreases from 0 to $-\pi/4$, the excitation energy of the elementary magnon around $p = \pi$ decreases until the gap in the system becomes zero (see Figure 3.16). Simultaneously, the entanglement increases as can be noticed by the Schmidt-values shifting upwards. At $\theta = -0.24\pi$, the elementary magnon has a slightly negative excitation energy at $p = \pi$. While this is of course an artefact of the low value of the bond dimension $D = 24$, since the critical point is not until $\theta = -0.25\pi$, it does indicate a tendency of these magnons to condense, resulting in a ground state that breaks translation invariance down to invariance under shifts over two sites. Indeed, for $\theta < -\pi/4$ the ground state of the system has a dimer configuration.

While a zero (negative) excitation energy of the elementary magnon at $p = \pi$ results in zero (negative) excitation energies for two-magnon excitations with total momentum $p = 0$, the excitation energies found with our ansatz are positive at $p = 0$, as required by the optimality of our uniform matrix product state approximation. The negative energy for the elementary excitation at $p = \pi$ indicates that we could have found a lower energy density if we would have used a two-periodic matrix product state with bond dimension $D = 24$.

The same analysis can be repeated for θ increasing from 0 to $\pi/4$, which is sketched in Figure 3.17. For θ slightly larger than 0, the excitation energy of the elementary magnon around $p = \pi$ increases, resulting in smaller correlation length and a decrease of the entanglement entropy (as indicated by the Schmidt values shifting downwards). Indeed, at $\theta = \arctan(1/3) \approx 0.1024\pi$ this is the AKLT-model, for which the ground state has an exact matrix product state representation with $D = 2$. For $\theta = 0.10\pi$, the importance of the Schmidt coefficients λ_α for $\alpha > 2$ has strongly decreased. If θ is increased further, the excitation energy of the elementary magnon starts to decrease around $p = 2\pi/3$ and eventually a zero mode develops. Once again, the excitation energy is slightly negative for $\theta = 0.24\pi$, which is an artefact of the small bond dimension $D = 24$. This could again be interpreted as an indication for condensation of elementary magnons with momentum $2\pi/3$ in the phase transition at $\theta = \pi/4$, which would result in the breaking of translation invariance down to invariance under shifts over three sites. However, in the exact solution no such trimerization occurs and the model remains critical throughout $\theta \in [\pi/4, \pi/2)$. Hence, while the matrix product state approximation and derived methods for excitations can provide valuable information about the phase of a system and the nature of a phase transition, such information is not always reliable and should be used carefully.

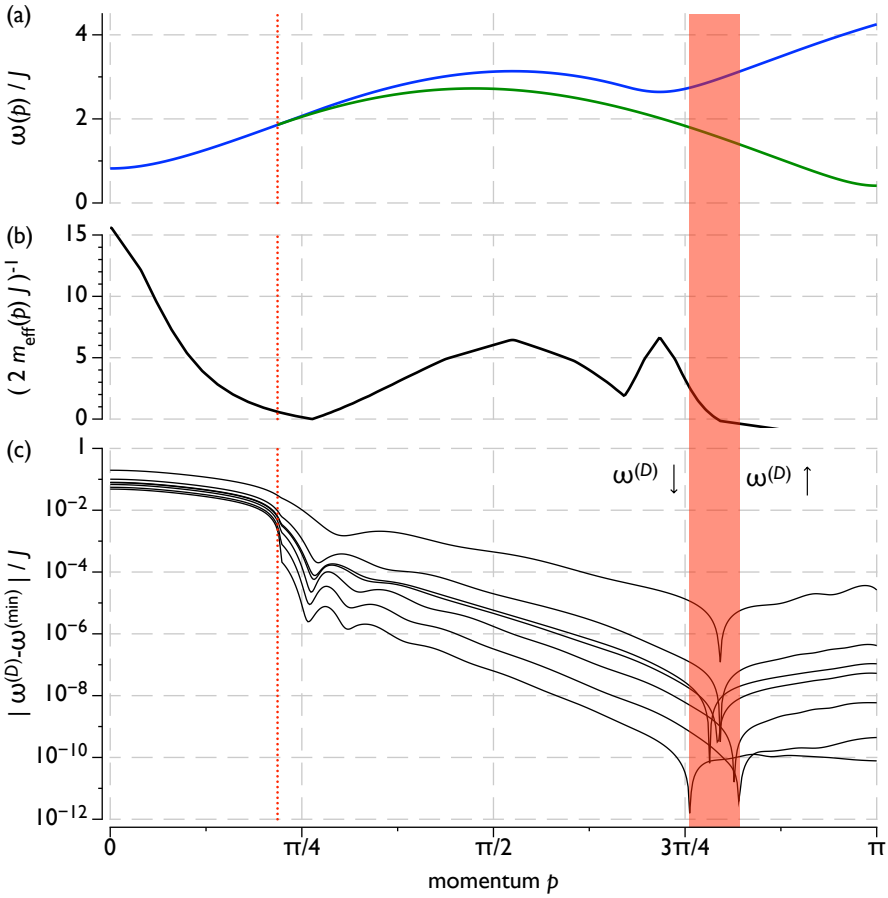

Figure 3.13: (a) One-magnon curve (green line) and the minimum of the two-magnon band (blue line) obtained at $D = 208$. (b) Effective mass $m_{\mathrm{eff}}(p)$ for the two-magnon bound state. (c) The convergence of the one-magnon curve as a function of D: $|\omega^{(D)}(p) - \omega^{(\mathrm{min})}(p)|$ is plotted for $D = 24, 48, 64, 72, 96, 120, 142$, where $\omega^{(\mathrm{min})}(p)$ is equal to $\omega^{(D=208)}(p)$ for $p > p_{\mathrm{abs}}$ and equal to the minimum of the two-magnon band for $p < p_{\mathrm{abs}}$. The red dashed line indicates the position of p_{abs}, based on the estimate of Eq. (3.173). The red area shows the transition region from elementary point-like excitation to a two-magnon bound state.

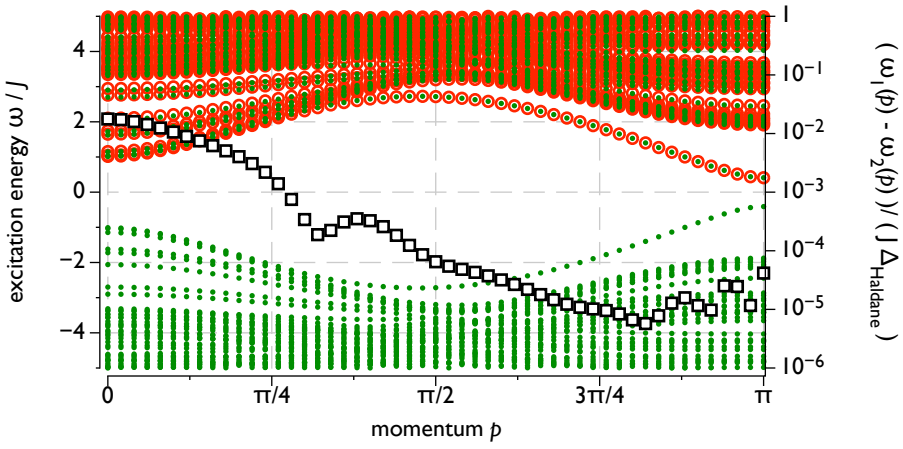

Figure 3.14: Comparison of the excitation spectrum ω obtained with the linearized flow equation of the time-dependent variational principle [Eq. (3.165)] (green dots) with the excitation spectrum obtained with our variational ansatz for excitations (red circles), for the Heisenberg model studied at bond dimension $D = 24$. Also shown is the difference between the dispersion relations $\omega_1(p)$ (obtained with the variational ansatz) and $\omega_2(p)$ (obtained with the linearized flow equation) for the lowest excitation (black squares).

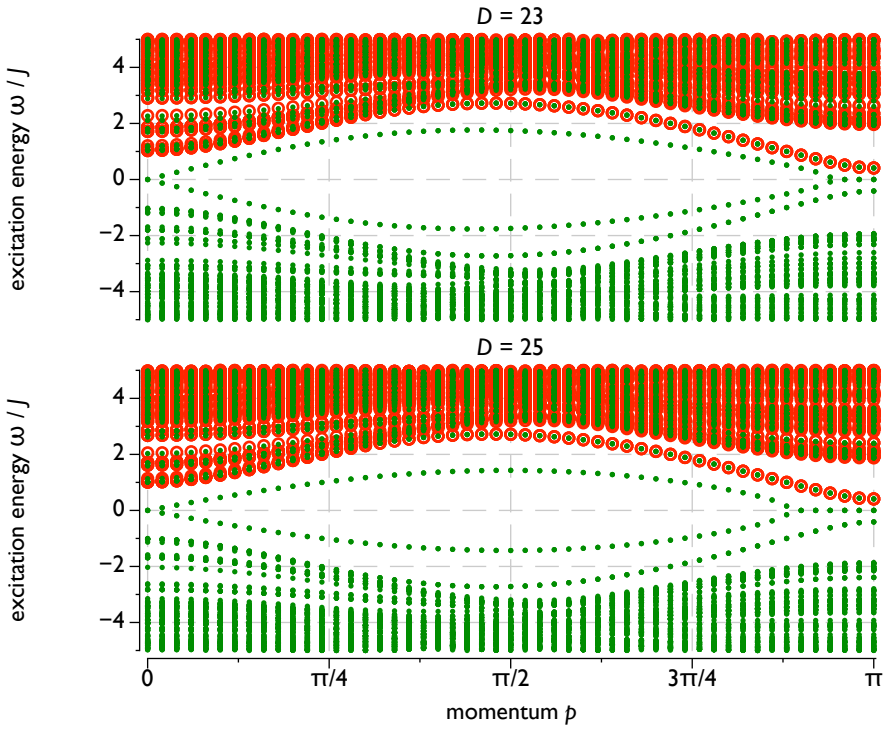

Figure 3.15: Similar comparison of the excitation spectrum ω obtained with the linearized flow equation of the time-dependent variational principle [Eq. (3.165)] (green dots) with the excitation spectrum obtained with our variational ansatz for excitations (red circles), for the Heisenberg model at bond dimension $D = 23$ and bond dimension $D = 25$.

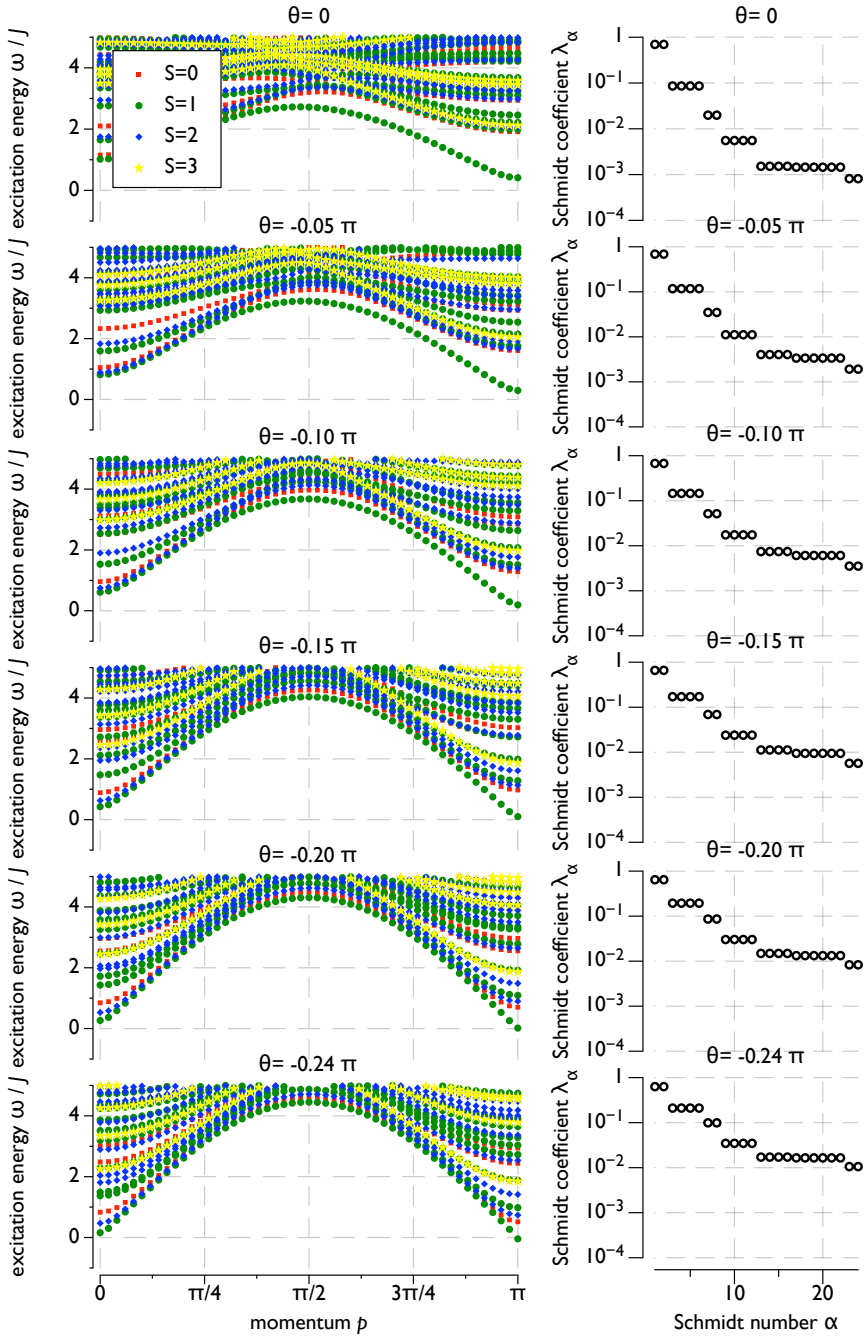

Figure 3.16: Excitation spectrum (left) and Schmidt spectrum (right) for the bilinear-biquadratic antiferromagnetic Heisenberg model in the region $\theta \in (-\pi/4, 0]$ obtained with a matrix product state ansatz with bond dimension $D = 24$.

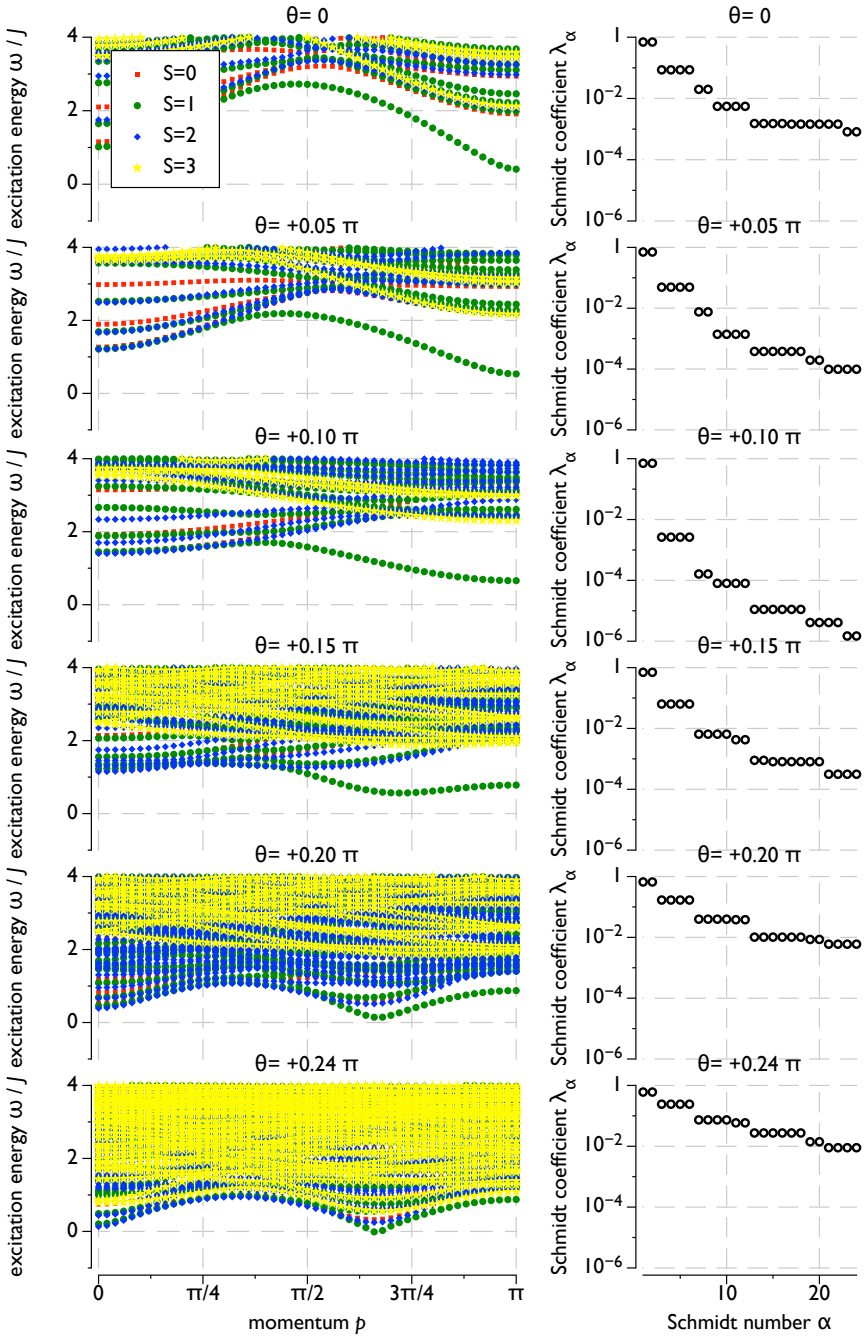

Figure 3.17: Excitation spectrum (left) and Schmidt spectrum (right) for the bilinear-biquadratic antiferromagnetic Heisenberg model in the region $\theta \in [0, \pi/4)$ obtained with a matrix product state ansatz with bond dimension $D = 24$.

$S = 1/2$ and $S = 1$ XXZ antiferromagnet

To study topologically non-trivial excitations in systems with spontaneous symmetry breaking, we now turn towards the anisotropic XXZ antiferromagnet, for which the Hamiltonian is given by

$$\hat{H}_{\text{XXZ}} = J \sum_{n\in\mathbb{Z}} \hat{S}^x_n \hat{S}^x_{n+1} + \hat{S}^y_n \hat{S}^y_{n+1} + \Delta \hat{S}^z_n \hat{S}^z_{n+1}, \tag{3.176}$$

with $J > 0$. We study this model both for $S = 1/2$ spins ($\hat{S}^{x,y,z} = \hat{\sigma}^{x,y,z}/2$) and for $S = 1$ spins. The anisotropy parameter explicitly breaks the SU(2) invariance, reducing it to a $\mathrm{U}(1) \times \mathbb{Z}_2$ symmetry, where U(1) contains the elements $\{\exp(\mathrm{i}\theta \sum_n \hat{S}^z_n)$, and the $\mathbb{Z}_2$ group contains the elements $\{\hat{\mathbb{1}}, \exp\left(\mathrm{i}\pi \sum_n \hat{S}^x_n\right)\}$. We could just as well have chosen $\hat{S}^y$ in the definition of $\mathbb{Z}_2$, or any linear combination $\cos(\theta)\hat{S}^x + \sin(\theta)\hat{S}^y$ to which $\hat{S}^x$ is transformed by an element from U(1). For Δ sufficiently large, this model transforms into the classical Ising model $\hat{H} \sim \sum_n \hat{S}^z_n \hat{S}^z_{n+1}$ and has antiferromagnetic order corresponding to the local order parameter $(-1)^n \hat{S}^z_n$. Since this spontaneous symmetry breaking also induces a breaking of translation invariance, we apply a spin flip $\exp(\mathrm{i}\pi \hat{S}^x)$ to every second site, so as to obtain a new Hamiltonian

$$\hat{H}'_{\text{XXZ}} = J \sum_{n\in\mathbb{Z}} \hat{S}^x_n \hat{S}^x_{n+1} - \hat{S}^y_n \hat{S}^y_{n+1} - \Delta \hat{S}^z_n \hat{S}^z_{n+1}, \tag{3.177}$$

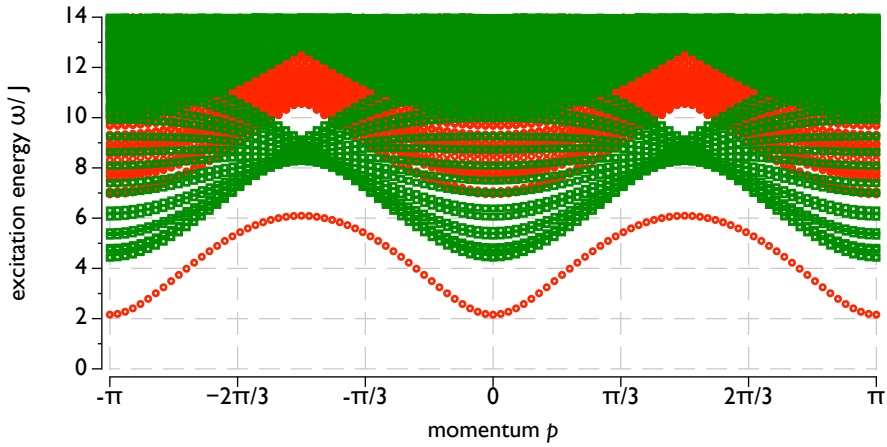

Figure 3.18: Spectrum of the lowest lying excitations of the $S = 1/2$ XXZ antiferromagnet with anisotropy parameter $\Delta = 4$ at $D = 33$. Red circles indicate of topologically non-trivial excitations whereas green squares indicate topologically trivial excitations.

Let us first discuss the $S = 1/2$ case, where the XXZ model is exactly solvable for all values of Δ using the Bethe ansatz [359]. The antiferromagnetic phase is realized all the way up to the critical value $\Delta_c = 1$, where the model turns into the critical $S = 1/2$

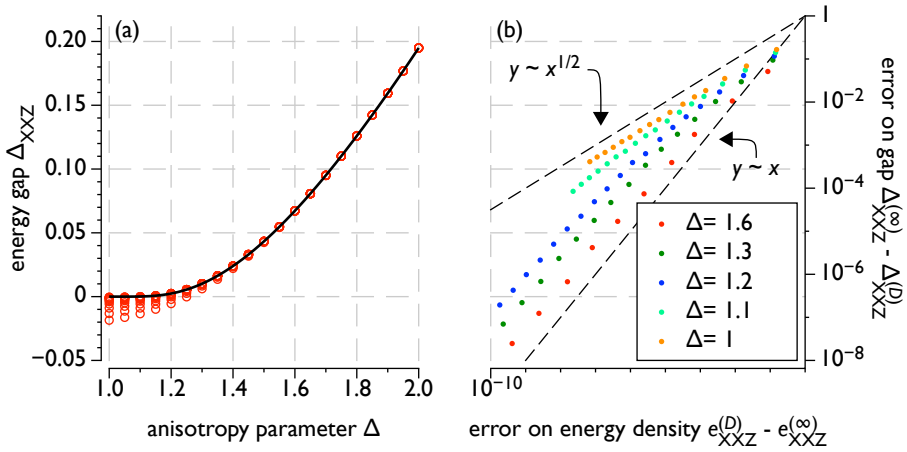

Figure 3.19: (a) Simulation results for $\Delta^{(D)}_{XXZ}$ as function of the anisotropy parameter Δ, obtained with our ansatz for topologically non-trivial excitations for various values of the bond dimension D ranging from $D = 10$ up to $D = 512$ (red circles), as well as the exact result $\Delta^{(\infty)}_{XXZ} = \Delta_{XXZ}$ obtained with the Bethe ansatz (solid black line). (b) Error on the results for the gap $\Delta^{(\infty)}_{XXZ} - \Delta^{(D)}_{XXZ}$ versus error on the ground state energy density $e^{(D)}_{XXZ} - e^{(\infty)}_{XXZ}$ for various values of the bond dimension D ranging from $D = 10$ to $D = 512$.

Heisenberg model and full SU(2) invariance is recovered, hence forbidding symmetry breaking. Figure 3.18 displays the full spectrum of excited states obtained with our ansatz at $D = 33$ for $\Delta = 4$, resulting in $(q-1)D^2 = 1089$ topologically non-trivial and 1089 topologically trivial excitations (full diagonalization becomes computationally demanding for much larger values of D). As pointed out by Fadeev and Takhtajan in [360], the elementary particle excitations in the symmetry broken phase are topologically non-trivial kinks, and all topologically trivial excitations are compound states containing an even number of kinks, in full accordance with our numerical results. The energy gap of the XXZ model is the value of the kink dispersion relation at its minima, *i.e.* at $p = 0$ and $p = \pi$. Because this gap belongs to a topologically non-trivial excitation that only comes in pairs on lattices with periodic boundary conditions, the value of the energy gap calculated in [359] using the Bethe ansatz on a lattice with periodic boundary conditions is twice the exact value $\omega(0)/J = \omega(\pi)/J = \Delta_{XXZ}$. The exact gap Δ_{XXZ} as function of the anisotropy parameter Δ is given by

$$\Delta_{XXZ} = \frac{\pi}{2}\frac{\sinh(\Phi)}{\Phi}\sum_{n=-\infty}^{+\infty}\frac{1}{\cosh\left(\frac{(2n+1)\pi^2}{2\Phi}\right)}, \quad \text{with } \Phi = \operatorname{arccosh}(\Delta). \tag{3.178}$$

Figure 3.19(b) shows results for $\Delta^{(D)}_{XXZ}$ as function of the anisotropy parameter Δ, as obtained with our variational ansatz for topologically non-trivial excitations with bond dimension D. Estimated values are now smaller than the exact result and, contrary to the case of topologically trivial excitations, can be negative even at momentum zero.

Positivity of the results is no longer guaranteed. The Bethe ansatz also provides us with an exact value for the energy density e_{XXZ} in the ground state as function of the anisotropy parameter Δ, which is given by

$$e_{\text{XXZ}} = \sinh(\Phi) \sum_{n=-\infty}^{+\infty} \frac{1}{1+\exp(2\Phi|n|)}, \quad \text{with } \Phi = \operatorname{arccosh}(\Delta). \tag{3.179}$$

We can then compare the error between the ground state energy $e^{(D)}_{\text{XXZ}}$ density obtained with a uniform matrix product state with bond dimension D and the exact result $e^{(\infty)}_{\text{XXZ}} = e_{\text{XXZ}}$ (where $e^{(D)}_{\text{XXZ}} > e^{(\infty)}_{\text{XXZ}}$ due to the variational principle) with the error between $\Delta^{(D)}_{\text{XXZ}}$ and the exact result $\Delta^{(\infty)}_{\text{XXZ}} = \Delta_{\text{XXZ}}$ given in Eq. (3.178). For small values of D, the error on the ground state energy density converges quadratically faster than the error of the energy gap. Hence, the energy gap converges much slower like most other observables that do not commute with the Hamiltonian. But for $\Delta > 1$, when a finite gap is present in the system, there is a transition point from where the error on the energy gap starts to decrease equally fast as the error on the ground state energy. The corresponding value of D is determined by the natural width of the excitation. Beyond this value of D, the largest contribution to the error of the gap is due to the subtraction of a ground state energy density that is too large, just as was the case for the topologically trivial excitation in the $S = 1$ Heisenberg antiferromagnet of the previous paragraph. The offset between the error on the energy density and the error on the gap can roughly be interpreted as the number of times the energy density has been subtracted and thus as the width of the excitation. For example, around $\Delta = 1.6$ the difference between both errors is roughly one order of magnitude, whereas the size of the gap and thus the inverse width of the excitation is about 0.1 in natural units. As Δ approaches the critical value $\Delta = 1$, the width of the excitation and thus the value of D at the transition point increases. At $\Delta = 1$, this transition point has shifted to infinity, and the gap converges only as the square root of the energy for arbitrarily large values of the bond dimension D.

As a final example, we now examine the XXZ antiferromagnet for $S = 1$. This model is no longer exactly solvable, but has an more interesting excitation spectrum with several elementary excitations. For $\Delta = 1$, we recognize the $S = 1$ Heisenberg antiferromagnet which has no symmetry breaking and is in a gapped, topologically ordered phase. There is a phase transition to a symmetry broken state for some critical value $\Delta_c > 1$. This model was studied by Mikeska in [361] with a mean field approach and the critical point was pinpointed at $\Delta_c \approx 2$. In the classical limit $\Delta \to \infty$, the ground states are the antiferromagnetic states $|\cdots\uparrow\downarrow\uparrow\downarrow\uparrow\downarrow\cdots\rangle$ and $|\cdots\downarrow\uparrow\downarrow\uparrow\downarrow\uparrow\cdots\rangle$. On top of that, the following elementary excitations can be found

(a) kinks with $\omega = 2\Delta J$: $|\cdots\uparrow\downarrow\uparrow\uparrow\downarrow\uparrow\cdots\rangle$ (a1) and $|\cdots\uparrow\downarrow\uparrow 0\downarrow\uparrow\cdots\rangle$ (a2)

(b) spin deviation state with $\omega = 2\Delta J$: $|\cdots\uparrow\downarrow\uparrow 0\uparrow\downarrow\cdots\rangle$

(c) topologically non-trivial bound state with $\omega = 3\Delta J$: $|\cdots\uparrow\downarrow 00\downarrow\uparrow\cdots\rangle$

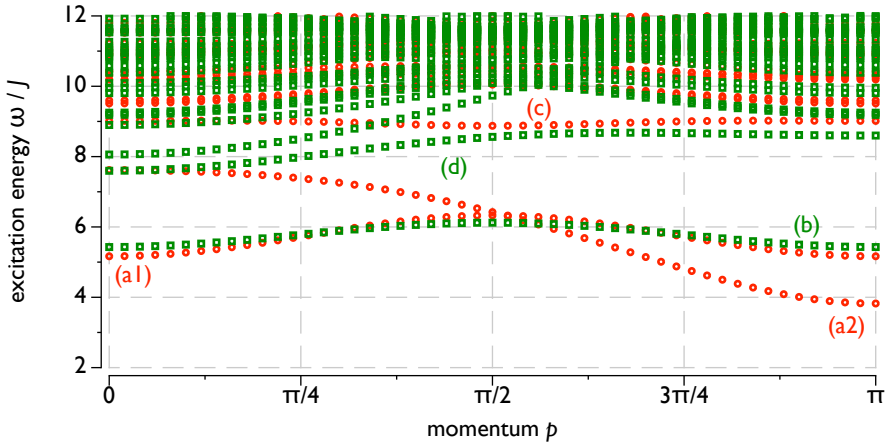

Figure 3.20: Spectrum of the lowest lying excitations of the $S = 1$ XXZ antiferromagnet with anisotropy parameter $\Delta = 3$ at $D = 32$. Red circles indicate topologically non-trivial excitations whereas green squares indicate topologically trivial excitations. We refer to the text for more information about the indicated branches.

(d) topologically trivial bound state with $\omega = 3\Delta J$: $|\cdots \uparrow\downarrow 00 \uparrow\downarrow \cdots\rangle$

These states are expected to exist at finite Δ throughout the antiferromagnetic phase. Fig 3.20 shows the lowest lying excited states for $\Delta = 3$ with the different elementary excitations indicated. Of the three states with energy ω around 2Δ, the kink (a2) receives a first order correction from the kinetic term $\hat{S}^x_n \hat{S}^x_{n+1} + \hat{S}^y_n \hat{S}^y_{n+1}$, resulting in large opposing energy changes around momentum $p = 0$ and $p = \pi$. States $(a1)$ and (b) only receive second order corrections from the kinetic term and are less strongly affected (and have corrections in the same direction). States (c) and (d) are only marginally stable and will be absorbed in the first continuous band of topologically non-trivial and topologically trivial excitations if Δ is further lowered. (Note that excitation (c) cannot decay into topologically trivial excitations and is still stable at $\Delta = 3$, according to Fig. 3.20). These results proof that our ansätze for topologically trivial and non-trivial excitations are able to produce the full set of elementary excitations, and is able to accurately obtain their excitation energy away from the critical point.

4. Summary and conclusion

In this chapter, we have discussed in great detail the matrix product state as a variational ansatz. The properties of physical states within the variational manifold $\mathcal{M}_{\mathrm{MPS}}$ as well as the properties of the matrix product state representation $\Psi : \mathbb{A}_{\mathrm{MPS}} \mapsto \mathcal{M}_{\mathrm{MPS}}$ have been surveyed. All of this is well known in the literature. We have however contributed by performing the same study to the tangent plane $\mathbb{T}_{\mathrm{MPS}}$. A precarious study of the properties of the tangent plane had not yet been developed, as its use only became

clear through the application of the time-dependent variational principle and the recent introduction of the ansatz for momentum eigenstates in [346].

In the second section we have applied the time-dependent variational principle to the variational class of matrix product states, and illustrated numerically (for uniform matrix product states) how this defines a new algorithm that has the same computational efficiency as existing algorithms based on the time-evolving block decimation, while solving a number of important issues of such algorithms. Translation invariance and other symmetries are automatically preserved, both for real and imaginary time simulations. Using the time-dependent variational principle with imaginary time evolution results in a very powerful algorithm to find solutions of the time-independent variational principle. For real time evolution, a symmetric integrator of the flow equations was implemented that is extremely stable and preserves first integrals over long simulation times.

In the third section, it was shown how the tangent plane $\mathbb{T}_{\mathrm{MPS}}$ constructed at a variationally optimal (uniform) matrix product state defines a natural ansatz for studying low-lying excitations of one-dimensional quantum spin chains. This ansatz can easily be generalized to also include topologically non-trivial excitations (kinks or domain walls) in systems with (discrete) symmetry breaking. We have illustrated how this variational strategy can be implemented efficiently, and we have obtained some very accurate results for dispersion relations of elementary excitations in quantum spin chains.

4

CONTINUOUS MATRIX PRODUCT STATES FOR QUANTUM FIELDS

In the previous chapter we have introduced a variational ansatz that counters Feynman's second and third objection for extended lattice systems: $\mathscr{M}_{\mathrm{MPS}}$ is a manifold of non-Gaussian ansatz states that allow for an efficient evaluation of expectation values. Since matrix product states do not naturally overcome Feynman's first objection, they do fail at critical points where $\xi_c/a \to \infty$. However, because they are so efficient, the bond dimension D that determines the variational flexibility can be chosen very large and critical behavior can be approached very closely.

For field theories, few methods —variational or otherwise— allow to work directly in the continuum. Numerical approaches require a finite number of degrees of freedom in order to fit the problem in the memory of a computer. For compact systems such as nuclei, atoms and molecules, an expansion into a finite-dimensional basis is possible, but for extended systems this eventually results in a discretization to an effective lattice system. This chapter introduces a new variational ansatz for field theories in $d = 1$ spatial dimensions that was developed by Verstraete and Cirac in 2010 [362]. This ansatz is formulated in the continuum and does not require an underlying lattice approximation. It can be considered to be the continuum limit of a special subclass of matrix product states and is therefore called the *continuous matrix product state*. Most results that were obtained with matrix product states in the previous chapter can also be derived for continuous matrix product states. The discrete operations that were required in the previous chapter will naturally be cast into a continuum form. Due to the very short history of these states, most of the results in this chapter have not yet been published, nor are there any other publications to compare to. These results were derived in collaboration with J. Ignacio Cirac, Tobias J. Osborne and Frank Verstraete.

1. Definition and properties of the manifold $\mathscr{M}_{\mathrm{cMPS}}$

Consider a one-dimensional continuum $\mathscr{R} = [-L/2, +L/2]$ that accommodates N bosonic and/or fermionic particle species, created and annihilated by the operators $\hat{\psi}_\alpha^\dagger$ and $\hat{\psi}_\alpha$ with $\alpha = 1, \ldots, N$. These satisfy the general commutation or anticommutation

relations

$$\hat{\psi}_\alpha(x)\hat{\psi}_\beta(y) - \eta_{\alpha,\beta}\hat{\psi}_\beta(y)\hat{\psi}_\alpha(x) = 0, \quad \hat{\psi}_\alpha(x)\hat{\psi}^\dagger_\beta(y) - \eta_{\alpha,\beta}\hat{\psi}^\dagger_\beta(y)\hat{\psi}_\alpha(x) = \delta_{\alpha,\beta}\delta(x-y), \tag{4.1}$$

where $\eta_{\alpha,\beta} = -1$ if both α and β represent fermionic particles and $\eta_{\alpha,\beta} = 1$ as soon as one of the two particles species α or β is bosonic. We always write sums over the species index α explicitly and do not use Einstein's summation convention with respect to this index.

We can generalize the Fock construction from Section 1.2 of Chapter 1 to this problem in order to obtain the Hilbert space $\mathbb{H}^{(\mathrm{F})}_{\mathscr{R}}$. We define the variational manifold of continuous matrix product states $\mathscr{M}_{\mathrm{cMPS(D)}} \in \mathbb{H}^{(\mathrm{F})}_{\mathscr{R}}$ as

$$\mathscr{M}_{\mathrm{cMPS}} = \{|\Psi[Q,R_1,\ldots,R_N]\rangle \mid \forall Q : \mathscr{R} \to \mathbb{C}^{D\times D}; \forall R_\alpha : \mathscr{R} \to \mathbb{C}^{D\times D}, \forall \alpha = 1,\ldots,N\}, \tag{4.2}$$

where the continuous matrix product state $|\Psi[Q,R_1,\ldots,R_N]\rangle$ with bond dimension D is given by

$$|\Psi[Q,R_1,\ldots,R_N]\rangle \triangleq \operatorname{tr}\left(B\mathcal{P}\exp\left[\int_{-L/2}^{+L/2} \mathrm{d}x\, Q(x)\otimes\hat{\mathbb{1}} + \sum_{\alpha=1}^{N} R_\alpha(x)\otimes\hat{\psi}^\dagger_\alpha(x)\right]\right)|\Omega\rangle, \tag{4.3}$$

with $\mathcal{P}\exp$ the path ordered exponential (that orders arguments increasingly from left to right) and $|\Omega\rangle$ the empty vacuum that is annihilated by $\hat{\psi}_\alpha(x)$, $\forall\alpha = 1,\ldots,N$. B is a $D\times D$ matrix that acts in the ancilla space $\mathbb{C}^D$ and encodes the boundary conditions. For a system with periodic boundary conditions one can choose $B = \mathbb{1}_D$. In case of open boundary conditions, we can choose $B = \boldsymbol{v}_{\mathrm{R}}\boldsymbol{v}_{\mathrm{L}}^\dagger$ with $\boldsymbol{v}_{\mathrm{L}}$ and $\boldsymbol{v}_{\mathrm{R}}$ D-dimensional boundary vectors. We do not include B in the set of variational parameters, as it can often be completely fixed and does not enter in physical expectation values in the thermodynamic limit. In contrast to the case of generic matrix product states at finite lattices, we cannot use a space-dependent bond dimension $D(x)$, since the required continuity of D in combination with its discrete character enforces a constant value. Neither can we absorb the boundary vectors into the matrices $Q(-L/2)$, $R_\alpha(L/2)$ and $Q(L/2)$, $R_\alpha(L/2)$ in the case of open boundary conditions.

Henceforth, we compactly denote a continuous matrix product state $|\Psi[Q,R_1,\ldots,R_n]\rangle$ as $|\Psi[Q,\{R_\alpha\}]\rangle$. It will always be clear from the context how many and which particle species are present. Most of the derivations in this chapter will for the sake of simplicity and ease of notation be restricted to a single bosonic particle, for which the continuous matrix product state is denoted as $|\Psi[Q,R]\rangle$. The variational manifold $\mathscr{M}_{\mathrm{cMPS}(D)}$ is not a vector space, since the representation of the sum of two elements $|\Psi[Q,\{R_\alpha\}]\rangle + |\Psi[Q',\{R'_\alpha\}]\rangle$ requires in the most general case a continuous matrix

product state $|\tilde{\Psi}[\tilde{Q},\{\tilde{R}_\alpha\}]\rangle \in \mathscr{M}_{\text{cMPS}(\tilde{D})}$ with bond dimension $\tilde{D}=2D$, where we choose $(\forall x \in [-L/2,+L/2])$

$$\begin{aligned}\tilde{Q}(x) &= Q(x)\oplus Q'(x),\\ \tilde{R}_\alpha(x) &= R_\alpha(x)\oplus R'_\alpha(x), \qquad\qquad \forall \alpha=1,\ldots,N\\ \tilde{B} &= B\oplus B'.\end{aligned}$$

The variational manifold does however contain almost complete rays of states, since for any state $|\Psi[Q,\{R_\alpha\}]\rangle \in \mathscr{M}_{\text{cMPS}(D)}$ and any $\lambda \in \mathbb{C}_0 = \mathbb{C}\setminus\{0\}$ we can also represent $\lambda|\Psi[Q,\{R_\alpha\}]\rangle$ as a continuous matrix product state with bond dimension D as $|\Psi[Q',\{R'_\alpha\}]\rangle$, where $Q'(x)=Q(x)+\mu(x)\mathbb{1}_D$ and $R'_\alpha(x)=R_\alpha(x)$ with

$$\exp\Big(\int_{-L/2}^{+L/2} \mathrm{d}x\, \mu(x)\Big)=\lambda.$$

A special case is obtained for $\lambda=0$, since this requires to redefine $Q(x)$ as $Q'(x)=Q(x)-\infty\mathbb{1}_D$. Hence, the null state is not contained within $\mathscr{M}_{\text{cMPS}(D)}$ but only in its closure. Correspondingly, the variational manifold $\mathscr{M}_{\text{cMPS}(D')}$ with $D'<D$ is not a subset of $\mathscr{M}_{\text{cMPS}(D)}$. For example, if the boundary matrices are fixed to $B'=\mathbb{1}_{D'}$ and $B=\mathbb{1}_D$ (periodic boundary conditions), then a representation of the continuous matrix product state $|\Psi'[Q',\{R'_\alpha\}]\rangle$ with bond dimension D' as a continuous matrix product state $|\Psi[Q,\{R_\alpha\}]\rangle$ with bond dimension $D>D'$ requires $Q=Q'\oplus(-\infty\times\mathbb{1}_{D-D'})$ and $R_\alpha = R'_\alpha\oplus(0\times\mathbb{1}_{D-D'})$, hence $\mathscr{M}_{\text{cMPS}(D')}$ is only included in the closure of $\mathscr{M}_{\text{cMPS}(D)}$.

The embedding of $|\Psi[Q,\{R_\alpha\}]\rangle \in \mathscr{M}_{\text{cMPS}(D)}$ in the Fock space $\mathbb{H}^{(\mathrm{F})}_{\mathscr{R}}$ for finite $|\mathscr{R}|$ can be made explicit by rewriting it as

$$\begin{aligned}|\Psi[Q,\{R_\alpha\}]\rangle = &\\ \sum_{k=0}^{+\infty}\sum_{\alpha_1,\ldots,\alpha_k=1}^{N}&\int_{-L/2\le x_1\le\cdots\le x_k\le L/2} \mathrm{d}x_1\cdots\mathrm{d}x_k\,\phi_{\alpha_1,\ldots,\alpha_k}(x_1,\ldots,x_k)\\ &\times\hat{\psi}^\dagger_{\alpha_1}(x_1)\cdots\hat{\psi}^\dagger_{\alpha_k}(x_k)|\Omega\rangle \qquad (4.4)\end{aligned}$$

with

$$\begin{aligned}\phi_{\alpha_1,\ldots,\alpha_k}(x_1,\ldots,x_k)=&\\ \mathrm{tr}\Big[B\mathcal{P}\mathrm{e}^{\int_{-L/2}^{x_1}Q(y)\mathrm{d}y}R_{\alpha_1}(x_1)&\mathcal{P}\mathrm{e}^{\int_{x_1}^{x_2}Q(y)\mathrm{d}y}\cdots R_{\alpha_k}(x_k)\mathcal{P}\mathrm{e}^{\int_{x_k}^{L/2}Q(y)\mathrm{d}y}\Big]. \qquad (4.5)\end{aligned}$$

Note that the k-particle wave functions $\phi_{\alpha_1,\ldots,\alpha_k}(x_1,\ldots,x_k)$ are only defined for $x_1\le\cdots\le x_k$. It can be extended to any order of the arguments by using the commutativity or anticommutativity of the creation operators that multiply it in Eq. (4.4). Put differently,

for any order of the arguments we can define

$$\phi_{\alpha_1,\ldots,\alpha_k}(x_1,\ldots,x_k) = \langle\Omega|\hat{\psi}_{\alpha_k}(x_k)\cdots\hat{\psi}_{\alpha_1}(x_1)|\Psi[Q,\{R_\alpha\}]\rangle\,. \tag{4.6}$$

The non-relativistic kinetic energy requires that these functions are sufficiently regular, which imposes certain constraints on the matrix functions Q and R_α that are to be discussed in Subsection 1.3. We do thus not yet attempt to define the parameter space of the variational manifold $\mathscr{M}_{\mathrm{cMPS}(D)}$. As for matrix product states, there is a parameter redundancy in the continuous matrix product state representation. For example, if $B = \mathbb{1}_D$ (periodic boundary conditions) the physical state is invariant under a redefinition $Q(x) \leftarrow gQ(x)g^{-1}$ and $R_\alpha(x) \leftarrow gR_\alpha(x)g^{-1}$ with $g \in \mathrm{GL}(\mathbb{C},D)$. The full set of local gauge transformations that leave the physical state invariant is constructed in Subsection 1.5.

We can already define the tangent plane $\mathbb{T}_{\mathscr{M}_{\mathrm{cMPS}}}[Q,\{R_\alpha\}] = \mathbb{T}_{\mathrm{cMPS}}[Q,\{R_\alpha\}]$ at a certain point $|\Psi[Q,\{R_\alpha\}]\rangle \in \mathscr{M}_{\mathrm{cMPS}}$. For further reference, we first define

$$\hat{U}(y,z) = \mathcal{P}\exp\left[\int_y^z \mathrm{d}x\, Q(x)\otimes\hat{\mathbb{1}} + \sum_{\alpha=1}^{N} R_\alpha(x)\otimes\hat{\psi}^\dagger_\alpha(x)\right], \tag{4.7}$$

where $\hat{U}(y,z) \in \mathbb{L}(\mathbb{H}\otimes\mathbb{C}^D)$ with $\mathbb{C}^D$ the ancilla space, *i.e.* it is a $D\times D$ matrix of operators. The matrix functions Q and R_α that appear in $\hat{U}(y,z)$ will always be clear from the context. If now the collective index i combines both virtual (matrix) indices (α,β), we define a general tangent vector $|\Phi[V,\{W_\alpha\};Q,\{R_\alpha\}]\rangle$ as

$$\begin{aligned}
|\Phi[V,\{W_\alpha\};Q,\{R_\alpha\}]\rangle &= |\Phi^{[Q,\{R_\alpha\}]}[V,\{W_\alpha\}]\rangle \\
&= \int_{-L/2}^{+L/2}\mathrm{d}x\left(V^i(x)\frac{\delta}{\delta Q^i(x)} + \sum_{\beta=1}^{N} W^i_\beta(x)\frac{\delta}{\delta R^i_\beta(x)}\right)|\Psi[Q,\{R_\alpha\}]\rangle \\
&= \int_{-L/2}^{+L/2}\mathrm{d}x\,\mathrm{tr}\left[B\hat{U}(-L/2,x)\left(V(x)\otimes\hat{\mathbb{1}} + \sum_{\beta=1}^{N} W_\beta(x)\otimes\hat{\psi}^\dagger_\beta(x)\right)\hat{U}(x,L/2)\right]|\Omega\rangle\,.
\end{aligned} \tag{4.8}$$

Note that by choosing $V = \mathbb{1}_D$ and $W_\alpha = 0$ ($\forall\alpha = 1,\ldots,N$) we obtain

$$|\Phi[V,\{W_\alpha\};Q,\{R_\alpha\}]\rangle = |\mathscr{R}|\,|\Psi[Q,\{R_\alpha\}]\rangle = L\,|\Psi[Q,\{R_\alpha\}]\rangle\,,$$

so that $|\Psi[Q,\{R_\alpha\}]\rangle \in \mathbb{T}_{\mathrm{cMPS}}[Q,\{R_\alpha\}]$. The orthogonal complement of $|\Psi[Q,\{R_\alpha\}]\rangle$ in $\mathbb{T}_{\mathrm{cMPS}}[Q,\{R_\alpha\}]$ is denoted as $\mathbb{T}^\perp_{\mathrm{cMPS}}[Q,\{R_\alpha\}]$.

1.1. The continuum limit of matrix product states

The continuous matrix product state $|\Psi[Q,\{R_\alpha\}]\rangle$ was originally constructed in [362] as the continuum limit of a certain subclass of matrix product states. Let us explain this construction in some more detail. We approximate the continuum $\mathscr{R}=[-L/2,L/2]$ by a lattice $\mathscr{L}$ with lattice spacing a and $N=L/a$ sites, where at the end we send $a\to 0$. On every site of the lattice we can create and annihilate particles of type α by acting with the creation and annihilation operators $\hat{c}^\dagger_\alpha(n)$ and $\hat{c}_\alpha(n)$. The local basis on site n thus consists of the states $|0\rangle_n$ (no particles), $|\alpha\rangle_n=c^\dagger_\alpha(n)|0\rangle_n$, $|\alpha,\beta\rangle_n=c^\dagger_\alpha(n)c^\dagger_\beta(n)|0\rangle_n$, … On this lattice, we can define a matrix product state $|\Psi[A]\rangle$ with matrices $A^s(n)$ where s can take values 0, α, (α,β), … If the local basis is infinite-dimensional, this matrix product state definition is only formal, *i.e.* it cannot be used for practical computations. In the limit $a\to 0$, the number of sites L/a in the lattice $\mathscr{L}$ goes to infinity. As we have concluded in the previous chapter, the matrix product state representation is not restricted to a single Fock space in the thermodynamic limit and different matrix product states are generally orthogonal due to the infrared orthogonality catastrophe. Since we now aim to create quantum field states within the Fock space $\mathbb{H}^{(\mathrm{F})}_{\mathscr{R}}$, we need to restrict to a special subclass of matrix product states where the total number of particles is finite (on average: so that $\langle\hat{N}\rangle$ is finite). Since a finite number of particles has to be distributed over a diverging number of sites L/a, most of the sites in the lattice $\mathscr{L}$ will on average be empty. So A^0 will have to be the dominant matrix, and it turns out that the continuous matrix product state $|\Psi[Q,\{R_\alpha\}]\rangle\in\mathbb{H}^{(\mathrm{F})}_{\mathscr{R}}$ can be obtained from the continuum limit ($a\to 0$) of the matrix product state $|\Psi[A]\rangle\in\mathbb{H}_{\mathscr{L}}$ by identifying $\hat{\psi}^\dagger_\alpha(na)=\hat{c}^\dagger_\alpha(n)/\sqrt{a}$ and

$$\begin{aligned}
A^0(n)&=\mathbb{1}_D+aQ(na),\\
A^\alpha(n)&=\sqrt{a}R_\alpha(na),\\
A^{(\alpha,\beta)}(n)&=\begin{cases}\frac{a}{2}[R_\alpha(na)R_\beta(na)+\eta_{\alpha,\beta}R_\beta(na)R_\alpha(na)], & \alpha\neq\beta\\ \frac{a}{2}R_\alpha(na)^2, & \alpha=\beta\end{cases}\\
&\ldots
\end{aligned}\tag{4.9}$$

together with $|\Omega\rangle=|\mathbf{0}\rangle=\otimes_{n\in\mathscr{L}}|0\rangle_n$, $\forall n=-L/2a,-L/2a+1,\ldots,+L/2a-1$. This equivalence can be obtained from a Taylor expansion of the exp-operator, and is only completely mathematically rigorous when the entries of Q and R_α are finite and the operators $\hat{\psi}^\dagger(x)$ are bounded (*i.e.* not for bosons). Most results for continuous matrix product states in the remainder of this chapter can be derived from this correspondence with matrix product states, but we aim to derive these results directly in the continuum as much as possible.

The correspondence with matrix product states is useful for concluding that the entanglement of one half of the chain with the other half (in the case of open boundary

conditions) is limited by the upper bound $\log D$. By restricting to matrix product states within a single Fock space in the thermodynamic limit, we avoid the orthogonality catastrophe. The infrared orthogonality catastrophe of matrix product states in the thermodynamic limit would turn into an ultraviolet catastrophe when this infinitely-sized lattice $\mathscr{L}$ would correspond to the continuum limit of a finitely sized continuum $\mathscr{R}$. Physically, this ultraviolet catastrophe is avoided because the finite number of particles induce a physical cutoff a_{phys} that is given, not by the lattice spacing $a \to 0$ but by $a_{\text{phys}} = \rho^{-d} = \rho^{-1}$ with $\rho = \langle \hat{N} \rangle / L$ the particle density. Note however that continuous matrix product states still obey the infrared orthogonality catastrophe when formulated in the thermodynamic limit (see Subsection 1.6). The presence of a physical length scale can be detected from the physical dimensions of Q and R_α, which are given by $[Q] = \ell^{-1}$ and $[R] = \ell^{-1/2}$ with ℓ a generic length dimension. The nature of the physical cutoff a_{phys} and its relation to Q and R_α is discussed in Subsection 1.6. Shifting the cutoff from the lattice spacing a to a physical value a_{phys} is a very important step in the definition of continuous matrix product states. Matrix product states with finite bond dimension D have a finite amount of entanglement to which corresponds in general a finite range of fluctuations ξ_c/a. Hence, they have in general a finite dimensionless correlation length $\tilde{\xi} = \xi_c/a$. As a is scaled to zero while $\tilde{\xi}$ remains finite, the physical correlation length ξ_c would also scale to zero. It is because the physical cutoff is shifted to a finite value a_{phys} (with thus $a_{\text{phys}}/a \to \infty$) that continuous matrix product states are able to combine a finite amount of entanglement with a finite physical correlation length ξ_c (with thus $\xi_c/a \to \infty$ but with ξ_c/a_{phys} finite). The physical correlation length ξ_c is computed in Subsection 1.6.

1.2. Alternative constructions

Rather than trying to construct a continuous matrix product state as the continuum limit of a matrix product state, we could also try to directly define the continuum limit of the processes that define matrix product states. Unfortunately, the process of sequential Schmidt decompositions has no straightforward generalization to the continuum and neither has the definition of valence bond solids. One can however define a continuum version of the sequential generation process that creates matrix product states, based on the paradigm of continuous measurement [363]. The resulting process for creating continuous matrix product states is described in [276].

Continuous matrix product states through continuous measurement

As in the discrete case, let the ancilla start in a state $v_R \in \mathbb{H}_{\text{ancilla}} = \mathbb{C}^D$. This ancilla can be interpreted as a resonating cavity with D internal levels, in which there is a particle source that creates particles of type α ($\alpha = 1, \ldots, N$). These particles gradually leave the cavity due to cavity losses. Since particles leaving the cavity at different times occupy different positions in space (since they travel at a certain speed which we set equal to one),

the resulting configuration of particles can be interpreted as a static spatially distributed quantum state. For a compact cavity (*i.e.* a zero-dimensional system), the resulting quantum state is one-dimensional. By abstracting the process, a $(d-1)$-dimensional cavity can be used to encode a d-dimensional holographic quantum state. We refer to [276] for the general case, and henceforth restrict to the $d=1$ case that produces continuous matrix product states.

Between two particle emissions, the cavity evolves according to a Hamiltonian $K \in \mathbb{L}(\mathbb{H}_{\text{ancilla}})$ (a Hermitean $D \times D$ matrix), whereas the physical state outside the cavity does not evolve. By observing the particles that are emitted from the cavity, we are continuously measuring the state of the cavity (*i.e.* ancilla). The process of continuous measurement as described in [363] also requires to be formulated as the continuum limit of a discrete process. Let thus the total Hamiltonian $\hat{H} \in \mathbb{L}(\mathbb{C}^D \otimes \mathbb{H})$ of the cavity (ancilla) and the physical system outside the cavity be given by

$$\begin{aligned}\hat{H}(t) = K(-t) \otimes \hat{\mathbb{1}}_D \\ + \sqrt{a} \sum_{n=-L/2a}^{L/2a-1} \delta(t-na) \sum_{\alpha=1}^{N} \mathrm{i}R_\alpha(-t) \otimes \hat{c}_\alpha^\dagger(-n) - \mathrm{i}R_\alpha(-t)^\dagger \otimes \hat{c}_\alpha(-n). \quad (4.10)\end{aligned}$$

A few remarks are in order. Firstly, this Hamiltonian is totally unrelated to any physical Hamiltonian for which the state of the physical system might approximate the ground state. This Hamiltonian models the evolution of the ancilla and its interaction with the physical system as a measurement process. The matrices K and R_α contain the variational parameters that make up the variational manifold of physical states. The measurement process is run for $t \in [-L/2, +L/2]$. The actual measurement by emission of particles is restricted to discrete times $t = na$, with $n = -L/2a, -L/2a+1, \ldots, +L/2a-1$. When a particle α is emitted (created) by $\hat{c}_\alpha^\dagger$ at time $t = na$, it ends up at spatial position $x = -t$ at the end of the process. The emission is accompanied by an interaction with the cavity, as dictated by the $D \times D$ matrix $R_\alpha(-t)$. The unitarity of quantum mechanical evolution requires that the Hamiltonian also contains the Hermitian conjugate term which absorbs a particle of type α at time $t = na$. Since the initial state outside the cavity was $|\Omega\rangle$, no particle will be present at time $t = na$ before one has been emitted. The interaction term in $\hat{H}(t)$ only implies that particles can be —but not necessarily have to be— emitted at every discrete time event $t = na$. In the end, we send $a \to 0$ in order to obtain a continuous measurement. Finally, the overall coupling strength of this interaction terms scales as $\sqrt{a}$, which can be motivated by the fact that a stronger coupling (lower power of a) would result in the quantum Zeno effect (continuous measurement of the ancilla state would prevent any evolution at all) whereas a weaker coupling (higher power of a) would result in trivial dynamics of the ancilla (no measurement or interaction at all). At the end of the measurement ($t = L$) we project the ancilla onto the state v_{L} in order to decouple it from the physical state. We hence obtain

$$|\Psi[Q,\{R_\alpha\}]\rangle = \lim_{a\to 0} \boldsymbol{v}_{\mathrm{L}}^\dagger \mathcal{T}\exp\left(-\mathrm{i}\int_{-L/2}^{+L/2} \mathrm{d}t\, \hat{H}(t)\right) \boldsymbol{v}_{\mathrm{R}}\,|\Omega\rangle =$$
$$\boldsymbol{v}_{\mathrm{L}}^\dagger \mathcal{P}\exp\left(-\mathrm{i}\int_{-L/2}^{+L/2} \mathrm{d}x\, K(x)\otimes\hat{\mathbb{1}} + \sum_{\alpha=1}^{N} \mathrm{i}R_\alpha(x)\otimes\hat{\psi}_\alpha^\dagger(x) - \mathrm{i}R_\alpha(x)^\dagger\otimes\hat{\psi}_\alpha(x)\right)\boldsymbol{v}_{\mathrm{R}}\,|\Omega\rangle\,,$$

where we have identified $\hat{c}_\alpha(n) = \sqrt{a}\,\hat{\psi}_\alpha(na)$ and introduced $x = -t$. Note that the time-ordered exponential $\mathcal{T}\exp$ orders its arguments increasingly from right to left, whereas the path-ordered exponential $\mathcal{P}\exp$ is here defined to order its arguments increasingly from left to right. The resulting expression does not yet correspond exactly to Eq. (4.3) but it can easily be brought in the required form. We therefore repartition the integral over $x\in[-L/2,+L/2]$ into infinitesimal patches $x\in[na-a/2,na+a/2]$ and use the Baker-Campbell-Hausdorff formula to prove

$$\begin{aligned}
&\exp\left(-\mathrm{i}\int_{na-a/2}^{na+a/2} \mathrm{d}x\, K(x)\otimes\hat{\mathbb{1}} + \sum_{\alpha=1}^{N} \mathrm{i}R_\alpha(x)\otimes\hat{\psi}_\alpha^\dagger(x) - \mathrm{i}R_\alpha(x)^\dagger\otimes\hat{\psi}_\alpha(x)\right)\\
&\quad= \exp\left(-\mathrm{i}\int_{na-a/2}^{na+a/2} \mathrm{d}x\, K(x)\otimes\hat{\mathbb{1}} + \sum_{\alpha=1}^{N} \mathrm{i}R_\alpha(x)\otimes\hat{\psi}_\alpha^\dagger(x)\right)\\
&\qquad\times \exp\left(+\mathrm{i}\int_{na-a/2}^{na+a/2} \mathrm{d}x\, \mathrm{i}R_\alpha(x)^\dagger\otimes\hat{\psi}_\alpha(x)\right)\\
&\qquad\times \exp\left(\frac{1}{2}\int_{na-a/2}^{na+a/2}\mathrm{d}x\int_{na-a/2}^{na+a/2}\mathrm{d}y \sum_{\alpha=1}^{N}\left[\mathrm{i}R_\alpha(x)^\dagger\otimes\hat{\psi}_\alpha(x), K(y)\otimes\hat{\mathbb{1}}\right]\right.\\
&\qquad\qquad\left. + \sum_{\alpha,\beta=1}^{N}\left[\mathrm{i}R_\alpha(x)^\dagger\otimes\hat{\psi}_\alpha(x), \mathrm{i}R_\beta(y)\otimes\hat{\psi}_\beta^\dagger(y)\right] + \dots\right)\\
&\quad= \exp\left(-\mathrm{i}\int_{na-a/2}^{na+a/2} \mathrm{d}x\, K(x)\otimes\hat{\mathbb{1}} + \sum_{\alpha=1}^{N} \mathrm{i}R_\alpha(x)\otimes\hat{\psi}_\alpha^\dagger(x)\right)\\
&\qquad\times \exp\left(+\mathrm{i}\int_{na-a/2}^{na+a/2} \mathrm{d}x\, \mathrm{i}R_\alpha(x)^\dagger\otimes\hat{\psi}_\alpha(x)\right)\\
&\qquad\times \exp\left(-\frac{1}{2}\int_{na-a/2}^{na+a/2}\mathrm{d}x \sum_{\alpha=1}^{N} R_\alpha^\dagger(x)R_\alpha(x)\otimes\hat{\mathbb{1}}\right.\\
&\qquad\qquad + \frac{1}{2}\int_{na-a/2}^{na+a/2}\mathrm{d}x\int_{na-a/2}^{na+a/2}\mathrm{d}y \sum_{\alpha=1}^{N}\left[\mathrm{i}R_\alpha(x)^\dagger, K(y)\right]\otimes\hat{\psi}_\alpha(x)\\
&\qquad\qquad \left. + \frac{1}{2}\int_{na-a/2}^{na+a/2}\mathrm{d}x\int_{na-a/2}^{na+a/2}\mathrm{d}y \sum_{\alpha,\beta=1}^{N}\left[\mathrm{i}R_\alpha^\dagger(x), \mathrm{i}R_\beta(y)\right]_\pm \otimes \hat{\psi}_\beta^\dagger(y)\hat{\psi}_\alpha(x) + \dots\right).
\end{aligned}$$

The dots $(\dots)$ in this equation represent higher order terms, which all produce corrections of $\mathcal{O}(a^2)$ or higher and are unimportant when we restore $a\to 0$. Note that we do not need to use a path-ordered exponential since these infinitesimal patches are assumed

to be ordered correctly (*i.e.* with n increasing from left to right). This partition into infinitesimally small patches that are correctly ordered is precisely the definition of the path-ordered exponential. Since this operator is going to act on $|\Omega\rangle$, all terms that end with $\hat{\psi}_\alpha(x)$ do not contribute at $\mathcal{O}(a)$ and we can write

$$\exp\left(-\mathrm{i}\int_{na-a/2}^{na+a/2}\mathrm{d}x\,K(x)\otimes\hat{\mathbb{1}}+\sum_{\alpha=1}^{N}\mathrm{i}R_\alpha(x)\otimes\hat{\psi}_\alpha^\dagger(x)-\mathrm{i}R_\alpha(x)^\dagger\otimes\hat{\psi}_\alpha(x)\right)|\Omega\rangle=$$
$$\exp\left(\int_{na-a/2}^{na+a/2}\mathrm{d}x\,\left[-\mathrm{i}K(x)-\frac{1}{2}\sum_{\alpha=1}^{N}R_\alpha(x)^\dagger R_\alpha(x)\right]\otimes\hat{\mathbb{1}}+\sum_{\alpha=1}^{N}\mathrm{i}R_\alpha(x)\otimes\hat{\psi}_\alpha^\dagger(x)\right)|\Omega\rangle,$$

which eventually leads to

$$|\Psi[Q,\{R_\alpha\}]\rangle=\boldsymbol{v}_{\mathrm{L}}^\dagger\mathcal{P}\exp\left(\int_{-L/2}^{+L/2}\mathrm{d}x\,Q(x)\otimes\hat{\mathbb{1}}+\sum_{\alpha=1}^{N}R_\alpha(x)\otimes\hat{\psi}_\alpha^\dagger(x)\right)\boldsymbol{v}_{\mathrm{R}}|\Omega\rangle \tag{4.11}$$

with

$$Q(x)=-\mathrm{i}K(x)-\frac{1}{2}\sum_{\alpha=1}^{N}R_\alpha(x)^\dagger R_\alpha(x). \tag{4.12}$$

This construction allows to introduce a unitary operator $\hat{U}(y,z)\in\mathbb{L}(\mathbb{C}^D\otimes\mathbb{H})$

$$\hat{U}(y,z)=\mathcal{P}\exp\left(-\mathrm{i}\int_z^y\mathrm{d}x\,K(x)\otimes\hat{\mathbb{1}}+\sum_{\alpha=1}^{N}\mathrm{i}R_\alpha(x)\otimes\hat{\psi}_\alpha^\dagger(x)-\mathrm{i}R_\alpha(x)^\dagger\otimes\hat{\psi}_\alpha(x)\right). \tag{4.13}$$

As proven above, the former operator is equivalent to the operator $\hat{U}(y,z)$ defined in Eq. (4.7) only when acting on the empty physical vacuum $|\Omega\rangle$. But where the latter is not unitary in general, the former is. The unitary operator in Eq. (4.13) conserves the norm of $\boldsymbol{v}_{\mathrm{R}}\otimes|\Omega\rangle$. This does not imply that the continuous matrix product state $|\Psi[Q,\{R_\alpha\}]\rangle$ is automatically normalized to unity, because the definition also involves a projection to $\boldsymbol{v}_{\mathrm{L}}$. But the unitarity of $\hat{U}(y,z)$ in Eq. (4.13) does guarantee that $|\Psi[Q,\{R_\alpha\}]\rangle$ can easily be normalized and has no norm that diverges or goes to zero in the large volume limit. We return to the specific parameterization of $Q(x)$ as in Eq. (4.12) with K a Hermitian matrix in Subsection 1.5.

From a physical perspective, this construction is important as it clearly sketches the holographic properties of the continuous matrix product state. The physical state of a one-dimensional system is described by a zero-dimensional boundary theory. The spatial coordinate of the physical system acts as a time coordinate in the boundary theory. The physical state is created because the boundary theory interacts with the physical system, where the position of the interaction shifts linearly in time. This interaction results in the boundary theory not being at equilibrium, as will become clear in the following subsections. This holographic property is of course strongly related with the intrinsic

area law for entanglement that is present in continuous matrix product states.

Continuous matrix product states and exactly solvable models

As for matrix product states, it has been established in [364] that the Bethe ansatz solution of an exactly solvable model can be written in terms of a continuous matrix product state representation. We do not further explore this connection.

1.3. Regularity properties

In Eq. (4.6) we have defined the k-particle wave functions $\phi_{\alpha_1,\ldots,\alpha_k}(x_1,\ldots,x_k)$. For $x_1 \leq \cdots \leq x_k$ these are completely specified by Eq. (4.5). However, for general choices of the matrix functions Q and R_α, the extension of Eq. (4.5) to all orders of its arguments will not satisfy the required properties that a physical k-particle wave function should satisfy. For example, the k-particle wave functions should be differentiable in each of its arguments if the state has to produce a finite kinetic energy.

We can check the regularity of the k-particle wave functions by immediately evaluating the kinetic energy in second quantization. The kinetic energy operator $\hat{T}$ is given by

$$\hat{T} = \int_{-L/2}^{+L/2} \hat{t}(x)\,\mathrm{d}x, \tag{4.14}$$

where the kinetic energy density $\hat{t}(x)$ at position x is given by

$$\hat{t}(x) = \sum_{\alpha=1}^{N} \frac{1}{2m_\alpha} \left(\frac{\mathrm{d}\hat{\psi}_\alpha^\dagger}{\mathrm{d}x}(x)\right)\left(\frac{\mathrm{d}\hat{\psi}_\alpha}{\mathrm{d}x}(x)\right). \tag{4.15}$$

Let us try to compute the kinetic energy expectation value $\langle\Psi[\overline{Q},\{\overline{R}_\alpha\}]|\hat{T}|\Psi[Q,\{R_\alpha\}]\rangle$ by first evaluating

$$\hat{\psi}_\alpha(x)|\Psi[Q,\{R_\beta\}]\rangle = \mathrm{tr}\left[B\hat{V}_\alpha(-L/2,x)R_\alpha(x)\hat{U}(x,+L/2)\right]|\Omega\rangle,$$

with $\hat{U}(y,z)$ given in Eq. (4.7) and $\hat{V}_\alpha(y,z) \in \mathbb{L}(\mathbb{C}^D \otimes \mathbb{H})$ similarly defined as

$$\hat{V}_\alpha(y,z) = \mathcal{P}\exp\left[\int_y^z \mathrm{d}x\, Q(x)\otimes\hat{\mathbb{1}} + \sum_{\beta=1}^{N}\eta_{\alpha,\beta}R_\beta(x)\otimes\hat{\psi}_\beta^\dagger(x)\right]. \tag{4.16}$$

It is clear that $\hat{\psi}_\alpha(x)\hat{U}(y,z) = \hat{V}_\alpha(y,z)\hat{\psi}_\alpha(x)$ if $x \notin [y,z]$. We can easily derive

$$\frac{\mathrm{d}}{\mathrm{d}y}\hat{U}(y,z) = -\left(Q(y)\otimes\hat{\mathbb{1}} + \sum_{\alpha=1}^{N} R_\alpha(y)\otimes\hat{\psi}_\alpha^\dagger(y)\right)\hat{U}(y,z),$$

$$\frac{\mathrm{d}}{\mathrm{d}z}\hat{U}(y,z) = +\hat{U}(y,z)\left(Q(z)\otimes\hat{\mathbb{1}} + \sum_{\alpha=1}^{N} R_\alpha(z)\otimes\hat{\psi}^\dagger_\alpha(z)\right),$$
$$\frac{\mathrm{d}}{\mathrm{d}y}\hat{V}_\alpha(y,z) = -\left(Q(y)\otimes\hat{\mathbb{1}} + \sum_{\beta=1}^{N}\eta_{\alpha,\beta}R_\beta(y)\otimes\hat{\psi}^\dagger_\beta(y)\right)\hat{V}_\alpha(y,z),$$
$$\frac{\mathrm{d}}{\mathrm{d}z}\hat{V}_\alpha(y,z) = +\hat{V}_\alpha(y,z)\left(Q(z)\otimes\hat{\mathbb{1}} + \sum_{\beta=1}^{N}\eta_{\alpha,\beta}R_\beta(z)\otimes\hat{\psi}^\dagger_\beta(z)\right),$$

which we can use to obtain

$$\begin{aligned}\frac{\mathrm{d}}{\mathrm{d}x}&\hat{\psi}_\alpha(x)|\Psi[Q,\{R_\beta\}]\rangle \\ &= \mathrm{tr}\left[B\hat{V}_\alpha(-L/2,x)\left([Q(x),R_\alpha(x)] + \frac{\mathrm{d}R_\alpha}{\mathrm{d}x}(x)\right)\hat{U}(x,+L/2)\right]|\Omega\rangle \\ &\quad + \mathrm{tr}\left[B\hat{V}_\alpha(-L/2,x)\left(\sum_{\beta=1}^{N}\left[\eta_{\alpha,\beta}R_\beta(x)R_\alpha(x)\right.\right.\right. \\ &\qquad\qquad \left.\left.\left. - R_\alpha(x)R_\beta(x)\right]\otimes\hat{\psi}^\dagger_\beta(x)\right)\hat{U}(x,+L/2)\right]|\Omega\rangle\,. \quad (4.17)\end{aligned}$$

Different terms in the expectation value of the kinetic energy density $\hat{t}(x)$ are proportional to

$$\langle\Psi[\overline{Q},\{\overline{R}_\alpha\}]|(\mathrm{d}\hat{\psi}^\dagger(x)/\mathrm{d}x)(\mathrm{d}\hat{\psi}(x)/\mathrm{d}x)|\Psi[Q,\{R_\alpha\}]\rangle = \|(\mathrm{d}\hat{\psi}(x)/\mathrm{d}x)|\Psi[Q,\{R_\alpha\}]\rangle\|^2.$$

Since the term on the second line of Eq. (4.17) has particles of any species $\beta = 1,\ldots,N$ being created at the fixed position x, this term is not normalizable. Put differently, $\|(\mathrm{d}\hat{\psi}(x)/\mathrm{d}x)|\Psi[Q,\{R_\alpha\}]\rangle\|^2$ contains a divergent contribution $\delta(0)$ (in position space), unless we impose

$$\eta_{\alpha,\beta}R_\beta(x)R_\alpha(x) - R_\alpha(x)R_\beta(x) = 0, \quad \forall x\in\mathscr{R}. \quad (4.18)$$

Hence the matrices R_α should have the same statistics as the particle creation operators to which they couple. For systems with a single species of bosons, the *regularity condition* in Eq. (4.18) is automatically fulfilled. For systems with multiple species of bosons, it requires that any two matrices $R_\alpha(x)$ and $R_\beta(x)$ at the same spatial point x commute. If α is a fermionic particle species, the corresponding matrix $R_\alpha(x)$ has to satisfy $R_\alpha(x)^2 = 0$, $\forall x\in\mathscr{R}$. When two particles of fermionic type α approach each other, there is a corresponding factor $R_\alpha(y)\mathcal{P}\exp(\int_y^z \mathrm{d}x\, Q(x))R_\alpha(z)$ in the k-particle wave function $\phi_{\alpha_1,\ldots,\alpha,\alpha,\ldots\alpha_k}(x_1,\ldots,y,z,\ldots,x_k)$. For $y\to z$, the exponential factor continuously evolves towards $\mathbb{1}_D$, so that the k-particle wave function continuously becomes zero. Hence, the finiteness of the kinetic energy requires that two fermionic particles of the same type

cannot come arbitrarily close together and thus imposes Pauli's principle.

Differentiability of the wave function is sufficient for a finite kinetic energy, which is by far the most important physical requirement of the wave function. It is also possible to impose higher regularity constraints on the k-particle wave functions. Assuming that Eq. (4.18) is fulfilled, the second order derivative $(\mathrm{d}^2\hat{\psi}_\alpha(x)/\mathrm{d}x^2)|\Psi[Q,\{R_\beta\}]\rangle$ contains a contribution with infinite norm unless

$$\left[\frac{\mathrm{d}R_\alpha}{\mathrm{d}x}(x)+[Q(x),R_\alpha(x)],R_\beta(x)\right]_\mp=0, \tag{4.19}$$

where $[\cdot,\cdot]_\mp$ is a commutator $(-)$ or anticommutator $(+)$ for $\eta=\pm1$. If Q and R_α obey all equations to have a 'well defined' derivative up to order n, so that the state $(\mathrm{d}^n\hat{\psi}(x)/\mathrm{d}x^n)|\Psi[Q,\{R_\beta\}]\rangle$ is normalizable, the sufficient condition to eliminate all harmful contributions from $(\mathrm{d}^{n+1}\hat{\psi}(x)/\mathrm{d}x^{n+1})|\Psi[Q,\{R_\beta\}]\rangle$ is

$$\begin{aligned}\Bigg[\frac{\mathrm{d}^n}{\mathrm{d}x^n}R_\alpha(x)+\frac{\mathrm{d}^{n-1}}{\mathrm{d}x^{n-1}}[Q(x),R_\alpha(x)]+\frac{\mathrm{d}^{n-2}}{\mathrm{d}x^{n-2}}[Q(x),[Q(x),R_\alpha(x)]]\\ +\ldots+[Q(x),[\ldots,[Q(x),R(x)]]\ldots],R_\beta(x)\Bigg]_\mp=0.\end{aligned} \tag{4.20}$$

We can also impose regularity of the mixed derivatives of the k-particle wave function, by first evaluating $\hat{\psi}_\alpha(x)\hat{\psi}_\beta(y)|\Psi[Q,\{R_\gamma\}]\rangle$

$$\begin{aligned}&\hat{\psi}_\alpha(x)\hat{\psi}_\beta(y)|\Psi[Q,\{R_\gamma\}]\rangle=\\ &\quad\theta(y-x)\mathrm{tr}\left[B\hat{W}_{\alpha,\beta}(-L/2,x)\eta_{\beta,\alpha}R_\alpha(x)\hat{V}_\beta(x,y)R_\beta(y)\hat{U}(y,+L/2)\right]|\Omega\rangle\\ &\quad+\theta(x-y)\mathrm{tr}\left[B\hat{W}_{\alpha,\beta}(-L/2,y)R_\beta(y)\hat{V}_\alpha(y,x)R_\alpha(x)\hat{U}(x,+L/2)\right]|\Omega\rangle\end{aligned}$$

with

$$\hat{W}_{\alpha,\beta}(y,z)=\mathcal{P}\exp\left[\int_y^z\mathrm{d}x\,Q(x)\otimes\hat{\mathbb{1}}+\sum_{\gamma=1}^N\eta_{\alpha,\gamma}\eta_{\beta,\gamma}R_\gamma(x)\otimes\hat{\psi}_\gamma^\dagger(x)\right]. \tag{4.21}$$

Note that the regularity condition in Eq. (4.18) is sufficient for the annihilation of two particles $\hat{\psi}_\alpha(x)\hat{\psi}_\beta(y)|\Psi[Q,\{R_\gamma\}]\rangle$ to be continuous at $x=y$. By firstly differentiating to x, we obtain

$$\begin{aligned}&\left(\frac{\mathrm{d}\hat{\psi}_\alpha}{\mathrm{d}x}(x)\right)\hat{\psi}_\beta(y)|\Psi[Q,\{R_\gamma\}]\rangle\\ &=\theta(y-x)\mathrm{tr}\left[B\hat{W}_{\alpha,\beta}(-L/2,x)\eta_{\beta,\alpha}\left(\frac{\mathrm{d}R_\alpha}{\mathrm{d}x}(x)+\left[Q(x),R_\alpha(x)\right]\right)\right.\end{aligned}$$

$$\times \hat{V}_\beta(x,y)R_\beta(y)\hat{U}(y,+L/2)\Big]\,|\Omega\rangle$$
$$+\theta(x-y)\,\mathrm{tr}\Big[B\hat{W}_{\alpha,\beta}(-L/2,y)R_\beta(y)\hat{V}_\alpha(y,x)$$
$$\times\Big(\frac{\mathrm{d}R_\alpha}{\mathrm{d}x}(x)+[Q(x),R_\alpha(x)]\Big)\hat{U}(x,+L/2)\Big]\,|\Omega\rangle\,,$$

where we have assumed the regularity condition in Eq. (4.18) to hold. This allows to eliminate the fixed insertion of particles at position x as well as the terms obtained from differentiating the Heaviside functions (*i.e.* the therms proportional to $\delta(x-y)$). Such terms would indeed arise if $\hat{\psi}_\alpha(x)\hat{\psi}_\beta(y)|\Psi[Q,\{R_\gamma\}]\rangle$ were not continuous at $x=y$. If we now also differentiate with respect to y, we obtain a divergent contribution

$$-\delta(x-y)\,\mathrm{tr}\Big[B\hat{W}_{\alpha,\beta}(-L/2,x)\Big[R_\beta(x),\frac{\mathrm{d}R_\alpha}{\mathrm{d}x}(x)+[Q(x),R_\alpha(x)]\Big]_\mp\hat{U}(x,+L/2)\Big]\,|\Omega\rangle\,.$$

If we differentiated with respect to y first, and then to x, the divergent contribution is

$$\delta(x-y)\,\mathrm{tr}\Big[B\hat{W}_{\alpha,\beta}(-L/2,x)\Big[\frac{\mathrm{d}R_\beta}{\mathrm{d}x}(x)+[Q(x),R_\beta(x)],R_\alpha(x)\Big]_\mp\hat{U}(x,+L/2)\Big]\,|\Omega\rangle\,.$$

Since we are working under assumption of the regularity condition $[R_\beta(x),R_\alpha(x)]_\mp=0$ [Eq. (4.18)], it is easy to show that $[R_\beta(x),\mathrm{d}R_\alpha(x)/\mathrm{d}x]_\mp=-[\mathrm{d}R_\beta(x)/\mathrm{d}x,R_\alpha(x)]$ and also $[R_\beta(x),[Q(x),R_\alpha(x)]]_\mp=-[[Q(x),R_\beta(x)],R_\alpha(x)]_\mp$, so that both diverging contributions are equal. By imposing

$$\Big[\frac{\mathrm{d}R_\beta}{\mathrm{d}x}(x)+[Q(x),R_\beta(x)],R_\alpha(x)\Big]_\mp=-\Big[R_\beta(x),\frac{\mathrm{d}R_\alpha}{\mathrm{d}x}(x)+[Q(x),R_\alpha(x)]\Big]_\mp=0 \tag{4.22}$$

the mixed derivative $(\mathrm{d}\hat{\psi}_\alpha(x)/\mathrm{d}x)(\mathrm{d}\hat{\psi}_\beta(y)/\mathrm{d}y)|\Psi[Q(x),\{R_\gamma\}]\rangle$ is well defined and normalizable.

We conclude this subsection by investigating what else can be learned from the physical considerations concerning particle statistics. The regularity conditions [Eq. (4.18)] already require that the matrices R_α behave as the corresponding operators $\hat{\psi}_\alpha$ in terms of commutation and anticommutation relations. In a physical system, we should not have fermionic condensates, *i.e.* $\langle\Psi|\hat{\psi}_\alpha(x)|\Psi\rangle=0$ if particle species α is fermionic. This is a consequence of the invariance of an physical Hamiltonian $\hat{H}$ under the action of the parity operator $\hat{P}$, which flips the sign of any fermionic operator ($\hat{P}\hat{\psi}_\alpha(x)\hat{P}=\eta_{\alpha,\alpha}\hat{\psi}_\alpha(x)$) and is thus idempotent ($\hat{P}=\hat{P}^{-1}=\hat{P}^\dagger$). Note that $\hat{P}$ is not equivalent to the spatial parity (reflection) operator $\hat{\Pi}$ introduced in Subsection 1.4 of Chapter 1, which is not

necessarily idempotent for fermionic systems. We can construct $\hat{P}$ as

$$\hat{P} = \exp\left[\mathrm{i}\pi \sum_{\alpha \text{ fermionic}} \hat{N}_\alpha\right] = \exp\left[\mathrm{i}\pi \sum_{\alpha \text{ fermionic}} \int_{\mathscr{R}} \mathrm{d}x\, \hat{\psi}^\dagger_\alpha(x)\hat{\psi}_\alpha(x)\right]. \tag{4.23}$$

Physical states satisfy $\hat{P}|\Psi\rangle = \mathrm{e}^{\mathrm{i}\phi}|\Psi\rangle$, where the idempotence of $\hat{P}$ requires $\phi = 0$ or $\phi = \pi$. Physical states thus consist completely of a superposition of states, all of which have either an even or an odd number of fermions. Imposing this same property for continuous matrix product states requires to explicitly incorporate the $\mathbb{Z}_2$ symmetry (with group elements $\{\hat{\mathbb{1}}, \hat{P}\}$) in the matrix structure of R_α and Q. Since $\hat{P}|\Psi[Q,\{R_\alpha\}]\rangle = |\Psi[Q,\{\eta_{\alpha,\alpha}R_\alpha\}]\rangle$, we should also be able to define a virtual operator $P \in \mathbb{L}(\mathbb{C}^D)$ such that $PQP^{-1} = Q$ and $PR_\alpha P^{-1} = \eta_{\alpha,\alpha}R_\alpha$. This operator can in principle be x-dependent, but we should then be able to apply a local gauge transformation (see Subsection 1.5) in order to make P space-independent. In addition, it is clear from the definition that P is idempotent ($P = P^{-1}$). If we can assume that P is diagonalizable, then P divides the ancilla space $\mathbb{C}^D$ into a sector with positive parity (eigenspace of eigenvalue $+1$) and a sector with negative parity (eigenspace of -1). A global gauge transformation brings P into the diagonal form

$$P = \begin{bmatrix} \mathbb{1}_{D^{(+)}} & 0_{D^{(+)}\times D^{(-)}} \\ 0_{D^{(-)}\times D^{(+)}} & -\mathbb{1}_{D^{(-)}} \end{bmatrix} \tag{4.24}$$

with $D^{(+)} + D^{(-)} = D$. The required transformation behavior of Q and R_α then requires the following decomposition

$$Q = \begin{bmatrix} Q^{(+)} & 0_{D^{(+)}\times D^{(-)}} \\ 0_{D^{(-)}\times D^{(+)}} & Q^{(-)} \end{bmatrix}, \tag{4.25}$$

$$R_\alpha = \begin{bmatrix} R_\alpha^{(+)} & 0_{D^{(+)}\times D^{(-)}} \\ 0_{D^{(-)}\times D^{(-)}} & R_\alpha^{(-)} \end{bmatrix} \qquad \text{(particle species } \alpha \text{ is bosonic)}, \tag{4.26}$$

$$R_\alpha = \begin{bmatrix} 0_{D^{(+)}\times D^{(+)}} & R_\alpha^{(+-)} \\ R_\alpha^{(-+)} & 0_{D^{(-)}\times D^{(-)}} \end{bmatrix} \qquad \text{(particle species } \alpha \text{ is fermionic)}. \tag{4.27}$$

In the continuous matrix product state $|\Psi[Q,\{R_\alpha\}]\rangle$, all contributions with either an even or an odd number of fermions in Eq. (4.4) drop out, depending on the boundary matrices B. If only states with an even number of fermions are allowed, B should have a decomposition as

$$B = \begin{bmatrix} B^{(+)} & 0_{D^{(+)}\times D^{(-)}} \\ 0_{D^{(-)}\times D^{(+)}} & B^{(-)} \end{bmatrix}, \tag{4.28}$$

whereas a decomposition of the form

$$B = \begin{bmatrix} 0_{D^{(+)}\times D^{(+)}} & B_\alpha^{(+-)} \\ B_\alpha^{(-+)} & 0_{D^{(-)}\times D^{(-)}} \end{bmatrix} \tag{4.29}$$

is required to select only states with an odd number of fermions.

1.4. Computation of expectation values

The analog of the transfer matrix $\breve{E}(n) = \breve{E}_{\mathbb{1}}(n)$ of the matrix product state $|\Psi[A]\rangle$ (see Subsection 1.4 of the previous chapter) for the continuous matrix product state $|\Psi[Q,\{R_\alpha\}]\rangle$ is given by the transfer matrix $\breve{T}$ defined as

$$\breve{T}(x) = Q(x)\otimes \mathbb{1}_D + \mathbb{1}_D \otimes \overline{Q(x)} + \sum_{\alpha=1}^{N} R_\alpha(x)\otimes \overline{R_\alpha(x)}. \tag{4.30}$$

To this transfer matrix, we can also associate linear maps $\mathcal{T}^{(x)} : \mathbb{L}(\mathbb{C}^D) \mapsto \mathbb{L}(\mathbb{C}^D)$ and $\widetilde{\mathcal{T}}^{(x)} : \mathbb{L}(\mathbb{C}^D) \mapsto \mathbb{L}(\mathbb{C}^D)$ that maps virtual operators f ($D\times D$ matrices) as

$$\mathcal{T}^{(x)}(f) = Q(x)f + fQ(x)^\dagger + \sum_{\alpha=1}^{N} R_\alpha(x) f R_\alpha(x)^\dagger, \tag{4.31}$$

$$\widetilde{\mathcal{T}}^{(x)}(f) = fQ(x) + Q(x)^\dagger f + \sum_{\alpha=1}^{N} R_\alpha(x)^\dagger f R_\alpha(x). \tag{4.32}$$

If $|\Psi[A]\rangle$ is the matrix product state with matrices A as in Eq. (4.9), then the transfer operator $\breve{T}(x)$ is related to the transfer operator $\breve{E}(n)$ of the matrix product state $|\Psi[A]\rangle$ by $\breve{E}(n) = \breve{\mathbb{1}} + a\breve{T}(na) + \mathcal{O}(a^2)$. The normalization of the continuous matrix product state $|\Psi[Q,\{R_\alpha\}]\rangle$ is given by

$$\langle\Psi[\overline{Q},\{\overline{R}_\alpha\}]|\Psi[Q,\{R_\alpha\}]\rangle = \operatorname{tr}\left[\left(B\otimes\overline{B}\right)\mathcal{P}\exp\left(\int_{-L/2}^{+L/2}\breve{T}(x)\,\mathrm{d}x\right)\right] \tag{4.33}$$

The expectation value of any normally ordered operator $\hat{O} =: O[\{\hat{\psi}_\alpha^\dagger\},\{\hat{\psi}_\beta\}] :$ can be computed by first acting with all annihilation operators $\hat{\psi}_\alpha(x)$ on $|\Psi[Q,\{R_\beta\}]\rangle$ as we did in the previous subsection. We therefore use

$$\hat{\psi}_\alpha(x)\hat{U}(y,z) = \hat{V}_\alpha(y,z)R_\alpha(x)\hat{U}(x,z) + \eta_{\alpha,\alpha}\hat{V}_\alpha(y,z)\hat{\psi}_\alpha(x) \tag{4.34}$$

where the second term does not contribute since it acts on $|\Omega\rangle$. Similarly applying all creation operators $\hat{\psi}_\alpha^\dagger(x)$ in $\hat{O}$ to $\langle\Psi[\overline{Q},\{\overline{R}_\beta\}]|$, we can then evaluate the overlap. We

therefore generalize the definition of the transfer operator as

$$\check{T}_\alpha(x) = Q(x)\otimes \mathbb{1}_D + \mathbb{1}_D \otimes \overline{Q(x)} + \sum_{\beta=1}^{N} \eta_{\alpha,\beta} R_\gamma(x) \otimes \overline{R_\gamma(x)}, \tag{4.35}$$

$$\check{T}_{\alpha,\beta}(x) = Q(x)\otimes \mathbb{1}_D + \mathbb{1}_D \otimes \overline{Q(x)} + \sum_{\gamma=1}^{N} \eta_{\alpha,\gamma}\eta_{\beta,\gamma} R_\gamma(x) \otimes \overline{R_\gamma(x)}. \tag{4.36}$$

Note that $\check{T}_{\alpha,\alpha}(x) = \check{T}(x)$ since $\eta_{\alpha,\beta}^2 = 1$. We can for example evaluate the correlation function

$$\begin{aligned} G^{\alpha,\beta}(x,y) &= \langle \Psi[\overline{Q},\{\overline{R}_\alpha\}] | \hat{\psi}_\alpha^\dagger(x)\hat{\psi}_\beta(y) \Psi[Q,\{R_\alpha\}]\rangle \\ &= \theta(x-y)\,\mathrm{tr}\Big[\big(B\otimes\overline{B}\big)\mathcal{P}\mathrm{e}^{\int_{-L/2}^{+x}\check{T}_{\alpha,\beta}(z)\mathrm{d}z} \big(R_\beta(y)\otimes\mathbb{1}_D\big)\mathcal{P}\mathrm{e}^{\int_y^x \check{T}_\alpha(z)\mathrm{d}z} \\ &\qquad\qquad \times \big(\mathbb{1}_D\otimes\overline{R_\alpha(x)}\big)\mathcal{P}\mathrm{e}^{\int_x^{+L/2}\check{T}(z)\mathrm{d}z}\Big] \\ &\quad + \theta(y-x)\,\mathrm{tr}\Big[\big(B\otimes\overline{B}\big)\mathcal{P}\mathrm{e}^{\int_{-L/2}^{+x}\check{T}_{\alpha,\beta}(z)\mathrm{d}z} \big(\mathbb{1}_D\otimes\overline{R_\alpha(x)}\big)\mathcal{P}\mathrm{e}^{\int_x^y \check{T}_\beta(z)\mathrm{d}z} \\ &\qquad\qquad \times \big(R_\beta(y)\otimes\mathbb{1}_D\big)\mathcal{P}\mathrm{e}^{\int_y^{+L/2}\check{T}(z)\mathrm{d}z}\Big]. \end{aligned} \tag{4.37}$$

Note that all quantities in this expression, even if we could store and manipulate variables with a fully continuous x-dependence, are $D^2\times D^2$ matrices. Since such matrices need to be multiplied, this is an operation with computational complexity of $\mathcal{O}(D^6)$, or $\mathcal{O}(D^5)$ if we exploit the tensor product structure.

For physical systems, we can further simplify Eq. (4.37). When only bosonic particle species are present, all $\eta_{\alpha,\beta}=1$ and $\check{T}=\check{T}_\alpha=\check{T}_{\alpha,\beta}$. In case of the presence of fermionic particle species, we should incorporate the $\mathbb{Z}_2$ parity symmetry discussed in the previous subsection. We can then define an idempotent parity superoperator $\check{P}=P\otimes\overline{P}$ and we obtain $\check{P}\check{T}\check{P}=\check{T}$, as well as $\check{P}\check{T}_\alpha\check{P}=\check{T}_\alpha$ and $\check{P}\check{T}_{\alpha,\beta}\check{P}=\check{T}_{\alpha,\beta}$. This allows to conclude that $\langle\Psi[\overline{Q},\{\overline{R}_\alpha\}]|\hat{\psi}_\alpha^\dagger(x)\hat{\psi}_\beta(y)|\Psi[Q,\{R_\alpha\}]\rangle = 0$ if only one of the two particle species α or β is of fermionic nature. But when α and β are both bosonic or both fermionic, $\check{T}_{\alpha,\beta}=\check{T}$ and $\check{T}_\alpha=\check{T}_\beta$.

In case of open boundary conditions, we can define virtual density matrices $l(x), r(x)\in \mathbb{L}(\mathbb{C}^D)$ which are defined through the initial conditions $l(-L/2)=\boldsymbol{v}_\mathrm{L}\boldsymbol{v}_\mathrm{L}^\dagger$ and $r(+L/2)=\boldsymbol{v}_\mathrm{R}\boldsymbol{v}_\mathrm{R}^\dagger$ and the first order differential equation

$$\frac{\mathrm{d}}{\mathrm{d}x}l(x) = \widetilde{\mathcal{T}}^{(x)}\big(l(x)\big), \qquad\qquad \frac{\mathrm{d}}{\mathrm{d}x}r(x) = -\mathcal{T}^{(x)}\big(r(x)\big). \tag{4.38}$$

To these density matrices $l(x)$ and $r(x)$ we associate vectors $|l(x)\rangle\!\rangle, |r(x)\rangle\!\rangle \in \mathbb{C}^D\otimes\overline{\mathbb{C}^D}$ in

the ancilla product space. Formally, the solution is given by

$$(l(x)| = (l(-L/2)|\mathcal{P}\mathrm{e}^{\int_{-L/2}^{x}\breve{T}(y)\,\mathrm{d}y},$$
$$|r(x)) = \mathcal{P}\mathrm{e}^{\int_{x}^{+L/2}\breve{T}(y)\,\mathrm{d}y}|r(+L/2)).$$

We can hence write

$$\langle\Psi[\overline{Q},\{\overline{R}_\alpha\}]|\Psi[Q,\{R_\alpha\}]\rangle = \left(l(-L/2)\middle|\mathcal{P}\exp\left[\int_{-L/2}^{+L/2}\breve{T}(x)\,\mathrm{d}x\right]\middle|r(+L/2)\right)$$
$$= (l(x)|r(x)) = \mathrm{tr}\left[l(x)r(x)\right], \quad \forall x\in\mathscr{R}. \tag{4.39}$$

From the correspondence with completely positive maps, it can be shown that both maps $\mathcal{T}^{(x)}$ and $\widetilde{\mathcal{T}}^{(x)}$ preserve the positivity of the virtual density matrices $l(x)$ and $r(x)$, so that the norm is guaranteed to be positive. Note that, for the special parameterization of $Q(x)$ in the continuous measurement interpretation [Eq. (4.12)], we can write the determining differential equation for $r(x)$ as

$$\frac{\mathrm{d}}{\mathrm{d}x}r(x) = -\mathcal{T}^{(x)}\big(r(x)\big) =$$
$$-\mathrm{i}[K(x),r(x)] - \frac{1}{2}\sum_{\alpha=1}^{N}\{R_\alpha(x)^\dagger R_\alpha(x), r(x)\} + \sum_{\alpha=1}^{N}R_\alpha(x)r(x)R_\alpha(x)^\dagger. \tag{4.40}$$

This is a master equation in Lindblad form, that describes the non-equilibrium Markov dynamics of the ancilla (*i.e.* the cavity). Starting from a pure state $r(L/2) = v_{\mathrm{R}}v_{\mathrm{R}}^\dagger$ at $t = -x = -L/2$, it evolves through interaction with the physical system (through the interaction operators R_α). At a general time $t = -x$, the density matrix $r(x)$ is no longer pure: non-equilibrium evolution is a dissipative process. Note that the evolution is trace preserving, since tracing the equation above results in $\mathrm{d}\,\mathrm{tr}[r(x)]/\mathrm{d}x = 0$. In addition, the corresponding map $\widetilde{\mathcal{T}}^{(x)}$ satisfies $\widetilde{\mathcal{T}}^{(x)}(\mathbb{1}_D) = 0$.

In systems which only contain bosons, all $\eta_{\alpha,\beta} = 1$ and there is no need to introduce $\breve{T}_\alpha(x)$, $\breve{T}_{\alpha,\beta}(x)$, etc. We can then deduce all expectation values of normally ordered operators $\hat{O} =: O[\{\hat{\psi}_\alpha^\dagger\},\{\hat{\psi}_\alpha\}]:$ from a generating functional $Z[\{\bar{J}_\alpha\},\{J_\alpha\}]$ as (see [276])

$$\langle\Psi[\overline{Q},\{\overline{R}_\alpha]|:O[\{\hat{\psi}_\beta^\dagger\},\{\hat{\psi}_\beta\}]:|\Psi[Q,\{R_\alpha\}]\rangle =$$
$$O\left[\left\{\frac{\delta}{\delta\bar{J}_\beta}\right\},\left\{\frac{\delta}{\delta J_\beta}\right\}\right]Z[\{\bar{J}_\alpha\},\{J_\alpha\}]\Big|_{\bar{J}_\alpha J_\alpha=0} \tag{4.41}$$

with $\delta\,/\delta J_\alpha$ the functional derivative with respect to J_α, and

$$Z[\{\bar{J}_\alpha\},\{J_\alpha\}] = \mathrm{tr}\left[(B\otimes\overline{B})\mathcal{P}\exp\left\{\int_{-L/2}^{+L/2}\mathrm{d}x\,\check{T}(x) + \sum_{\alpha=1}^{N} J_\alpha(x)[R_\alpha(x)\otimes 1_D] + \bar{J}_\alpha(x)[1_D\otimes\overline{R_\alpha(x)}]\right\}\right], \quad (4.42)$$

which for a system with open boundary conditions results in

$$Z[\{\bar{J}_\alpha\},\{J_\alpha\}] = \left(l(-L/2)\middle|\mathcal{P}\exp\left\{\int_{-L/2}^{+L/2}\mathrm{d}x\,\check{T}(x) + \sum_{\alpha=1}^{N} J_\alpha(x)[R_\alpha(x)\otimes 1_D] + \bar{J}_\alpha(x)[1_D\otimes\overline{R_\alpha(x)}]\right\}\middle|r(+L/2)\right). \quad (4.43)$$

Let us now illustrate this approach by defining a generic Hamiltonian for a single-boson system with open boundary conditions

$$\hat{H} = \hat{T} + \hat{V} + \hat{W} = \int_{-L/2}^{+L/2}\mathrm{d}x\,\frac{1}{2m}\left(\frac{\mathrm{d}}{\mathrm{d}x}\hat{\psi}^\dagger(x)\right)\left(\frac{\mathrm{d}}{\mathrm{d}x}\hat{\psi}(x)\right) + \int_{-L/2}^{+L/2}\mathrm{d}x\,v(x)\hat{\psi}^\dagger(x)\hat{\psi}(x) + \frac{1}{2}\int_{-L/2}^{+L/2}\mathrm{d}x\int_{-L/2}^{+L/2}\mathrm{d}y\,w(x,y)\hat{\psi}^\dagger(x)\hat{\psi}^\dagger(y)\hat{\psi}(y)\hat{\psi}(x) \quad (4.44)$$

describing particles with mass m that interact with an external potential $v(x)$ and with each other through two-particle interaction $w(x,y) = w(y,x)$. Using Eq. (4.41) we find (henceforth omitting the arguments Q and R in the state $|\Psi\rangle$)

$$\langle\Psi|\hat{\psi}^\dagger(x)\hat{\psi}(x)|\Psi\rangle = (l(x)|R(x)\otimes\overline{R}(x)|r(x)), \quad (4.45)$$

and

$$\langle\Psi|\hat{\psi}^\dagger(x)\hat{\psi}^\dagger(y)\hat{\psi}(y)\hat{\psi}(x)|\Psi\rangle = \theta(y-x)(l(x)|R(x)\otimes\overline{R(x)}\mathcal{P}\mathrm{e}^{\int_x^y \mathrm{d}z\,\check{T}(z)}R(y)\otimes\overline{R(y)}|r(y)) + \theta(x-y)(l(y)|R(y)\otimes\overline{R(y)}\mathcal{P}\mathrm{e}^{\int_y^x \mathrm{d}z\,\check{T}(z)}R(x)\otimes\overline{R(x)}|r(x)). \quad (4.46)$$

Defining $R_x^{(l)}(x) = R(x)^\dagger l(x) R(x)$ for every $x\in[-L/2,+L/2]$ and solving

$$\frac{\mathrm{d}}{\mathrm{d}y}(R_x^{(l)}(y)| = (R_x^{(l)}(y)|\check{T}(y) \quad (4.47)$$

for every $y\in[x,L/2]$, we can write the expectation value of the potential and interaction

energy as

$$\langle\Psi|\hat{V}|\Psi\rangle = \int_{-L/2}^{+L/2} \mathrm{d}x\, v(x)(l(x)|R(x)\otimes\overline{R(x)}|r(x)), \tag{4.48}$$

$$\langle\Psi|\hat{W}|\Psi\rangle = \int_{-L/2}^{+L/2} \mathrm{d}x \int_{x}^{+L/2} \mathrm{d}y\, w(x,y)(R_x^{(l)}(y)|R(y)\otimes\overline{R(y)}|r(y)). \tag{4.49}$$

To evaluate the expectation value of the kinetic energy, we compute

$$\begin{aligned}
&\langle\Psi|\left(\frac{\mathrm{d}}{\mathrm{d}x}\hat{\psi}^\dagger(x)\right)\left(\frac{\mathrm{d}}{\mathrm{d}x}\hat{\psi}(x)\right)|\Psi\rangle = \lim_{x\to y}\frac{\mathrm{d}^2}{\mathrm{d}x\mathrm{d}y}\langle\Psi|\hat{\psi}^\dagger(x)\hat{\psi}(y)|\Psi\rangle \\
&= \lim_{x\to y}\frac{\mathrm{d}^2}{\mathrm{d}x\mathrm{d}y}\Big[\theta(y-x)(l(x)|(1_D\otimes\overline{R(x)})\mathcal{P}\mathrm{e}^{\int_x^y \mathrm{d}z\,\check{T}(z)}(R(y)\otimes 1_D)|r(y)) \\
&\qquad + \theta(x-y)(l(y)|(R(y)\otimes 1_D)\mathcal{P}\mathrm{e}^{\int_y^x \mathrm{d}z\,\check{T}(z)}(1_D\otimes\overline{R(x)})\}|r(x))\Big] \\
&= \lim_{x\to y}\frac{\mathrm{d}}{\mathrm{d}x}\Big[\theta(y-x)\big(l(x)\big|\big(1_D\otimes\overline{R(x)}\big)\mathcal{P}\mathrm{e}^{\int_x^y \mathrm{d}z\,\check{T}(z)} \\
&\qquad\qquad \times\Big\{\big[\check{T}(y),R(y)\otimes 1_D\big] + \big(\mathrm{d}R(y)/\mathrm{d}y\otimes 1_D\big)\Big\}\big|r(y)\big) \\
&\qquad + \theta(x-y)\big(l(y)\big|\Big\{\big[\check{T},R(y)\otimes 1_D\big] + \big(\mathrm{d}R(y)/\mathrm{d}y\otimes 1_D\big)\Big\} \\
&\qquad\qquad \times\mathcal{P}\mathrm{e}^{\int_y^x \mathrm{d}z\,\check{T}(z)}\big(1_D\otimes\overline{R(x)}\big)\big|r(x)\big)\Big].
\end{aligned}$$

We have used the defining equations [Eq. (4.38)] in the computation of $\mathrm{d}(l(y)|/\mathrm{d}y = (l(y)|\check{T}(y)$ and $\mathrm{d}|l(y))/\mathrm{d}y = -\check{T}(y)|l(y))$. Since $\check{T}(y) = Q(y)\otimes 1_D + 1_D\otimes\overline{Q(y)} + R(y)\otimes\overline{R(y)}$, we obtain $[\check{T}(y),R(y)\otimes 1_D] = [Q(y),R(y)]\otimes 1_D$ and thus

$$\begin{aligned}
&\langle\Psi|\Big(\frac{\mathrm{d}}{\mathrm{d}x}\hat{\psi}^\dagger(x)\Big)\Big(\frac{\mathrm{d}}{\mathrm{d}x}\hat{\psi}(x)\Big)|\Psi\rangle = \\
&\lim_{x\to y}\Big[\theta(y-x)\big(l(x)\big|1_D\otimes\big([\overline{Q(x)},\overline{R(x)}] + \mathrm{d}\overline{R(x)}/\mathrm{d}x\big)\mathcal{P}\mathrm{e}^{\int_x^y \mathrm{d}z\,\check{T}(z)} \\
&\qquad\qquad \times\big([Q(y),R(y)] + \mathrm{d}R(y)/\mathrm{d}y\big)\otimes 1_D\big|r(y)\big) \\
&\qquad + \theta(x-y)\big(l(y)\big|\big([Q(y),R(y)] + \mathrm{d}R(y)/\mathrm{d}y\big)\otimes 1_D\mathcal{P}\mathrm{e}^{\int_y^x \mathrm{d}z\,\check{T}(z)} \\
&\qquad\qquad \times 1_D\otimes\big(1_D\otimes[\overline{Q(x)},\overline{R(x)}] + \mathrm{d}\overline{R(x)}/\mathrm{d}x\big)\big|r(x)\big)\Big],
\end{aligned}$$

where we used the same trick. Note that derivatives with respect to the Heaviside functions (which would produce a diverging contribution $\delta(x-y)$) nicely cancel for both derivatives to y and to x. As noted in the previous subsection, the regularity

condition Eq. (4.18) is automatically fulfilled for the case of a single boson. We thus obtain

$$\langle\Psi|\hat{T}|\Psi\rangle = \frac{1}{2m}\int_{-L/2}^{+L/2} \mathrm{d}x \, \big(l(x)\big|\big([Q(x),R(x)] + \mathrm{d}R(x)/\mathrm{d}x\big) \otimes \big([\overline{Q(x)},\overline{R(x)}] + \mathrm{d}\overline{R(x)}/\mathrm{d}x\big)\big|r(x)\big). \quad (4.50)$$

Note that this result could also be obtained by the general strategy outlined at the beginning of this section, *i.e.* by acting directly on the continuous matrix product state with the operators $\hat{\psi}(x)$ and $\mathrm{d}\hat{\psi}(x)/\mathrm{d}x$ and only afterwards computing the expectation values. However, the generating function approach is very general and relates nicely to the standard approach that is used to compute expectation values in quantum field theory. Note that, if we introduce $N = L/a$ discretization points in the interval $[-L/2,+L/2]$ on which to solve the integrals and differential equations, the scaling of our approach is $\mathcal{O}(N^2)$ if long-range interactions are present [due to the required computation of $R_x^{(l)}(y)$] and only $\mathcal{O}(N)$ if no long-range interactions are present [thus if $w(x,y) \sim \delta(x-y)$].

1.5. Gauge invariance in the manifold and its tangent plane

In the introduction of this section, we have already remarked that the continuous matrix product state representation is invariant under a global transformation $Q(x) \leftarrow \tilde{Q}(x) = gQ(x)g^{-1}$ and $R_\alpha(x) \leftarrow \tilde{R}_\alpha(x) = gR_\alpha(x)g^{-1}$, $\forall\alpha = 1,\ldots,N$, provided that we also transform the boundary matrix $B \leftarrow \tilde{B} = gBg^{-1}$. From the relationship with matrix product states, we expect to be also able to have invariance under local gauge transformations $g(x) \in \mathsf{GL}(\mathbb{C},D)$. By using the correspondence with matrix product states [Eq. (4.9)] and the gauge transformations for matrix product states constructed in Subsection 1.5 of the previous chapter, we can identify

$$\begin{aligned}
\tilde{A}^0(n) &= g((n-1)a)A^0(n)g(na)^{-1} \\
&= g((n-1)a)g(na)^{-1} + a\,g((n-1)a)Q(na)g(na)^{-1} \\
&= 1_D + a\left[-\frac{\mathrm{d}g}{\mathrm{d}x}(na)g(na) + g(na)Q(na)g(na)^{-1}\right] + \mathcal{O}(a^2), \\
\tilde{A}^\alpha(n) &= g((n-1)a)A^\alpha(n)g(na)^{-1} \\
&= \sqrt{a}\,g(na)R_\alpha(na)g(na)^{-1} + \mathcal{O}(a^{3/2}), \\
\tilde{A}^{(\alpha,\beta)}(n) &= g((n-1)a)A^{(\alpha,\beta)}g(na)^{-1} \\
&= \begin{cases} \frac{a}{2}[\tilde{R}_\alpha(na)\tilde{R}_\beta(na) + \eta_{\alpha,\beta}\tilde{R}_\beta(na)\tilde{R}_\alpha(na)] + \mathcal{O}(a^2), & \alpha \neq \beta \\ \frac{a}{2}\tilde{R}_\alpha(na)^2 + \mathcal{O}(a^2), & \alpha = \beta \end{cases} \\
&\ldots
\end{aligned}$$

The associated gauge transformation for the continuous matrix product state is thus given by

$$\tilde{Q}(x) = g(x)Q(x)g(x)^{-1} - \frac{\mathrm{d}g}{\mathrm{d}x}(x)g(x)^{-1}, \qquad \tilde{R}(x) = g(x)R(x)g(x)^{-1}, \tag{4.51}$$

where $\tilde{Q}(x)$ contains an additive contribution that can be recognized as the infinitesimal parallel transport, familiar from Yang-Mills gauge theory. Note that the gauge transformation $g(x)$ should be differentiable and thus continuous in order to obtain finite matrices $\tilde{Q}(x)$ and $\tilde{R}(x)$. We also need to transform the boundary matrix as $\tilde{B} = g(L/2)Bg(-L/2)^{-1}$. When B is fixed, we either need to restrict to gauge transformations with the boundary conditions $g(-L/2) = g(+L/2) = 1_D$ (in case of open boundary conditions) or with $g(-L/2) = g(+L/2)$ (in case of periodic boundary conditions where $B = \mathbb{1}_D$). As for matrix product states, we can use the gauge fixing conditions to impose a certain canonical form on the matrices $Q(x)$ and $R_\alpha(x)$. We restrict to the case of open boundary conditions where we have at our disposal virtual density matrices $l(x)$ and $r(x)$ which we assume to be positive and to have full rank. Under a gauge transformation, they are mapped to $\tilde{l}(x) = (g^{-1}(x))^\dagger l(x) g^{-1}(x)$ and $\tilde{r}(x) = g(x)r(x)g(x)^\dagger$. We can choose a gauge transformation $g(x) = l(x)^{1/2}$ so that $\tilde{l}(x) = \mathbb{1}_D$. Since

$$\frac{\mathrm{d}}{\mathrm{d}x}\tilde{l}(x) = \tilde{Q}(x)^\dagger \tilde{l}(x) + \tilde{l}(x)\tilde{Q}(x) + \sum_{\alpha=1}^{N} \tilde{R}_\alpha(x)^\dagger \tilde{l}(x) \tilde{R}_\alpha(x),$$

we can insert $\tilde{l}(x) = \mathbb{1}_D$ in order to find (henceforth dropping the tildes)

$$Q(x)^\dagger + Q(x) + \sum_{\alpha=1}^{N} R_\alpha(x)^\dagger R_\alpha(x) = 0. \tag{4.52}$$

This automatically implies that $Q(x)$ is of the form in Eq. (4.12). It is equivalent to the left orthonormalization condition of matrix product states. This does not fix the gauge freedom completely, and we can use the remaining gauge freedom $g(x) \in \mathrm{U}(D)$ to diagonalize $r(x)$ at every point x, hence obtaining the left-canonical form. Alternatively, we could have chosen to set $r(x) = \mathbb{1}_D$, which results in the right orthonormalization condition

$$Q(x) + Q(x)^\dagger + \sum_{\alpha=1}^{N} R_\alpha(x) R_\alpha(x)^\dagger = 0. \tag{4.53}$$

and implies that

$$Q(x) = -\mathrm{i}K(x) - \frac{1}{2}\sum_{\alpha=1}^{N} R_\alpha(x) R_\alpha(x)^\dagger \tag{4.54}$$

with $K(x)$ a Hermitian matrix. By then diagonalizing $l(x)$ we have obtained the right-canonical form. Note that the parameterization of matrices $Q(x)$ and $R_\alpha(x)$ that automatically satisfy the left or right orthonormalization condition is much easier then in the

case of matrix products states, where no explicit parameterization exists and such a condition has to be imposed manually by applying the corresponding gauge transformation. Unfortunately, the assumption of $l(x)$ and $r(x)$ having full rank fails near $x = -L/2$ or $x = +L/2$ respectively, since $l(-L/2) = \boldsymbol{v}_{\mathrm{L}}\boldsymbol{v}_{\mathrm{L}}^{\dagger}$ and $r(+L/2) = \boldsymbol{v}_{\mathrm{R}}\boldsymbol{v}_{\mathrm{R}}^{\dagger}$. This problem does not occur with matrix product states because the boundary vectors can there be absorbed into the matrices, resulting in a dynamic decrease of the bond dimension D near the boundary. As noted in the beginning of this section, the bond dimension cannot be space dependent for continuous matrix product states, which poses a problem that has yet to be overcome.

As in the previous chapter, the multiplicative gauge transformations induce an additive gauge equivalence in the tangent plane $\mathbb{T}_{\mathrm{cMPS}}$. Let $Q(\eta)$ and $R_\alpha(\eta)$ ($\forall \alpha = 1,\ldots,N$) be a one-parameter family of matrix functions, so that $Q(\eta) : \mathscr{R} \mapsto \mathbb{C}^{D\times D} : x \mapsto Q(x;\eta)$ and similarly for $R_\alpha(\eta)$. If we define $Q(0) = Q : x \mapsto Q(x)$, $R_\alpha(0) = R_\alpha : x \mapsto R_\alpha(x)$ together with $\mathrm{d}Q/\mathrm{d}\eta(0) = V : x \mapsto V(x)$ and $\mathrm{d}R_\alpha/\mathrm{d}\eta(0) = W_\alpha : x \mapsto W_\alpha(x)$, then we can write

$$\frac{\mathrm{d}}{\mathrm{d}\eta}\,|\Psi[Q(\eta),R_\alpha(\eta)]\rangle\bigg|_{\eta=0} = |\Phi[V,\{W_\alpha\};Q,\{R_\alpha\}]\rangle\,. \tag{4.55}$$

If we now chose a one-parameter family of gauge equivalent states, so that $Q(x;\eta) = g(x;\eta)Q(x)g(x;\eta)^{-1} - \frac{\partial g(x;\eta)}{\partial x}g(x;\eta)^{-1}$ and $R(x;\eta) = g(x;\eta)R(x)g(x;\eta)^{-1}$, where the one-parameter family of gauge transforms is given by $g(x;\eta) = \exp(\eta h(x))$ and $h(x) \in \mathbb{C}^{D\times D}$, $\forall x \in \mathscr{R}$, then we can use the gauge invariance of the continuous matrix product state representation to obtain $|\Psi[Q(x;\eta),R(x;\eta)]\rangle = |\Psi[Q(x),R(x)]\rangle$ and thus

$$|\Phi[\mathcal{M}_{\Phi}^{[Q]}[h],\{\mathcal{N}_{\Phi,\alpha}^{[R_\alpha]}[h]\};Q,\{R_\alpha\}]\rangle = 0, \tag{4.56}$$

where the maps $\mathcal{M}_{\Phi}^{[Q]}$ and $\mathcal{N}_{\Phi,\alpha}^{[R_\alpha]}$ ($\forall \alpha = 1,\ldots,N$) are given by

$$\mathcal{M}_{\Phi}^{[Q]}[h](x) = [h(x),Q(x)] - \frac{\mathrm{d}h}{\mathrm{d}x}(x), \qquad \mathcal{N}_{\Phi,\alpha}^{[R_\alpha]}[h](x) = [h(x),R_\alpha(x)]. \tag{4.57}$$

The maps $\mathcal{M}_{\Phi}^{[Q]}$ and $\mathcal{N}_{\Phi,\alpha}^{[R_\alpha]}$ thus establish a linear homomorphism from functions $h : \mathscr{R} \mapsto \mathbb{C}^{D\times D}$ to the kernel of the representation $|\Phi[V,\{W_\alpha\};Q,\{R_\alpha\}]\rangle$ of the tangent plane $\mathbb{T}_{\mathrm{cMPS}}[Q,\{R_\alpha\}]$. The counting argument is now less rigorous as in the discrete case. In general, we have D^2 parameters in $h(x)$ to eliminate D^2 degrees of freedom from $\{V(x),W_1(x),\ldots,W_N(x)\}$ at every point x. The only choice of h that does not produce a non-zero state in the kernel is the constant function $h(x) = c\mathbb{1}_D$ with $c \in \mathbb{C}$. However, since $\mathbb{T}_{\mathrm{cMPS}}[Q,\{R_\alpha\}]$ also contains $|\Psi[Q,\{R_\alpha\}]\rangle$, we have to impose orthogonality $\langle\Psi[\overline{Q},\{\overline{R}_\alpha\}]|\Phi[V,\{W_\alpha\};Q,\{R_\alpha\}]\rangle = 0$, where

$$\langle\Psi[\overline{Q},\{\overline{R}_\alpha\}]|\Phi[V,\{W_\alpha\};Q,\{R_\alpha\}]\rangle =$$

$$\int_{-L/2}^{+L/2} \mathrm{d}x\, (l(x)|V(x)\otimes \mathbb{1}_D + \sum_{\alpha=1}^{N} W_\alpha(x)\otimes \overline{R_\alpha(x)}|r(x)). \quad (4.58)$$

We can both fix the gauge of the state and restrict to tangent vectors $|\Phi[V(x), W(x)]\rangle \in \mathbb{T}^{\perp}_{\text{cMPS}}[Q, \{R_\alpha\}]$ by imposing that

$$(l(x)|\left[V(x)\otimes \mathbb{1}_D + \sum_{n=1}^{N} W_\alpha(x)\otimes \overline{R_\alpha(x)}\right] = 0, \quad (4.59)$$

to which we refer as the left gauge fixing condition. Analogously, we can also define a right gauge fixing condition

$$\left[V(x)\otimes \mathbb{1}_D + \sum_{\alpha=1}^{N} W_\alpha(x)\otimes \overline{R_\alpha(x)}\right] |r(x)) = 0. \quad (4.60)$$

Note that once again we can easily find a parameterization that respects these gauge fixing conditions. For the right gauge fixing condition, it is sufficient to parameterize V as $V(x) = \sum_{\alpha=1}^{N} W_\alpha(x) r(x) R_\alpha(x)^\dagger r(x)^{-1}$ and $W_\alpha(x)$ can be chosen freely. Similarly, the left gauge fixing is automatically satisfied by the parameterization $V(x) = \sum_{\alpha=1}^{N} l(x)^{-1} R_\alpha(x)^\dagger l(x) W_\alpha(x)$ where $W_\alpha(x)$ can be chosen freely.

Finally, note that we can even define a gauge transformation $g(x)$ for the continuous matrix product state $|\Psi[Q, \{R_\alpha\}]\rangle \in \mathscr{M}_{\text{cMPS}}$ so that

$$\tilde{Q}(x) = g(x)Q(x)g(x)^{-1} - \frac{\mathrm{d}g}{\mathrm{d}x}(x)g(x)^{-1} = 0. \quad (4.61)$$

It is sufficient to choose

$$g(x) = \mathcal{P}\exp\left[\int_{x_0}^{x} Q(y)\,\mathrm{d}y\right] \quad (4.62)$$

with x_0 some arbitrary starting point. Hence, the continuous matrix product state can now be written as

$$|\Psi[\{\tilde{R}_\alpha\}]\rangle = \mathrm{tr}\left(B\ \mathcal{P}\exp\left[\int_{-L/2}^{+L/2} \mathrm{d}x \sum_{\alpha=1}^{N} \tilde{R}_\alpha(x)\otimes \hat{\psi}^\dagger_\alpha(x)\right]\right)|\Omega\rangle\,. \quad (4.63)$$

This formulation is close in spirit to the bosonic mean field ansatz

$$|\varphi\rangle = \exp\left(\int_{-L/2}^{+L/2} \varphi(x)\hat{\psi}^\dagger(x)\,\mathrm{d}x\right)|\Omega\rangle$$

with φ a scalar (complex-valued) function, since it identifies the mean field ansatz with a continuous matrix product state with bond dimension $D = 1$. This mean field ansatz lies at the basis of the Gross-Pitaevskii equation [247, 248], that is still today used with

great success. Since all variational degrees of freedom are now contained in the matrices $\tilde{R}_\alpha(x)$, and all gauge degrees of freedom have been eliminated (except for a global gauge transformation if $B = \mathbb{1}_D$). The tangent plane is now spanned by the vectors

$$|\Phi[\{\tilde{W}_\alpha\};\{\tilde{R}_\alpha\}]\rangle = \int_{-L/2}^{+L/2} \mathrm{d}x\ \mathrm{tr}\left[B\ \mathcal{P}\mathrm{e}^{\int_{-L/2}^{x}\sum_{\alpha=1}^{N}\tilde{R}_\alpha(u)\otimes\hat{\psi}_\alpha^\dagger(y)\,\mathrm{d}y} \times\left(\sum_{\beta=1}^{N}\tilde{W}_\beta(x)\otimes\hat{\psi}_\beta^\dagger(x)\right)\mathcal{P}\mathrm{e}^{\int_{x}^{+L/2}\sum_{\alpha=1}^{N}\tilde{R}_\alpha(u)\otimes\hat{\psi}_\alpha^\dagger(y)\,\mathrm{d}y}\right]|\Omega\rangle\,. \quad (4.64)$$

However, we will not employ this particular formulation in the remainder of this section. For example, for a translation invariant state $|\Psi[Q,R_\alpha]\rangle$, the matrices Q and R_α are x-independent (see next subsection). This particular gauge transformation will map the x-independent matrices R_α to x-dependent matrices $\tilde{R}_\alpha(x) = \mathrm{e}^{+Qx}R_\alpha\mathrm{e}^{-Qx}$, so that translation invariance is less easily recognized.

1.6. Translation invariance and the thermodynamic limit

For the ground state of translation invariant Hamiltonians, we can use the manifold $\mathcal{M}_{\mathrm{ucMPS}}$ of uniform continuous matrix product states $|\Psi(Q,\{R_\alpha\})\rangle$, which are obtained from taking $Q(x) = Q$ and $R_\alpha(x) = R_\alpha$ constant x-independent $D\times D$ matrices in $|\Psi[Q,\{R_\alpha\}]\rangle$. This approach is valid both for a finite system with periodic boundary conditions ($B = \mathbb{1}_D$) or for a system in the thermodynamic limit ($|\mathscr{R}| = L \to \infty$ or thus $\mathscr{R} \to \mathbb{R}$). We henceforth restrict to this last case. The transfer operator $\breve{T} = Q\otimes 1_D + 1_D\otimes\overline{Q} + R\otimes\overline{R}$ also becomes translation invariant and $\mathcal{P}\exp[\int_y^z \mathrm{d}x\,\breve{T}] = \exp[\breve{T}(z-y)]$. The normalization of the state $|\Psi(Q,R)\rangle$ is given by $\lim_{L\to\infty}\mathrm{tr}\left[(B\otimes\overline{B})\exp(\breve{T}L)\right]$. If $\mu = \max_{\lambda\in\sigma(\breve{T})}\{\Re(\lambda)\}$, then $\langle\Psi(\overline{Q},\{\overline{R}_\alpha\})|\Psi(Q,\{R_\alpha\})\rangle \sim \lim_{L\to\infty}\exp(\mu L)$. Normalizing this state by multiplying it with $\exp(-\mu L)$ results in $Q \leftarrow Q - \mu/2\mathbb{1}_D$ and $\breve{T} \leftarrow \breve{T} - \mu\breve{\mathbb{1}}$, so that the new transfer operator $\breve{T}$ has at least one eigenvalue for which the real part is zero and no eigenvalue has a positive real part. Let us assume that the eigenvalue λ with $\Re\lambda = 0$ is unique. If $|r)$ is the corresponding right eigenvector, then we can write the eigenvalue equation as $\mathcal{T}(r) = \lambda r$ with r the associated virtual density matrix. Hermitian conjugation learns that $\mathcal{T}(r^\dagger) = \overline{\lambda}r^\dagger$, so that the uniqueness of the eigenvalue with $\Re\lambda = 0$ implies that $\lambda = \overline{\lambda} = 0$ and $r^\dagger = \mathrm{e}^{\mathrm{i}\phi}r$, where we can choose the phase of the eigenvector so that r is Hermitian. Similarly, the virtual density matrix l associated to the left eigenvector $|l)$ can also be chosen Hermitian. If these vectors are normalized such that $(l|r) = 1$, then $\lim_{L\to\infty}\exp(\breve{T}L) = |r)(l|$ and we obtain

$$\langle\Psi(\overline{Q},\{\overline{R}_\alpha\})|\Psi(Q,\{R_\alpha\})\rangle = (l|B\otimes\overline{B}|r) = (\boldsymbol{v}_{\mathrm{L}}^\dagger r\boldsymbol{v}_{\mathrm{L}})(\boldsymbol{v}_{\mathrm{R}}^\dagger l\boldsymbol{v}_{\mathrm{R}}), \quad (4.65)$$

where the last equation is valid in the case of open boundary conditions. A full categorization of the eigenvalue structure of $\breve{T}$ can be obtained by identifying

$$\breve{T} = \lim_{a\to 0} \frac{1}{a} \ln \breve{E} \tag{4.66}$$

with $\breve{E}$ the corresponding transfer operator of the uniform matrix product state $|\Psi(A)\rangle$ with A related to Q and R_α as in Eq. (4.9). Clearly then, the transfer operator $\breve{E}$ of a pure matrix product state has a single eigenvalue 1 that maps to the eigenvalue zero of $\breve{T}$, while all other eigenvalues of $\breve{E}$ lie strictly within the unit circle and map to eigenvalues of $\breve{T}$ with strictly negative real part.

For uniform continuous matrix product states, the gauge invariance is restricted to global transformations $Q \leftarrow \tilde{Q} = gQg^{-1}$ and $R_\alpha \leftarrow \tilde{R}_\alpha = gR_\alpha g^{-1}$ with $g \in \mathrm{GL}(\mathbb{C}, D)$. This gauge transformation can be used to impose the left or right orthonormalization conditions. Left orthonormalization boils down to fixing the left eigenvector l of eigenvalue 0 to $l = \mathbb{1}_D$, which requires that $Q = -iK - 1/2\sum_{\alpha=1}^{N} R_\alpha^\dagger R_\alpha$ with K a Hermitian matrix. The remaining unitary gauge equivalence can be used to diagonalize r, bringing Q and R_α in the left-canonical form. The right-canonical form is obtained analogously. In principle, an exact computation of the left and right eigenvectors l and r corresponding to the eigenvalue with largest real part λ of the transfer operator $\breve{T}$ are computationally costly operations $[\mathcal{O}(D^6)]$. By using an explicit parameterization of the left-canonical form in terms of R_α and the Hermitian matrix K, we know exactly that $\lambda = 0$ and $l = \mathbb{1}_D$. It is then possible to obtain r with an iterative solver with computational efficiency $\mathcal{O}(D^3)$.

By imposing the physical requirements discussed at the end of Subsection 1.3, we can define the parity superoperator $\breve{P}$ as in Subsection 1.4. Since $\breve{P}\breve{T}\breve{P} = \breve{T}$, we can expect that the left and right eigenvectors $|l)$ and $|r)$ corresponding to the zero eigenvalue satisfy $(l|\breve{P} = (l|$ and $\breve{P}|r) = |r)$, or thus $P^\dagger l P = l$ and $PrP^\dagger = r$. Note that we can always choose the gauge such that P is Hermitian. In addition, it is easy to proof that $\breve{T}_\alpha$ also has an eigenvalue zero even if α refers to a fermionic particle species so that $\breve{T}_\alpha \neq \breve{T}$. The corresponding left and right eigenvectors are in that case given by $lP = P^\dagger l$ and $Pr = rP^\dagger$. We now assume that the boundary vectors are chosen so that only states with an even number of fermions are allowed, so that $(\boldsymbol{v}_{\mathrm{L}}^\dagger r \boldsymbol{v}_{\mathrm{L}})(\boldsymbol{v}_{\mathrm{R}}^\dagger l \boldsymbol{v}_{\mathrm{R}}) \neq 0$. We can then compute correlation functions as

$$\begin{aligned} C_{\alpha,\beta}(x,y) &= \langle \Psi(\overline{Q}, \{\overline{R}_\alpha\}) | \hat{\psi}_\alpha^\dagger(x) \hat{\psi}_\beta(y) | \Psi(Q, \{R_\alpha\}) \rangle \\ &= \theta(x-y)(l|[R_\beta \otimes \mathbb{1}_D] \mathcal{P} \mathrm{e}^{\breve{T}_\alpha (x-y)} [\mathbb{1}_D \otimes \overline{R_\alpha}]|r) \\ &\quad + \theta(y-x)(l|[\mathbb{1}_D \otimes \overline{R_\alpha}] \mathcal{P} \mathrm{e}^{\breve{T}_\alpha (y-x)} [R_\beta \otimes \mathbb{1}_D]|r), \end{aligned} \tag{4.67}$$

where we have used the physical requirement $\breve{T}_{\alpha,\beta} = \breve{T}$ and $\breve{T}_\alpha = \breve{T}_\beta$ for non-vanishing correlation functions (see Subsection 1.4). Note that we have introduced a new symbol C

for these correlation functions, because they are set apart from the correlation functions G and its connected counterpart Γ defined in Subsection 2.2 of Chapter 1 by the fact that $\hat{\psi}_\alpha$ and $\hat{\psi}^\dagger_\beta$ do not form a complete set of operators (when bosons are present). The correlation function $C_{\alpha,\beta}(x,y)$ is translation invariant and we define $C_{\alpha,\beta}(x,y) = C_{\alpha,\beta}(y-x)$. When α is bosonic and β fermionic, we automatically have $C_{\alpha,\beta}(x) = 0$ if the parity considerations from Subsection 1.3 are correctly built in. In the long range limit, we obtain $\lim_{|x|\to\infty} C_{\alpha,\beta}(x) = (l|R_\beta \otimes \mathbb{1}_D|r)(l|\mathbb{1}_D \otimes \overline{R_\alpha}|r)$. When both α and β refer to fermionic particle species, this limiting value is automatically zero (also under the assumption that parity is correctly built into the matrices). When both indices refer to bosonic particles, a non-zero value is possible in the case of Bose-Einstein condensation. We should then define a connected correlation function, which decays exponentially as $\lim_{|x|\to\infty} C_{\alpha,\beta}(x) = \mathcal{O}(\exp[-|x|/\xi_c])$ with $\xi_c = (\Re\lambda_1)^{-1}$, where λ_1 is the eigenvalue of $\hat{T}_\alpha$ with second largest real part (*i.e.* skipping eigenvalue $\lambda_0 = 0$). Clearly, $C_{\alpha,\beta}(x)$ is continuous at $x = 0$. We can then compute the first derivative, which is only continuous at $x = 0$ if we impose the regularity conditions in Eq. (4.18). This is another way to derive these conditions. If Eq. (4.18) is satisfied, then the second derivative of $C_{\alpha,\beta}(x)$ at $x = 0$ (which gives the expectation value of the kinetic energy density $\hat{t}$ up to a factor $-1/2m$) is finite and automatically continuous. The third derivative is then finite but will not be continuous in general, without imposing further conditions as in Eq. (4.19) or Eq. (4.20).

We define the Fourier transformed correlation function

$$n_{\alpha,\beta}(p,p') = \int_{-\infty}^{+\infty} \frac{\mathrm{d}x}{2\pi} \int_{-\infty}^{+\infty} \frac{\mathrm{d}x}{2\pi}\, C_{\alpha,\beta}(x,y) \mathrm{e}^{\mathrm{i}px - \mathrm{i}p'y} = \delta(p'-p) n_{\alpha,\beta}(p) \tag{4.68}$$

with

$$\begin{aligned} n_{\alpha,\beta}(p) &= \int_{-\infty}^{+\infty} \frac{\mathrm{d}x}{2\pi} C_{\alpha,\beta}(x) \mathrm{e}^{-\mathrm{i}px}, \\ &= (l|[\mathbb{1}_D \otimes \overline{R_\alpha}](-\check{T}_\alpha + \mathrm{i}p)^{-1}[R_\beta \otimes \mathbb{1}_D]|r) \\ &\quad + (l|[R_\beta \otimes \mathbb{1}_D](-\check{T}_\alpha - \mathrm{i}p)^{-1}[\mathbb{1}_D \otimes \overline{R_\alpha}]|r). \end{aligned} \tag{4.69}$$

This expression is in principle ill-defined at $p = 0$ since $\check{T}_\alpha$ has an eigenvalue zero. By defining a projector $\check{Q} = \check{\mathbb{1}} - |r)(l|$ and introducing the notation $\check{Q}(-\check{T}_\alpha \pm \mathrm{i}p)^{-1}\check{Q} = (-\check{T}_\alpha \pm \mathrm{i}p)^{\mathsf{P}}$, we can rewrite $n_{\alpha,\beta}(p)$ as

$$\begin{aligned} n_{\alpha,\beta}(p) &= 2\pi\delta(p)(l|\mathbb{1}_D \otimes \overline{R_\alpha}|r)(l|R_\beta \otimes \mathbb{1}_D|r) \\ &\quad + (l|[\mathbb{1}_D \otimes \overline{R_\alpha}](-\check{T}_\alpha + \mathrm{i}p)^{\mathsf{P}}[R_\beta \otimes \mathbb{1}_D]|r) \\ &\quad + (l|[R_\beta \otimes \mathbb{1}_D](-\check{T}_\alpha - \mathrm{i}p)^{\mathsf{P}}[\mathbb{1}_D \otimes \overline{R_\alpha}]|r). \end{aligned} \tag{4.70}$$

The first term is only present for bosonic particles that have condensed. It would also

disappear in the proper Fourier transformation of the connected correlation function. The large-p behavior of $n_{\alpha,\beta}(p)$ follows from the regularity of $C_{\alpha,\beta}(x)$. If the regularity conditions in Eq. (4.18) are satisfied, then the momentum-space correlation function $n_{\alpha,\beta}(p)$ decays for large values of p as $\mathcal{O}(\Lambda^4/p^4)$ (observe that $n_{\alpha,\beta}(p)$ is a dimensionless quantity). The eigenvalue spectrum of $\hat{T}_\alpha$ thus provides a definition for an ultraviolet cutoff scale $a = \Lambda^{-1}$. If we define Fourier transformed field operators $\hat{\Psi}(p)$ —no confusion between the state Ψ and the momentum-space operator $\hat{\Psi}$ should arise— as

$$\hat{\Psi}(p) = \frac{1}{\sqrt{2\pi}} \int_{-\infty}^{+\infty} \mathrm{d}x\, \hat{\psi}(x) \mathrm{e}^{-\mathrm{i}px}, \tag{4.71}$$

then it is easy to see why we have used the suggestive notation $n_{\alpha,\beta}$ for the Fourier transform of $C_{\alpha,\beta}$. We obtain

$$\langle \Psi(\overline{Q}, \{\overline{R}_\alpha\}) | \hat{\Psi}^\dagger_\alpha(p) \hat{\Psi}_\beta(p') | \Psi(Q, \{R_\alpha\}) \rangle = \delta(p - p') n_{\alpha,\beta}(p). \tag{4.72}$$

Hence, $n_{\alpha,\beta}(p)$ describes the occupation number of momentum levels. Rather than defining the ultraviolet cutoff scale $a = \Lambda^{-1}$ through the total particle density

$$\rho_{\alpha,\beta} = \int_{-\infty}^{+\infty} \frac{\mathrm{d}p}{2\pi}\, n_{\alpha,\beta}(p), \tag{4.73}$$

we have now defined a cutoff scale through the large momentum behavior of the momentum occupation number $n_{\alpha,\beta}(p)$.

For two pure uniform continuous matrix product states $|\Psi(Q, \{R_\alpha\})\rangle$ and $|\Psi(Q', \{R'_\alpha\})\rangle$ we can define a superoperator $\check{S} = Q' \otimes \mathbb{1}_D + \mathbb{1}_D \otimes \overline{Q} + \sum_{\alpha=1}^N R'_\alpha \otimes \overline{R_\alpha}$ so that the $\langle \Psi(Q, \{R_\alpha\}) | \Psi(Q', \{R'_\alpha\}) \rangle$ decays as $\lim_{L\to+\infty} \exp(\lambda L)$, with λ the eigenvalue with largest real part of $\hat{S}$. If the two uniform continuous matrix product states are inequivalent, $\Re(\lambda) < 0$ and there is an infrared orthogonality catastrophe. If $\Re(\lambda) = 0$, then we can define a phase $\phi = \Im(\lambda)$ and a gauge transformation $g \in \mathrm{GL}(D;\mathbb{C})$ such that $Q' = gQg^{-1} + \mathrm{i}\phi$ and $R'_\alpha = gR_\alpha g^{-1}$. With f being the right eigenvector corresponding to eigenvalue $\lambda = \mathrm{i}\phi$ of $\check{S}$, g can be obtained as $g = fr^{-1}$.

Let us also illustrate how to compute the expectation value of a translation invariant Hamiltonian. The generic Hamiltonian in Eq. (4.44) becomes translation invariant for $v(x) = v$ and $w(x,y) = w(y-x)$ with $w(x) = w(-x)$. Since the uniform continuous matrix product state is extensive, expectation values are proportional to the volume and it makes more sense to compute the expectation values of the kinetic, potential and interaction energy densities $\hat{t}$, $\hat{v}$ and $\hat{w}$. We obtain

$$\langle \Psi(\overline{Q}, \{\overline{R}_\alpha\}) | \hat{t} | \Psi(Q, \{R_\alpha\}) \rangle = \frac{1}{2m} (l | [Q,R] \otimes [\overline{Q}, \overline{R}] | r), \tag{4.74}$$

$$\langle \Psi(\overline{Q}, \{\overline{R}_\alpha\}) | \hat{v} | \Psi(Q, \{R_\alpha\}) \rangle = v (l | R \otimes \overline{R} | r), \tag{4.75}$$

$$\langle\Psi(\overline{Q},\{\overline{R}_\alpha\})|\hat{w}|\Psi(Q,\{R_\alpha\})\rangle = \int_0^{+\infty} \mathrm{d}z\, w(z)(l|R\otimes\overline{R}\mathrm{e}^{\check{T}z}R\otimes\overline{R}|r). \tag{4.76}$$

If $w(z)$ has a Laplace transform $\mathcal{L}[w](\sigma) = \int_0^{+\infty} \mathrm{d}z\, w(z)\exp(-\sigma z)$ that is defined for $\Re\sigma \geq 0$, we obtain

$$\langle\Psi|\hat{w}|\Psi\rangle = (l|R\otimes\overline{R}\,\mathcal{L}[w](-\check{T})R\otimes\overline{R}|r). \tag{4.77}$$

Note that translation invariance has allowed to parameterize a field theory with a continuous number of degrees of freedom by a discrete number of degrees of freedom. Having l and r, the computational cost is $\mathcal{O}(D^6)$ when long-range interactions are present, since we then have to compute an arbitrary function $\mathcal{L}[w]$ of the transfer operator $\check{T}$. If only strictly local interactions are present $w(x-y)\sim\delta(x-y)$, the interaction energy (density) can be computed with computational complexity of $\mathcal{O}(D^3)$ just like the potential and the kinetic energy density. In special cases of long-range interactions for which $\mathcal{L}[w]$ is extremely simple (*e.g.* exponentially decaying interaction), an implementation with computational cost $\mathcal{O}(D^3)$ can be constructed iteratively.

Finally we can construct the tangent vectors of $|\Psi(Q,\{R_\alpha\})\rangle$. As in Subsection 1.6 of the previous chapter, it is fruitful to consider the complete tangent plane $\mathbb{T}_{\mathrm{cMPS}}$ at the special uniform point $|\Psi(Q,\{R_\alpha\})\rangle$, rather than to restrict to the tangent vectors in $\mathbb{T}_{\mathscr{M}_{\mathrm{ucMPS}}}(Q,\{R_\alpha\}) = \mathbb{T}_{\mathrm{ucMPS}}(Q,\{R_\alpha\})$. We can then decompose the complete tangent plane into sectors $\mathbb{T}_{\Phi_p}$ of momentum $p\in\mathbb{R}$ by introducing Fourier modes $V(x) = V\mathrm{e}^{\mathrm{i}px}$ and $W_\alpha(x) = W_\alpha\mathrm{e}^{\mathrm{i}px}$ in the generic tangent vectors of Eq. (4.8), hence defining

$$|\Phi_p(V,\{W_\alpha\};Q,\{R_\alpha\})\rangle = |\Phi_p^{(Q,\{R_\alpha\})}(V,\{W_\alpha\})\rangle = \int_{-\infty}^{+\infty}\mathrm{d}x\,\mathrm{e}^{\mathrm{i}px}\boldsymbol{v}_{\mathrm{L}}^\dagger\hat{U}(-\infty,x)\left(V\otimes\hat{\mathbb{1}} + \sum_{\alpha=1}^{N} W_\alpha\otimes\hat{\psi}_\alpha^\dagger(x)\right)\hat{U}(x,+\infty)\boldsymbol{v}_{\mathrm{R}}|\Omega\rangle\,. \tag{4.78}$$

As before, a one-parameter family of local gauge transformations $g(x;s) = \exp(s\,h(x))$ with $h(x)\in\mathfrak{gl}(D;\mathbb{C})$ induces a map to the kernel of the representation Φ_p of $\mathbb{T}_{\Phi_p}$ by setting $h(x) = h\mathrm{e}^{\mathrm{i}px}$, so that

$$|\Phi_p(\mathcal{M}_{\Phi_p}^{(Q)}(h),\{\mathcal{N}_{\alpha,\Phi_p}^{(R_\alpha)}(h)\};Q,\{R_\alpha\})\rangle = 0,$$

with

$$\mathcal{M}_{\Phi_p}^{(Q)}(h) = [h,Q] - \mathrm{i}ph \qquad \text{and} \qquad \mathcal{N}_{\alpha,\Phi_p}^{(R_\alpha)}(h) = [h,R_\alpha],\quad \forall\alpha = 1,\ldots,N. \tag{4.79}$$

We henceforth omit the superscript notation of Q and R_α. The dimension of the kernel of the map Φ_p is thus D^2-dimensional, except at $p=0$. This can easily be proven, since for every non-zero $h\in\mathfrak{gl}(D;\mathbb{C})$, $\mathcal{M}_{\Phi_p}(h)\neq 0$ or $\mathcal{N}_{\alpha,\Phi_p}(h)\neq 0$, $\forall\alpha = 1,\ldots,N$. Indeed,

suppose that $\mathcal{M}_{\Phi_p}(h) = 0$ and $\mathcal{N}_{\Phi_p}(h) = 0$. Imposing that

$$\mathcal{M}_{\Phi_p}(h)r + \sum_{\alpha=1}^{N} \mathcal{N}_{\alpha,\Phi_p}(h) r R_\alpha^\dagger = 0$$

results in $\breve{T}|hr) = \mathrm{i}p|hr)$ which has no non-trivial solution except at $p = 0$, where we find $h = c\mathbb{1}_D$ with $c \in \mathbb{C}$. At nonzero momenta, we can use a gauge fixing condition to reduce the number of parameters by D^2. At $p = 0$, we can only reduce the number of parameters by $D^2 - 1$ through gauge fixing. But whereas $\langle\Psi(\overline{Q}, \{\overline{R}_\alpha\})|\Phi_p(V, \{W_\alpha\})\rangle = 0$ for all nonzero momenta p, we obtain $\langle\Psi(\overline{Q}, \{\overline{R}_\alpha\})|\Phi_0(V, \{W_\alpha\})\rangle \sim (l|V \otimes 1_D + W \otimes R|r)$, where the proportionality factor is given by $\int_{-\infty}^{+\infty} \mathrm{d}x = |\mathbb{R}| = +\infty$. We thus need to impose orthogonality to $|\Psi(Q,R)\rangle$ manually at $p = 0$, which allows to discard one additional parameter. For any momentum p, we can uniquely fix the gauge of any tangent vector in $\mathbb{T}_{\Phi_p}^{\perp}$ by setting $(l|V \otimes 1_D + W \otimes R = 0$ or $V \otimes 1_D + W \otimes R|r) = 0$, corresponding to the left and right gauge fixing conditions respectively.

1.7. Symmetries and quantum phases

As for matrix product states in Subsection 1.7 of the previous chapter, a continuous matrix product state can be made to satisfy certain symmetry constraints. Translation invariance, for one, has been studied in the previous section. Translation invariant continuous matrix product states are obtained by the uniform representation where the matrices Q and R_α x-independent, although an x-dependent gauge transform produces a non-uniform continuous matrix product state that is still translation invariant. Whether $\mathscr{M}_{\text{cMPS}}$ also contains translation invariant states that do not allow a uniform representation without increasing the bond dimension D is unknown, but seems likely.

Other spacetime symmetries, invariance under parity and time reversal transformations in particular, can be treated much as in the case of matrix product states and produce the same results. Ground states of systems which are time-reversal invariant —for simplicity defined as Hamiltonians having real coefficients with respect to an expansion in the operators $\hat{\psi}_\alpha(x)$ and $\hat{\psi}_\alpha^\dagger(x)$— can be represented with real matrices Q and R_α. If the ground state of a parity invariant Hamiltonian is being approximated, a representation with complex-valued symmetric matrices Q and R_α can be used. Unfortunately, both choices of gauge are incompatible. Time-reversal invariance combined with parity invariant does not allow to represent the continuous matrix product state with real, symmetric matrices Q and R_α. Such a choice would produce a real, symmetric transfer operator $\breve{T}$ with real eigenvalues, so that all correlations decay monotonically. No periodic fluctuations (*e.g.* Friedel oscillations [365]) that are commonly associated to systems with finite density would be allowed in such a continuous matrix product state.

For internal symmetry transformations $\hat{U}$ that act as

$$\hat{U}\hat{\psi}^\dagger_\alpha(x)\hat{U}^\dagger = \sum_\beta u_{\alpha,\beta}\hat{\psi}^\dagger_\beta(x) \tag{4.80}$$

we obtain $\hat{U}|\Omega\rangle = |\Omega\rangle$ and

$$\hat{U}|\Psi[Q,\{R_\alpha\}]\rangle = |\Psi[Q,\{\sum_\beta u_{\alpha,\beta}R_\beta\}]\rangle\,. \tag{4.81}$$

If the continuous matrix product state is to be invariant under this transformation, the requirement is the existence of a gauge transformation g_u such that

$$g_u Q g_u^{-1} = Q, \qquad\qquad g_u R_\alpha g_u^{-1} = \sum_\beta R_\beta u_{\beta,\alpha}. \tag{4.82}$$

If $\hat{U}$ belongs to a symmetry group S, the matrices g_u also constitute a representation of S and the matrices Q and R_α transform as a scalar and as a vector respectively. Together with the fact that the regularity condition Eq. (4.18) requires the matrices R_α to satisfy the same (anti)commutation rules as the operators $\hat{\psi}^\dagger_\alpha$, it is clear that Q and R_α are not simply matrices with numbers but act as a physical objects in the ancilla space. The holographic property of continuous matrix product states is thus even more manifest as in the case of matrix product states. This insight may also provide a way to generalize the concept continuous matrix product states to higher dimensions or to states with an infinite-dimensional ancilla.

2. Time-dependent variational principle and excitations

We can now apply the time-dependent variational principle to $\mathscr{M}_{\text{cMPS}}$, as well as the ansatz for studying the spectrum of low-lying excitations in $\mathbb{T}_{\text{cMPS}}$. These techniques were discussed in Chapter 2 and applied to the class of matrix product states in Section 2 and Section 3 of the previous chapter respectively. We derive in this section all necessary formula for computing with continuous matrix product states and their tangent vectors, but omit a detailed discussion of the interpretation, which is analogous to the previous chapter. In addition, we henceforth restrict to systems with a single bosonic particle species for the sake of notational simplicity and apply our approach to the general Hamiltonian in Eq. (4.44). Most results can trivially be generalized to the more general case with an arbitrary number of particles present (at least when the regularity conditions in Eq. (4.18) and the physical requirements concerning fermion parity are satisfied). Occasionally, we state some comments regarding this generalization.

The time-dependent variational principle was first applied to the setting of continuous matrix product states (see [366]) and only afterwards to matrix product states. While

the time-dependent variational principle solves some fundamental issues with the time-evolving block decimation based on the Lie-Trotter-Suzuki decomposition for matrix product states, it was more urgently required for continuous matrix product states as these are not susceptible to a treatment based on the Lie-Trotter-Suzuki decomposition. The distinction between a 'two-site' operator such as the kinetic energy and a one-site operator such as a local interaction disappears in the continuum. Another indication for the impossibility of applying the time-evolving block decimation in the continuum, is the fact that it works on matrix product states by locally increasing the bond dimension between two sites (after which a reduction onto a matrix product state with original bond dimension is required). In a continuous matrix product state, a local increase of bond dimension is impossible. Luckily, the time-dependent variational principle provides an approach for simulating time evolution without ever leaving the variational manifold $\mathscr{M}_{\mathrm{cMPS}}$.

2.1. Time-dependent variational principle for generic continuous matrix product states

The time-dependent variational principle for the manifold $\mathscr{M}_{\mathrm{cMPS}}$ of generic continuous matrix product states $|\Psi[Q,R]\rangle$ as defined in Eq. (4.3) is based on a computation of the tangent vector

$$\frac{\mathrm{d}}{\mathrm{d}t}|\Psi[Q(t),R(t)]\rangle = |\Phi[V(t),W(t);Q(t),R(t)]\rangle$$

with $V(t): x \mapsto V(x;t) = \partial Q(x;t)/\partial t$ and $W(t): x \mapsto W(x;t) = \partial R(x;t)/\partial t$. We first compute some relevant quantities. The overlap between two tangent vectors is given by

$$\begin{aligned}\langle \Phi[\overline{V},\overline{W}]|\Phi[V',W']\rangle = &\int_{-L/2}^{+L/2}\mathrm{d}x\,(l(x)|W'(x)\otimes\overline{W(x)}|r(x)) \\ &+\int_{-L/2}^{+L/2}\mathrm{d}x\int_{x}^{+L/2}\mathrm{d}y\,\Big(l(x)\Big|\Big[V'(x)\otimes 1_D + W'(x)\otimes\overline{R(x)}\Big]\mathcal{P}\mathrm{e}^{\int_x^y \mathrm{d}z\,\check{T}(z)} \\ &\qquad\qquad\times\Big[1_D\otimes\overline{V(y)}+R(y)\otimes\overline{W(y)}\Big]|r(y)\Big) \\ &+\int_{-L/2}^{+L/2}\mathrm{d}x\int_{-L/2}^{x}\mathrm{d}y\,\Big(l(y)\Big|\Big[1_D\otimes\overline{V(y)}+R(y)\otimes\overline{W(y)}\Big]\mathcal{P}\mathrm{e}^{\int_y^x \mathrm{d}z\,\check{T}(z)} \\ &\qquad\qquad\times\Big[V'(x)\otimes 1_D + W'(x)\otimes\overline{R(x)}\Big]\Big|r(x)\Big). \end{aligned} \tag{4.83}$$

To compute more complex expectation values, we first evaluate $(-L/2 < x < +L/2)$

$$\hat{\psi}(x)|\Phi[V,W]\rangle = v_{\mathrm{L}}^{\dagger}\hat{U}(-L/2,x)W(x)\hat{U}(x,L/2)v_{\mathrm{R}}|\Omega\rangle$$

$$
\begin{aligned}
&+\int_{-L/2}^{x}\mathrm{d}y\,\boldsymbol{v}_{\mathrm{L}}^{\dagger}\hat{U}(-L/2,y)\left(V(y)\otimes\hat{\mathbb{1}}+W(y)\otimes\hat{\psi}^{\dagger}(y)\right)\\
&\qquad\times\hat{U}(y,x)R(x)\hat{U}(x,L/2)\boldsymbol{v}_{\mathrm{R}}|\Omega\rangle\\
&+\int_{x}^{L/2}\mathrm{d}y\,\boldsymbol{v}_{\mathrm{L}}^{\dagger}\hat{U}(-L/2,x)R(x)\hat{U}(x,y)\\
&\qquad\times\left(V(y)\otimes\hat{\mathbb{1}}+W(y)\otimes\hat{\psi}^{\dagger}(y)\right)\hat{U}(y,L/2)\boldsymbol{v}_{\mathrm{R}}|\Omega\rangle\,. \qquad (4.84)
\end{aligned}
$$

We also obtain that (without loss of generality we can set $-L/2<x<y<+L/2$)

$$
\begin{aligned}
\hat{\psi}(y)\hat{\psi}(x)|\Phi[V,W]\rangle=&\int_{-L/2}^{x}\mathrm{d}z\,\boldsymbol{v}_{\mathrm{L}}^{\dagger}\hat{U}(-L/2,z)\left(V(z)\otimes\hat{\mathbb{1}}+W(z)\otimes\hat{\psi}^{\dagger}(z)\right)\\
&\times\hat{U}(z,x)R(x)\hat{U}(x,y)R(y)\hat{U}(y,L/2)\boldsymbol{v}_{\mathrm{R}}|\Omega\rangle\\
&+\int_{x}^{y}\mathrm{d}z\,\boldsymbol{v}_{\mathrm{L}}^{\dagger}\hat{U}(-L/2,x)R(x)\hat{U}(x,z)\left(V(z)\otimes\hat{\mathbb{1}}+W(z)\otimes\hat{\psi}^{\dagger}(z)\right)\\
&\times\hat{U}(z,y)R(y)\hat{U}(y,L/2)\boldsymbol{v}_{\mathrm{R}}|\Omega\rangle\\
&+\int_{y}^{L/2}\mathrm{d}z\,\boldsymbol{v}_{\mathrm{L}}^{\dagger}\hat{U}(-L/2,x)R(x)\hat{U}(x,y)R(y)\hat{U}(y,z)\\
&\times\left(V(z)\otimes\hat{\mathbb{1}}+W(z)\otimes\hat{\psi}^{\dagger}(z)\right)\hat{U}(z,L/2)\boldsymbol{v}_{\mathrm{R}}|\Omega\rangle\\
&+\boldsymbol{v}_{\mathrm{L}}^{\dagger}\hat{U}(-L/2,x)W(x)\hat{U}(x,y)R(y)\hat{U}(y,L/2)\boldsymbol{v}_{\mathrm{R}}|\Omega\rangle\\
&+\boldsymbol{v}_{\mathrm{L}}^{\dagger}\hat{U}(-L/2,x)R(x)\hat{U}(x,y)W(y)\hat{U}(y,L/2)\boldsymbol{v}_{\mathrm{R}}|\Omega\rangle\,. \qquad (4.85)
\end{aligned}
$$

In addition, Eq. (4.84) allows to derive

$$
\begin{aligned}
\frac{\mathrm{d}}{\mathrm{d}x}\hat{\psi}(x)|\Phi[V,W]\rangle=&\int_{-L/2}^{x}\mathrm{d}y\,\boldsymbol{v}_{\mathrm{L}}^{\dagger}\hat{U}(-L/2,y)\left(V(y)\otimes\hat{\mathbb{1}}+W(y)\otimes\hat{\psi}^{\dagger}(y)\right)\\
&\times\hat{U}(y,x)\left([Q(x),R(x)]+\frac{\mathrm{d}R}{\mathrm{d}x}(x)\right)\hat{U}(x,L/2)\boldsymbol{v}_{\mathrm{R}}|\Omega\rangle\\
&+\int_{x}^{L/2}\mathrm{d}y\,\boldsymbol{v}_{\mathrm{L}}^{\dagger}\hat{U}(-L/2,x)\left([Q(x),R(x)]+\frac{\mathrm{d}R}{\mathrm{d}x}(x)\right)\hat{U}(x,y)\\
&\times\left(V(y)\otimes\hat{\mathbb{1}}+W(y)\otimes\hat{\psi}^{\dagger}(y)\right)\hat{U}(y,L/2)\boldsymbol{v}_{\mathrm{R}}|\Omega\rangle\\
&+\boldsymbol{v}_{\mathrm{L}}^{\dagger}\hat{U}(-L/2,x)\left(V(x)\otimes\hat{\mathbb{1}}+W(x)\otimes\hat{\psi}^{\dagger}(x)\right)R(x)\hat{U}(x,L/2)\boldsymbol{v}_{\mathrm{R}}|\Omega\rangle\\
&-\boldsymbol{v}_{\mathrm{L}}^{\dagger}\hat{U}(-L/2,x)R(x)\left(V(x)\otimes\hat{\mathbb{1}}+W(x)\otimes\hat{\psi}^{\dagger}(x)\right)\hat{U}(x,L/2)\boldsymbol{v}_{\mathrm{R}}|\Omega\rangle\\
&+\boldsymbol{v}_{\mathrm{L}}^{\dagger}\hat{U}(-L/2,x)\Big([Q(x),W(x)]+[R(x),W(x)]\otimes\hat{\psi}^{\dagger}(x)\\
&\qquad+\frac{\mathrm{d}W}{\mathrm{d}x}(x)\Big)\hat{U}(x,L/2)\boldsymbol{v}_{\mathrm{R}}|\Omega\rangle\,,
\end{aligned}
$$

which we can reorder to give

$$\begin{aligned}\frac{\mathrm{d}}{\mathrm{d}x}\hat{\psi}(x)|\Phi[V,W]\rangle = &\int_{-L/2}^{x}\mathrm{d}y\,\boldsymbol{v}_{\mathrm{L}}^{\dagger}\hat{U}(-L/2,y)\left(V(y)\otimes\hat{\mathbb{1}}+W(y)\otimes\hat{\psi}^{\dagger}(y)\right)\\ &\times\hat{U}(y,x)\left([Q(x),R(x)]+\frac{\mathrm{d}R}{\mathrm{d}x}(x)\right)\hat{U}(x,L/2)\boldsymbol{v}_{\mathrm{R}}|\Omega\rangle\\ +&\int_{x}^{L/2}\mathrm{d}y\,\boldsymbol{v}_{\mathrm{L}}^{\dagger}\hat{U}(-L/2,x)\left([Q(x),R(x)]+\frac{\mathrm{d}R}{\mathrm{d}x}(x)\right)\\ &\times\hat{U}(x,y)\left(V(y)\otimes\hat{\mathbb{1}}+W(y)\otimes\hat{\psi}^{\dagger}(y)\right)\hat{U}(y,L/2)\boldsymbol{v}_{\mathrm{R}}|\Omega\rangle\\ +&\boldsymbol{v}_{\mathrm{L}}^{\dagger}\hat{U}(-L/2,x)\Big([Q(x),W(x)]\\ &+[V(x),R(x)]+\frac{\mathrm{d}W}{\mathrm{d}x}(x)\Big)\hat{U}(x,L/2)\boldsymbol{v}_{\mathrm{R}}|\Omega\rangle\,. \quad (4.86)\end{aligned}$$

Note that the term with $\hat{\psi}^{\dagger}(x)$ at the fixed position x drops out, since single boson systems automatically satisfy the regularity properties. For a system with multiple species of particles, $\mathrm{d}\hat{\psi}_{\alpha}(x)/\mathrm{d}x\,|\Phi[V,\{W_{\beta}\}]\rangle$ has a contribution containing

$$\begin{aligned}\sum_{\beta=1}^{N}\Big[&\eta_{\alpha,\beta}W_{\beta}(x)R_{\alpha}(x)-R_{\alpha}(x)W_{\beta}(x)\\ &+\eta_{\alpha,\beta}R_{\beta}(x)W_{\alpha}(x)-W_{\alpha}(x)R_{\beta}(x)\Big]\otimes\hat{\psi}_{\beta}^{\dagger}(x). \quad (4.87)\end{aligned}$$

This norm-divergent contribution disappears if Eq. (4.18) is satisfied at every time t, since imposing the regularity condition at all times implies that

$$\frac{\partial}{\partial t}\left[\eta_{\alpha,\beta}R_{\beta}(x;t)R_{\alpha}(x;t)-R_{\alpha}(x;t)R_{\beta}(x;t)\right]=0$$

with $R_{\alpha}(x;t)=R_{\alpha}(x)$ and $\partial R_{\alpha}(x;t)/\partial t=W_{\alpha}(x)$. This indeed results in Eq. (4.87).

For the generic Hamiltonian of Eq. (4.44), we obtain for the projection of the kinetic energy

$$\begin{aligned}&\langle\Phi[\overline{V},\overline{W}]|\hat{T}|\Psi[Q,R]\rangle=\\ &\quad\frac{1}{2m}\int_{-L/2}^{+L/2}\mathrm{d}x\,(l(x)|\big([Q(x),R(x)]+\frac{\mathrm{d}R}{\mathrm{d}x}(x)\big)\\ &\qquad\otimes\big([\overline{Q(x)},\overline{W(x)}]+[\overline{V(x)},\overline{R(x)}]+\overline{\frac{\mathrm{d}W}{\mathrm{d}x}(x)}\big)|r(x))\end{aligned}$$

$$+\frac{1}{2m}\int_{-L/2}^{+L/2}\mathrm{d}x\int_{x}^{+L/2}\mathrm{d}y\,(l(x)|\big([Q(x),R(x)]+\frac{\mathrm{d}R}{\mathrm{d}x}(x)\big)\otimes\big(\overline{[Q(x),R(x)]}+\overline{\frac{\mathrm{d}R}{\mathrm{d}x}(x)}\big)$$
$$\times\mathcal{P}\mathrm{e}^{\int_x^y\mathrm{d}z\,\check{T}(z)}\big[1_D\otimes\overline{V(y)}+R(y)\otimes\overline{W(y)}\big]|r(y))$$
$$+\frac{1}{2m}\int_{-L/2}^{+L/2}\mathrm{d}x\int_{-L/2}^{x}\mathrm{d}y\,(l(y)|\big[1_D\otimes\overline{V(y)}+R(y)\otimes\overline{W(y)}\big]\mathcal{P}\mathrm{e}^{\int_y^x\mathrm{d}z\,\check{T}(z)}$$
$$\times\big([Q(x),R(x)]+\frac{\mathrm{d}R}{\mathrm{d}x}(x)\big)\otimes\big(\overline{[Q(x),R(x)]}+\overline{\frac{\mathrm{d}R}{\mathrm{d}x}(x)}\big)|r(x)),\quad(4.88)$$

for the projection of the potential energy

$$\langle\Phi[\overline{V},\overline{W}]|\hat{V}|\Psi[Q,R]\rangle=\int_{-L/2}^{+L/2}\mathrm{d}x\,(l(x)|\big(R(x)\otimes\overline{W(x)}\big)|r(x))$$
$$+\int_{-L/2}^{+L/2}\mathrm{d}x\int_{x}^{+L/2}\mathrm{d}y\,v(x)(l(x)|\big(R(x)\otimes\overline{R(x)}\big)\mathcal{P}\mathrm{e}^{\int_x^y\mathrm{d}z\,\check{T}(z)}$$
$$\times\big[1_D\otimes\overline{V(y)}+R(y)\otimes\overline{W(y)}\big]|r(y))$$
$$+\int_{-L/2}^{+L/2}\mathrm{d}x\int_{-L/2}^{x}\mathrm{d}y\,v(x)(l(y)|\big[1_D\otimes\overline{V(y)}+R(y)\otimes\overline{W(y)}\big]$$
$$\times\mathcal{P}\mathrm{e}^{\int_y^x\mathrm{d}z\,\check{T}(z)}\big(R(x)\otimes\overline{R(x)}\big)|r(x)),\quad(4.89)$$

and for the projection of the interaction energy

$$\langle\Phi[\overline{V},\overline{W}]|\hat{W}|\Psi[Q,R]\rangle=$$
$$\int_{-L/2}^{+L/2}\mathrm{d}x\int_{x}^{+L/2}\mathrm{d}y\int_{y}^{+L/2}\mathrm{d}z\,w(x,y)(l(x)|\big(R(x)\otimes\overline{R(x)}\big)\mathcal{P}\mathrm{e}^{\int_x^y\mathrm{d}u\,\check{T}(u)}$$
$$\times\big(R(y)\otimes\overline{R(y)}\big)\times\mathcal{P}\mathrm{e}^{\int_y^z\mathrm{d}u'\,\check{T}(u')}\big[1_D\otimes\overline{V(z)}+R(z)\otimes\overline{W(z)}\big]|r(z))$$
$$+\int_{-L/2}^{+L/2}\mathrm{d}x\int_{x}^{+L/2}\mathrm{d}y\int_{-L/2}^{y}\mathrm{d}z\,w(x,y)(l(z)|\big[1_D\otimes\overline{V(z)}+R(z)\otimes\overline{W(z)}\big]$$
$$\times\mathcal{P}\mathrm{e}^{\int_z^x\mathrm{d}u\,\check{T}(u)}\big(R(x)\otimes\overline{R(x)}\big)\mathcal{P}\mathrm{e}^{\int_x^y\mathrm{d}u'\,\check{T}(u')}\big(R(y)\otimes\overline{R(y)}\big)|r(y))$$
$$+\int_{-L/2}^{+L/2}\mathrm{d}x\int_{x}^{+L/2}\mathrm{d}y\int_{x}^{y}\mathrm{d}z\,w(x,y)(l(x)|\big(R(x)\otimes\overline{R(x)}\big)\mathcal{P}\mathrm{e}^{\int_x^z\mathrm{d}u\,\check{T}(u)}$$
$$\times\big[1_D\otimes\overline{V(z)}+R(z)\otimes\overline{W(z)}\big]\mathcal{P}\mathrm{e}^{\int_z^y\mathrm{d}u'\,\check{T}(u')}\big(R(y)\otimes\overline{R(y)}\big)|r(y))$$
$$+\int_{-L/2}^{+L/2}\mathrm{d}x\int_{x}^{+L/2}\mathrm{d}y\,w(x,y)(l(x)|\big(R(x)\otimes\overline{W(x)}\big)\mathcal{P}\mathrm{e}^{\int_x^y\mathrm{d}u\,\check{T}(u)}\big(R(y)\otimes\overline{R(y)}\big)|r(y))$$
$$+\int_{-L/2}^{+L/2}\mathrm{d}x\int_{x}^{+L/2}\mathrm{d}y\,w(x,y)(l(x)|\big(R(x)\otimes\overline{R(x)}\big)\mathcal{P}\mathrm{e}^{\int_x^y\mathrm{d}u\,\check{T}(u)}\big(R(y)\otimes\overline{W(y)}\big)|r(y)).$$
$$(4.90)$$

If we now want to apply the time dependent variational principle, we need to look for the tangent vector $|\Phi[V^*(t), W^*(t))]\rangle$ (where we henceforth omit the explicit inclusion of $Q(t)$ and $R(t)$ in the notation of the tangent vectors) that is obtained as

$$\{V^*(t), W^*(t)\} = \min_{\{V,W\}} \Big\| |\Phi[V,W]\rangle - \left(\hat{H} - H[\overline{Q(t)}, \overline{R(t)}; Q(t), R(t)]\right) |\Psi[Q(t), R(t)]\rangle \Big\|^2 \quad (4.91)$$

with $H[\overline{Q(t)}, \overline{R(t)}; Q(t), R(t)] = \langle \Psi[\overline{Q(t)}, \overline{R(t)}] | \hat{H} | \Psi[Q(t), R(t)]\rangle$. Since this problem is quadratic in the combined variables V and W, we can expand the norm as

$$\begin{aligned} \Big\| |\Phi[V,W]\rangle - \hat{P}_0[\overline{Q}, \overline{R}; Q, R] \hat{H} |\Psi[Q(t), R(t)]\rangle \Big\|^2 = \\ \langle \Phi[\overline{V}, \overline{W}] | \Phi[V,W]\rangle - \langle \Phi[\overline{V}, \overline{W}] | \hat{P}_0[\overline{Q}, \overline{R}; Q, R] \hat{H} | \Psi[Q,R]\rangle \\ - \langle \Psi[\overline{Q}, \overline{R}] | \hat{H} \hat{P}_0[\overline{Q}, \overline{R}; Q, R] | \Phi[V,W]\rangle + \text{constant} \end{aligned}$$

and differentiate (functional derivative) with respect to $\overline{V(x)}$ and $\overline{W(x)}$. The resulting equation for $V(x)$ and $W(x)$ is strongly non-local. However, by using the left gauge fixing condition

$$(l(x)|[V(x) \otimes 1_D + W(x) \otimes \overline{R(x)}] = 0, \quad (4.92)$$

we can eliminate all non-local terms in the overlap, in order to obtain

$$\langle \Phi[\overline{V}, \overline{W}] | \Phi[V,W]\rangle = \int_{-L/2}^{+L/2} \mathrm{d}x (l(x)| W(x) \otimes \overline{W(x)} | r(x)).$$

In addition, this choice of gauge ensures that $|\Phi[V,W]\rangle \perp |\Psi[Q,R]\rangle$ so that

$$\langle \Phi[\overline{V}, \overline{W}] | \hat{P}_0[\overline{Q}, \overline{R}; Q, R] = \langle \Phi[\overline{V}, \overline{W}] | .$$

This choice of gauge also eliminates the third term in Eq. (4.88) and (4.89) and the second term in Eq. (4.90). We now define

$$\begin{aligned} (F(x)| = \int_{-L/2}^{x} \mathrm{d}y \, (l(y)| \Big[\frac{1}{2m} \left([Q(y), R(y)] + \frac{\mathrm{d}R}{\mathrm{d}y}(y) \right) \otimes \left([\overline{Q(y)}, \overline{R(y)}] + \frac{\mathrm{d}\overline{R}}{\mathrm{d}y}(y) \right) \\ + v(y) R(y) \otimes \overline{R(y)} \Big] \mathcal{P} \mathrm{e}^{\int_y^x \mathrm{d}z \, \check{T}(z)} \\ + \int_{-L/2}^{x} \mathrm{d}y \int_y^x \mathrm{d}z \, w(y,z) (R_y^{(l)}(z) | R(z) \otimes \overline{R(z)} \mathcal{P} \mathrm{e}^{\int_z^x \mathrm{d}u \, \check{T}(u)}, \end{aligned} \quad (4.93)$$

where $R_y^{(l)}(z)$ was defined in Eq. (4.47). We can thus obtain $(F(x)|$ from solving the

differential equation

$$\frac{\mathrm{d}}{\mathrm{d}x}(F(x)| = (l(x)|\Bigg[\frac{1}{2m}\big([Q(x),R(x)] + \frac{\mathrm{d}R}{\mathrm{d}x}(x)\big) \otimes \big([\overline{Q(x)},\overline{R(x)}] + \frac{\mathrm{d}\overline{R}}{\mathrm{d}x}(x)\big) + v(x)R(x)\otimes\overline{R(x)}\Bigg] + (F(x)|\breve{T}(x) + \int_{-L/2}^{x}\mathrm{d}y\, w(y,x)(R_y^{(l)}(x)|R(x)\otimes\overline{R(x)} \quad (4.94)$$

with initial condition $F(-L/2) = l(-L/2)$. The last term contains an additional integral due to the presence of a long-range interactions. It would disappear for $w(x,y) \sim \delta(x-y)$. Similar to the definition of $R_x^{(l)}(y)$, we also introduce a quantity $R_x^{(r)}(y)$ by setting $R_x^{(r)}(x) = R(x)r(x)R(x)^\dagger$ for every $x \in [-L/2,+L/2]$ and solving

$$\frac{\mathrm{d}}{\mathrm{d}y}|R_x^{(r)}(y)) = -T(y)|R_x^{(r)}(y))$$

for every $y \in [-L/2,x]$. Using the assumption that the left gauge fixing condition is satisfied, we obtain

$$\begin{aligned}
&\langle\Phi[\overline{V},\overline{W}]|\hat{H}|\Psi[Q,R]\rangle = \\
&\quad\int_{-L/2}^{+L/2}\mathrm{d}y\,(F(y)|\big[1_D\otimes\overline{V(y)} + R(y)\otimes\overline{W(y)}\big]|r(y)) \\
&\quad+\int_{-L/2}^{+L/2}\mathrm{d}x\int_x^{+L/2}\mathrm{d}z\int_x^z\mathrm{d}y\, w(x,z)(R_x^{(l)}(y)|\big[1_D\otimes\overline{V(y)} + R(y)\otimes\overline{W(y)}\big]|R_z^{(r)}(y)) \\
&\quad+\int_{-L/2}^{+L/2}\mathrm{d}y\,(l(y)|\Bigg[\frac{1}{2m}\Big([Q(y),R(y)] + \frac{\mathrm{d}R}{\mathrm{d}y}(y)\Big) \\
&\qquad\qquad\otimes\Big([\overline{Q(y)},\overline{W(y)}] + [\overline{V(y)},\overline{R(y)}] + \overline{\frac{\mathrm{d}W}{\mathrm{d}y}(y)}\Big) \\
&\qquad\qquad + v(y)R(y)\otimes\overline{W(y)}\Bigg]|r(y)) \\
&\quad+\int_{-L/2}^{+L/2}\mathrm{d}y\int_{-L/2}^{y}\mathrm{d}x\, w(x,y)(R_x^{(l)}(y)|R(y)\otimes\overline{W(y)}|r(y)) \\
&\qquad\qquad+\int_{-L/2}^{+L/2}\mathrm{d}y\int_y^{+L/2}\mathrm{d}x\, w(y,x)(l(y)|R(y)\otimes\overline{W(y)}|R_x^{(r)}(y)). \quad (4.95)
\end{aligned}$$

We now explicitly parameterize $V(x) = \mathcal{V}_\Phi[Y](x) = -l(x)^{-1}R(x)^\dagger l(x)^{1/2}Y(x)r(x)^{-1/2}$ and $W(x) = \mathcal{W}_\Phi[Y](x) = l(x)^{-1/2}Y(x)r(x)^{-1/2}$ in terms of a single matrix function $Y : \mathscr{R} \mapsto \mathbb{C}^{D\times D} : x \mapsto Y(x)$ that contains all degrees of freedom. This parameterization automatically satisfies the left gauge fixing condition and has an effective Gram matrix

that is given by

$$\langle\Phi[\overline{\mathcal{V}_\Phi}[\overline{X}],\overline{\mathcal{W}_\Phi}[\overline{X}]]|\Phi[\mathcal{V}_\Phi[Y],\mathcal{W}_\Phi[Y]]\rangle = \int_{-L/2}^{+L/2} \mathrm{d}y\ \mathrm{tr}\left\{X(y)^\dagger Y(y)\right\}.$$

We thus obtain

$$Y^*(x;t) = \frac{\delta}{\delta Y(x)^\dagger}\langle\Phi[\overline{\mathcal{V}_\Phi}[\overline{Y}],\overline{\mathcal{W}_\Phi}[\overline{Y}]]|\hat{H}|\Psi[Q(t),R(t)]\rangle. \tag{4.96}$$

and with this $V^*(t) = \mathcal{V}_\Phi[Y^*(t)]$ and $W^*(t) = \mathcal{W}_\Phi[Y^*(t)]$. This equation can rightfully be called the *quantum Gross-Pitaevskii equation*, since it reduces to the ordinary Gross-Pitaevskii equation if $D = 1$, for the particular choice of gauge in Eq. (4.63). We don't need to solve any differential equation in terms of the unknowns $V^*(x)$ and $W^*(x)$. However, we do of course need to solve differential equations in Eq. (4.38) and Eq. (4.94) in order to obtain $l(x)$, $r(x)$ and $F(x)$. These differential equations are entirely formulated in terms of $Q(x)$ and $R(x)$, which are known functions. They can thus be solved efficiently ($\mathcal{O}(D^3)$) with any standard numerical integrator. Other integrals that appear in Eq. (4.94) and Eq. (4.95) are a consequence of having long-range interactions and will disappear if $w(x,y) \sim \delta(x-y)$. While the evaluation of the expectation value of the Hamiltonian $\hat{H}$ with long range interactions for the continuous matrix product state $|\Psi[Q,\{R_\alpha\}]\rangle$ requires $\mathcal{O}(N^2D^3)$ operations —with N the number of discretization points on which the differential equations and integrals are solved—, the application of the time-dependent variational principle requires in general $\mathcal{O}(N^3D^3)$ operations. For a strictly local interaction $w(x,y) \sim \delta(x-y)$, $\mathcal{O}(ND^3)$ operations suffices both for the evaluation of the expectation value of $\hat{H}$ as for the application of the time-dependent variational principle. As final note, we point out that the representation of $V(x)$ and $W(x)$ in terms of $Y(x)$ might be ill-defined near the boundaries, as $l(-L/2)$ ($r(+L/2)$) is singular so that $l(x)$ ($r(x)$) will be ill-conditioned near $x = -L/2$ ($x = +L/2$).

2.2. Time-dependent variational principle for uniform continuous matrix product states

The application of the time-dependent variational principle cleans up significantly for the case of uniform continuous matrix product states. In principle, we only need the set of momentum zero tangent vectors $|\Phi_0(V,W)\rangle$ for the application of the time-dependent variational principle to the variational class of uniform continuous matrix product states. However, we state results for general tangent states $|\Phi_p(V,W)\rangle$ with arbitrary momentum p, as we need these results in the following subsections on excitations. We can recycle some results from the previous subsection by setting $Q(x) = Q$, $R(x) = R$, $W(x) = We^{ipx}$ and $V(x) = Ve^{ipx}$ and taking the thermodynamic limit $L \to \infty$.

Let ($l|$ and $|r$) the left and right eigenvectors corresponding to the zero eigenvalue of

the transfer matrix $\check{T}$. As in Subsection 1.6, we define $\check{Q} = \mathbb{1} - |r)(l|$ and $(-\check{T} \pm \mathrm{i}p)^{\mathsf{P}} = \check{Q}(-\check{T} \pm \mathrm{i}p)^{-1}\check{Q}$. Note that only for $p = 0$ this is a true pseudo-inverse. We can easily evaluate the scalar product $\langle \Phi_p(\overline{V}, \overline{W}) | \Phi_{p'}(V', W') \rangle$ as

$$\begin{aligned}
&\langle \Phi_p(\overline{V}, \overline{W}) | \Phi_{p'}(V', W') \rangle = \\
&2\pi\delta(p'-p) \Big[2\pi\delta(p)(l|V' \otimes 1_D + W' \otimes \overline{R}|r)(l|1_D \otimes \overline{V} + R \otimes \overline{W}'|r) + (l|W' \otimes \overline{W}|r) \\
&\qquad + (l|(1_D \otimes \overline{V} + R \otimes \overline{W})(-\check{T} - \mathrm{i}p)^{\mathsf{P}}(V' \otimes 1_D + W' \otimes \overline{R})|r) \\
&\qquad\quad + (l|(V' \otimes 1_D + W' \otimes \overline{R})(-\check{T} + \mathrm{i}p)^{\mathsf{P}}(1_D \otimes \overline{V} + R \otimes \overline{W})|r) \Big] . \qquad (4.97)
\end{aligned}$$

States with different momenta are automatically orthogonal. As usual, states with a definite momentum in an infinite system cannot be orthogonalized to a finite constant: they satisfy a δ normalization. For $p = 0$, there is a divergence inside the factor multiplying $\delta(p - p')$. This divergence is unphysical and disappears if we impose orthogonality with respect to the state $|\Psi(Q,R)\rangle$, which boils down to

$$\langle \Psi(\overline{Q}, \overline{R}) | \Phi_0(V, W) \rangle = 2\pi\delta(0)(l|V \otimes 1_D + W \otimes \overline{R}|r) = 0 \qquad (4.98)$$

for all states $|\Phi_0(V, W)\rangle$. For $p \neq 0$, they are automatically orthogonal to the translation invariant uniform cMPS $|\Psi(Q,R)\rangle$ and there is no physical nor mathematical need for additional constraints. We can impose the left gauge fixing requirement, $(l|[V \otimes 1_D + W \otimes \overline{R}] = 0$, which eliminates all but the second term in Eq. (4.97) and automatically imposes orthogonality at $p = 0$.

The overlap $\langle \Phi_k(\overline{V}, \overline{W}) | \hat{H} | \Psi(Q,R) \rangle$ can be evaluated as

$$\begin{aligned}
&\langle \Phi_p(\overline{V}, \overline{W}) | \hat{H} | \Psi(Q,R) \rangle = 2\pi\delta(p) \\
&\quad \times \Big[2\pi\delta(p)(l|\frac{1}{2m}[Q,R] \otimes [\overline{Q}, \overline{R}] + v(R \otimes \overline{R}) \\
&\qquad\qquad + (R \otimes \overline{R})\mathcal{L}[w](-\check{T})(R \otimes \overline{R})|r)(l|1_D \otimes \overline{V} + R \otimes \overline{W}|r) \\
&\qquad + (l| \Big(\frac{1}{2m}[Q,R] \otimes [\overline{Q}, \overline{R}] + v(R \otimes \overline{R}) + (R \otimes \overline{R})\mathcal{L}[w](-\check{T})(R \otimes \overline{R}) \Big) \\
&\qquad\qquad (-\check{T})^{\mathsf{P}} (1_D \otimes \overline{V} + R \otimes \overline{W})|r) \\
&\qquad + (l|(1_D \otimes \overline{V} + R \otimes \overline{W})(-\check{T})^{\mathsf{P}} \\
&\qquad\quad \Big(\frac{1}{2m}[Q,R] \otimes [\overline{Q}, \overline{R}] + v(R \otimes \overline{R}) + (R \otimes \overline{R})\mathcal{L}[w](-\check{T})(R \otimes \overline{R}) \Big)|r) \\
&\qquad + \int_0^{+\infty} \mathrm{d}x \int_0^x \mathrm{d}y\, w(x)(l|(R \otimes \overline{R})\mathrm{e}^{\check{T}y}(1_D \otimes \overline{V} + R \otimes \overline{W})\mathrm{e}^{\check{T}(x-y)}(R \otimes \overline{R})|r) \\
&\qquad + (l|\frac{1}{2m}[Q,R] \otimes \big([\overline{Q}, \overline{W}] + [\overline{V}, \overline{R}] \big) + vR \otimes \overline{W}
\end{aligned}$$

$$+(R\otimes\overline{W})\mathcal{L}[w](-\check{T})(R\otimes\overline{R})+(R\otimes\overline{R})\mathcal{L}[w](-\check{T})(R\otimes\overline{W})|r)\Big]. \quad (4.99)$$

The prefactor illustrates that only the set of tangent vectors with momentum zero can have a non-zero overlap with the evolution vector for uniform continuous matrix product states. It cancels with the diverging prefactor in the normalization of $|\Phi_0(\overline{V},\overline{W})\rangle$. The first term in the square brackets contains the divergent contribution of $\langle\Psi(Q,R)|\hat{H}|\Psi(Q,R)\rangle$, which disappears by replacing $\hat{H}$ by $\hat{H}-H(\overline{Q},\overline{R},Q,R)$ in the evolution vector, or just by imposing the orthogonality $\langle\Psi_0(\overline{V},\overline{W})|\Psi(Q,R)\rangle$, as follows from the second factor in this term. The term on the third line will once again disappear by using the left gauge fixing condition. Note also that

$$(l|\left(\frac{1}{2m}[Q,R]\otimes[\overline{Q},\overline{R}]+vR\otimes\overline{R}+R\otimes\overline{R}\mathcal{L}[w](-T)R\otimes\overline{R}\right)(-\check{T})^{\mathsf{P}}$$

is the steady state solution $(F|$ as predicted from Eq. (4.94). The fourth line below the equality sign is only present for long range interactions and disappears if $w(x,y)\sim\delta(x-y)$. Evaluating it for general interactions w is easiest by diagonalizing $\check{T}$, which is an operation with computational cost of $\mathcal{O}(D^6)$. If $\check{T}=\sum_{k=1}^{D^2}\lambda^{(k)}|r^{(k)})(l^{(k)}|$ with $\lambda^{(1)}=0$, $|r^{(1)})=|r)$ and $(l^{(1)}|=(l|$, we can compute

$$\begin{aligned}
&\int_0^{+\infty}\mathrm{d}x\int_0^x\mathrm{d}y\,w(x)(l|(R\otimes\overline{R})\mathrm{e}^{\check{T}y}\big(1_D\otimes\overline{V}+R\otimes\overline{W}\big)\mathrm{e}^{\check{T}(x-y)}(R\otimes\overline{R})|r)\\
&\quad=\sum_{\alpha,\beta=1}^{D^2}(l|R\otimes\overline{R}|r_\alpha)(l_\alpha|\big(1_D\otimes\overline{V}+R\otimes\overline{W}\big)|r_\beta)(l_\beta|R\otimes\overline{R}|r)\\
&\qquad\qquad\times\int_0^{+\infty}\mathrm{d}x\int_0^x\mathrm{d}y\,w(x)\mathrm{e}^{(\lambda_\alpha-\lambda_\beta)y}\mathrm{e}^{\lambda_\beta x}\\
&\quad=\sum_{\alpha,\beta=1}^{D^2}(l|R\otimes\overline{R}|r_\alpha)(l_\alpha|\big(1_D\otimes\overline{V}+R\otimes\overline{W}\big)|r_\beta)(l_\beta|R\otimes\overline{R}|r)\\
&\qquad\qquad\times\int_0^{+\infty}\mathrm{d}x\,w(x)\left(\delta_{\alpha,\beta}x\mathrm{e}^{\lambda_\alpha x}+(1-\delta_{\alpha,\beta})\frac{\mathrm{e}^{\lambda_\alpha x}-\mathrm{e}^{\lambda_\beta x}}{\lambda_\alpha-\lambda_\beta}\right)\\
&\quad=\sum_{\alpha,\beta=1}^{D^2}(l|R\otimes\overline{R}|r_\alpha)(l_\alpha|\big(1_D\otimes\overline{V}+R\otimes\overline{W}\big)|r_\beta)(l_\beta|R\otimes\overline{R}|r)\\
&\qquad\times\left(-\delta_{\alpha,\beta}\mathcal{L}'[w](-\lambda_\alpha)+(1-\delta_{\alpha,\beta})\frac{\mathcal{L}[w](-\lambda_\alpha)-\mathcal{L}'[w](-\lambda_\beta)}{\lambda_\alpha-\lambda_\beta}\right), \quad (4.100)
\end{aligned}$$

with $\mathcal{L}'[w]=\mathcal{L}[-xw]$ and thus $-\mathcal{L}'[w](-\lambda_\alpha)=\frac{\mathrm{d}}{\mathrm{d}\lambda_\alpha}\mathcal{L}[w](-\lambda_\alpha)$ the derivative of the Laplace transform of w. At first sight, it seems as if computing $(l_\alpha|\big(1_D\otimes\overline{V}+R\otimes\overline{W}\big)|r_\beta)$ for all $\alpha,\beta=1,\ldots,D^2$ will be a $\mathcal{O}(D^4D^3)=\mathcal{O}(D^7)=$ operation. However, we can first compute $(l_\alpha|\big(1_D\otimes\overline{V}+R\otimes\overline{W}\big)$ for all $\alpha=1,\ldots,D^2$, which is a $\mathcal{O}(D^2D^3)=\mathcal{O}(D^5)$

operation and store this result. The computation of $(l_\alpha|(1_D \otimes \overline{V} + R \otimes \overline{W})|r_\beta)$ for a single combination (α,β) is then only $\mathcal{O}(D^2)$, and the total cost is $\mathcal{O}(D^6)$. At no point does the memory cost exceeds $\mathcal{O}(D^4)$.

If only local interactions $[w(x) \sim \delta(x)]$ are present, we can use iterative methods to compute the inverses of $\check{T}$ and to obtain a $\mathcal{O}(D^3)$ method. Also, if all long-range interactions are of the exponential type $[w(x) = \sum_{\alpha=1}^{k} c_\alpha \exp(-\mu_\alpha x)$ with $k \ll D^2]$, then we obtain

$$\int_0^{+\infty} \mathrm{d}x \int_0^x \mathrm{d}y\, w(x)(l|(R\otimes\overline{R})\mathrm{e}^{\check{T}y}(1_D\otimes\overline{V}+R\otimes\overline{W})\mathrm{e}^{\check{T}(x-y)}(R\otimes\overline{R})|r) = \sum_{\alpha=1}^{k} c_\alpha (l|(R\otimes\overline{R})(\mu_\alpha-\check{T})^{-1}(1_D\otimes\overline{V}+R\otimes\overline{W})(\mu_\alpha-\check{T})^{-1}(R\otimes\overline{R})|r) \quad (4.101)$$

and we can try to compute all functions of $\check{T}$ with iterative methods in order to obtain an approach with computational cost $\mathcal{O}(kD^3)$.

To impose the left gauge fixing condition, we can use a parameterization where $V = \mathcal{V}_{\Phi_p}(Y) = -l^{-1}R^\dagger l^{1/2} Y r^{-1/2}$ and $W = \mathcal{W}_{\Phi_p}(Y) = l^{-1/2} Y r^{-1/2}$. Inserting this parameterization allows to determine $Y^*(t)$ as

$$2\pi\delta(0)Y^*(t) = \frac{\partial}{\partial Y^\dagger}\langle \Phi_0(\overline{\mathcal{V}_{\Phi_0}}(\overline{Y}),\overline{\mathcal{W}_{\Phi_0}}(\overline{Y}))|\hat{H}|\Psi(Q(t),R(t))\rangle \quad (4.102)$$

and thus $V^*(t) = \mathcal{V}_{\Phi_0}(Y^*(t))$ and $W^*(t) = \mathcal{W}_{\Phi_0}(Y^*(t))$. We can combine this with the left orthonormalization gauge for Q,R, so that $l = 1_D$ and $Q = K - \frac{1}{2}R^\dagger R$ with K an antihermitian matrix. In an imaginary time algorithm with time step, we would update R as $R(t+\mathrm{d}t) = R(t) - \mathrm{d}t\, W^*(t)$ and $Q(t+\mathrm{d}t) = Q(t) - \mathrm{d}t\, V^*(t) = K(t) - \frac{1}{2}R^\dagger(t)R(t) + \mathrm{d}t R^\dagger(t) W^*(t)$. This update rule only conserves the left orthonormalization gauge to first order, since $Q(t+\mathrm{d}t)$ is no longer of the format $Q(t+\mathrm{d}t) = K(t+\mathrm{d}t) - \frac{1}{2}R(t+\mathrm{d}t)^\dagger R(t+\mathrm{d}t)$. However, if we completely eliminate Q, we can obtain the first order update rule for K as $K(t+\mathrm{d}t) = K(t) + \frac{\mathrm{d}t}{2}\left(R(t)^\dagger W^*(t) - W^*(t)^\dagger R(t)\right)$. This produces the same update rule for $Q(t+\mathrm{d}t)$ up to a correction of second order in $\mathrm{d}t$, but produces a new antihermitean matrix $K(t+\mathrm{d}t)$, so that the left orthonormalization gauge is conserved exactly! We still have the freedom to apply a unitary gauge transform to $K(t+\mathrm{d}t)$ and $R(t+\mathrm{d}t)$, in order to *e.g.* diagonalize $r(t+\mathrm{d}t)$.

As for the case of matrix product states, we can in principle derive local convergence and error measures $\tilde{\eta}(\overline{Q},\overline{R};Q,R)$ and $\tilde{\epsilon}(\overline{Q},\overline{R};Q,R)$ for the uniform continuous matrix product state $|\Psi[Q,R]\rangle$. The convergence measure is simply given by $\tilde{\eta}(\overline{Q},\overline{R};Q,R) = \mathrm{tr}((Y^*)^\dagger Y^*)$ with Y^* the optimal value for the parameterization of the tangent vector as defined above. The expression for the error measure becomes very cumbersome for the case of long-range interactions, and diverges for the case of short range interactions, since ΔH^2 contains the expectation value of $\int \mathrm{d}x \int \mathrm{d}y\, \langle \hat{\psi}^\dagger(x)^2 \hat{\psi}(x)^2 \hat{\psi}^\dagger(y)^2 \hat{\psi}(y)^2\rangle$. On

bringing this expression in normal order, we encounter $\int \mathrm{d}x\, \langle \hat{\psi}^\dagger(x)^2 \hat{\psi}(x)\hat{\psi}^\dagger(x)\hat{\psi}(x)^2\rangle$ which produces a $\delta(0)$. Hence, we do not attempt to derive general expressions for the error measure. Finally, we can also develop a strategy to dynamically expand the variational manifold by increasing the bond dimension D of the continuous matrix product state at a certain time during the evolution. This is discussed in Subsection 2.1 of Appendix A.

2.3. Ansatz for topologically trivial excited states

We now define an ansatz for momentum eigenstates, that is suited to describe low-lying, point-like excitations of translation invariant Hamiltonians, such as the generic Hamiltonian of Eq. (4.44) with $v(x) = v$ and $w(x,y) = w(x-y)$. Our ansatz consists of simply taking the states $|\Phi_p(V,W)\rangle$ living in the tangent plane $\mathbb{T}^\perp_{\Phi_p}(Q,R)$ of the uniform continuous matrix product state $|\Psi(Q,R)\rangle \in \mathscr{M}_{\mathrm{ucMPS}}$ that best approximates the ground state of the Hamiltonian. In order to apply the variational principle, which boils down to the Rayleigh-Ritz method, we need to compute $\langle \Phi_p(\overline{V},\overline{W})|\Phi_{p'}(V,W)\rangle$, which was determined in the previous section, and $\langle \Phi_p(\overline{V},\overline{W})|\hat{H}|\Phi_{p'}(V,W)\rangle$, which is determined next.

Evaluating the expectation value of the Hamiltonian is a bit more involved. First of all, we need to evaluate the full Hamiltonian, not only the Hamiltonian density. But, this expectation value contains a divergent contribution $\langle \Psi(\overline{Q},\overline{R})|\hat{H}|\Psi(Q,R)\rangle = H(\overline{Q},\overline{R};Q,R) = \int_{-\infty}^{+\infty} \mathrm{d}x\, h(\overline{Q},\overline{R};Q,R)$ from the ground state energy, which is an extensive quantity. The best way to make sure that we subtract this infinite constant correctly, is to redefine the Hamiltonian as

$$\hat{H} \leftarrow \hat{H} - \int_{-\infty}^{+\infty} \mathrm{d}x\, h(\overline{Q},\overline{R};Q,R), \tag{4.103}$$

with

$$h(\overline{Q},\overline{R};Q,R) = \langle l|\frac{1}{2m}([Q,R]\otimes[\overline{Q},\overline{R}]) + vR\otimes\overline{R} + (R\otimes\overline{R})\mathcal{L}[w](-\check{T})(R\otimes\overline{R})|r\rangle\,. \tag{4.104}$$

Correspondingly, the energy density is redefined as

$$\begin{aligned}\hat{h}(x) = \frac{1}{2m}\Big(\frac{\mathrm{d}\hat{\psi}^\dagger}{\mathrm{d}x}(x)\Big)\Big(\frac{\mathrm{d}\hat{\psi}}{\mathrm{d}x}(x)\Big) + v\hat{\psi}^\dagger(x)\hat{\psi}(x) \\ + \int_{-\infty}^{+\infty} \mathrm{d}y\, w(y)\hat{\psi}^\dagger(x)\hat{\psi}^\dagger(x+y)\hat{\psi}(x+y)\hat{\psi}(x) - h(\overline{Q},\overline{R};Q,R)\hat{\mathbb{1}}.\end{aligned} \tag{4.105}$$

We can use the translation non-invariant results from the Subsection 2.1 in order to obtain

$$\begin{aligned}\hat{\psi}(x)|\Phi_p(V,W)\rangle &= \mathrm{e}^{\mathrm{i}px}\,\langle \boldsymbol{v}_L|\hat{U}(-\infty,x)W\hat{U}(x,+\infty)|\boldsymbol{v}_R\rangle\,|\Omega\rangle \\ &+\int_{-\infty}^{x}\mathrm{d}y\,\mathrm{e}^{\mathrm{i}py}\boldsymbol{v}_L^\dagger\hat{U}(-\infty,y)\left(V\otimes\hat{\mathbb{1}}+W\otimes\hat{\psi}^\dagger(y)\right) \\ &\qquad\times\hat{U}(y,x)R\hat{U}(x,+\infty)\boldsymbol{v}_R\,|\Omega\rangle \\ &+\int_{x}^{+\infty}\mathrm{d}y\,\mathrm{e}^{\mathrm{i}py}\boldsymbol{v}_L^\dagger\hat{U}(-\infty,x)R\hat{U}(x,y) \\ &\qquad\times\left(V\otimes\hat{\mathbb{1}}+W\otimes\hat{\psi}^\dagger(y)\right)\hat{U}(y,+\infty)\boldsymbol{v}_R\,|\Omega\rangle \end{aligned} \tag{4.106}$$

and

$$\begin{aligned}\hat{\psi}(y)\hat{\psi}(x)|\Phi_p(V,W)\rangle &= \mathrm{e}^{\mathrm{i}px}\boldsymbol{v}_{\mathrm{L}}^\dagger\hat{U}(-\infty,x)W\hat{U}(x,y)R\hat{U}(y,+\infty)\boldsymbol{v}_{\mathrm{R}}\,|\Omega\rangle \\ &+\mathrm{e}^{\mathrm{i}py}\boldsymbol{v}_{\mathrm{L}}^\dagger\hat{U}(-L/2,x)R\hat{U}(x,y)W\hat{U}(y,+\infty)\boldsymbol{v}_{\mathrm{R}}\,|\Omega\rangle \\ &+\int_{-\infty}^{x}\mathrm{d}z\,\mathrm{e}^{\mathrm{i}pz}\boldsymbol{v}_{\mathrm{L}}^\dagger\hat{U}(-\infty,z)\left(V\otimes\hat{\mathbb{1}}+W\otimes\hat{\psi}^\dagger(z)\right) \\ &\qquad\times\hat{U}(z,x)R\hat{U}(x,y)R\hat{U}(y,+\infty)\boldsymbol{v}_{\mathrm{R}}\,|\Omega\rangle \\ &+\int_{x}^{y}\mathrm{d}z\,\mathrm{e}^{\mathrm{i}pz}\boldsymbol{v}_{\mathrm{L}}^\dagger\hat{U}(-\infty,x)R\hat{U}(x,z)\left(V\otimes\hat{\mathbb{1}}+W\otimes\hat{\psi}^\dagger(z)\right) \\ &\qquad\times\hat{U}(z,y)R\hat{U}(y,+\infty)\boldsymbol{v}_{\mathrm{R}}\,|\Omega\rangle \\ &+\int_{y}^{+\infty}\mathrm{d}z\,\mathrm{e}^{\mathrm{i}pz}\boldsymbol{v}_{\mathrm{L}}^\dagger\hat{U}(-\infty,x)R\hat{U}(x,y)R(y,z) \\ &\qquad\times\left(V\otimes\hat{\mathbb{1}}+W\otimes\hat{\psi}^\dagger(z)\right)\hat{U}(z,+\infty)\boldsymbol{v}_{\mathrm{R}}\,|\Omega\rangle \end{aligned} \tag{4.107}$$

as well as

$$\begin{aligned}&\frac{\mathrm{d}}{\mathrm{d}x}\hat{\psi}(x)|\Phi_p(V,W)\rangle = \\ &\quad\mathrm{e}^{\mathrm{i}px}\boldsymbol{v}_L^\dagger\hat{U}(-\infty,x)([V,R]+[Q,W]+\mathrm{i}pW)\,\hat{U}(x,+\infty)\boldsymbol{v}_R\,|\Omega\rangle \\ &\quad+\int_{-\infty}^{x}\mathrm{d}y\,\mathrm{e}^{\mathrm{i}py}\boldsymbol{v}_L^\dagger\hat{U}(-\infty,y)\left(V\otimes\hat{\mathbb{1}}+W\otimes\hat{\psi}^\dagger(y)\right) \\ &\qquad\times\hat{U}(y,x)[Q,R]\hat{U}(x,+\infty)\boldsymbol{v}_R\,|\Omega\rangle \\ &\quad+\int_{x}^{+\infty}\mathrm{d}y\,\mathrm{e}^{\mathrm{i}py}\boldsymbol{v}_L^\dagger\hat{U}(-\infty,x)[Q,R]\hat{U}(x,y) \\ &\qquad\times\left(V\otimes\hat{\mathbb{1}}+W\otimes\hat{\psi}^\dagger(y)\right)\hat{U}(y,+\infty)\boldsymbol{v}_R\,|\Omega\rangle\,. \end{aligned} \tag{4.108}$$

We can now collect everything and evaluate the general overlap:

$$\langle\Phi_p(\overline{V},\overline{W})|\hat{H}|\Phi_{p'}(V',W')\rangle = 2\pi\delta(p'-p)\times$$

$$
\begin{aligned}
&\Big\{\Big[\Big(l\Big|\frac{1}{2m}([V',R]+[Q,W']+\mathrm{i}pW')\otimes([\overline{V},\overline{R}]+[\overline{Q},\overline{W}]-\mathrm{i}p\overline{W})\\
&\qquad\qquad+vW'\otimes\overline{W}\\
&\qquad+(W'\otimes\overline{W})\mathcal{L}[w](-\check{T})(R\otimes\overline{R})+(R\otimes\overline{R})\mathcal{L}[w](-\check{T})(W'\otimes\overline{W})\Big|r\Big)\\
&+\Big(l\Big|(W'\otimes\overline{W})(-\check{T})^{\mathsf{P}}\Big(\frac{1}{2m}[Q,R]\otimes[\overline{Q},\overline{R}]\\
&\qquad\qquad+vR\otimes\overline{R}+(R\otimes\overline{R})\mathcal{L}[w](-\check{T})(R\otimes\overline{R})\Big)\Big|r\Big)\\
&+\Big(l\Big|\Big(\frac{1}{2m}[Q,R]\otimes[\overline{Q},\overline{R}]+vR\otimes\overline{R}\\
&\qquad\qquad+(R\otimes\overline{R})\mathcal{L}[w](-\check{T})(R\otimes\overline{R})\Big)(-\check{T})^{\mathsf{P}}(W'\otimes\overline{W})\Big|r\Big)\\
&\qquad+\int_0^{+\infty}\mathrm{d}x\int_0^x\mathrm{d}y\,w(x)\Big(l\Big|(R\otimes\overline{R})\mathrm{e}^{\check{T}y}(W'\otimes\overline{W})\mathrm{e}^{\check{T}(x-y)}(R\otimes\overline{R})\Big|r\Big)\Big]\\
&+\Big[\Big(l\Big|(W'\otimes\overline{R})\mathcal{L}[w](-\check{T}+\mathrm{i}p)(R\otimes\overline{W})\Big|r\Big)\\
&\qquad\qquad+\Big(l\Big|(R\otimes\overline{W})\mathcal{L}[w](-\check{T}-\mathrm{i}p)(W'\otimes\overline{R})\Big|r\Big)\Big]\\
&+\Big[\Big(l\Big|(V'\otimes\mathbb{1}_D+W'\otimes\overline{R})(-\check{T}+\mathrm{i}p)^{\mathsf{P}}\\
&\qquad\times\Big(\frac{1}{2m}[Q,R]\otimes([\overline{Q},\overline{W}]+[\overline{V},\overline{R}]-\mathrm{i}p\overline{W})+vR\otimes\overline{W}\\
&\qquad\qquad+(R\otimes\overline{W})\mathcal{L}[w](-\check{T})(R\otimes\overline{R})\\
&\qquad\qquad+(R\otimes\overline{R})\mathcal{L}[w](-\check{T}+\mathrm{i}p)(R\otimes\overline{W})\Big)\Big|r\Big)\\
&+\Big(l\Big|\Big(\frac{1}{2m}[Q,R]\otimes([\overline{Q},\overline{W}]+[\overline{V},\overline{R}]-\mathrm{i}p\overline{W})+vR\otimes\overline{W}\\
&\qquad+(R\otimes\overline{W})\mathcal{L}[w](-\check{T}-\mathrm{i}p)(R\otimes\overline{R})\\
&\qquad+(R\otimes\overline{R})\mathcal{L}[w](-\check{T})(R\otimes\overline{W})\Big)\\
&\qquad\qquad\times(-\check{T}-\mathrm{i}p)^{\mathsf{P}}(V'\otimes\mathbb{1}_D+W'\otimes\overline{R})\Big|r\Big)\\
&+\int_0^{+\infty}\mathrm{d}x\int_0^x\mathrm{d}y\,w(x)\Big(l\Big|(R\otimes\overline{R})\mathrm{e}^{\check{T}y}(V'\otimes\mathbb{1}_D+W'\otimes\overline{R})\\
&\qquad\qquad\times\mathrm{e}^{(\check{T}-\mathrm{i}p)(x-y)}(R\otimes\overline{W})\Big|r\Big)\\
&+\int_0^{+\infty}\mathrm{d}x\int_0^x\mathrm{d}y\,w(x)\Big(l\Big|(R\otimes\overline{W})\mathrm{e}^{(\check{T}+\mathrm{i}p)y}\\
&\qquad\qquad\times(V'\otimes\mathbb{1}_D+W'\otimes\overline{R})\mathrm{e}^{\check{T}(x-y)}(R\otimes\overline{R})\Big|r\Big)\Big]
\end{aligned}
$$

$$
\begin{aligned}
&+\Big[\Big(l\Big|(\mathbb{1}_D\otimes\overline{V}+R\otimes\overline{W})(-\check{T}-\mathrm{i}p)^{\mathsf{P}}\\
&\qquad\times\Big(\frac{1}{2m}([Q,W']+[V',R]+\mathrm{i}pW')\otimes[\overline{Q},\overline{R}]+vW'\otimes\overline{R}\\
&\qquad\qquad+(W'\otimes\overline{R})\mathcal{L}[w](-\check{T})(R\otimes\overline{R})\\
&\qquad\qquad+(R\otimes\overline{R})\mathcal{L}[w](-\check{T}-\mathrm{i}p)(W'\otimes\overline{R})\Big)\Big|r\Big)\\
&+\Big(l\Big|\Big(\frac{1}{2m}([Q,W']+[V',R]+\mathrm{i}pW')\otimes[\overline{Q},\overline{R}]+vW'\otimes\overline{R}\\
&\qquad+(W'\otimes\overline{R})\mathcal{L}[w](-\check{T}+\mathrm{i}p)(R\otimes\overline{R})\\
&\qquad+(R\otimes\overline{R})\mathcal{L}[w](-\check{T})(W'\otimes\overline{R})\Big)\\
&\qquad\qquad\times(-\check{T}+\mathrm{i}p)^{\mathsf{P}}(\mathbb{1}_D\otimes\overline{V}+R\otimes\overline{W})\Big|r\Big)\\
&+\int_0^{+\infty}\mathrm{d}x\int_0^x\mathrm{d}y\,w(x)\Big(l\Big|(R\otimes\overline{R})\mathrm{e}^{\check{T}y}(\mathbb{1}_D\otimes\overline{V}+R\otimes\overline{W})\\
&\qquad\qquad\mathrm{e}^{(\check{T}+\mathrm{i}p)(x-y)}(W'\otimes\overline{R})\Big|r\Big)\\
&+\int_0^{+\infty}\mathrm{d}x\int_0^x\mathrm{d}y\,w(x)\Big(l\Big|(W'\otimes\overline{R})\mathrm{e}^{(\check{T}-\mathrm{i}p)y}\\
&\qquad\qquad(\mathbb{1}_D\otimes\overline{V}+R\otimes\overline{W})\mathrm{e}^{\check{T}(x-y)}(R\otimes\overline{R})\Big|r\Big)\Big]\\
&+\Big[\Big(l\Big|(V'\otimes\mathbb{1}_D+W'\otimes\overline{R})(-\check{T}+\mathrm{i}p)^{\mathsf{P}}(\mathbb{1}_D\otimes\overline{V}+R\otimes\overline{W})(-\check{T})^{\mathsf{P}}\\
&\qquad\times\Big(\frac{1}{2m}[Q,R]\otimes[\overline{Q},\overline{R}]+vR\otimes\overline{R}+(R\otimes\overline{R})\mathcal{L}[w](-\check{T})(R\otimes\overline{R})\Big)\Big|r\Big)\\
&+\Big(l\Big|(\mathbb{1}_D\otimes\overline{V}+R\otimes\overline{W})(-\check{T}-\mathrm{i}p)^{\mathsf{P}}(V'\otimes\mathbb{1}_D+W'\otimes\overline{R})(-\check{T})^{\mathsf{P}}\\
&\qquad\times\Big(\frac{1}{2m}[Q,R]\otimes[\overline{Q},\overline{R}]+vR\otimes\overline{R}+(R\otimes\overline{R})\mathcal{L}[w](-\check{T})(R\otimes\overline{R})\Big)\Big|r\Big)\\
&+\Big(l\Big|\Big(\frac{1}{2m}[Q,R]\otimes[\overline{Q},\overline{R}]+vR\otimes\overline{R}+(R\otimes\overline{R})\mathcal{L}[w](-\check{T})(R\otimes\overline{R})\Big)\\
&\qquad\times(-\check{T})^{\mathsf{P}}(V'\otimes\mathbb{1}_D+W'\otimes\overline{R})(-\check{T}+\mathrm{i}p)^{\mathsf{P}}(\mathbb{1}_D\otimes\overline{V}+R\otimes\overline{W})\Big|r\Big)\\
&+\Big(l\Big|\Big(\frac{1}{2m}[Q,R]\otimes[\overline{Q},\overline{R}]+vR\otimes\overline{R}+(R\otimes\overline{R})\mathcal{L}[w](-\check{T})(R\otimes\overline{R})\Big)\\
&\qquad\times(-\check{T})^{\mathsf{P}}(\mathbb{1}_D\otimes\overline{V}+R\otimes\overline{W})(-\check{T}-\mathrm{i}p)^{\mathsf{P}}(V'\otimes\mathbb{1}_D+W'\otimes\overline{R})\Big|r\Big)\\
&+\Big(l\Big|(V'\otimes\mathbb{1}_D+W'\otimes\overline{R})(-\check{T}+\mathrm{i}p)^{\mathsf{P}}\Big(\frac{1}{2m}[Q,R]\otimes[\overline{Q},\overline{R}]+vR\otimes\overline{R}\\
&\qquad+(R\otimes\overline{R})\mathcal{L}[w](-\check{T}+\mathrm{i}p)(R\otimes\overline{R})\Big)(-\check{T}+\mathrm{i}p)^{\mathsf{P}}(\mathbb{1}_D\otimes\overline{V}+R\otimes\overline{W})\Big|r\Big)\\
&+\Big(l\Big|(\mathbb{1}_D\otimes\overline{V}+R\otimes\overline{W})(-\check{T}-\mathrm{i}p)^{\mathsf{P}}\Big(\frac{1}{2m}[Q,R]\otimes[\overline{Q},\overline{R}]+vR\otimes\overline{R}
\end{aligned}
$$

$$
\begin{aligned}
&+(R\otimes\overline{R})\mathcal{L}[w](-\check{T}-\mathrm{i}p)(R\otimes\overline{R})\Big)(-\check{T}-\mathrm{i}p)^{\mathsf{P}}(V'\otimes\mathbb{1}_D+W'\otimes\overline{R})\Big|r\Big)\\
&+\int_0^{+\infty}\mathrm{d}x\int_0^x\mathrm{d}y\int_0^y\mathrm{d}z\,w(x)\Big(l\Big|(R\otimes\overline{R})\mathrm{e}^{\check{T}z}(V'\otimes\mathbb{1}_D+W'\otimes\overline{R})\mathrm{e}^{(\check{T}-\mathrm{i}p)(y-z)}\\
&\qquad\times(\mathbb{1}_D\otimes\overline{V}+R\otimes\overline{W})\mathrm{e}^{\check{T}(x-y)}(R\otimes\overline{R})\Big|r\Big)\\
&+\int_0^{+\infty}\mathrm{d}x\int_0^x\mathrm{d}y\int_0^y\mathrm{d}z\,w(x)\Big(l\Big|(V'\otimes\mathbb{1}_D+W'\otimes\overline{R})\mathrm{e}^{(\check{T}-\mathrm{i}p)z}(R\otimes\overline{R})\\
&\qquad\times\mathrm{e}^{(\check{T}-\mathrm{i}p)(y-z)}(\mathbb{1}_D\otimes\overline{V}+R\otimes\overline{W})\mathrm{e}^{\check{T}(x-y)}(R\otimes\overline{R})\Big|r\Big)\\
&+\int_0^{+\infty}\mathrm{d}x\int_0^x\mathrm{d}y\int_0^y\mathrm{d}z\,w(x)\Big(l\Big|(R\otimes\overline{R})\mathrm{e}^{\check{T}z}(V'\otimes\mathbb{1}_D+W'\otimes\overline{R})\mathrm{e}^{(\check{T}-\mathrm{i}p)(y-z)}\\
&\qquad\times(R\otimes\overline{R})\mathrm{e}^{(\check{T}-\mathrm{i}p)(x-y)}(\mathbb{1}_D\otimes\overline{V}+R\otimes\overline{W})\Big|r\Big)\\
&+\int_0^{+\infty}\mathrm{d}x\int_0^x\mathrm{d}y\int_0^y\mathrm{d}z\,w(x)\Big(l\Big|(R\otimes\overline{R})\mathrm{e}^{\check{T}z}(\mathbb{1}_D\otimes\overline{V}+R\otimes\overline{W})\mathrm{e}^{(\check{T}+\mathrm{i}p)(y-z)}\\
&\qquad\times(V'\otimes\mathbb{1}_D+W'\otimes\overline{R})\mathrm{e}^{\check{T}(x-y)}(R\otimes\overline{R})\Big|r\Big)\\
&+\int_0^{+\infty}\mathrm{d}x\int_0^x\mathrm{d}y\int_0^y\mathrm{d}z\,w(x)\Big(l\Big|(\mathbb{1}_D\otimes\overline{V}+R\otimes\overline{W})\mathrm{e}^{(\check{T}+\mathrm{i}p)z}(R\otimes\overline{R})\\
&\qquad\times\mathrm{e}^{(\check{T}+\mathrm{i}p)(y-z)}(V'\otimes\mathbb{1}_D+W'\otimes\overline{R})\mathrm{e}^{\check{T}(x-y)}(R\otimes\overline{R})\Big|r\Big)\\
&+\int_0^{+\infty}\mathrm{d}x\int_0^x\mathrm{d}y\int_0^y\mathrm{d}z\,w(x)\Big(l\Big|(R\otimes\overline{R})\mathrm{e}^{\check{T}z}(\mathbb{1}_D\otimes\overline{V}+R\otimes\overline{W})\mathrm{e}^{(\check{T}+\mathrm{i}p)(y-z)}\\
&\qquad\times(R\otimes\overline{R})\mathrm{e}^{(\check{T}+\mathrm{i}p)(x-y)}(V'\otimes\mathbb{1}_D+W'\otimes\overline{R})\Big|r\Big)\Big]\\
&+\Big(l\Big|V'\otimes\mathbb{1}_D+W'\otimes\overline{R}\Big|r\Big)\Big[2\pi\delta(p)\Big(\dots\Big)+\dots\Big]\\
&\qquad+\Big(l\Big|\mathbb{1}_D\otimes\overline{V}+R\otimes\overline{W}\Big|r\Big)\Big[2\pi\delta(p)\Big(\dots\Big)+\dots\Big]\Big\}.
\end{aligned}
$$

As the Hamiltonian is a translation invariant operator, it conserves the momentum and we once again find a $\delta(p'-p)$ factor. The need for imposing $(l|V\otimes 1_D+W\otimes\overline{R}|r)=0$ for $p=0$ is once again apparent, as we would have divergences in the excitation energy without this requirement. We have not explicitly computed the diverging terms, nor the remaining finite terms that are present in principle when $p\neq 0$. All terms with integrals disappear for strictly local interactions $[w(x-y)\sim\delta(x-y)]$. Terms are grouped in square brackets for clarity. The first pair of square brackets contain all terms where (V,W) and (V',W') act on the same location. The second pair contains terms where both pairs act precisely on the location of the two points of the interaction. The third pair contains all terms where (V',W') acts on a point of the Hamiltonian. Vice versa for the fourth pair. The fifth pair contains all terms where there are four different points: one for (V,W), one for (V',W') and two for (the interaction term of) the Hamiltonian.

Since we can order these four points in 4! ways, but where the order of the two terms in the interaction is irrelevant, we have $4!/2 = 12$ terms. The final terms are, as said in the beginning of this paragraph, terms that will disappear if we use a left or right gauge fixing condition so that $(l|V \otimes 1_D + W \otimes \overline{R}|r) = 0$ (also at nonzero momentum). They have not been worked out explicitly. Note that for either two choices of gauge fixing condition, additional terms will disappear in the other groups.

Clearly, the expressions for $\langle \Phi_p(\overline{V}, \overline{W}) | \Phi_{p'}(V', W') \rangle$ and $\langle \Phi_p(\overline{V}, \overline{W}) | \hat{H} | \Phi_{p'}(V', W') \rangle$ are bilinear in the combined variables $(\overline{V}, \overline{W})$ and (V', W'). They thus define a generalized eigenvalue problem for which we can define an $2D^2 \times 2D^2$ effective norm and Hamiltonian matrix N_{Φ_p} and H_{Φ_p} as

$$\langle \Phi_p(\overline{V}, \overline{W}) | \Phi_{p'}(V', W') \rangle = 2\pi\delta(p' - p) \begin{bmatrix} \boldsymbol{V}^\dagger & \boldsymbol{W}^\dagger \end{bmatrix} N_{\Phi_p} \begin{bmatrix} \boldsymbol{V} \\ \boldsymbol{W} \end{bmatrix} \tag{4.109a}$$

$$\langle \Phi_p(\overline{V}, \overline{W}) | \check{H} | \Phi_{p'}(V', W') \rangle = 2\pi\delta(p' - p) \begin{bmatrix} \boldsymbol{V}^\dagger & \boldsymbol{W}^\dagger \end{bmatrix} H_{\Phi_p} \begin{bmatrix} \boldsymbol{V} \\ \boldsymbol{W} \end{bmatrix} \tag{4.109b}$$

where $\boldsymbol{V}$ and $\boldsymbol{W}$ represent the D^2-dimensional vectors containing the entries of the matrices V and W. We can now determine low lying excited states with momentum p by solving the generalized eigenvalue problem

$$H_{\Phi_p} \begin{bmatrix} \boldsymbol{V} \\ \boldsymbol{W} \end{bmatrix} = \Delta E \, N_{\Phi_p} \begin{bmatrix} \boldsymbol{V} \\ \boldsymbol{W} \end{bmatrix}, \tag{4.110}$$

where the eigenvalue ΔE gives the excitation energy. However, both N_{Φ_p} and H_{Φ_p} have D^2 eigenvalues zero, corresponding to pure gauge states in the tangent plane. These zeros are eliminated by imposing the gauge fixing condition and restricting the number of parameters to D^2. If we use the parameterization $W = \mathcal{W}_{\Phi_p}(Y) = l^{-1/2} Y r^{-1/2}$ and $V = \mathcal{V}_{\Phi_p}(Y) = l^{-1} R^\dagger l^{1/2} Y r^{-1/2}$, the effective norm matrix reduces to $\mathbb{1}_{D^2}$ and the generalized eigenvalue problem is transformed into an ordinary eigenvalue problem. When no long-range interactions are present, the application of H_{Φ_p} to a vector can be implemented with a total computational cost of $\mathcal{O}(D^3)$ using iterative solvers for $(-\check{T})^{\mathsf{P}}$ and $(-\check{T} \pm \mathrm{i}p)^{\mathsf{P}}$. The eigenvalue problem can then also be solved iteratively with computational cost of $\mathcal{O}(D^3)$.

2.4. Ansatz for topologically non-trivial excited states

If the Hamiltonian $\hat{H}$ has a symmetry breaking phase, where two inequivalent ground state (approximations) $|\Psi(Q_1, R_1)\rangle$ and $|\Psi(Q_2, R_2)\rangle$ can be found, we can propose an

ansatz for topologically non-trivial excitations as

$$|\Xi_p(V,W)\rangle = \int_{-\infty}^{+\infty} \mathrm{d}x\, \mathrm{e}^{\mathrm{i}px} \boldsymbol{v}_{\mathrm{L}}^\dagger \hat{U}_1(-\infty,x)\left(V\otimes\hat{\mathbb{1}} + W\otimes\hat{\phi}^\dagger(x)\right)\hat{U}_2(x,+\infty)\boldsymbol{v}_{\mathrm{R}}|\Omega\rangle\,, \tag{4.111}$$

where

$$\hat{U}_1(y,z) = \mathcal{P}\exp\left[\int_y^z \mathrm{d}x\, Q_1\otimes\hat{\mathbb{1}} + R_1\otimes\hat{\phi}^\dagger(x)\right],$$
$$\hat{U}_2(y,z) = \mathcal{P}\exp\left[\int_y^z \mathrm{d}x\, Q_2\otimes\hat{\mathbb{1}} + R_2\otimes\hat{\phi}^\dagger(x)\right].$$

We can repeat the same analysis for this ansatz. Little will change with respect to the previous subsection. If we define

$$\check{T}_{11} = Q_1\otimes\mathbb{1}_D + \mathbb{1}_D\otimes\overline{Q}_1 + R_1\otimes\overline{R}_1, \tag{4.112}$$
$$\check{T}_{22} = Q_2\otimes\mathbb{1}_D + \mathbb{1}_D\otimes\overline{Q}_2 + R_2\otimes\overline{R}_2, \tag{4.113}$$
$$\check{T}_{12} = Q_1\otimes\mathbb{1}_D + \mathbb{1}_D\otimes\overline{Q}_2 + R_1\otimes\overline{R}_2, \tag{4.114}$$
$$\check{T}_{21} = Q_2\otimes\mathbb{1}_D + \mathbb{1}_D\otimes\overline{Q}_1 + R_2\otimes\overline{R}_1, \tag{4.115}$$

and furthermore define l_1 (l_2) and r_1 (r_2) as the left and right eigenvector of $\check{T}_{11}$ ($\check{T}_{22}$) corresponding to eigenvalue zero, then we obtain

$$\begin{aligned}\langle\Xi_p(\overline{V},\overline{W})|\Xi_{p'}(V',W')\rangle = 2\pi\delta(p'-p)\Big[&(l_1|W'\otimes\overline{W}|r_2)\\ &+(l|(1_D\otimes\overline{V}+R\otimes\overline{W})(-\check{T}_{12}-\mathrm{i}p)^{-1}(V'\otimes 1_D+W'\otimes\overline{R})|r)\\ &+(l|(V'\otimes 1_D+W'\otimes\overline{R})(-\check{T}_{21}+\mathrm{i}p)^{-1}(1_D\otimes\overline{V}+R\otimes\overline{W})|r)\Big].\end{aligned} \tag{4.116}$$

Similarly to Subsection 3.3 of the previous chapter, symmetry breaking requires that $\mu = \min_{\lambda\in\sigma(\check{T}_{12})}\Re(\lambda) < 0$. This results in a simplification, since no regularization is required, no pseudo-inverses have to be defined and disconnected contributions are automatically absent. For evaluating $\langle\Xi_p(\overline{V},\overline{W})|\hat{H}|\Xi_{p'}(V',W')\rangle$, we can reuse the expression for $\langle\Phi_p(\overline{V},\overline{W})|\hat{H}|\Phi_{p'}(V',W')\rangle$ from the previous subsection, where we substitute $\check{T}_{11}$ for any transfer operator $\check{T}$ appearing to the left of both (V,W) and (V',W'), $\check{T}_{22}$ for any transfer operator $\check{T}$ appearing to the right of both (V,W) and (V',W'), $\check{T}_{12}+\mathrm{i}p$ for any virtual operator $\check{T}+\mathrm{i}p$ appearing in between (V,W) and (V',W') and, finally, $\check{T}_{21}-\mathrm{i}p$ for any virtual operator $\check{T}-\mathrm{i}p$ appearing in between (V',W') and (V,W). Since we assume all eigenvalues of $\check{T}_{12}$ and $\check{T}_{21}$ have a real part that is strictly negative, we can replace the specially defined inverse $^{\mathsf{P}}$ by a regular inverse and no disconnected contributions can appear in $\langle\Xi_p(\overline{V},\overline{W})|\hat{H}|\Xi_{p'}(V',W')\rangle$.

3. Examples

Non-relativistic free bosons

As a benchmark, we now start with the approximation of a free theory with continuous matrix product states. A non-relativistic free (quadratic) boson model can be obtained by adding a number-violating term $\hat{\psi}(x)\hat{\psi}(x)$ and its Hermitian conjugate. The Hamiltonian we choose to study is given by

$$\hat{H} = \int_{-\infty}^{+\infty} \left[\left(\frac{\mathrm{d}\hat{\psi}^\dagger}{\mathrm{d}x}(x) \right) \left(\frac{\mathrm{d}\hat{\psi}}{\mathrm{d}x}(x) \right) + \mu \hat{\psi}^\dagger(x)\hat{\psi}(x) - \nu \left(\hat{\psi}^\dagger(x)\hat{\psi}^\dagger(x) + \hat{\psi}(x)\hat{\psi}(x) \right) \right] \mathrm{d}x. \quad (4.117)$$

Let $\hat{\Psi}(p)$ denote the Fourier transform of $\hat{\psi}(p)$. This quadratic theory can be solved by a Bogoliubov transformation according to

$$\begin{cases} \hat{\Psi}(p) = \cosh\big(f(p)\big)\hat{\Xi}(p) + \sinh\big(f(p)\big)\hat{\Xi}^\dagger(-p), \\ \hat{\Psi}^\dagger(p) = \cosh\big(f(p)\big)\hat{\Xi}^\dagger(p) + \sinh\big(f(p)\big)\hat{\Xi}(-p), \end{cases} \quad (4.118)$$

with Bogoliubov angle $f(p)$ given by

$$f(p) = \frac{1}{2}\operatorname{arctanh}\left(\frac{2\nu}{p^2+\mu} \right). \quad (4.119)$$

The Hamiltonian in Eq. (4.117) can then be written as

$$\hat{H} = \int_{-\infty}^{+\infty} \omega(p)\hat{\Xi}^\dagger(p)\hat{\Xi}(p) + \int_{-\infty}^{+\infty} e_0(\mu,\nu)\,\mathrm{d}x \quad (4.120)$$

with the dispersion relation $\omega(p)$ of the elementary excitations created by $\hat{\Xi}^\dagger(p)$ given by

$$\omega(p) = \sqrt{(p^2+\mu)^2 - 4\nu^2} \quad (4.121)$$

and the ground state energy density $e_0(\mu,\nu)$ given by

$$e_0(\mu,\nu) = \frac{1}{2}\int_{-\infty}^{+\infty} \frac{\mathrm{d}p}{2\pi} \left[\sqrt{(p^2+\mu)^2 - 4\nu^2} - (p^2+\mu) \right]. \quad (4.122)$$

The elementary excitation has an energy gap $\omega(0) = \Delta = \sqrt{\mu^2 - 4\nu^2}$, and hence becomes

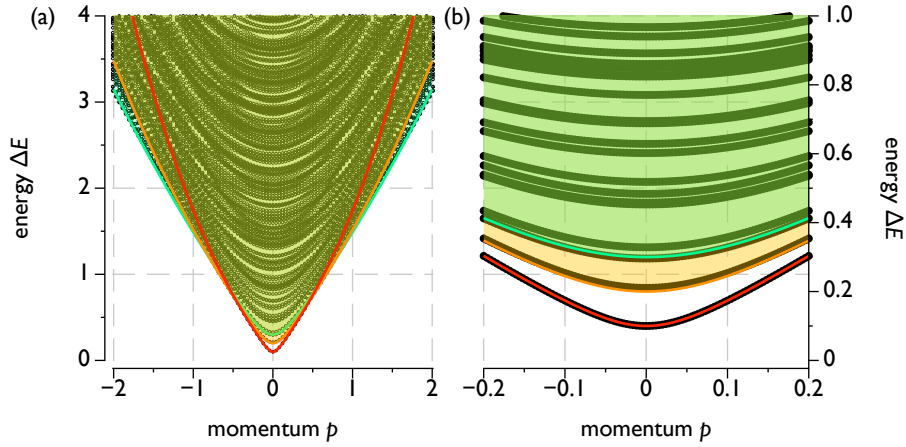

Figure 4.1: (a) Spectrum of excitation energies (black dots) as function of momentum p for the free boson model described by the Hamiltonian Eq. (4.117) for the choice of parameters $\nu = 1/2$, $\mu = \sqrt{1+\Delta^2}$ and $\Delta = 0.1$, obtained with the ansatz $|\Phi(V, W; Q, R)\rangle$ with bond dimension $D = 41$. (b) Detail of (a) around momentum zero. The red line indicates the fundamental excitation with $\Delta E = \omega(p)$, the yellow shaded area represents the band of two-particle excitations with minimal energy $2\omega(p/2)$ and the green shaded area represents the band of three-particle excitations with minimal energy $3\omega(p/3)$.

gapless at the critical point $\nu = \mu/2$. There is no real quantum phase transition since the Hamiltonian is ill-defined for $\nu > \mu/2$.

We now study this model with the continuous matrix product state ansatz. While the Hamiltonian in Eq. (4.117) is not of the form that was used in the previous sections, the generalization for the additional terms is straightforward. Figure 4.1 shows the excitation spectrum of the free boson model of Eq. (4.117) for the choice of parameters $\nu = 1/2$, $\mu = \sqrt{1+\Delta^2}$ and $\Delta = 0.1$, obtained with the ansatz $|\Phi(V, W; Q, R)\rangle$ for excitations with bond dimension $D = 41$ as described in the previous section. The parameter Δ determines the exact gap $\Delta = \omega(p = 0)$ of the fundamental excitation. At this value of the bond dimension, the fundamental excitation is almost exactly reproduced, as is visible in Figure 4.1(a). But Figure 4.1(b) indicates that also many higher order excitations are reproduced that fall within the continuum of two-, three- or more-particle excitations. For $\Delta \ll 1$, we can interpret $\mu \approx 2\nu = 1$ as the ultraviolet cutoff in the model, and Δ as the infrared cutoff. The range of interacting energy scales is thus equal to $1/\Delta$, which has the value 10 in the results of Figure 4.1.

The accuracy on both the estimation of the ground state energy density with $|\Psi(Q, R)\rangle$ and on the estimation of the gap with $|\Phi(V, W; Q, R)\rangle$ for values $\Delta = 0.1$, $\Delta = 0.01$ and $\Delta = 0$ is shown in Figure 4.2. As for the results of the antiferromagnetic XXZ lattice model in the previous chapter, the error on the gap scales as the square root of the error on the ground state energy density for small values of D, but then shifts to a linear proportionality as D increases for gapped systems. For the critical case $\Delta = 0$, the square

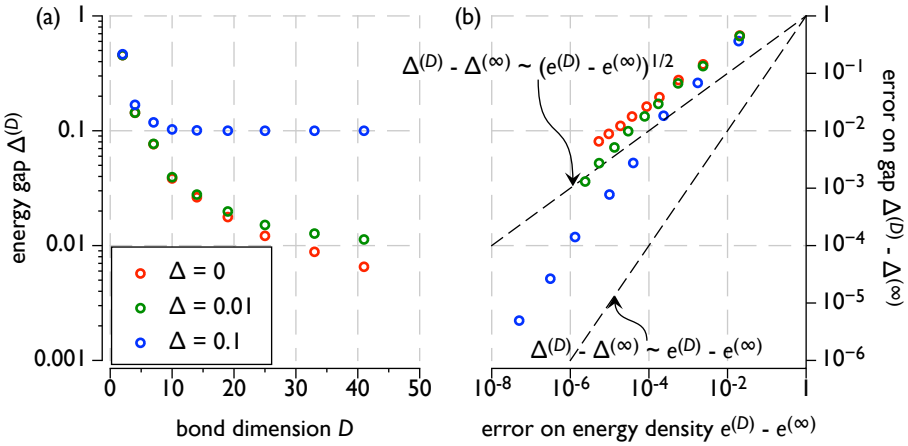

Figure 4.2: (a) Estimated value of the gap $\Delta^{(D)}$ as function of the bond dimension D for values of the exact gap $\Delta = \Delta^{(\infty)} = 0$, 0.01 and 0.1. (b) Error on the estimation of the gap versus error on the estimation of the ground state energy density for different values of the bond dimension $D = 2$, 4, 7, 10, 14, 19, 25, 33 and 41 and for different values of the exact gap $\Delta = \Delta^{(\infty)} = 0$, 0.01 and 0.1.

root dependency is observed for all values of the bond dimension D.

Lieb-Liniger model

We now study an interacting non-relativistic boson model that is exactly solvable. We therefore consider the one-dimensional model with Hamiltonian

$$\hat{H} - \mu\hat{N} = \int_{-\infty}^{+\infty} \left[\left(\frac{\mathrm{d}\hat{\psi}^\dagger}{\mathrm{d}x}(x) \right) \left(\frac{\mathrm{d}\hat{\psi}}{\mathrm{d}x}(x) \right) + g\left(\hat{\psi}^\dagger(x)\right)^2 \left(\hat{\psi}(x)\right)^2 - \mu\hat{\psi}^\dagger(x)\hat{\psi}(x) \right] \mathrm{d}x, \tag{4.123}$$

which describes non-relativistic bosons that interact through a simple δ interaction with coupling constant g. We have explicitly separated the chemical potential term with chemical potential μ that is responsible for creating a non-trivial ground state. The ground state of this Hamiltonian was exactly determined by Lieb and Liniger in [367], and the excitation spectrum by Lieb in [16]. This model has a continuous U(1) symmetry corresponding to number preservation, which is spontaneously broken for $d > 1$ resulting in Bose-Einstein condensation and the formation of a superfluid. For all temperatures T in $d = 1$, and for $T > 0$ in $d = 2$, this symmetry is restored due to Coleman's theorem or the Mermin-Wagner theorem (see Subsection 1.4 of Chapter 1). In particular, the ground state ($T = 0$) of the one-dimensional system (Lieb-Liniger model) does not break the U(1) symmetry.

If we were to approximate the ground state by a mean-field construction using a factorized

coherent state

$$|\Psi[\varphi]\rangle = \hat{D}[\varphi]\,|\Omega\rangle = \exp\left[-\frac{1}{2}\int |\varphi(x)|^2\,\mathrm{d}x\right]\left[\int \varphi(x)\hat{\psi}^\dagger(x)\,\mathrm{d}x\right]|\Omega\rangle\,, \tag{4.124}$$

with $\varphi(x)$ a scalar-valued complex field and $\hat{D}[\varphi]$ the unitary displacement operator

$$\hat{D}(\varphi) = \exp\left[\int \left(\varphi(x)\hat{\psi}^\dagger(x) - \overline{\varphi}(x)\hat{\psi}(x)\right)\,\mathrm{d}x\right], \tag{4.125}$$

then the variational optimum would be given by any uniform solution satisfying

$$|\varphi(x)| = \sqrt{\frac{\mu}{2g}}. \tag{4.126}$$

Hence, the mean field solution breaks the symmetry. If we choose the real solution $\varphi(x) = \varphi_0(x) = \sqrt{2\mu/g}$ and define a transformed Hamiltonian $\hat{H}' = \hat{D}[\varphi_0]^\dagger \hat{H} \hat{D}[\varphi_0]$, then the quadratic part of $\hat{H}'$ corresponds to the free boson Hamiltonian of the previous section at the critical point $\nu = \mu/2$. The massless excitations then correspond to the Goldstone modes resulting from this artificial symmetry breaking. The exact solution in $d = 1$ has no symmetry breaking but remains critical, *i.e.* the low-lying excitations are gapless.

Note that this factorized coherent state is included in the continuous matrix product state ansatz by choosing $R(x) = \varphi(x)\mathbb{1}_D$ and $Q(x) = -|\varphi(x)|^2/2 \times \mathbb{1}_D$. However, for bond dimension $D > 1$, this solution is no longer the variational optimum, and the energy can be lowered by restoring the symmetry and creating entanglement in the state. In order to now study the Lieb-Liniger model, we define the energy density $e(g,\rho)$ as

$$\begin{aligned} e(g,\rho) &= \langle\Psi(\overline{Q},\overline{R})|\left(\frac{\mathrm{d}\hat{\psi}^\dagger}{\mathrm{d}x}(x)\right)\left(\frac{\mathrm{d}\hat{\psi}}{\mathrm{d}x}(x)\right) + g\left(\hat{\psi}^\dagger(x)\right)^2\left(\hat{\psi}(x)\right)^2|\Psi(Q,R)\rangle\,, \\ &= (l|[Q,R]\otimes[\overline{Q},\overline{R}] + gR^2\otimes\overline{R}^2|r), \end{aligned} \tag{4.127}$$

where the particle density ρ is given by

$$\rho = \langle\Psi(\overline{Q},\overline{R})|\hat{\psi}^\dagger(x)\hat{\psi}(x)|\Psi(Q,R)\rangle = (l|R\otimes\overline{R}|r) \tag{4.128}$$

and is determined by the chemical potential μ. Since ρ has the dimension of $1/\ell$, with ℓ a characteristic length, and e has a dimension $1/\ell^3$ (due to our choice of units in which $\frac{\hbar^2}{2m} = 1$), the dimensionless quantity $e(g,\rho)/\rho^3$ can only depend on the dimensionless quantity $\gamma = g/\rho$. To this dimensional analysis corresponds a physical scale transformation, which can also be realized in the continuous matrix product state by defining a transformation

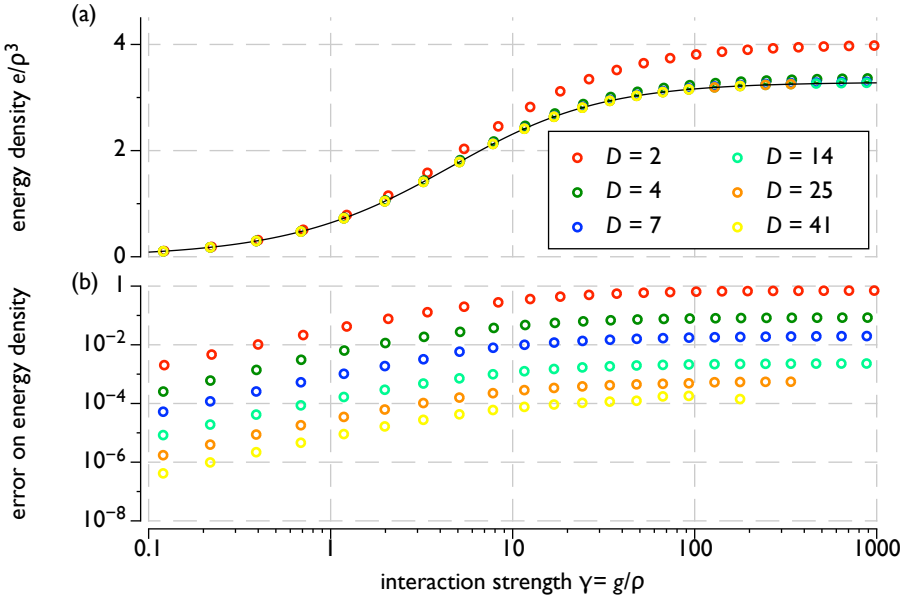

Figure 4.3: (a) Normalized ground state energy density e/ρ^3 for different values of the normalized interaction strength $\gamma = g/\rho$ and for different values of D, as compared to the exact value (black line) (b) Absolute error on the ground state energy density.

$Q = cQ$ and $R' = \sqrt{c}R$. We obtain

$$e(g,\rho) = (l|[Q',R'] \otimes [\overline{Q}',\overline{R}'] + g(R')^2 \otimes (\overline{R}')^2|r) = c^3 e(g/c,\rho/c)$$

and thus, by choosing $c = \rho$,

$$e(g,\rho) = \rho^3 e(g/\rho,1). \tag{4.129}$$

The compatibility of the continuous matrix product state ansatz with these scale transformations is essential for the conclusion that the numerical results at finite values of the bond dimension D also depend only on the dimensionless quantity $\gamma = g/\rho$. We first study the ground state of the Lieb Liniger model, which is always critical. Figure 4.3 depicts the accuracy in the approximation of the ground state energy density for different values of γ and for different values of the bond dimension D. Since the Lieb Liniger model is critical, the accuracy only improves slowly, but nevertheless it is possible to obtain values that are accurate up to order 10^{-6} for modest values of the bond dimension $D \approx 40$.

We can now also evaluate other properties of our approximate ground state, as well as the approximation to the excited states that can be obtained with the ansatz $|\Phi(V,W)\rangle\!\rangle$. The local order parameter for the U(1) symmetry is given by the expectation value $o = \langle\Psi(\overline{Q},\overline{R})|\hat{\psi}(x)|\Psi(Q,R)\rangle$ and can be normalized as $o/\rho^{1/2}$. The exact ground state

of the Lieb-Liniger model cannot break this continuous symmetry since the global order parameter $\hat{O} = \int \hat{\psi}(x)\mathrm{d}x$ does not commute with the Hamiltonian; it has a fixed number of particles so that $o = \langle\hat{\psi}\rangle = 0$. In addition, being in a critical phase, the exact energy gap Δ, which can be normalized as Δ/ρ^2, is zero. Figure 4.4 shows results for the order parameter and for the gap as obtained with our continuous matrix product state approximation. As for the critical case of the previous example, the error on the energy gap scales roughly as the square root of the error on the energy density. However, the error on the order parameter is very large and decreases very slowly. The reason is of course to be sought in the fact that the continuous matrix product state was not constructed to be a state with a fixed particle number, but as a generalization of a coherent state with a superposition over different particle numbers. Hence, $\langle\Psi(\overline{Q},\overline{R})|\hat{\psi}(x)|\Psi(Q,R)\rangle$ is not automatically zero and in fact turns out to be quite large. Hence, the continuous matrix product state still describes a symmetry broken state. The particular choice to which the time-dependent variational principle converges is determined by our initial state, which is the symmetry-broken coherent state ($D = 1$) with $R = \sqrt{\mu/(2g)}$. Any solution with $\tilde{Q} = Q$ and $\tilde{R} = \mathrm{e}^{\mathrm{i}\alpha}R$, $\forall\alpha \in [0, 2\pi)$ would be an equally good approximation to the ground state, so that there is a whole valley of minima in the variational manifold. If we were to apply the full generalized eigenvalue equation resulting from the linearized flow equations of the time-dependent variational principle, we would in fact recover a massless excitation corresponding to variations of the state along this valley, *i.e.* this is the Goldstone boson resulting from this artificial symmetry breaking. With our variational approach towards excitations, we do not recover the massless mode, but as the bond dimension D increases and the approximation improves, the mass gap $\Delta^{(D)}$ resulting from this variational approach is converging towards the exact value $\Delta^{(\infty)} = 0$.

Let us conclude this section by looking at the complete spectra obtained for different values of γ. Lieb has computed two types of elementary excitations of the Hamiltonian $\hat{H}$ (without the chemical potential term) in [16], both of which do not change the particle number (so that the chemical potential term has no influence). However, these two types of excitations are not independent, since either of them form a complete set, and one type of excitation can be interpreted as a multi-particle excitation of the other type. With our approach, we compute a set of excitations of $\hat{H} - \mu\hat{N}$ which can change the particle number, as illustrated in Figure 4.5. Clearly, Lieb's type II excitation corresponds to the elementary excitation with lowest possible energy. However, the exact solution of this excitation is only defined for $|p| < \pi\rho$, whereas this excitation smoothly continues in our numeric results. In addition, as $\gamma = c/\rho$ increases, new low-energy regions around $p = \pm 2\pi\rho$ develop, corresponding to the *umklapp* excitations of the free fermion model, to which the Lieb-Liniger model is strongly related in the $\gamma \to \infty$ limit.

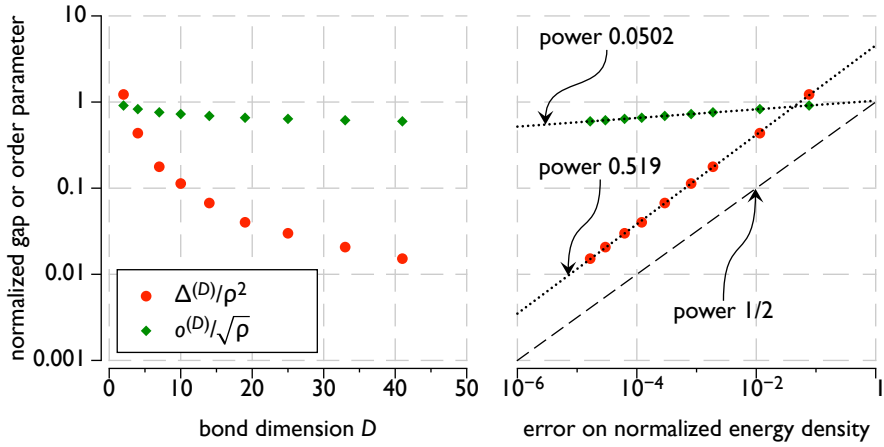

Figure 4.4: Normalized value of the order parameter $o/\rho^{1/2}$ and of the energy gap Δ/ρ^2 obtained with our continuous matrix product state ansatz, as function of the bond dimension D and as function of the error on the ground state energy density e/ρ^3, for a value $\gamma = g/\rho \approx 2$. Since the exact values of o and Δ are zero, these values are also equal to the corresponding error.

4. Summary and conclusions

In this chapter, we have introduced the variational manifold of continuous matrix product states, the natural extension of matrix product states to the setting of one-dimensional quantum field theories. Definitions and properties of these states are given in Section 1, while the necessary machinery to apply the time-dependent variational principle and to study excitations has been developed in Section 2. Section 3 completes this chapter by studying two exemplary benchmark models.

Continuous matrix product states are extensive non-Gaussian states that allow for an efficient evaluation of expectation values. The natural ultraviolet cutoff on the lattice has been replaced by an effective ultraviolet cutoff given by the inter-particle distance, which can be optimally chosen for any given Hamiltonian. As for matrix product states, continuous matrix product states have a finite amount of bipartite entanglement and are in theory restricted to systems which have both a finite ultraviolet cutoff and a finite infrared cutoff, *i.e.* gapped non-relativistic systems. However, as shown in the examples, reasonable results for the ground state energy and the excitation spectrum can also be obtained for critical non-relativistic systems. According to Feynman's "sensitivity to high frequencies", one should of course be careful with the computation of observables that truly depend on low frequencies, such as the expectation value of the order parameter.

In Chapter 6 we will also apply the continuous matrix product state ansatz to relativistic systems, in order to investigate the effect of having no ultraviolet cutoff.

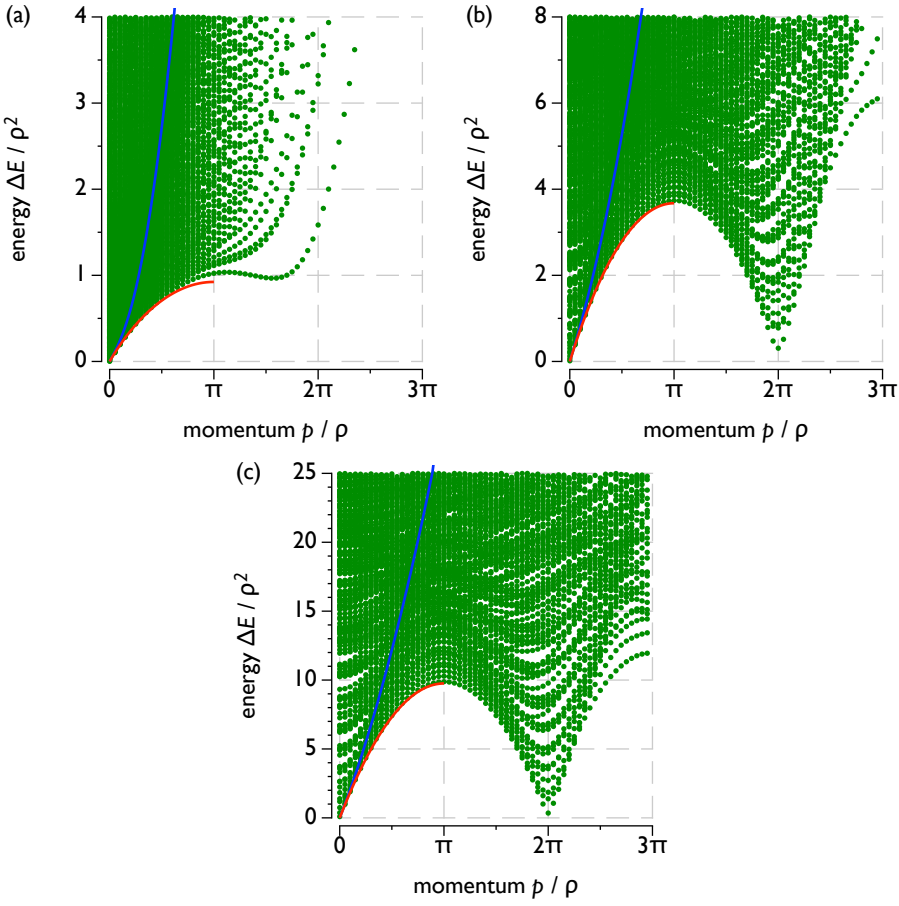

Figure 4.5: Spectra obtained with our ansatz $|\Phi(V,W)\rangle$ with bond dimension $D = 33$, for $\gamma \approx 0.12$ (a), $\gamma \approx 1.98$ (b) and $\gamma \approx 337.47$ (c). Also shown are the 'elementary excitations' of type I (blue line) and type II (red line) according to [16].

5

Entanglement renormalization

This chapter introduces the concept of *entanglement renormalization*, which is a real-space renormalization group transformation that acts on quantum states in an arbitrary number of spatial dimensions d. It was introduced for lattice systems by Vidal in 2005 [368]. Entanglement renormalization defines a variational ansatz that is called *multi-scale entanglement renormalization ansatz* [369]. It is related to matrix product states and its higher-dimensional generalizations within the more general framework of tensor network states. It differs by the fact that the tensor network for the multi-scale entanglement renormalization ansatz has a $(d+1)$-dimensional structure, where the additional dimension can be interpreted as the renormalization scale and thus as a holographic dimension (see Subsection 3 of Chapter 1).

Entanglement renormalization on the lattice corresponds to a discrete renormalization group transformation and has proven to indeed inhibit all the expected properties of renormalization. Different states in the same phase are renormalized to the same fixed point. Unlike matrix product states, the multi-scale entanglement renormalization ansatz is also capable of describing ground states of critical quantum models. These correspond to non-trivial fixed points of the entanglement renormalization scheme and hence become scale-invariant. From the linearized renormalization transformation at the fixed point the critical exponents can be derived with great accuracy. Entanglement renormalization also respects the intrinsic quantum mechanical properties of renormalization. Entanglement decreases monotonically along the renormalization scale and true quantum phases with topological order can also be characterized by fixed points of the renormalization process. In addition, as a variational ansatz the multi-scale entanglement renormalization ansatz answers each of Feynman's concerns (Subsection 4.2 of Chapter 2). Just like the (continuous) matrix product state ansatz, the multi-scale entanglement renormalization ansatz is a non-Gaussian extensive state that allows for an efficient evaluation of expectation values (for $d = 1, 2, \ldots$). But due to the intrinsic multi-scale aspect, it also naturally overcomes Feynman's first argument regarding the sensitivity to high frequencies. Variational parameters living at the long-range scales do not attempt to minimize the energy by modifying the short-range degrees of freedom, since these have already been "integrated out".

There is also a qualitative agreement between the way that entanglement is created in the multi-scale entanglement renormalization ansatz and the postulate by Ryu and

Takayanagi for computing entanglement with the AdS/CFT correspondence (Subsection 2.5 of Chapter 1). In order to investigate this relationship further, it would be beneficial to be able to define entanglement renormalization as a continuous process with infinitesimally small renormalization steps. Such infinitesimal steps are impossible on the lattice and require to define entanglement renormalization for ground states of quantum field theories. Since the process of grouping sites has no meaning in the continuum, a generalization to the continuum is not straightforward. In collaboration with Tobias J. Osborne and Frank Verstraete, we have been able to propose a continuum limit of the multi-scale entanglement renormalization ansatz, which is described in Section 2. But we first recapitulate the conceptual elements of entanglement renormalization on the lattice.

1. Entanglement renormalization on the lattice

This section surveys the concept of entanglement renormalization on the lattice and the results obtained with it, based on the outstanding review by Vidal [370]. Consider hereto a lattice $\mathscr{L}$ of sites with Hilbert space $\mathbb{H}_{\text{site}}$ and $\mathbb{H}_{\mathscr{L}} = \mathbb{H}_{\text{site}}^{\otimes|\mathscr{L}|}$. Let $\hat{H} \in \mathbb{L}(\mathbb{H}_{\mathscr{L}})$ be a Hamiltonian for this lattice system and $|\Psi\rangle$ its corresponding ground state. We now construct a renormalization group transformation that acts directly on the quantum state $|\Psi\rangle$, and learn that inverting this transformation gives rise to a variational class.

1.1. Renormalization of quantum states

Traditional renormalization schemes are based on the partition function (Section 3 of Chapter 1), which can be related to the density matrix $\hat{\rho} \sim \lim_{\beta\to+\infty} \exp(-\beta\hat{H}) \sim |\Psi\rangle\langle\Psi|$. The standard approach for relativistic theories is to integrate out a shell of spacetime momenta $(\omega, \vec{p})$ with $e^{-s}\Lambda \leq ||(\omega, \vec{p})|| \leq \Lambda$. For non-relativistic quantum systems at zero temperature, we can also devise a scheme where we integrate out modes with spatial momentum $e^{-s}\Lambda \leq ||\vec{p}|| \leq \Lambda$ over all time scales or frequencies ω. We then don't need to introduce a cutoff in the (imaginary) time direction and the resulting partition function uniquely defines a new Hamiltonian $\hat{H}(s)$ so that $\hat{\rho}(s) \sim \lim_{\beta\to+\infty} \exp(-\beta\hat{H}(s)) \sim |\Psi(s)\rangle\langle\Psi(s)|$. We can now try to completely formulate this renormalization process in terms of quantum mechanical operations. Intuitively, integrating out modes with spatial momentum $e^{-s}\Lambda \leq ||\vec{p}|| \leq \Lambda$ boils down to a partial trace so that $\hat{\rho}(s) = \mathcal{R}_s(\hat{\rho}) = \text{tr}_{e^{-s}\Lambda<||\vec{p}||<\Lambda}(\hat{\rho})$. However, this trace integrates out all modes which have momentum $e^{-s}\Lambda \leq ||p|| \leq \Lambda$ at $\tau = -\beta/2 = -\infty$ and at $\tau = +\beta/2 = +\infty$. Only for free theories does the momentum of these modes not change during the evolution over $-\infty < \tau < +\infty$ and do the two schemes agree. Indeed, for free theories there is no entanglement between the momentum modes and $\hat{\rho}(s)$ is still a pure density matrix that allows to define a state $|\Psi(s)\rangle$ such that $\hat{\rho}(s) = |\Psi(s)\rangle\langle\Psi(s)|$. For interacting theories, the entanglement between the modes that are traced out and the rest of the

system results in a mixed density matrix $\hat{\rho(s)}$ and no renormalized state $|\Psi(s)\rangle$ can be defined.

To overcome this problem, we now attempt to define a renormalization group transformation that acts directly on states $|\Psi\rangle$. Consider the renormalization group transformation $|\Psi\rangle \mapsto |\Psi'\rangle = R(|\Psi\rangle)$ that eliminates degrees of freedom, so that $|\Psi'\rangle$ lives in a smaller Hilbert space $\mathbb{H}'_{\mathscr{L}}$ and R represents a map $R : \mathbb{H}_{\mathscr{L}} \mapsto \mathbb{H}'_{\mathscr{L}}$. Since we are now focussing on real-space transformations R and the real-space degrees of freedom live on lattice sites, $\mathbb{H}'_{\mathscr{L}}$ should correspond to the Hilbert space $\mathbb{H}_{\mathscr{L}'}$ of a smaller lattice $\mathscr{L}'$. Since all transformation that can be performed on quantum systems are linear, it should be possible to construct R as a linear homomorphism $R \in \mathrm{Hom}(\mathbb{H}_{\mathscr{L}'}, \mathbb{H}_{\mathscr{L}})$. As for the Wilsonian effective action, the resulting state $|\Psi'\rangle = R|\Psi\rangle$ contains less information. Given only $|\Psi'\rangle$, it is no longer possible to compute the expectation value of any physical observable $\hat{O} \in \mathbb{L}(\mathbb{H}_{\mathscr{L}})$. However, since we also know R, we can define an associated linear map $\mathcal{R} : \mathbb{L}(\mathbb{H}_{\mathscr{L}}) \mapsto \mathbb{L}(\mathbb{H}_{\mathscr{L}'}) : \hat{O} \mapsto \hat{O}' = \mathcal{R}(\hat{O})$ that is given by $\hat{O}' = \mathcal{R}(\hat{O}) = R\hat{O}R^\dagger$. If we require that $\mathcal{R}(\hat{\mathbb{1}}) = \hat{\mathbb{1}}'$ with $\hat{\mathbb{1}}'$ the identity operator in $\mathbb{H}_{\mathscr{L}'}$, we obtain $RR^\dagger = \hat{\mathbb{1}}'$ so that R is an isometry. Rather than integrating out or tracing out degrees of freedom we now project out these degrees of freedom and R represents the projection matrix from $\mathbb{H}_{\mathscr{L}}$ to $\mathbb{H}_{\mathscr{L}'}$. We now require that

$$\langle\Psi'|\hat{O}'|\Psi'\rangle = \langle\Psi|R^\dagger R\hat{O}R^\dagger R|\Psi\rangle \approx \langle\Psi|\hat{O}|\Psi\rangle\,. \tag{5.1}$$

Hence $R^\dagger$ contains the information to restore the high-energy degrees of freedom in $|\Psi'\rangle$. This requires $R^\dagger R|\Psi\rangle \approx |\Psi\rangle$, so that $|\Psi\rangle$ is (approximately) contained in the support of the orthogonal projection operator $R^\dagger R$. In addition, the renormalization group transformation on quantum states also defines a scheme to obtain a renormalized Hamiltonian $\hat{H}' = \mathcal{R}(\hat{H})$.

By reiterating the renormalization group transform we obtain

$$\langle\Psi|\hat{O}|\Psi\rangle \approx \langle\Psi'|\hat{O}'|\Psi'\rangle \approx \langle\Psi''|\hat{O}''|\Psi''\rangle \approx \ldots \tag{5.2}$$

In the end, $|\Psi'''\rangle = R'''\cdots R'R|\Psi\rangle$ becomes trivial, especially for finite lattices $\mathscr{L}$, since $\mathscr{L}'''$ will have only a few sites left. For example, we can then exactly diagonalize $\hat{H}''' = R'''\cdots R'R\hat{H}R^\dagger R'^\dagger\cdots R'''^\dagger$ and find $|\Psi'''\rangle$ as ground state. Define $|0\rangle = |\Psi'''\rangle = R'''\cdots R'R|\Psi\rangle$ so that

$$\langle\Psi|\hat{O}|\Psi\rangle \approx \langle\Psi'''|\hat{O}'''|\Psi'''\rangle = \langle 0|\hat{O}'''|0\rangle = \langle 0|R'''\cdots R'R\hat{O}R^\dagger R'^\dagger\cdots R'''^\dagger|0\rangle \tag{5.3}$$

It is easy to choose the final R''' so that $|0\rangle$ becomes some fixed state. We can now interpret $R^\dagger(R')^\dagger\cdots(R''')^\dagger|0\rangle$ for different choices of R, R', …and a fixed end state $|0\rangle$ as a class of variational ansätze and optimize over R, R', …using the variational principle.

Note that White's density matrix renormalization group (Subsection 3.4 of Chapter 1)

also follows this general scheme. The renormalization group transformation on quantum states R is defined as a transformation $R : \mathbb{C}^D \otimes \mathbb{H}_{\mathscr{L}} \mapsto \mathbb{C}^D \otimes \mathbb{H}_{\mathscr{L}'}$, *i.e.* the lattice is extended with an ancilla space $\mathbb{C}^D$. In every renormalization step, one site is projected out by defining a map $R : \mathbb{C}^D \otimes \mathbb{H}_{\text{site}} \mapsto \mathbb{C}^D$. After $|\mathscr{L}|$ renormalization steps, the lattice $\mathscr{L}$ has been completely absorbed into the ancilla space $\mathbb{C}^D$. The physical state $|\Psi\rangle$, extended with some initial state for the ancilla v_{L}, has been mapped to a state $v_{\text{R}} = (R''' \cdots R' R v_{\text{L}} \otimes |\Psi\rangle) \in \mathbb{C}^D$, as sketched in Figure 5.1. All physical operators $\hat{O}$ are first extended to $\mathbb{L}(\mathbb{C}^D \otimes \mathbb{H}_{\mathscr{L}})$ as $v_{\text{L}} v_{\text{L}}^\dagger \otimes \hat{O}$ and are then transformed into virtual operators $O \in \mathbb{L}(\mathbb{C}^D)$, which is sketched in Figure 5.2. We thus obtain

$$(v_{\text{L}}^\dagger \otimes \langle\Psi|)(v_{\text{L}} v_{\text{L}}^\dagger \otimes \hat{O})(v_{\text{L}} \otimes |\Psi\rangle) \approx v_{\text{R}}^\dagger O v_{\text{R}}$$

By fixing v_{L} and v_{R} and considering $R, R', \ldots$ as variational parameters, we define the class of matrix product states $\mathscr{M}_{\text{MPS}}$ as in Figure 5.3. If R removes sites 1, R' removes site 2 and so on, and we now define $R = R(1)$, $R' = R(2)$, …, then we can relate this to the matrices $A^s(n)$ in the matrix product state as $A^s_{\alpha,\beta}(n) = [R(n)^\dagger]_{(\alpha,s);\beta} = [\overline{R(n)}]_{\beta;(\alpha,s)}$. This construction strongly resembles the sequential generation picture described in Subsection 1.3 of Chapter 3. However, as already announced in Section 3.5 of Chapter 1, the density matrix renormalization group does not satisfy the required properties of a good renormalization scheme: fixed points do not correspond to ground states of critical models. In every step, the next set of degrees of freedom that are to be projected out are not degrees of freedom living at the shortest length scale but just the degrees of freedom of the next site. The degrees of freedom of this site influence the physics at all length scales, which is why matrix product states do also suffer from Feynman's "sensitivity to high frequencies" near critical points. The same remarks apply to continuous matrix product states as well.

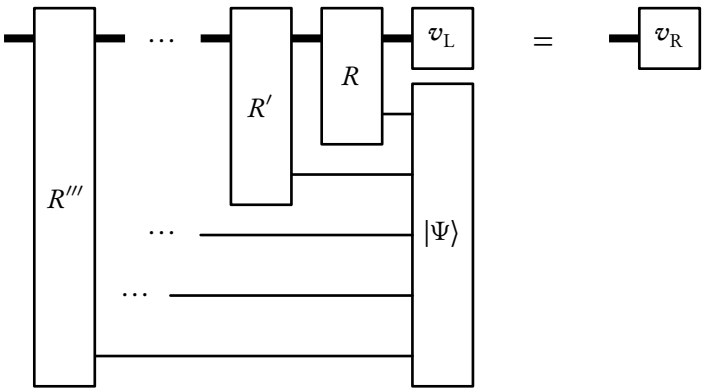

Figure 5.1: The density matrix renormalization group as a renormalization process on quantum states.

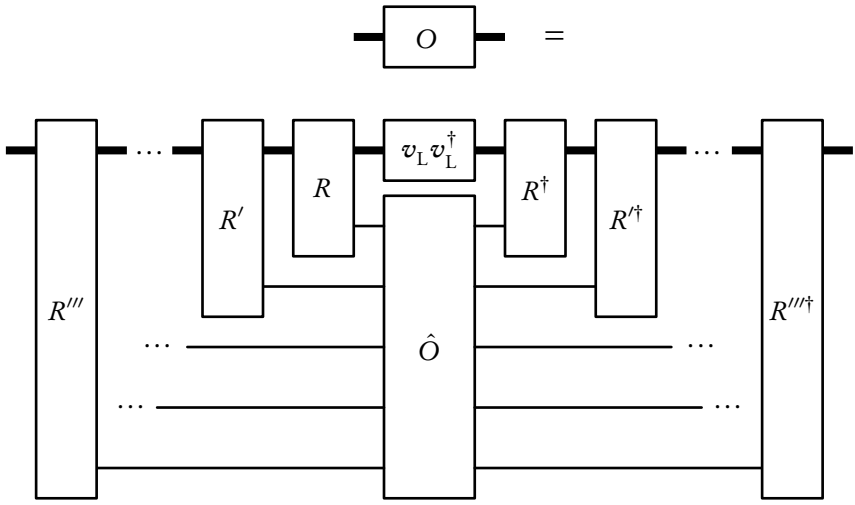

Figure 5.2: The corresponding renormalization scheme of operators $\hat{O}$.

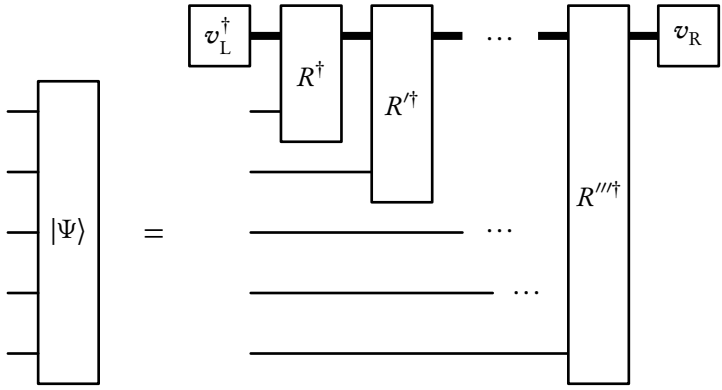

Figure 5.3: The class of variational ansatz states $\mathscr{M}_{\mathrm{MPS}}$ as defined by the renormalization scheme above.

1.2. Disentangling degrees of freedom

As for the real-space renormalization group transformations developed by Kadanoff and others for lattice models in statistical physics, we can construct R by course graining the lattice, *i.e.* by grouping blocks $\mathcal{B}$ of b^d sites into an effective site with Hilbert space $\mathbb{H}_{\text{site}'}$ so that $\dim \mathbb{H}_{\text{site}'} = q' \leq \dim \mathbb{H}_{\text{site}}^{\otimes b^d} = q^{b^d}$ with $q = \dim \mathbb{H}_{\text{site}}$ and d the number of spatial dimensions. In the spirit of familiar renormalization group transformations we would have $q' = q$, *i.e.* we replace b^d spins by one effective spin and short range fluctuations within the block $\mathcal{B}$ of b^d spins have been removed. Let us define $w^\dagger \in \mathrm{Hom}(\mathbb{H}_{\text{site}'}, \mathbb{H}_{\text{site}}^{\otimes b})$ as the isometry ($ww^\dagger = \hat{\mathbb{1}}$) that maps b^d sites onto a single effective site. We have explicitly included the Hermitian conjugation since the resulting variational ansatz will be defined in terms of $(w^\dagger)^\dagger = w$. We can now group all sites $n \in \mathcal{L}$ in blocks $\mathcal{B}_{n'}$ ($n' \in \mathcal{L}'$) of b^d sites, with $|\mathcal{L}'| = |\mathcal{L}|/b^d$. We then define $R = \bigotimes_{n' \in \mathcal{L}'} w_{n'}^\dagger$. For translation invariant states, we can choose all isometries $w_{n'}$ equal as is sketched in Figure 5.4 for $d = 1$ and $b = 2$. The associated map $\mathcal{R}$ for operators is displayed in Figure 5.5. The resulting variational class depicted in Figure 5.6 is the class of tree tensor network states [371], and allows an efficient evaluation of expectation values when $q', q'', \ldots$ can be chosen small (*e.g.* $\mathcal{O}(q)$).

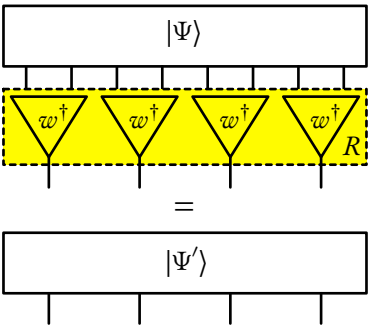

Figure 5.4: A quantum analog of Kadanoff's spin blocking with $b = 2$ for one-dimensional quantum states.

Unfortunately, this last requirement is exactly where the blocking scheme fails. In order to obtain the required behavior $R^\dagger R\,|\Psi\rangle \approx |\Psi\rangle$, the local projectors $w_b w_b^\dagger$ should project onto the support of the reduced density matrix of the corresponding block $\mathcal{B}$ of ℓ sites. But because the block is strongly entangled with the rest of the state, the Schmidt decomposition of $|\Psi\rangle$ with respect to a bipartition into a block $\mathcal{B}$ and the rest of the system, written as

$$|\Psi\rangle = \sum_{\alpha=1}^{q^\ell} \lambda_\alpha\, |\Psi_\alpha^{(\mathcal{B})}\rangle\, |\Psi_\alpha^{(\mathcal{L}\setminus\mathcal{B})}\rangle \tag{5.4}$$

contains many non-zero Schmidt-coefficients: $\lambda_\alpha \neq 0$ for $\alpha = 1, \ldots, q'$. We can lower-bound q' by $\exp[S(\mathcal{B})]$ with $S(\mathcal{B})$ the entanglement entropy of a block $\mathcal{B}$ of b^d sites, as discussed in Subsection 2.4 of Chapter 1. In particular, for one-dimensional critical systems we can use the scaling law in Eq. (1.66) to infer that $q' \geq \exp(c/6 \log b)$ and thus $q'' \geq \exp(c/6 \log b^2) \approx (q')^2$ and so on. The short range quantum fluctuations thus accumulate, resulting in a rapid increase in the required Schmidt dimension. This behavior was to be expected. We try to reduce the degrees of freedom by discarding the

quantum fluctuations within a block of b^d sites. But the partition of the lattice into such blocks is arbitrary, and the same short-range fluctuations exist across the boundaries of these blocks. The area law allows some benefit from discarding short range fluctuations within a block (see *e.g.* [372]) in comparison to exact diagonalization, where we would need a double exponential scaling $q' = q^{b^d}$, $q'' = q^{(b^d)^2}, \ldots$ However, the cross-boundary fluctuations are still responsible for a large entanglement between each block and the rest of the system. We should thus also try to eliminate these short-range fluctuations before trying to reduce the number of degrees of freedom within a single block.

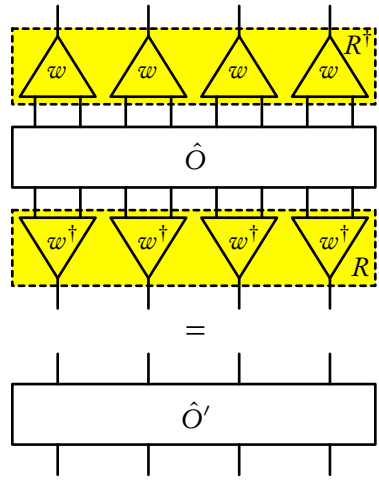

Figure 5.5: Kadanoff's associated blocking transformation of operators.

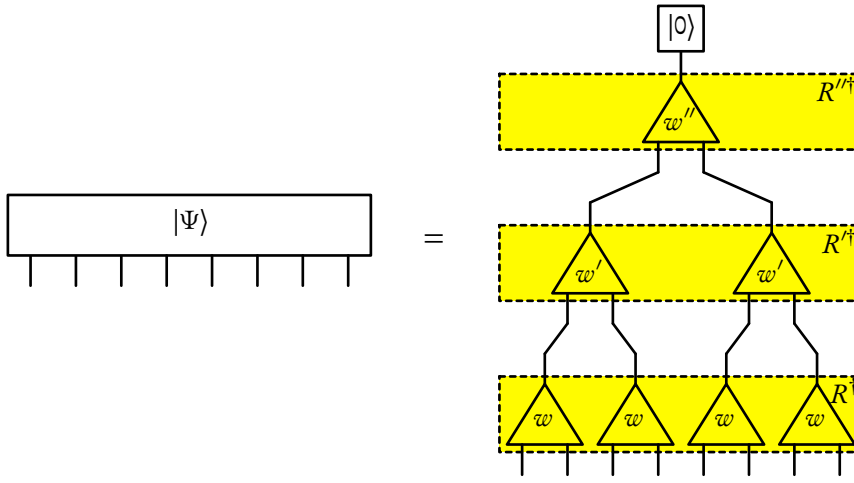

Figure 5.6: The variational class of tree tensor network states $\mathscr{M}_{\mathrm{TTNS}}$ as defined by the quantum analog of Kadanoff's blocking scheme defined above.

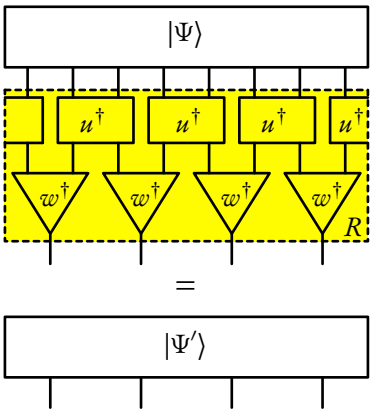

Figure 5.7: The entanglement renormalization step with $b = 2$ for one-dimensional quantum states with periodic boundary conditions.

This naturally leads to the process of entanglement renormalization as was first defined in [368], the renormalization transformation R of which is sketched in Figure 5.7 for one-dimensional systems. The renormalization step R now also contains unitary operators $u^\dagger \in \mathbb{L}(\mathbb{H}_{\text{site}}^{\otimes 2})$ that act on the two neighboring sites of different blocks $\mathscr{B}$ and $\mathscr{B}'$. This construction can be generalized in a number of ways to higher dimensions, but important is to act with unitary operators across the boundaries of neighboring blocks. These unitary operators are appropriately called *disentanglers*. The resulting variational ansatz is called the multi-scale entanglement renormalization ansatz and is sketched in Figure 5.8. This variational class was studied in great detail in [369] and allows to efficiently evaluate expectation values when q', q'', ... remain small. Unlike in the previous case, this is now a valid assumption. Even with $q = q' = q'' = \ldots$ this ansatz allows for algebraically decaying correlation functions and can thus be used to describe both critical and non-critical systems. In Subsection 1.4, we recapitulate the argument that shows how the multi-scale entanglement renormalization ansatz produces an area law for the entanglement entropy $S^{(\mathscr{A})}$ of a spatial region $\mathscr{A}$ in arbitrary dimensions $d > 1$, while allowing logarithmic violations compatible with the conformal field theory result of Eq. (1.66) for $d = 1$. Since the lowest layers $R^\dagger$ effectively eliminate the degrees of freedom living at the shortest length scale, the variational parameters in the higher layers u' and w' only influence the long-range behavior of the wave function. These parameters do thus not suffer from Feynman's sensitivity to high frequencies. The only downside is that the arbitrariness of grouping blocks of b spins together results in a general instance of this variational class not being translationally invariant, even when all transformations u and w within a single layer are chosen to be identical.

Let us now compare this renormalization scheme to a scheme based on tracing out degrees of freedom in the density matrix $\hat{\rho} = |\Psi\rangle\langle\Psi|$. When $q = q' = q'' = \ldots$, we can rewrite the isometries w, w', ... as a b^d-site unitary operators $\tilde{w}$ where $b^d - 1$ of the input sites are in a fixed state $|0\rangle$, as in Figure 5.9(a) for $b = 2$ and $d = 1$. The Hermitian conjugate transformation $w^\dagger$ appearing in the renormalization group transformation R acting on quantum states can then be written as a unitary transformation $\tilde{w}^\dagger$ followed by a projection of $b - 1$ of the b sites onto the reference state $|0\rangle$. Let us now denote the successive action of $u^\dagger$ and $\tilde{w}^\dagger$ as $\tilde{R}$, so that R consists of the unitary quantum cirquit $\tilde{R}$ followed by the projection onto $|0\rangle$. In the ideal case, where $R^\dagger R|\Psi\rangle = |\Psi\rangle$, this implies that $\tilde{R}$ is able to completely disentangle $|\mathscr{L} \setminus \mathscr{L}'| = |\mathscr{L}|(b^d - 1)/b^d$ degrees of freedom,

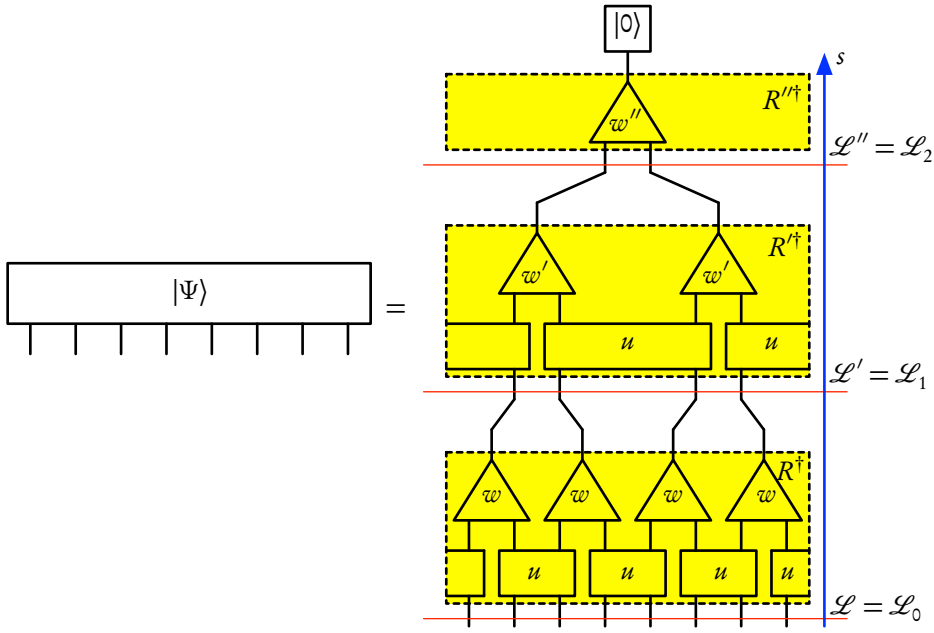

Figure 5.8: The multi-scale entanglement renormalization ansatz with $b = 2$ for one-dimensional systems with periodic boundary conditions.

so that $\tilde{R}|\Psi\rangle = |\Psi'\rangle \otimes |0\rangle^{\otimes|\mathscr{L}\setminus\mathscr{L}'|}$. In that case, there is no difference between projecting onto the fixed states $|0\rangle$ or just tracing these degrees of freedom, so that

$$\hat{\rho}' = \mathrm{tr}_{\mathscr{L}\setminus\mathscr{L}'}\left[\tilde{R}\hat{\rho}\tilde{R}^\dagger\right] = |\Psi'\rangle\langle\Psi'|(\mathrm{tr}[|0\rangle\langle 0|])^{|\mathscr{L}\setminus\mathscr{L}'|} = |\Psi'\rangle\langle\Psi'|. \tag{5.5}$$

In the general case where such a complete disentanglement is not exactly obtainable, we should explicitly include a projection $\hat{P}_{\mathscr{L}\setminus\mathscr{L}'} = (|0\rangle\langle 0|)^{\otimes|\mathscr{L}\setminus\mathscr{L}'|}$ in order to obtain

$$\hat{\rho}' = \mathcal{R}(\hat{\rho}) = R\hat{\rho}R^\dagger = \mathrm{tr}_{\mathscr{L}\setminus\mathscr{L}'}\left[\hat{P}_{\mathscr{L}\setminus\mathscr{L}'}\tilde{R}\hat{\rho}\tilde{R}^\dagger\right] = |\Psi'\rangle\langle\Psi'|. \tag{5.6}$$

Hence, we have generalized the intuitive tracing operation from the beginning of the previous subsection to a more general format, where we first operate on the density matrix $\hat{\rho}$ before tracing out degrees of freedom. This operation includes a unitary transformation that tries to disentangle the degrees of freedom, followed by a projection that ensures that the resulting density matrix is pure even when the disentanglement was not complete. Since the following renormalization steps no longer act on the disentangled degrees of freedom, we can postpone the projection step until the very end. Reversing this process defines the multi-scale entanglement renormalization ansatz as a special quantum circuit acting on the initial state $|0\rangle^{\otimes|\mathscr{L}|}$, as depicted in Figure 5.10.

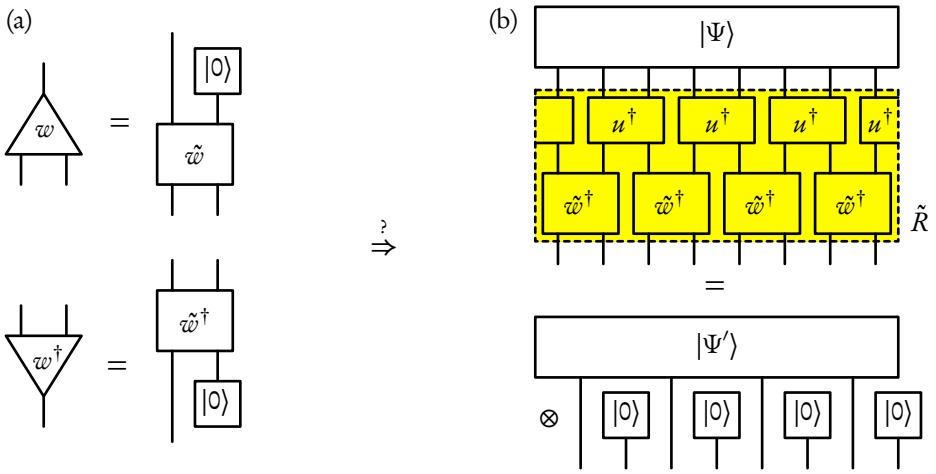

Figure 5.9: (a) The isometry w can for $b = 2$ be recast as a two-site unitary operator $\tilde{w}$ with a reference state $|0\rangle$ acting as fixed input for one site; the projection $w^\dagger$ acts as a unitary transformation $\tilde{w}^\dagger$ after which one output is projected onto the fixed state $|0\rangle$. (b) The renormalization group transformation R acting on quantum states can now be interpreted as a unitary quantum circuit that tries to completely disentangle half of the degrees of freedom.

1.3. Fixed points, quantum phases and critical exponents

Further evidence that the process of entanglement renormalization defines a proper renormalization group transformation comes from numerically applying it to test models and investigating its fixed point structure. Numerical investigation of critical and non-critical spin models chains have been conducted in [373] for $d = 1$ and in [374, 375] for $d = 2$ and agree well with Monte-Carlo results. For two-dimensional models, the multi-scale entanglement renormalization ansatz has also proven to be successful to describe systems that are not accessible by Monte Carlo techniques, *i.e.* frustrated antiferromagnets [376] and interacting fermion systems [377, 378], both at finite size and in the thermodynamic limit. These simulations learn that for non-critical models (*e.g.* disordered phases or symmetry breaking ordered phases), the tensors u and w become trivial after a number of layers s such that $\tilde{\xi}_c/b^s \lesssim 1$, with $\tilde{\xi}_c = \xi_c/a$ the dimensionless correlation length in terms of the number of lattice spacings a. Hence, the layers above layer s can be omitted. As an active renormalization process, the ground state $|\Psi\rangle$ has been completely disentangled after the application of s renormalization steps $R, R', \ldots$ In contrast, for critical models the transformations u and w can be chosen equal for the successive layers, with a possible transient regime in the first few layers. Hence, the low-energy behavior of the ground state of critical models becomes scale invariant. The multi-scale entanglement renormalization can also describe phases with topological order [379, 380]. While these models are non-critical and all fluctuations can be projected out with a finite number of s layers, the resulting state is not completely disentangled. In a system of finite size, the top tensor w''' introduces a global entanglement in the system

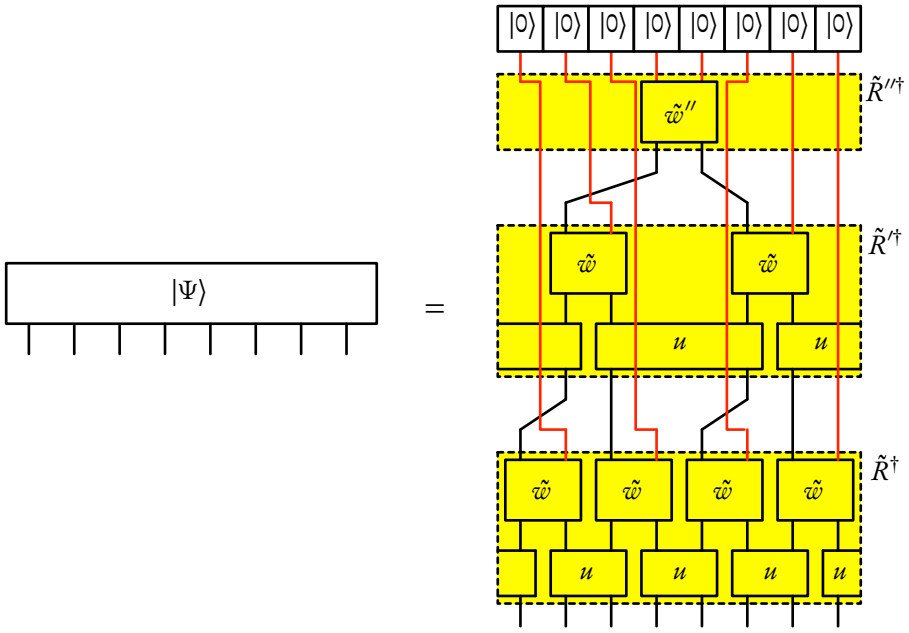

Figure 5.10: The multi-scale entanglement renormalization ansatz as a unitary quantum circuit acting on a fixed input state $|0\rangle^{\otimes|\mathcal{L}|}$.

that lives at the scale of the system size. This entanglement gives rise to the topological entanglement entropy γ discussed in Subsection 2.4 of Chapter 1 [see Eq. (1.72)]. Very recently, the multi-scale entanglement renormalization ansatz has even been applied to a simple $\mathbb{Z}_2$ lattice gauge theory [381], where the local symmetry can be incorporated in the tensor network. Accurate estimates for the energy gap and the Wilson loop can be obtained.

As a valid renormalization group transformation, entanglement renormalization should also enable us to compute scaling exponents and the corresponding scaling operators near critical points through linearization of the fixed point transformation law. In the current scheme of renormalization of quantum states, the renormalization group transformation law $\mathcal{R}(\hat{O}) = R\hat{O}R^\dagger$ can already be considered as this linearization. For the scheme of entanglement renormalization, R contains the tensors u and w of a scale-invariant multi-scale entanglement renormalization ansatz representation of the ground state of a critical model. Non-linear contributions to the renormalization group transformation law of operators are obtained by taking into account the change in u and w under the substitution $\hat{H} \leftarrow \hat{H} + \eta\hat{O}$. The transformation $\mathcal{R}(\hat{O})$ is depicted in terms of u and w in Figure 5.11(a) for $b = 2$ and $d = 1$. We can use $u^\dagger \hat{\mathbb{1}} u = \hat{\mathbb{1}}'$ and $w^\dagger \hat{\mathbb{1}} w = \hat{\mathbb{1}}'$ to note that local operators, which act as $\hat{\mathbb{1}}$ on most sites, are mapped to local operators. In particular, for the binary one-dimensional scheme ($b = 2$ and $d = 1$) of Figure 5.11(a), all operators with finite support are automatically contracted onto three-site operators

after a number of successive iterations. Hence, as a proper renormalization group transformation, the map $\mathcal{R}$ does not induce long-range interactions. While this is a general feature of entanglement renormalization, the number of sites to which all local operators converge is specific to the chosen implementation. For $b = 3$ and $d = 1$, all local operators are contracted to two-site operators. We are now interested in the eigenvalues $\lambda^{(\alpha)}$ and corresponding operators $\hat{O}^{(\alpha)}$ of $\mathcal{R}$ —so that $\mathcal{R}(\hat{O}^{(\alpha)}) = \lambda^{(\alpha)}\hat{O}^{(\alpha)}$— since these define the scaling operators and scaling exponents. The scaling exponents Δ are then obtained as $-\log \lambda^{(\alpha)}/\log b$. For $b = 2$, all eigenoperators are either three-site operators or have an infinitely large support. Note that the map $\mathcal{R}$ is b-periodic, *i.e.* it is only translation invariant under shifts over b sites. The output $\hat{O}' = \mathcal{R}(\hat{O})$ for a local operator depends on the position of the operator. It is therefore better to define for local operators an averaged map $\mathcal{A}(\hat{O})$ which is called the ascending superoperator and is sketched in Figure 5.11(b). Local scaling operators and corresponding scaling exponents are obtained from the eigenvalues and eigenoperators of $\mathcal{A}$ in [382, 383, 384] for one-dimensional critical spin models and are in very good agreement with the exact results from conformal field theory. In addition, the transformation law $\mathcal{R}$ can also be used to obtain non-local scaling operators [385], which consist of a local operator times a semi-infinite string (*i.e.* like the Mandelstam operators for creating topologically non-trivial excitations introduced in Section 3 of Chapter 3). Finally, the multi-scale entanglement renormalization ansatz can be used to study boundary critical phenomena and obtain boundary scaling operators [386].

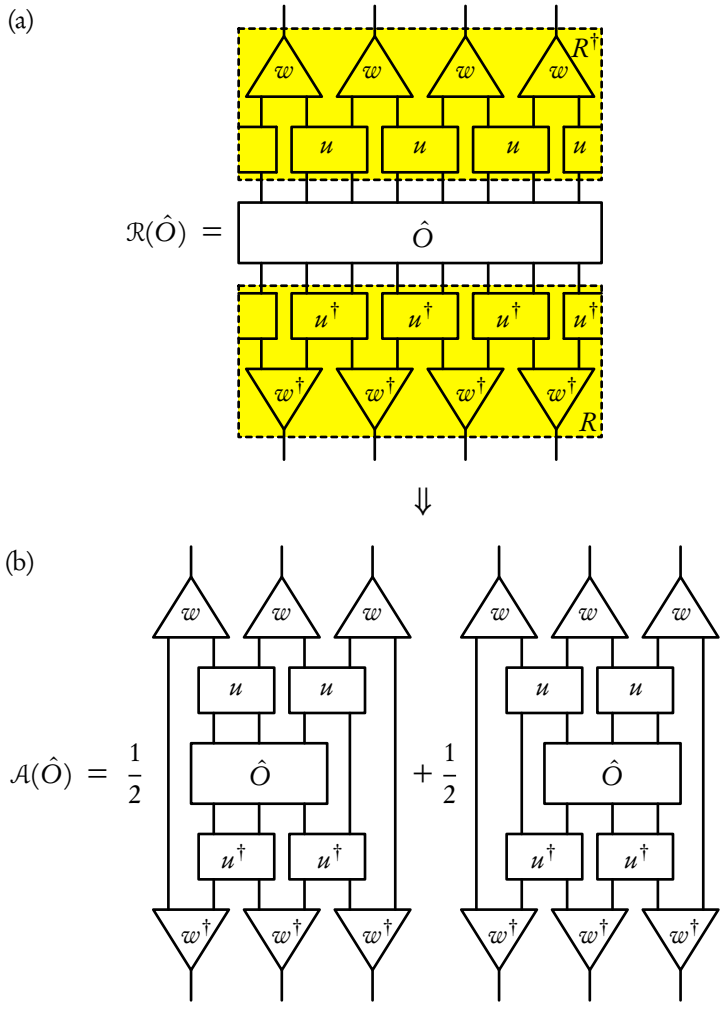

Figure 5.11: (a) The entanglement renormalization step induces a renormalization group transformation law for operators $\hat{O}' = \mathcal{R}(\hat{O})$. (b) An averaged renormalization group transformation law for local operators $\hat{O}' = \mathcal{A}(\hat{O})$ with $\mathcal{A}$ the ascending superoperator.

1.4. Scaling of entanglement

The success of the multi-scale entanglement renormalization ansatz can of course be explained by the precarious way it deals with entanglement. Entanglement is created by quantum fluctuations of degrees of freedom living at different length scales and thus has itself a multi-scale structure. Let us now label the lattices $\mathscr{L}, \mathscr{L}', \ldots$ appearing through successive renormalization steps as $\mathscr{L}_s$, with s labeling the number of renormalization steps (so that $\mathscr{L} = \mathscr{L}_0, \mathscr{L}' = \mathscr{L}_1, \ldots$). A block $\mathscr{B}_s$ of n^d sites at lattice $\mathscr{L}_s$ corresponds to n^{sd} sites on the original lattice. For one-dimensional critical models, the entanglement entropy of $\mathscr{B}_s$ with the rest of the lattice would thus be given by $S^{(\mathscr{B}_s)} = (c+\bar{c})/6 \log n^s \sim s \log n$ if no entanglement had been renormalized away. The entanglement entropy of a block with a fixed number of sites would thus increases linearly in s, corresponding with an exponential increase of the required dimension of the effective sites in the case of tree tensor networks. As was illustrated in [368], the disentanglers are able to reduce this scaling down to a constant (s-independent) entanglement entropy $S^{(\mathscr{B}_s)}$ for critical models, whereas the entanglement entropy $S^{(\mathscr{B}_s)}$ scales to zero for non-critical models (if the absence of topological order is assumed). As discussed in the previous section, the successive renormalization steps acting on $|\Psi\rangle$ produce a disentangled state after s steps such that $\tilde{\xi}_c / b^s \lesssim 1$.

This observation of course explains why the multi-scale entanglement renormalization ansatz is able to accurately describe ground states of critical models even with $q = q' = q'' = \ldots$. Let us now reverse this argument and analyze directly how entanglement is created in the multi-scale entanglement renormalization ansatz for an arbitrary number d of spatial dimensions. Let ρ be the density matrix of a block $\mathscr{B}$ of n^d sites in $\mathscr{L}$. The density matrix $\hat{\rho}$ is obtained from a density matrix $\hat{\rho}'$ corresponding to a block $\mathscr{B}'$ of sites in lattice $\mathscr{L}'$, and so on. The corresponding transformation is sketched for $d = 1$ and $b = 2$ in Figure 5.12. Let us reintroduce the index s that labels the lattice $\mathscr{L}_s$ on which $\hat{\rho}_s$ is defined. If the disentanglers act only between nearest neighbors across the boundary of blocks of linear size b, then the linear size n_{s+1} of $\hat{\rho}_{s+1}$ is given in terms of the linear size n_s of $\hat{\rho}_s$ as $n_{s+1} = \lceil (n_s + 2)/b \rceil$. Hence, the linear size of ρ_s decreases up to some constant value

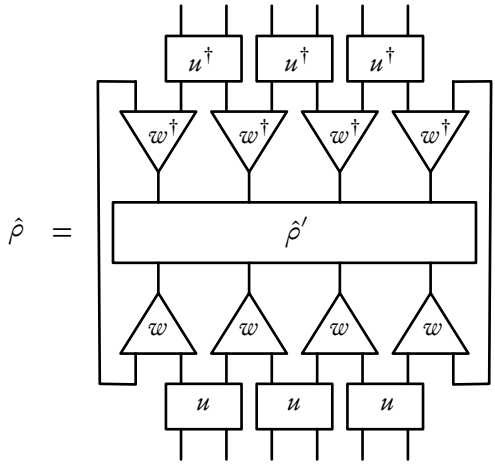

Figure 5.12: Creation of entanglement in the multi-scale entanglement renormalization ansatz for a local reduced density matrix $\hat{\rho}'$ that is obtained from a smaller reduced density matrix $\hat{\rho}'$ in a higher layer.

$\overline{n} = n_{\overline{s}}$ after $\overline{s} \approx \log_b n$ renormalization steps. In the most extreme case, $\hat{\rho}_{\overline{s}}$ is in a totally mixed state, so that $S(\hat{\rho}_{\overline{s}}) = \overline{n}^d \log q$, where we still assume that $q = q' = \ldots = q_s$. In every step, the $\hat{\rho}_s$ is obtained from $\hat{\rho}_{s+1}$ by some isometric transformations (which do not increase the entropy) followed by tracing out approximately $2d\, n_s^{(d-1)}$ boundary sites, where tracing out one site increases the entanglement by at most $\log q$. Hence, we obtain

$$\hat{S}^{(\mathscr{B})} \leq \overline{n}^d \log q + \sum_{s=0}^{\overline{s}} 2d\, n_s^{(d-1)} \log q. \tag{5.7}$$

For $d = 1$ this leads to

$$\hat{S}^{(\mathscr{B})} \lesssim \frac{2 \log q}{\log b} \log n + \text{cst} \sim \log|\mathscr{B}|, \tag{5.8}$$

while for $d > 1$ it results in

$$\hat{S}^{(\mathscr{B})} \lesssim \overline{n}^d \log q + 2d\, n^{(d-1)} \log q \sum_{s=0}^{\log_b n} b^{-s(d-1)} = k 2 n^{(d-1)} + \text{cst} \sim |\partial \mathscr{B}|. \tag{5.9}$$

We have ignored the constant term for large blocks $\mathscr{B}$. Hence, the sum over the different layers is able to create a logarithmic violation of the area law in $d = 1$ but not in higher dimensions. As a result, certain fermionic models with logarithmic violations to the area law in $d > 1$ cannot be captured by the multi-scale entanglement renormalization ansatz. A solution to this problem is provided by a generalized tensor network structure where at each renormalization step the theory branches into two or more decoupled theories [387, 388], the so-called *branching multi-scale entanglement renormalization ansatz*.

Finally, we return to the nature of the additional dimension s that is present in the tensor network structure of the multi-scale entanglement renormalization ansatz. We have given ample proof that s labels the renormalization scale. But can we now also interpret s as a holographic dimension? A first step towards such a correspondence was provided in [389] and further explored in [388]. If we now reverse the postulate of Ryu and Takayanagi [Eq. (1.78) in Subsection 2.5 of Chapter 1], we can define the geometry of this additional dimension through entanglement. The length or surface of a block $\mathscr{B} \subset \mathscr{L}$ of sites can be defined to be proportional to its entanglement $S^{(\mathscr{B})}$. The corresponding geodesic or minimal surface is then obtained as the connection of all the bonds that are responsible for creating $S^{(\mathscr{B})}$, *i.e.* all bonds that had to be traced out in order to obtain $\hat{\rho}^{(\mathscr{B})}$. This definition endows the bulk containing the collection of all lattices $\mathscr{L}, \mathscr{L}', \mathscr{L}'', \ldots$ with the structure of a discrete anti-de Sitter space. Such a discrete anti-de Sitter space has also been recovered in an explicit construction of holographic duals for large N lattice gauge theory [390].

2. Entanglement renormalization for quantum fields

Jutho Haegeman, Tobias J. Osborne, Henri Verschelde, Frank Verstraete.
"*Entanglement renormalization for quantum fields*".
arXiv:1102.5524 (2011).

Despite the many interesting properties of the entanglement renormalization prescription for quantum lattice systems, we can isolate two drawbacks. The first one was already mentioned in the previous section: entanglement renormalization defines a variational ansatz that can not easily be made translation invariant. Secondly, while the choice $q = q' = q'' = ...$ already produces a variational ansatz with the correct entanglement and correlation structure, a small increase of q_s in the lowest layers is in general required in order to obtain truly accurate results. This can be easily understood. In the discrete entanglement renormalization scheme, we are trying to eliminate a large fraction $(b-1)/b$ of all degrees of freedom in a single layer. Rephrased in terms of the quantum circuit $\tilde{R}$, we are trying to disentangle a large fraction of all degrees of freedom by a very simple quantum circuit consisting of a layer of two-site unitary operators u followed by a shifted layer of b-site unitary operators $\tilde{w}$ [see Figure 5.9(b)].

This last issue has two easy solutions. Either we can try to increase the complexity of the quantum circuit (see *e.g.* [278]), which might very quickly jeopardize the efficient contractibility of the tensor network, or we can try to take infinitesimally small renormalization steps. However, being able to define infinitesimal renormalization group transformations forces us to abandon the lattice $\mathscr{L}$ and move to the continuum $\mathscr{R}$. As we show momentarily, this also enables us to overcome the first problem and formulate a variational ansatz for field theories that can easily be made translation invariant. A continuum formulation is also very appealing from the theoretical point of view, since it will facilitate further research regarding the connection with the AdS/CFT correspondence.

2.1. Towards a continuum formulation of entanglement renormalization

We first introduce a continuum formulation of entanglement renormalization as a renormalization group transformation acting on quantum states. Through the strategy of the previous section, this renormalization group transformation automatically defines a variational ansatz that is discussed in the next subsection. Extracting a continuum limit from the entanglement renormalization scheme for lattice systems starts from the observation that there is some asymmetry in the definition of the entanglement renormalization process of *e.g.* Figure 5.7 ($d = 1$ and $b = 2$), since entanglement between an even and odd nearest neighbor site is removed with a disentangler $u^\dagger$, whereas entanglement between an odd and even nearest neighbor site is removed by an isometry $w^\dagger$. We can eliminate this assymetry by redefining $w^\dagger = w_0^\dagger v^\dagger$ where $v^\dagger$ is a disentangler

acting on odd-even pairs and $w_0^\dagger$ is a fixed isometry. For the unitary quantum circuit of Figure 5.9(b), the same substitution results in $\tilde{w}^\dagger = \tilde{w}_0^\dagger v^\dagger$, with $\tilde{w}_0^\dagger$ a fixed unitary operator. The resulting tensor network is displayed in Figure 5.13. While we have of course performed a trivial substitution, this allows for a level of abstraction that is required in order to obtain a continuum limit.

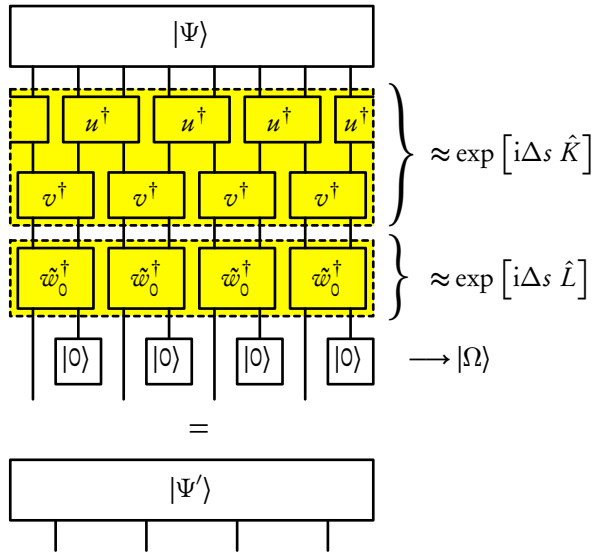

Figure 5.13: A reinterpretation of the entanglement renormalization process required to obtain the continuum limit.

We can now interpret the double layer of disentanglers $u^\dagger$ and $v^\dagger$ as a first order Lie-Trotter-Suzuki decomposition of an evolution operator $\exp(\mathrm{i}\Delta s\hat{K})$ with respect to a nearest neighbor Hamiltonian $\hat{K} = \sum_{n\in\mathcal{L}} \hat{k}_{n,n+1}$. In the original definition of s as the number of discrete renormalization steps, we would have $\Delta s = 1$. However, for reasons that are explained in the next paragraph, we now redefine dimension s such that a single layer corresponds to $\Delta s = \log b$, with $b = 2$ in Figure 5.13. This picture immediately explains and cures the two shortcomings of the multi-scale entanglement renormalization ansatz for lattice systems. Firstly, for translation invariant systems we expect that we are able to choose $\hat{K}$ translation invariant. This will result in all disentanglers $u = v = \exp(\mathrm{i}\Delta s\hat{k})$ being equal. But as a general feature of the Lie-Trotter-Suzuki decomposition that also plagues the Time-Evolving Block Decimation (see Subsection 2 of Chapter 3), the decomposition of a translation invariant operator is not translation invariant. Secondly, it explains why keeping q constant in the multi-scale entanglement renormalization ansatz cannot provide highly accurate results: the two layers of shifted disentanglers are only a rough first order approximation of the large evolution step $\exp(\mathrm{i}\Delta s\hat{K})$ with $\Delta s = \mathcal{O}(1)$. A better ansatz would be to include in each renormalization step R several layers of shifted disentanglers representing a higher order Lie-Suzuki-Trotter decomposition, but this destroys the efficient contractibility of the

tensor network. It is now straightforward how to define $\exp(\mathrm{i}\Delta s\hat{K})$ in the continuum, since it suffices to replace $\hat{K}$ by a field theory Hamiltonian defined in terms of creation and annihilation operators $\hat{\psi}^\dagger_\alpha(\vec{x})$ and $\hat{\psi}_\alpha(\vec{x})$, $\vec{x}\in\mathscr{R}$. One subtlety should not be ignored. On the lattice, $\hat{K}$ disentangles degrees of freedom at the shortest length scale available in the lattice, *i.e.* degrees of freedom living at the scale of the lattice spacing. In the continuum, such a length scale is missing and we should manually include a cutoff $a=\Lambda^{-1}$ in the definition of $\hat{K}$. This is the scale at which $\hat{K}$ acts to disentangle degrees of freedom. This situation is similar to Wilson's renormalization group discussed in Section 3 of Chapter 1: without the introduction of an explicit cutoff this process can not be defined in the continuum. When required, we can always send $\Lambda\to\infty$ at the end of the process.

We still have to deal with the isometries $w_0^\dagger$, or alternatively the unitary operators $\tilde{w}_0^\dagger$ followed by the projection onto the ancillas $|0\rangle$. By removing sites from the lattice, we obtain a coarser lattice with lattice spacing $a'=ba$. However, operators and states on the lattice have no notion of the physical length of the lattice spacing. All distances are naturally measured in terms of lattice spacings. Hence, the operator $\hat{K}'$ of renormalization step R' naturally disentangles degrees of freedom living at scale $a'=ba$. This is no longer true in the continuum: we either need to redefine the explicit cutoff in $\hat{K}'$ or we need to apply a scale transformation that brings degrees of freedom living at scale Λ/b back to the cutoff scale Λ. These two solutions are of course complementary and both have there merits, as we illustrate in the remainder of this chapter. The last point of view is however closest to the original formulation of Wilson's renormalization group, where such an explicit scale transformation is also present. We can thus interpret $w_0^\dagger$ as applying this scale transformation. For example, if every lattice site can either be empty ($|0\rangle$) or occupied ($|1\rangle=\hat{c}^\dagger|0\rangle$) by a particle, then choosing $w_0^\dagger=|0\rangle\langle 00|+|1\rangle(\langle 01|+\langle 10|)/\sqrt{2}$ acts naturally as a scale transformation on a single particle state $|\varphi\rangle=\sum_{n\in\mathscr{L}}\varphi_n\hat{c}_n^\dagger|\mathbf{0}\rangle$ with $|\mathbf{0}\rangle=|0\rangle^{\otimes|\mathscr{L}|}$, since

$$|\varphi'\rangle=(w_0^\dagger)^{\otimes|\mathscr{L}'|}|\varphi\rangle=\sum_{n\in\mathscr{L}'}\frac{\varphi_{2n-1}+\varphi_{2n}}{\sqrt{2}}(\hat{c}'_n)^\dagger|\mathbf{0}'\rangle\,. \tag{5.10}$$

In the continuum, there is no easy way to project onto a continuous subspace of degrees of freedom and it is easier to use the unitary quantum circuit with unitary operators $\tilde{w}_0^\dagger$ of Figure 5.13, where the projection step can be postponed until the very end of the process. We can then identify the unitary operation $(\tilde{w}_0^\dagger)^{\otimes|\mathscr{L}'|}$ with a scaling transformation, which is indeed a unitary operation in quantum field theories. Let $\hat{L}$ be the generator of scaling transformations in d spatial dimensions, which in terms of the field creation and annihilation operators $\hat{\psi}^\dagger_\alpha(\vec{x})$ and $\hat{\psi}_\alpha(\vec{x})$ is given by

$$\hat{L}=-\frac{\mathrm{i}}{2}\sum_{\alpha=1}^{N}\int \mathrm{d}^d x\,\hat{\psi}^\dagger_\alpha(\vec{x})\left[\vec{x}\cdot\vec{\nabla}\hat{\psi}_\alpha(\vec{x})\right]-\left[\vec{x}\cdot\vec{\nabla}\hat{\psi}^\dagger_\alpha(\vec{x})\right]\hat{\psi}_\alpha(\vec{x}). \tag{5.11}$$

Since the different field species α decouple, we continue henceforth with a single species. We define

$$\hat{\psi}^\dagger(\vec{x};s) = \mathrm{e}^{\mathrm{i}s\hat{L}}\hat{\psi}^\dagger(\vec{x})\mathrm{e}^{-\mathrm{i}s\hat{L}} \tag{5.12}$$

so that

$$\frac{\partial}{\partial s}\hat{\psi}^\dagger(\vec{x};s) = \mathrm{i}[\hat{L},\hat{\psi}^\dagger(\vec{x};s)]. \tag{5.13}$$

Since $\hat{L}(s) = \mathrm{e}^{\mathrm{i}s\hat{L}}\hat{L}\mathrm{e}^{-\mathrm{i}s\hat{L}} = \hat{L}$ we immediately obtain

$$\frac{\partial}{\partial s}\hat{\psi}^\dagger(\vec{x};s) = -\frac{1}{2}\vec{\nabla}\cdot(\vec{x}\hat{\psi}^\dagger(\vec{x};s)) - \frac{1}{2}\vec{x}\cdot\vec{\nabla}\hat{\psi}^\dagger(\vec{x};s) = -\vec{x}\cdot\vec{\nabla}\hat{\psi}^\dagger(\vec{x};s) - \frac{d}{2}\hat{\psi}^\dagger(\vec{x};s) \tag{5.14}$$

and thus

$$\hat{\psi}^\dagger(\vec{x};s) = \mathrm{e}^{-sd/2}\hat{\psi}^\dagger(\mathrm{e}^{-s}\vec{x}). \tag{5.15}$$

If we now define a single particle state as $|\varphi\rangle = \int \mathrm{d}^d x\, \varphi(\vec{x})\hat{\psi}^\dagger(\vec{x})|\Omega\rangle$ with $|\Omega\rangle$ the vacuum that is annihilated by every $\hat{\psi}(\vec{x})$, we obtain

$$|\varphi'\rangle = \mathrm{e}^{\mathrm{i}\Delta s\hat{L}}|\varphi\rangle = \int \mathrm{d}^d x\, \varphi(\vec{x})\hat{\psi}^\dagger(\vec{x};\Delta s)\mathrm{e}^{\mathrm{i}\Delta s\hat{L}}|\Omega\rangle = \mathrm{e}^{-d\Delta s/2}\int \mathrm{d}^d x'\, \varphi(\mathrm{e}^{\Delta s}\vec{x}')\hat{\psi}^\dagger(\vec{x}')|\Omega\rangle \tag{5.16}$$

since $\hat{L}|\Omega\rangle = 0$. Setting $\Delta s = \log b$ establishes the relationship between Eq. (5.16) and its discrete version Eq. (5.10) for $d = 1$ and $b = 2$. However, in the continuum we are no longer restricted to choosing Δs equal to the logarithm of an integer, and we can hence define a infinitesimal entanglement renormalization step by sending $\Delta s \to 0$ and iterating this process infinitely many times. Every infinitesimal renormalization step $\mathrm{d}s$ at total renormalization scale s will disentangle the degrees of freedom living at momentum scale $[\mathrm{e}^{-s-\mathrm{d}s}\Lambda, \mathrm{e}^{-s}\Lambda]$ until all modes have been disentangled. Note that here and in the remainder of this chapter, even though we speak about momentum scales according to common practice, these intervals of scales should not be interpreted as having sharp cutoffs in momentum space. We are in fact free to implement the cutoff however we deem appropriate. This disentangling process is generated by the operator $\hat{K}(s)$, which can depend on the scale s. Note that due to the rescaling step, $\hat{K}(s)$ always disentangles degrees of freedom effectively living at the momentum cutoff scale $[\mathrm{e}^{-\mathrm{d}s}\Lambda, \Lambda]$, but that this corresponds to the physical momentum scale $[\mathrm{e}^{-s-\mathrm{d}s}\Lambda, \mathrm{e}^{-s}\Lambda]$. In principle, this process continues forever ($s \to \infty$). However, for non-critical systems we can expect that at a scale $\bar{s}$ such that $\xi_\mathrm{c} \ll \mathrm{e}^{\bar{s}}\Lambda^{-1}$, the state has been transformed into a fully disentangled reference state $|\Omega\rangle$ and can thus be projected onto it (in the assumed absence of topological order). Put differently, $\hat{K}(s)$ converges to zero for $s \gg \log(\xi_\mathrm{c}\Lambda)$. For critical systems, on the other hand, the scale invariance of the low-energy behavior of the theory allows to assume that $\hat{K}(s)$ develops a horizontal asymptote for $s \to \infty$, *i.e.* it becomes effectively constant after some possible transient regime.

2.2. Continuous entanglement renormalization ansatz

The infinitesimal entanglement renormalization transformation introduced in the previous subsection immediately defines a variational ansatz for quantum field theories, to which we henceforth refer to as the *continuous entanglement renormalization ansatz*

$$|\Psi[\hat{K}]\rangle \triangleq \mathcal{S}\exp\left[-\mathrm{i}\int_{s_a}^{s_\xi} \hat{K}(s) + \hat{L}\,\mathrm{d}s\right]|\Omega\rangle\,. \tag{5.17}$$

Here, $a = \Lambda^{-1}$ represents the minimal length scale cutoff and s can run from s_a up to s_ξ such that $\mathrm{e}^{s_\xi - s_a} \gg \xi_c/a = \xi_c\Lambda$. We can always fix one of the two end points of the integration interval, such as $s_a = 0$. The operation $\mathcal{S}\exp$ represents a *scale ordered* exponential where the argument is ordered for *increasing values* of the scale parameter s from left to right, *i.e.* the argument for s_a appears completely at the left while the argument for s_ξ appears completely to the right acting on $|\Omega\rangle$. $|\Omega\rangle$ represents a completely unentangled reference state (for systems without topological order). For non-relativistic field theories defined in terms of creation and annihilation operators $\hat{\psi}^\dagger_\alpha(\vec{x})$ and $\hat{\psi}_\alpha(\vec{x})$, we can choose $|\Omega\rangle$ as the vacuum that is annihilated by all annihilation operators $\hat{\psi}_\alpha(\vec{x})$. The variational parameters are now given by the (possible s-dependent) Hermitian operator $\hat{K}$ of the form

$$\hat{K}(s) = \int \mathrm{d}^d x\, \hat{k}(\vec{x}; s), \tag{5.18}$$

where $\hat{k}(\vec{x}; s)$ has non-trivial support in a small region of approximate linear size $a = \Lambda^{-1}$ around the point $\vec{x}$. It is easy to show that a translation invariant choice $\hat{K}(s)$ ($\forall s \in [s_a, s_\xi]$) produces a translation invariant quantum state. While $\hat{L}$ is in itself not translation invariant, a dilatation of a translation invariant state is always again translation invariant. More formally,

$$\exp(-\mathrm{i}\vec{x}_0 \cdot \hat{\vec{P}})\hat{L}\exp(+\mathrm{i}\vec{x}_0 \cdot \hat{\vec{P}}) = \hat{L} - \vec{x}_0 \cdot \hat{\vec{P}} \tag{5.19}$$

with the momentum operator $\hat{\vec{P}}$ given by

$$\hat{\vec{P}} = -\mathrm{i}\int \mathrm{d}^d x\, \hat{\psi}^\dagger(\vec{x})\vec{\nabla}\hat{\psi}(\vec{x}). \tag{5.20}$$

The second term in Eq. (5.19) does not contribute when acting on a translation invariant state. Similarly, for $\hat{K}(s)$ rotation invariant ($\forall s \in [s_a, s_\xi]$), the resulting state $|\Psi[\hat{K}]\rangle$ is rotation invariant.

By redefining $s = -t$ and $s_a = -t_a$ and $s_\xi = -t_\xi$ we can reformulate Eq. (5.17) as

$$|\Psi[\hat{K}]\rangle = \mathcal{T}\exp\left[-\mathrm{i}\int_{t_\xi}^{t_a} \hat{K}(-t) + \hat{L}\,\mathrm{d}t\right]|\Omega\rangle\,, \tag{5.21}$$

with $\mathcal{T}\exp$ an ordinary time-ordered exponential that orders its arguments for *decreasing*

values of t from left to right. Finally, we also define the unitary circuit that prepares the continuous entanglement renormalization ansatz as

$$\hat{U}(s_a, s_\xi) = \mathcal{S} \exp\left[-\mathrm{i}\int_{s_a}^{s_\xi} \hat{K}(s) + \hat{L}\,\mathrm{d}s\right]. \tag{5.22}$$

Note that we have always assumed to be working in the thermodynamic limit, in order to be able to define continuous scale transformations. Hence, $\hat{U}(s_a, s_\xi)$ does not represent a proper unitary transformation, since it transforms one state $|\Omega\rangle$ to another state $|\Psi[\hat{K}]\rangle$ that probably does not live in the same Hilbert space. Since $\hat{K}(s)$ is assumed to have a cutoff, the resulting orthogonalization catastrophe is only of infrared nature (see Subsection 1.2 of Chapter 1). We henceforth ignore this potential problem.

Let us now interpret our ansatz as an active quantum circuit that transforms the unentangled reference state $|\Omega\rangle$ into a highly entangled state $|\Psi\rangle$. Initially the operator $\hat{K}(s_\xi)$ entangles degrees of freedom in $|\Omega\rangle$ that are living in the range of scales up to momentum scale Λ during an infinitesimal 'renormalization time' $\mathrm{d}s$. Then, an infinitesimal dilation $\mathrm{d}s\hat{L}$ is applied that transports these degrees of freedoms to longer length scales and new unentangled degrees of freedom that were originally living above momentum scale Λ are introduced at scale Λ. This process is then iterated. Note that the decomposition of $\hat{K}(s) + \hat{L}$ into two parts is somewhat artificial, since only the action of the sum is well defined. The decomposition is based on $\hat{K}(s)$ being fully responsible for creation all entanglement. The scaling part $\hat{L}$ does not increase or reduce the entanglement. In particular, the scaling transformation maps any unentangled state into an unentangled state. This property alone is not sufficient to fully specify $\hat{L}$ and we can still add to $\hat{L}$ an operator that has the same property, *i.e.* a strictly local operator that contains only the field operators and no derivatives thereof. In most systems, there is a well-defined generator of physical scaling transformations, that contains two parts: one part is responsible for transforming the argument $\vec{x}$ of local operators by acting as $\vec{x}\cdot\vec{\nabla}$, while the second part is responsible for generating the canonical scaling dimensions. Adding a strictly local operator in the definition of $\hat{L}$ (and subtracting it again in $\hat{K}$) changes the canonical scaling dimensions. As we show in the next paragraph, it is also beneficial to choose a reference state that is scale invariant ($\hat{L}|\Omega\rangle$). In some cases, it is useful to use the freedom in the definition of $\hat{L}$ for this. After having fixed $\hat{L}$, there are still many different choices of $\hat{K}(s)$ that result in the same physical state $|\Psi[\hat{K}]\rangle$. Hence, as the other variational classes encountered in the previous chapters, the continuous entanglement renormalization ansatz also has a gauge invariance. This is discussed in Subsection 2.5.

In principle we always have to set $s_\xi - s_a \to +\infty$. For ground states of non-critical systems, we expect that $\hat{K}(s)$ automatically converges to zero for $s \to +\infty$ by applying the variational principle, so that arbitrarily good approximations can be obtained with a finite range of renormalization scales $[s_a, s_\xi]$. For critical systems on the other hand, we expect that the variational principle forces $\hat{K}(s)$ to develop a non-zero horizontal

asymptote. We test this premise for an explicit example in the Section 3.

2.3. Renormalization group flow

We now establish how to evaluate expectation values and illustrate how this naturally lead to a renormalization group transformation law for operators in a Hamiltonian framework. Expectation values are given by

$$\langle\Psi[\hat{K}]|\hat{O}|\Psi[\hat{K}]\rangle = \langle\Omega|\hat{U}(s_a,s_\xi)^\dagger\hat{O}\hat{U}(s_a,s_\xi)|\Omega\rangle = \langle\Psi(s)|\hat{O}_{\mathrm{R}}(s)|\Psi(s)\rangle\,,\quad \forall s\in[s_a,s_\xi] \tag{5.23}$$

where we have defined a renormalized operator $\hat{O}_{\mathrm{R}}(s)$ and a renormalized state $|\Psi_{\mathrm{R}}(s)\rangle$ at renormalization scale s as

$$\hat{O}_{\mathrm{R}}(s) = \hat{U}(s_a,s)^\dagger\hat{O}\hat{U}(s_a,s),\qquad |\Psi_{\mathrm{R}}(s)\rangle = \hat{U}(s_a,s)^\dagger|\Psi[\hat{K}]\rangle = \hat{U}(s,s_\xi)|\Omega\rangle\,. \tag{5.24}$$

In particular, at $s = s_\xi$, $|\Psi_{\mathrm{R}}(s_\xi)\rangle = |\Omega\rangle$, so that evaluating the operator $\hat{O}$ defined at the ultraviolet cutoff scale s_a with respect to $|\Psi[\hat{K}]\rangle$ boils down to evaluating the renormalized operator $\hat{O}_{\mathrm{R}}(s_\xi)$ at the infrared scale s_ξ with respect to the reference state $|\Omega\rangle$. For any renormalization scale s, we can indeed interpret $\hat{O}_{\mathrm{R}}(s)$ as the renormalized operator, where all quantum fluctuations between momentum scales $\mathrm{e}^{-s}\Lambda$ and Λ have been integrated out. However, $\hat{O}_{\mathrm{R}}(s)$ is still defined with respect to an effective cutoff Λ due to the additional scaling transformation in $\hat{U}$. The *renormalization group equation* for the renormalized operator $\hat{O}_{\mathrm{R}}(s)$ is given by

$$\frac{\mathrm{d}}{\mathrm{d}s}\hat{O}_{\mathrm{R}}(s) = \mathrm{i}[\hat{K}(s)+\hat{L},\hat{O}_{\mathrm{R}}(s)]. \tag{5.25}$$

For critical systems, we expect that $\hat{K}(s)$ becomes s-independent. If the commutator $\mathrm{i}[\hat{K}+\hat{L},\cdot]$ has eigenoperators $\hat{O}^{(\alpha)}$ with corresponding eigenvalues $\lambda^{(\alpha)}$, so that

$$\mathrm{i}[\hat{K}+\hat{L},\hat{O}^{(\alpha)}] = \lambda^{(\alpha)}\hat{O}^{(\alpha)}, \tag{5.26}$$

then operator $\hat{O}^{(\alpha)}$ is a scaling operator and $\lambda^{(\alpha)}$ is the corresponding scaling exponent: $\hat{O}^{(\alpha)}_{\mathrm{R}}(s) = \mathrm{e}^{\lambda_\alpha s}\hat{O}^{(\alpha)}$. For local operators, this behavior is to restricted. Any local operator $\hat{O}(\vec{x})$ that is defined as a homogeneous polynomial of degree n in terms of the field operators $\hat{\psi}_\alpha(\vec{x})$ and $\hat{\psi}^\dagger_\alpha(\vec{x})$ satisfies

$$[\hat{L},\hat{O}(\vec{x})] = -\vec{x}\cdot\vec{\nabla}\hat{O}(\vec{x}) - \frac{nd}{2}\hat{O}(\vec{x}) \tag{5.27}$$

with thus $nd/2$ the canonical scaling dimension. Hence, if $\hat{O}(\vec{x})$ satisfies

$$[\hat{K}+\hat{L},\hat{O}(\vec{x})] = -\vec{x}\cdot\vec{\nabla}\hat{O}(\vec{x}) - \lambda\hat{O}(\vec{x}), \tag{5.28}$$

then $\hat{O}(\vec{x})$ is a local scaling operator with scaling dimension λ, and its renormalization group flow is given by

$$\hat{O}_{\mathrm{R}}(\vec{x};s) = \mathrm{e}^{-s\lambda}\hat{O}(\mathrm{e}^{-s}\vec{x}) \tag{5.29}$$

If $\hat{O}(\vec{x})$ is homogenous in the field operators so that it has a well defined canonical scaling dimension $nd/2$, then we can define $\lambda - nd/2$ as the anomalous scaling dimension.

Note that the renormalized operators $\hat{O}_{\mathrm{R}}(s)$ correspond roughly to the operator $\hat{O}$ in the Heisenberg picture with respect to the s-dependent Hamiltonian $\hat{K}(s)+\hat{L}$, the only difference being the fact that $\hat{U}$ contains a scale ordered exponential that orders its arguments in the reverse direction. Hence, the first argument $\hat{K}(s)+\hat{L}$ of the commutator is still defined in the 'Schrödinger picture' and should not be 'renormalized'. This difference is only present when $\hat{K}(s)$ actually depends on s, since otherwise $\hat{K}_{\mathrm{R}}(s)+\hat{L}_{\mathrm{R}}(s) = \hat{K}+\hat{L}$. By considering $\hat{L}$ as a free Hamiltonian and $\hat{K}$ as the interactive part, we can introduce another picture that is complementary to the interaction picture. We thereto define the physically renormalized operator $\hat{O}_{\mathrm{P}}(s)$ as

$$\hat{O}_{\mathrm{P}}(s) = \mathrm{e}^{-\mathrm{i}(s-s_a)\hat{L}}\hat{O}_{\mathrm{R}}(s)\mathrm{e}^{+\mathrm{i}(s-s_a)\hat{L}} = \mathrm{e}^{-\mathrm{i}(s-s_a)\hat{L}}\hat{U}(s_a,s)^{\dagger}\hat{O}\hat{U}(s_a,s)\mathrm{e}^{+\mathrm{i}(s-s_a)\hat{L}}. \tag{5.30}$$

It straightforwardly follows that $\hat{O}_{\mathrm{P}}(s)$ is defined by

$$\hat{O}_{\mathrm{P}}(s) = \mathrm{i}[\hat{K}'(s), \hat{O}_L(s)] \tag{5.31}$$

with

$$\hat{K}'(s) = \mathrm{e}^{-\mathrm{i}(s-s_a)\hat{L}}\hat{K}(s)\mathrm{e}^{+\mathrm{i}(s-s_a)\hat{L}}. \tag{5.32}$$

The physically renormalized operator $\hat{O}_{\mathrm{P}}(s)$ is equal to the renormalized operator $\hat{O}_{\mathrm{R}}(s)$ up to the fact that the excess scaling has been removed, so that it is truly defined with respect to a physical momentum cutoff $\mathrm{e}^{-s}\Lambda$. It arises from $\hat{O}$ by disentangling all modes living at momentum scale in the interval $[\mathrm{e}^{-s}\Lambda, \Lambda]$. Note that these modes have not yet been projected out, they have only been disentangled. Correspondingly, $\hat{K}'(s)$ is now an operator that disentangles mode at the scale-dependent physical cutoff $\mathrm{e}^{-s}\Lambda$. Hence, even if $\hat{K}$ is s-independent, $\hat{K}'(s)$ is not. We also define the physically renormalized states $|\Psi_{\mathrm{P}}(s)\rangle$

$$|\Psi_{\mathrm{P}}(s)\rangle = \mathrm{e}^{-\mathrm{i}(s-s_a)\hat{L}}|\Psi_{\mathrm{R}}(s)\rangle = \mathrm{e}^{-\mathrm{i}(s-s_a)\hat{L}}\hat{U}(s,s_\xi)|\Omega\rangle\,, \tag{5.33}$$

so that all expectation values can be obtained as

$$\langle\Psi[\hat{K}]|\hat{O}|\Psi[\hat{K}]\rangle = \langle\Psi_{\mathrm{P}}(s)|\hat{O}_{\mathrm{P}}(s)|\Psi_{\mathrm{P}}(s)\rangle\,, \quad \forall s \in [s_a, s_\xi]. \tag{5.34}$$

We obtain

$$\frac{\mathrm{d}}{\mathrm{d}s}|\Psi_{\mathrm{P}}(s)\rangle = \mathrm{i}\hat{K}'(s)|\Psi_{\mathrm{P}}(s)\rangle \tag{5.35}$$

and $|\Psi_{\mathrm{P}}(s_\xi)\rangle = \mathrm{e}^{-\mathrm{i}(s_\xi - s_a)\hat{L}}|\Omega\rangle$. If the reference state is now chosen to be scale invariant, as

was announced in the previous subsection, we can use $|\Psi_{\mathrm{P}}(s_\xi)\rangle = |\Omega\rangle$ to redefine

$$|\Psi_{\mathrm{P}}(s)\rangle = \mathcal{S} \exp\left[-\mathrm{i}\int_s^{s_\xi} \hat{K}'(s)\,\mathrm{d}s\right]|\Omega\rangle\,. \tag{5.36}$$

This corresponds to the interpretation given to $\hat{K}'(s)$ given above, but now in an active sense: $\hat{K}'(s)$ entangles degrees of freedom immediately at the correct scale $\mathrm{e}^{-s}\Lambda$ and there is no need for $\hat{L}$ to bring these freshly entangled degrees of freedom to the correct scale. The scale invariance of $|\Omega\rangle$ implies that degrees of freedom at all scales were identical before being entangled. When introducing new unentangled degrees of freedom, it does not matter from which scale they are coming since all scales are identical in $|\Omega\rangle$. We can then also write

$$|\Psi[\hat{K}]\rangle = |\Psi_{\mathrm{P}}(s_a)\rangle = \mathcal{S} \exp\left[-\mathrm{i}\int_{s_a}^{s_\xi} \hat{K}'(s)\,\mathrm{d}s\right]|\Omega\rangle\,, \tag{5.37}$$

and we can use this formulation as an alternative definition of the continuous entanglement renormalization ansatz. But as for the Wilsonian renormalization group, the additional scale transformations in the original definition of $|\Psi[\hat{K}]\rangle$ is better suited to detect a critical point, as indicated by $\hat{K}(s)$ developing a non-zero horizontal asymptote.

2.4. Entanglement and correlations

As for the multi-scale entanglement renormalization ansatz for lattice systems, it is easy to proof that the continuous entanglement renormalization ansatz supports algebraically decaying correlations and a logarithmic violation of the area law for $d = 1$ spatial dimension. Regarding the correlations, it is sufficient to look at state $|\Psi[\hat{K}]\rangle$ with $\hat{K}$ being s-independent and translation invariant. Let $\hat{O}^{(\alpha)}(\vec{x})$ and $\hat{O}^{(\alpha')}(\vec{x}')$ be two local scaling operators. The operator $\hat{C}^{(\alpha,\alpha')}(\vec{x},\vec{x}') = \hat{O}^{(\alpha)}(\vec{x})\hat{O}^{(\alpha')}(\vec{x}')$ that produces the correlation function as expectation value renormalizes as $\hat{C}_{\mathrm{R}}^{(\alpha,\alpha')}(\vec{x},\vec{x}';s) = \mathrm{e}^{s[\lambda^{(\alpha)}+\lambda^{(\alpha')}]}\hat{O}^{(\alpha)}(\mathrm{e}^{-s}\vec{x})\hat{O}^{(\beta)}(\mathrm{e}^{-s}\vec{x}')$ as long as $\mathrm{e}^{-s}|\vec{x}-\vec{x}'| \gg a = \Lambda^{-1}$. If for $\bar{s} \approx \log(|\vec{x}-\vec{x}'|\Lambda)$ we obtain $\langle\Psi_{\mathrm{R}}(\bar{s})|\hat{O}^{(\alpha)}(\mathrm{e}^{-\bar{s}}\vec{x})\hat{O}^{(\beta)}(\mathrm{e}^{-\bar{s}}\vec{x}')|\Psi_{\mathrm{R}}(\bar{s})\rangle = c$ then we can write

$$\langle\Psi[\hat{K}]|\hat{C}^{(\alpha,\alpha')}(\vec{x},\vec{x}')|\Psi[\hat{K}]\rangle \approx \mathrm{e}^{\bar{s}[\lambda^{(\alpha)}+\lambda^{(\alpha')}]}c \sim |\vec{x}-\vec{x}'|^{\lambda^{(\alpha)}+\lambda^{(\alpha')}}. \tag{5.38}$$

For computing the entanglement entropy of a spatial region $\mathscr{A}$, we can use the results regarding entanglement growth under quantum mechanical (time) evolution of Subsection 2.5 of Chapter 1. Using the variable $t = -s$ and the operator $\hat{K}'(s)$, we can define

$$|\Psi_{\tilde{\mathrm{P}}}(t)\rangle = \mathcal{T} \exp\left[-\mathrm{i}\int_{t_\xi}^{t} \hat{K}'(-t)\,\mathrm{d}t\right]|\Omega\rangle \tag{5.39}$$

so that $|\Psi_{\tilde{\mathrm{P}}}(t)\rangle = |\Psi_{\mathrm{P}}(-t)\rangle$. $\hat{K}'(-t)$ is a local Hamiltonian with momentum cutoff $\mathrm{e}^{t-t_a}\Lambda$. Clearly, the entanglement entropy of region $\mathscr{A}$ in $|\Omega\rangle$ is zero. The entanglement remains very small as long as $\mathrm{e}^{t_a-t}a \gg L$ with L the linear size of region $\mathscr{A}$. For these time scales, the region $\mathscr{A}$ is much smaller then the minimal region on which $\hat{K}'(-t)$ acts and very little entanglement is being created. Let now $\overline{t} \approx t_a - \log L/a = t_a - \log L\Lambda$ and let the entropy of region $\mathscr{A}$ in $|\Psi_{\tilde{\mathrm{P}}}(\overline{t})\rangle$ be given by some small constant k. In generalizing Eq. (1.75) to the continuum, we have to assume that we have to measure the boundary $|\partial\mathscr{A}|$ of region $\mathscr{A}$ in terms of the cutoff, so that we obtain

$$\frac{\mathrm{d}}{\mathrm{d}t}S^{(\mathscr{A})}(t) \leq c|\partial\mathscr{A}|(\Lambda\mathrm{e}^{t-t_a})^{d-1}, \tag{5.40}$$

and thus

$$S^{(\mathscr{A})} = S^{(\mathscr{A})}(t_a) \leq k + c\int_{\overline{t}}^{t_a} |\partial\mathscr{A}|\Lambda^{d-1}\mathrm{e}^{(t-t_a)(d-1)}\,\mathrm{d}t. \tag{5.41}$$

Hence, for $d = 1$ we recover

$$S^{(\mathscr{A})} \leq k + 2c\int_{\overline{t}}^{t_a} \mathrm{d}t = 2c\log L/a + k, \tag{5.42}$$

while for $d > 1$ we obtain

$$\begin{aligned} S^{(\mathscr{A})} &\leq k + c|\partial\mathscr{A}|\int_{\overline{t}}^{t_a} \Lambda^{d-1}\mathrm{e}^{(t-t_a)(d-1)}\,\mathrm{d}t \\ &= \frac{c}{d-1}|\partial\mathscr{A}|\Lambda^{d-1}\left[1 - \frac{1}{(L\Lambda)^{(d-1)}}\right] + k \sim |\partial\mathscr{A}|\Lambda^{d-1}. \end{aligned} \tag{5.43}$$

These results are of course no surprise. We can now define a continuous path or surface of points (x, s) for which the corresponding operators $\hat{k}(x, s)$ contributes to the generation of the entanglement of $\mathscr{A}$. This could then be contrasted to the minimal surfaces of Ryu and Takayanagi [Eq. (1.78) in Subsection 2.5 of Chapter 1], in order to establish a connection between the continuous entanglement renormalization ansatz and the holographic duality between anti-de Sitter space and conformal field theories.

2.5. Gauge invariance of the continuous entanglement renormalization ansatz

As for the Wilsonian renormalization group flow described in Subsection 3.3 of Chapter 1, there is a massive gauge invariance or reparameterization invariance in the entanglement renormalization scheme, since many different choices of $\hat{K}$ produce (for a fixed choice of $\hat{L}$) the same state $|\Psi[\hat{K}]\rangle$. This is also the case in the multi-scale entanglement renormalization ansatz for lattice systems, where we can act with a one-site unitary operator and its inverse on the legs of two tensors that are contracted in the tensor

network. For the continuous entanglement renormalization ansatz, we can define infinitesimal layers $\hat{U}(s, s+\mathrm{d}s) = \exp(-\mathrm{i}\mathrm{d}s[\hat{K}(s)+\hat{L}]) \approx \exp[-\mathrm{i}\mathrm{d}s\hat{K}(s)]\exp[-\mathrm{i}\mathrm{d}s\hat{L}]$ and insert between every two layers $\hat{U}(s-\mathrm{d}s, s)\hat{U}(s, s+\mathrm{d}s)$ a unitary gauge transformation $\hat{G}(s)$ and its inverse as $\hat{G}(s)\hat{G}^\dagger(s)$, where we absorb the first factor into $\hat{U}(s-\mathrm{d}s, s)$ and the second factor into $\hat{U}(s, s+\mathrm{d}s)$. We obtain invariance under the gauge transformation $\hat{U}(s, s+\mathrm{d}s) \leftarrow \hat{U}'(s, s+\mathrm{d}s)$ where

$$
\begin{aligned}
&\hat{U}'(s, s+\mathrm{d}s) \\
&\quad = \hat{G}(s)^\dagger \exp\left[-\mathrm{i}\mathrm{d}s\hat{K}(s)\right] \exp\left[-\mathrm{i}\mathrm{d}s\hat{L}\right] \hat{G}(s+\mathrm{d}s) \\
&\quad = \exp\left[-\mathrm{i}\mathrm{d}s\hat{G}(s)^\dagger\hat{K}(s)\hat{G}(s)\right] \hat{G}(s)^\dagger \mathrm{e}^{-\mathrm{i}\mathrm{d}s\hat{L}}\hat{G}(s+\mathrm{d}s)\mathrm{e}^{+\mathrm{i}\mathrm{d}s\hat{L}} \exp\left[-\mathrm{i}\mathrm{d}s\hat{L}\right] \\
&\quad = \exp\left[-\mathrm{i}\mathrm{d}s\hat{G}(s)^\dagger\hat{K}(s)\hat{G}(s)\right] \hat{G}(s)^\dagger \\
&\qquad\qquad \times \left\{\hat{G}(s) + \mathrm{d}s\frac{\mathrm{d}}{\mathrm{d}s}\hat{G}(s) - \mathrm{i}\mathrm{d}s\left[\hat{L}, \hat{G}(s)\right]\right\} \exp\left[-\mathrm{i}\mathrm{d}s\hat{L}\right] \\
&\quad = \exp\left[-\mathrm{i}\mathrm{d}s\left(\hat{G}(s)^\dagger\hat{K}(s)\hat{G}(s) + \mathrm{i}\hat{G}^\dagger\frac{\mathrm{d}}{\mathrm{d}s}\hat{G}(s) + \hat{G}(s)^\dagger\left[\hat{L}, \hat{G}(s)\right]\right)\right] \exp\left[-\mathrm{i}\mathrm{d}s\hat{L}\right].
\end{aligned}
$$

Hence, the continuous entanglement renormalization ansatz $|\Psi[\hat{K}]\rangle$ is invariant under a substitution of the variational parameters $\hat{K} \leftarrow \hat{K}'$, where the gauge transformed operator $\hat{K}'(s)$ is given by

$$
\begin{aligned}
\hat{K}'(s) &= \hat{G}(s)^\dagger\hat{K}(s)\hat{G}(s) + \mathrm{i}\hat{G}^\dagger\frac{\mathrm{d}}{\mathrm{d}s}\hat{G}(s) + \hat{G}(s)^\dagger\left[\hat{L}, \hat{G}(s)\right] \\
&= \hat{G}(s)^\dagger\hat{K}(s)\hat{G}(s) + \mathrm{i}\hat{G}^\dagger\frac{\mathrm{d}}{\mathrm{d}s}\hat{G}(s) + \hat{G}(s)^\dagger\hat{L}\hat{G}(s) - \hat{L}.
\end{aligned}
\tag{5.44}
$$

The gauge transformation $\hat{G}$ thus consists of an s-dependent unitary operator, where we require $\hat{G}(s_a) = \hat{\mathbb{1}}$. At s_ξ, we either need to accompany the gauge transformation by a transformation of the reference state as $|\Omega\rangle \leftarrow |\Omega'\rangle = \hat{G}(s_\xi)^\dagger|\Omega\rangle$, or we need to restrict to choices $\hat{G}(s_\xi)^\dagger$ that leave the reference state invariant. If $\hat{K}$ is translation invariant, then $\hat{G}$ should also be translation invariant to produce a translation invariant $\hat{K}'$. However, applying a translation non-invariant gauge transformation to a translation invariant choice $\hat{K}$ indicates that translation invariant states $|\Psi[\hat{K}]\rangle$ can be represented by a translation non-invariant choice $\hat{K}'$. The same argument applies to rotation invariance and other symmetries.

For critical theories, we expect that $\hat{K}(s)$ becomes s-independent after some transient regime, *i.e.* that $\hat{K}(s)$ develops a horizontal asymptote for $s \to +\infty$. Clearly, applying an s-dependent gauge transformation might transform this horizontal asymptote into a general s-dependent behavior with no converging limit. As for Wilson's renormalization scheme, we need to impose certain renormalization conditions that fix the gauge invariance in order to be able to detect the presence of a horizontal asymptote

$\lim_{s\to+\infty}\hat{K}(s)=\hat{K}\neq\hat{0}$ for critical theories.

Finally, we investigate the effect of an infinitesimal gauge transformation generated by $\hat{J}$ as $\hat{G}(s)=\exp[\mathrm{i}\eta\hat{J}(s)]$. We obtain for the corresponding transformation of $\hat{K}$:

$$\hat{K}'=\hat{K}+\eta\left(-\frac{\mathrm{d}}{\mathrm{d}s}\hat{J}(s)+\mathrm{i}\left[\hat{K}(s)+\hat{L},\hat{J}(s)\right]\right). \tag{5.45}$$

The shift in $\hat{K}$ for an infinitesimal gauge transformation is equal in form to the renormalization group flow equation for renormalized operators $\hat{O}_{\mathrm{R}}(s)$. This correspondence might be related to the correspondence between the Callan-Symanzik equation and the equations of motion for the bulk fields in the holographic renormalization scheme, and might thus provide another angle in which the equivalence between the continuous entanglement renormalization scheme and the AdS/CFT duality might be investigated.

3. Entanglement renormalization of free field theories

Let us now apply the continuous entanglement renormalization ansatz to free field theories —quadratic and translation-invariant theories— where we can hopefully compute everything analytically. Since the exact ground state is a Gaussian state, we can construct a Gaussian continuous entanglement renormalization ansatz where $\hat{K}$ contains only quadratic interactions. We show how this already illustrates many of the general claims and predictions of the previous section.

3.1. Scaling in momentum space

Since free theories can be solved exactly, we first determine the pure scaling case $\hat{K}(s)=0$ in momentum space. In real space, we can generalize Eq. (5.15) to learn that

$$\hat{\psi}_{\mathrm{R}}(\vec{x};s)=\mathrm{e}^{+\mathrm{i}(s-s_a)\hat{L}}\hat{\psi}(\vec{x})\mathrm{e}^{-\mathrm{i}(s-s_a)\hat{L}}=\mathrm{e}^{-(s-s_a)\frac{d}{2}}\hat{\psi}\left(\mathrm{e}^{-(s-s_a)}\vec{x}\right). \tag{5.46}$$

Defining momentum-space operators via

$$\hat{\Psi}(\vec{p})\triangleq\frac{1}{(2\pi)^{d/2}}\int_{-\infty}^{\infty}e^{-\mathrm{i}\vec{p}\cdot\vec{x}}\hat{\psi}(\vec{x})\,\mathrm{d}^dx, \tag{5.47}$$

we obtain

$$\hat{L}=\frac{\mathrm{i}}{2}\int\left\{\hat{\Psi}^\dagger(\vec{p})\left[\vec{p}\cdot\vec{\boldsymbol{\nabla}}\hat{\Psi}(\vec{p})\right]-\left[\vec{p}\cdot\vec{\boldsymbol{\nabla}}\hat{\Psi}^\dagger(\vec{p})\right]\hat{\Psi}(\vec{p})\right\}\mathrm{d}^dp \tag{5.48}$$

with $\vec{\blacktriangledown}$ the gradient operator in momentum space ($\vec{e}_\mu \cdot \vec{\blacktriangledown} = \partial\ /\partial\, p^\mu$, $\forall \mu = 1,\ldots,d$). This scaling operator automatically results in

$$\hat{\Psi}_{\mathrm{R}}(\vec{p};s) = e^{(s-s_a)\frac{d}{2}}\hat{\Psi}(e^{s-s_a}\vec{p}). \tag{5.49}$$

Note that in the pure scaling case, $\hat{K}(s) = 0$ also implies $\hat{K}'(s) = 0$ so that $\hat{\psi}_{\mathrm{P}}(\vec{x};s) = \hat{\psi}(\vec{x})$ and $\hat{\Psi}_{\mathrm{P}}(\vec{p};s) = \hat{\Psi}(\vec{p})$.

3.2. Gaussian continuous entanglement renormalization ansatz

A Gaussian continuous entanglement renormalization ansatz can be defined as being generated by a choice of $\hat{K}(s)$ that is quadratic in the field operators. A quadratic choice of $\hat{K}(s)$ only generates a Gaussian state if the unitary circuit $\hat{U}(s_a, s_\xi)$ acts on a Gaussian reference state $|\Omega\rangle$. The reference vacuum $|\Omega\rangle$ should in principle not contain any variational degrees of freedom, as any local unitary that would transform $|\Omega\rangle$ to a better reference state could also be absorbed into the unitary quantum circuit $\hat{U}(s_a, s_\xi)$. Nevertheless, it is sometimes beneficial to allow some degree of variational freedom in $|\Omega\rangle$. For the non-relativistic examples in the next subsection, we fix $|\Omega\rangle$ to the vacuum of the annihilation operators $\hat{\psi}(\vec{x})$.

Since free field theories can be solved by an appropriate Bogoliubov transformation in momentum space, it is sufficient to investigate states $|\Psi[\hat{K}]\rangle$ that can be prepared with an operator $\hat{K}(s)$ that generates Bogoliubov transformations. We define

$$\hat{K}(s) = \frac{\mathrm{i}}{2}\int \left[G(\vec{p};s)\hat{\Psi}^\dagger(\vec{p})\hat{\Psi}^\dagger(-\vec{p}) - \overline{G(\vec{p};s)}\hat{\Psi}(-\vec{p})\hat{\Psi}(\vec{p})\right] \mathrm{d}^d\, p. \tag{5.50}$$

Since $\hat{\Psi}^\dagger(\vec{p})\hat{\Psi}^\dagger(-\vec{p})$ is even (odd) in the argument $\vec{p}$ for bosons (fermions), we can without loss of generalization impose that $G(\vec{p};s)$ is even (odd) in the argument $\vec{p}$, since the odd (even) part cancels anyway. In order to end up with a strictly local operator, $G(\vec{p};s)$ should be polynomial in the argument $\vec{p}$. Since the scale variable s is dimensionless, $\hat{K}(s)$ should be as well. Hence, the function $G(\vec{p};s)$ should be dimensionless, which can be realized by using the yet-to-be introduced ultraviolet cutoff length scale a, or the momentum cutoff $\Lambda = a^{-1}$. We thus define

$$G(\vec{p};s) = g(\vec{p}/\Lambda, s) = \gamma(\vec{p}/\Lambda, s)r(||\vec{p}||/\Lambda) \tag{5.51}$$

where $\gamma(\vec{p}/\Lambda, s)$ is an even or odd polynomial in its first argument, with the s-dependent coefficients acting as the variational parameters, and where $r(\kappa)$ is a fixed cutoff function with natural cutoff 1, such as the normal distribution

$$r(\kappa) = \exp(-\kappa^2). \tag{5.52}$$

Note that any cutoff function adds a non-polynomial contribution to $g(\vec{p}/\Lambda, s)$, so that

$\hat{K}(s)$ is only local up to $\mathcal{O}(a)$. If $g(\vec{p}/\Lambda, s)$ were a pure polynomial then $\hat{K}(s)$ would be strictly local but would act nontrivially on all momenta $\vec{p}$ and would not exhibit any cutoff behavior. We can, equivalently, interpret $\hat{K}(s)$ as a strictly local combination (polynomial in $\vec{p}$)

$$\hat{K}(s) = \frac{\mathrm{i}}{2}\int \left[\gamma(\vec{p}/\Lambda, s)\hat{\Psi}_r^\dagger(\vec{p})\hat{\Psi}_r^\dagger(-\vec{p}) - \overline{\gamma(\vec{p}/\Lambda, s)}\hat{\Psi}_r(-\vec{p})\hat{\Psi}_r(\vec{p})\right] \mathrm{d}^d p \tag{5.53}$$

of regularized or smoothed operators $\hat{\psi}_r(\vec{x})$ given by

$$\hat{\psi}_r(\vec{p}) = \frac{1}{\sqrt{2\pi}a}\int \hat{\psi}(\vec{x}')\exp\left(-\frac{||\vec{x}-\vec{x}'||^2}{2a^2}\right)\mathrm{d}^d x' \;\leftrightarrow\; \hat{\Psi}_r(\vec{p}) = \hat{\Psi}(\vec{p})\exp\left(-\frac{||\vec{p}||^2}{2\Lambda^2}\right).$$

For the remainder of this section, it is easier to combine the polynomial $\gamma(\vec{p}/\Lambda, s)$ and the cutoff function $r(||\vec{p}/\Lambda||)$ into a single function $g(\vec{p}/\Lambda, s)$ than to work with smoothed operators. Note finally that for a Hamiltonian with real coefficients with respect to the real-space operators $\hat{\Psi}(\vec{x})$ and $\hat{\Psi}^\dagger(\vec{x})$, it should be possible to choose $\exp(\mathrm{i}\hat{K}(s))$ such that it is real when expressed in terms of the operators $\hat{\Psi}(\vec{x})$ and $\hat{\Psi}^\dagger(\vec{x})$. This requires that $\mathrm{i}\hat{K}(s)$ has real coefficients with respect to the real-space operators. For bosons, $g(\vec{p}/\Lambda, s)$ is even in $\vec{p}$ and should be chosen real. For fermions, $g(\vec{p}/\Lambda, s)$ is odd in $\vec{p}$ and should be chosen imaginary.

Bosons

Let's warm up by integrating the renormalization group equation [Eq. (5.25)] for the field operators when we have an s-independent operator $\hat{K}$ with $g(\vec{p}/\Lambda, s) = \varphi(\vec{p}/\Lambda)$ (with φ an even complex-valued function) while temporarily ignoring the scaling, *i.e.* setting $\hat{L} = 0$. We choose the convenient definition $s_a = 0$. Since $\hat{K} = \mathrm{e}^{\mathrm{i}\hat{K}s}\hat{K}\mathrm{e}^{-\mathrm{i}\hat{K}s}$, so that

$$\hat{K} = \frac{\mathrm{i}}{2}\int \left[\varphi(\vec{p}/\Lambda, s)\hat{\Psi}_{\mathrm{R}}^\dagger(\vec{p}; s)\hat{\Psi}_{\mathrm{R}}^\dagger(-\vec{p}; s) - \overline{\varphi(\vec{p}/\Lambda, s)}\hat{\Psi}_{\mathrm{R}}(-\vec{p}; s)\hat{\Psi}_{\mathrm{R}}(\vec{p}; s)\right] \mathrm{d}^d p \tag{5.54}$$

with $\hat{\Psi}_{\mathrm{R}}(\vec{p}; s) = \mathrm{e}^{\mathrm{i}\hat{K}s}\hat{\Psi}(\vec{p})\mathrm{e}^{-\mathrm{i}\hat{K}s}$, we obtain

$$\frac{\partial}{\partial s}\hat{\Psi}_{\mathrm{R}}(\vec{p}; s) = \varphi(\vec{p}/\Lambda)\hat{\Psi}_{\mathrm{R}}^\dagger(-\vec{p}; s), \quad \text{and} \quad \frac{\partial}{\partial s}\hat{\Psi}_{\mathrm{R}}^\dagger(\vec{p}; s) = \overline{\varphi(\vec{p}/\Lambda)}\hat{\Psi}_{\mathrm{R}}(-\vec{p}; s), \tag{5.55}$$

which can be integrated ($\forall s > 0$) as

$$\hat{\Psi}_{\mathrm{R}}(\vec{p}; s) = \cosh(|\varphi(\vec{p}/\Lambda)|s)\hat{\Psi}(\vec{p}) + \frac{\varphi(\vec{p}/\Lambda)}{|\varphi(\vec{p}/\Lambda)|}\sinh(|\varphi(\vec{p}/\Lambda)|s)\hat{\Psi}^\dagger(-\vec{p}), \tag{5.56}$$

and its hermitian conjugate. Without the scaling transformation the evolution under $\hat{K}$ does not approach a limit when s grows to $+\infty$.

If we now assume that $g(\vec{p};s)$ is a real-valued function and include the scaling, we can put forward as general solution for the renormalization group flow of the field operators:

$$\hat{\Psi}_{\mathrm{R}}(\vec{p};s) = \cosh\left(f(\vec{p};s)\right) e^{s\frac{d}{2}} \hat{\Psi}(e^s\vec{p}) + \sinh\left(f(\vec{p};s)\right) e^{s\frac{d}{2}} \hat{\Psi}^\dagger(-e^s\vec{p}), \tag{5.57}$$

and Hermitian conjugate, where the Bogoliubov angle $f(\vec{p};s)$ should be even in $\vec{p}$. Substituting this expression into the renormalization group flow equation [Eq. (5.25)], we obtain

$$\frac{\partial}{\partial s}\hat{\Psi}_{\mathrm{R}}(\vec{p};s) - \mathrm{i}\left[\hat{L},\hat{\Psi}_{\mathrm{R}}(\vec{p};s)\right] = \frac{\partial f(\vec{p};s)}{\partial s}\left[\sinh\left(f(\vec{p};s)\right) e^{s\frac{d}{2}} \hat{\Psi}(e^s\vec{p}) + \cosh\left(f(\vec{p};s)\right) e^{s\frac{d}{2}} \hat{\Psi}^\dagger(-e^s\vec{p})\right],$$

which should equal

$$\mathrm{i}\left[\hat{K}(s),\hat{\Psi}_{\mathrm{R}}(\vec{p};s)\right] = g(e^s\vec{p};s)\left[\sinh\left(f(\vec{p};s)\right) e^{s\frac{d}{2}} \hat{\Psi}(e^s\vec{p}) + \cosh\left(f(\vec{p};s)\right) e^{s\frac{d}{2}} \hat{\Psi}^\dagger(-e^s\vec{p})\right].$$

We thus find

$$f(\vec{p};s) = \int_0^s g(e^w\vec{p}/\Lambda, w)\,\mathrm{d}w \tag{5.58}$$

where we've used the initial value condition $f(\vec{p},0) = 0$. At the level s_ξ of evaluation, the Bogoliubov angle $f(\vec{p})$ is given by $f(\vec{p};s_\xi)$. We can always take $s_\xi = +\infty$ for both critical and non-critical systems. In non-critical systems, $g(\vec{p}/\Lambda,s)$ automatically goes to zero for $s \gg \mathcal{O}(\log(\xi_c/a)) = \mathcal{O}(\log(\xi_c\Lambda))$. Because $g(\vec{p}/\Lambda,s)$ is expected to decay rapidly when the norm of its first argument $|\vec{p}/\Lambda|$ grows beyond one, the Bogoliubov angle will be very small for all $||\vec{p}|| > \Lambda$. For all $||\vec{p}|| < \Lambda$, it will be determined by the value of g at scales $0 \leq s \lesssim \mathcal{O}(\log||\vec{p}||/\Lambda)$ and the integral converges for all $\vec{p}$ with $||\vec{p}|| > 0$. At zero momentum, we find

$$f(\vec{0}) = \int_0^{+\infty} g(\vec{0},w)\,\mathrm{d}w \tag{5.59}$$

and the convergence of this integral depends on the choice of $g(\vec{0},s)$.

Fermions

We study an analogous choice for $\hat{K}$ in the fermionic case. If we once again start with an s-independent operator $\hat{K}$ (thus $g(\vec{p}/\Lambda,s) = \varphi(\vec{p}/\Lambda)$ with φ now a complex-

valued odd function) and temporarily ignore the scaling, *i.e.* we set $\hat{L}=0$, we obtain an renormalization group equation [Eq. (5.25)] for the field operators

$$\frac{\partial}{\partial s}\hat{\Psi}_{\mathrm{R}}(\vec{p};s)=\varphi(\vec{p}/\Lambda)\hat{\Psi}^{\dagger}_{\mathrm{R}}(-\vec{p};s),\quad\text{and}\quad\frac{\partial}{\partial s}\hat{\Psi}^{\dagger}_{\mathrm{R}}(\vec{p};s)=\overline{\varphi(\vec{p}/\Lambda)}\hat{\Psi}_{\mathrm{R}}(-\vec{p};s),\tag{5.60}$$

which can be integrated ($\forall s>0$) to produce

$$\hat{\Psi}_{\mathrm{R}}(\vec{p};s)=\cos\left(|\varphi(\vec{p}/\Lambda)|s\right)\hat{\Psi}(\vec{p})+\frac{\varphi(\vec{p}/\Lambda)}{|\varphi(\vec{p}/\Lambda)|}\sin\left(|\varphi(\vec{p}/\Lambda)|s\right)\hat{\Psi}^{\dagger}(-\vec{p}),\tag{5.61}$$

and its hermitian conjugate. We now turn back to the general case, were we assume that $g(k,s)$ is a real-valued function and reintroduce the scaling. We put forward the following general solution of the renormalization group flow equation

$$\hat{\Psi}_{\mathrm{R}}(\vec{p};s)=\cos\left(f(\vec{p};s)\right)e^{s\frac{d}{2}}\hat{\Psi}(e^{s}\vec{p})+\sin\left(f(\vec{p};s)\right)e^{s\frac{d}{2}}\hat{\Psi}^{\dagger}(-e^{s}\vec{p}),\tag{5.62}$$

and complex conjugate, where the Bogoliubov angle $f(\vec{p};s)$ should now be odd in $\vec{p}$. Substituting this expression into the renormalization group equation, we obtain

$$\frac{\partial}{\partial s}\hat{\Psi}_{\mathrm{R}}(\vec{p};s)-\mathrm{i}\left[\hat{L},\hat{\Psi}_{\mathrm{R}}(\vec{p};s)\right]=\\ \frac{\partial f(\vec{p};s)}{\partial s}\left[-\sin\left(f(\vec{p};s)\right)e^{s\frac{d}{2}}\hat{\Psi}(e^{s}\vec{p})+\cos\left(f(\vec{p};s)\right)e^{s\frac{d}{2}}\hat{\psi}^{\dagger}(-e^{s}\vec{p})\right],$$

which should equal

$$\mathrm{i}\left[\hat{K}(s),\hat{\Psi}_{\mathrm{R}}(\vec{p};s)\right]=\\ g(e^{s}\vec{p};s)\left[-\sin\left(f(\vec{p};s)\right)e^{-s\frac{d}{2}}\hat{\Psi}(e^{s}\vec{p})+\cos\left(f(\vec{p};s)\right)e^{-s\frac{s}{2}}\hat{\Psi}^{\dagger}(-e^{s}\vec{p})\right].$$

We thus find

$$f(\vec{p};s)=\int_{0}^{s}g(e^{w}\vec{p}/\Lambda,w)\,\mathrm{d}w\tag{5.63}$$

where we have used the initial value condition $f(\vec{p},0)=0$. Similar considerations as for bosons apply. Note that, because $g(\vec{p}/\Lambda,s)$ is odd in its first argument, we must have $g(\vec{0},s)=0$ and $f(\vec{0},s)=0$ and thus

$$f(\vec{0})=\lim_{s_{\xi}\to+\infty}f(\vec{0},s)=0.\tag{5.64}$$

The order of the limits is of course important, and it could just as well be that

$$f(\vec{0})=\lim_{|\vec{p}|\to 0}f(\vec{p})\neq 0.\tag{5.65}$$

Since $f(\vec{p})$ is an odd function, this limit does not exist (*i.e.* is direction-dependent) if it is not zero.

3.3. Example 1: applying the variational principle to a non-relativistic boson system

Here we apply the variational principle to the Gaussian continuous entanglement renormalization ansatz as introduced in the previous subsection. We use the parameterization

$$g(\vec{p}/\Lambda, s) = \gamma(\vec{p}/\Lambda, s) r(|\vec{p}/\Lambda|) \tag{5.66}$$

with $\gamma(\vec{p}/\Lambda, s)$ an even (respectively, odd) polynomial in the first argument for bosons (respectively, fermions) with s-dependent coefficients that constitute the set of variational parameters and $r(\kappa)$ is a fixed function that is cut off beyond $\kappa > 1$. As we show in the example below, we can already obtain quite accurate results by terminating $\gamma(\vec{p}; s)$ at the lowest order in $\vec{p}$. For the bosonic model, this boils down to choosing $\gamma(\vec{p}; s) = \chi(s)$. The resulting Bogoliubov angle $f(\vec{p}) = \lim_{s_\xi \to \infty} f(\vec{p}; s_\xi)$ can acquire an arbitrary $\vec{p}$-dependence thanks to s-dependence of $\chi(s)$ and the presence of a cutoff. Note that the energy expectation value $E = \langle \Psi[\hat{K}] | \hat{H} | \Psi[\hat{K}] \rangle = \langle \Omega | \hat{H}_{\mathrm{R}}(s_\xi) | \Omega \rangle$ is a *functional* of the variational parameters. The variational method thus boils down to choosing $\chi(s)$ such that the *functional derivative* of $E[\chi]$ with respect to $\chi(s)$ is zero:

$$\frac{\delta}{\delta \chi(s)} E[\chi] = 0. \tag{5.67}$$

Many non-relativistic models are naturally described with creation and annihilation operators $\psi^\dagger(x)$ and $\psi(x)$. Since most non-relativistic models are characterized by a finite density of particles, the exact ground state $|\Psi\rangle$ will typically not contain particles with very large momenta, i.e. $\hat{\Psi}(\vec{p})|\Psi\rangle \approx 0$ for $|\vec{p}|$ sufficiently large. If we choose $|\Omega\rangle$ as the vacuum annihilated by all annihilation operators ($\hat{\psi}(\vec{x})|\Omega\rangle = 0$, so that $\hat{\Psi}(\vec{p})|\Omega\rangle = 0$), then all particles in the resulting Gaussian entanglement renormalization ansatz $|\Psi[\hat{K}]\rangle$ are created by $\hat{K}$ and live below the ultraviolet momentum cutoff Λ. We now study a Gaussian model of non-relativistic bosons, governed by the Hamiltonian

$$\hat{H}(\mu, \nu) = \int \left[\left(\vec{\nabla} \hat{\psi}^\dagger(\vec{x}) \right) \cdot \left(\vec{\nabla} \hat{\psi}(\vec{x}) \right) + \mu \hat{\psi}^\dagger(\vec{x}) \hat{\psi}(\vec{x}) - \nu \left(\hat{\psi}^\dagger(\vec{x})^2 + \hat{\psi}(\vec{x})^2 \right) \right] \mathrm{d}^d x, \tag{5.68}$$

where $0 \leq 2\nu \leq \mu$ is required for this model to be well defined. In terms of the momentum space operators $\hat{\Psi}(\vec{p})$, the Hamiltonian is given as

$$\hat{H}(\mu, \nu) = \int \left[\left(||\vec{p}||^2 + \mu \right) \hat{\Psi}^\dagger(\vec{p}) \hat{\Psi}(\vec{p}) - \nu \left(\hat{\Psi}^\dagger(\vec{p}) \hat{\Psi}^\dagger(-\vec{p}) + \hat{\Psi}(\vec{p}) \hat{\Psi}(-\vec{p}) \right) \right] \mathrm{d}^d p. \tag{5.69}$$

This model is the d-dimensional generalization of the one-dimensional model to which the continuous matrix product state ansatz was applied in the previous chapter. It is solved by a Bogoliubov transformation with the exact Bogoliubov angle

$$f_{\text{exact}}(\vec{p}) = \frac{1}{2}\operatorname{arctanh}\left(\frac{2\nu}{||\vec{p}||^2+\mu}\right). \tag{5.70}$$

As for the one-dimensional model, the momentum space density $\langle\Psi|\hat{\Psi}^\dagger(\vec{p})\hat{\Psi}(\vec{p})|\Psi\rangle$ goes as $4\nu^2/||\vec{p}||^4$ for large $||\vec{p}||$, so that we can interpret $\sqrt{2\nu}$ as the ultraviolet momentum cutoff. The energy gap is given by $\sqrt{\mu^2-4\nu^2}$, which explains the requirement $\mu \geq 2\nu$. At $\mu = 2\nu$, the correlation length diverges and the model becomes critical. There is no real quantum phase transition since the Hamiltonian is ill-defined for $\mu < 2\nu$.

In order to study this model using the Gaussian continuous entanglement renormalization ansatz $|\Psi[\hat{K}]\rangle$, we first compute the renormalized Hamiltonian $\hat{H}_{\text{R}}(s)$; the integrand becomes

$$\begin{aligned}
e^s(||\vec{p}||^2+\mu)&\left(\cosh[f(\vec{p};s)]\hat{\Psi}^\dagger(e^s\vec{p})+\sinh[f(\vec{p};s)]\hat{\Psi}(-e^s\vec{p})\right)\\
&\qquad\times\left(\cosh[f(\vec{p};s)]\hat{\Psi}(e^s\vec{p})+\sinh[f(\vec{p};s)]\hat{\Psi}^\dagger(-e^s\vec{p})\right)\\
-e^s\nu\Big\{&\left(\cosh[f(\vec{p};s)]\hat{\Psi}^\dagger(e^s\vec{p})+\sinh[f(\vec{p};s)]\hat{\Psi}(-e^s\vec{p})\right)\\
&\qquad\times\left(\cosh[f(\vec{p};s)]\hat{\Psi}^\dagger(-e^s\vec{p})+\sinh[f(\vec{p};s)]\hat{\Psi}(e^s\vec{p})\right)\\
&\quad+\left(\cosh[f(\vec{p};s)]\hat{\Psi}(e^s\vec{p})+\sinh[f(\vec{p};s)]\hat{\Psi}^\dagger(-e^s\vec{p})\right)\\
&\qquad\times\left(\cosh[f(\vec{p};s)]\hat{\Psi}(-e^s\vec{p})+\sinh[f(\vec{p};s)]\hat{\Psi}^\dagger(e^s\vec{p})\right)\Big\}.
\end{aligned}$$

The energy expectation value $E[\chi] = \langle\Omega|\hat{H}_{\text{R}}(s_\xi)|\Omega\rangle$ is thus given by

$$E[\chi] = e^{s_\xi}\int \delta(e^{s_\xi}\vec{p}-e^{s_\xi}\vec{p})\left[(\vec{p}^2+\mu)\sinh[f(\vec{p})]^2-2\nu\sinh[f(\vec{p})]\cosh[f(\vec{p})]\right]\mathrm{d}^d p, \tag{5.71}$$

with $f(\vec{p}) = f(\vec{p};s_\xi)$ and where $e^s\delta(e^s\vec{p}-e^s\vec{p}) = \delta(\vec{0}) = |\mathscr{R}|/(2\pi)^d = |\mathbb{R}|^d/(2\pi)^d$ gives the familiar volume factor, as energy is an extensive quantity. This illustrates a first property: our ansatz is clearly extensive. We define the energy density as

$$e[\chi] = \frac{1}{(2\pi)^d}\int\left[(||\vec{p}||^2+\mu)\sinh[f(\vec{p})]^2-2\nu\sinh[f(\vec{p})]\cosh[f(\vec{p})]\right]\mathrm{d}^d p. \tag{5.72}$$

We apply the variational principle by demanding the stationarity of $e[\chi]$ under variations in $\chi(s)$. Note that from Eq. (5.58) we obtain the functional derivative

$$\frac{\delta f(k)}{\delta\chi(s)} = r(e^s||\vec{p}||/\Lambda), \tag{5.73}$$

so the chain rule gives us ($\forall s \in [0, +\infty)$)

$$\frac{\delta e[\chi]}{\delta \chi(s)} = \int \frac{\mathrm{d}^d p}{(2\pi)^d} \left\{ (||\vec{p}||^2 + \mu) \sinh[2f(\vec{p})] - 2\nu \cosh[2f(\vec{p})] \right\} r(e^s ||\vec{p}||/\Lambda) = 0. \tag{5.74}$$

Since the integrand is an even function in k, this is a highly non-trivial relation that fixes $\chi(s)$ completely. Eq. (5.74) illustrates a second property of the continuous entanglement renormalization ansatz. The variation of the ground state energy (density) with respect to the variational parameter $\chi(s)$ at scale s contains all contributions to the energy coming from modes with $||\vec{p}|| < e^{-s}\Lambda$. The variational optimization with respect to $\chi(s)$ is thus not influenced by the dominating energy contributions from modes at higher momentum scale. Whereas the variational optimization with respect to other variational classes is usually dominated by these modes, the entanglement renormalization ansatz (both for the continuum and for the lattice) allows for a clear separation of scales and thus a way to overcome Feynman's "sensitivity to high frequencies" (see Subection 4.2 of Chapter 2). While this is of course always possible for free theories, we expect the same result to hold for interacting models with the general (*i.e.* non-Gaussian) continuous entanglement renormalization ansatz. If the cutoff is correctly implemented (*e.g.* through smoothed field operators), interaction terms contain a higher power of the field operators, and are more strongly suppressed in the scaling process.

In order to proceed, it is useful to choose $r(\kappa) = \theta(1 - |\kappa|)$, with θ the Heaviside step function. While this results in a highly non-local operator in real space, it allows an easy solution of the integral equations. Better behaved cutoff functions produce similar results, but require the solution of a more difficult set of integral equations. With the sharp cutoff, Eq. (5.74) tells us that the argument should be zero for all $||\vec{p}|| \leq \Lambda$. We thus need to reproduce the exact Bogoliubov angle $f(\vec{p}) = f_{\text{exact}}(\vec{p})$ from Eq. (5.70) up to the momentum cutoff $||\vec{p}|| \leq \Lambda$. Indeed, we can write ($\forall s \in [0, +\infty)$)

$$\frac{\delta e[\chi]}{\delta \chi(s)} = \int_0^{\mathrm{e}^{-s}\Lambda} \frac{2p^{d-1}\,\mathrm{d}p}{(4\pi)^{\frac{d}{2}}\Gamma(d/2)} \left\{ (p^2 + \mu) \sinh[2\tilde{f}(p)] - 2\nu \cosh[2\tilde{f}(p)] \right\} = 0. \tag{5.75}$$

where we have used that $f(\vec{p}) = \tilde{f}(||\vec{p}||)$. Differentiating with respect to s does indeed result in

$$\tilde{f}(p) = \frac{1}{2} \operatorname{arctanh} \left[\frac{2\nu}{p^2 + \mu} \right] \theta(\Lambda - p). \tag{5.76}$$

Since

$$f(\vec{p}) = \tilde{f}(||\vec{p}||) = \int_0^{+\infty} \chi(s)\theta(1 - \mathrm{e}^s ||\vec{p}||/\Lambda)\,\mathrm{d}s = \int_0^{\log(\Lambda/||\vec{p}||)} \chi(s)\,\mathrm{d}s \tag{5.77}$$

we can differentiate with respect to $|\vec{p}|$ in order to obtain

$$\begin{aligned}\chi(s) &= \frac{2(\nu/\Lambda^2)e^{-2s}}{(e^{-2s}+\mu/\Lambda^2)^2-4(\nu/\Lambda^2)^2}+\frac{1}{2}\operatorname{arctanh}\left[\frac{2\nu/\Lambda^2}{1+\mu/\Lambda^2}\right]\delta(s)\\ &= \frac{2\nu/\Lambda^2}{(e^{-2s}+[\mu^2/\Lambda^4-4\nu^2/\Lambda^4]e^{+2s})+2\mu/\Lambda^2}+\frac{1}{2}\operatorname{arctanh}\left[\frac{2\nu/\Lambda^2}{1+\mu/\Lambda^2}\right]\delta(s).\end{aligned} \tag{5.78}$$

This expression has been rewritten in terms of the dimensionless variables μ/Λ^2 and ν/Λ^2. It contains a singular contribution at $s=0$. Since $f(\vec{p})=0$ for $||\vec{p}||>\Lambda$, while the exact Bogoliubov angle f_{exact} becomes only exactly zero at infinite momentum, this δ-peak acts so as to immediately eliminate the error for $||\vec{p}||=\Lambda$. However, for $||\vec{p}||^2 \gg \mu$, the exact angle $f_{\text{exact}}(\vec{p})$ approaches zero very quickly (namely as $\mathcal{O}(\nu/||\vec{p}||^2)$), and so does the amplitude of the δ contribution. By choosing $\Lambda^2 \gg \mathcal{O}(\mu) \approx \mathcal{O}(\nu)$, the second part can be ignored, resulting in an error $|f(\vec{p})-f_{\text{exact}}(\vec{p})| < \mathcal{O}(\mu/\Lambda^2)$. If we were to further increase Λ, the deepest layers of the continuous entanglement renormalization ansatz between the value s for which $\Lambda^2 e^{-2s} \approx \mathcal{O}(\mu)$ and $s=s_a=0$ would have little effect as $\hat{K}(s)\approx 0$. Non-relativistic systems do indeed possess a natural cut off at momenta $||\vec{p}||$ much larger then the particle density.

Note that the distribution $\chi(s)$ is peaked at $s=\frac{1}{2}\log[\Lambda^2/\Delta]$, where $\Delta=(\mu^2-4\nu^2)^{1/2}$ represents the energy gap of the system. In a non-relativistic system, the gap scales as the square of the momentum scale. The disentangling strength $\chi(s)$ thus increases up to the scale s for which $\Delta = e^{-2s}\Lambda^2$, and then decreases to a horizontal asymptote $\chi(s)=0$ for $s\to+\infty$. Thus, $\chi(s)\approx 0$ for $s \gg \log(\Lambda^2/\Delta)+\mathcal{O}(\log(\Lambda^2/\mu))$ and so we can safely stop the integration of the renormalization group flow at a scale $s=s_\xi$ satisfying this relation. As $2\nu\to\mu$ the distribution never reaches its peak, but rather develops a nonzero horizontal asymptote: $\lim_{s\to+\infty}\chi(s)=1/2$. For $4\nu\to\mu$ the system becomes critical and we need to integrate all the way up to $s_\xi\to+\infty$ in order to obtain a correct description of the infinite range of fluctuations existing in the system. Hence, the expected behavior regarding gapped and critical phases is recovered automatically by applying the variational principle. At criticality, neither the state $|\Psi[\hat{K}]\rangle$ nor the exact ground state $|\Psi\rangle$ are scale invariant: non-relativistic ground states have a finite density of particles. True scale invariance is only possible when the ultraviolet cutoff $\Lambda\to+\infty$. However, the appearance of a horizontal asymptote indicates that the system effectively becomes scale invariant far up in the renormalization group flow, if we have moved far away from the cutoff region that was set by the finite density of particles.

For the s-independent horizontal asymptote $\chi=1/2$, we obtain

$$\begin{aligned}\mathrm{i}[\hat{K}+\hat{L},\hat{\Psi}(\vec{p})] &= \frac{1}{2}\hat{\Psi}^\dagger(-\vec{p})\theta(\Lambda-||\vec{p}||)+\frac{d}{2}\hat{\Psi}(\vec{p})+\vec{p}\cdot\vec{\nabla}\hat{\Psi}(\vec{p}),\\ \mathrm{i}[\hat{K}+\hat{L},\hat{\Psi}^\dagger(\vec{p})] &= \frac{1}{2}\hat{\Psi}(-\vec{p})\theta(\Lambda-||\vec{p}||)+\frac{d}{2}\hat{\Psi}^\dagger(\vec{p})+\vec{p}\cdot\vec{\nabla}\hat{\Psi}^\dagger(\vec{p}).\end{aligned}$$

Below the cutoff $||\vec{p}|| < \Lambda$, we can thus create scaling operators

$$\hat{\phi}(\vec{p}) \sim (\hat{\Psi}(\vec{p}) + \hat{\Psi}^\dagger(-\vec{p})) \quad \Rightarrow \quad \mathrm{i}[\hat{K} + \hat{L}, \hat{\phi}(\vec{p})] = -\frac{-d-1}{2}\hat{\phi}(\vec{p}) + \vec{p}\cdot\vec{\nabla}\hat{\phi}(\vec{p}), \quad (5.79)$$

$$\hat{\pi}(\vec{p}) \sim \mathrm{i}(\hat{\Psi}(\vec{p}) - \hat{\Psi}^\dagger(-\vec{p})) \quad \Rightarrow \quad \mathrm{i}[\hat{K} + \hat{L}, \hat{\pi}(\vec{p})] = -\frac{-d+1}{2}\hat{\pi}(\vec{p}) + \vec{p}\cdot\vec{\nabla}\hat{\pi}(\vec{p}), \quad (5.80)$$

with scaling dimension $(-d-1)/2$ for $\hat{\phi}(\vec{p})$ and $(-d+1)/2$ for $\hat{\pi}(\vec{p})$. Correspondingly, the real space fields $\hat{\phi}(\vec{x})$ and $\hat{\pi}(\vec{x})$ have scaling dimensions $(d-1)/2$ and $(d+1)/2$ respectively, and can be recognized as the field operator and the canonical momentum of the (uncharged) Klein-Gordon model. Hence, the low-energy behavior of $\hat{H}(\mu, \nu)$ in the critical limit $\mu = 2\nu$ is described by the massless Klein-Gordon model in d spatial dimensions. Slightly away from criticality, we can expect that the low-energy behavior corresponds to a massive Klein-Gordon theory. We return to this in Section 3 of Chapter 6.

3.4. Example 2: entanglement renormalization and non-relativistic fermions

Let us now study the most simple fermionic system, described by the Hamiltonian

$$\hat{H}(\mu) = \int \left[\left(\vec{\nabla}\hat{\psi}^\dagger(\vec{x})\right) \cdot \left(\vec{\nabla}\hat{\psi}(\vec{x})\right) - \mu\hat{\psi}^\dagger(\vec{x})\hat{\psi}(\vec{x}) \right] \mathrm{d}^d x. \quad (5.81)$$

This model is solved by filling the momentum levels up to the Fermi momentum $p_\mathrm{F} = \sqrt{\mu}$ (in these units where $2m = 1$). In terms of the Bogoliubov transformation, we have $f_\mathrm{exact}(\vec{p}) = \frac{\pi}{2}\theta(p_\mathrm{F} - ||\vec{p}||)$. We already detect a problem, since our Gaussian continuous entanglement renormalization ansatz was only able to produce Boguliubov angles $f(\vec{p})$ that are odd in the argument $\vec{p}$ for fermionic systems. We could immediately have known that this would be problematic, since we cannot construct a rotation-invariant function $f(\vec{p})$ that is odd in $\vec{p}$. Indeed, the continuous entanglement renormalization ansatz $|\Psi[\hat{K}]\rangle$ with a local operator $\hat{K}$ cannot describe such free fermion systems, since it does not support the logarithmic violation of the entropic area law exhibited by these systems, except for $d = 1$. Note that the argument based on rotation invariance is no longer valid for relativistic systems, where different fermion species (different Dirac indices) are present and a wider range of operators $\hat{K}(s)$ can be constructed that are rotation invariant. Correspondingly, the ground state of the relativistic free fermion model (Dirac fermions) does not violate the area law for entanglement entropy (except for $d = 1$ in case of massless fermions). This is discussed in the next chapter.

Let us now first analyze the non-relativistic free fermion model for the case of $d = 1$ spatial dimension, where a logarithmic violation is a general feature of the continuous entanglement renormalization ansatz when $\hat{K}(s)$ develops a non-zero horizontal asymptote

for $s \to +\infty$. We use a simple form of $\hat{K}$, namely

$$\hat{K}(s) = \frac{\mathrm{i}}{2}\int_{-\infty}^{+\infty} \chi(s)\left(\frac{p}{\Lambda}\right)^{2n+1} r(|p|/\Lambda)\left[\hat{\Psi}^\dagger(p)\hat{\Psi}^\dagger(-p) - \hat{\Psi}(-p)\hat{\Psi}(p)\right] \mathrm{d}p \tag{5.82}$$

with n some integer. In principle, we can restrict to $n = 0$, but there is some merit to choosing $n > 0$ as is shown below. The renormalized Hamiltonian is given by

$$\begin{aligned}\hat{H}_{\mathrm{R}}(s) = \int_{-\infty}^{+\infty} \mathrm{d}p\,(p^2-\mu)\left(\cos[f(p;s)]\,e^{\frac{s}{2}}\hat{\Psi}^\dagger(e^s p) + \sin[f(p;s)]\,e^{\frac{s}{2}}\hat{\Psi}(-e^s p)\right)\\ \times\left(\cos[f(p;s)]\,e^{\frac{s}{2}}\hat{\Psi}(e^s p) + \sin[f(p;s)]\,e^{\frac{s}{2}}\hat{\Psi}^\dagger(-e^s p)\right)\end{aligned} \tag{5.83}$$

and we can thus define the energy (density) functional as

$$e[\chi] = \int_{-\infty}^{+\infty} \frac{\mathrm{d}p}{2\pi}(p^2-\mu)\sin[f(p)]^2 \tag{5.84}$$

with $f(p) = f(p; s_\xi)$. Since we now have

$$\frac{\delta f(p)}{\delta \chi(s)} = \left(e^s\frac{p}{\Lambda}\right)^{2n+1} r(\mathrm{e}^s|p|/\Lambda) \tag{5.85}$$

the variational degrees of freedom $\chi(s)$ should be tuned such that

$$\frac{\delta e}{\delta \chi(s)}[\chi] = \int_{-\infty}^{+\infty}\frac{\mathrm{d}p}{2\pi}(p^2-\mu)\sin[2f(p)]\left(e^s\frac{p}{\Lambda}\right)^{2n+1} r(\mathrm{e}^s|p|/\Lambda) = 0, \quad \forall s \in [0,+\infty). \tag{5.86}$$

Since the integrand is even in p, this is a non-trivial relation. Clearly, the energy function $e[\chi]$ has stationary points for any configurations where $f(p) = 0$ or $f(p) = \pm\pi/2$ for any $p \in \mathbb{R}$. The only true minimum is when $f(p) = \pm\pi/2$ for $|p| < p_{\mathrm{F}}$ and $f(p) = 0$ for $|p| > p_{\mathrm{F}}$. Since

$$f(p) = \int_0^{+\infty} \chi(s)\left(\mathrm{e}^s\frac{p}{\Lambda}\right)^{2n+1} r(\mathrm{e}^s|p|/\Lambda)\,\mathrm{d}s \tag{5.87}$$

it can be made compatible with the choice

$$f_{\mathrm{exact}}(p) = \mathrm{sgn}(p)\frac{\pi}{2}\theta(p_{\mathrm{F}} - |p|), \tag{5.88}$$

which is also odd in p. We thus need to solve

$$\int_0^{+\infty} \chi(s)\mathrm{e}^{(2n+1)s} r(\mathrm{e}^s|p|/\Lambda)\,\mathrm{d}s = \frac{\pi}{2}\left(\frac{\Lambda}{|p|}\right)^{2n+1}\theta(p_{\mathrm{F}} - |p|). \tag{5.89}$$

Let us again take the sharp cutoff function $r(\kappa) = \theta(1-|\kappa|)$ and differentiate the left and right hand side of this equation with respect to $|p|$ in order to obtain

$$\chi\left(\log(\Lambda/|p|)\right)\left(\frac{\Lambda}{|p|}\right)^{2n+1}\left(-\frac{1}{|p|}\right) = \frac{\pi}{2}\left(-(2n+1)\frac{\Lambda^{2n+1}}{|p|^{2n+1}}\right)\theta(p_{\mathrm{F}}-|p|) - \frac{\pi}{2}\left(\frac{\Lambda}{|p|}\right)^{2n+1}\delta(p-p_{\mathrm{F}}).$$

By inserting $|p| = \mathrm{e}^{-s}\Lambda$ we obtain

$$\begin{aligned}\chi(s) &= (2n+1)\frac{\pi}{2}\theta(p_{\mathrm{F}}-\mathrm{e}^{-s}\Lambda) + \frac{\pi}{2}p_{\mathrm{F}}\delta(\mathrm{e}^{-s}\Lambda - p_{\mathrm{F}}) \\ &= (2n+1)\frac{\pi}{2}\theta\left(s-\log(\Lambda/p_{\mathrm{F}})\right) + \frac{\pi}{2}\delta\left(s-\log(\Lambda/p_{\mathrm{F}})\right).\end{aligned} \tag{5.90}$$

The disentangling strength $\chi(s)$ is exactly zero for $s < \log(\Lambda/p_{\mathrm{F}})$, so that p_{F} represents the physical cutoff momentum. The sharp δ-spike is a consequence of the sharp Fermi surface in combination with the sharp cutoff function $r(\kappa) = \theta(1-|\kappa|)$. The sudden jump in $f(p)$ at the Fermi surface p_{F} results in a strong spike in $\chi(s)$ around $s = \log(\Lambda/p_{\mathrm{F}})$ for any cutoff function $r(|p|/\Lambda)$. Since $f(\pm\Lambda) = 0 = f_{\mathrm{exact}}(\pm\Lambda)$, the equality of the derivatives ensures that $f(p) = 0 = f_{\mathrm{exact}}(p)$ for all $p \neq 0$. The continuous entanglement renormalization ansatz representation of the ground state is thus exact. Indeed, we find

$$f(p) = \frac{\pi}{2}\left[\mathrm{sgn}(p) - \left(\frac{p}{p_{\mathrm{F}}}\right)^{2n+1}\right]\theta(p_{\mathrm{F}}-|p|) + \frac{\pi}{2}\left(\frac{p}{p_{\mathrm{F}}}\right)^{2n+1}\theta(p_{\mathrm{F}}-|p|). \tag{5.91}$$

The first, respectively second, term corresponds to the first, respectively second, term of Eq. (5.90) for $\chi(s)$. This illustrates that for $|p| < p_{\mathrm{F}}$, the importance of the δ-spike at $s = \log(\Lambda/p_{\mathrm{F}})$ decreases for increasing values of n. For $s \to 0$ [and in fact for any $s > \log(\Lambda/p_{\mathrm{F}})$], the disentangling strength $\chi(s)$ has a non-zero horizontal asymptote of value $(2n+1)\pi/2$, which indicates the criticality of the model and is responsible for power-law decay of correlations and for the logarithmic violation of the area law for entanglement entropy.

There is no obvious way to generalize this construction for the ground state of the free fermion model to higher dimensions. On the one hand, we expect that a rotation invariant ground state can be constructed using a rotation invariant choice for $\hat{K}(s)$. On the other hand, it is clear that it is impossible to create a rotation invariant $\hat{K}(s)$ that is odd in $\vec{p}$. While there are no rotations in $d = 1$, the above construction $\hat{K}(s)$ already violates parity invariance. We can safely expect that it is impossible to cast the ground state of the free fermion model for a higher number of dimensions $d > 1$ in the form of a continuous entanglement renormalization ansatz with a local operator $\hat{K}(s)$, since this construction is incompatible with the logarithmic violation to the area law observed

for free fermions. A more general construction could correspond to the continuum formulation of the branching multi-scale entanglement renormalization ansatz proposed in [387, 388].

4. Summary and conclusion

In this chapter we have introduced the continuous entanglement renormalization ansatz. As we have illustrated, this variational ansatz naturally overcomes all of Feynman's criticisms. It is extensive and in general (for arbitrary non-quadratic choices of $\hat{K}$) non-Gaussian. It naturally allows to decompose the system in different scales, and variational parameters living at one scale are not influenced by the energy contributions coming from higher momenta: the variational parameters are not 'too' sensitive to high frequencies.

Our set of variational parameters is now a $d+1$ dimensional continuum of operators $\hat{k}(\vec{x};s)$ defined in terms of field operators. Clearly we have come a long way from the discrete set of matrices that constituted the set of variational parameters for the matrix product state of Chapter 3. This much wider variational class has both advantages and disadvantages. From a practical point of view, we have moved away from a variational class that easily allows for a numerical black-box implementation. It is not immediately clear how to use this variational class beyond what is analytically feasible (*i.e.* the subclass of Gaussian continuous entanglement renormalization ansatz states). We have only tested this approach for free field theories, for which a Gaussian state provides the correct solution. In principle we can also apply the Gaussian continuous entanglement renormalization ansatz to interacting theories. This results in a complicated method for doing mean field theory, which could nevertheless provide valuable information regarding criticality and renormalization.

It remains to be seen whether a numeric or analytic implementation of the variational optimization process for interacting theories can be constructed. The success of the multi-scale entanglement renormalization ansatz should proof that, if such an implementation exists, the continuous entanglement renormalization ansatz should also be able to accurately describe ground states of interacting theories. As long as we are able to accurately compute $\hat{O}_{\mathrm{R}}(s)$ and from this expectation values $\langle\Psi[\hat{K}]|\hat{O}|\Psi[\hat{K}]\rangle = \langle\Omega|\hat{O}_{\mathrm{R}}(s_\xi)|\Omega\rangle$, the variational principle guarantees that it will tune $\hat{K}$ in the best way possible at all scales. Maybe this is the variational strategy that Feynman was dreaming of.

Disadvantages and advantages of the continuous entanglement renormalization ansatz go hand in hand. For example, the use of a Lie-Trotter-Suzuki-like structure in the multi-scale entanglement renormalization ansatz for lattice systems was the reason for the absence of translation invariant instances but also allowed for efficient contractibility. In the continuum formulation, translation invariance is easily obtained by choosing $\hat{k}(\vec{x};s)$ equal for all $\vec{x}$, but the Lie-Trotter-Suzuki decomposition is no longer accessible for

evaluating the renormalization group flow. The previous chapter on continuous matrix product states might provide a solution by using *e.g.* the time-dependent variational principle in a variational subclass of operator space to evaluate $\hat{O}_{\mathrm{R}}(s)$.

The use of operators in the variational class also has many benefits. As with continuous matrix product states, we are no longer restricted to theories for which the local dimension q is finite. Even stronger, the continuous entanglement renormalization ansatz can be applied to field theories which are not even formulated in terms of non-relativistic creation- and annihilation operators, since we can construct $\hat{k}(\vec{x};s)$ from any set of field operators that define the theory. For example, by using only gauge-independent operators $\hat{F}_{i,j}(\vec{x})$ in $\hat{k}(\vec{x};s)$, it is easy to construct a unitary circuit $\hat{U}(s_a, s_\xi)$ that is gauge invariant. In addition, the analytic structure of our ansatz will hopefully facilitate the quest of finding the relation of entanglement renormalization with holographic renormalization and the AdS/CFT correspondence.

6

Applications to relativistic theories

In the previous chapters we have introduced different variational classes for both lattice systems and field theories. All of these ansätze are non-Gaussian and extensive. In addition, they allow for an efficient evaluation of expectation values (the non-Gaussian continuous entanglement renormalization ansatz is still a bit of a puzzle). We now investigate how Feynman's first criticism, namely the "sensitivity to high frequencies", manifests itself when these variational ansätze are applied to relativistic theories.

In the first section, we employ the matrix product state to study a relativistic fermion model that has been discretized, so that the degrees of freedom are living on a lattice with lattice spacing a. We need to take the continuum limit $a \to 0$ in order to recover the expected results for the field theory. In doing so, we require that the physical correlation length ξ_c remains constant, so that $\tilde{\xi}_c = \xi_c/a \to \infty$ and the model becomes critical. We know that matrix product states eventually fail in this limit. The second section eliminates the necessity of taking a continuum limit by using the continuous matrix product state to study the field theory in the continuum. This approach has proven fruitful in Chapter 4 to study non-relativistic field theories with $\xi_c/a \to \infty$. The success of this approach was due to the fact that the original lattice spacing is replaced by a different ultraviolet length scale such as the inter-particle separation $a_{\text{phys}} = \rho^{-1/d}$. When $\xi_c/a_{\text{phys}} \to \infty$, the continuous matrix product state faces the same problems as the matrix product state. When applying the continuous matrix product state to relativistic theories, the lack of a physical ultraviolet cutoff (*i.e.* $a_{\text{phys}} = 0$) will indeed trigger Feynman's "sensitivity to high frequencies" and forces us to manually introduce a cutoff. In the third section, we show how using the (Gaussian) continuous entanglement renormalization ansatz to describe (free) field theories allows to overcome this problem. While we need to introduce some ultraviolet cutoff $a = \Lambda^{-1}$ in order to define the process, we can safely send $a \to 0$ at the end of the process.

1. Relativistic fermions on the lattice

Before the development of continuum ansätze that can directly approximate ground states of quantum field theories, the only way to numerically study quantum field theories was on the lattice. This is not too bad, since the lattice naturally provides an

ultraviolet regularization of quantum field theories: the momentum space is rendered finite and the number of 'high frequencies' that plague most variational techniques is manageable. Also with non-variational techniques such as Monte Carlo sampling of the path integral, a discretization of the field theory to the lattice is required. In the end, we have to take the continuum limit by sending the lattice spacing $a \to 0$. At the same time, we need to keep the physical correlation length $\xi_c = \tilde{\xi}_c a$ constant, so we also have to vary coupling constants $\lambda(a)$, which generates the renormalization group flow discussed in Subsection 3.3 of Chapter 1. Since $a \to 0$ requires $\tilde{\xi}_c \to \infty$, the lattice theory becomes critical and the possibility of Feynman's 'sensitivity to high frequencies' comes back into play. Note that Monte Carlo based techniques suffer from their own problems in this limit (*e.g.* critical slowing down).

In this section, we apply the variational manifold $\mathcal{M}_{\mathrm{MPS}}$ of matrix product states introduced in Chapter 3 to one-dimensional relativistic field theories that have been mapped to a lattice. Since the numerical implementation of matrix product states requires a finite dimensional local Hilbert space, we restrict to fermionic theories. Bosonic theories can be studied by restricting the maximal number of bosons that can occupy a single site [391]. We first introduce the most important properties of relativistic fermions that we would like to recover in our simulation, and discuss some peculiarities regarding the mapping to the lattice.

1.1. A brief survey of relativistic fermions for one spatial dimension

In $d = 1$ spatial dimensions, relativistic fermions are described by a 2-component Dirac spinor $\psi(x)$ with components $\psi_\alpha(x)$, $\alpha = 1, 2$. The relativistic kinetic energy of the fermion field is given by

$$\hat{H}_{\mathrm{kinetic}} = \int_{-\infty}^{+\infty} \left[-\frac{\mathrm{i}}{2} \hat{\psi}^\dagger(x) \alpha^x \frac{\mathrm{d}\hat{\psi}}{\mathrm{d}x}(x) + \frac{\mathrm{i}}{2} \frac{\mathrm{d}\hat{\psi}^\dagger}{\mathrm{d}x}(x) \alpha^x \hat{\psi}(x) \right] \mathrm{d}x$$
$$= \int_{-\infty}^{+\infty} \left[-\mathrm{i} \hat{\psi}^\dagger(x) \alpha^x \frac{\mathrm{d}\hat{\psi}}{\mathrm{d}x}(x) \right] \mathrm{d}x \quad (6.1)$$

with α^x the 2×2 Dirac matrix acting on the spinor components. By choosing the Dirac matrices α^x and β (which features in the mass term) as $\alpha^x = \sigma^y$ and $\beta = \sigma^z$, we obtain a Hamiltonian with real coefficients. To this kinetic term, we can add potential terms such as the mass term, resulting in the Dirac Hamiltonian

$$\hat{H}_{\mathrm{D}} = \int_{-\infty}^{+\infty} \left[-\frac{\mathrm{i}}{2} \hat{\psi}^\dagger(x) \alpha^x \frac{\mathrm{d}\hat{\psi}}{\mathrm{d}x}(x) + \frac{\mathrm{i}}{2} \frac{\mathrm{d}\hat{\psi}^\dagger}{\mathrm{d}x}(x) \alpha^x \hat{\psi}(x) + m \hat{\psi}^\dagger(x) \beta \hat{\psi}(x) \right] \mathrm{d}x, \quad (6.2)$$

or interaction terms. One particularly interesting model for interacting relativistic fermions in $d = 1$ is the Gross-Neveu model [392], where N flavors of massless fermions interact through a quartic potential as described by

$$\hat{H}_{\mathrm{GN}} = \int_{-\infty}^{+\infty} \Bigg[-\frac{\mathrm{i}}{2} \sum_{b=1}^{N} \hat{\psi}_b^\dagger(x) \alpha^x \frac{\mathrm{d}\hat{\psi}_b}{\mathrm{d}x}(x) + \frac{\mathrm{i}}{2} \sum_{b=1}^{N} \frac{\mathrm{d}\hat{\psi}_b^\dagger}{\mathrm{d}x}(x) \alpha^x \hat{\psi}_b(x) - \frac{g^2}{2} \left(\sum_{b=1}^{N} \hat{\psi}_b^\dagger(x) \beta \hat{\psi}_b(x) \right)^2 \Bigg] \mathrm{d}x. \quad (6.3)$$

Note that the field ψ now both has a spinor index α and a flavor index b. This Hamiltonian is derived from the Gross-Neveu action

$$S_{\mathrm{GN}} = \int \mathrm{d}t \int \mathrm{d}x \left(\sum_{b=1}^{N} \psi_b^\dagger(x,t) \left[\gamma^0 \frac{\partial}{\partial t} - \mathrm{i}\gamma^1 \frac{\partial}{\partial x} \right] \psi_b(x,t) + \frac{g^2}{2} \left[\sum_{b=1}^{N} \psi_b^\dagger(x,t) \gamma^0 \psi_b(x,t) \right]^2 \right). \quad (6.4)$$

Here we have introduced Dirac's γ-matrices as

$$\gamma^0 = \gamma_0 = \beta, \qquad \gamma^1 = -\gamma_1 = \beta\alpha^x, \quad (6.5)$$

and we also define

$$\gamma^5 = \gamma_5 = \gamma^0\gamma^1 = \alpha^x. \quad (6.6)$$

Let us now discuss the properties of relativistic fermions. Physical models will always be invariant under the U(1) transformations $\hat{\psi}(x) \leftarrow \exp(\mathrm{i}\theta)\hat{\psi}(x)$, which induces conservation of charge or particle number

$$\hat{N} = \int_{-\infty}^{+\infty} \mathrm{d}x\, \hat{\psi}^\dagger(x)\hat{\psi}(x). \quad (6.7)$$

The kinetic energy is also invariant under the chiral rotation $\hat{\psi}(x) \leftarrow \exp(\mathrm{i}\theta\gamma^5)\hat{\psi}(x)$. This invariance is explicitly broken by the mass term. Chiral invariance (and the breaking thereof) plays a very important role in the standard model: coupling fermions to gauge fields results in a spontaneous breaking of chiral invariance that is generally associated to the dynamic generation of mass. Since chiral invariance is a continuous symmetry, it cannot be broken for $d = 1$. We can however define a discrete chiral transformation $\hat{\psi}(x) \leftarrow \gamma^5\hat{\psi}(x)$ ($\theta = \pi/2$). Discrete chiral invariance still forbids the presence of a mass, since it maps $m \to -m$. However, the Gross-Neveu model is invariant under discrete chiral transformations but breaks this symmetry spontaneously, which also results in the dynamic generation of mass. Chiral invariance is also the source of the problems

that arise when trying to discretize the fermion field in order to put it on a lattice, as we explore in the next subsection.

1.2. Mapping fermions to the lattice

We first define how to discretize our fermion models and map them to lattice models that return the correct continuum results when the proper continuum limit $a \to 0$ is taken. Introducing a lattice with lattice spacing a, we can set

$$\hat{\psi}(x = ja) \to \frac{\hat{\phi}(j)}{\sqrt{a}} \quad \text{with } \{\hat{\phi}^\dagger_\alpha(j), \hat{\phi}_\beta(j')\} = \delta_{\alpha,\beta}\delta_{j,j'}. \tag{6.8}$$

The first problem one encounters when mapping relativistic Dirac fermions to the lattice is the notorious "fermion doubling problem". If one discretizes n of the $(d+1)$ spacetime dimensions using a naive scheme to discretize the derivatives in the kinetic term in the Hamiltonian or action, the resulting lattice theory has 2^n different low-energy regions in its Brillouin zone, which should be interpreted as 2^n different species. This fermion doubling is often attributed to the presence of a single (instead of a double) derivative. It is a feature of the classical equations of motion and also occurs in *e.g.* studies of acoustics and (classical) electromagnetism using the finite-difference time-domain method. The problem can there completely be overcome by using a staggered configuration of the discretization points for the different fields, resulting in *e.g.* the Yee cell for electromagnetism [393]. For relativistic fermions, the same idea results in the staggered fermion approach of Kogut and Susskind [394, 395]. However, this approach is not able to remove all doublers. Clearly, the problem turns out to be more fundamental and is in fact related to the chiral symmetry of the kinetic energy. The no-go theorem of Nielsen and Ninomiya ensures that every local, unitary and chirally symmetric lattice theory will have a degenerate excitation spectrum, with at least two independent fermion flavors [396, 397, 398]. Solutions to circumvent the fermion doubling problem include using Wilson fermions [399], which explicitly break chiral symmetry, overlap fermions, which are highly nonlocal, or domain wall fermions, which require an additional spatial dimension to be introduced. Recently, there has been renewed interest in the construction of so-called minimally doubled models, where the number of fermions has been reduced to the minimal number of two, inspired by the two-dimensional realization in graphene [400].

Luckily, there is one case that escapes the Nielsen-Ninomiya no-go theorem, which is the Hamiltonian lattice (only spatial dimension is discretized) in $d = 1$. Here, the staggered formulation of Kogut and Susskind is able to eliminate all doublers (since there is only one). A key ingredient of the staggered formulation is to choose an asymmetric definition for the lattice version of the derivative of the fields, for example by using the

left and right lattice derivative according to

$$\frac{\mathrm{d}\hat{\psi}_1}{\mathrm{d}x}(ja) \to \frac{\hat{\phi}_1(j+1) - \hat{\phi}_1(j)}{a\sqrt{a}}, \tag{6.9a}$$

$$\frac{\mathrm{d}\hat{\psi}_2}{\mathrm{d}x}(ja) \to \frac{\hat{\phi}_2(j) - \hat{\phi}_2(j-1)}{a\sqrt{a}}. \tag{6.9b}$$

It is then possible to stagger the two components of the Dirac equation to single-component fermionic fields $\hat{c}$ living on subsequent sites of an auxiliary lattice of twice the number of sites. With the definition

$$\hat{\phi}_1(j) \to (-1)^j \hat{c}(2j-1), \qquad \hat{\phi}_2(j) \to (-1)^{j+1} \hat{c}(2j), \tag{6.10}$$

we obtain for the lattice version of the kinetic energy term in the Hamiltonian

$$\hat{H}'_{\text{kinetic}} = \frac{1}{a} \sum_n \hat{c}(n)^\dagger \hat{c}(n+1) + \hat{c}(n+1)^\dagger \hat{c}(n). \tag{6.11}$$

This relativistic kinetic energy thus boils down to a typical lattice hopping term that also appears in non-relativistic models such as the Hubbard model. However, whereas $\hat{c}$ would represent a single fermion flavor in non-relativistic models, the even and odd sites should here be interpreted as representing the two different components of the Dirac spinor. Rather than interpreting Eq. (6.9) as an asymmetric lattice prescription of derivatives, we could also reinterpret the discretization scheme as

$$\hat{\psi}_1(x = (j-1/2)a) \to \frac{\hat{c}(2j-1)}{\sqrt{a}} \quad \text{and} \quad \hat{\psi}_2(x = ja) \to \frac{\hat{c}(2j)}{\sqrt{a}}. \tag{6.12}$$

The different spinor components are 'sampled' at different spatial locations so that the derivative of a component is required in between the two sampling points of that component, hence resulting in a symmetric prescription of the derivative.

Charge conservation is still expressed by the invariance under $\mathsf{U}(1)$ transformations $\hat{c}(n) \leftarrow \exp(\mathrm{i}\theta)\hat{c}(n)$, $\forall n$. Chiral transformations are more difficult. Since we do not longer discretize different components of the spinor at the same point in space, we can no longer define a continuous chiral transformation that mixes these two components. In higher dimensions d, the staggered fermion construction results in N different fermion species ($N = 2$ species on the Hamiltonian lattice for $d = 3$, $N = 4$ species on the Euclidean lattice for $d = 3$) that survive in the continuum limit. In the continuum description of N massless fermions, the chiral symmetry mixes with the $\mathsf{SU}(N)$ symmetry to produce a $\mathsf{SU}(N)_\mathsf{L} \otimes \mathsf{SU}(N)_\mathsf{R}$ symmetry. In the lattice model, only a single one-dimensional symmetry is present, which corresponds to the axial isospin transformation of the continuum.

We can however still define a lattice version of the discrete chiral transformation $\hat{\psi}(x) \leftarrow$

$\gamma^5\hat{\psi}(x)$. We hereto define the transformation $\{\hat{\phi}_1(j) \leftarrow -\mathrm{i}\hat{\phi}_2(j), \hat{\phi}_2(j) \leftarrow +\mathrm{i}\hat{\phi}_1(j+1)\}$. In terms of Eq. (6.12), this transformation formula indicates that we also have to shift the discretization points by half a lattice site in order to define a map between $\hat{\phi}_1$ and $\hat{\phi}_2$. Using Eq. (6.10), we obtain as discrete chiral transformation $\hat{c}(n) \leftarrow \mathrm{i}\hat{c}(n+1) = \mathrm{i}\hat{T}\hat{c}(n)\hat{T}^{-1}$. Up to a redundant phase factor that can be gauged away using the U(1) fermion number symmetry, a discrete chiral transformation is obtained by shifting the lattice over a single site. Hence, the translation invariance of $\hat{H}'_{\text{kinetic}}$ in Eq. (6.11) is partly due to the chiral invariance and partly due to the translation invariance of the continuum formulation. Other terms that are translation invariant in the continuum, such as the mass term, are only invariant under shifts over two sites. For example, the lattice version of the Dirac Hamiltonian is given by

$$\hat{H}'_{\mathrm{D}} = \frac{1}{a}\sum_n \hat{c}(n)^\dagger \hat{c}(n+1) + \hat{c}(n+1)^\dagger \hat{c}(n) + (-1)^n \tilde{m}\hat{c}(n)^\dagger \hat{c}(n), \tag{6.13}$$

with $\tilde{m} = ma$ the dimensionless mass. Under a discrete chiral transformation (shift over a single site), the mass term changes sign.

Chirally invariant field theories should thus map to translation invariant lattice models. Spontaneous breaking of (discrete) chiral symmetry in the continuum is then mapped to a breaking of translation invariance, which result in a gapped phase (dynamic generation of mass). For the Gross-Neveu interaction term, we obtain

$$\begin{aligned}
&-\frac{g^2}{2}\int \mathrm{d}x \left[\sum_{b=1}^N \hat{\psi}_b^\dagger(x)\beta\hat{\psi}_b(x)\right]^2 \\
&\quad\mapsto -\frac{g^2}{2a}\sum_j \left[\sum_{b=1}^N \hat{c}_b(2j-1)^\dagger \hat{c}_b(2j-1) - \hat{c}_b(2j)^\dagger \hat{c}_b(2j)\right]^2 \\
&\quad= -\frac{g^2}{2a}\sum_j \Bigg[\sum_{b,b'=1}^N \hat{c}_b(2j-1)^\dagger \hat{c}_b(2j-1)\hat{c}_{b'}(2j-1)^\dagger \hat{c}_{b'}(2j-1) \\
&\qquad\qquad + \sum_{b,b'=1}^N \hat{c}_b(2j)^\dagger \hat{c}_b(2j)\hat{c}_{b'}(2j)^\dagger \hat{c}_{b'}(2j) \\
&\qquad\qquad - 2\sum_{b,b'=1}^N \hat{c}_b(2j-1)^\dagger \hat{c}_b(2j-1)\hat{c}_{b'}(2j)^\dagger \hat{c}_{b'}(2j)\Bigg].
\end{aligned}$$

Clearly, this expression is not invariant under our lattice definition of discrete chiral transformations (*i.e.*ăshifts over single sites). Since we are free to make changes up to order a, as was also done in the definition of the discrete chiral transformation on the lattice, we can redefine the Gross-Neveu Hamiltonian on the lattice as

$$\hat{H}'_{\mathrm{GN}} = \frac{1}{a}\sum_n \sum_{b=1}^N \hat{c}_b(n)^\dagger \hat{c}_b(n+1) + \hat{c}_b(n+1)^\dagger \hat{c}_b(n)$$

$$-\frac{g^2}{2a}\sum_n\sum_{b,b'=1}^{N}\hat{n}_b(n)\hat{n}_{b'}(n)+\frac{g^2}{2a}\sum_n\sum_{b,b'=1}^{N}\hat{n}_b(n)\hat{n}_{b'}(n+1). \quad (6.14)$$

We have introduced the number operators $\hat{n}_b(n)=\hat{c}_b(n)^\dagger\hat{c}_b(n)$. No confusion between the number operator $\hat{n}$ and the site index n should arise. This definition of $\hat{H}'_{\mathrm{GN}}$ has the expected properties and will be studied with the matrix product state ansatz in the next subsection.

Finally, we can map $\hat{H}'_{\mathrm{GN}}$ to a spin Hamiltonian using the Jordan-Wigner transformation

$$\hat{c}_b(n)=\left[\prod_{b'=1}^{b-1}\prod_{m'=-\infty}^{+\infty}\hat{\sigma}^z_{b'}(m')\right]\left[\prod_{m=-\infty}^{n-1}\hat{\sigma}^z_b(m)\right]\hat{\sigma}^+_b(n), \quad (6.15a)$$

$$\hat{c}_b(n)\dagger=\left[\prod_{b'=1}^{b-1}\prod_{m'=-\infty}^{+\infty}\hat{\sigma}^z_{b'}(m')\right]\left[\prod_{m=-\infty}^{n-1}\hat{\sigma}^z_b(m)\right]\hat{\sigma}^-_b(n). \quad (6.15b)$$

The string of operators $\hat{\sigma}^z_{b'}$ over flavors $b'<b$ will not contribute. We obtain

$$\begin{aligned}\hat{H}'_{\mathrm{GN}}=&\frac{1}{a}\sum_n\sum_{b=1}^{N}\hat{\sigma}^-_b(n)\hat{\sigma}^+_b(n+1)+\hat{\sigma}^-_b(n+1)\hat{\sigma}^+_b(n)\\&-\frac{g^2}{8a}\sum_n\sum_{b,b'=1}^{N}\hat{\sigma}^z_b(n)\hat{\sigma}^z_{b'}(n)+\frac{g^2}{8a}\sum_n\sum_{b,b'=1}^{N}\hat{\sigma}^z_b(n)\hat{\sigma}^z_{b'}(n+1),\\=&\frac{1}{2a}\sum_n\sum_{b=1}^{N}\hat{\sigma}^x_b(n)\hat{\sigma}^x_b(n+1)+\hat{\sigma}^y_b(n+1)\hat{\sigma}^y_b(n)\\&-\frac{g^2}{8a}\sum_n\sum_{b,b'=1}^{N}\hat{\sigma}^z_b(n)\hat{\sigma}^z_{b'}(n)+\frac{g^2}{8a}\sum_n\sum_{b,b'=1}^{N}\hat{\sigma}^z_b(n)\hat{\sigma}^z_{b'}(n+1).\end{aligned} \quad (6.16)$$

Hence, the Gross-Neveu model can also be interpreted as a multi-layer spin model with an antiferromagnetic nearest neighbor coupling and a ferromagnetic coupling between the sites on the same spatial location. In the next subsection, we study some more properties of this model and then try to recover these from simulations based on matrix product states.

1.3. Excitations in the Gross-Neveu model

We now study the properties of the Hamiltonian in Eq. (6.16) using the uniform matrix product state ansatz. Before discussing the results, let us provide a short summary of the properties of the continuum model that we hope to reproduce. The Gross-Neveu model defined by the action S_{GN} in Eq. (6.4) was first proposed by Gross and Neveu

in [392] as a simple model to gain deeper insight in some of the non-perturbative properties of quantum chromodynamics, and has since been thoroughly studied. The four-fermion interaction triggers the dynamical breaking of the chiral symmetry of the massless fermions, resulting in a dynamically generated fermion mass m_{F}. Obviously, this is a non-perturbative effect, since the chiral invariance prohibits a mass term at all orders of perturbation theory. Dynamical mass generation is strongly connected to asymptotic freedom, as was argued by Gross and Neveu. The β-function of the Gross-Neveu model can easily be computed and exhibits the property of asymptotic freedom, as expected. The Gross-Neveu model was first studied in the large N limit. The ground state properties were obtained by Gross and Neveu in their original paper, and the spectrum of bound states by Dashen, Hasslacher and Neveu in [401]. Later, Zamolodchikov and Zamolodchikov calculated the exact S-matrix of the elementary fermions for the finite N-model [402], and Karowski and Thun calculated the complete S-matrix [403]. The exact mass gap was computed by Forgacs, Niedermayer and Weisz [404, 405]. Recent studies of the Gross-Neveu model are mainly concerned with the phase diagram at finite temperature and finite chemical potential.

We can now state some results obtained in the large N limit or with exact methods, using dimensional regularization in the $\overline{\mathrm{MS}}$ scheme, which is a modification of the minimal subtraction scheme (MS). The evolution of the coupling constant under renormalization group transformations is described by the β-function

$$\beta(g) = \mu \frac{\mathrm{d}g(\mu)}{\mathrm{d}\mu} = -\frac{N-1}{2\pi} g(\mu)^3 + \frac{N-1}{4\pi^2} g(\mu)^5 + \mathcal{O}(g(\mu)^7), \tag{6.17}$$

which allows for the definition of a renormalization group invariant mass scale

$$M = \mu g(\mu)^{\frac{1}{N-1}} \mathrm{e}^{-\frac{\pi}{(N-1)g(\mu)^2}} \left(1 + \mathcal{O}(g(\mu)^2)\right). \tag{6.18}$$

One exception is $N = 1$, where the β-function is identically zero and the Gross-Neveu model describes a critical system with exact conformal invariance at the quantum level. There are no masses ($M = 0$) and thus, no chiral symmetry breaking occurs. In correspondence, for $N = 1$ the lattice Hamiltonian $\hat{H}'_{\mathrm{GN}}$ reduces to the XXZ model with dimensionless anisotropy parameter $\Delta = g^2/4$. For $\Delta < 1$ ($g < 2$), this is a critical model with a conformally invariant low energy region.

For all $N > 1$, the breaking of discrete chiral symmetry produces a two-dimensional vacuum subspace and we denote the ground states of maximal symmetry breaking (see Subection 1.4 of Chapter 1) as $|\Psi^{\pm}\rangle$. The order parameter for the chiral symmetry breaking is given by the composite operator $\overline{\psi}(x)\psi(x)$, which acquires a finite vacuum expectation value

$$\sigma_{\pm} = \pm\sigma_0 = g^2(N-1) \frac{\langle \Psi^{\pm} | \sum_{a=1}^{N} \hat{\psi}_a^{\dagger}(x) \gamma^0 \hat{\psi}_a(x) | \Psi^{\pm} \rangle}{N} =$$

$$g^2(N-1)\langle\Psi^{\pm}|\hat{\bar{\psi}}_a^{\dagger}(x)\gamma^0\hat{\psi}_a(x)|\Psi^{\pm}\rangle, \quad (6.19)$$

where this last ground state expectation value is independent of the flavor a. The appearance of the prefactor $g^2(N-1)$ will immediately be clarified. In fact, this factor also appears in Eq. (6.17) and Eq. (6.18) and can therefore be defined as an effective coupling strength λ

$$\lambda = g^2(N-1). \quad (6.20)$$

Due to the property of entanglement monogamy (see Subsection 2.2 of Chapter 1), the entanglement between the different flavors disappears in the limit $N \to \infty$. The ground state of the Gross-Neveu Hamiltonian is then a product state over the different flavors, and we can use the definition of σ_0 above to write down an effective mean-field Hamiltonian for a single fermion flavor a as

$$\hat{H}_{\text{mean field}} = \int_{-\infty}^{+\infty} \left[-\mathrm{i}\hat{\bar{\psi}}_a^{\dagger}(x)\alpha^x \frac{\mathrm{d}\hat{\psi}_a}{\mathrm{d}x}(x) + \sigma_{\pm}\hat{\bar{\psi}}_a^{\dagger}(x)\beta\hat{\psi}_a(x) + \frac{g^2}{2}\left(\hat{\bar{\psi}}_a^{\dagger}(x)\beta\hat{\psi}_a(x)\right)^2 \right] \mathrm{d}x \quad (6.21)$$

The order parameter $\sigma_{\pm}$ thus appears as a mass for the elementary fermions (note that a relativistic mass can be negative, since this is equivalent to switching particles and antiparticles). The proper $N \to \infty$ limit is thus obtained by keeping $\lambda = g^2(N-1)$ constant. Hence, $g^2 = \lambda/(N-1) \to 0$ and the self-interaction of the flavor in the mean field Hamiltonian disappears, reducing the mean field Hamiltonian to a free theory. The value of the order parameter σ_0 can then self-consistently be obtained since it represents the mass of a free Dirac theory for which $\langle\hat{\bar{\psi}}^{\dagger}\gamma^0\hat{\psi}\rangle = \lambda\sigma_0$. Hence, σ_0 represents the dynamically generated fermion mass m_{F} for $N \to \infty$. For finite N, σ_0 is not a renormalization group invariant, and the relation between σ and the fermion mass m_{F} requires higher order corrections due to the self interaction and due to the entanglement between the different flavors. The fermion mass m_{F} should always be a renormalization group invariant and is thus proportional to the mass scale M of Eq. (6.18). In the $\overline{\mathrm{MS}}$ scheme, the exact expression is given by

$$m_{\mathrm{F}} = \frac{(4\mathrm{e})^{\frac{1}{2(N-1)}}}{\Gamma\left(1-\frac{1}{2(N-1)}\right)} M. \quad (6.22)$$

While the Gross-Neveu model clearly has $\mathrm{SU}(N)$ flavor symmetry, it can in fact be shown that this symmetry can be enlarged to a full $\mathrm{O}(2N)$ symmetry between the different Majorana-components. The appearance of the the factors $2(N-1)$ in the exact results is a consequence of this being the Coxeter number of the $\mathrm{O}(2N)$ group [406]. The complete excitation spectrum of the Gross-Neveu model can be subdivided in a topologically trivial and a nontrivial sector, which can also be categorized according to the representations of $\mathrm{O}(2N)$. The topologically non-trivial sector contains the Callen-Coleman-Gross-Zee kink, which interpolates between the two degenerate vacua and has a mass m_{K}. These

excitations can also be understood in terms of the mean field construction using a spatially dependent background field $\sigma(x)$ that is able to bind elementary fermions in a self-consistent way [407, 408]. At $x \to \pm\infty$, we must have $\sigma(x) = \sigma_+$ or $\sigma(x) = \sigma_-$, hence describing topologically trivial or topologically non-trivial excitations when both limits are equal or opposite. The resulting excitations and degeneracies are of course compatible. For example, kinks transform according to the two spinor representations of the $O(2N)$ group, each of which has dimension 2^{N-1}. The self-consistent kink background $\sigma(x)$ is a reflectionless potential with an N-fold degenerate bound state, in which the N fermion flavors can either bind or not bind, thus producing a $Q_K = 2^N$ degenerate topologically non-trivial excitation. The topologically trivial excitations can be understood as a bound state of a kink and anti-kink, which are held together by the fermions binding to the background field. They are labeled by a principle quantum number $n = 1, \ldots, N-2$ and have masses

$$m_n = 2m_K \sin\left(\frac{\pi n}{2(N-1)}\right). \tag{6.23}$$

Note that the large-N result predicts a factor N instead of $N-1$ in the denominator of the argument of the sine function in the equation above. The substitution $N \to N-1$ is also based on the Coxeter number of the $O(2N)$ symmetry group. It predicts that for $n = N-1$, the bound state is no longer stable ($m_{N-1} = 2m_K$) and separates into an unbound kink and anti-kink pair. The bound state $n = 1$ describes the fundamental massive fermion of the Gross-Neveu model, which implies that $m_1 = m_F$ and that the fundamental fermion is only part of the stable spectrum for $N > 2$. For $N > 2$, states with n odd are fermionic and states with n even are bosonic. For each n, the bound states can be labeled by a second quantum number $r = n, n-2, \ldots, \geq 0$, which indicates that these states transform according to the antisymmetric tensor representation of rank r under $O(2N)$ transformations, so that $Q_{n,r} = \binom{2N}{r}$. For example, the state at $n = 1$ transforms according to the fundamental representation and has dimensionality $2N$, whereas the state at $n = 2$ contains a subspace of dimension $2N(2N-1)/2$ that transforms as an antisymmetric matrix and a subspace of dimension 1 that transforms as a scalar.

We now try to recover this excitation spectrum by applying the uniform matrix product state ansatz and the resulting ansatz for excitations (see Chapter 3) to the lattice Hamiltonian (6.16) in the continuum limit $a \to 0$. However, since a only appears as a prefactor, the true continuum limit is obtained by a correct scaling of the coupling constant $g(a)$ as dictated by the asymptotic freedom of the Gross-Neveu model:

$$\lim_{a \to 0} g(a) \to 0. \tag{6.24}$$

Hence, the continuum limit is obtained by taking the limit towards the critical point $g = 0$. Due to the sharp increase of the site dimension as function of the number of flavors ($q = 2^N$), we restrict to the cases $N = 2$ and $N = 3$. The number of flavors also

has a strong influence on the attainable accuracy, especially in the critical continuum limit $g \to 0$. For N massless free fermions, which is equivalent to N copies of the XX model, the entanglement entropy of one half of the chain is N times larger than the entanglement entropy of a single fermion flavor. This dominating term will also be present in the continuum limit $g \to 0$, so that the dimension D of the matrices should also scale exponentially in N in order to obtain comparable accuracies as for the single flavor model. As N increases, it very rapidly becomes unfeasible to probe deeply into the continuum limit.

Because of the antiferromagnetic spatial ordering, we perform a spin flip on every second site, and actually use the Hamiltonian

$$\begin{aligned}\hat{H}''_{\mathrm{GN}} =& \frac{1}{2a}\sum_n \sum_{b=1}^{N} \hat{\sigma}_b^x(n)\hat{\sigma}_b^x(n+1) - \hat{\sigma}_b^y(n+1)\hat{\sigma}_b^y(n) \\ &- \frac{g^2}{8a}\sum_n \sum_{b,b'=1}^{N} \hat{\sigma}_b^z(n)\hat{\sigma}_{b'}^z(n) - \frac{g^2}{8a}\sum_n \sum_{b,b'=1}^{N} \hat{\sigma}_b^z(n)\hat{\sigma}_{b'}^z(n+1).\end{aligned} \tag{6.25}$$

In the lattice Hamiltonian, two neighboring sites correspond to the two components of the Dirac spinor at a single location. Hence, the lattice momentum p corresponds to a physical momentum $p_{\mathrm{phys}} = (2p \mod 2\pi)/a$. The charge conjugation symmetry of the original fermion model result in the spectrum of this Hamiltonian being similar around $p = 0$ and $p = \pi$. Both sectors produce equal types of excitations with the same physical momentum $p_{\mathrm{phys}} = 0$. They correspond to states with an eigenvalue $+1$ ($p = 0$) or -1 ($p = \pi$) with respect to the charge conjugation operation. When trying to reproduce the spectrum of the continuum model at p_{phys}, we should thus double any degeneracy we find in the excitation spectrum of our lattice model at momentum $p = 0$. However, the lattice model does not share the full $\mathrm{SO}(2N)$ symmetry with the continuum model, and is only invariant under $\mathrm{SU}(N)$ flavor transformations. We thus expect to find other degeneracies dictated by the smaller group $\mathrm{SU}(N)$ for our lattice model, and can only hope that the correct degeneracies are properly restored in the continuum limit.

While not directly related to the continuum limit, it is intuitive to first look at the strong coupling limit $g \to \infty$. The Hamiltonian $\hat{H}''_{\mathrm{GN}}$ of Eq. (6.25) then turns into a classical Ising-like model with N spins per site with ferromagnetic interaction. Since we do not expect any phase transition throughout the range $g \in (0, +\infty)$, we can already try to connect the different states to associated excitations in the spectrum of the continuum model. The ground state of this classical model is a fully polarized state, with all spins on every site either all up or all down. These states will thus flow into the two symmetry broken ground states for $g \to 0$. We first look at topologically non-trivial states. The fundamental kink and anti-kink are obtained by gluing the two classical ground states to each other. The resulting domain wall has an excitation energy and degeneracy

$$m'_{\mathrm{K}} = m'_{\mathrm{K},0} = N^2 \frac{g^2}{4a}, \qquad Q'_{\mathrm{K}} = Q'_{\mathrm{K},0} = 2. \tag{6.26}$$

We treat kink and anti-kink as different states, but obtain a two-fold degeneracy by counting the two momentum sectors around $p = 0$ and $p = \pi$, which both contribute to the sector $p_{\text{phys}} = 0$. We use single primes for the notation of the masses and the degeneracies since $\hat{H}'_{\text{GN}}$ and $\hat{H}''_{\text{GN}}$ should produce the same spectrum (up to shifts over momentum π which have no effect on the spectrum). Aside from the fundamental kinks, we can also create states that start with all spins up, then have a single site with $n < N$ spins up and $N - n$ spins down, and then all spins down. These are also topologically non-trivial states with mass and degeneracy

$$m'_{\text{K},n} = \big(N^2 + 2n(N-n)\big)\frac{g^2}{4a}, \qquad Q'_{\text{K},n} = 2\frac{N!}{n!(N-n)!}. \tag{6.27}$$

Unlike in the continuum, adding additional fermions (spin flips) to the fundamental kink now costs energy. We can hope that that this energy cost disappears in the continuum limit $g \to 0$. However, not all of the states above can become degenerate with the fundamental kink for $g \to 0$, since $\sum_{n=0}^{N-1} Q'_{\text{K},n} > Q_{\text{K}} = 2^N$. In the large g limit, we can treat the kinetic term as a perturbation. The masses of these topologically non-trivial states undergo first order shifts. It is thus not a priori impossible that the energy of some states is lowered and they will eventually become degenerate with the fundamental kink, while the energy of other states is shifted upwards and they are driven into the continuum. Topologically trivial states in the large g limit are obtained by flipping n of the N spins on a single site. The resulting excitation energy m_n and degeneracy Q_n are given by (again counting both momentum sectors)

$$m'_n = \big(2nN + 2n(N-n)\big)\frac{g^2}{4a} = 2n(2N-n)\frac{g^2}{4a}, \quad Q'_n = 2\binom{N}{n} = 2\frac{N!}{n!(N-n)!}. \tag{6.28}$$

The state $n = 1$ with a single flipped spin has degeneracy $2N$ and can be related to the fundamental fermion in the continuum. However, unlike in the continuum, it is already stable for $N = 2$. In the large g-limit, the states here constructed are only unstable for $n = N$. We then find $m_N = 2m_{\text{K},0}$, so that the state with N flipped spins decays into two fundamental kinks. The degeneracies of the states with $n > 1$ bare no resemblance to those predicted by the $O(2N)$ of the continuum. In addition, we now have too few states to account for all expected topologically trivial states in the continuum and additional states with flipped spins on neighboring sites will have to be mixed in. The topologically trivial states here constructed are stable at first order when the kinetic term is treated as a perturbation. The masses m'_n only receive corrections at second order in the perturbation, which are always negative. A complete classification of the spectrum and a group theoretic study of how it can possibly evolve into the continuum spectrum for general values of N is beyond the scope of this section.

We now focus on the cases $N = 2$ and $N = 3$ for which we study the continuum limit using the matrix product state ansatz. Figure 6.1 depicts the spectrum of $\hat{H}''_{\text{GN}}$ for $N = 2$ and $\lambda = 4$ ($g = 2$), which is still in the large g regime but already with large

corrections. This spectrum was obtained using our ansatz for excitations with bond dimension $D = 12$. We have also indicated the zeroth order energies for the fundamental kink [$m'_{\mathrm{K},0}$ in Eq. (6.26)], the kink with bound fermion [$m'_{\mathrm{K},1}$ in Eq. (6.27)] and the fundamental fermion [m'_1 in Eq. (6.28)]. It is clear that the fundamental kink and fundamental fermion only receive small second order corrections (necessarily negative) around momentum $p = 0$ and $p = \pi$, whereas the kink with bound fermion receives large first order corrections which are opposite at $p = 0$ and $p = \pi$. Indeed, if we define the lattice kinetic energy —our perturbation term—

$$\begin{aligned}\hat{H}''_{\mathrm{kinetic}} &= \frac{1}{2a}\sum_n \sum_{b=1}^{N} \hat{\sigma}^x_b(n)\hat{\sigma}^x_b(n+1) - \hat{\sigma}^y_b(n+1)\hat{\sigma}^y_b(n) \\ &= \sum_n \sum_{b=1}^{N} \hat{\sigma}^+(n)\hat{\sigma}^+(n+1) + \hat{\sigma}^-(n)\hat{\sigma}^-(n) \end{aligned} \tag{6.29}$$

and label the two kink states with bound fermion as

$$|\mathrm{K}_{1,1}\rangle = \left|\begin{matrix}\cdots & \uparrow & \uparrow & \downarrow & \cdots \\ \cdots & \uparrow & \downarrow & \downarrow & \cdots\end{matrix}\right\rangle, \qquad |\mathrm{K}_{1,2}\rangle = \left|\begin{matrix}\cdots & \uparrow & \downarrow & \downarrow & \cdots \\ \cdots & \uparrow & \uparrow & \downarrow & \cdots\end{matrix}\right\rangle, \tag{6.30}$$

then we obtain

$$\hat{H}''_{\mathrm{kinetic}}|\mathrm{K}_{1,1}\rangle \sim (\hat{T} + \hat{T}^{-1})|\mathrm{K}_{1,b}\rangle + \ldots \tag{6.31}$$

with $\hat{T}$ the shift operator. If we create momentum superpositions of the states $|\mathrm{K}_{1,i}\rangle$ with momentum p, then we can write $\hat{H}''_{\mathrm{kinetic}}$ in the two-dimensional subspace spanned by the basis $\{|\mathrm{K}^{(p)}_{1,1}\rangle, |\mathrm{K}^{(p)}_{1,2}\rangle\}$ as

$$[\hat{H}''_{\mathrm{kinetic}}] = \begin{bmatrix} 0 & \frac{2}{a}\cos p \\ \frac{2}{a}\cos p & 0 \end{bmatrix}. \tag{6.32}$$

Hence, the degeneracy between the levels $|\mathrm{K}^{(p)}_{1,1}\rangle$ and $|\mathrm{K}^{(p)}_{1,2}\rangle$ is lifted for all momenta $p \neq \pi/2$, by attributing to the linear combinations $|\mathrm{K}^{(p)}_{1,\pm}\rangle = |\mathrm{K}^{(p)}_{1,1}\rangle \pm |\mathrm{K}^{(p)}_{1,2}\rangle$ a first order energy shift $\pm 2/a\cos(p)$.

We now investigate whether the lowest of these two energies does eventually combine with the energy of the fundamental kink in the continuum limit $g \to 0$. In addition, we also examine whether the lowest topologically trivial excitation, which is still stable at the value of g in Figure 6.1, becomes unstable in the continuum limit. We therefore compute the two lowest topologically non-trivial excitation energies as well as the two lowest topologically trivial excitation energies for decreasing values of $\lambda = (N-1)g^2$ up to $\lambda \approx 2/3$ with our ansatz for excitations. We use different values of the bond dimension ranging up to $D = 512$ in order to obtain mass estimates $m^{(D)}$. We then use

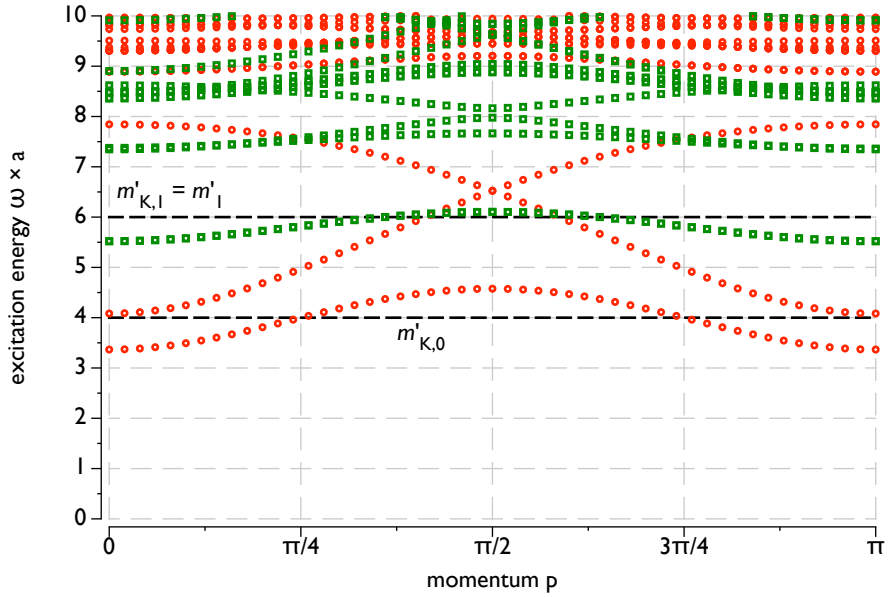

Figure 6.1: Spectrum of the Gross-Neveu lattice Hamiltonian $\hat{H}''_{\mathrm{GN}}$ (see Eq. (6.25)) for $N = 2$ and $g = 2$ using our ansatz for lattice excitations with bond dimension $D = 12$. Also indicated are the zeroth order excitation energies obtained in the large g limit.

the approach of Subsection 3.5 of Chapter 3 to obtain an estimate $m^{(\infty)}$ (*i.e.* a fit based on a power-law scaling of the differences $|m^{(D)} - m^{(\infty)}|$ as a function of the local state error $\tilde{\varepsilon}$ as in Figure 3.10). The results are displayed in Figure 6.2. The mass of the fundamental fermion quickly rises above the value of twice the mass of the fundamental kink. Since we know that two fundamental kinks with momentum $p = 0$ can appear together to form a topologically trivial state with an excitation energy that is twice the kink mass, this clearly shows the inadequacy of our ansatz to describe multi-particle excitations. In addition, the extrapolation of $m^{(\infty)}$ based on a power law scaling of the deviations as function of the local state error $\tilde{\varepsilon}$ is no longer suitable for multi-particle excitations. The ratio of the mass of the kink with bound fermion and the mass of the fundamental kink first decreases as the coupling constant g is decreased, but then starts to rise again and finally seems to saturate around a value of $m_{\text{kink+bound fermion}}/m_{\text{fundamental kink}} \approx 1.2$. At this point, we are already quite deep in teh continuum limit, since the kink mass is around 0.02 in lattice units, so the corresponding correlation length spans around 50 sites. While the relative uncertainty on the mass estimates $m^{(\infty)}$ is quite large for the points furthest in the continuum regime —due to two flavors each contributing to the amount of entanglement— it dos not supersede the order of 1 %. Hence, the mass ratio of about 1.2 around $\lambda \approx 2/3$ will not shift substantially by improving the approximation. Two possible explanations easily come to mind. It might be that we have to probe much deeper into the continuum limit before the theoretically expected mass ratio of 1 is obtained. Another possibility is that the low energy region of our lattice

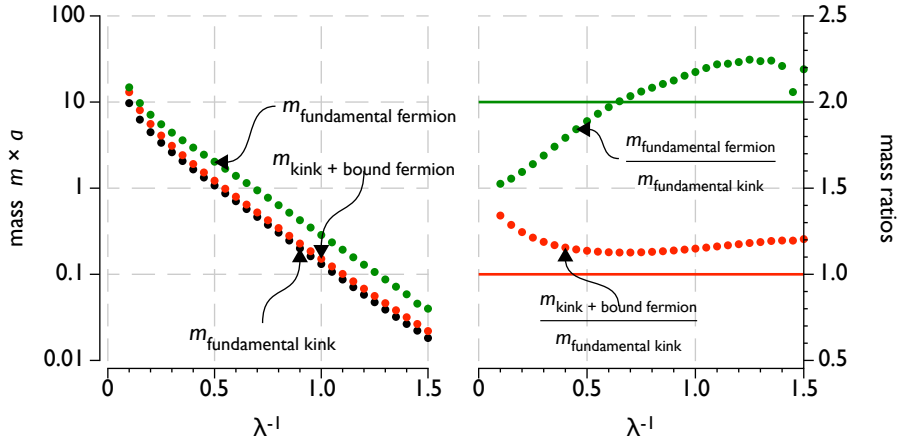

Figure 6.2: Masses of the elementary excitations of the Gross-Neveu lattice Hamiltonian $\hat{H}''_{\mathrm{GN}}$ as function of the inverse coupling constant $\lambda^{-1} = [(N-1)g^2]^{-1}$, as extrapolated from the results of our ansatz for lattice excitations for different values of the bond dimension ranging up to $D \approx 500$.

Hamiltonian $\hat{H}''_{\mathrm{GN}}$ for $N = 2$ in the critical limit (continuum limit) is not described by the $N = 2$ Gross-Neveu field theory, but rather flows towards a different fixed point under renormalization group transformations. Since our lattice model does not have the full $\mathrm{O}(2N)$ invariance of the Gross-Neveu model but only $\mathrm{SU}(N)$ invariance, this argument is not completely improbable. There is a priori no reason to assume that the $\mathrm{O}(2N)$ symmetry should automatically be restored in the continuum, and a different field theory with only $\mathrm{SU}(N)$ flavor symmetry might describe the low-energy behavior of $\hat{H}''_{\mathrm{GN}}$ in the critical limit.

We now repeat this analysis for the $N = 3$ case. Since the entanglement is even larger due to the additional flavor, the attainable accuracy in the continuum limit will be even smaller. The spectrum of $\hat{H}''_{\mathrm{GN}}$ for $N = 2$ and $\lambda = 4$ ($g = \sqrt{2}$) is depicted in Figure 6.3, as obtained obtained using our ansatz for excitations with bond dimension $D = 9$. The fundamental kink and fundamental fermion have received small second order energy contributions, which are negative around $p = 0$ and $p = \pi$. For $N = 3$, the zeroth order energy for the kink with one or two bound fermions is degenerate in the large g limit. These states are mixed by the kinetic term $\hat{H}''_{\mathrm{kinetic}}$ as defined in Eq. (6.29). Indeed, let us define the states

$$|\mathrm{K}_{1,1}\rangle = \left|\begin{matrix}\cdots & \uparrow & \uparrow & \downarrow & \cdots \\ \cdots & \uparrow & \uparrow & \downarrow & \cdots \\ \cdots & \uparrow & \downarrow & \downarrow & \cdots\end{matrix}\right\rangle, \qquad |\mathrm{K}_{2,1}\rangle = \left|\begin{matrix}\cdots & \uparrow & \downarrow & \downarrow & \cdots \\ \cdots & \uparrow & \downarrow & \downarrow & \cdots \\ \cdots & \uparrow & \uparrow & \downarrow & \cdots\end{matrix}\right\rangle,$$

$$|\mathrm{K}_{1,2}\rangle = \left|\begin{matrix}\cdots & \uparrow & \uparrow & \downarrow & \cdots \\ \cdots & \uparrow & \downarrow & \downarrow & \cdots \\ \cdots & \uparrow & \uparrow & \downarrow & \cdots\end{matrix}\right\rangle, \qquad |\mathrm{K}_{2,2}\rangle = \left|\begin{matrix}\cdots & \uparrow & \downarrow & \downarrow & \cdots \\ \cdots & \uparrow & \uparrow & \downarrow & \cdots \\ \cdots & \uparrow & \downarrow & \downarrow & \cdots\end{matrix}\right\rangle,$$

$$|\mathrm{K}_{1,3}\rangle = \left|\begin{matrix}\cdots & \uparrow & \downarrow & \downarrow & \cdots \\ \cdots & \uparrow & \uparrow & \downarrow & \cdots \\ \cdots & \uparrow & \uparrow & \downarrow & \cdots\end{matrix}\right\rangle, \qquad |\mathrm{K}_{2,3}\rangle = \left|\begin{matrix}\cdots & \uparrow & \uparrow & \downarrow & \cdots \\ \cdots & \uparrow & \downarrow & \downarrow & \cdots \\ \cdots & \uparrow & \downarrow & \downarrow & \cdots\end{matrix}\right\rangle.$$

We can then write expressions such as

$$\hat{H}''_{\text{kinetic}}\,|\mathrm{K}_{1,i}\rangle \sim \hat{T}\,|\mathrm{K}_{2,i}\rangle + \ldots \tag{6.33}$$

Making momentum superpositions of the states $|\mathrm{K}_{1,i}\rangle$ and $|\mathrm{K}_{2,i}\rangle$, we can write the perturbation $\hat{H}''_{\text{kinetic}}$ within the two-dimensional subspaces spanned by $\{|\mathrm{K}^{(p)}_{1,i}\rangle, |\mathrm{K}^{(p)}_{2,i}\rangle\}$ as

$$[\hat{H}''_{\text{kinetic}}] = \begin{bmatrix} 0 & \frac{1}{a}\mathrm{e}^{-\mathrm{i}p} \\ \frac{1}{a}\mathrm{e}^{\mathrm{i}p} & 0 \end{bmatrix}. \tag{6.34}$$

Hence, the degeneracy between the levels $|\mathrm{K}^{(p)}_{1,i}\rangle$ and $|\mathrm{K}^{(p)}_{2,i}\rangle$ is lifted and the linear combinations $|\mathrm{K}^{(p)}_{1,i}\rangle \pm |\mathrm{K}^{(p)}_{2,i}\rangle$ are given an energy shift $\pm 1/a$. The first order energy correction is thus momentum independent. The momentum dependence of these levels in Figure 6.3 is a result of second and higher order corrections, which explains why the shift is equal and not opposite for momenta $p = 0$ and $p = \pi$. The degeneracy between the three levels $i = 1,2,3$ does of course remain, and these levels transform according to the fundamental representation of SU(3). Combining the sectors around momentum $p = 0$ and momentum $p = \pi$, we can hope that they constitute a fundamental representation of O(6) in the continuum limit. Note finally that the topologically trivial state with $n = 2$ fermions is still stable at the current value of g. In fact, there is one more topologically trivial stable state at the current value of g. This is a state that transforms according to the trivial representation of SU(3) and was lying in the two-kink continuum for $g = \infty$. However, it is stabilized by the second order energy shift of the kinetic part of the Hamiltonian. This seems to be compatible with the fact that the second topologically trivial state in the continuum Gross-Neveu spectrum, while being unstable again, contains a state that transforms according to the trivial representation of the O(6) group. However, there should be 15 remaining states that transform according to an antisymmetric tensor of rank 2. The total degeneracy of this level is thus 16, while we have only 8 states in the expected energy range (4 at momentum $p = 0$ and 4 at momentum $p = \pi$). Since these states should become unstable in the continuum limit anyway, we cannot access them with our ansatz and we make no further attempt of trying to find all of them.

Figure 6.3 shows the masses obtained with our ansatz for various values of λ ranging down to $\lambda = 2/3$. As before, we have computed mass estimates $m^{(D)}$ for different values of the bond dimension D ranging up to $D \approx 500$, and then extrapolated these results to find an estimate $m^{(\infty)}$. The mass ratio of the fundamental fermion, which is now stable, and the fundamental kink seems to converge to the correct value of $2\sin(\pi/4) = \sqrt{2}$. Also, the kink state with bound fermion seems to become degenerate with the fundamental kink for $g \to 0$. However, the relative uncertainty on these ratios

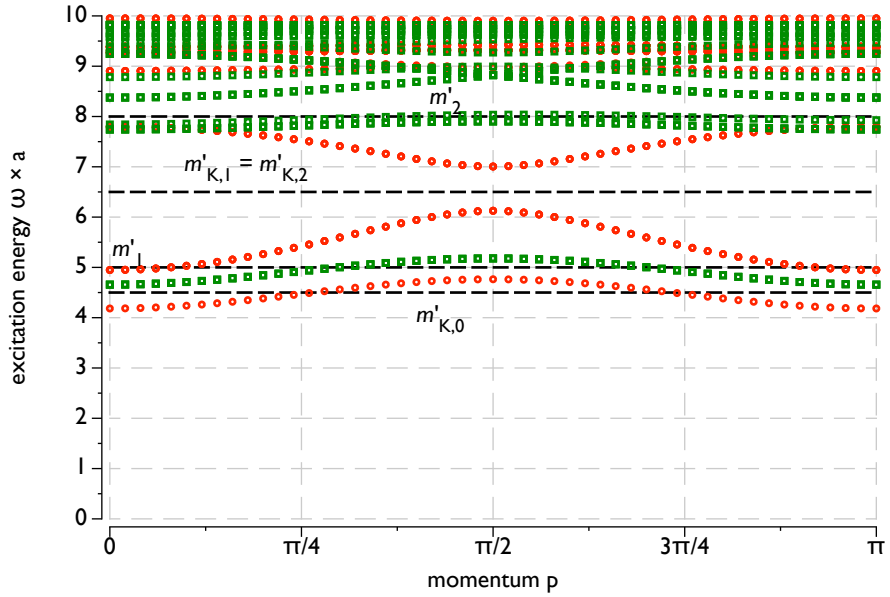

Figure 6.3: Spectrum of the Gross-Neveu lattice Hamiltonian $\hat{H}''_{\mathrm{GN}}$ (see Eq. (6.25)) for $N = 3$ and $g = \sqrt{2}$ using our ansatz for lattice excitations with bond dimension $D = 9$. Also indicated are the zeroth order excitation energies obtained in the large g limit.

is of the order of a few percent. In addition, the limiting behavior is only setting in so we would need to probe deeper into the continuum limit with higher accuracy in order to be able to conclude that the low-energy behavior of the lattice model under study is described by the $N = 3$ Gross-Neveu field theory in the critical limit. It is also not clear why our lattice model would flow to the Gross-Neveu field theory under the action of the renormalization group for $N = 3$, but not for $N = 2$. Unfortunately, going to larger values of N is almost impossible without drastically increasing the bond dimension D.

Clearly, the matrix product state approximation performed less well for the model under study in this section then for the spin models that were studied in Section 3. This is not due to the relativistic aspect of the current model. While studying the relativistic field theory requires that we take the continuum limit and approach closely to the critical point, computing with the matrix product state approximation is sufficiently efficient to allow to go to large values of the bond dimension where there is enough variability to also capture long range correlations. The main problem with the current model is that each fermion flavor or spin flavor contributes equally to the entanglement entropy, so that the total entanglement entropy is roughly N times higher than for a single spin model with comparable correlation length. However, the structure of this entanglement is quite trivial, since for large N the exact ground state will be very close to state that factorizes over the different flavors due to the monogamy property of entanglement.

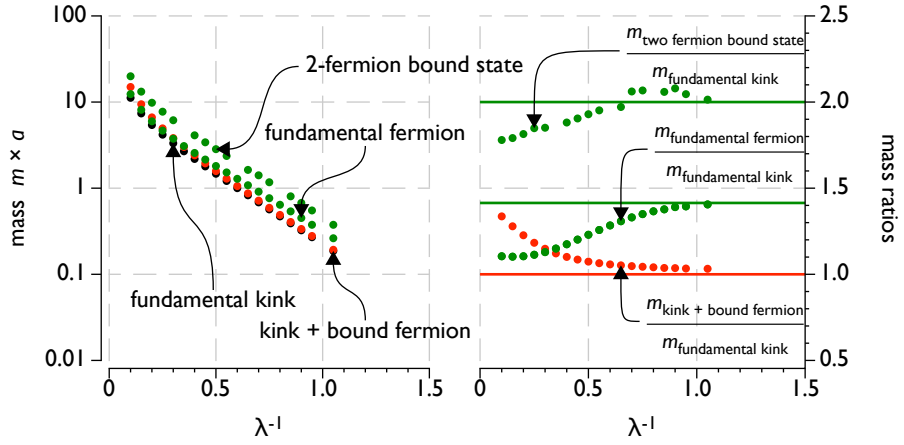

Figure 6.4: Masses of the elementary excitations of the Gross-Neveu lattice Hamiltonian $\hat{H}''_{\mathrm{GN}}$ as function of the inverse coupling constant $\lambda^{-1} = [(N-1)g^2]^{-1}$, as extrapolated from the results of our ansatz for lattice excitations for different values of the bond dimension ranging up to $D \approx 500$.

We can then approximate the ground state by a direct product of independent matrix product states over each flavor, which is an approach that we pursue using continuous matrix product states in the next section. However, there is no easy way to systematically improve this product state or to find a suitable middle way between the a mean field product of matrix product states and a single matrix product states where all flavors are included in a single physical index, which was the approach of the current section. Larger bond dimensions could be obtained by implementing explicit symmetry considerations, but this too becomes very complex for the general SU(N) group.

2. Relativistic fermions with continuous matrix product states

Jutho Haegeman, J. Ignacio Cirac, Tobias J. Osborne, Henri Verschelde, Frank Verstraete. "*Applying the variational principle to* $(1+1)$*-dimensional quantum field theories*". Physical Review Letters 105, 251601 (2010).

2.1. Introduction

In the previous section we have applied the matrix product state formalism to study a relativistic fermion model that was discretized and put on a lattice. When scaling the results back to the continuum limit, the model approaches criticality and the matrix product state approximation worsens. Since we also have a variational ansatz that is in itself a continuum limit of the matrix product state, we now investigate what

happens when we immediately apply this continuous matrix product state to a relativistic field theory. As we will show in this section, the absence of a physical cutoff a_{phys} in relativistic theories ($a_{\text{phys}} = 0$) implies $\xi_c/a_{\text{phys}} \to \infty$ and the sensitivity to high frequencies now becomes catastrophic: there are an infinite amount of high-energy modes and all physical expectation values obtained with our variational ansatz would be totally wrong. Feynman's criticism manifests itself in a very particular way and the only solution is to manually introduce an ultraviolet cutoff lengthscale $a = \Lambda^{-1}$.

Once again, we restrict to fermionic theories (in $d = 1$), since these are naturally defined in terms of creation and annihilation operators $\hat{\psi}_\alpha(x)$ and $\hat{\psi}^\dagger(x)_\alpha$ that can be used in the definition of the continuous matrix product state. The index α now runs over the values $\alpha = 1,2$ and labels the two components of the Dirac spinor in $d = 1$ spatial dimension. Since the ground state of relativistic field theories should definitely be translation invariant for $d = 1$, we can try to approximate this ground state with the uniform continuous matrix product state $|\Psi(Q,R_1,R_2)\rangle\rangle$ with bond dimension D. In order to satisfy the regularity condition Eq. (4.18), the matrices R_1 and R_2 have to anticommute. A representation for these matrices that automatically satisfies this property is constructed in Subsection 2.2 of Appendix A. The state $|\Phi(Q,R_1,R_2)\rangle\rangle$ arises by acting with the path-ordered exponential $\hat{U}(-\infty,+\infty)$ [see Eq. (4.7)] on the empty vacuum $|\Omega\rangle$, for which all levels are empty ($\hat{\psi}_\alpha|\Omega\rangle = 0$). For free Dirac fermions, the path-ordered exponential should thus fill the Dirac sea.

The kinetic energy term of relativistic fermions was already introduced in the previous section. With respect to the continuous matrix product state $|\Psi(Q,R_1,R_2)\rangle\rangle$, we obtain for the kinetic energy density (henceforth omitting the arguments of $|\Psi\rangle\rangle$)

$$\begin{aligned} -\frac{\mathrm{i}}{2}\langle\Psi|\hat{\psi}^\dagger(x)\alpha^x\frac{\mathrm{d}\hat{\psi}}{\mathrm{d}x}(x)|\Psi\rangle + \frac{\mathrm{i}}{2}\langle\Psi|\frac{\mathrm{d}\hat{\psi}^\dagger}{\mathrm{d}x}(x)\alpha^x\hat{\psi}(x)|\Psi\rangle \\ = \Im\Big\{\sum_{\alpha,\beta=1}^{2}\sigma^y_{\alpha\beta}(l|[Q,R_\alpha]\otimes\overline{R}_\beta|r)\Big\}, \\ = -(l|[Q,R_1]\otimes\overline{R}_2|r) + (l|[Q,R_2]\otimes\overline{R}_1|r). \end{aligned} \tag{6.35}$$

In order to obtain real coefficients, we have again chosen the convention $\alpha^x = \sigma^y$ and $\beta = \sigma^z$ for the Dirac matrices. The D^2-component vector $(l|$ and $|r)$ are, respectively, the left and right eigenvectors of the transfer operator $\breve{T} = Q\otimes\mathbb{1} + \mathbb{1}\otimes\overline{Q} + \sum_{\alpha=1}^{2} R_\alpha\otimes\overline{R}_\alpha$ corresponding to eigenvalue zero (see Subsection 1.6 of Chapter 4). We focus on the kinetic energy density as it is the dominant term in the ultraviolet region, which is the region responsible for divergences and for Feynman's first criticism. Eq. (6.35) indicates that the kinetic energy density is finite —and thus regularized— as long as the $D\times D$ matrices Q and R_α have finite entries. This regularization can be understood as a consequence of the internal momentum cutoff Λ that is built into the continuous matrix product state. As discussed in Subsection 1.6 of Chapter 4, the momentum occupation number $n_{\alpha,\beta}(p)$ [see Eq. (4.72)] decays for large values of the momentum as $\mathcal{O}(\Lambda^4/p^4)$

with Λ determined by the eigenvalues of the transfer operator $\check{T}$, provided that the regularity conditions [Eq. (4.18)] are satisfied. Since the relativistic kinetic energy is proportional to the momentum p, a p^{-4} decay of the momentum occupation number is indeed sufficient to regularize every relativistic field theory. Hence, Λ can be interpreted as a soft momentum cutoff.

2.2. Avoiding Feynman's criticism

We can now investigate how Feynman's "sensitivity to high frequencies" manifests itself for the continuous matrix product state. The problem is situated in the ability to describe a scale transformation $x \mapsto cx$ ($c > 0$) by an equivalent transformation $Q' = cQ$ and $R'_\alpha = \sqrt{c} R_\alpha$. Since this transformation does not change ($|l$ and $|r$), the kinetic energy density is simply multiplied by a factor c^2. In renormalizable theories, the kinetic energy has the highest scaling dimension, together with other terms with dimensionless coupling constants. These are thus the dominant terms in the ultraviolet region. However, in contrast to the non-relativistic case, the relativistic kinetic energy is not a positive definite operator and can acquire a negative expectation value. If $|\Psi[Q, R_1, R_2]\rangle$ is a continuous matrix product state for which the sum of terms with highest scaling dimension has a negative energy expectation value, then the total ground state energy can always be decreased by a scale transformation with c sufficiently large. Any variational optimization method will thus try to push $c \to \infty$, in order to approximate the divergent (kinetic) energy of the exact solution. Under such a transformation, the momentum occupation changes to $n'_{\alpha,\beta}(k) = n_{\alpha,\beta}(k/c)$ and the intrinsic cutoff determined by n' is given by $\Lambda' = c\Lambda$. Hence, the variational principle does not like the effective cutoff that is imposed by the continuous matrix product state and tries to shift it to infinity for relativistic theories.

This change of scale will be accompanied by a worse description of the low frequency region, as predicted by Feynman. The precise underlying cause for this effect in our variational class is that a cMPS can only accurately describe states with a finite amount of entanglement. The maximal entanglement entropy in a one-dimensional system with energy gap $\Delta \approx \xi_c^{-1}$ (in the relativistic case) and momentum or energy cutoff Λ is roughly given by $S \sim \log(\Lambda/\Delta)$, and a continuous matrix product state with bond dimension D proportional to $\mathcal{O}(\exp(S))$ should suffice to provide a good description. If D is too low to obtain a good approximation of the exact ground state, the variational method makes compromises in that part of the frequency spectrum that contributes least to the ground state energy, *i.e.* the low-frequency region. In non-relativistic systems, the cutoff is set by the particle density or thus by the chemical potential. But in a relativistic Hamiltonian, there is no physical cutoff and we only have the intrinsic momentum cutoff Λ of the cMPS. If we start from a cMPS with negative energy expectation value, the variational method can quickly lower the energy by shifting the cutoff to $\Lambda' = c\Lambda$ with $c \to \infty$. As c goes to infinity, all low-energy modes will eventually fall into the region that is poorly described and the description of any observable quantity will be

completely wrong for every finite value of the bond dimension D. This is schematically illustrated in Figure 6.5 for a free field theory, where we have single-particle energy levels that should be filled if they correspond to a negative energy level.

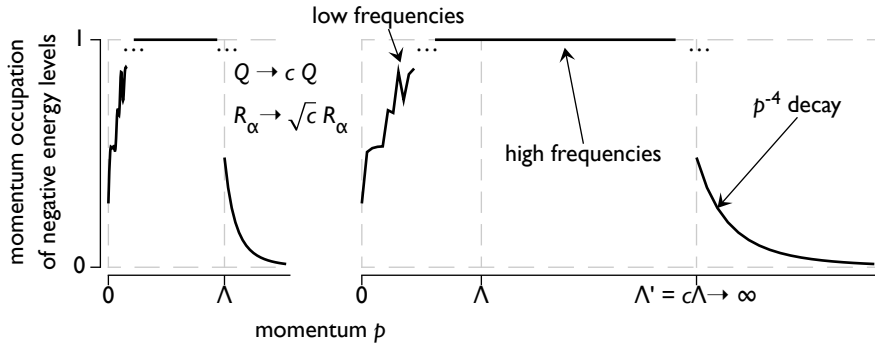

Figure 6.5: Hypothetical momentum distribution of an optimal cMPS for a free fermionic theory: high-frequency degrees of freedom are well-approximated up to a cutoff Λ, after which the momentum occupation decays as p^{-4}. Also shown is the effect of a scale transformation.

A solution is now straightforward as we can prevent c from running to infinity by imposing a constraint on the matrices Q and R_α: since Q has the dimension of a momentum and R_α has the dimension of the square root of a momentum, constraining the *norm* of Q and R_α prevents c from running and regularizes the resulting theory by introducing a scale, *i.e.* a dimensionful parameter, into the system, similar to what happens in analytical regularization techniques or lattice regularization. In the sequel, we will constrain the norm of the commutator $[Q,R_\alpha]$ by fixing the expectation value of $(\mathrm{d}\hat{\psi}^\dagger/\mathrm{d}x)(\mathrm{d}\hat{\psi}/\mathrm{d}x)$. Indeed, the expectation value of this operator is given by

$$\langle\Psi(\overline{Q},\overline{R}_1,\overline{R}_2)|(\mathrm{d}\hat{\psi}^\dagger/\mathrm{d}x)(\mathrm{d}\hat{\psi}/\mathrm{d}x)|\Psi(Q,R_1,R_2)\rangle = \sum_{\alpha=1}^{2}(l|[Q,R_\alpha]\otimes[\overline{Q},\overline{R}_\alpha]|r) \quad (6.36)$$

and —with l and r positive definite matrices— can rightfully be interpreted as a norm of $[Q,R_\alpha]$. In order to fix this expectation value, we add this term to the Hamiltonian with a Lagrange multiplier $1/\Lambda$, *i.e.* $\hat{H}_{\text{cutoff}} = \Lambda^{-1}\int \mathrm{d}x\,(\mathrm{d}\hat{\psi}^\dagger/\mathrm{d}x)(\mathrm{d}\hat{\psi}/\mathrm{d}x)$. This apparently arbitrary choice is motivated by the requirement that the constraint needs to penalize high values of the momentum p, to which $[Q,R_\alpha]$ is related by the calculational rules of continuous matrix product states. H_{cutoff} gives a p^2 contribution in momentum space, which is low enough to ensure a finite result in combination with a momentum occupation that decays as p^{-4}. It is, however, also strong enough to penalize high frequency modes, even the ones that give a contribution $-|p|$ to the (kinetic) energy. Put differently, it is a positive definite term with a higher scaling dimension than the relativistic kinetic energy. As such, it is non-renormalizable, which by means of Wilson's renormalization group indicates that it will be irrelevant for the description of the low-

frequency modes and cannot strongly influence the expectation value of observable quantities. Note that it also respects the chiral symmetry of the kinetic energy term. It does of course break relativistic invariance, which is inevitable when introducing a momentum cutoff in a Hamiltonian framework. We expect that any other norm constraint with similar properties and respecting the symmetries of the system should also work.

2.3. Casimir energy of the Dirac field

We now illustrate our arguments by applying them to relativistic fermion models. As a benchmark, we first consider free Dirac fermions with mass m, as described by the Hamiltonian $\hat{H}_{\mathrm{D}}$ given in Eq. (6.2). In the exact ground state of $\hat{H}_{\mathrm{D}} + \hat{H}_{\mathrm{cutoff}}$, the regularization procedure introduces a sharp cutoff at

$$p_{\mathrm{cutoff}} = \Lambda(1/2 + (1/4 + m^2/\Lambda^2)^{1/2})^{1/2}, \tag{6.37}$$

which is equal to Λ up to corrections of $\mathcal{O}(m^2/\Lambda^2)$. The cMPS ansatz will not be able to reproduce this sharp cutoff because it decays as p^{-4}. Indeed, this cutoff is not expected to be reproduced very well, because the new Hamiltonian is gapless at $p = \pm p_{\mathrm{cutoff}}$. However, this is not a problem, as we do not expect these high-frequency modes to influence physical properties. Note that both zeros in the dispersion relation occur at physically different momenta and do thus not result in fermion doubling.

Since we do not aim at reproducing the exact solution in the high-frequency regime, we cannot compare the corresponding energy as a measure of the accuracy of our solution. Instead, we have computed the momentum occupation of the exact positive (particle) and negative (antiparticle) levels according to the definitions

$$\langle \Psi(\overline{Q}, \overline{R}_1, \overline{R}_2) | \hat{a}^\dagger(p) \hat{a}(p') | \Psi(Q, R_1, R_2) \rangle = \delta(p' - p) n^{++}(p), \tag{6.38a}$$

$$\langle \Psi(\overline{Q}, \overline{R}_1, \overline{R}_2) | \hat{b}^\dagger(p) \hat{b}(p') | \Psi(Q, R_1, R_2) \rangle = \delta(p' - p) n^{--}(p), \tag{6.38b}$$

$$\langle \Psi(\overline{Q}, \overline{R}_1, \overline{R}_2) | \hat{a}^\dagger(p) \hat{b}(p') | \Psi(Q, R_1, R_2) \rangle = \delta(p' - p) n^{+-}(p), \tag{6.38c}$$

with $\hat{a}(p)$ the annihilator of particles with momentum p, and $\hat{b}(p)$ the creator of antiparticles with momentum $-p$, which is a slightly different convention from standard field theory books. These expectation values can be computed from $n_{\alpha,\beta}(p)$ using the relation with $\hat{\Psi}_\alpha(p)$, the Fourier transform of $\hat{\psi}_\alpha(x)$,

$$\hat{a}(p) = \frac{m + \omega(p)}{\sqrt{2\omega(p)[m + \omega(p)]}} \hat{\Psi}_1(p) - \frac{\mathrm{i}p}{\sqrt{2\omega(p)[m + \omega(p)]}} \hat{\Psi}_2(p), \tag{6.39a}$$

$$\hat{b}(p) = -\frac{\mathrm{i}p}{\sqrt{2\omega(p)[m + \omega(p)]}} \hat{\Psi}_1(p) + \frac{m + \omega(p)}{\sqrt{2\omega(p)[m + \omega(p)]}} \hat{\Psi}_2(p), \tag{6.39b}$$

with $\omega(p) = \sqrt{m^2 + p^2}$.

The results corresponding to the optimal uniform continuous matrix product state are shown in Figure 6.6. The exact solution has the Dirac sea filled ($n^{--}(p) = 1$) all the way up to p_{cutoff}, after which $n^{--}(p) = 0$ for $|p| > p_{\text{cutoff}}$, and $n^{++}(p) = n^{+-}(p) = 0$, $\forall\, p$. These results were obtained using a continuous matrix product state where Q and R_α act on an ancilla Hilbert space $\mathbb{H}_{\text{ancilla}} = \mathbb{C}^2 \otimes \mathbb{C}^2 \otimes \mathbb{C}^D$, so that the bond dimension is given by $4D$. The first two two-dimensional Hilbert spaces in $\mathbb{H}_{\text{ancilla}}$ accommodate auxiliary fermions which are used to impose the anticommutation relations on R_α. This construction can be found in Subsection 2.2 of Appendix A. It is clear from the results of Figure 6.6 that the low-energy behavior is approximated very well for the massive Dirac theory, and the accuracy greatly increases by increasing D. As anticipated, the cutoff behavior is approximated less well. In the case $m = 0$, the theory is critical and the low-energy behavior is also approximated less well. Here, Feynman's sensitivity to high frequencies is still at work since $\xi_c/a = \Lambda/m = +\infty$. Critical theories cannot be well described with (continuous) matrix product states. However, from the fact that $|n^{+-}| \approx 0$ for $m = 0$, we see that the algorithm automatically converges to a continuous matrix product state respecting chiral symmetry, except at $D = 2$.

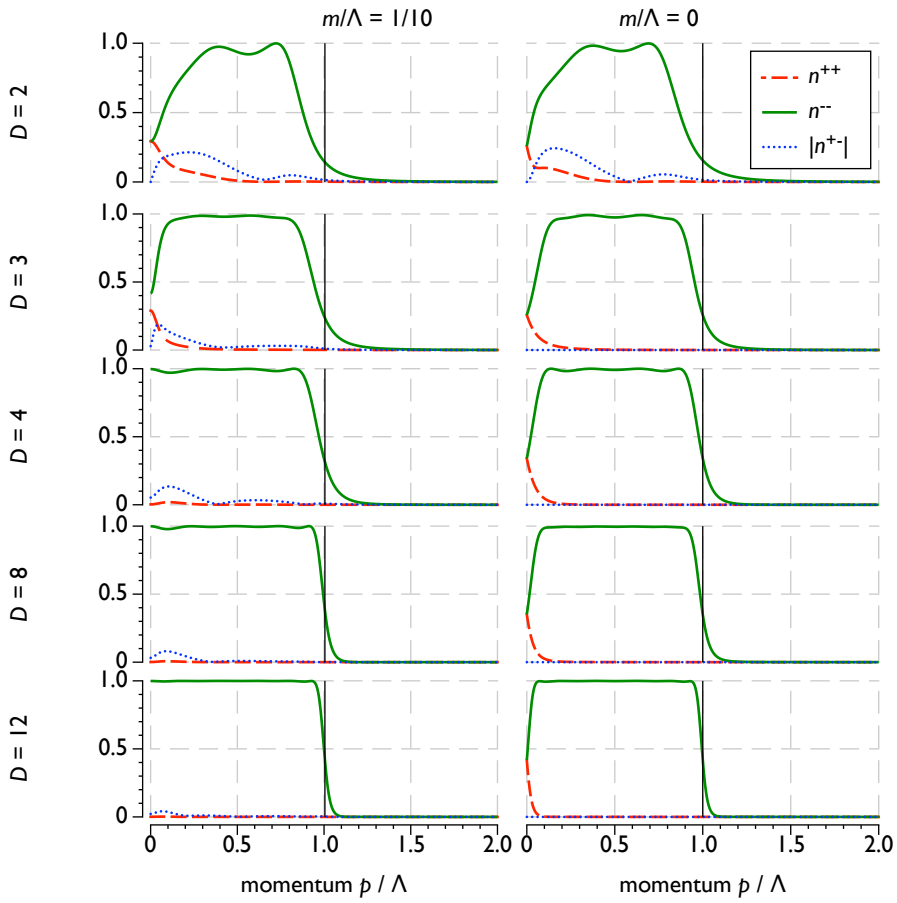

Figure 6.6: Momentum occupation of the antiparticle levels $n^{--}(k)$, the particle levels $n^{++}(k)$ and the mixing $|n^{+-}(k)|$ in a continuous matrix product state approximation of the ground state of the Dirac field with mass m. The ancilla space of the continuous matrix product state is $\mathbb{C}^2 \otimes \mathbb{C}^2 \otimes \mathbb{C}^D$. The vertical line indicates the position of the exact cutoff p_{cutoff} according to Eq. (6.37).

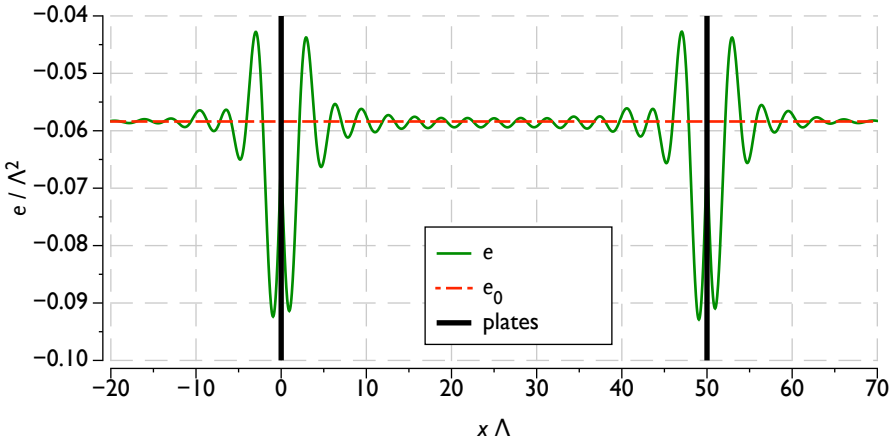

Figure 6.7: Energy density e for Dirac fermions with $m/\Lambda = 1/10$ in a system where 'plates' are present at position $x = 0$ and $x = 50/\Lambda$. These plates enforce the bag-model boundary conditions. The ground state energy density e_0 in the infinite vacuum is plotted for comparison.

To give a non-trivial example of what can be done with this approach we have also calculated the Casimir energy of the massive Dirac field. We simply recycle the matrices Q and R_α from the simulation above, and add suitable operators $B(x)$ to the ansatz at the location of the 'plates' or defects ($x = 0$ and $x = L$), which impose the correct boundary conditions. The boundary conditions only fix a part of these operators, the remaining elements can be used to optimize the energy with fixed Q and R_α. While a more complete approach would be to use x-dependent matrices Q and R_α, this simple approach works already quite well. It is similar in spirit to the ansatz we have used to study excitations in Chapter 3 and Chapter 4. By transferring information through the ancilla system, the boundary effect can spread over some distance $\mathcal{O}(\xi_c)$. All boundary effects can be incorporated in the boundary operators B. For relativistic fermions, one typically imposes the bag-model boundary conditions $(1 + in\gamma^x)\psi = 0$, where $\gamma^x = -i\sigma^x$ in our convention, and the outward normal $n = -1$ at $x = 0$ and $n = +1$ at $x = L$. Since these boundary conditions completely shield the fermions in the three different regions of space ($x < 0$, $0 < x < L$ and $x > L$), we can replace the boundary operators by appropriate left and right vectors in the ancilla, so that $B(0) = \boldsymbol{v}_R \boldsymbol{v}_L^\dagger$ and $B(L) = \boldsymbol{w}_R \boldsymbol{w}_L^\dagger$. The vectors are thus chosen such that $(R_1 + R_2)\boldsymbol{v}_R = (R_1 + R_2)\boldsymbol{w}_R = 0$ and $\boldsymbol{v}_L^\dagger(R_1 - R_2) = \boldsymbol{w}_L^\dagger(R_1 - R_2) = 0$. Using the structure of R_1 and R_2 (see Subsection 2.2 of Appendix A) one can show that these equations have a $2D$-dimensional solution space, and we can choose the particular solution that optimizes the energy. For the regions $x < 0$ and $x > L$, the energy is quadratic in respectively $\boldsymbol{v}_R$ and $\boldsymbol{w}_L$, and the solution follows straightforwardly. For the region $0 < x < L$, the energy is biquadratic in both $\boldsymbol{v}_L$ and $\boldsymbol{w}_R$ simultaneously. This optimization problem can be solved with a variational sweeping procedure, where we first optimize $\boldsymbol{v}_L$ for a fixed $\boldsymbol{w}_R$, then optimize $\boldsymbol{w}_R$ and then repeat this process until convergence.

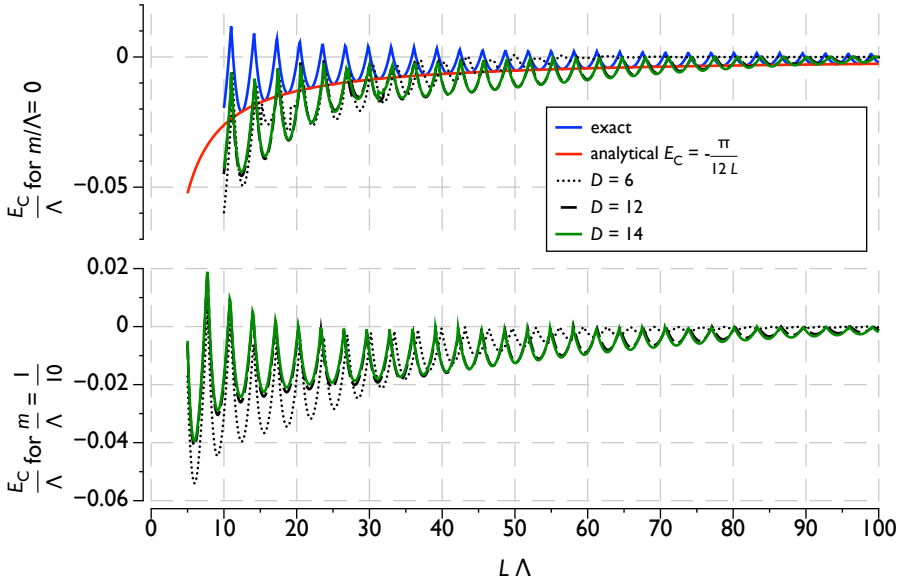

Figure 6.8: The total Casimir energy as a function of the distance L between the 'plates'. For $m = 0$, the exact Casimir energy, both in our model with cutoff, and analytically through zeta function regularization, is also displayed.

In Figure 6.7 we show the energy density for a particular configuration of 'plates' in the $(1+1)$-dimensional free-fermion model. A clear manifestation of the Fermi surface at a finite momentum p_{cutoff} is present in the form of Friedel oscillations. The Casimir energy E_C as a function of the distance L between the plates is plotted in Figure 6.8. The presence of the momentum cutoff, and thus of a finite particle density, also introduces a strong oscillatory behavior in $E_C(L)$, which was already observed in studies of the interaction energy between defects in one-dimensional quantum liquids [409, 410]. Local minima correspond to values of L where the number of allowed modes is such that the density of fermions between the plates is exactly equal to the density of fermions outside the plates. The sharp maxima appear when this condition is most strongly violated. In the limit $p_{\text{cutoff}} \to \infty$, the density of fermions is infinite, both in between and outside the plates, and the equal density condition is always satisfied. So the physical Casimir energy, which is expected to be cutoff independent, can be found by the envelope of the local minima. This is illustrated for the $m = 0$ case, where the exact solution in our model is compared to the value of the Casimir energy for massless Dirac fermions in $(1+1)$ dimensions, as calculated with zeta-function regularization, i.e. $E_C(L) = -\frac{\pi}{12L}$. Note that the Casimir energy will always have an asymptotic exponential decay when computed using a continuous matrix product state approximation, but that it can be well approximated at intermediate values of L. Because the Casimir energy is a *difference* of energies, approximate results can be lower than the exact solutions, as was also noticed for excitation energies. This is clearly the case in Figure 6.8. We attribute this effect to

the fact that the additional degrees of freedom present in the boundary vectors allow one to further optimize the energy in their immediate vicinity. Nevertheless, the qualitative behavior of the energy is already reproduced by this simple approach. For $m \neq 0$, exact results are much more difficult to obtain and we only show the approximative result.

2.4. Symmetry breaking in the Gross-Neveu model

As a final proof of principle, we study a theory with interactions. We therefore recycle the Gross-Neveu model that was discussed at length in the previous section. The Gross-Neveu Hamiltonian $\hat{H}_{\mathrm{GN}}$ is given in Eq. (6.3). We now study the large N behavior of the theory, and employ as a variational ansatz a product state of continuous matrix product states across the different fermion flavors. Because the exact ground state has S_N flavor symmetry (which is a subgroup of the actual $\mathsf{O}(2N)$ symmetry of the model), the nearest product state should also be invariant under S_N [411]. We can thus use the same continuous matrix product state for every flavor. This amounts to a Hartree-Fock approximation of the theory, where the self-interaction of the flavor is treated exactly, and the self-consistent mean-field approach is only applied to the interactions between different flavors. We add the same cutoff term $\hat{H}_{\mathrm{cutoff}}$ to the Hamiltonian for every fermion flavor, so as to respect the flavor symmetry. Since this term introduces our regularization parameter Λ, we know that the coupling constant g will have to depend on Λ in order to have a consistent theory. In the $N \to \infty$ limit, we can solve this problem exactly, and we obtain the well-known result for $\sigma = \lambda \langle \chi | \hat{\psi}^\dagger \sigma^z \hat{\psi} | \chi \rangle$ (with $\lambda = N g^2$)

$$\frac{\pi}{\lambda} = \int_0^{p_{\mathrm{cutoff}}} \frac{\mathrm{d}p}{\sqrt{\sigma^2 + p^2}} \quad \Rightarrow \quad |\sigma| \approx 2\Lambda \mathrm{e}^{-\frac{\pi}{\lambda(\Lambda)}}$$

where $p_{\mathrm{cutoff}} \approx \Lambda$ if $|\sigma| \ll \Lambda$. This indicates that the cutoff fixing term $\hat{H}_{\mathrm{cutoff}}$ has no effect other then what it is meant to do, *i.e.* introducing a cutoff. With the current Hartree-Fock ansatz based on continuous matrix product states, we can calculate an approximation for any λ and N. Numerical results with the mean-field approach are illustrated in Figure 6.9 for $N = \infty$. At strong coupling ($\lambda > 1$) they agree very well with the exact result. The discrepancies between the exact solution and the cMPS approximation for $N = \infty$ are clearly finite-D effects. They become more pronounced as σ / Λ gets smaller, since σ is exactly equal to the mass gap in the $N = \infty$ limit.

3. Relativistic fields with the continuous entanglement renormalization

In the previous section, we have shown that continuous matrix product states can be used to study relativistic field theories (in $d = 1$ spatial dimension), provided that we introduce

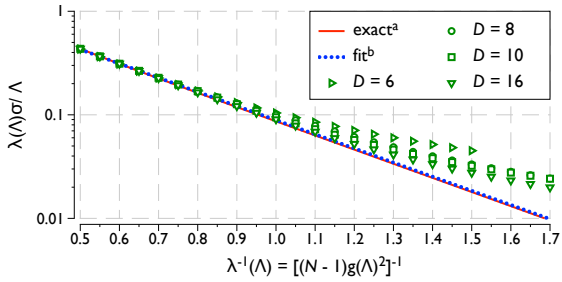

Figure 6.9: Expectation value of $\sigma = \langle\chi|\hat{\psi}^\dagger\sigma^z\hat{\psi}|\chi\rangle$ in the Gross-Neveu model as function of $\lambda(\Lambda)$ for $N=\infty$. A fit of the form $c_1 e^{-c_2/\lambda}$ to the numerical results for $\lambda^{-1}\leq 1$ at $D=16$ results in $c_2 = 3.142^{+0.047}_{-0.047}$ and $c_1 = 2.057^{+0.074}_{-0.072}$, to be compared to the exact values $c_1=2$ and $c_2=\pi$ (see main text).

an ultraviolet momentum cutoff Λ. The accuracy of the ground state approximation depends on the ratio $\xi_c\Lambda$, and we should choose the bond dimension as $\log D \sim \log(\xi_c\Lambda)$. For critical field theories, the continuous matrix product state approximation will always fail. So let us now try to use the continuous entanglement renormalization ansatz for the description of relativistic ground states. As before, we have to introduce a cutoff in order to define our ansatz. However, the continuous entanglement renormalization ansatz puts no restriction on $\xi_c\Lambda$ and we can even send $\Lambda\to\infty$ at the end of the process. Since we have not (yet) developed how to evaluate expectation values of interacting theories, we restrict to a description of free field theories using the Gaussian continuous entanglement renormalization ansatz.

3.1. Dirac fermions in $(1+1)$ dimensions

We start again with discussing relativistic fermions in one spatial dimension, described by $\hat{H}=\hat{H}_{\rm D}$ in Eq. (6.2). For each of the two Dirac components $\hat{\psi}_\alpha(x)$ —or $\hat{\Psi}_\alpha(p)$ in momentum space— we can use the generator of scale transformations $\hat{L}$ in Eq. (5.48). Since we have now two fermion flavors, the quadratic operator $\hat{K}(s)$ featuring in the Gaussian continuous entanglement renormalization ansatz can be more general and we are no longer restricted to odd Bogoliubov angles $f(-p)=-f(p)$. We now show that we can use the choice

$$\hat{K}(s)=\int \mathrm{d}p\, g(p;s)\left[\hat{\Psi}_1^\dagger(p)\hat{\Psi}_2(p)+\hat{\Psi}_2^\dagger(p)\hat{\Psi}_1(p)\right]=\mathrm{i}\int \mathrm{d}p\, g(p;s)\hat{\Psi}^\dagger(p)\gamma^1\hat{\Psi}(p), \quad (6.40)$$

with γ^1 defined in Eq. (6.5) and where we still choose $g(-p;s)=-g(p;s)$ even if this is not necessary. Since the Dirac Hamiltonian has real coefficients in real space, we can use that $g(p;s)$ contains only odd powers of p to show that $\mathrm{i}\hat{K}(s)$ has real coefficients with

respect to the real-space operators $\hat{\psi}_\alpha(x)$ and $\hat{\psi}^\dagger_\alpha(x)$. We now obtain

$$\hat{\Psi}_{1,\mathrm{R}}(p;s) = \cos(f(p;s))e^{s/2}\hat{\Psi}_1(e^s p) - \mathrm{i}\sin(f(p;s))e^{s/2}\hat{\Psi}_2(e^s p), \tag{6.41}$$

$$\hat{\Psi}_{2,\mathrm{R}}(p;s) = \cos(f(p;s))e^{s/2}\hat{\Psi}_2(e^s p) - \mathrm{i}\sin(f(p;s))e^{s/2}\hat{\Psi}_1(e^s p), \tag{6.42}$$

where the Bogoliubov angle satisfies $\frac{\partial}{\partial s}f(p,s) = g(e^s p, s)$ and we have again chosen $s_a = 0$. We can then compute the renormalized Hamiltonian as

$$\begin{aligned}
\hat{H}_{\mathrm{R}}(s) = \int \mathrm{d}p\ \Big[& -\mathrm{i}p\hat{\Psi}^\dagger_1(p;s)\hat{\Psi}_2(p;s) + \mathrm{i}p\hat{\Psi}^\dagger_2(p;s)\hat{\Psi}_1(p;s) \\
& + m\hat{\Psi}^\dagger_1(p;s)\hat{\Psi}_1(p;s) - m\hat{\Psi}^\dagger_2(p;s)\hat{\Psi}_2(p;s)\Big] \\
= \int \mathrm{d}p\, e^s\, & [-p\sin(2f(p;s)) + m\cos(2f(p;s))] \\
& \times \left[\hat{\Psi}^\dagger_1(e^s p)\hat{\Psi}_1(e^s p) - \hat{\Psi}^\dagger_2(e^s p)\hat{\Psi}_2(e^s p)\right] \\
& - \mathrm{i}e^s\, [p\cos(2f(p;s)) + m\sin(2f(p;s))] \\
& \times \left[\hat{\Psi}^\dagger_1(e^s p)\hat{\Psi}_2(e^s p) - \hat{\Psi}^\dagger_2(e^s p)\hat{\Psi}_1(e^s p)\right].
\end{aligned}$$

By setting $f(p) = f(p, s_\xi)$ and choosing $|\Omega\rangle$ such that $\hat{\Psi}_1(p)|\Omega\rangle = \hat{\Psi}^\dagger_2(p)|\Omega\rangle = 0$, we obtain for the energy functional

$$\begin{aligned}
E[\chi] = \langle\Omega|\hat{H}_{\mathrm{R}}(s_\xi)|\Omega\rangle &= -\int \mathrm{d}p\, \delta(e^s p - e^s p)e^s\, [-p\sin(2f(p)) + m\cos(2f(p))] \\
&= -\int \mathrm{d}x \int \frac{\mathrm{d}p}{2\pi}\, [-p\sin(2f(p)) + m\cos(2f(p))],
\end{aligned} \tag{6.43}$$

where we now use the minimal form $g(p/\Lambda, s) = \chi(s)p/\Lambda\Gamma(|p|/\Lambda)$ with $\chi(s)$ representing the variational degrees of freedom. As expected, the energy is extensive, but now the energy density diverges: for $|p| > \Lambda$, we have $f(p) = 0$ so that this region contributes a diverging part $-m\int_{|p|>\Lambda}\mathrm{d}p/2\pi$ to the integral. We can remove this divergence by subtracting from this energy the value $\langle\Omega|\hat{H}_{\mathrm{R}}(s_a)|\Omega\rangle = \langle\Omega|\hat{H}|\Omega\rangle$ that the vacuum $|\Omega\rangle$ would produce without the action of the unitary network $\hat{U}(s_\xi, s_a)$. We define the regularized energy density as

$$e_{\mathrm{reg}}[\chi] = -\int \frac{\mathrm{d}p}{2\pi}\left(-p\sin\left(2f(p)\right) - m\left[1 - \cos\left(2f(p)\right)\right]\right). \tag{6.44}$$

Using the functional derivative

$$\frac{\delta}{\delta\chi(s)}f(p) = e^s\frac{p}{\Lambda}\Gamma\left(e^s\frac{|p|}{\Lambda}\right), \tag{6.45}$$

in combination with the chain rule, we obtain the requirement ($\forall s \in [0, s_\xi]$)

$$\frac{\delta e_{\rm reg}[\chi]}{\delta \chi(s)} = \int \frac{{\rm d}p}{2\pi} \left[p\cos(2f(p)) + m\sin(2f(p)) \right] 2\frac{p}{\Lambda} e^s \Gamma\left(e^s \frac{|p|}{\Lambda} \right) = 0. \tag{6.46}$$

Since the integrand is an even function in p, this is a nontrivial relation. If we send $s_\xi \to \infty$ and again choose the sharp momentum cutoff $\Gamma(\kappa) = \theta(1-|\kappa|)$, this integral equation translates to

$$\left[p\cos(2f(p)) + m\sin(2f(p)) \right] = 0, \quad \forall |p| < \Lambda. \tag{6.47}$$

As expected, we need to reproduce the exact Bogoliubov angle below the cutoff, so that

$$f(p) = f_{\rm exact}(p)\theta(\Lambda - |p|) = -\frac{1}{2}\arcsin\left[\frac{p}{\sqrt{m^2+p^2}} \right] \theta(\Lambda - |p|). \tag{6.48}$$

This should be compared with

$$f(p) = \lim_{s_\xi \to \infty} \int_0^{s_\xi} g(e^s k; s)\,{\rm d}s = \frac{p}{\Lambda} \int_0^{\log(\Lambda/|p|)} {\rm e}^s \chi(s)\,{\rm d}s.$$

Differentiating the relation

$$\int_0^{\log(\Lambda/|p|)} {\rm e}^s \chi(s)\,{\rm d}s = -\frac{\Lambda}{2p}\arcsin\left[\frac{p}{\sqrt{m^2+p^2}} \right] \theta(\Lambda - |p|) = \\ -\frac{\Lambda}{2|p|}\arcsin\left[\frac{|p|}{\sqrt{m^2+p^2}} \right] \theta(\Lambda - |p|)$$

with respect to $|p|$ learns that

$$\chi(s) = -\frac{1}{2}\arcsin\left[\frac{{\rm e}^{-s}}{\sqrt{m^2/\Lambda^2 + {\rm e}^{-2s}}} \right] + \frac{{\rm e}^{-s} m/\Lambda}{2(m^2/\Lambda^2 + {\rm e}^{-2s})} \\ - \delta(s)\frac{1}{2}\arcsin\left[\frac{1}{\sqrt{m^2/\Lambda^2 + 1}} \right]. \tag{6.49}$$

There is now a diverging contribution at $s = 0$, that immediately sends the Bogoliubov angle from $f(p) = 0$ to $f(p) = -\arcsin[(m^2/\Lambda^2 + 1)^{-1/2}]/2$. The amplitude of this δ-spike does not decrease by increasing Λ, since every finite value of Λ is still infinitely far away from the physical cutoff (which does not exist or thus lies at infinity). For

arbitrary momenta p, this divergent part of the 'disentangling strength' $\chi(s)$ in the lowest layer contributes a term $p/\Lambda \arcsin[(m^2/\Lambda^2+1)^{-1/2}]/2$ to $f(p)$, so that its effect can be ignored and the δ-spike can be omitted in the limit $\Lambda \to \infty$.

The behavior at large values of s can be obtained from a Taylor expansion of the defining relation Eq. (6.49)

$$\lim_{s\to\infty} \chi(s) = -\frac{1}{3}\left(\frac{\Lambda}{m}\right)^3 e^{-3s} + \mathcal{O}(e^{-5s}),$$

from which we infer that for $s \gg \log(\Lambda/m)$, $\chi(s) \approx 0$ and we can stop the integration of the RG flow. Hence, for the massive case ($m \neq 0$), it is sufficient to choose $s_\xi \gg \log(\Lambda/m)$, which was to be expected as $m = \xi_c^{-1}$ is the energy gap of the model and thus defines the correlation length. Note, however, that as we try to restore the exact behavior for arbitrarily large p by setting $\Lambda \to \infty$ we automatically find the requirement $s_\xi \to \infty$. Indeed, any relativistic model exhibits quantum fluctuations across an infinite range of scales.

For the massless case $m = 0$, we obtain $\chi(s) = -\pi/4$ for $s > 0$. We then obtain

$$\mathrm{i}[\hat{K}, \hat{\Psi}_\alpha(p)] = (\pi/4)(p/\Lambda)\gamma^1_{\alpha,\beta}\hat{\Psi}_\beta(p), \qquad \text{for } |p| < \Lambda. \tag{6.50}$$

While we need a finite cutoff scale Λ to define the action of the continuous entanglement renormalization ansatz, we can send $\Lambda \to \infty$ for the computation of the critical exponents. Hence, the disentangler $\hat{K}$ does not contribute to the critical exponents, and the scaling operators are just the field operators $\hat{\Psi}_\alpha(x)$ and $\hat{\Psi}^\dagger_\alpha(x)$ with their canonical scaling dimension. This was to be expected for a free theory.

3.2. Dirac fermions in $(3+1)$ dimensions

The Dirac Hamiltonian for massive fermions with mass m in $(3+1)$ dimensions is given by

$$\hat{H} = \int \hat{\psi}^\dagger(\vec{x})\left(-\mathrm{i}\vec{\alpha}\cdot\vec{\nabla} + m\beta\right)\hat{\psi}(\vec{x})\,\mathrm{d}^3x, \tag{6.51}$$

with the Dirac spinor $\hat{\psi}(\vec{x})$ now containing four components, and the Dirac matrices $\vec{\alpha}$ and β given by

$$\alpha^i = \begin{bmatrix} 0 & \sigma^i \\ \sigma^i & 0 \end{bmatrix} = \sigma^x \otimes \sigma^i, \qquad \beta = \begin{bmatrix} \mathbb{1} & 0 \\ 0 & -\mathbb{1} \end{bmatrix} = \sigma^z \otimes \mathbb{1}, \tag{6.52}$$

and $\mathbb{1} = \mathbb{1}_2$ the 2×2 unit matrix. We now try to generalize $\hat{K}(s)$ from Eq. (6.40) to

$$\hat{K}(s) = \mathrm{i}\int \chi(s)\Gamma(\|\vec{p}\|/\Lambda)\left[\hat{\Psi}^\dagger(\vec{p})\left(\frac{\vec{p}\cdot\vec{\gamma}}{\Lambda}\right)\hat{\Psi}(\vec{p})\right]\mathrm{d}^3p, \tag{6.53}$$

with $\vec{\gamma}$ the spatial components Dirac's γ matrices given by

$$\gamma^0 = \gamma_0 = \beta \qquad\qquad \gamma^i = -\gamma_i = \beta\alpha^i. \tag{6.54}$$

The renormalization trajectories of the field operators are now given by

$$\hat{\Psi}_{\mathrm{R}}(\vec{p};s) = \cos\left(f(||\vec{p}||;s)\right)e^{s/2}\hat{\Psi}(e^s\,\vec{p}) + \sin\left(f(||\vec{p}||;s)\right)e^{s/2}\left(\frac{\vec{p}}{||\vec{p}||}\cdot\vec{\gamma}\right)\hat{\Psi}(e^s\,p), \tag{6.55}$$

with

$$\frac{\partial f}{\partial s}(p;s) = \chi(s)\frac{\mathrm{e}^s\,p}{\Lambda}\Gamma(p\mathrm{e}^s/\Lambda). \tag{6.56}$$

The renormalized Hamiltonian is thus given by

$$\begin{aligned}\hat{H}_{\mathrm{R}}(s) = \int \mathrm{d}^3\,p\,\Big[&\mathrm{e}^s\cos\left(2f(||\vec{p}||;s)\right)\hat{\Psi}^\dagger(\mathrm{e}^s\,\vec{p})\left(\vec{p}\cdot\vec{\alpha}+m\beta\right)\hat{\Psi}(\mathrm{e}^s\,\vec{p})\\ &+\mathrm{e}^s\sin\left(2f(||\vec{p}||;s)\right)\hat{\Psi}^\dagger(\mathrm{e}^s\,\vec{p})\left(\vec{p}\cdot\vec{\alpha}+m\beta\right)\left(\beta\frac{\vec{\alpha}\cdot\vec{p}}{||\vec{p}||}\right)\hat{\Psi}(\mathrm{e}^s\,\vec{p})\Big].\end{aligned} \tag{6.57}$$

If we now define the vacuum $|\Omega\rangle$ such that

$$\hat{\psi}_1(\vec{x})|\Omega\rangle = \hat{\psi}_2(\vec{x})|\Omega\rangle = \hat{\psi}_3^\dagger(\vec{x})|\Omega\rangle = \hat{\psi}_4^\dagger(\vec{x})|\Omega\rangle = 0, \qquad \forall x, \tag{6.58}$$

then we obtain

$$\begin{aligned}E_{\mathrm{reg}}[\chi] &= \langle\Omega|\hat{H}_{\mathrm{R}}(s_\xi)|\Omega\rangle - \langle\Omega|\hat{H}|\Omega\rangle\\ &= -2\int \mathrm{d}^3x\int\frac{\mathrm{d}^3\,p}{(2\pi)^3}\left[m\left(\cos\left(2f(||\vec{p}||)\right)-1\right)-||\vec{p}||\sin\left(2f(||\vec{p}||)\right)\right],\end{aligned} \tag{6.59}$$

with $f(||\vec{p}||) = f(||\vec{p}||;s_\xi)$. The variational principle requires that

$$\frac{\delta e_{\mathrm{reg}}[\chi]}{\delta\chi(s)} = 2\int\frac{\mathrm{d}^3\,p}{(2\pi)^3}\left[m\sin\left(2f(||\vec{p}||)\right)+||\vec{p}||\cos\left(2f(||\vec{p}||)\right)\right]2\frac{||\vec{p}||}{\Lambda}\chi(s)\Gamma(||\vec{p}||/\Lambda\mathrm{e}^s). \tag{6.60}$$

If we choose again the hard momentum cutoff function $\Gamma(\kappa) = \theta(1-|\kappa|)$, then the variational principle imposes the same condition as in Eq. (6.47). Hence we obtain the same solution $\chi(s)$ as in Eq. (6.49).

What can we learn from this? In contrast to the case of non-relativistic fermions discussed in Section 3.4 of the previous chapter, it is possible to create a rotation invariant quadratic expression that is odd in the momentum $\vec{p}$ for the multi-component relativistic fermion spinor. In fact, we can rewrite the fundamental operator featuring in $\hat{K}(s)$ in a relativistic

fashion as

$$\hat{\Psi}^\dagger(\vec{p})(\vec{p}\cdot\vec{\gamma})\hat{\Psi}(\vec{p}) = -\hat{\overline{\Psi}}(\vec{p})(p_i\gamma^0\gamma^i)\hat{\Psi}(\vec{p}) = \frac{\mathrm{i}}{2}p_i\hat{\overline{\Psi}}(\vec{p})\sigma^{0i}\hat{\Psi}(\vec{p})$$

with $\overline{\Psi} = \Psi\gamma^0$ and

$$\sigma^{\mu\nu} = \frac{\mathrm{i}}{2}[\gamma^\mu, \gamma^\nu]. \tag{6.61}$$

It can easily be shown that the bilinear $\hat{\overline{\psi}}(\vec{x})\sigma^{\mu\nu}\hat{\psi}(\vec{x})$ transforms as an antisymmetric tensor under a general Lorentz transformations $x^\mu \leftarrow \Lambda^\mu_{\ \nu}x^\nu$. Hence, the combination $p_i\hat{\overline{\Psi}}(\vec{p})\sigma^{0i}\hat{\Psi}(\vec{p})$ featuring in $\hat{K}(s)$ transforms as the zero-component of a four-vector. It is invariant under rotations but not under Lorentz boosts. This was to be expected, since we are working in a Hamiltonian framework where we are imposing a cutoff in momentum space, which is a manifestly Lorentz non-invariant operation.

Note that the representation of the ground state of the higher-dimensional Dirac field as a (Gaussian) continuous entanglement renormalization ansatz implies that this ground state satisfies the area law, both for nonzero and zero mass m. More precisely, with the hard momentum cutoff we have filled the Dirac sea up to $||\vec{p}|| \leq \Lambda$. In the massless case, this looks very much like a Fermi sea with Fermi momentum $k_{\mathrm{F}} = \Lambda$. However, unlike the Fermi sea this massless Dirac sea does not produce a logarithmic divergence of the area law for entanglement entropy.

3.3. Klein-Gordon bosons in $(d+1)$ dimensions

As a final example we study relativistic free (scalar, uncharged) bosons with mass m in $(d+1)$ dimensions, which are described by the Klein Gordon Hamiltonian

$$\begin{aligned}\hat{H} &= \int \mathrm{d}^d x\, \frac{1}{2}\left[\hat{\pi}(\vec{x})^2 + \left(\vec{\nabla}\hat{\phi}(\vec{x})\right)^2 + m^2\hat{\phi}(\vec{x})^2\right], \\ &= \int \mathrm{d}^d p\, \frac{1}{2}\left[\hat{\Pi}(\vec{p})\hat{\Pi}(-\vec{p}) + (|\vec{p}|^2 + m^2)\hat{\Phi}(\vec{p})\hat{\Phi}(-\vec{p})\right],\end{aligned} \tag{6.62}$$

where the field operator $\hat{\phi}(\vec{x})$ and its conjugate momentum $\hat{\pi}(\vec{x})$ are hermitian operators satisfying the canonical commutation relation $[\hat{\phi}(\vec{x}), \hat{\pi}(\vec{x}')] = \mathrm{i}\delta(\vec{x}-\vec{x}')$, and the corresponding momentum-space operators satisfy $\hat{\Phi}(\vec{p})^\dagger = \hat{\Phi}(-\vec{p})$, $\hat{\Pi}(\vec{p})^\dagger = \hat{\Pi}(-\vec{p})$ and $[\hat{\Phi}(\vec{p}), \hat{\Pi}(-\vec{p}')] = \mathrm{i}\delta(\vec{p}-\vec{p}')$.

We have already encountered the operators $\hat{\phi}(\vec{x})$ and $\hat{\pi}(\vec{x})$ as scaling operators in the critical limit of the non-relativistic boson model studied in Subsection 3.3 of Chapter 4. Their scaling dimension was modified from the value $d/2$ for the creation and annihilation operators $\hat{\psi}(\vec{x})$ and $\hat{\psi}^\dagger(\vec{x})$ to respectively $(d-1)/2$ for $\hat{\phi}(\vec{x})$ and $(d+1)/2$ for $\hat{\pi}(\vec{x})$. Whether we formulate the unitary operator of the continuous entanglement

renormalization ansatz in terms of the creation and annihilation operators $\hat{\psi}(\vec{x})$ and $\hat{\psi}^\dagger(\vec{x})$ or in terms of the field operator $\hat{\phi}(\vec{x})$ and its canonical conjugate momentum $\hat{\pi}(\vec{x})$ does not make any difference, since both are trivially equivalent. What does make a difference, however, is whether we use the non-relativistic scaling generator $\hat{L}$ that generates equal scaling dimensions $d/2$ for $\hat{\phi}(\vec{x})$ and $\hat{\pi}(\vec{x})$, or we define a new relativistic scaling generator $\hat{L}'$ given by

$$\begin{aligned}\hat{L}' &= -\frac{1}{2}\int \mathrm{d}^d x \left[\hat{\pi}(\vec{x})\vec{x}\cdot\vec{\nabla}\hat{\phi}(\vec{x}) + \vec{x}\cdot\vec{\nabla}\hat{\phi}(\vec{x})\hat{\pi}(\vec{x})\right. \\ &\qquad\left. + \frac{d-1}{2}\hat{\phi}(\vec{x})\hat{\pi}(\vec{x}) + \frac{d-1}{2}\hat{\pi}(\vec{x})\hat{\phi}(\vec{x})\right], \\ &= +\frac{1}{2}\int \mathrm{d}^d p \left[\hat{\Pi}(-\vec{p})\vec{p}\cdot\vec{\boldsymbol{\nabla}}\hat{\Phi}(\vec{p}) + \vec{p}\cdot\vec{\boldsymbol{\nabla}}\hat{\Phi}(\vec{p})\hat{\Pi}(-\vec{p})\right. \\ &\qquad\left. + \frac{d+1}{2}\hat{\Pi}(-\vec{p})\hat{\Phi}(\vec{p}) + \frac{d+1}{2}\hat{\Phi}(\vec{p})\hat{\Pi}(-\vec{p})\right].\end{aligned} \tag{6.63}$$

Indeed, in the pure scaling case $\hat{K} = 0$, the scaling operator $\hat{L}' = \hat{U}(0,s)^\dagger \hat{U}(0,s)$ results in the renormalization group equations

$$\begin{aligned}\frac{\partial}{\partial s}\hat{\phi}_{\mathrm{R}}(\vec{x};s) &= \mathrm{i}[\hat{L}'(s), \hat{\phi}_{\mathrm{R}}(\vec{x};s)] = -\left(\vec{x}\cdot\vec{\nabla} + \frac{d-1}{2}\right)\phi_{\mathrm{R}}(\vec{x};s), \\ \frac{\partial}{\partial s}\pi_{\mathrm{R}}(\vec{x};s) &= \mathrm{i}[\hat{L}'(s), \hat{\pi}_{\mathrm{R}}(\vec{x};s)] = -\left(\vec{x}\cdot\vec{\nabla} + \frac{d+1}{2}\right)\pi_{\mathrm{R}}(\vec{x};s),\end{aligned}$$

from which we obtain

$$\hat{\phi}_{\mathrm{R}}(\vec{x};s) = e^{-s\frac{d-1}{2}}\hat{\phi}(e^{-s}\vec{x}), \qquad \hat{\pi}_{\mathrm{R}}(\vec{x};s) = e^{-s\frac{d+1}{2}}\hat{\pi}(e^{-s}\vec{x}), \tag{6.64}$$

and, for the momentum space operators,

$$\hat{\Phi}_{\mathrm{R}}(\vec{p};s) = e^{s\frac{d+1}{2}}\hat{\Phi}(e^{s}\vec{p}), \qquad \hat{\Pi}_{\mathrm{R}}(\vec{p};s) = e^{s\frac{d-1}{2}}\hat{\Pi}(e^{s}\vec{p}). \tag{6.65}$$

Hence, the relativistic scaling generator $\hat{L}'$ automatically produces the correct relativistic scaling dimensions, which agree with the physical units of these operators.

In order to fully specify the Gaussian continuous entanglement renormalization ansatz $|\Psi[\hat{K}]\rangle$, we also have to define a Gaussian reference state $|\Omega\rangle$. A general factorized Gaussian state with width Δ^{-1} can be defined via

$$\left[\sqrt{\frac{\Delta}{2}}\hat{\phi}(\vec{x}) + \mathrm{i}\sqrt{\frac{1}{2\Delta}}\hat{\pi}(\vec{x})\right]|\Omega\rangle = 0, \tag{6.66}$$

where the operator between the square brackets can of course be interpreted as one particular choice of annihilation operator $\hat{\psi}(\vec{x})$ depending on an energy scale Δ. However, this reference state is not invariant under the relativistic scaling transformation because $|\Omega'\rangle = e^{isL}|\Omega\rangle$ is an equivalent factorized Gaussian state with inverse width $\Delta' = e^s\Delta$. Only the very singular choices $\Delta = 0$ or $\Delta = +\infty$ produce a reference vacuum $|\Omega\rangle$ that is invariant under relativistic scaling transformations.

For any inverse width Δ, the reference state $|\Omega\rangle$ is however invariant under the action of the non-relativistic scaling transformation generated by $\hat{L}$, which is in terms of the fields $\hat{\phi}(\vec{x})$ and $\hat{\pi}(\vec{x})$ given by

$$\hat{L} = -\frac{1}{2}\int \mathrm{d}^d x \left[\hat{\pi}(\vec{x})\vec{x}\cdot\vec{\nabla}\hat{\phi}(\vec{x}) + \vec{x}\cdot\vec{\nabla}\hat{\phi}(\vec{x})\hat{\pi}(\vec{x}) + \frac{d}{2}\hat{\phi}(\vec{x})\hat{\pi}(\vec{x}) + \frac{d}{2}\hat{\pi}(\vec{x})\hat{\phi}(\vec{x})\right]. \tag{6.67}$$

Since $\hat{L}$ also generates the desired scaling behavior of the arguments, we use the operator L in combination with $K(s)$. Below the cutoff, only the effect of $\hat{K}(s) + L = \hat{K}'(s) + \hat{L}'$ is uniquely defined and we can absorb the correction for the relativistic scaling dimensions in $\hat{K}(s)$, as happened automatically in the critical limit of the non-relativistic boson model in the previous chapter. Above the cutoff, the scaling of modes is irrelevant if $\hat{L}|\Omega\rangle = 0$. Let us now investigate the effect of choosing $\hat{K}(s)$ as

$$K(s) = \int \mathrm{d}^d p\, \frac{1}{2}\left[g(\vec{p}/\Lambda, s)\hat{\Phi}(\vec{p})\hat{\Pi}(-\vec{p}) + \overline{g(\vec{p}/\Lambda, s)}\hat{\Pi}(-\vec{p})\hat{\Phi}(\vec{p})\right], \tag{6.68}$$

which results in renormalization trajectories

$$\hat{\Phi}_{\mathrm{R}}(\vec{p}; s) = \mathrm{e}^{+f(+\vec{p};s)}\mathrm{e}^{+s\frac{d}{2}}\hat{\Phi}(\mathrm{e}^s\vec{p}), \tag{6.69}$$

$$\hat{\Pi}_{\mathrm{R}}(\vec{p}; s) = \mathrm{e}^{-f(-\vec{p};s)}\mathrm{e}^{-s\frac{d}{2}}\hat{\Pi}(\mathrm{e}^s\vec{p}), \tag{6.70}$$

with

$$f(\vec{p}; s) = \int_0^s \frac{g(e^w\vec{p}/\Lambda, w) + \overline{g(-e^w\vec{p}/\Lambda, w)}}{2}\,\mathrm{d}w. \tag{6.71}$$

We can choose $g(\vec{p}/\Lambda, s)$ a real-valued function that is even in the first argument, so that $f(\vec{p}; s) = f(-\vec{p}; s)$. We again parameterize $g(\vec{p}/\Lambda, s)$ as $\gamma(\vec{p}/\Lambda, s)\Gamma(||\vec{p}||/\Lambda)$ with Γ the cutoff function. In addition, it turns out to be sufficient to take the lowest order form $\gamma(\vec{p}/\Lambda, s) = \chi(s)$. Note that $\hat{K}(s)$ is rotation invariant (trivially) but also transforms as the zero component of a relativistic four-vector under general Lorentz transformations, since $\hat{\phi}(\vec{x})$ is a relativistic scalar while $\hat{\pi}(\vec{x}) \sim \mathrm{d}\hat{\phi}(\vec{x})/\mathrm{d}t$. This was also the case for the operator $\hat{K}(s)$ of Eq. (6.53) for the free Dirac field.

In order to evaluate the energy functional, we first calculate $\hat{H}_{\mathrm{R}}(s)$ as

$$\hat{H}_{\mathrm{R}}(s) = \int \mathrm{d}^d p\, \frac{1}{2}\Big[e^{-2f(\vec{p};s)}e^{sd}\hat{\Pi}(e^s\vec{p})\hat{\Pi}(-e^s\vec{p})$$

$$+(||\vec{p}||^2+m^2)e^{+2f(\vec{p};s)}e^{sd}\hat{\Phi}(e^s\vec{p})\hat{\Phi}(-e^s\vec{p})\Big]. \quad (6.72)$$

Using the gaussian reference state with width Δ^{-1} we obtain

$$\langle\Omega|\widehat{\phi}(\vec{p})\widehat{\phi}(\vec{p}')|\Omega\rangle=\frac{1}{2\Delta}\delta(\vec{p}+\vec{p}') \qquad \langle\Omega|\widehat{\pi}(\vec{p})\widehat{\pi}(\vec{p}')|\Omega\rangle=\frac{\Delta}{2}\delta(\vec{p}+\vec{p}'), \quad (6.73)$$

and thus find

$$\begin{aligned}E[\chi]&=\langle\Omega|\hat{H}_{\mathrm{R}}(s_\xi)|\Omega\rangle-\langle\Omega|\hat{H}|\Omega\rangle\\&=\int \mathrm{d}^dx\int\frac{\mathrm{d}^dp}{(2\pi)^d}\frac{1}{4}\left[(e^{-2f(\vec{p})}-1)\Delta+\frac{|\vec{p}|^2+m^2}{\Delta}(e^{+2f(\vec{p})}-1)\right], \quad (6.74)\end{aligned}$$

where $f(\vec{p})=f(\vec{p};s_\xi)$ and we have once again subtracted the energy expectation value of the reference vacuum, in order to eliminate the diverging contribution coming from the modes above the cutoff. The variational optimization results in

$$\frac{\delta e[\chi]}{\delta\chi(s)}=-\int\frac{\mathrm{d}^dp}{(2\pi)^d}\frac{1}{2}\left[e^{-2f(\vec{p})}\Delta-\frac{|\vec{p}|^2+m^2}{\Delta}e^{+2f(\vec{p})}\right]\Gamma(|\vec{p}|/\Lambda e^{-s})=0. \quad (6.75)$$

Using the hard cutoff function $\Gamma(\kappa)=\theta(1-|\kappa|)$, the variational principle tries to set $f(\vec{p})$ equal to the exact solution

$$f(\vec{p})=f_{\mathrm{exact}}(\vec{p})\theta(\Lambda-||\vec{p}||)=-\frac{1}{2}\log\left(\frac{\sqrt{m^2+||\vec{p}||^2}}{\Delta}\right)\theta(\Lambda-||\vec{p}||), \quad (6.76)$$

up to the cutoff $||\vec{p}||\leq\Lambda$. By sending $s_\xi\to\infty$, we can write

$$f(\vec{p})=\int_0^{\log(\Lambda/||\vec{p}||}\chi(w)\,\mathrm{d}w, \quad (6.77)$$

and by differentiating $f(\vec{p})=f_{\mathrm{exact}}(\vec{p})\theta(\Lambda-||\vec{p}||)$ with respect to $||\vec{p}||$, we find

$$\chi(s)=\frac{1}{2}\frac{e^{-2s}}{e^{-2s}+(m/\Lambda)^2}-\frac{1}{2}\log\left(\frac{\sqrt{m^2+\Lambda^2}}{\Delta}\right)\delta(s). \quad (6.78)$$

As before, we have a diverging contribution in the lowest layer ($s=0$) that immediately imposes the correct solution for the momenta at $||\vec{p}||=\Lambda$. We still have the inverse width Δ of the reference vacuum as a variational parameter, and we can now choose $\Delta\approx\Lambda$, so that the amplitude of the δ-spike goes to zero if we send $\Lambda\to\infty$. The δ-spike would not feature at all if we set $\Delta=\sqrt{m^2+\Lambda^2}$, but this is only possible because we can exactly solve this free theory. For $s\ll\log(\Lambda/m)$ —and thus for all s in the massless case— the

disentangling strength $\chi(s)$ is (approximately) equal to $\chi(s) \approx 1/2$, which restores the correct relativistic scaling dimensions of $\hat{\phi}(\vec{x})$ and $\hat{\pi}(\vec{x})$. However, for $s \gg \log(\Lambda/m)$, the disentangling strength goes to zero and we can stop the integration at some finite $s_\xi \gg \log(\Lambda/m)$. Hence, at the trivial massive fixed point, the non-relativistic scaling operator $\hat{L}$ generates the correct scaling dimensions. Put differently, at the massive fixed point the scaling operators are given by the non-relativistic creation and annihilation operator.

4. Summary and conclusion

In this final chapter we have illustrated how the three variational ansätze that were introduced in this dissertation can be applied to relativistic field theories. Using matrix product states involves writing down a lattice Hamiltonian for which the field theory describes the low energy behavior close to its critical point. The nice thing is that the lattice provides a natural cutoff that regularizes the field theory. Since this was pretty much the only method available until recently, a lot of research on good lattice Hamiltonians exist. However, this does not imply that the construction of a suitable Hamiltonian is problem free, especially not for relativistic fermions, which are plagued by the fermion doubling problem. Since we have to study the lattice Hamiltonian in the vicinity of its critical point, one can argue whether matrix product states are an adequate choice. While using the multi-scale entanglement renormalization ansatz might be a better alternative, matrix product states are sufficiently efficient to produce a high accuracy deep in the continuum limit, *i.e.* when the correlation length is already of the order of 100 sites. Using the approach constructed in Chapter 3, they easily allow to determine the excitation spectrum, which is one of the main interesting quantities.

The development of continuous matrix product states has opened a new alternative for studying relativistic field theories. While these do not require to discretize the field theory —and thus allow to overcome such problems as the fermion doubling problem— another kind or regularization still has to be provided. We have taken a first step in showing how such a regularization scheme for fermionic theories can be constructed. Bosonic theories and gauge theories will however require different strategies, so that additional research is required in this direction. In addition, a further investigation of the effect of the regularization procedure on *e.g.* the low energy excitation spectrum is still in order.

The most natural ansatz for relativistic field theories is without doubt the continuous entanglement renormalization ansatz. This ansatz has no intrinsic difficulties with the infinite range of quantum fluctuations that is present in relativistic theories. In addition, it naturally defines a renormalization group flow that can be used to extract scaling operators, which are also very important in the study of relativistic field theories. Of course, this approach is currently only applicable to free theories and it remains to be seen

whether a truly variational strategy for interacting theories can be developed. If such an approach turns out to be feasible, the continuous entanglement renormalization ansatz might provide a completely new and very powerful toolbox for the non-perturbative study of relativistic field theories.

Conclusions and outlook

"A conclusion is the place where you get tired of thinking."
Martin Henry Fischer, in *Encore : A Continuing Anthology* (1945).

Having come at the end of this dissertation, what can we conclude to have learned? We have successfully developed a few new variational methods and ansätze for quantum lattice systems and quantum field theories in Chapters 3, 4 and 5. Individual conclusions about these approaches were already provided at the end of the respective chapters. If there is one unifying conclusion to be made, then it is most certainly that we are at the very interesting crossing point where different branches of theoretical physics —each of which has its individual merits— join together and allow for revolutionary new breakthroughs. The combined effort of quantum information theory, condensed matter physics, renormalization group theory and even quantum gravity and black-hole physics have resulted in powerful new methods and ideas to study and think about quantum many body systems. Indeed, a systematic study of entanglement in condensed matter systems has resulted in the area law for entanglement entropy, which strongly hints towards a holographic principle as exists in quantum gravity theories. Numerical renormalization based on insights regarding this area law has provided us with a general class of tensor network states that have now grown to be more than a mere variational ansatz to be used in numerical implementations. They are now deployed as theoretical tools to study in general terms the possible phases of quantum systems, including exotic phases such as topological order. They can be used to obtain new proofs for old theorems and maybe even proof new theorems. This is a very exciting area of research that has certainly not yet come to rest. Intriguing possibilities await to be discovered.

Let us now use the remainder of this chapter to present a personal outlook on future research that can sprout from our modest contributions. Most research has up till now been focussed on lattice systems, using matrix product states and higher dimensional generalizations, *i.e.* projected entangled pair states, or using the multiscale entanglement renormalization ansatz. We were able to develop a new algorithm for simulating time evolution as well as provide a new ansatz for studying excitations and obtain accurate estimates of the dispersion relation of spin systems. Essential for both developments was a systematic study of the tangent plane of the variational manifold with a full characterization of the gauge invariance. The implementation of the time-dependent variational principle can be used in imaginary time as an optimization method for finding the variationally optimal representation of the ground state within the variational manifold. This approach is very stable, can achieve high accuracy and automatically respects all symmetries of the system. An implementation for a lattice with open boundary conditions was also outlined but not tested. It will certainly be interesting to see how this algorithm

would compete with the traditional variational sweeping procedure, both in terms of accuracy and in terms of computational efficiency. The presented algorithms can also be further improved by explicitly incorporating symmetries. A more challenging project would be to try apply the same methods to the variational manifold of projected entangled pair states. In particular, the prospect of having a simple yet accurate method for determining dispersion relations of two-dimensional (and maybe even three-dimensional) lattice systems is very enticing. However, we can no longer expect to be able to choose a gauge condition that locally maps the metric of the manifold to the unit matrix, and a complex approximative implementation with many iterative operations will be required. But as long as the computational complexity scales polynomially, this will eventually become a feasible strategy as computing power increases. Contrastingly, the multiscale entanglement renormalization ansatz by Vidal does not easily lend itself to a similar treatment, since it is impossible to characterize the translation invariant instances in the variational manifold, and the tangent plane cannot simply be decomposed in different momentum sectors.

A very recent breakthrough is the formulation of variational ansätze that can go arbitrarily far beyond mean field theory and can be directly applied to quantum fields. The correspondence between the continuous matrix product state and the well-studied matrix product state should allow a rapid transition of the many algorithms that were developed for the latter, enabling for example to study one-dimensional quantum field theories at finite temperature. We have already developed a strategy to apply the continuous matrix product state to relativistic fermion theories in Section 2 of Chapter 6. While relativistic bosons require a different regularization strategy, they should also be amenable to a treatment with continuous matrix product states. There is also the question of higher-dimensional generalizations of the continuous matrix product state. While some ideas are already floating around, it remains to be seen whether they also allow a numeric black box implementation that can be used to study all kinds of interesting field theories. If not, then it is still worthwhile to construct such generalizations as a theoretical tool.

Last but not least there is the continuous entanglement renormalization ansatz. At this point, only free theories have been studied using a Gaussian restriction of the full ansatz. This Gaussian ansatz can also be applied to interacting theories, resulting in a complicated way of doing mean field theory, but which may nevertheless provide interesting results or insights. As soon as the operator $\hat{K}(s)$, which now contains all variational degrees of freedom, contains higher powers of the field operators, an exact integration of the renormalization group equation for operators, and hence an exact evaluation of expectation values, is no longer feasible. However, it might be possible to find approximative integration schemes that are still very accurate. Renormalization group theory has learned that most operators generated by the renormalization group equation are irrelevant anyway and quickly scale away. Finding a strategy to implement the variational principle for the non-Gaussian continuous entanglement renormalization ansatz would provide us with an exciting new tool to study field theories of all kinds. Since it is variational, such an approach would be self-correcting since the available de-

grees of freedom in $\hat{K}(s)$ would be optimally tuned to approximate the exact ground state as well as possible. And since degrees of freedom with different label s act on different length scales, there is no 'sensitivity to high frequencies' that could potentially harm this approach. Another intriguing line of research is also to find a formal connection between the process of entanglement renormalization and the AdS/CFT correspondence using the continuous entanglement renormalization ansatz. In fact, since the AdS/CFT correspondence is only a conjecture, such a connection might eventually result in a proof of the AdS/CFT correspondence. And since the continuous entanglement renormalization ansatz is not limited to conformal theories, it might even enable us to construct holographic duals of non-conformal field theories.

A

Some more calculations

This appendix provides some additional details that have been omitted from Chapters 3 and 4 because of their technicality. Section 1 is concerned with the matrix product state ansatz. An explicit expression for the matrix $M_{\Upsilon_{p,-p}}$ that appears in the linearization of the time-dependent variational principle is developed. Section 2 fills in the missing pieces regarding the continuous matrix product state ansatz. Firstly, we develop a construction to expand the variational manifold by going to a larger value of the bond dimension D within a simulation according to the time-dependent variational principle. The second subsection explains how the matrices Q and R_α for the application of the continuous matrix product state to relativistic fermion systems in Chapter 6 are parameterized.

1. Additional results for matrix product states

1.1. The matrix $M_{\Upsilon_{-p,p}}$

In Subsection 3.4 of Chapter 3 we have introduced states $|\Upsilon_{p_+,p_-}(B_+,B_-;A)\rangle$ living in the double tangent plane of the variational manifold $\mathscr{M}_{\text{uMPS}}$ at the point $|\Psi(A)\rangle$ [see Eq. (3.163)]. We have also defined a $D^2d \times D^2d$ matrix $M_{\Upsilon_{p,-p}}$ as

$$\langle \Upsilon_{\tilde{p},-p}(\overline{B_+},\overline{B_-};A)|\hat{H}-H(\overline{A},A)|\Psi(A)\rangle = 2\pi\delta(\tilde{p}-p)\boldsymbol{B}_+^\dagger M_{\Upsilon_{p,-p}}\overline{\boldsymbol{B}_-}$$

Using a derivation similar to the one in Subsection 3.2 of Chapter 3, we obtain

$$\begin{aligned}
&\langle \Upsilon_{p_+,p_-}(\overline{B_+},\overline{B_-})|\hat{H}-H(\overline{A},A)|\Psi(A)\rangle = 2\pi\delta(p_+ + p_-)\times \\
&\Big\{ \mathrm{e}^{+\mathrm{i}p_+}(l|\check{H}^{AA}_{B_+B_-}|r) + \mathrm{e}^{-\mathrm{i}p_+}(l|\check{H}^{AA}_{B_-B_+}|r) \\
&\quad + \mathrm{e}^{+\mathrm{i}p_+}(l|\check{E}^A_{B_+}(\check{\mathbb{1}}-\mathrm{e}^{+\mathrm{i}p_+}\check{E})^{\mathsf{P}}\check{E}^A_{B_-}(\check{\mathbb{1}}-\check{E})^{\mathsf{P}}\check{H}^{AA}_{AA}|r) \\
&\quad + \mathrm{e}^{-\mathrm{i}p_+}(l|\check{E}^A_{B_-}(\check{\mathbb{1}}-\mathrm{e}^{-\mathrm{i}p_+}\check{E})^{\mathsf{P}}\check{E}^A_{B_+}(\check{\mathbb{1}}-\check{E})^{\mathsf{P}}\check{H}^{AA}_{AA}|r) \\
&\quad + \mathrm{e}^{+\mathrm{i}p_+}(l|\check{H}^{AA}_{AA}(\check{\mathbb{1}}-\check{E})^{\mathsf{P}}\check{E}^A_{B_+}(\check{\mathbb{1}}-\mathrm{e}^{+\mathrm{i}p_+}\check{E})^{\mathsf{P}}\check{E}^A_{B_-}|r)
\end{aligned}$$

$$
\begin{aligned}
&+\mathrm{e}^{-\mathrm{i}p_+}(l|\check{H}^{AA}_{AA}(\check{\mathbb{1}}-\check{E})^{\mathsf{P}}\check{E}^{A}_{B_-}(\check{\mathbb{1}}-\mathrm{e}^{-\mathrm{i}p_+}\check{E})^{\mathsf{P}}\check{E}^{A}_{B_+}|r)\\
&+\mathrm{e}^{+\mathrm{i}p_+}(l|\check{E}^{A}_{B_+}(\check{\mathbb{1}}-\mathrm{e}^{+\mathrm{i}p_+}\check{E})^{\mathsf{P}}\check{H}^{AA}_{B_-A}|r)+\mathrm{e}^{-\mathrm{i}p_+}(l|\check{E}^{A}_{B_-}(\check{\mathbb{1}}-\mathrm{e}^{-\mathrm{i}p_+}\check{E})^{\mathsf{P}}\check{H}^{AA}_{B_+A}|r)\\
&+\mathrm{e}^{+2\mathrm{i}p_+}(l|\check{E}^{A}_{B_+}(\check{\mathbb{1}}-\mathrm{e}^{+\mathrm{i}p_+}\check{E})^{\mathsf{P}}\check{H}^{AA}_{AB_-}|r)+\mathrm{e}^{-2\mathrm{i}p_+}(l|\check{E}^{A}_{B_-}(\check{\mathbb{1}}-\mathrm{e}^{-\mathrm{i}p_+}\check{E})^{\mathsf{P}}\check{H}^{AA}_{AB_+}|r)\\
&+\mathrm{e}^{+\mathrm{i}p_+}(l|\check{H}^{AA}_{AB_+}(\check{\mathbb{1}}-\mathrm{e}^{+\mathrm{i}p_+}\check{E})^{\mathsf{P}}\check{E}^{A}_{B_-}|r)+\mathrm{e}^{-\mathrm{i}p_+}(l|\check{H}^{AA}_{AB_-}(\check{\mathbb{1}}-\mathrm{e}^{-\mathrm{i}p_+}\check{E})^{\mathsf{P}}\check{E}^{A}_{B_+}|r)\\
&+\mathrm{e}^{+2\mathrm{i}p_+}(l|\check{H}^{AA}_{B_+A}(\check{\mathbb{1}}-\mathrm{e}^{+\mathrm{i}p_+}\check{E})^{\mathsf{P}}\check{E}^{A}_{B_-}|r)+\mathrm{e}^{-2\mathrm{i}p_+}(l|\check{H}^{AA}_{B_-A}(\check{\mathbb{1}}-\mathrm{e}^{-\mathrm{i}p_+}\check{E})^{\mathsf{P}}\check{E}^{A}_{B_+}|r)\\
&+\mathrm{e}^{+3\mathrm{i}p_+}(l|\check{E}^{A}_{B_+}(\check{\mathbb{1}}-\mathrm{e}^{+\mathrm{i}p_+}\check{E})^{\mathsf{P}}\check{H}^{AA}_{AA}(\check{\mathbb{1}}-\mathrm{e}^{+\mathrm{i}p_+}\check{E})^{\mathsf{P}}\check{E}^{A}_{B_-}|r)\\
&+\mathrm{e}^{-3\mathrm{i}p_+}(l|\check{E}^{A}_{B_-}(\check{\mathbb{1}}-\mathrm{e}^{-\mathrm{i}p_+}\check{E})^{\mathsf{P}}\check{H}^{AA}_{AA}(\check{\mathbb{1}}-\mathrm{e}^{-\mathrm{i}p_+}\check{E})^{\mathsf{P}}\check{E}^{A}_{B_+}|r)\\
&+(l|\check{E}^{A}_{B_+}|r)\Big[\Big(2\pi\delta(p_+)-1-\mathrm{e}^{-\mathrm{i}p_+}\Big)\\
&\qquad\qquad\times\Big((l|\check{H}^{AA}_{B_-A}|r)+(l|\check{E}^{A}_{B_-}(\check{\mathbb{1}}-\check{E})^{\mathsf{P}}\check{H}^{AA}_{AA}|r)\Big)\\
&\qquad+\Big(2\pi\delta(p_+)-1-\mathrm{e}^{+\mathrm{i}p_+}\Big)\\
&\qquad\qquad\times\Big((l|\check{H}^{AA}_{AB_-}|r)+(l|\check{H}^{AA}_{AA}(\check{\mathbb{1}}-\check{E})^{\mathsf{P}}\check{E}^{A}_{B_-}|r)\Big)\\
&\qquad-\mathrm{e}^{-\mathrm{i}2p_+}(l|\check{E}^{A}_{B_-}(\check{\mathbb{1}}-\check{E})^{\mathsf{P}}(\check{\mathbb{1}}-\mathrm{e}^{-\mathrm{i}p_+}\check{E})^{\mathsf{P}}\check{H}^{AA}_{AA}|r)\\
&\qquad\qquad-\mathrm{e}^{+\mathrm{i}2p_+}(l|\check{H}^{AA}_{AA}(\check{\mathbb{1}}-\check{E})^{\mathsf{P}}(\check{\mathbb{1}}-\mathrm{e}^{+\mathrm{i}p_+}\check{E})^{\mathsf{P}}\check{E}^{A}_{B_-}|r)\Big]\\
&+(l|\check{E}^{A}_{B_-}|r)\Big[\Big(2\pi\delta(p_+)-1-\mathrm{e}^{+\mathrm{i}p_+}\Big)\\
&\qquad\qquad\times\Big((l|\check{H}^{AA}_{B_+A}|r)+(l|\check{E}^{A}_{B_+}(\check{\mathbb{1}}-\check{E})^{\mathsf{P}}\check{H}^{AA}_{AA}|r)\Big)\\
&\qquad+\Big(2\pi\delta(p_+)-1-\mathrm{e}^{-\mathrm{i}p_+}\Big)\\
&\qquad\qquad\times\Big((l|\check{H}^{AA}_{AB_+}|r)+(l|\check{H}^{AA}_{AA}(\check{\mathbb{1}}-\check{E})^{\mathsf{P}}\check{E}^{A}_{B_+}|r)\Big)\\
&\qquad-\mathrm{e}^{+\mathrm{i}2p_+}(l|\check{E}^{A}_{B_+}(\check{\mathbb{1}}-\check{E})^{\mathsf{P}}(\check{\mathbb{1}}-\mathrm{e}^{+\mathrm{i}p_+}\check{E})^{\mathsf{P}}\check{H}^{AA}_{AA}|r)\\
&\qquad\qquad-\mathrm{e}^{-\mathrm{i}2p_+}(l|\check{H}^{AA}_{AA}(\check{\mathbb{1}}-\check{E})^{\mathsf{P}}(\check{\mathbb{1}}-\mathrm{e}^{-\mathrm{i}p_+}\check{E})^{\mathsf{P}}\check{E}^{A}_{B_+}|r)\Big]\Big\}. \qquad \text{(A.1)}
\end{aligned}
$$

As was shown in Subsection 3.4 of Chapter 3, at the variational optimum where

$$\langle\Phi(B;A)|\hat{H}-H(\overline{A},A)|\Psi(A)\rangle=0,$$

we can also use gauge transformation on B_+ and B_- to eliminate *e.g.* the disconnected terms in the last six lines, as well as some other terms in this expression.

2. Additional results for continuous matrix product states

2.1. Dynamic expansion of the variational manifold

This subsection is restricted to the case of uniform continuous matrix product states for the sake of simplicity, but it can straightforwardly be generalized to generic continuous matrix product states. For the generic translation invariant Hamiltonian, the exact evolution vector looks like

$$\begin{aligned}[\hat{H} - H(\overline{Q},\overline{R};Q,R)]\,|\Psi(Q,R)\rangle &= -H(\overline{Q},\overline{R};Q,R)\,|\Psi(Q,R)\rangle \\ &+ \int_{-\infty}^{+\infty} \mathrm{d}x\, \boldsymbol{v}_{\mathrm{L}}^{\dagger}\hat{U}(-\infty,x)\Big(vR\otimes\hat{\phi}^{\dagger}(x)\Big)\hat{U}(x,+\infty)\boldsymbol{v}_{\mathrm{R}}\,|\Omega\rangle \\ &+ \int_{-\infty}^{+\infty} \mathrm{d}x\, \boldsymbol{v}_{\mathrm{L}}^{\dagger}\hat{U}(-\infty,x)\Big([Q,R]\otimes\frac{\mathrm{d}\hat{\phi}^{\dagger}}{\mathrm{d}x}(x)\Big)\hat{U}(x,+\infty)\boldsymbol{v}_{\mathrm{R}}\,|\Omega\rangle \\ &+ \int_{-\infty}^{+\infty} \mathrm{d}x \int_{-\infty}^{+\infty} \mathrm{d}y\, \boldsymbol{v}_{\mathrm{L}}^{\dagger}\hat{U}(-\infty,x)\Big(R\otimes\hat{\phi}^{\dagger}(x)\Big)w(x-y) \\ &\qquad\qquad \times \hat{U}(x,y)\Big(R\otimes\hat{\phi}^{\dagger}(y)\Big)\hat{U}(y,+\infty)\boldsymbol{v}_{\mathrm{R}}\,|\Omega\rangle\,. \end{aligned} \tag{A.2}$$

If we apply the time-dependent variational principle to the Hamiltonian $\hat{H}$, we try to approximate the exact evolution vector by tangent vectors given by

$$|\Phi_0(V,W)\rangle = \int_{-\infty}^{+\infty} \mathrm{d}x\, \boldsymbol{v}_{\mathrm{L}}^{\dagger}\hat{U}(-\infty,x)\left(V\otimes\hat{\mathbb{1}} + W\otimes\hat{\phi}^{\dagger}(x)\right)\hat{U}(x,+\infty)\boldsymbol{v}_{\mathrm{R}}\,|\Omega\rangle\,. \tag{A.3}$$

If at some point in the evolution, the error $\tilde{\varepsilon}(\overline{Q(t)},\overline{R(t)};Q(t),R(t))$ between the exact evolution and the projected evolution in $\mathscr{M}_{\mathrm{ucMPS}(D)}$ grows too large, we can try to dynamically expand the variational manifold by increasing the bond dimension D to some new value $\widetilde{D} > D$. As mentioned in Section 1 of Chapter 4, a continuous matrix product state with $|\Psi[Q,R]\rangle$ with bond dimension D cannot be exactly represented as a continuous matrix product state $|\widetilde{\Psi}[\widetilde{Q},\widetilde{R}]\rangle \in \mathscr{M}_{\mathrm{cMPS}(\widetilde{D})}$ for systems of finite size $|\mathscr{R}| = L$. For example, in case of a uniform continuous matrix product state on a finite system with periodic boundary conditions, the choice

$$\widetilde{Q} = \begin{bmatrix} Q & 0 \\ 0 & \alpha\times\mathbb{1}_{\widetilde{D}-D} \end{bmatrix}, \qquad \widetilde{R} = \begin{bmatrix} R & 0 \\ 0 & 0 \end{bmatrix} \tag{A.4}$$

results in $|\widetilde{\Psi}(\widetilde{Q},\widetilde{R})\rangle = |\Psi(Q,R)\rangle + \mathrm{e}^{\alpha L}|\Omega\rangle$, so we need to take $\alpha\to-\infty$ for an exact representation. In the thermodynamic limit $L\to\infty$, any negative value would suffice. For systems with open boundary conditions, which is the scenario we are always working

in, it is sufficient that the boundary vectors are given by

$$\widetilde{v}_{\mathrm{L}} = \begin{bmatrix} v_{\mathrm{L}} \\ 0 \end{bmatrix}, \qquad \widetilde{v}_{\mathrm{R}} = \begin{bmatrix} v_{\mathrm{R}} \\ 0 \end{bmatrix}, \tag{A.5}$$

to ensure that $|\widetilde{\Psi}(\widetilde{Q},\widetilde{R})\rangle = |\Psi(Q,R)\rangle$ for every value of α. We hence set $\alpha = 0$, but will automatically recover such a contribution in the remainder of this subsection.

For the evolution over the time step $\mathrm{d}t$, we can now use the larger variations $\widetilde{\mathrm{d}Q}$ and $\widetilde{\mathrm{d}R}$ given by

$$\widetilde{\mathrm{d}Q} = \begin{bmatrix} \mathrm{d}Q_{00} & \mathrm{d}Q_{01} \\ \mathrm{d}Q_{10} & \mathrm{d}Q_{11} \end{bmatrix}, \qquad \widetilde{\mathrm{d}R} = \begin{bmatrix} \mathrm{d}R_{00} & \mathrm{d}R_{01} \\ \mathrm{d}R_{10} & \mathrm{d}R_{11} \end{bmatrix}. \tag{A.6}$$

As for the case of matrix product states, we have to choose $\mathrm{d}Q_{00}$ and $\mathrm{d}R_{00}$ of $\mathcal{O}(\mathrm{d}t)$, $\mathrm{d}Q_{01}$, $\mathrm{d}Q_{10}$, $\mathrm{d}R_{01}$ and $\mathrm{d}R_{10}$ of $\mathcal{O}(\mathrm{d}t^{1/2})$ and $\mathrm{d}Q_{11}$ and $\mathrm{d}R_{11}$ of $\mathcal{O}(\mathrm{d}t^{0})$. We then obtain up to order $\mathrm{d}t$

$$|\mathrm{d}\Psi\rangle = |\Psi(\widetilde{Q}+\widetilde{\mathrm{d}Q},\widetilde{R}+\widetilde{\mathrm{d}R})\rangle - |\Psi(Q,R)\rangle = |\mathrm{d}\Psi_0\rangle + |\mathrm{d}\Psi_1\rangle \tag{A.7}$$

with

$$|\mathrm{d}\Psi_0\rangle = |\Phi_0(\mathrm{d}Q_{00},\mathrm{d}R_{00})\rangle \tag{A.8}$$

and

$$\begin{aligned} |\mathrm{d}\Psi_1\rangle = \int_{-\infty}^{+\infty}\mathrm{d}x\int_{x}^{+\infty}\mathrm{d}y\, v_{\mathrm{L}}^{\dagger}\hat{U}(-\infty,x)\Big(\mathrm{d}Q_{01}\otimes\hat{\mathbb{1}}+\mathrm{d}R_{01}\otimes\hat{\psi}^{\dagger}(x)\Big)\hat{U}_{11}(x,y) \\ \times\Big(\mathrm{d}Q_{10}\otimes\hat{\mathbb{1}}+\mathrm{d}R_{10}\otimes\hat{\psi}^{\dagger}(x)\Big)\hat{U}(y,+\infty)v_{\mathrm{R}}|\Omega\rangle \end{aligned} \tag{A.9}$$

where $\hat{U}_{11}(x,y) = \mathcal{P}\exp\left\{\int_x^y \mathrm{d}z\,\mathrm{d}Q_{11}\otimes\hat{\mathbb{1}}+\mathrm{d}R_{11}\otimes\hat{\psi}^{\dagger}(z)\right\}$. We have to determine the optimal choice for $\widetilde{\mathrm{d}Q}$ and $\widetilde{\mathrm{d}R}$ by minimizing the distance between the exact evolution vector and $|\mathrm{d}\Psi\rangle$. In order to do so, we can use gauge freedom and orthonormality to the ground state to impose

$$(l|\mathrm{d}Q_{00}\otimes 1_D + \mathrm{d}R_{00}\otimes\overline{R} = 0 \tag{A.10a}$$

$$(l|\mathrm{d}Q_{01}\otimes 1_D + \mathrm{d}R_{01}\otimes\overline{R} = 0 \tag{A.10b}$$

$$\mathrm{d}Q_{10}\otimes 1_D + \mathrm{d}R_{10}\otimes\overline{R}|r) = 0 \tag{A.10c}$$

such that $\langle\mathrm{d}\Psi_0|\mathrm{d}\Psi_1\rangle = 0$ and $\langle\Psi(\overline{Q},\overline{R})|\mathrm{d}\Psi_1\rangle = 0$. As a result, the optimization with respect to $\mathrm{d}Q_{00}$ and $\mathrm{d}R_{00}$ can be dealt with independent of the optimization with respect to $\mathrm{d}Q_{01}$, $\mathrm{d}Q_{10}$, $\mathrm{d}Q_{11}$, $\mathrm{d}R_{01}$, $\mathrm{d}R_{11}$ and $\mathrm{d}R_{11}$, using the scheme outlined in Subsection 2.2 of Chapter 4. We furthermore find

$$\langle\mathrm{d}\Psi_1|\mathrm{d}\Psi_1\rangle = 2\pi\delta(0)(l|\big(\mathrm{d}R_{01}\otimes\overline{\mathrm{d}R}_{01}\big)(-\breve{T}_{11})^{-1}\big(\mathrm{d}R_{10}\otimes\overline{\mathrm{d}R}_{10}\big)|r) \tag{A.11}$$

with $\breve{T}_{11} = \mathrm{d}Q_{11} \otimes \mathbb{1}_{\tilde{D}-D} + \mathbb{1}_{\tilde{D}-D} \otimes \overline{\mathrm{d}Q}_{11} + \mathrm{d}R_{11} \otimes \overline{\mathrm{d}R}_{11}$.

The evaluation of $\langle \mathrm{d}\Psi_1 | \hat{H} | \Psi(Q,R) \rangle$ is a bit more involved. We first compute

$$
\begin{aligned}
&\hat{\psi}(x)|\mathrm{d}\Psi_1\rangle = \\
&\quad \int_x^{+\infty} \mathrm{d}y \int_y^{+\infty} \mathrm{d}z\, \boldsymbol{v}_{\mathrm{L}}^\dagger \hat{U}(-\infty,x) R \hat{U}(x,y) \Big(\mathrm{d}Q_{01} \otimes \hat{\mathbb{1}} + \mathrm{d}R_{01} \otimes \hat{\psi}^\dagger(y) \Big) \\
&\qquad\qquad \times \hat{U}_{11}(y,z) \Big(\mathrm{d}Q_{10} \otimes \hat{\mathbb{1}} + \mathrm{d}R_{10} \otimes \hat{\psi}^\dagger(z) \Big) \hat{U}(z,+\infty) \boldsymbol{v}_{\mathrm{R}} |\Omega\rangle \\
&\quad + \int_x^{+\infty} \mathrm{d}z\, \boldsymbol{v}_{\mathrm{L}}^\dagger \hat{U}(-\infty,x) \mathrm{d}R_{01} \hat{U}_{11}(x,z) \\
&\qquad\qquad \times \Big(\mathrm{d}Q_{10} \otimes \hat{\mathbb{1}} + \mathrm{d}R_{10} \otimes \hat{\psi}^\dagger(z) \Big) \hat{U}(z,+\infty) \boldsymbol{v}_{\mathrm{R}} |\Omega\rangle \\
&\quad + \int_{-\infty}^{x} \mathrm{d}y \int_x^{+\infty} \mathrm{d}z\, \boldsymbol{v}_{\mathrm{L}}^\dagger \hat{U}(-\infty,y) \Big(\mathrm{d}Q_{01} \otimes \hat{\mathbb{1}} + \mathrm{d}R_{01} \otimes \hat{\psi}^\dagger(y) \Big) \hat{U}_{11}(y,x) \mathrm{d}R_{11} \\
&\qquad\qquad \times \hat{U}_{11}(x,z) \Big(\mathrm{d}Q_{10} \otimes \hat{\mathbb{1}} + \mathrm{d}R_{10} \otimes \hat{\psi}^\dagger(z) \Big) \hat{U}(z,+\infty) \boldsymbol{v}_{\mathrm{R}} |\Omega\rangle \\
&\quad + \int_{-\infty}^{x} \mathrm{d}y\, \boldsymbol{v}_{\mathrm{L}}^\dagger \hat{U}(-\infty,y) \Big(\mathrm{d}Q_{01} \otimes \hat{\mathbb{1}} + \mathrm{d}R_{01} \otimes \hat{\psi}^\dagger(y) \Big) \\
&\qquad\qquad \times \hat{U}_{11}(y,x) \mathrm{d}R_{10} \hat{U}(x,+\infty) \boldsymbol{v}_{\mathrm{R}} |\Omega\rangle \\
&\quad + \int_{-\infty}^{x} \mathrm{d}z \int_{-\infty}^{z} \mathrm{d}y\, \boldsymbol{v}_{\mathrm{L}}^\dagger \hat{U}(-\infty,y) \Big(\mathrm{d}Q_{01} \otimes \hat{\mathbb{1}} + \mathrm{d}R_{01} \otimes \hat{\psi}^\dagger(y) \Big) \hat{U}_{11}(y,z) \\
&\qquad\qquad \times \Big(\mathrm{d}Q_{10} \otimes \hat{\mathbb{1}} + \mathrm{d}R_{10} \otimes \hat{\psi}^\dagger(z) \Big) \hat{U}(z,x) R \hat{U}(x,+\infty) \boldsymbol{v}_{\mathrm{R}} |\Omega\rangle .
\end{aligned}
$$

Then, we can compute

$$
\begin{aligned}
&\frac{\mathrm{d}\hat{\psi}}{\mathrm{d}x}(x)|\mathrm{d}\Psi_1\rangle = \\
&\quad \int_x^{+\infty} \mathrm{d}y \int_y^{+\infty} \mathrm{d}z\, \boldsymbol{v}_{\mathrm{L}}^\dagger \hat{U}(-\infty,x) [Q,R] \hat{U}(x,y) \Big(\mathrm{d}Q_{01} \otimes \hat{\mathbb{1}} + \mathrm{d}R_{01} \otimes \hat{\psi}^\dagger(y) \Big) \\
&\qquad\qquad \times \hat{U}_{11}(y,z) \Big(\mathrm{d}Q_{10} \otimes \hat{\mathbb{1}} + \mathrm{d}R_{10} \otimes \hat{\psi}^\dagger(z) \Big) \hat{U}(z,+\infty) \boldsymbol{v}_{\mathrm{R}} |\Omega\rangle \\
&\quad - \int_x^{+\infty} \mathrm{d}z\, \boldsymbol{v}_{\mathrm{L}}^\dagger \hat{U}(-\infty,x) R \Big(\mathrm{d}Q_{01} \otimes \hat{\mathbb{1}} + \mathrm{d}R_{01} \otimes \hat{\psi}^\dagger(x) \Big) \\
&\qquad\qquad \hat{U}_{11}(x,z) \Big(\mathrm{d}Q_{10} \otimes \hat{\mathbb{1}} + \mathrm{d}R_{10} \otimes \hat{\psi}^\dagger(z) \Big) \hat{U}(z,+\infty) \boldsymbol{v}_{\mathrm{R}} |\Omega\rangle \\
&\quad + \int_x^{+\infty} \mathrm{d}z\, \boldsymbol{v}_{\mathrm{L}}^\dagger \hat{U}(-\infty,x) \Big[\big(Q \otimes \hat{\mathbb{1}} + R \otimes \hat{\psi}^\dagger(x) \big) \mathrm{d}R_{01} \\
&\qquad\qquad - \mathrm{d}R_{01} \big(Q_{11} \otimes \hat{\mathbb{1}} + R_{11} \otimes \hat{\psi}^\dagger(x) \big) \Big] \\
&\qquad\qquad \times \hat{U}_{11}(x,z) \Big(\mathrm{d}Q_{10} \otimes \hat{\mathbb{1}} + \mathrm{d}R_{10} \otimes \hat{\psi}^\dagger(z) \Big) \hat{U}(z,+\infty) \boldsymbol{v}_{\mathrm{R}} |\Omega\rangle
\end{aligned}
$$

$$
\begin{aligned}
&- \boldsymbol{v}_{\mathrm{L}}^{\dagger}\hat{U}(-\infty,x)\mathrm{d}R_{01}\Big(\mathrm{d}Q_{10}\otimes\hat{\mathbb{1}}+\mathrm{d}R_{10}\otimes\hat{\psi}^{\dagger}(x)\Big)\hat{U}(x,+\infty)\boldsymbol{v}_{\mathrm{R}}|\Omega\rangle\\
&+\int_{-\infty}^{x}\mathrm{d}y\int_{x}^{+\infty}\mathrm{d}z\,\boldsymbol{v}_{\mathrm{L}}^{\dagger}\hat{U}(-\infty,y)\Big(\mathrm{d}Q_{01}\otimes\hat{\mathbb{1}}+\mathrm{d}R_{01}\otimes\hat{\psi}^{\dagger}(y)\Big)\hat{U}_{11}(y,x)\\
&\qquad\times[\mathrm{d}Q_{11},\mathrm{d}R_{11}]\hat{U}_{11}(x,z)\Big(\mathrm{d}Q_{10}\otimes\hat{\mathbb{1}}+\mathrm{d}R_{10}\otimes\hat{\psi}^{\dagger}(z)\Big)\hat{U}(z,+\infty)\boldsymbol{v}_{\mathrm{R}}|\Omega\rangle\\
&+\int_{x}^{+\infty}\mathrm{d}z\,\boldsymbol{v}_{\mathrm{L}}^{\dagger}\hat{U}(-\infty,x)\Big(\mathrm{d}Q_{01}\otimes\hat{\mathbb{1}}+\mathrm{d}R_{01}\otimes\hat{\psi}^{\dagger}(x)\Big)\mathrm{d}R_{11}\\
&\qquad\times\hat{U}_{11}(x,z)\Big(\mathrm{d}Q_{10}\otimes\hat{\mathbb{1}}+\mathrm{d}R_{10}\otimes\hat{\psi}^{\dagger}(z)\Big)\hat{U}(z,+\infty)\boldsymbol{v}_{\mathrm{R}}|\Omega\rangle\\
&-\int_{-\infty}^{x}\mathrm{d}y\,\boldsymbol{v}_{\mathrm{L}}^{\dagger}\hat{U}(-\infty,y)\Big(\mathrm{d}Q_{01}\otimes\hat{\mathbb{1}}+\mathrm{d}R_{01}\otimes\hat{\psi}^{\dagger}(y)\Big)\hat{U}_{11}(y,x)\\
&\qquad\times\mathrm{d}R_{11}\Big(\mathrm{d}Q_{10}\otimes\hat{\mathbb{1}}+\mathrm{d}R_{10}\otimes\hat{\psi}^{\dagger}(x)\Big)\hat{U}(x,+\infty)\boldsymbol{v}_{\mathrm{R}}|\Omega\rangle\\
&+\int_{-\infty}^{x}\mathrm{d}y\,\boldsymbol{v}_{\mathrm{L}}^{\dagger}\hat{U}(-\infty,y)\Big(\mathrm{d}Q_{01}\otimes\hat{\mathbb{1}}+\mathrm{d}R_{01}\otimes\hat{\psi}^{\dagger}(y)\Big)\hat{U}_{11}(y,x)\\
&\qquad\times\Big[\big(\mathrm{d}Q_{11}\otimes\hat{\mathbb{1}}+\mathrm{d}R_{11}\otimes\hat{\psi}^{\dagger}(x)\big)\mathrm{d}R_{10}-\mathrm{d}R_{10}\big(Q\otimes\hat{\mathbb{1}}+R\otimes\hat{\psi}^{\dagger}(x)\big)\Big]\\
&\qquad\times\hat{U}(x,+\infty)\boldsymbol{v}_{\mathrm{R}}|\Omega\rangle\\
&+\boldsymbol{v}_{\mathrm{L}}^{\dagger}\hat{U}(-\infty,x)\Big(\mathrm{d}Q_{01}\otimes\hat{\mathbb{1}}+\mathrm{d}R_{01}\otimes\hat{\psi}^{\dagger}(x)\Big)\mathrm{d}R_{10}\hat{U}(x,+\infty)\boldsymbol{v}_{\mathrm{R}}|\Omega\rangle\\
&+\int_{-\infty}^{x}\mathrm{d}z\int_{-\infty}^{z}\mathrm{d}y\,\boldsymbol{v}_{\mathrm{L}}^{\dagger}\hat{U}(-\infty,y)\Big(\mathrm{d}Q_{01}\otimes\hat{\mathbb{1}}+\mathrm{d}R_{01}\otimes\hat{\psi}^{\dagger}(y)\Big)\hat{U}_{11}(y,z)\\
&\qquad\times\Big(\mathrm{d}Q_{10}\otimes\hat{\mathbb{1}}+\mathrm{d}R_{10}\otimes\hat{\psi}^{\dagger}(z)\Big)\hat{U}(z,x)[Q,R]\hat{U}(x,+\infty)\boldsymbol{v}_{\mathrm{R}}|\Omega\rangle\\
&+\int_{-\infty}^{x}\mathrm{d}y\,\boldsymbol{v}_{\mathrm{L}}^{\dagger}\hat{U}(-\infty,y)\Big(\mathrm{d}Q_{01}\otimes\hat{\mathbb{1}}+\mathrm{d}R_{01}\otimes\hat{\psi}^{\dagger}(y)\Big)\hat{U}_{11}(y,x)\\
&\qquad\times\Big(\mathrm{d}Q_{10}\otimes\hat{\mathbb{1}}+\mathrm{d}R_{10}\otimes\hat{\psi}^{\dagger}(x)\Big)R\hat{U}(x,+\infty)\boldsymbol{v}_{\mathrm{R}}|\Omega\rangle\,.
\end{aligned}
$$

At first sight, this expression contains many contributions $\hat{\psi}^{\dagger}(x)$ at the fixed position x, which could result in a divergent contribution to the kinetic energy. It can however easily be seen that they all cancel, resulting in

$$
\begin{aligned}
&\frac{\mathrm{d}\hat{\psi}}{\mathrm{d}x}(x)|\mathrm{d}\Psi_1\rangle=\\
&\quad\int_{x}^{+\infty}\mathrm{d}y\int_{y}^{+\infty}\mathrm{d}z\,\boldsymbol{v}_{\mathrm{L}}^{\dagger}\hat{U}(-\infty,x)[Q,R]\hat{U}(x,y)\Big(\mathrm{d}Q_{01}\otimes\hat{\mathbb{1}}+\mathrm{d}R_{01}\otimes\hat{\psi}^{\dagger}(y)\Big)\\
&\qquad\times\hat{U}_{11}(y,z)\Big(\mathrm{d}Q_{10}\otimes\hat{\mathbb{1}}+\mathrm{d}R_{10}\otimes\hat{\psi}^{\dagger}(z)\Big)\hat{U}(z,+\infty)\boldsymbol{v}_{\mathrm{R}}|\Omega\rangle\\
&\quad+\int_{-\infty}^{x}\mathrm{d}y\int_{x}^{+\infty}\mathrm{d}z\,\boldsymbol{v}_{\mathrm{L}}^{\dagger}\hat{U}(-\infty,y)\Big(\mathrm{d}Q_{01}\otimes\hat{\mathbb{1}}+\mathrm{d}R_{01}\otimes\hat{\psi}^{\dagger}(y)\Big)\hat{U}_{11}(y,x)[\mathrm{d}Q_{11},\mathrm{d}R_{11}]\\
&\qquad\times\hat{U}_{11}(x,z)\Big(\mathrm{d}Q_{10}\otimes\hat{\mathbb{1}}+\mathrm{d}R_{10}\otimes\hat{\psi}^{\dagger}(z)\Big)\hat{U}(z,+\infty)\boldsymbol{v}_{\mathrm{R}}|\Omega\rangle
\end{aligned}
$$

$$
\begin{aligned}
&+\int_{-\infty}^{x}\mathrm{d}z\int_{-\infty}^{z}\mathrm{d}y\,\boldsymbol{v}_{\mathrm{L}}^{\dagger}\hat{U}(-\infty,y)\Big(\mathrm{d}Q_{01}\otimes\hat{\mathbb{1}}+\mathrm{d}R_{01}\otimes\hat{\psi}^{\dagger}(y)\Big)\hat{U}_{11}(y,z)\\
&\qquad\qquad\times\Big(\mathrm{d}Q_{10}\otimes\hat{\mathbb{1}}+\mathrm{d}R_{10}\otimes\hat{\psi}^{\dagger}(z)\Big)\hat{U}(z,x)[Q,R]\hat{U}(x,+\infty)\boldsymbol{v}_{\mathrm{R}}|\Omega\rangle\\
&+\int_{x}^{+\infty}\mathrm{d}z\,\boldsymbol{v}_{\mathrm{L}}^{\dagger}\hat{U}(-\infty,x)\Big(Q\mathrm{d}R_{01}-R\mathrm{d}Q_{01}+\mathrm{d}Q_{01}\mathrm{d}R_{11}-\mathrm{d}R_{01}\mathrm{d}Q_{11}\Big)\\
&\qquad\qquad\times\hat{U}_{11}(x,z)\Big(\mathrm{d}Q_{10}\otimes\hat{\mathbb{1}}+\mathrm{d}R_{10}\otimes\hat{\psi}^{\dagger}(z)\Big)\hat{U}(z,+\infty)\boldsymbol{v}_{\mathrm{R}}|\Omega\rangle\\
&+\int_{-\infty}^{x}\mathrm{d}y\,\boldsymbol{v}_{\mathrm{L}}^{\dagger}\hat{U}(-\infty,y)\Big(\mathrm{d}Q_{01}\otimes\hat{\mathbb{1}}+\mathrm{d}R_{01}\otimes\hat{\psi}^{\dagger}(y)\Big)\hat{U}_{11}(y,x)\\
&\qquad\qquad\times\Big(\mathrm{d}Q_{10}R-\mathrm{d}R_{10}Q+\mathrm{d}Q_{11}\mathrm{d}R_{10}-\mathrm{d}R_{11}\mathrm{d}Q_{10}\Big)\hat{U}(x,+\infty)\boldsymbol{v}_{\mathrm{R}}|\Omega\rangle\\
&\qquad\qquad+\boldsymbol{v}_{\mathrm{L}}^{\dagger}\hat{U}(-\infty,x)\Big(\mathrm{d}Q_{01}\mathrm{d}R_{10}-\mathrm{d}R_{01}\mathrm{d}Q_{10}\Big)\mathrm{d}R_{10}\hat{U}(x,+\infty)\boldsymbol{v}_{\mathrm{R}}|\Omega\rangle\,.
\end{aligned}
$$

Due to the gauge fixing conditions in Eq. (A.10), all terms with integrals over y and z will disappear from the final expression for $\langle \mathrm{d}\Psi_1|(\mathrm{d}\hat{\psi}^{\dagger}(x)/\mathrm{d}x)(\mathrm{d}\hat{\psi}(x)/\mathrm{d}x)|\Psi(Q,R)\rangle$, so that only the last term survives. In the same way, we can deal with the interaction term, and we eventually obtain

$$
\begin{aligned}
\langle \mathrm{d}\Psi_1|\hat{H}|\Psi(Q,R)\rangle &= 2\pi\delta(0)\times\Big[(l|[Q,R]\otimes\big(\overline{\mathrm{d}Q}_{01}\overline{\mathrm{d}R}_{10}-\overline{\mathrm{d}R}_{01}\overline{\mathrm{d}Q}_{10}\big)|r)\\
&+(l|\big(R\otimes\overline{\mathrm{d}R}_{01}\big)\mathcal{L}[w](-\check{T}_1)\big(R\otimes\overline{\mathrm{d}R}_{10}\big)|r)\\
&+\int_0^{+\infty}\mathrm{d}x\int_0^{+\infty}\mathrm{d}y\int_0^{+\infty}\mathrm{d}z\,w(x+y+z)(l|\big(R\otimes\overline{R}\big)\mathrm{e}^{\check{T}x}\big(1_D\otimes\overline{\mathrm{d}Q}_{01}+R\otimes\overline{\mathrm{d}R}_{01}\big)\\
&\qquad\qquad\times\mathrm{e}^{\check{T}_1 y}\big(1_D\otimes\overline{\mathrm{d}Q}_{10}+R\otimes\overline{\mathrm{d}R}_{10}\big)\mathrm{e}^{\check{T}z}\big(R\otimes\overline{R}\big)|r)\Big]
\end{aligned}
\tag{A.12}
$$

where $\check{T}_1 = Q\otimes\mathbb{1}_{\tilde{D}-D}+\mathbb{1}_D\otimes\overline{\mathrm{d}Q}_{11}+R\otimes\overline{\mathrm{d}R}_{11}$. Note that the external potential v does not feature. While we could try to proceed a little bit further with the general case of long range interactions, this soon becomes very complicated. Most relevant is the scenario of strictly local interactions $w(x-y)=c\,\delta(x-y)$, for which

$$
\begin{aligned}
&\langle \mathrm{d}\Psi_1|\hat{H}|\Psi(Q,R)\rangle =\\
&\quad 2\pi\delta(0)\Big[(l|[Q,R]\otimes\big(\overline{\mathrm{d}Q}_{01}\overline{\mathrm{d}R}_{10}-\overline{\mathrm{d}R}_{01}\overline{\mathrm{d}Q}_{10}\big)|r)+c(l|R^2\otimes\big(\overline{\mathrm{d}R}_{01}\overline{\mathrm{d}R}_{10}\big)|r)\Big]
\end{aligned}
$$

If we set $\mathrm{d}R_{11}=0$ and $\mathrm{d}Q_{11}=\alpha 1_{\tilde{D}-D}$ with $\alpha\in\mathbb{R}$ then we also find

$$
\langle \mathrm{d}\Psi_1|\mathrm{d}\Psi_1\rangle = 2\pi\delta(0)\frac{1}{\alpha^2}(l|(\mathrm{d}R_{01}\mathrm{d}R_{10})\otimes(\overline{\mathrm{d}R}_{01}\overline{\mathrm{d}R}_{10})|r)
$$

The two insertions $\mathrm{d}R_{01}$ and $\mathrm{d}R_{10}$ can appear at positions x and y with a weight proportional to $\exp(\alpha|x-y|)$, so that only for $\alpha\to-\infty$ they are truly localized together. This

is the same α from the beginning of the paragraph, which now necessarily reappears in order to obtain a finite norm (up to the volume factor $2\pi\delta(0)$) for $|\mathrm{d}\Psi_1\rangle$.

We can use these expressions to find the best $\mathrm{d}R_{01}$ and $\mathrm{d}R_{10}$. The corresponding $\mathrm{d}Q_{01}$ and $\mathrm{d}Q_{10}$ are completely specified by the gauge fixing conditions in Eq. (A.10) as

$$\mathrm{d}Q_{01} = -l^{-1}R^\dagger l\,\mathrm{d}R_{01}, \qquad \mathrm{d}Q_{10} = -\mathrm{d}Q_{10}\,r R^\dagger r^{-1},$$

so that we can rewrite

$$\langle \mathrm{d}\Psi_1|\hat{H}|\Psi(Q,R)\rangle = 2\pi\delta(0)\Big[(l|\big(-R[Q,R]+[Q,R]R+cR^2\big)\otimes\big(\overline{\mathrm{d}R}_{01}\overline{\mathrm{d}R}_{10}\big)|r)\Big].$$

Setting $X = \alpha^{-1}l^{1/2}\mathrm{d}R_{01}\mathrm{d}R_{10}r^{1/2}$, we obtain

$$\langle \mathrm{d}\Psi_1|\mathrm{d}\Psi_1\rangle = 2\pi\delta(0)\,\mathrm{tr}[X^\dagger X], \tag{A.13}$$

$$\langle \mathrm{d}\Psi_1|\hat{H}|\Psi(Q,R)\rangle = 2\pi\delta(0)\alpha\,\mathrm{tr}[X^\dagger l^{1/2}(-R[Q,R]+[Q,R]R+cR^2)r^{1/2}]. \tag{A.14}$$

We thus need to find the $D\times D$ matrix X with maximal rank $\widetilde{D}-D$ that minimizes

$$||X-\alpha l^{1/2}(-R[Q,R]+[Q,R]R+cR^2)r^{1/2}||^2 \tag{A.15}$$

with $||\cdot||$ the Hilbert-Schmidt norm. We can hence obtain X from a singular value decomposition of $\alpha l^{1/2}(-R[Q,R]+[Q,R]R+cR^2)r^{1/2}$, where we only retain the $\widetilde{D}-D$ largest singular values. From this, we also obtain $\mathrm{d}R_{01}$ and $\mathrm{d}R_{10}$. Having obtained the optimal values for $\mathrm{d}R_{01}$ and $\mathrm{d}R_{10}$ —and thus also for $\mathrm{d}Q_{01}$ and $\mathrm{d}Q_{10}$— we can update $\widetilde{Q}$ and $\widetilde{R}$, where we should in principle use $\alpha=-\infty$, given the remark above. In practice, we need to find a finite value of α for which our small step is valid.

2.2. Representation of a two-fermion system

In Section 2 of Chapter 6 we have used the continuous matrix product state ansatz to describe relativistic fermion systems which are described by a two-component spinor field. The regularity condition Eq. (4.18) of Chapter 4 requires that the matrices $\{R_\alpha,\alpha=1,2\}$ have 'Fermi statistics' and thus satisfy

$$\{R_\alpha,R_\beta\}=0. \tag{A.16}$$

This relation has been derived from the necessity of having a finite non-relativistic kinetic energy, and it is not immediately obvious that we should also impose this condition for relativistic systems. However, any fermionic system with any number of negative energy levels would have a diverging energy if we would not impose the condition $R^2=0$, since this would allow to stack infinitely many fermions in the same level. Put differently, the condition $R^2=0$ —or the more general condition of Eq. (A.16) in case of several fermions— imposes, through the continuity of the wave function, the Pauli principle,

which is also valid in relativistic systems. Hence, for free relativistic Dirac fermions there would be two sources of divergences if this condition was not imposed: both the fact that there are infinitely many energy levels with negative energy and the fact that infinitely many fermions can be put in each of these levels. Only the first of these is physical.

We could try to start with an initial choice of matrices $\{R_\alpha\}$ that satisfy Eq. (A.16) and then apply the general evolution in imaginary time according to the time dependent variational principle, as discussed in Chapter 4, in order to obtain optimized matrices. The regularity condition of the tangent vectors in Eq. (4.87) ensures that the regularity condition remains fulfilled up to first order. However, higher order corrections will be present and slowly the matrices will start to violate Eq. (A.16). We could try to reimpose the regularity condition exactly after every step, but there is no straightforward strategy to map a general set of matrices $\{R_\alpha\}$ to a nearby set $\{R'_\alpha\}$ that satisfies the required condition. It is therefore better to use an explicit parameterization that always satisfies Eq. (A.16) exactly. This will constrain the allowed set of gauge transformations, so that we cannot choose a gauge condition for the tangent vectors that maps the metric to the identity matrix. We then have to use the full flow equations of the time-dependent variational principle including the computation of the inverse of the transfer matrix. It is therefore a good idea to restrict the parameterization such that all gauge freedom has been eliminated, because the metric would be singular otherwise.

The easiest parameterization for a general set $\{R_\alpha, \alpha, 1, \ldots, n\}$ matrices is given by

$$R_\alpha = g_\alpha c_\alpha \otimes \mathbb{1}_{\tilde{D}} \tag{A.17}$$

where $\{c_\alpha, \alpha = 1, \ldots, n\}$ is a set of virtual fermion annihilation operators, that can be parameterized as

$$c_n = \Big(\bigotimes_{k<n} \sigma_k^z\Big) \otimes \sigma_n^-. \tag{A.18}$$

The auxiliary space is thus given by the Kronecker product of the Hilbert space $(\mathbb{C}^2)^{\otimes n}$ of these n auxiliary fermions and an additional $\tilde{D}$ dimensional Hilbert space $\mathbb{C}^{\tilde{D}}$ on which we impose no constraints (for now). In principle, we should assign to the R_α matrices some non-trivial commuting matrices $\tilde{R}_\alpha$ on the $\tilde{D}$ dimensional space: $R_\alpha = c_\alpha \otimes \tilde{R}_\alpha$ with the additional condition $[\tilde{R}_\alpha, \tilde{R}_\beta] = 0$. The remaining gauge freedom is in itself not sufficient to be able to transform each $\tilde{R}_\alpha$ to the form $g_\alpha \mathbb{1}_{\tilde{D}}$. The physical picture of continuous matrix product states being defined through continuous measurement (see Subsection 1.2 of Chapter 4) does allow to interpret R_α as a virtual fermion (inside the cavity) that is annihilated whenever a physical fermion (outside the cavity) is created. The parameter g_α acts as a coupling strength. Alternatively, we can interpret this parameterization as a restricted variational ansatz, with g_α the minimal amount of variational freedom that is required in order to be compatible with the scaling transformation $Q \leftarrow cQ$ and $R \leftarrow \sqrt{c}R$, which plays a crucial role in Section 2 of Chapter 6. However, it turns out that even in the larger variational space, the time-dependent variational

principle automatically converges towards a solution within this restricted space, *i.e.* where $\tilde{R}_\alpha \sim \mathbb{1}_{\tilde{D}}$.

Since we have used the picture of continuous measurement to define the R_α matrices, we now also parameterize Q as

$$Q = \mathrm{i}K - \frac{1}{2}\sum_\alpha R_\alpha^\dagger R_\alpha \tag{A.19}$$

with K a Hermitian matrix. Since the Hamiltonians under consideration have real coefficients, we should also be able to choose Q real and we thus replace $\mathrm{i}K$ by a real skew-symmetric matrix S. In order to impose parity preservation in the physical system, and thus to have $\langle\psi_\alpha\rangle = \langle\psi_\alpha^\dagger\rangle = 0$, we also have to define some kind of parity in the auxiliary system. To this end, we define a parity operator

$$P = \prod_{\alpha=1}^{n}\left(1 - 2c_\alpha^\dagger c_\alpha\right) \otimes \tilde{P} \tag{A.20}$$

where $\tilde{P}$ is some $\tilde{D}\times\tilde{D}$ matrix which acts as a parity operator in the $\tilde{D}$-dimensional part of the auxiliary space. The parameterization of R_α is compatible with additional gauge transformations in the $\tilde{D}$-dimensional subspace of the auxiliary space. These gauge transformation should be orthogonal in order to preserve the parameterization of Q. In the first place, we can diagonalize $\tilde{P}$, which will of course only have eigenvalues $+1$ and -1. The degeneracy $\tilde{D}_+$ and $\tilde{D}_-$ of these eigenvalues (with $\tilde{D}_+ + \tilde{D}_- = \tilde{D}$) results in the gauge freedom not being completely fixed, and additional gauge transformations in the subspaces with positive and negative parity are still possible.

In order to preserve parity, the skew-symmetric matrix S should be parity preserving, *i.e.* $PSP = S$. For the case of $n = 2$, such as for the relativistic Dirac Hamiltonian in Chapter 4, we can use a parameterization

$$S = \begin{bmatrix} S_{11}^+ & S_{12}^- & S_{13}^- & S_{14}^+ \\ -(S_{12}^-)^{\mathrm{T}} & S_{22}^+ & S_{23}^+ & S_{24}^- \\ -(S_{13}^-)^{\mathrm{T}} & -(S_{23}^+)^{\mathrm{T}} & S_{33}^+ & S_{34}^- \\ -(S_{14}^+)^{\mathrm{T}} & -(S_{24}^-)^{\mathrm{T}} & -(S_{34}^-)^{\mathrm{T}} & S_{44}^+ \end{bmatrix} \tag{A.21}$$

$$R_1 = g_1 \begin{bmatrix} 0 & 0 & \mathbb{1} & 0 \\ 0 & 0 & 0 & \mathbb{1} \\ 0 & 0 & 0 & 0 \\ 0 & 0 & 0 & 0 \end{bmatrix} \tag{A.22}$$

$$R_2 = g_2 \begin{bmatrix} 0 & \mathbb{1} & 0 & 0 \\ 0 & 0 & 0 & 0 \\ 0 & 0 & 0 & -\mathbb{1} \\ 0 & 0 & 0 & 0 \end{bmatrix} \tag{A.23}$$

where the elements are matrices in the $\tilde{D}$ dimensional space. The matrices S^+_{11}, S^+_{22}, S^+_{33} and S^+_{44} on the diagonal should be skew-symmetric, while there is no such restriction on the off-diagonal blocks. The superscript $\pm$ indicates the parity of these matrices with respect to $\tilde{P}$, i.e. $\tilde{P} S^+_{kl} \tilde{P} = S^+_{kl}$ and $\tilde{P} S^-_{kl} \tilde{P} = -S^-_{kl}$. If we order the eigenvalues of $\tilde{P}$ as first all $+1$'s, followed by all -1's, than these matrices will have a block diagonal form

$$S^+_{kl} = \begin{bmatrix} S^{++}_{kl} & 0 \\ 0 & S^{--}_{kl} \end{bmatrix}, \qquad S^-_{kl} = \begin{bmatrix} 0 & S^{+-}_{kl} \\ S^{-+}_{kl} & 0 \end{bmatrix}. \tag{A.24}$$

Finally, in order to fix the gauge freedom completely, we can further fix the parameterization of one of these H_{kl} matrices. The best approach is to work on a matrix with positive parity, as we can then choose the orthogonal transformations on the $+$ and the $-$ subspace independently. The matrices on the diagonal are not the best candidates, because the fact that they are skew-symmetric implies that they will commute with a linear combination of the generators of all possible orthogonal transformations, and that we will not be able to fix the gauge completely. So the remaining possibilities are H^+_{23} or H^+_{14}. We have chosen the latter one. With

$$H^+_{14} = \begin{bmatrix} H^{++}_{14} & 0 \\ 0 & H^{--}_{14} \end{bmatrix},$$

fixing the gauge boils down to choosing a fixed format for H^{++}_{14} and H^{--}_{14} that is always obtainable from a general matrix by performing on orthogonal transformation. Since we can always write a general matrix as a sum of a symmetric and a skew-symmetric matrix, we can choose the orthogonal transformation such that it diagonalizes the symmetric part. We thus choose a representation in which H^{++}_{14} and H^{--}_{14} are skew-symmetric, except for the fact that the diagonal elements are non-zero. Since this final choice completely eliminates all gauge freedom, the tangent vectors resulting from this parameterization will all be linearly independent and their Gram matrix will not have zero eigenvalues. It can then safely be inverted in the application of the time-dependent variational principle.

Bibliography

[1] J. von Neumann, "Wahrscheinlichkeitstheoretischer Aufbau der Quantenmechanik," *Göttinger Nachrichten* **1** (1927) 245.

[2] L. Van Hove, "Les difficultés de divergences pour un modèle de champ quantifié," *Physica* **18** (1952) 145.

[3] K. O. Friedrichs, "Mathematical aspects of the quantum theory of fields parts I and II," *Communications on Pure and Applied Mathematics* **4** (1951) 161.

[4] K. O. Friedrichs, "Mathematical aspects of the quantum theory of fields. Part III. Boson field in interaction with a given source distribution," *Communications on Pure and Applied Mathematics* **5** (1952) 349.

[5] K. O. Friedrichs, "Mathematical aspects of the quantum theory of fields. Part IV. Occupation number representation and fields of different kinds," *Communications on Pure and Applied Mathematics* **5** (1952) 1.

[6] K. O. Friedrichs, "Mathematical aspects of the quantum theory of fields. Part V. Fields modified by linear homogeneous forces," *Communications on Pure and Applied Mathematics* **6** (1953) 1.

[7] G. G. Emch, *Algebraic Methods in Statistical Mechanics and Quantum Field Theory*, vol. XXVI of *Monographs and Texts in Physics and Astronomy*. Wiley-Interscience, 1972.

[8] F. Strocchi, *An Introduction to the Mathematical Structure of Quantum Mechanics: A Short Course for Mathematicians*, vol. 28 of *Advanced Series in Mathematical Physics*. World Scientific, 2008.

[9] I. Galfand and M. A. Naimark, "On the Imbedding of Normed Rings into the Ring of Operators in Hilbert Space," *Matematicheskii Sbornik* **12 [54]** (1943) 197. `http://mi.mathnet.ru/eng/msb6155`.

[10] I. E. Segal, "Postulates for General Quantum Mechanics," *The Annals of Mathematics* **48** (1947) 930. `http://www.jstor.org/stable/1969387`.

[11] V. Fock, "Konfigurationsraum und zweite Quantelung," *Zeitschrift für Physik A* **75** (1932) 622.

[12] N. Bogoljubov, "On a new method in the theory of superconductivity," *Il Nuovo Cimento* **7** (1958) 794.

[13] P. W. Anderson, "Infrared Catastrophe in Fermi Gases with Local Scattering Potentials," *Physical Review Letters* **18** (1967) 1049.

[14] R. Haag, "On quantum field theories," *Matematisk-fysiske Meddelelser* **29** (1955) 1. `http://cdsweb.cern.ch/record/212242/files/p1.pdf`.

[15] R. Haag, *Local Quantum Physics: Fields, Particles, Algebras*. Springer, 1996.

[16] E. H. Lieb, "Exact Analysis of an Interacting Bose Gas. II. The Excitation Spectrum," *Physical Review* **130** (1963) 1616.

[17] E. P. Wigner, *Gruppentheorie und ihre Anwendung*. Friedrich Vieweg und Sohn, 1931.

[18] F. Strocchi, *Symmetry Breaking*, vol. 643 of *Lecture Notes in Physics*. Springer, 2005.

[19] R. Rajaraman, *Solitons and Instantons: An Introduction to Solitons and Instantons in Quantum Field Theory*. North-Holland, 1982.

[20] Y. Nambu, "Quasi-Particles and Gauge Invariance in the Theory of Superconductivity," *Physical Review* **117** (1960) 648.

[21] J. Goldstone, "Field theories with superconductor solutions," *Nuovo Cimento* **19** (1961) 154.

[22] J. Goldstone, A. Salam, and S. Weinberg, "Broken symmetries," *Physical Review* **127** (1962) 965.

[23] R. V. Lange, "Nonrelativistic Theorem Analogous to the Goldstone Theorem," *Physical Review* **146** (1966) 301.

[24] S. Coleman, "There are no Goldstone bosons in two dimensions," *Communications in Mathematical Physics* **31** (1973) 259.

[25] N. D. Mermin and H. Wagner, "Absence of Ferromagnetism or Antiferromagnetism in One- or Two-Dimensional Isotropic Heisenberg Models," *Physical Review Letters* **17** (1966) 1133.

[26] P. C. Hohenberg, "Existence of Long-Range Order in One and Two Dimensions," *Physical Review* **158** (1967) 383.

[27] S. Elitzur, "Impossibility of spontaneously breaking local symmetries," *Physical Review D* **12** (1975) 3978.

[28] F. Englert and R. Brout, "Broken Symmetry and the Mass of Gauge Vector Mesons," *Physical Review Letters* **13** (1964) 321.

[29] P. W. Higgs, "Broken Symmetries and the Masses of Gauge Bosons," *Physical Review Letters* **13** (1964) 508.

[30] G. S. Guralnik, C. R. Hagen, and T. W. B. Kibble, "Global Conservation Laws and Massless Particles," *Physical Review Letters* **13** (1964) 585.

[31] J. A. Hertz, "Quantum critical phenomena," *Physical Review B* **14** (1976) 1165.

[32] S. Sachdev, *Quantum Phase Transitions*. Cambridge University Press, 2nd ed., 2011.

[33] L. D. Landau, "Theory of phase transformations. I," *Physikalische Zeitschrift der Sowjetunion* **11** (1937) 26.

[34] L. D. Landau, "Theory of phase transformations. II," *Physikalische zeitschrift der Sowjetunion* **11** (1937) 545.

[35] V. L. Ginzburg and L. D. Landau, "Concerning the theory of superconductivity," *Soviet Journal of Experimental and Theoretical Physics* **20** (1950) 1064.

[36] K. G. Wilson and J. Kogut, "The renormalization group and the ϵ expansion," *Physics Reports* **12** (1974) 75.

[37] X. G. Wen, "Topological Orders in Rigid States," *International Journal of Modern Physics B* **4** (1990) 239.

[38] M. A. Levin and X.-G. Wen, "String-net condensation: A physical mechanism for topological phases," Phys. Rev. B **71** (2005) 045110, `arXiv:cond-mat/0404617`.

[39] R. B. Laughlin, "Anomalous Quantum Hall Effect: An Incompressible Quantum Fluid with Fractionally Charged Excitations," *Physical Review Letters* **50** (1983) 1395.

[40] D. C. Tsui, H. L. Stormer, and A. C. Gossard, "Two-Dimensional Magnetotransport in the Extreme Quantum Limit," *Physical Review Letters* **48** (1982) 1559.

[41] X. G. Wen, *Quantum Field Theory of Many Body Systems—From the Origin of Sound to an Origin of Light and Electrons*. Oxford University Press, 2004.

[42] A. Uhlmann, "The "transition probability" in the state space of a *-algebra," *Reports on Mathematical Physics* **9** (1976) 273.

[43] R. Jozsa, "Fidelity for Mixed Quantum States," *Journal of Modern Optics* **41** (1994) 2315.

[44] P. Zanardi and N. Paunković, "Ground state overlap and quantum phase transitions," Phys. Rev. E **74** (2006) 031123, arXiv:quant-ph/0512249.

[45] S. Chen, L. Wang, Y. Hao, and Y. Wang, "Intrinsic relation between ground-state fidelity and the characterization of a quantum phase transition," Phys. Rev. A **77** (2008) 032111, arXiv:0801.0020.

[46] H.-Q. Zhou and J. P. Barjaktarevič, "FAST TRACK COMMUNICATION: Fidelity and quantum phase transitions," *Journal of Physics A Mathematical General* **41** (2008) 2001.

[47] M. M. Rams and B. Damski, "Quantum Fidelity in the Thermodynamic Limit," *Physical Review Letters* **106** (2011) 055701, arXiv:1010.1048.

[48] P. Zanardi, P. Giorda, and M. Cozzini, "Information-Theoretic Differential Geometry of Quantum Phase Transitions," *Physical Review Letters* **99** (2007) 100603.

[49] L. Campos Venuti and P. Zanardi, "Quantum Critical Scaling of the Geometric Tensors," *Physical Review Letters* **99** (2007) 095701, arXiv:0705.2211.

[50] H.-Q. Zhou, J.-H. Zhao, H.-L. Wang, and B. Li, "FAST TRACK COMMUNICATION Singularities in fidelity surfaces for quantum phase transitions: a geometric perspective," *Journal of Physics A Mathematical General* **44** (2011) 042002.

[51] S.-J. Gu, "Fidelity Approach to Quantum Phase Transitions," *International Journal of Modern Physics B* **24** (2010) 4371.

[52] S. Garnerone, D. Abasto, S. Haas, and P. Zanardi, "Fidelity in topological quantum phases of matter," Phys. Rev. A **79** (2009) 032302, arXiv:0901.3807.

[53] E. Schrödinger, "Die gegenwärtige Situation in der Quantenmechanik," *Naturwissenschaften* **23** (1935) 807.

[54] A. Einstein, B. Podolsky, and N. Rosen, "Can Quantum-Mechanical Description of Physical Reality Be Considered Complete?," *Physical Review* **47** (1935) 777.

[55] J. S. Bell, "On the Problem of Hidden Variables in Quantum Mechanics," *Reviews of Modern Physics* **38** (1966) 447.

[56] J. F. Clauser, M. A. Horne, A. Shimony, and R. A. Holt, "Proposed Experiment to Test Local Hidden-Variable Theories," *Physical Review Letters* **23** (1969) 880.

[57] R. F. Werner, "Quantum states with Einstein-Podolsky-Rosen correlations admitting a hidden-variable model," *Physical Review A* **40** (1989) 4277.

[58] E. Schmidt, "Zur Theorie der linearen und nichtlinearen Integralgleichungen," *Mathematische Annalen* **63** (1907) 433.

[59] L. Amico, R. Fazio, A. Osterloh, and V. Vedral, "Entanglement in many-body systems," *Reviews of Modern Physics* **80** (2008) 517, arXiv:quant-ph/0703044.

[60] M. B. Plenio and S. Virmani, "An introduction to entanglement measures," arXiv:quant-ph/0504163.

[61] V. Vedral, M. B. Plenio, M. A. Rippin, and P. L. Knight, "Quantifying Entanglement," *Physical Review Letters* **78** (1997) 2275, arXiv:quant-ph/9702027.

[62] T.-C. Wei and P. M. Goldbart, "Geometric measure of entanglement and applications to bipartite and multipartite quantum states," Phys. Rev. A **68** (2003) 042307, arXiv:quant-ph/0307219.

[63] D. Petz, "Quasi-entropies for finite quantum systems," *Reports on Mathematical Physics* **23** (1986) 57.

[64] O. E. Lanford III and D. W. Robinson, "Mean entropy of states in quantum-statistical mechanics," *Journal of Mathematical Physics* **9** (1968) 1120.

[65] E. H. Lieb and M. B. Ruskai, "A Fundamental Property of Quantum-Mechanical Entropy," *Physical Review Letters* **30** (1973) 434.

[66] M. M. Wolf, F. Verstraete, M. B. Hastings, and J. I. Cirac, "Area Laws in Quantum Systems: Mutual Information and Correlations," *Physical Review Letters* **100** (2008) 070502, `arXiv:0704.3906`.

[67] F. Verstraete, M. Popp, and J. I. Cirac, "Entanglement versus Correlations in Spin Systems," *Physical Review Letters* **92** (2004) 027901, `arXiv:quant-ph/0307009`.

[68] D. Kaszlikowski, A. Sen(de), U. Sen, V. Vedral, and A. Winter, "Quantum Correlation without Classical Correlations," *Physical Review Letters* **101** (2008) 070502, `arXiv:0705.1969`.

[69] V. Coffman, J. Kundu, and W. K. Wootters, "Distributed entanglement," Phys. Rev. A **61** (2000) 052306, `arXiv:quant-ph/9907047`.

[70] M. Koashi and A. Winter, "Monogamy of quantum entanglement and other correlations," Phys. Rev. A **69** (2004) 022309, `arXiv:quant-ph/0310037`.

[71] B. M. Terhal, "Is entanglement monogamous?," *IBM Journal of Research and Development* **48** (2004) 71.

[72] T. J. Osborne and F. Verstraete, "General Monogamy Inequality for Bipartite Qubit Entanglement," *Physical Review Letters* **96** (2006) 220503, `arXiv:quant-ph/0502176`.

[73] D. Dieks, "Communication by EPR devices," *Physics Letters A* **92** (1982) 271.

[74] W. K. Wootters and W. H. Zurek, "A single quantum cannot be cloned," *Nature* **299** (1982) 802.

[75] L. Masanes, A. Acin, and N. Gisin, "General properties of nonsignaling theories," Phys. Rev. A **73** (2006) 012112, `arXiv:quant-ph/0508016`.

[76] B. Toner and F. Verstraete, "Monogamy of Bell correlations and Tsirelson's bound," `arXiv:quant-ph/0611001`.

[77] M. Seevinck, "Monogamy of Correlations vs. Monogamy of Entanglement," `arXiv:0908.1867`.

[78] B. Toner, "Monogamy of non-local quantum correlations," *Royal Society of London Proceedings Series A* **465** (2009) 59, `arXiv:quant-ph/0601172`.

[79] M. M. Wolf, F. Verstraete, and J. I. Cirac, "Entanglement and Frustration in Ordered Systems," `arXiv:quant-ph/0311051`.

[80] M. M. Wolf, F. Verstraete, and J. I. Cirac, "Entanglement Frustration for Gaussian States on Symmetric Graphs," *Physical Review Letters* **92** (2004) 087903, `arXiv:quant-ph/0307060`.

[81] S. Kirkpatrick, "Frustration and ground-state degeneracy in spin glasses," *Physical Review B* **16** (1977) 4630.

[82] G. Toulouse, "Theory of Frustration Effect in Spin Glasses," *Communications in Physics* **2** (1977) 115.

[83] J. Villain, "Spin glass with non-random interactions," *Journal of Physics C* **10** (1977) 1717.

[84] A. Fine, "Joint distributions, quantum correlations, and commuting observables," *Journal of Mathematical Physics* **23** (1982) 1306.

[85] L. Pauling, "The Structure and Entropy of Ice and of Other Crystals with Some Randomness of Atomic Arrangement," *Journal of the American Chemical Society* **57** (1935) 2680.

[86] G. Misguich and C. Lhuillier, "Two-dimensional quantum antiferromagnets," in *Frustrated spin systems*, H. T. Diep, ed. World Scientific, 2005. arXiv:cond-mat/0310405.

[87] S. M. Giampaolo, G. Adesso, and F. Illuminati, "Probing Quantum Frustrated Systems via Factorization of the Ground State," *Physical Review Letters* **104** (2010) 207202, arXiv:0906.4451.

[88] C. M. Dawson and M. A. Nielsen, "Frustration, interaction strength, and ground-state entanglement in complex quantum systems," Phys. Rev. A **69** (2004) 052316, arXiv:quant-ph/0401061.

[89] C. Brukner and V. Vedral, "Macroscopic Thermodynamical Witnesses of Quantum Entanglement," arXiv:quant-ph/0406040.

[90] G. Tóth, "Entanglement witnesses in spin models," Phys. Rev. A **71** (2005) 010301, arXiv:quant-ph/0406061.

[91] M. R. Dowling, A. C. Doherty, and S. D. Bartlett, "Energy as an entanglement witness for quantum many-body systems," Phys. Rev. A **70** (2004) 062113, arXiv:quant-ph/0408086.

[92] S. M. Giampaolo, G. Gualdi, A. Monras, and F. Illuminati, "Theory of classical and quantum frustration in quantum many-body systems," arXiv:1103.0022.

[93] J. W. Essam and M. E. Fisher, "Padé Approximant Studies of the Lattice Gas and Ising Ferromagnet below the Critical Point," *The Journal of Chemical Physics* **38** (1963) 802.

[94] B. Widom, "Surface Tension and Molecular Correlations near the Critical Point," *The Journal of Chemical Physics* **43** (1965) 3892.

[95] B. Widom, "Equation of State in the Neighborhood of the Critical Point," *The Journal of Chemical Physics* **43** (1965) 3898.

[96] L. P. Kadanoff, "Scaling laws for Ising models near T_c," *Physics* **2** (1966) 263.

[97] H. L. Haselgrove, M. A. Nielsen, and T. J. Osborne, "Entanglement, correlations, and the energy gap in many-body quantum systems," Phys. Rev. A **69** (2004) 032303, arXiv:quant-ph/0308083.

[98] B. Nachtergaele and R. Sims, "Lieb-Robinson Bounds and the Exponential Clustering Theorem," *Communications in Mathematical Physics* **265** (2006) 119, arXiv:math-ph/0506030.

[99] M. B. Hastings and T. Koma, "Spectral Gap and Exponential Decay of Correlations," *Communications in Mathematical Physics* **265** (2006) 781, arXiv:math-ph/0507008.

[100] M. C. Arnesen, S. Bose, and V. Vedral, "Natural Thermal and Magnetic Entanglement in the 1D Heisenberg Model," *Physical Review Letters* **87** (2001) 017901, arXiv:quant-ph/0009060.

[101] D. Gunlycke, V. M. Kendon, V. Vedral, and S. Bose, "Thermal concurrence mixing in a one-dimensional Ising model," Phys. Rev. A **64** (2001) 042302, arXiv:quant-ph/0102137.

[102] K. M. O'connor and W. K. Wootters, "Entangled rings," Phys. Rev. A **63** (2001) 052302, arXiv:quant-ph/0009041.

[103] T. J. Osborne and M. A. Nielsen, "Entanglement in a simple quantum phase transition," Phys. Rev. A **66** (2002) 032110, arXiv:quant-ph/0202162.

[104] A. Osterloh, L. Amico, G. Falci, and R. Fazio, "Scaling of entanglement close to a quantum phase transition," Nature **416** (2002) 608, arXiv:quant-ph/0202029.

[105] S.-J. Gu, H.-Q. Lin, and Y.-Q. Li, "Entanglement, quantum phase transition, and scaling in the XXZ chain," Phys. Rev. A **68** (2003) 042330, arXiv:quant-ph/0307131.

[106] F. Verstraete, M. A. Martín-Delgado, and J. I. Cirac, "Diverging Entanglement Length in Gapped Quantum Spin Systems," *Physical Review Letters* **92** (2004) 087201, arXiv:quant-ph/0311087.

[107] G. Vidal, J. I. Latorre, E. Rico, and A. Kitaev, "Entanglement in Quantum Critical Phenomena," *Physical Review Letters* **90** (2003) 227902, arXiv:quant-ph/0211074.

[108] J. I. Latorre, E. Rico, and G. Vidal, "Ground state entanglement in quantum spin chains," arXiv:quant-ph/0304098.

[109] M. B. Hastings, "An area law for one-dimensional quantum systems," *Journal of Statistical Mechanics: Theory and Experiment* **8** (2007) 24, arXiv:0705.2024.

[110] D. Gottesman and M. B. Hastings, "Entanglement versus gap for one-dimensional spin systems," *New Journal of Physics* **12** (2010) 025002, arXiv:0901.1108.

[111] M. B. Plenio, J. Eisert, J. Dreißig, and M. Cramer, "Entropy, Entanglement, and Area: Analytical Results for Harmonic Lattice Systems," *Physical Review Letters* **94** (2005) 060503, arXiv:quant-ph/0405142.

[112] M. Cramer, J. Eisert, M. B. Plenio, and J. Dreißig, "Entanglement-area law for general bosonic harmonic lattice systems," Phys. Rev. A **73** (2006) 012309, arXiv:quant-ph/0505092.

[113] M. M. Wolf, "Violation of the Entropic Area Law for Fermions," *Physical Review Letters* **96** (2006) 010404, arXiv:quant-ph/0503219.

[114] D. Gioev and I. Klich, "Entanglement Entropy of Fermions in Any Dimension and the Widom Conjecture," *Physical Review Letters* **96** (2006) 100503, arXiv:quant-ph/0504151.

[115] B. Swingle, "Entanglement Entropy and the Fermi Surface," *Physical Review Letters* **105** (2010) 050502, arXiv:0908.1724.

[116] X. Chen, Z.-C. Gu, and X.-G. Wen, "Local unitary transformation, long-range quantum entanglement, wave function renormalization, and topological order," Phys. Rev. B **82** (2010) 155138, arXiv:1004.3835.

[117] S. Bachmann, S. Michalakis, B. Nachtergaele, and R. Sims, "Automorphic Equivalence within Gapped Phases of Quantum Lattice Systems," arXiv:1102.0842.

[118] M. B. Hastings, "Solving gapped Hamiltonians locally," Phys. Rev. B **73** (2006) 085115, arXiv:cond-mat/0508554.

[119] N. de Beaudrap, M. Ohliger, T. J. Osborne, and J. Eisert, "Solving Frustration-Free Spin Systems," *Physical Review Letters* **105** (2010) 060504, arXiv:1005.3781.

[120] H. Casini, "Geometric entropy, area and strong subadditivity," *Classical and Quantum Gravity* **21** (2004) 2351, arXiv:hep-th/0312238.

[121] H. Casini and M. Huerta, "A finite entanglement entropy and the c-theorem," *Physics Letters B* **600** (2004) 142, arXiv:hep-th/0405111.

[122] J. L. Cardy and I. Peschel, "Finite-size dependence of the free energy in two-dimensional critical systems," *Nuclear Physics B* **300** (1988) 377.

[123] C. Holzhey, F. Larsen, and F. Wilczek, "Geometric and renormalized entropy in conformal field theory," *Nuclear Physics B* **424** (1994) 443.

[124] P. Calabrese and J. Cardy, "Entanglement entropy and quantum field theory," *Journal of Statistical Mechanics: Theory and Experiment* **6** (2004) 2, arXiv:hep-th/0405152.

[125] L. Bombelli, R. K. Koul, J. Lee, and R. D. Sorkin, "Quantum source of entropy for black holes," Phys. Rev. D **34** (1986) 373.

[126] M. Srednicki, "Entropy and area," *Physical Review Letters* **71** (1993) 666, arXiv:hep-th/9303048.

[127] H. Casini and M. Huerta, "Entanglement entropy in free quantum field theory," *Journal of Physics A Mathematical General* **42** (2009) 4007, arXiv:0905.2562.

[128] H. Casini and M. Huerta, "Universal terms for the entanglement entropy in 2+1 dimensions," *Nuclear Physics B* **764** (2007) 183, arXiv:hep-th/0606256.

[129] A. Kitaev and J. Preskill, "Topological Entanglement Entropy," *Physical Review Letters* **96** (2006) 110404, arXiv:hep-th/0510092.

[130] M. Levin and X.-G. Wen, "Detecting Topological Order in a Ground State Wave Function," *Physical Review Letters* **96** (2006) 110405, arXiv:cond-mat/0510613.

[131] P. Fendley, M. P. A. Fisher, and C. Nayak, "Topological Entanglement Entropy from the Holographic Partition Function," *Journal of Statistical Physics* **126** (2007) 1111, arXiv:cond-mat/0609072.

[132] S. Das and S. Shankaranarayanan, "How robust is the entanglement entropy-area relation?," Phys. Rev. D **73** (2006) 121701, arXiv:gr-qc/0511066.

[133] S. Das and S. Shankaranarayanan, "Where are the black-hole entropy degrees of freedom?," *Classical and Quantum Gravity* **24** (2007) 5299, arXiv:gr-qc/0703082.

[134] S. Das, S. Shankaranarayanan, and S. Sur, "Power-law corrections to entanglement entropy of horizons," Phys. Rev. D **77** (2008) 064013, arXiv:0705.2070.

[135] V. Alba, M. Fagotti, and P. Calabrese, "Entanglement entropy of excited states," *Journal of Statistical Mechanics: Theory and Experiment* **10** (2009) 20, arXiv:0909.1999.

[136] L. Masanes, "Area law for the entropy of low-energy states," Phys. Rev. A **80** (2009) 052104, arXiv:0907.4672.

[137] S. Bravyi, M. B. Hastings, and F. Verstraete, "Lieb-Robinson Bounds and the Generation of Correlations and Topological Quantum Order," *Physical Review Letters* **97** (2006) 050401, arXiv:quant-ph/0603121.

[138] J. Eisert and T. J. Osborne, "General Entanglement Scaling Laws from Time Evolution," *Physical Review Letters* **97** (2006) 150404, arXiv:quant-ph/0603114.

[139] E. H. Lieb and D. W. Robinson, "The finite group velocity of quantum spin systems," *Communications in Mathematical Physics* **28** (1972) 251.

[140] M. B. Hastings, "Lieb-Schultz-Mattis in higher dimensions," Phys. Rev. B **69** (2004) 104431, arXiv:cond-mat/0305505.

[141] B. Nachtergaele, Y. Ogata, and R. Sims, "Propagation of Correlations in Quantum Lattice Systems," *Journal of Statistical Physics* **124** (2006) 1, arXiv:math-ph/0603064.

[142] M. Cramer, A. Serafini, and J. Eisert, "Locality of dynamics in general harmonic quantum systems," arXiv:0803.0890.

[143] B. Nachtergaele, H. Raz, B. Schlein, and R. Sims, "Lieb-Robinson Bounds for Harmonic and Anharmonic Lattice Systems," *Communications in Mathematical Physics* **286** (2009) 1073, arXiv:0712.3820.

[144] D. Poulin, "Lieb-Robinson Bound and Locality for General Markovian Quantum Dynamics," *Physical Review Letters* **104** (2010) 190401, arXiv:1003.3675.

[145] I. Prémont-Schwarz, A. Hamma, I. Klich, and F. Markopoulou-Kalamara, "Lieb-Robinson bounds for commutator-bounded operators," Phys. Rev. A **81** (2010) 040102, arXiv:0912.4544.

[146] B. Nachtergaele and R. Sims, "Lieb-Robinson Bounds in Quantum Many-Body Physics," arXiv:1004.2086.

[147] N. Schuch, S. K. Harrison, T. J. Osborne, and J. Eisert, "Information propagation for interacting particle systems," arXiv:1010.4576.

[148] J. D. Bekenstein, "Black holes and entropy," *Physical Review D* **7** (1973) 2333.

[149] J. M. Bardeen, B. Carter, and S. W. Hawking, "The four laws of black hole mechanics," *Communications in Mathematical Physics* **31** (1973) 161.

[150] S. W. Hawking, "Black hole explosions?," *Nature* **248** (1974) 30.

[151] C. Holzhey, F. Larsen, and F. Wilczek, "Geometric and renormalized entropy in conformal field theory," *Nuclear Physics B* **424** (1994) 443, arXiv:hep-th/9403108.

[152] S. Das, S. Shankaranarayanan, and S. Sur, "Black hole entropy from entanglement: A review," arXiv:0806.0402.

[153] G. 't Hooft, "Dimensional Reduction in Quantum Gravity," arXiv:gr-qc/9310026.

[154] L. Susskind, "The world as a hologram," *Journal of Mathematical Physics* **36** (1995) 6377, arXiv:hep-th/9409089.

[155] R. Bousso, "The holographic principle," *Reviews of Modern Physics* **74** (2002) 825, arXiv:hep-th/0203101.

[156] J. Maldacena, "The large-n limit of superconformal field theories and supergravity," *International Journal of Theoretical Physics* **38** (1999) 1113.

[157] S. S. Gubser, I. R. Klebanov, and A. M. Polyakov, "Gauge theory correlators from non-critical string theory," *Physics Letters B* **428** (1998) 105.

[158] E. Witten, "Anti-de Sitter space and holography," *Advances in Theoretical and Mathematical Physics* **2** (1998) 253, arXiv:hep-th/9802150.

[159] S. Ryu and T. Takayanagi, "Holographic Derivation of Entanglement Entropy from the anti de Sitter Space/Conformal Field Theory Correspondence," *Physical Review Letters* **96** (2006) 181602, arXiv:hep-th/0603001.

[160] S. Ryu and T. Takayanagi, "Aspects of holographic entanglement entropy," *Journal of High Energy Physics* **8** (2006) 45, arXiv:hep-th/0605073.

[161] M. Headrick and T. Takayanagi, "Holographic proof of the strong subadditivity of entanglement entropy," Phys. Rev. D **76** (2007) 106013, arXiv:0704.3719.

[162] T. Nishioka, S. Ryu, and T. Takayanagi, "Holographic entanglement entropy: an overview," *Journal of Physics A Mathematical General* **42** (2009) 4008, arXiv:0905.0932.

[163] H. Casini, M. Huerta, and R. C. Myers, "Towards a derivation of holographic entanglement entropy," *Journal of High Energy Physics* **5** (2011) 36, arXiv:1102.0440.

[164] P. W. Anderson, "More Is Different: Broken symmetry and the nature of the hierarchical structure of science," *Science* **177** (1972) 393. http://www.jstor.org/pss/1734697.

[165] H. A. Bethe, "The Electromagnetic Shift of Energy Levels," *Physical Review* **72** (1947) 339.

[166] J. Schwinger, "On Quantum-Electrodynamics and the Magnetic Moment of the Electron," *Physical Review* **73** (1948) 416.

[167] W. E. Lamb and R. C. Retherford, "Fine Structure of the Hydrogen Atom by a Microwave Method," *Physical Review* **72** (1947) 241.

[168] P. Kusch and H. M. Foley, "The Magnetic Moment of the Electron," *Physical Review* **74** (1948) 250.

[169] S. Tomonaga, "On a Relativistically Invariant Formulation of the Quantum Theory of Wave Fields," *Progress of Theoretical Physics* **1** (1946) 27.

[170] J. Schwinger, "Quantum Electrodynamics. I. A Covariant Formulation," *Physical Review* **74** (1948) 1439.

[171] J. Schwinger, "Quantum Electrodynamics. II. Vacuum Polarization and Self-Energy," *Physical Review* **75** (1949) 651.

[172] J. Schwinger, "Quantum Electrodynamics. III. The Electromagnetic Properties of the Electron—Radiative Corrections to Scattering," *Physical Review* **76** (1949) 790.

[173] R. P. Feynman, "Space-Time Approach to Quantum Electrodynamics," *Physical Review* **76** (1949) 769.

[174] R. P. Feynman, "The Theory of Positrons," *Physical Review* **76** (1949) 749.

[175] R. P. Feynman, "Mathematical Formulation of the Quantum Theory of Electromagnetic Interaction," *Physical Review* **80** (1950) 440.

[176] F. J. Dyson, "The Radiation Theories of Tomonaga, Schwinger, and Feynman," *Physical Review* **75** (1949) 486.

[177] F. J. Dyson, "The *S* Matrix in Quantum Electrodynamics," *Physical Review* **75** (1949) 1736.

[178] W. E. Thirring, "Zum Wert der Renormalisationskonstanten," *Zeitschrift Naturforschung Teil A* **6** (1951) 462.

[179] G. Källen, "Non perturbation theory approach to renormalization technique," *Physica* **19** (1953) 850.

[180] N. Bogoliubow and O. Parasiuk, "Über die Multiplikation der Kausalfunktionen in der Quantentheorie der Felder," *Acta Mathematica* **97** (1957) 227.

[181] K. Hepp, "Proof of the Bogoliubov-Parasiuk theorem on renormalization," *Communications in Mathematical Physics* **2** (1966) 301.

[182] W. Zimmermann, "Convergence of Bogoliubov's method of renormalization in momentum space," *Communications in Mathematical Physics* **15** (1969) 208.

[183] H. Epstein and V. Glaser, "The role of locality in perturbation theory," *Annales de l'Institute Henri Poincaré* **19** (1973) 2011.

[184] E. C. G. Stueckelberg and A. Petermann, "Normalization of constants in the quanta theory," *Helvetica Physica Acta* **26** (1953) 499.

[185] M. Gell-Mann and F. E. Low, "Quantum Electrodynamics at Small Distances," *Physical Review* **95** (1954) 1300.

[186] C. G. Callan, "Broken Scale Invariance in Scalar Field Theory," *Physical Review D* **2** (1970) 1541.

[187] K. Symanzik, "Small distance behaviour in field theory and power counting," *Communications in Mathematical Physics* **18** (1970) 227.

[188] K. Symanzik, "Small-distance-behaviour analysis and Wilson expansions," *Communications in Mathematical Physics* **23** (1971) 49.

[189] K. G. Wilson, "The renormalization group: Critical phenomena and the Kondo problem," *Reviews of Modern Physics* **47** (1975) 773.

[190] K. G. Wilson, "Model of Coupling-Constant Renormalization," *Physical Review D* **2** (1970) 1438.

[191] K. G. Wilson, "Renormalization Group and Critical Phenomena. I. Renormalization Group and the Kadanoff Scaling Picture," Phys. Rev. B **4** (1971) 3174.

[192] K. G. Wilson, "Renormalization Group and Critical Phenomena. II. Phase-Space Cell Analysis of Critical Behavior," Phys. Rev. B **4** (1971) 3184.

[193] K. G. Wilson and M. E. Fisher, "Critical Exponents in 3.99 Dimensions," *Physical Review Letters* **28** (1972) 240.

[194] K. G. Wilson, "Feynman-Graph Expansion for Critical Exponents," *Physical Review Letters* **28** (1972) 548.

[195] F. J. Wegner, "Corrections to Scaling Laws," *Physical Review B* **5** (1972) 4529.

[196] F. J. Wegner, "Some invariance properties of the renormalization group," *Journal of Physics C* **7** (1974) 2098.

[197] F. J. Wegner, *Phase Transitions and Critical Phenomena*, vol. 6, ch. The Critical State, General Aspects. Academic Press, 1976.

[198] J. Zinn-Justin, "Perturbation series at large orders in quantum mechanics and field theories: Application to the problem of resummation," *Physics Reports* **70** (1981) 109.

[199] A. M. Polyakov, "Interaction of goldstone particles in two dimensions. Applications to ferromagnets and massive Yang-Mills fields," *Physics Letters B* **59** (1975) 79.

[200] A. A. Migdal, "Gauge transitions in gauge and spin lattice systems," *Soviet Journal of Experimental and Theoretical Physics* **42** (1975) 743.

[201] E. Brézin, J. Zinn-Justin, and J. C. Le Guillou, "Anomalous dimensions of composite operators near two dimensions for ferromagnets with $o(n)$ symmetry," *Physical Review B* (1976) no. 11, 4976.

[202] T. Niemeijer and J. M. J. van Leeuwen, "Wilson Theory for Spin Systems on a Triangular Lattice," *Physical Review Letters* **31** (1973) 1411.

[203] T. Niemeyer and J. V. Leeuwen, "Wilson theory for 2-dimensional Ising spin systems," *Physica* **71** (1974) 17.

[204] L. P. Kadanoff and A. Houghton, "Numerical evaluations of the critical properties of the two-dimensional ising model," *Physical Review B* **11** (1975) 377.

[205] L. Onsager, "Crystal Statistics. I. A Two-Dimensional Model with an Order-Disorder Transition," *Physical Review* **65** (1944) 117.

[206] V. L. Berezinskiĭ, "Destruction of Long-range Order in One-dimensional and Two-dimensional Systems having a Continuous Symmetry Group I. Classical Systems," *Soviet Journal of Experimental and Theoretical Physics* **32** (1971) 493.

[207] V. L. Berezinskiĭ, "Destruction of Long-range Order in One-dimensional and Two-dimensional Systems Possessing a Continuous Symmetry Group. II. Quantum Systems," *Soviet Journal of Experimental and Theoretical Physics* **34** (1972) 610.

[208] J. M. Kosterlitz and D. J. Thouless, "Ordering, metastability and phase transitions in two-dimensional systems," *Journal of Physics C: Solid State Physics* (1973) no. 7, 1181.

[209] J. M. Kosterlitz, "The critical properties of the two-dimensional xy model," *Journal of Physics C: Solid State Physics* **7** (1974) 1046.

[210] F. J. Wegner and A. Houghton, "Renormalization group equation for critical phenomena," *Physical Review A* **8** (1973) 401.

[211] J. Polchinski, "Renormalization and effective lagrangians," *Nuclear Physics B* **231** (1984) 269.

[212] B. Delamotte, "An Introduction to the Nonperturbative Renormalization Group," `arXiv:cond-mat/0702365`.

[213] C. Wetterich, "Average action and the renormalization group equations," *Nuclear Physics B* **352** (1991) 529.

[214] E. T. Akhmedov, "A remark on the AdS/CFT correspondence and the renormalization group flow," *Physics Letters B* **442** (1998) 152.

[215] V. Balasubramanian and P. Kraus, "Spacetime and the Holographic Renormalization Group," *Physical Review Letters* **83** (1999) 3605, arXiv:hep-th/9903190.

[216] J. de Boer, E. Verlinde, and H. Verlinde, "On the holographic renormalization group," *Journal of High Energy Physics* **2000** (2000) 003, arXiv:hep-th/9912012.

[217] M. Bianchi, D. Z. Freedman, and K. Skenderis, "Holographic renormalization," *Nuclear Physics B* **631** (2002) 159, arXiv:hep-th/0112119.

[218] M. Fukuma, S. Matsuura, and T. Sakai, "Holographic Renormalization Group," *Progress of Theoretical Physics* **109** (2003) 489, arXiv:hep-th/0212314.

[219] D. Radicevic, "Connecting the Holographic and Wilsonian Renormalization Groups," arXiv:1105.5825.

[220] M. E. Fisher, S.-k. Ma, and B. G. Nickel, "Critical Exponents for Long-Range Interactions," *Physical Review Letters* **29** (1972) 917.

[221] K. G. Wilson, "Model hamiltonians for local quantum field theory," *Physical Review* **140** (1965) B445.

[222] S. R. White and R. M. Noack, "Real-space quantum renormalization groups," *Physical Review Letters* **68** (1992) 3487.

[223] S. R. White, "Density matrix formulation for quantum renormalization groups," *Physical Review Letters* **69** (1992) 2863.

[224] S. R. White, "Density-matrix algorithms for quantum renormalization groups," Phys. Rev. B **48** (1993) 10345.

[225] K. Hallberg, "Density Matrix Renormalization: A Review of the Method and its Applications," arXiv:cond-mat/0303557.

[226] U. Schollwöck, "The density-matrix renormalization group," *Reviews of Modern Physics* **77** (2005) 259, arXiv:cond-mat/0409292.

[227] S. Östlund and S. Rommer, "Thermodynamic Limit of Density Matrix Renormalization," *Physical Review Letters* **75** (1995) 3537, arXiv:cond-mat/9503107.

[228] S. Rommer and S. Öautstlund, "Class of ansatz wave functions for one-dimensional spin systems and their relation to the density matrix renormalization group," Phys. Rev. B **55** (1997) 2164, arXiv:cond-mat/9606213.

[229] F. Verstraete, J. I. Cirac, J. I. Latorre, E. Rico, and M. M. Wolf, "Renormalization-Group Transformations on Quantum States," *Physical Review Letters* **94** (2005) 140601, arXiv:quant-ph/0410227.

[230] J. I. Latorre, C. A. Lütken, E. Rico, and G. Vidal, "Fine-grained entanglement loss along renormalization-group flows," Phys. Rev. A **71** (2005) 034301, arXiv:quant-ph/0404120.

[231] R. Orús, "Entanglement and majorization in (1+1) -dimensional quantum systems," Phys. Rev. A **71** (2005) 052327, arXiv:quant-ph/0501110.

[232] H. Casini and M. Huerta, "A c-theorem for entanglement entropy," *Journal of Physics A Mathematical General* **40** (2007) 7031, arXiv:cond-mat/0610375.

[233] J. W. Rayleigh, "In Finding the Correction for the Open End of an Organ-Pipe," *Philosophical Transactions* **161** (1870) 77.

[234] W. Ritz, "Über eine neue Methode zur Lösung gewisser Variationsprobleme der mathematischen Physik," *Journal für die reine und angewandte Mathematik* **135** (1908) 1.

[235] D. R. Hartree, "The Wave Mechanics of an Atom with a Non-Coulomb Central Field. Part I. Theory and Methods," *Mathematical Proceedings of the Cambridge Philosophical Society* **24** (1928) 89.

[236] D. R. Hartree, "The Wave Mechanics of an Atom with a Non-Coulomb Central Field. Part II. Some Results and Discussion," *Mathematical Proceedings of the Cambridge Philosophical Society* **24** (1928) 111.

[237] V. Fock, "Näherungsmethode zur Lösung des quantenmechanischen Mehrkörperproblems," *Zeitschrift für Physik A* **61** (1930) 126.

[238] J. C. Slater, "Note on hartree's method," *Physical Review* **35** (1930) 210.

[239] D. A. Huse and E. D. Siggia, "The density distribution of a weakly interacting bose gas in an external potential," *Journal of Low Temperature Physics* **46** (1982) 137.

[240] P. Hohenberg and W. Kohn, "Inhomogeneous Electron Gas," *Physical Review* **136** (1964) 864.

[241] W. Kohn and L. J. Sham, "Self-Consistent Equations Including Exchange and Correlation Effects," *Physical Review* **140** (1965) 1133.

[242] P. W. Anderson, "Limits on the Energy of the Antiferromagnetic Ground State," *Physical Review* **83** (1951) 1260.

[243] T. J. Osborne, "Lower Bound for the Ground-State Energy Density of a 1D Quantum Spin System," `arXiv:cond-mat/0508428`.

[244] P. A. M. Dirac, "On the Annihilation of Electrons and Protons," *Mathematical Proceedings of the Cambridge Philosophical Society* **26** (1930) 376.

[245] J. Frenkel, *Wave Mechanics, Advanced General Theory*. Oxford, 1934.

[246] P. Kramer and M. Saraceno, *Geometry of the Time-Dependent Variational Principle in Quantum Mechanics*, vol. 140 of *Lecture Notes in Physics*. Springer, 1981.

[247] E. P. Gross, "Structure of a quantized vortex in boson systems," *Il Nuovo Cimento* **20** (1961) 454.

[248] L. P. Pitaevskii, "Vortex Lines in an Imperfect Bose Gas," *Soviet Journal of Experimental and Theoretical Physics* **13** (1961) 451.

[249] A. K. Kerman and S. E. Koonin, "Hamiltonian formulation of time-dependent variational principles for the many-body system," *Annals of Physics* **100** (1976) 332.

[250] D. Bohm and D. Pines, "A Collective Description of Electron Interactions: III. Coulomb Interactions in a Degenerate Electron Gas," *Physical Review* **92** (1953) 609.

[251] P. G. de Gennes, *Superconductivity of Metals and Alloys*. Benjamin, 1966.

[252] R. P. Feynman, "Difficulties in applying the variational principle to quantum field theories," in *Proceedings of the International Workshop on Variational Calculations in Quantum Field Theory held in Wangarooge, West Germany, 1-4 September 1987*, L. Polley and D. E. L. Pottinger, eds. World Scientific, 1988.

[253] J. Čížek, "On the Correlation Problem in Atomic and Molecular Systems. Calculation of Wavefunction Components in Ursell-Type Expansion Using Quantum-Field Theoretical Methods," *Journal of Chemical Physics* **45** (1966) 4256.

[254] D. Schütte, Z. Weihong, and C. J. Hamer, "Coupled cluster method in hamiltonian lattice field theory," *Physical Review D* **55** (1997) 2974.

[255] B. H. J. McKellar, C. R. Leonard, and L. C. L. Hollenberg, "Coupled Cluster Methods for Lattice Gauge Theories," *International Journal of Modern Physics B* **14** (2000) 2023.

[256] A. Wichmann, D. Schütte, B. C. Metsch, and V. Wethkamp, "Coupled cluster method in Hamiltonian lattice field theory: SU(2) glueballs," *Physical Review D* **65** (2002) 094511.

[257] F. Verstraete, V. Murg, and J. I. Cirac, "Matrix product states, projected entangled pair states, and variational renormalization group methods for quantum spin systems," *Advances in Physics* **57** (2008) 143, arXiv:0907.2796.

[258] J. I. Cirac and F. Verstraete, "Renormalization and tensor product states in spin chains and lattices," *Journal of Physics A Mathematical General* **42** (2009) 4004, arXiv:0910.1130.

[259] U. Schollwöck, "The density-matrix renormalization group in the age of matrix product states," *Annals of Physics* **326** (2011) 96, arXiv:1008.3477.

[260] G. Vidal, "Efficient Classical Simulation of Slightly Entangled Quantum Computations," *Physical Review Letters* **91** (2003) 147902, arXiv:quant-ph/0301063.

[261] K. Okunishi, Y. Hieida, and Y. Akutsu, "Universal asymptotic eigenvalue distribution of density matrices and corner transfer matrices in the thermodynamic limit," Phys. Rev. E **59** (1999) 6227, arXiv:cond-mat/9810239.

[262] F. Verstraete and J. I. Cirac, "Matrix product states represent ground states faithfully," Phys. Rev. B **73** (2006) 094423, arXiv:cond-mat/0505140.

[263] N. Schuch, M. M. Wolf, F. Verstraete, and J. I. Cirac, "Entropy Scaling and Simulability by Matrix Product States," *Physical Review Letters* **100** (2008) 030504, arXiv:0705.0292.

[264] P. Anderson, "Resonating valence bonds: A new kind of insulator?," *Materials Research Bulletin* **8** (1973) 153.

[265] P. Anderson, "The Resonating Valence Bond State in La2CuO4 and Superconductivity," *Science* **235** (1987) 1196.

[266] S. A. Kivelson, D. S. Rokhsar, and J. P. Sethna, "Topology of the resonating valence-bond state: Solitons and high-T_c superconductivity," *Physical Review B* **35** (1987) 8865.

[267] I. Affleck, T. Kennedy, E. H. Lieb, and H. Tasaki, "Rigorous results on valence-bond ground states in antiferromagnets," *Physical Review Letters* **59** (1987) 799.

[268] I. Affleck, T. Kennedy, E. H. Lieb, and H. Tasaki, "Valence bond ground states in isotropic quantum antiferromagnets," *Communications in Mathematical Physics* **115** (1988) 477.

[269] F. Verstraete and J. I. Cirac, "Valence-bond states for quantum computation," Phys. Rev. A **70** (2004) 060302, arXiv:quant-ph/0311130.

[270] F. Verstraete, D. Porras, and J. I. Cirac, "Density Matrix Renormalization Group and Periodic Boundary Conditions: A Quantum Information Perspective," *Physical Review Letters* **93** (2004) 227205, arXiv:cond-mat/0404706.

[271] F. Verstraete and J. I. Cirac, "Renormalization algorithms for Quantum-Many Body Systems in two and higher dimensions," arXiv:cond-mat/0407066.

[272] M. Fannes, B. Nachtergaele, and R. F. Werner, "Valence bond states on quantum spin chains as ground states with spectral gap," *Journal of Physics A Mathematical General* **24** (1991) .

[273] D. Perez-Garcia, F. Verstraete, M. M. Wolf, and J. I. Cirac, "Matrix Product State Representations," arXiv:quant-ph/0608197.

[274] C. Saavedra, K. M. Gheri, P. Törmä, J. I. Cirac, and P. Zoller, "Controlled source of entangled photonic qubits," *Physical Review A* **61** (2000) 062311.

[275] C. Schön, E. Solano, F. Verstraete, J. I. Cirac, and M. M. Wolf, "Sequential Generation of Entangled Multiqubit States," *Physical Review Letters* **95** (2005) 110503, arXiv:quant-ph/0501096.

[276] T. J. Osborne, J. Eisert, and F. Verstraete, "Holographic Quantum States," *Physical Review Letters* **105** (2010) 260401, arXiv:1005.1268.

[277] M. C. Bañuls, D. Pérez-García, M. M. Wolf, F. Verstraete, and J. I. Cirac, "Sequentially generated states for the study of two-dimensional systems," Phys. Rev. A **77** (2008) 052306, arXiv:0802.2472.

[278] C. M. Dawson, J. Eisert, and T. J. Osborne, "Unifying Variational Methods for Simulating Quantum Many-Body Systems," *Physical Review Letters* **100** (2008) 130501, arXiv:0705.3456.

[279] F. C. Alcaraz and M. J. Lazo, "LETTER TO THE EDITOR: The Bethe ansatz as a matrix product ansatz," *Journal of Physics A Mathematical General* **37** (2004) , arXiv:cond-mat/0304170.

[280] F. C. Alcaraz and M. J. Lazo, "Exact solutions of exactly integrable quantum chains by a matrix product ansatz," *Journal of Physics A Mathematical General* **37** (2004) 4149, arXiv:cond-mat/0312373.

[281] H. Katsura and I. Maruyama, "Derivation of the matrix product ansatz for the Heisenberg chain from the algebraic Bethe ansatz," *Journal of Physics A Mathematical General* **43** (2010) 175003, arXiv:0911.4215.

[282] J. I. Cirac and G. Sierra, "Infinite matrix product states, conformal field theory, and the Haldane-Shastry model," Phys. Rev. B **81** (2010) 104431, arXiv:0911.3029.

[283] A. E. B. Nielsen, G. Sierra, and J. I. Cirac, "Violation of the area law and long-range correlations in infinite-dimensional-matrix product states," Phys. Rev. A **83** (2011) 053807, arXiv:1103.2205.

[284] E. C. Sudarshan, P. M. Mathews, and J. Rau, "Stochastic Dynamics of Quantum-Mechanical Systems," *Physical Review* **121** (1961) 920.

[285] A. Jamiołkowski, "Linear transformations which preserve trace and positive semidefiniteness of operators," *Reports on Mathematical Physics* **3** (1972) 275.

[286] M.-D. Choi, "Completely positive linear maps on complex matrices," *Linear Algebra and its Applications* **10** (1975) 285.

[287] P. Arrighi and C. Patricot, "On quantum operations as quantum states," *Annals of Physics* **311** (2004) 26.

[288] P. Pippan, S. R. White, and H. G. Evertz, "Efficient matrix-product state method for periodic boundary conditions," Phys. Rev. B **81** (2010) 081103.

[289] B. Pirvu, F. Verstraete, and G. Vidal, "Exploiting translational invariance in matrix product state simulations of spin chains with periodic boundary conditions," Phys. Rev. B **83** (2011) 125104, arXiv:1005.5195.

[290] A. W. Sandvik and G. Vidal, "Variational Quantum MonteCarlo Simulations with Tensor-Network States," *Physical Review Letters* **99** (2007) 220602, arXiv:0708.2232.

[291] V. Murg, F. Verstraete, and J. I. Cirac, "Variational study of hard-core bosons in a two-dimensional optical lattice using projected entangled pair states," Phys. Rev. A **75** (2007) 033605, arXiv:cond-mat/0611522.

[292] H. C. Jiang, Z. Y. Weng, and T. Xiang, "Accurate Determination of Tensor Network State of Quantum Lattice Models in Two Dimensions," *Physical Review Letters* **101** (2008) 090603, arXiv:0806.3719.

[293] L. Wang, I. Pižorn, and F. Verstraete, "Monte Carlo simulation with tensor network states," Phys. Rev. B **83** (2011) 134421, arXiv:1010.5450.

[294] F. Verstraete, J. J. García-Ripoll, and J. I. Cirac, "Matrix Product Density Operators: Simulation of Finite-Temperature and Dissipative Systems," *Physical Review Letters* **93** (2004) 207204, arXiv:cond-mat/0406426.

[295] M. Zwolak and G. Vidal, "Mixed-State Dynamics in One-Dimensional Quantum Lattice Systems: A Time-Dependent Superoperator Renormalization Algorithm," *Physical Review Letters* **93** (2004) 207205, arXiv:cond-mat/0406440.

[296] G. M. Crosswhite, A. C. Doherty, and G. Vidal, "Applying matrix product operators to model systems with long-range interactions," Phys. Rev. B **78** (2008) 035116, arXiv:0804.2504.

[297] I. P. McCulloch, "Infinite size density matrix renormalization group, revisited," arXiv:0804.2509.

[298] B. Pirvu, V. Murg, J. I. Cirac, and F. Verstraete, "Matrix product operator representations," *New Journal of Physics* **12** (2010) 025012, arXiv:0804.3976.

[299] M. Fannes, B. Nachtergaele, and R. F. Werner, "Finitely correlated states on quantum spin chains," *Communications in Mathematical Physics* **144** (1992) 443.

[300] G. Vidal, "Classical Simulation of Infinite-Size Quantum Lattice Systems in One Spatial Dimension," *Physical Review Letters* **98** (2007) 070201, arXiv:cond-mat/0605597.

[301] N. Schuch, D. Perez-Garcia, and I. Cirac, "Classifying quantum phases using Matrix Product States and PEPS," arXiv:1010.3732.

[302] S. Singh, H.-Q. Zhou, and G. Vidal, "Simulation of one-dimensional quantum systems with a global SU(2) symmetry," *New Journal of Physics* **12** (2010) 033029, arXiv:cond-mat/0701427.

[303] S. Singh, R. N. C. Pfeifer, and G. Vidal, "Tensor network decompositions in the presence of a global symmetry," Phys. Rev. A **82** (2010) 050301, arXiv:0907.2994.

[304] I. P. McCulloch and M. Gulácsi, "The non-Abelian density matrix renormalization group algorithm," *Europhysics Letters* **57** (2002) 852, arXiv:cond-mat/0012319.

[305] I. P. McCulloch, "From density-matrix renormalization group to matrix product states," *Journal of Statistical Mechanics: Theory and Experiment* **10** (2007) 14, arXiv:cond-mat/0701428.

[306] M. Sanz, M. M. Wolf, D. Pérez-García, and J. I. Cirac, "Matrix product states: Symmetries and two-body Hamiltonians," Phys. Rev. A **79** (2009) 042308, arXiv:0901.2223.

[307] S. Singh, R. N. C. Pfeifer, and G. Vidal, "Tensor network states and algorithms in the presence of a global U(1) symmetry," Phys. Rev. B **83** (2011) 115125, arXiv:1008.4774.

[308] H.-L. Wang, J.-H. Zhao, B. Li, and H.-Q. Zhou, "Kosterlitz-Thouless Phase Transition and Ground State Fidelity: a Novel Perspective from Matrix Product States," arXiv:0902.1670.

[309] B. Nachtergaele, "The spectral gap for some spin chains with discrete symmetry breaking," *Communications in Mathematical Physics* **175** (1996) 565, arXiv:cond-mat/9410110.

[310] H.-Q. Zhou, "Deriving local order parameters from tensor network representations," arXiv:0803.0585.

[311] D. Pérez-García, M. M. Wolf, M. Sanz, F. Verstraete, and J. I. Cirac, "String Order and Symmetries in Quantum Spin Lattices," *Physical Review Letters* **100** (2008) 167202, arXiv:0802.0447.

[312] M. Cozzini, R. Ionicioiu, and P. Zanardi, "Quantum fidelity and quantum phase transitions in matrix product states," Phys. Rev. B **76** (2007) 104420, arXiv:cond-mat/0611727.

[313] H. H. Zhao, Z. Y. Xie, Q. N. Chen, Z. C. Wei, J. W. Cai, and T. Xiang, "Renormalization of tensor-network states," Phys. Rev. B **81** (2010) 174411, arXiv:1002.1405.

[314] C. Liu, L. Wang, A. W. Sandvik, Y.-C. Su, and Y.-J. Kao, "Symmetry breaking and criticality in tensor-product states," Phys. Rev. B **82** (2010) 060410, arXiv:1002.1657.

[315] M. M. Wolf, G. Ortiz, F. Verstraete, and J. I. Cirac, "Quantum Phase Transitions in Matrix Product Systems," *Physical Review Letters* **97** (2006) 110403, arXiv:cond-mat/0512180.

[316] J.-M. Zhu, "Quantum Phase Transitions in Matrix Product States," *Chinese Physics Letters* **25** (2008) 3574.

[317] K. A. Hallberg, "Density-matrix algorithm for the calculation of dynamical properties of low-dimensional systems," Phys. Rev. B **52** (1995) 9827, arXiv:cond-mat/9503094.

[318] S. Ramasesha, S. K. Pati, H. R. Krishnamurthy, Z. Shuai, and J. L. Bredas, "Low-Lying Electronic Excitations and Nonlinear Optic Properties of Polymers via Symmetrized Density Matrix Renormalization Group Method," arXiv:cond-mat/9609164.

[319] T. D. Kühner and S. R. White, "Dynamical correlation functions using the density matrix renormalization group," Phys. Rev. B **60** (1999) 335, arXiv:cond-mat/9812372.

[320] E. Jeckelmann, "Dynamical density-matrix renormalization-group method," Phys. Rev. B **66** (2002) 045114, arXiv:cond-mat/0203500.

[321] E. Jeckelmann, "Density-matrix renormalization group methods for momentum- and frequency-resolved dynamical correlation functions," arXiv:0808.2620.

[322] M. A. Cazalilla and J. B. Marston, "Time-Dependent Density-Matrix Renormalization Group: A Systematic Method for the Study of Quantum Many-Body Out-of-Equilibrium Systems," *Physical Review Letters* **88** (2002) 256403, arXiv:cond-mat/0109158.

[323] H. G. Luo, T. Xiang, and X. Q. Wang, "Comment on "Time-Dependent Density-Matrix Renormalization Group: A Systematic Method for the Study of Quantum Many-Body Out-of-Equilibrium Systems"," *Physical Review Letters* **91** (2003) 049701, arXiv:cond-mat/0212580.

[324] P. Schmitteckert, "Nonequilibrium electron transport using the density matrix renormalization group method," Phys. Rev. B **70** (2004) 121302, arXiv:cond-mat/0403759.

[325] G. Vidal, "Efficient Simulation of One-Dimensional Quantum Many-Body Systems," *Physical Review Letters* **93** (2004) 040502, arXiv:quant-ph/0310089.

[326] S. R. White and A. E. Feiguin, "Real-Time Evolution Using the Density Matrix Renormalization Group," *Physical Review Letters* **93** (2004) 076401, arXiv:cond-mat/0403310.

[327] A. J. Daley, C. Kollath, U. Schollwöck, and G. Vidal, "Time-dependent density-matrix renormalization-group using adaptive effective Hilbert spaces," *Journal of Statistical Mechanics: Theory and Experiment* **4** (2004) 5, arXiv:cond-mat/0403313.

[328] H. F. Trotter, "On the Product of Semi-Groups of Operators," *Proceedings of the American Mathematical Society* **10** (1959) 545. http://www.jstor.org/stable/2033649.

[329] M. Suzuki, "Generalized Trotter's formula and systematic approximants of exponential operators and inner derivations with applications to many-body problems," *Communications in Mathematical Physics* **51** (1976) 183.

[330] M. Suzuki, "Fractal decomposition of exponential operators with applications to many-body theories and monte carlo simulations," *Physics Letters A* **146** (1990) 319.

[331] J. J. Dorando, J. Hachmann, and G. K.-L. Chan, "Analytic response theory for the density matrix renormalization group," J. Chem. Phys. **130** (2009) 184111, arXiv:0901.3166.

[332] E. Hairer, C. Lubich, and G. Wanner, *Geometric Numerical Integration: Structure Preserving Algorithms for Ordinary Differential Equations*, vol. 31 of *Springer Series in Computational Mathematics*. Springer, 2004.

[333] M. den Nijs and M. Rommelse, "Preroughening transitions in crystal surfaces and valence-bond phases in quantum spin chains," *Physical Review B* **40** (1989) 4709.

[334] S. Qin, T.-K. Ng, and Z.-B. Su, "Edge states in open antiferromagnetic heisenberg chains," *Physical Review B* **52** (1995) 12844.

[335] F. D. M. Haldane, "Continuum dynamics of the 1-D Heisenberg antiferromagnet: Identification with the O(3) nonlinear sigma model," *Physics Letters A* **93** (1983) 464.

[336] F. D. M. Haldane, "Nonlinear Field Theory of Large-Spin Heisenberg Antiferromagnets: Semiclassically Quantized Solitons of the One-Dimensional Easy-Axis Néel State," *Physical Review Letters* **50** (1983) 1153.

[337] R. G. Pereira, S. R. White, and I. Affleck, "Exact Edge Singularities and Dynamical Correlations in Spin-1/2 Chains," *Physical Review Letters* **100** (2008) 027206.

[338] S. R. White and I. Affleck, "Spectral function for the $s = 1$ heisenberg antiferromagetic chain," *Physical Review B* **77** (2008) 134437.

[339] D. Porras, F. Verstraete, and J. I. Cirac, "Renormalization algorithm for the calculation of spectra of interacting quantum systems," Phys. Rev. B **73** (2006) 014410, `arXiv:cond-mat/0504717`.

[340] A. Bijl, J. de Boer, and A. Michels, "Properties of liquid helium II," *Physica* **8** (1941) 655.

[341] R. P. Feynman, "Atomic theory of the two-fluid model of liquid helium," *Physical Review* **94** (1954) 262.

[342] R. P. Feynman and M. Cohen, "Energy Spectrum of the Excitations in Liquid Helium," *Physical Review* **102** (1956) 1189.

[343] D. P. Arovas, A. Auerbach, and F. D. M. Haldane, "Extended Heisenberg models of antiferromagnetism: Analogies to the fractional quantum Hall effect," *Physical Review Letters* **60** (1988) 531.

[344] E. Bartel, A. Schadschneider, and J. Zittartz, "Excitations of anisotropic spin-1 chains with matrix product ground state," *European Physical Journal B* **31** (2003) 209, `arXiv:cond-mat/0301435`.

[345] S. G. Chung and L. Wang, "Entanglement perturbation theory for the elementary excitation in one dimension," *Physics Letters A* **373** (2009) 2277, `arXiv:1008.0346`.

[346] B. Pirvu, J. Haegeman, and F. Verstraete, "A matrix product state based algorithm for determining dispersion relations of quantum spin chains with periodic boundary conditions," `arXiv:1103.2735`.

[347] S. Mandelstam, "Soliton operators for the quantized sine-Gordon equation," *Physical Review D* **11** (1975) 3026.

[348] C. V. Kraus, N. Schuch, F. Verstraete, and J. I. Cirac, "Fermionic projected entangled pair states," Phys. Rev. A **81** (2010) 052338, `arXiv:0904.4667`.

[349] I. Pižorn and F. Verstraete, "Fermionic implementation of projected entangled pair states algorithm," Phys. Rev. B **81** (2010) 245110, `arXiv:1003.2743`.

[350] Z.-C. Gu, F. Verstraete, and X.-G. Wen, "Grassmann tensor network states and its renormalization for strongly correlated fermionic and bosonic states," `arXiv:1004.2563`.

[351] P. Jordan and E. Wigner, "Über das Paulische Äquivalenzverbot," *Zeitschrift für Physik A* **47** (1928) 631.

[352] P. Pfeuty, "The one-dimensional ising model with a transverse field," *Annals of Physics* **57** (1970) 79.

[353] J. B. Kogut, "An introduction to lattice gauge theory and spin systems," *Reviews of Modern Physics* **51** (1979) 659.

[354] T. Grover and T. Senthil, "Quantum spin nematics, dimerization, and deconfined criticality in quasi-1d spin-one magnets," *Physical Review Letters* **98** (2007) 247202.

[355] A. Läuchli, G. Schmid, and S. Trebst, "Spin nematics correlations in bilinear-biquadratic $S = 1$ spin chains," *Physical Review B* **74** (2006) 144426.

[356] S. Rachel and M. Greiter, "Exact models for trimerization and tetramerization in spin chains," *Physical Review B* **78** (2008) 134415.

[357] L. Tagliacozzo, T. R. de Oliveira, S. Iblisdir, and J. I. Latorre, "Scaling of entanglement support for matrix product states," Phys. Rev. B **78** (2008) 024410, arXiv:0712.1976.

[358] F. Pollmann, S. Mukerjee, A. M. Turner, and J. E. Moore, "Theory of Finite-Entanglement Scaling at One-Dimensional Quantum Critical Points," *Physical Review Letters* **102** (2009) 255701, arXiv:0812.2903.

[359] J. D. Cloizeaux and M. Gaudin, "Anisotropic linear magnetic chain," *Journal of Mathematical Physics* **7** (1966) 1384.

[360] L. D. Faddeev and L. A. Takhtajan, "What is the spin of a spin wave?," *Physics Letters A* **85** (1981) 375.

[361] H.-J. Mikeska, "Quantum solitons and the Haldane phase in antiferromagnetic spin chains," *Chaos, Solitons & Fractals* **5** (1995) 2585.

[362] F. Verstraete and J. I. Cirac, "Continuous Matrix Product States for Quantum Fields," *Physical Review Letters* **104** (2010) 190405, arXiv:1002.1824.

[363] C. M. Caves and G. J. Milburn, "Quantum-mechanical model for continuous position measurements," *Physical Review A* **36** (1987) 5543.

[364] I. Maruyama and H. Katsura, "Continuous Matrix Product Ansatz for the One-Dimensional Bose Gas with Point Interaction," *Journal of the Physical Society of Japan* **79** (2010) 073002, arXiv:1003.5463.

[365] J. Friedel, "Electronic structure of primary solid solutions in metals," *Advances in Physics* **3** (1954) 446.

[366] J. Haegeman, J. I. Cirac, T. J. Osborne, H. Verschelde, and F. Verstraete, "Applying the Variational Principle to (1+1)-Dimensional Quantum Field Theories," *Physical Review Letters* **105** (2010) 251601, arXiv:1006.2409.

[367] E. H. Lieb and W. Liniger, "Exact Analysis of an Interacting Bose Gas. I. The General Solution and the Ground State," *Physical Review* **130** (1963) 1605.

[368] G. Vidal, "Entanglement Renormalization," *Physical Review Letters* **99** (2007) 220405, arXiv:cond-mat/0512165.

[369] G. Vidal, "Class of Quantum Many-Body States That Can Be Efficiently Simulated," *Physical Review Letters* **101** (2008) 110501, arXiv:quant-ph/0610099.

[370] G. Vidal, "Entanglement Renormalization: an introduction," arXiv:0912.1651.

[371] Y.-Y. Shi, L.-M. Duan, and G. Vidal, "Classical simulation of quantum many-body systems with a tree tensor network," Phys. Rev. A **74** (2006) 022320, arXiv:quant-ph/0511070.

[372] L. Tagliacozzo, G. Evenbly, and G. Vidal, "Simulation of two-dimensional quantum systems using a tree tensor network that exploits the entropic area law," Phys. Rev. B **80** (2009) 235127, arXiv:0903.5017.

[373] G. Evenbly and G. Vidal, "Algorithms for entanglement renormalization," Phys. Rev. B **79** (2009) 144108, arXiv:0707.1454.

[374] L. Cincio, J. Dziarmaga, and M. M. Rams, "Multiscale Entanglement Renormalization Ansatz in Two Dimensions: Quantum Ising Model," *Physical Review Letters* **100** (2008) 240603, arXiv:0710.3829.

[375] G. Evenbly and G. Vidal, "Entanglement Renormalization in Two Spatial Dimensions," *Physical Review Letters* **102** (2009) 180406, arXiv:0811.0879.

[376] G. Evenbly and G. Vidal, "Frustrated Antiferromagnets with Entanglement Renormalization: Ground State of the Spin-(1)/(2) Heisenberg Model on a Kagome Lattice," *Physical Review Letters* **104** (2010) 187203, arXiv:0904.3383.

[377] P. Corboz, G. Evenbly, F. Verstraete, and G. Vidal, "Simulation of interacting fermions with entanglement renormalization," Phys. Rev. A **81** (2010) 010303, arXiv:0904.4151.

[378] P. Corboz and G. Vidal, "Fermionic multiscale entanglement renormalization ansatz," Phys. Rev. B **80** (2009) 165129, arXiv:0907.3184.

[379] M. Aguado and G. Vidal, "Entanglement Renormalization and Topological Order," *Physical Review Letters* **100** (2008) 070404, arXiv:0712.0348.

[380] R. König, B. W. Reichardt, and G. Vidal, "Exact entanglement renormalization for string-net models," Phys. Rev. B **79** (2009) 195123, arXiv:0806.4583.

[381] L. Tagliacozzo and G. Vidal, "Entanglement renormalization and gauge symmetry," Phys. Rev. B **83** (2011) 115127, arXiv:1007.4145.

[382] V. Giovannetti, S. Montangero, and R. Fazio, "Quantum Multiscale Entanglement Renormalization Ansatz Channels," *Physical Review Letters* **101** (2008) 180503, arXiv:0804.0520.

[383] R. N. C. Pfeifer, G. Evenbly, and G. Vidal, "Entanglement renormalization, scale invariance, and quantum criticality," Phys. Rev. A **79** (2009) 040301, arXiv:0810.0580.

[384] S. Montangero, M. Rizzi, V. Giovannetti, and R. Fazio, "Critical exponents with a multiscale entanglement renormalization Ansatz channel," Phys. Rev. B **80** (2009) 113103.

[385] G. Evenbly, P. Corboz, and G. Vidal, "Nonlocal scaling operators with entanglement renormalization," Phys. Rev. B **82** (2010) 132411, arXiv:0912.2166.

[386] G. Evenbly, R. N. C. Pfeifer, V. Picó, S. Iblisdir, L. Tagliacozzo, I. P. McCulloch, and G. Vidal, "Boundary quantum critical phenomena with entanglement renormalization," Phys. Rev. B **82** (2010) 161107, arXiv:0912.1642.

[387] G. Evenbly and G. Vidal, "Beyond the "entropic boundary law" with entanglement renormalization." Presented at "New Development of Numerical Simulations in Low-Dimensional Quantum Systems: From Density Matrix Renormalization Group to Tensor Network Formulations", Yukawa Institute for Theoretical Physics, Kyoto University, October 19th 2010. *Unpublished*.

[388] G. Evenbly and G. Vidal, "Tensor Network States and Geometry," *Journal of Statistical Physics* (2011) 185, arXiv:1106.1082.

[389] B. Swingle, "Entanglement Renormalization and Holography," arXiv:0905.1317.

[390] S.-S. Lee, "Holographic description of large N gauge theory," *Nuclear Physics B* **851** (2011) 143, arXiv:1011.1474.

[391] D. J. Weir, "Studying a relativistic field theory at finite chemical potential with the density matrix renormalization group," *Physical Review D* **82** (2010) 025003, arXiv:1003.0698.

[392] D. J. Gross and A. Neveu, "Dynamical symmetry breaking in asymptotically free field theories," Phys. Rev. D **10** (1974) 3235.

[393] K. Yee, "Numerical solution of initial boundary value problems involving maxwell's equations in isotropic media," *IEEE Transactions on Antennas and Propagation* **14** (1966) 302.

[394] J. Kogut and L. Susskind, "Hamiltonian formulation of Wilson's lattice gauge theories," *Physical Review D* **11** (1975) 395.

[395] L. Susskind, "Lattice fermions," *Physical Review D* **16** (1977) 3031.

[396] H. B. Nielsen and M. Ninomiya, "Absence of neutrinos on a lattice (I). Proof by homotopy theory," *Nuclear Physics B* **185** (1981) 20.

[397] H. B. Nielsen and M. Ninomiya, "Absence of neutrinos on a lattice (II). Intuitive topological proof," *Nuclear Physics B* **193** (1981) 173.

[398] H. B. Nielsen and M. Ninomiya, "A no-go theorem for regularizing chiral fermions," *Physics Letters B* **105** (1981) 219.

[399] K. G. Wilson in *Gauge Theories and Modern Field Theory : proceedings of a conference held at Northeastern University, Boston, September 26 and 27, 1975* , R. Arnowitt and P. Nath, eds. 1976.

[400] M. Creutz, "Four-dimensional graphene and chiral fermions," *Journal of High Energy Physics* **4** (2008) 17, `arXiv:0712.1201`.

[401] R. F. Dashen, B. Hasslacher, and A. Neveu, "Semiclassical bound states in an asymptotically free theory," Phys. Rev. D **12** (1975) 2443.

[402] A. B. Zamolodchikov and A. B. Zamolodchikov, "Exact S matrix of Gross-Neveu "elementary" fermions," *Physics Letters B* **72** (1978) 481.

[403] M. Karowski and H. J. Thun, "Complete s-matrix of the o(2n) gross-neveu model," *Nuclear Physics B* **190** (1981) 61.

[404] P. Forgács, F. Niedermayer, and P. Weisz, "The exact mass gap of the Gross-Neveu model (I). The thermodynamic Bethe ansatz," *Nuclear Physics B* **367** (1991) 123.

[405] P. Forgács, F. Niedermayer, and P. Weisz, "The exact mass gap of the Gross-Neveu model (II). The 1/N expansion," *Nuclear Physics B* **367** (1991) 144.

[406] P. Fendley, "Integrable Sigma Models," in *Integrable quantum field theories and their applications: Proceedings of the APCTP Winter School*, C. Ahn, C. Rim, and R. Sasaki, eds. World Scientific, 2001.

[407] J. Feinberg, "Kinks and bound states in the Gross-Neveu model," *Physical Review D* **51** (1995) 4503, `arXiv:hep-th/9408120`.

[408] J. Feinberg, "All about the static fermion bags in the Gross-Neveu model," *Annals of Physics* **309** (2004) 166–231, `arXiv:hep-th/0305240`.

[409] A. Recati, J. N. Fuchs, C. S. Peça, and W. Zwerger, "Casimir forces between defects in one-dimensional quantum liquids," *Physical Review A* **72** (2005) 023616, `arXiv:cond-mat/0505420`.

[410] J. N. Fuchs, A. Recati, and W. Zwerger, "Oscillating Casimir force between impurities in one-dimensional Fermi liquids," *Physical Review A* **75** (2007) 043615, `arXiv:cond-mat/0610659`.

[411] N. Duffield and R. F. Werner, "Local dynamics of mean-field quantum systems," *Helvetica Physica Acta* **65** (1992) 1016.